

**Xanthenes and benzophenones
from *Cyclopia genistoides* (honeybush):
chemical characterisation and
assessment of thermal stability**

Theresa Beelders

*Dissertation presented for the degree of
Doctor of Philosophy (Food Science)
in the Faculty of AgriScience at Stellenbosch University*



Supervisor: Prof. E. Joubert
Co-supervisors: Dr. D. de Beer
Dr. G.O. Sigge

March 2016

DECLARATION

By submitting this dissertation electronically, I declare that the entirety of the work contained therein is my own, original work, that I am the sole author thereof (save to the extent explicitly otherwise stated), that reproduction and publication thereof by Stellenbosch University will not infringe any third party rights and that I have not previously in its entirety or in part submitted it for obtaining any qualification.

This dissertation includes three original papers published in peer-reviewed journals and one unpublished publication. The development and writing of the papers (published and unpublished) were the principal responsibility of myself and for each of the cases where this is not the case, a declaration is included in the dissertation indicating the nature and extent of the contributions of co-authors.

Theresa Beelders

Date: March 2016

SUMMARY

Numerous health-promoting benefits may be derived from the consumption of honeybush tea, a herbal infusion prepared from the leaves and fine stems of the endemic Cape fynbos genus, *Cyclopia*. These health-promoting benefits are attributed to its phenolic constituents and therefore insight into the nature, quantities and biological activities of individual compounds are required. Information regarding the thermal stability of these compounds is also crucial, as the plant material is subjected to a high-temperature chemical oxidation process (“fermentation”) to develop the sought-after characteristic sensory attributes of the herbal tea product. In this study, the phenolic composition of *Cyclopia genistoides*, a commercially important species, was comprehensively characterised by high-performance liquid chromatography (HPLC) coupled with diode-array and mass spectrometric detection. A species-specific HPLC method was developed for the qualitative analysis of aqueous extracts prepared from “unfermented” and “fermented” *C. genistoides* plant material and was subsequently validated for the quantification of 18 phenolic compounds in these types of extracts. The major phenolic constituents included the C-glucosyl xanthone mangiferin (**1**) and its regio-isomer isomangiferin (**2**), and the benzophenone 3- β -D-glucopyranosyliriflophenone (**3**). The presence of novel benzophenone and xanthone derivatives in *C. genistoides* was demonstrated for the first time, including an iriflophenone-di-O,C-hexoside derivative, present in large quantities. This compound was isolated and unambiguously identified by nuclear magnetic resonance spectroscopy as 3- β -D-glucopyranosyl-4- β -D-glucopyranosyloxyiriflophenone (**4**) – a novel benzophenone unique to *Cyclopia*. 3- β -D-Glucopyranosylmaclurin (**5**), present in small quantities, was also isolated. The isolated benzophenones (**4** and **5**) exhibited mammalian α -glucosidase inhibitory activity, while **4** and **3** were also marginally effective in increasing glucose uptake in vitro. Compound **4** was ineffective as antioxidant in the DPPH assay, but the most effective in the ORAC assay, compared to the other compounds tested (**1**, **2**, **3**, **5**). Degradation of compounds **1-4** in *C. genistoides* plant material under simulated fermentation conditions (80 °C/24 h and 90 °C/16 h) followed first-order degradation kinetics and their thermal stability decreased in the order **4** > **2** > **3** > **1**. An increase in the degree of glucosylation significantly increased the thermal stability of the benzophenones, whereas glucosylation at C-4 of the dibenzo- γ -pyrone structure, as opposed to C-2, increased the stability of the tetrahydroxanthones in the plant material matrix. This was also confirmed for individual compounds (**1-5**) in aqueous model solutions (pH 5). Inclusion of **5** in the model systems provided additional insight into structure-stability relationships. Increased B-ring hydroxylation significantly increased the first-order degradation rate constants of the benzophenones. Oxidative coupling of the polyhydroxybenzophenone **5** with the formation of its corresponding xanthones (**1** and **2**) led to substantial increases in the thermal stability of **1** and **2** compared to that of **5**. Increased temperatures increased the degradation rates of all compounds in both the plant material matrix and model solutions. The thermal stability of **1**, tested at pH 3-7, was found to be pH-dependent, with increased degradation rates observed at higher pH. Thermally-induced reactions principally included isomerisation, dimerisation and cleavage of O-linked sugar moieties; conversion of all benzophenones to the xanthones occurred to varying degrees. Of special interest was the rapid and predominant conversion of **5** to **1** and **2**.

OPSOMMING

Die gebruik van heuningbostee, berei van die eg Suid-Afrikaanse fynbosgenus, *Cyclopia*, mag verskeie gesondheidsvoordele inhou wat grootliks toegeskryf kan word aan sy fenoliese samestelling. Inligting aangaande die aard, hoeveelhede en biologiese aktiwiteite van individuele verbindings word dus benodig. Die hitte-stabiliteit van die fenoliese verbindings is ook van kardinale belang, aangesien hulle blootgestel word aan hoë temperature tydens chemiese oksidasie (“fermentasie”) van die plantmateriaal – ’n proses wat noodsaaklik is om die hoogs-gesogte, karakteristieke sensoriese eienskappe van die kruie tee produk te ontwikkel. In hierdie studie is die fenoliese samestelling van *C. genistoides*, ’n kommersieël-belangrike spesie, in diepte gekarakteriseer deur middel van hoë-druk vloeistof chromatografie (HPLC) gekoppel aan ultraviolet-diode deteksie en massa spektrometrie. ’n Spesie-spesifieke HPLC metode is ontwikkel vir die kwalitatiewe analise van water ekstrakte wat van “ongefermenteerde” sowel as “gefermenteerde” *C. genistoides* plantmateriaal voorberei is. Die metode is vervolgens vir die kwantifisering van 18 fenoliese verbindings in hierdie tipe ekstrakte gevalideer. Die hoof fenoliese verbindings is geïdentifiseer as die *C*-glukosidiese xantoon mangiferien (**1**) en sy posisionele isomeer isomangiferien (**2**), sowel as die bensofenoon iriflofenoon-3-*C*-glukosied (**3**). Die aanwesigheid van unieke bensofenoon en xantoon-derivate is vir die eerste keer in *C. genistoides* aangedui, insluitende ’n iriflofenoon-di-*O,C*-glukosied afgeleide wat in hoë konsentrasies aanwesig was. Hierdie verbinding is geïsoleer en met behulp van kern magnetiese resonans spektroskopie as iriflofenoon-3-*C*-glukosied-4-*O*-glukosied (**4**) geïdentifiseer – ’n nuwe bensofenoon uniek aan *Cyclopia*. Maklurien-3-*C*-glukosied (**5**), aanwesig in klein hoeveelhede, is ook geïsoleer. Die geïsoleerde verbindings (**4** en **5**) het inhiberende aktiwiteit teenoor α -glukosidase, geïsoleer uit rotte, getoon, terwyl **4** en **3** ook marginaal effektief was om glukose-opname in selsisteme te bevorder. Verbinding **4** was onreaktief as antioksidant in die DPPH toets, maar die mees reaktiefste in die ORAC toets, in vergelyking met al die ander verbindings wat getoets is (**1**, **2**, **3**, **5**). Degradasie van die verbindings **1-4** in *C. genistoides* plantmateriaal onder gesimuleerde “fermentasie” kondisies (80 °C/24 h en 90 °C/16 h) het eerste-orde degradasie kinetika gevolg en hul hitte-stabiliteit het afgeneem in die volgorde **4** > **2** > **3** > **1**. ’n Toename in die graad van glukosilering het die hitte-stabiliteit van die bensofenone in die plantmateriaal matrig aansienlik verbeter, terwyl glukosilering op C-4 van die dibenso- γ -piroon struktuur, in plaas van C-2, die stabiliteit van die tetrahidroksiexantone verbeter het. Dit is ook vir individuele verbindings (**1-5**) in waterige model oplossings (pH 5) bevestig. Die insluiting van **5** in die modelsisteme het addisionele insig ten opsigte van struktuur-stabiliteitverwantskappe gebied. ’n Toename in die aantal hidroksie-groepe op die B-ring van die bensofenone het hul eerste-orde degradasie tempo’s aansienlik verhoog. Oksidatiewe koppeling van die polihidroksiebensofenoon **5** met die vorming van sy ooreenkomstige xantone (**1** en **2**) het die hitte-stabiliteit van **1** en **2**, in vergelyking met **5**, merkbaar verbeter. ’n Toename in reaksietemperatuur het die eerste-orde degradasie tempo’s van al die fenoliese verbindings in die plantmateriaal en in die modelsisteme laat toeneem. Die hitte stabiliteit van **1**, getoets by pH 3-7, was ook afhanklik van die pH van die waterige model sisteem, met hoër reaksie tempo’s waargeneem by hoër pH-vlakke. Hitte-geïnduseerde reaksies het hoofsaaklik dimerisasie, isomerisasie en afsplitsting van O-gekoppelde suiker eenhede behels. Omskakeling van die bensofenone na die xantone is ook tot verskeie mates waargeneem, waar die snelle en oorheersende omskakeling van **5** na **1** en **2** veral opvallend was.

ACKNOWLEDGEMENTS

My most sincere gratitude goes to my supervisor, Prof. Elizabeth Joubert, and to my so-supervisor, Dr. Dalene de Beer. Thank you for the guidance, advice and immense help offered throughout this study. It has been a privilege and pleasure to work with such experienced researchers.

Recognition goes to my co-supervisor, Dr. Gunnar Sigge (Food Science Department, Stellenbosch University), for his kind support and various inputs, especially in the preparation of my research seminars and the compilation of this thesis.

Dr Christiaan Malherbe (Post-Harvest and Wine Technology Division, ARC Infruitec-Nietvoorbij, Stellenbosch) is thanked for his immense help and practical assistance throughout my doctoral study, and also for conducting the α -glucosidase inhibitory assays.

Drr. Sithandiwe Mazibuko and Christo Muller (Diabetes Discovery Platform, South African Medical Research Council, Tygerberg), for conducting in vitro tests in several cell models to investigate the ability of target benzophenones to increase glucose uptake in vitro.

Dr Jaco Brand (Nuclear Magnetic Resonance Unit, Central Analytical Facility (CAF), Stellenbosch University), for NMR analyses and data interpretation.

Dr Marietjie Stander (Mass Spectrometry Unit, CAF, Stellenbosch University), for assisting with LC-MS analyses.

Mrs Wernich Kühn (Water Analysis Division, CAF, Stellenbosch University) is thanked for the enzyme robot assay and Mr Fletcher Hiten (Mass Spectrometry Unit, CAF, Stellenbosch University) for GC-MS analyses.

Mrs Marieta van der Rijst (Biometry Unit, ARC Infruitec-Nietvoorbij, Stellenbosch) and Prof Martin Kidd (Centre for Statistical Consultation, Department of Statistics and Actuarial Sciences, Stellenbosch University) are thanked for statistical data analysis.

Mr Fritz Joubert (Koksrivier, Pearly Beach, Western Cape, South Africa) is acknowledged for supplying plant material.

Dr Elize Willenburg (Post-Harvest and Wine Technology Division, ARC Infruitec-Nietvoorbij, Stellenbosch) is thanked for the isolation of isomangiferin from *C. genistoides*.

The following institutions and associations are acknowledged for providing research funding and other financial support:

- The National Research Foundation (IPRR Grant 85277 to E. Joubert and Thuthuka Grant 87849 to C.J. Malherbe)
- South African Department of Science and Technology (DST/CON 0133/2012).
- Agricultural Research Council (Economic Competitive Support Package for Agroprocessing)
- NRF-DST Professional Development Programme Doctoral Scholarship (NRF-DST Grant 78992 to E. Joubert)
- Stellenbosch University (Merit Bursary 2013, 2014 and 2015)
- Department of Science and Technology (Women in Science Awards, 2014).
- South African Association of Food Science and Technology (SAAFoST, Dreosti Award 2013).

*** Friends and family, thank you for all forms of encouragement and support, it is truly appreciated ***

TABLE OF CONTENTS

Declaration	i
Summary	ii
Opsomming	iii
Acknowledgements	iv
CHAPTER 1	
General Introduction	1
CHAPTER 2	
Literature Review	7
1. Introduction	8
2. Honeybush and its Phenolic Composition	8
2.1. Phenolic Composition of <i>Cyclopia</i> spp.	8
2.2. Quantitative Analysis of the Phenolic Composition of <i>Cyclopia</i> spp. by LC-DAD	12
2.3. Factors Affecting the Phenolic Composition of <i>Cyclopia</i> spp.	16
2.4. Bio-activity of <i>Cyclopia</i> Xanthone and Benzophenone Constituents	18
2.5. Concluding Remarks	19
3. Thermal Degradation Kinetics Modelling of Phenolic Acids and Flavonoids	19
3.1. Phenolic Acids	20
3.1.1. Thermal Stability of Chlorogenic Acids and Other Phenolic Acid Derivatives	20
3.1.2. Thermal Stability of Phenolic Acids under Sub- and Supercritical Water Conditions	25
3.2. Flavan-3-ols and Proanthocyanidins	27
3.2.1. Green Tea Flavan-3-ols	28
3.2.2. Thermal Stability of Monomeric Flavan-3-ols in Apple Juice, Grape Seed Extract and Cocoa	38
3.2.3. Proanthocyanidins	40
3.3. Dihydrochalcones, Flavanones, Dihydroflavonols, Flavonols and Flavones	44
3.3.1. Dihydrochalcones	44
3.3.2. Flavanones	51
3.3.3. Dihydroflavonols	52
3.3.4. Flavonols	53
3.3.5. Flavones	55
3.4. Isoflavones	57
3.5. Concluding Remarks	65
References	66

CHAPTER 3Comprehensive Phenolic Profiling of *Cyclopia genistoides* (L.) Vent.

by LC-DAD-ESI-MS and -MS/MS Reveals Novel Xanthone and Benzophenone Constituents	78
Declaration	79
Abstract	80
1. Introduction	81
2. Materials and Methods	81
2.1. Chemicals	81
2.2. Sample Preparation	82
2.3. HPLC-DAD Method Development	82
2.4. Optimised HPLC-DAD Method	82
2.5. LC-DAD-ESI-MS and –MS/MS Analyses	83
2.6. HPLC-DAD Method Validation	83
2.7. Quantification of Phenolic Compounds In Freeze-Dried Aqueous Extracts of <i>C. genistoides</i>	84
3. Results and Discussion	84
3.1. HPLC-DAD Method Development	84
3.2. LC-DAD-ESI-MS and -MS/MS Identification of Compounds Present in Hot Water Extracts of Unfermented and Fermented <i>C. genistoides</i>	86
3.2.1. Benzophenone Derivatives	87
3.2.2. Xanthone Derivatives	89
3.2.3. Flavanones	95
3.2.4. Amino Acids	96
3.2.5. Glycosylated Phenolic Acids	96
3.2.6. Flavones	99
3.2.7. Dihydrochalcones	99
3.3. HPLC-DAD Method Validation	99
3.4. Quantification of Phenolic Compounds	100
4. Conclusions	101
References	102
Supplementary Material Chapter 3	106

CHAPTER 4Structural Elucidation of the Novel *Cyclopia* Benzophenone 3- β -D-Glucopyranosyl-4- β -D-

glucopyranosyloxyiriflophenone and the Comparative Assessment of its Antidiabetic Potential	109
Declaration	110
Abstract	111
1. Introduction	112
2. Materials and Methods	113
2.1. General Experimental Procedures	113
2.2. Plant Material	113
2.3. Extraction and Isolation	113

2.4. Structural Elucidation	114
2.5. Determination of α -Glucosidase Inhibitory Activity	115
2.6. Assessment of Cellular 2-deoxy- ^3H -D-glucose (^3H -2-DOG) Uptake	116
3. Results and Discussion	117
3.1. Identification of Compounds 1 and 2	117
3.2. α -Glucosidase Inhibitory Activity of Benzophenones	118
3.3. The Ability of Benzophenones to Increase Glucose Uptake In Vitro	119
4. Conclusions	120
References	121

CHAPTER 5

Thermal Degradation Kinetics Modelling of Benzophenones and Xanthoness during High-Temperature Oxidation of <i>Cyclopia genistoides</i> (L.) Vent. Plant Material and the Effect on Total Antioxidant Capacity of Aqueous Extracts	123
Declaration	124
Abstract	125
1. Introduction	126
2. Materials and Methods	127
2.1. Chemicals	127
2.2. Thermal Degradation Kinetics Modelling	127
2.3. Evaluation of the Thermal Degradation Kinetics Model	128
2.4. Antioxidant Capacity of Selected Xanthoness and Benzophenones and the Effect of High-Temperature Oxidation on TAC of Aqueous Extracts	129
3. Results	130
3.1. Thermal Degradation Kinetics Modelling	130
3.2. Evaluation of the Thermal Degradation Kinetics Model	132
3.3. Effect of High-Temperature Oxidation on the Levels of Individual Phenolic Compounds in Hot Water Extracts	133
3.4. Antioxidant Capacity of Selected Xanthoness and Benzophenones and the Effect of High-Temperature Oxidation on TAC of Aqueous Extracts	135
4. Discussion	136
4.1. Thermal Degradation Kinetics Modelling and Evaluation of the Model	136
4.2. Effect of High-Temperature Oxidation on the Levels of Individual Phenolic Compounds in Hot Water Extracts	137
4.3. Antioxidant Capacity of Selected Xanthoness and Benzophenones and Effect of High-Temperature Oxidation on TAC of Aqueous Extracts	138
5. Conclusions	140
References	141
Supplementary Material Chapter 5	143

CHAPTER 6

Thermal Degradation Kinetics Modelling of Benzophenones and Xanthonones in Aqueous Model Systems: Structure-Stability Relationships, and Temperature and pH Effects	146
Abstract	147
1. Introduction	148
2. Materials and Methods	150
2.1. Chemicals	150
2.2. Optimisation and Validation of an UHPLC-DAD Method for Thermal Degradation Kinetics Experiments	150
2.3. Thermal Degradation Kinetics Experiments	151
2.4. Quantitative Determination of Target Xanthonones and Benzophenones in Thermally-Treated Solutions by UHPLC-DAD	152
2.5. Determination of Thermal Degradation Kinetic Parameters	152
2.6. Identification of Thermal Degradation Products by LC-DAD-ESI-MS and –MS/MS	153
2.7. Evolution of Mangiferin and Isomangiferin in Thermally-Treated Solutions of 3- β -D-Glucopyranosylmaclurin as a Function of Treatment Temperature and Time	154
3. Results and Discussion	155
3.1. Thermal Degradation Kinetics Modelling of Benzophenones and Xanthonones in Aqueous Model Systems (pH 5): Structure-Stability Relationships and Temperature Effects	156
3.2. Thermal Degradation Kinetics Modelling of the Xanthone Mangiferin in Aqueous Model Systems: pH and Temperature Effects	162
3.3. Identification of Thermal Degradation Products by LC-DAD-ESI-MS and –MS/MS	165
3.4. Evolution of Mangiferin and Isomangiferin in Thermally-Treated Solutions of 3- β -D-Glucopyranosylmaclurin as a Function of Treatment Temperature and Time	182
4. Conclusions	183
References	184
Supplementary Material Chapter 6	187

CHAPTER 7

General Discussion and Conclusions	203
References	213

NOTES

This dissertation is presented in the format prescribed by the Department of Food Science at Stellenbosch University. The structure is in the form of one or more research chapters (papers prepared for publication) and is prefaced by an introduction chapter with the study objectives, followed by a literature review chapter and culminating with a chapter for elaborating a general discussion and conclusion. The language, style and referencing format used are in accordance with the requirements of the *International Journal of Food Science and Technology*. This dissertation represents a compilation of manuscripts where each chapter is an individual entity and some repetition between chapters has, therefore, been unavoidable.

Please take note of the following:

1. The language, style and referencing format of research chapters that have been published have been changed according to the requirements of the *International Journal of Food Science and Technology*.
2. Minor formatting changes have been made throughout the thesis to ensure consistency.
3. With regard to the nomenclature: in cases where the structure of a compound was not elucidated in full (*e.g.* iriflophenone-di-*O,C*-hexoside), the *O* refers to a hexosyloxy moiety, and the *C* to a hexosyl moiety.

CHAPTER 1

General Introduction

The herbal tea, honeybush, is prepared from “unfermented” (green) and “fermented” (oxidised) plant material of various species of the genus *Cyclopia* Vent. (family Fabaceae; tribe Podalyriaceae), a leguminous shrub endemic to the Cape Floristic region of South Africa (Schutte, 1995; Du Toit *et al.*, 1998). Honeybush is recognised as one of the few indigenous South African plants that have made the transition from a local wild resource to a commercial product over the past 100 years (Joubert *et al.*, 2011). Most of the annual production is exported to the Netherlands, Germany, United Kingdom (UK) and United States of America (USA) (Joubert *et al.*, 2011).

The popularity of fermented honeybush as herbal tea is attributed to its characteristically slightly sweet taste, mild astringency and sweet-associated, floral, fruity, woody and plant-like aromas (Theron *et al.*, 2014). Other contributing factors are its relatively low tannin content (Marloth, 1925; Terblanche, 1982), caffeine-free status (Greenish, 1881) and mounting evidence supporting its health-promoting potential (as reviewed by Joubert *et al.*, 2008a). This herbal tea also represents a rich source of bio-active phenolic compounds not commonly found in other food and beverage products and may therefore contribute to a healthy diet (Joubert *et al.*, 2009). In terms of phenolic composition, only fermented *C. intermedia* (Ferreira *et al.*, 1998; Kamara *et al.*, 2003) and unfermented *C. subternata* (Kamara *et al.*, 2004; Kokotkiewicz *et al.*, 2012) have been characterised comprehensively, while recent studies have also focused on the isolation and identification of compounds from unfermented *C. genistoides* (Kokotkiewicz *et al.*, 2013; Malherbe *et al.*, 2014). Collectively, these studies indicate that *Cyclopia* extracts principally contain glycosylated compounds from the xanthone, benzophenone, dihydrochalcone, flavanone, flavone, isoflavone and flavonol phenolic sub-classes. The presence of a number of polyphenols, identified in these species, has also been confirmed in these and other *Cyclopia* species by liquid chromatography-mass spectrometry (Joubert *et al.*, 2008b; De Beer & Joubert, 2010; De Beer *et al.*, 2012; Malherbe *et al.*, 2014; Schulze *et al.*, 2014).

Harvested *Cyclopia* plant material is traditionally oxidised (fermented) at elevated temperatures, which results in the development of the characteristic sensory properties, including the dark-brown leaf and red-brown infusion colour of honeybush tea (Du Toit & Joubert, 1999). Du Toit & Joubert (1999) investigated the effects of processing temperatures (60, 70, 80 and 90 °C) on the extract and leaf colour, as well as the sensory quality of *C. maculata* (later re-classified as *C. buxifolia*; Joubert *et al.*, 2011) and *C. intermedia*. It was found that the development of optimal sweet-associated flavour depended on the fermentation temperature-time combinations, with higher temperatures needing shorter times. Fermentation at 70 °C for 60 h or 90 °C for 36 h produced the best flavoured tea. The latter temperature-time combination was also optimal for the development of the desired leaf and infusion colour. Colour development was principally ascribed to the oxidation of polyphenols during fermentation (Du Toit & Joubert, 1999), although this phenomenon was not investigated.

Theron (2012) subsequently re-evaluated the effect of fermentation temperature (80 and 90 °C) and time (8, 16, 24 and 32 h) on the sensory profile and polyphenolic composition of honeybush tea. The objective of the latter study was to establish the optimum fermentation temperature-time combination for *C. subternata*, *C. genistoides* and *C. maculata*, respectively. Fermentation was found to enhance positive and to decrease the negative aroma, flavour and taste attributes, rather than form new attributes. In order to produce honeybush tea with an optimal sensory profile, fermentation conditions of 80 °C/24 h or 90 °C/16 h were proposed, depending on the specific aroma note required.

While the aforementioned studies primarily focused on establishing the optimal fermentation conditions from a sensory perspective, compositional changes were also observed. Du Toit & Joubert (1999) noted that *C. maculata* (re-classified *C. buxifolia*) and *C. intermedia* showed progressive decreases in hot water soluble solids (SS) content and the polyphenolic content of the SS with increasing fermentation time, irrespective of the temperature used. The reduction in SS content was, amongst others, ascribed to the formation of insoluble products as a result of polymerisation of monomeric phenols (Du Toit & Joubert, 1999). Theron (2012) also reported that fermentation reduced the SS content,

total polyphenol content and concentrations of individual polyphenolic compounds, and that these losses were exacerbated with increased fermentation times and temperatures. Similarly, studies by Joubert *et al.* (2008b) and De Beer & Joubert (2010) showed that fermentation (70 °C for 60 h) resulted in significant reductions in extract yields and the total polyphenol and individual polyphenol contents of the aqueous extracts. The antioxidant capacity and antimutagenicity of the extracts prepared from the fermented plant material were also lower than those of the unfermented plant material, attributed to changes in phenolic composition and/or decreased levels of phenolic compounds (Van der Merwe *et al.*, 2006; Joubert *et al.*, 2008b).

While it is evident that the high-temperature oxidation process represents a crucial step in the production of a high-quality herbal tea product, it also leads to significant losses in phenolic content and biological activity. Knowledge regarding the thermal stability of *Cyclopia* phenolic constituents is therefore required so that their losses during fermentation may be predicted, and subsequently also minimised, to obtain a honeybush product with maximum biofunctionality. Similarly, when *Cyclopia* extracts are used as food ingredients in iced tea beverages and bread, amongst others, they are subject to heat treatment during processing, *e.g.* pasteurisation and baking, respectively.

The overall objective of this study was thus to investigate the thermal stability of the major xanthenes and benzophenones present in *Cyclopia genistoides*. The focus fell specifically on these constituents, in light of their relative abundance and biological significance. Previous studies have indicated that *C. genistoides* contains high levels of the bio-active C-glucosyl xanthone, mangiferin (as reviewed by Vyas *et al.* 2012), maximally present at levels of *ca.* 10% dry weight of the leaves (Joubert *et al.*, 2014). Of special interest is the antidiabetic properties of mangiferin, postulated to contribute to the hypoglycaemic effect observed when streptozotocin-induced diabetic rats were treated with aqueous extracts of *C. intermedia* and *C. maculata* (Muller *et al.*, 2011; Chellan *et al.*, 2014). Other major compounds reported to be present in *C. genistoides* include the xanthone isomangiferin (*ca.* 2%) and the benzophenone 3- β -D-glucopyranosylriflophenone (*ca.* 1%) (Joubert *et al.*, 2014). It has been found that isomangiferin improves glucose uptake by C2C12 muscle cells with the same efficacy as mangiferin (Schulze *et al.*, 2015). The benzophenone 3- β -D-glucopyranosylriflophenone has demonstrated α -glucosidase inhibitory (Feng *et al.*, 2011) and pro-apoptotic (Kokotkiewicz *et al.*, 2013) activities. Moreover, using on-line high-performance liquid chromatographic (HPLC) antioxidant assays, Malherbe *et al.* (2014) demonstrated antioxidant activities for both isomangiferin and 3- β -D-glucopyranosylriflophenone. 3- β -D-Glucopyranosylriflophenone exhibited no radical scavenging activity in the DPPH assay, but was as effective as mangiferin in the ORAC assay, and slightly less effective than mangiferin in the ABTS assay. Isomangiferin showed slightly lower antioxidant capacity than mangiferin against DPPH \cdot , but higher capacity against ABTS $^{++}$ and peroxy radicals (Malherbe *et al.*, 2014). The presence of the benzophenone 3- β -D-glucopyranosylmaclurin in unfermented *C. genistoides* (< 0.5% dry weight) was also recently demonstrated (Kokotkiewicz *et al.*, 2013). Although the biological activity of the latter minor benzophenone has not yet been assessed, it is expected that this compound will be highly reactive as antioxidant due to its ortho-diol structure, one of the structural features responsible for antioxidant activity of polyphenols (Rice-Evans *et al.*, 1996; Heim *et al.*, 2002).

In this study, these xanthone and benzophenone constituents, together with other related compound(s) of interest, were foremost characterised in terms of their thermal stability and also with respect to their biological activities (antioxidant, mammalian α -glucosidase inhibitory and glucose-uptake stimulatory activities). New compound(s), and/or those that were not commercially available, were isolated from *C. genistoides* and identified using appropriate analytical techniques. Thermal stability of the compounds when present in the *C. genistoides* plant material matrix was assessed under conditions simulating the fermentation process, used in herbal tea manufacture. Their thermal stabilities were also assessed in aqueous model solutions. By conducting stability assessments in aqueous model solutions, potential matrix

effects were reduced and fundamental insight into degradation pathways and/or possible interconversion reactions was obtained.

In this study, thermal degradation kinetics modelling (Van Boekel, 1996; 2008) was used as a tool to derive the basic kinetic information (*i.e.*, reaction order, reaction rate constants, etc.) for each compound in the respective systems. The effect of temperature on the degradation rate was evaluated by calculating the temperature coefficient of Van't Hoff (Bělehrádek, 1930) or the Arrhenius activation energy (Peleg *et al.*, 2012), where applicable. Comparison of the kinetic data, generated for the individual xanthones and benzophenones under the same conditions, provided insight into structure-stability relationships, a field that had yet to be explored for these sub-classes of phenolic compounds. To date, the thermal stability of the compounds from the xanthone and benzophenone phenolic sub-classes has not been assessed at all.

In order to monitor the evolution of the target xanthones, benzophenones and/or their degradation products upon thermal treatment, a high-resolution HPLC method coupled with diode-array detection (DAD) was required. Over the last three years, there has been significant advances in the analysis of *Cyclopia* phenolic compounds by HPLC-DAD. From the “generic” HPLC-DAD methods developed by Joubert *et al.* (2003) and De Beer & Joubert (2010), new methods have been developed and optimised to provide high-resolution chromatographic separation of a large number of phenolic compounds present in individual *Cyclopia* species (De Beer *et al.*, 2012; Schulze *et al.*, 2014). Such “species-specific” HPLC methods are required to accommodate qualitative and quantitative variation between the different *Cyclopia* species. Thus far, a species-specific HPLC method has not yet been developed for the analysis of phenolic compounds present in extracts from *C. genistoides*. Another aim of the current study was therefore to develop an HPLC method suitable for the qualitative and quantitative analysis of aqueous extracts prepared from unfermented and fermented *C. genistoides* plant material. The optimised HPLC method was coupled to high-resolution electrospray ionisation mass spectrometry (ESI-MS) to provide information on the accurate mass and proposed molecular formula of new phenolic constituents present in the unfermented and fermented *C. genistoides* extracts, and also in the thermally-treated samples. By resorting to tandem MS in combination with collision induced dissociation (CID) more detailed structural information was obtained.

REFERENCES

- Bělehrádek, J. (1930). Temperature coefficients in biology. *Biology Reviews*, **5**, 30-58.
- Chellan, N., Joubert, E., Strijdom, H., Roux, C., Louw, J. & Muller, C.J.F. (2014). Aqueous extract of unfermented honeybush (*Cyclopia maculata*) attenuates STZ-induced diabetes and β -cell cytotoxicity. *Planta Medica*, **80**, 622-629.
- De Beer, D. & Joubert, E. (2010). Development of HPLC method for *Cyclopia subternata* phenolic compound analysis and application to other *Cyclopia* spp. *Journal of Food Composition and Analysis*, **23**, 289-297
- De Beer, D., Schulze, A.E., Joubert, E., De Villiers, A., Malherbe, C.J. & Stander, M.A. (2012). Food ingredient extracts of *Cyclopia subternata* (honeybush): variation in phenolic composition and antioxidant capacity. *Molecules*, **17**, 14602-14624.
- Du Toit, J., Joubert, E. & Britz, T.J. (1998). Honeybush tea – A rediscovered indigenous South African herbal tea. *Journal of Sustainable Agriculture*, **12**, 67-84.
- Du Toit, J. & Joubert, E. (1999). Optimization of the fermentation parameters of honeybush tea (*Cyclopia*). *Journal of Food Quality*, **22**, 241-256.
- Feng, J., Yang, X.-W. & Wang, R.-F. (2011). Bio-assay guided isolation and identification of α -glucosidase inhibitors from the leaves of *Aquilaria sinensis*. *Phytochemistry*, **72**, 242-247.
- Ferreira, D., Kamara, B.I., Brandt, E.V. & Joubert, E. (1998). Phenolic compounds from *Cyclopia intermedia* (honeybush tea). 1. *Journal of Agricultural and Food Chemistry*, **46**, 3406-4310.
- Greenish, H.G. (1881). Cape tea. *The Pharmaceutical Journal and Transactions*, **11**, 549-551.
- Heim, K.E., Tagliaferro, A.R. & Bobilya, D.J. (2002). Flavonoid antioxidants: chemistry, metabolism and structure-activity relationships. *Journal of Nutritional Biochemistry*, **13**, 572-584.
- Joubert, E., Gelderblom, W.C.A., Louw, A. & De Beer, D. (2008a). South African herbal teas: *Aspalathus linearis*, *Cyclopia* spp. and *Athrixia phylicoides* – A review. *Journal of Ethnopharmacology*, **119**, 376-412.
- Joubert, E., Richards, E.S., Van der Merwe, J.D., De Beer, D., Manley, M. & Gelderblom, W.C.A. (2008b). Effect of species variation and processing on phenolic composition and *in vitro* antioxidant activity of aqueous extracts of *Cyclopia* spp. (honeybush tea). *Journal of Agricultural and Food Chemistry*, **56**, 954-963.
- Joubert, E., Gelderblom, W.C.A. & De Beer, D. (2009). Phenolic contribution of South African herbal teas to a healthy diet. *Natural Product Communications*, **4**, 701-718.
- Joubert, E., Joubert, M.E., Bester, C., De Beer, D. & De Lange, J.H. (2011). Honeybush (*Cyclopia* spp.): From local cottage industry to global markets – the catalytic and supporting role of research. *South African Journal of Botany*, **77**, 887-907.
- Joubert, E., De Beer, D., Hernández, I. & Munné-Bosch, S. (2014). Accumulation of mangiferin, isomangiferin, iriflophenone-3-*C*- β -glucoside and hesperidin in honeybush leaves (*Cyclopia genistoides* Vent.) in response to harvest time, harvest interval and seed source. *Industrial Crops and Products*, **56**, 74-82.
- Kamara, B.I., Brandt, E.V., Ferreira, D. & Joubert, E. (2003). Polyphenols from honeybush tea (*Cyclopia intermedia*). *Journal of Agricultural and Food Chemistry*, **51**, 3874-3879.
- Kamara, B.I., Brand, D.J., Brandt, E.V. & Joubert, E. (2004). Phenolic metabolites from honeybush tea (*Cyclopia intermedia*). *Journal of Agricultural and Food Chemistry*, **52**, 5391-5395.
- Kokotkiewicz, A., Luczkiewicz, M., Sowinski, P., Glod, D., Gorynski, K. & Bucinski, A. (2012). Isolation and structure elucidation of phenolic compounds from *Cyclopia subternata* Vogel (honeybush) intact plant and *in vitro* cultures. *Food Chemistry*, **133**, 1373-1382.

- Kokotkiewicz, A., Luczkiewicz, M., Pawlowska, J., Luczkiewicz, P., Sowinski, P., Witkowski, J., Bryl, E. & Bucinski, A. (2013). Isolation of xanthone and benzophenone derivatives from *Cyclopia genistoides* (L.) Vent. (honeybush) and their pro-apoptotic activity on synoviocytes from patients with rheumatoid arthritis. *Fitoterapia*, **90**, 199-208.
- Malherbe, C.J., Willenburg, E., De Beer, D., Bonnet, S.L., van der Westhuizen, J.H. & Joubert, E. (2014). Iriflophenone-3-C-glucoside from *Cyclopia genistoides*: Isolation and quantitative comparison of antioxidant capacity with mangiferin and isomangiferin using on-line HPLC antioxidant assays. *Journal of Chromatography B*, **951–952C**, 164-171
- Marloth, R. (1925). *The Flora of South Africa with Synoptical Tables of the Genera of the Higher Plants*. Pp.69-72. Cape Town: Darter Bros & Co.
- Muller, C.J.F., Joubert, E., Gabuza, K., De Beer, D., Fey, S.J. & Louw, J. (2011). Assessment of the antidiabetic potential of an aqueous extract of honeybush (*Cyclopia intermedia*) in streptozotocin and obese insulin resistant wistar rats. In: *Phytochemicals – Bioactivities and Impact on Health*, Prof. Iraj Rasooli (Ed.), ISBN: 978-953-307-424-5, InTech.
- Peleg, M., Normand, M.D. & Corradini, M.G. (2012). The Arrhenius equation revisited. *Critical Reviews in Food Science and Nutrition*, **52**, 830-851.
- Rice-Evans, C.A., Miller, N.J. & Paganga, G. (1996). Structure-antioxidant activity relationships of flavonoids and phenolic acids. *Free Radical Biology and Medicine*, **20**, 933-956.
- Schulze, A.E., De Beer, D., De Villiers, A., Manley, M. & Joubert, E. (2014). Chemometric analysis of chromatographic fingerprints shows potential of *Cyclopia maculata* (Andrews) Kies for production of standardized extracts with high xanthone content. *Journal of Agricultural and Food Chemistry*, **62**, 10542-10551.
- Schulze, A.E., De Beer, D., Mazibuko, S.E., Muller, C.J.F., Roux, C., Willenburg, E.L., Nyunai, N., Louw, J., Manley, M. & Joubert, E. (2015). Assessing similarity analysis of chromatographic fingerprints of *Cyclopia subternata* extracts as potential screening tool for *in vitro* glucose utilization. *Analytical and Bioanalytical Chemistry*, DOI 10.1007/s00216-015-9147-7.
- Schutte, A.L. (1995). A taxonomic study of the tribes Podalyrieae and Liparieae (Fabaceae). Ph.D. (Botany) Dissertation, Rand Afrikaans University, Johannesburg, South Africa.
- Terblanche, S.E. (1982). Report on Honeybush Tea. Department of Biochemistry, University of Port Elizabeth, Port Elizabeth, South Africa.
- Theron, K.A. (2012). Sensory and Phenolic Profiling of *Cyclopia* Species (Honeybush) and Optimisation of the Fermentation Conditions. MSc (Food Science) Thesis, Stellenbosch University, Stellenbosch, South Africa.
- Theron, K.A., Muller, M., Van der Rijst, M., Cronje, J.C., Le Roux, M. & Joubert, E. (2014). Sensory profiling of honeybush tea (*Cyclopia* species) and the development of a honeybush sensory wheel. *Food Research International*, **66**, 12-22.
- Van Boekel, M.A.J.S. (1996). Statistical aspects of kinetic modelling for food science problems. *Journal of Food Science*, **61**, 477-486.
- Van Boekel, M.A.J.S. (2008). Kinetic modeling of food quality: a critical review. *Comprehensive Reviews in Food Science and Food Safety*, **7**, 144-158.
- Van der Merwe, J.D., Joubert, E., Richards, E.S., Manley, M., Snijman, P.W., Marnewick, J.L. & Gelderblom, W.C.A. (2006). A comparative study on the antimutagenic properties of aqueous extracts of *Aspalathus linearis* (roobos), different *Cyclopia* spp. (honeybush) and *Camellia sinensis* teas. *Mutation Research*, **611**, 42-53.
- Vyas, A., Syeda, K., Ahmad, A., Padhye, S. & Sarkar, F.H. (2012). Perspectives on medicinal properties of mangiferin. *Mini-Reviews in Medicinal Chemistry*, **12**, 412-425.

CHAPTER 2

Literature Review

1. INTRODUCTION

The indigenous Cape fynbos plant, *Cyclopia* Vent. (family Fabaceae; tribe Podalyrieae) has a long history of localised use as herbal tea (Greenish, 1881; Marloth, 1913; Marloth, 1925; Watt & Breyer-Brandwijk, 1962). In recent years, honeybush herbal tea has gained prominence on both the local and international markets after concerted efforts to establish a formal honeybush industry in the 1990s. Both “unfermented” (green) and “fermented” (oxidised) honeybush are available to consumers, but the preferred product is the traditional fermented honeybush with its sought-after sweet-associated aroma, flavour and taste (Joubert *et al.*, 2011).

The paper by Greenish (1881) refers to “Cape-Tea”, a term used for several *Cyclopia* species, including *C. genistoides* (L.) Vent. This species currently represents one of the commercially-exploited *Cyclopia* species (Joubert *et al.*, 2011). Its natural habitat spans from the coastal areas of the West Coast to the Southern Coast of South Africa and commercial cultivation is mainly localised in the Overberg area (Joubert *et al.*, 2011).

The interest in honeybush as a commercial crop in the 1990s coincided with the demand of consumers world-wide for health-promoting foods and ingredients, due to increased awareness of the link between diet and prevention of life-style diseases. This prompted investigation of the phenolic composition of honeybush, partly to underpin studies on the health-promoting properties of this beverage, and partly to gain insight for value-adding opportunities (Joubert *et al.*, 2008a; Joubert *et al.*, 2011). The present review will provide an overview of the phenolic composition of *Cyclopia* spp., including recent advances and trends in the analysis of *Cyclopia* phenolic constituents by high-performance liquid chromatography (HPLC) and factors that affect the phenolic composition. To provide further context for the interest in these phenolic constituents, the bio-activity of xanthenes and benzophenones found in *Cyclopia* will be discussed briefly.

In view of the high-temperature oxidation step employed for the manufacture of fermented honeybush (Du Toit & Joubert, 1999), the second part of the review will discuss thermal degradation of different sub-classes of flavonoids to serve as background to the current investigation of the thermal stability of major honeybush polyphenols.

2. HONEYBUSH AND ITS PHENOLIC COMPOSITION

2.1. Phenolic Composition of *Cyclopia* spp.

To date, comprehensive studies utilising nuclear magnetic resonance (NMR) spectroscopy for the unambiguous identification of phenolic compounds in *Cyclopia* spp. have been limited to fermented *C. intermedia* (Ferreira *et al.*, 1998; Kamara *et al.*, 2003) and unfermented *C. subternata* (Kamara *et al.*, 2004; Kokotkiewicz *et al.*, 2012) (Table 1).

The first in-depth study by Ferreira *et al.* (1998) investigated the phenolic composition of a methanolic extract from the fermented leaves and stems of *C. intermedia*. The following compounds were identified by NMR spectroscopy (Table 1): a benzoic acid (*p*-coumaric acid), three isoflavones (formononetin, afrormosin and calycosin) and two methylenedioxy isoflavone derivatives (pseudobaptigen and fujikinetin), four flavanones (naringenin, eriodictyol, hesperetin and hesperidin), three coumestans (medicagol, flemichapparin and sophoracoumestan B), two xanthenes (mangiferin and isomangiferin) and one flavone (luteolin).

Table 1 Phenolic composition of *Cyclopia* spp.

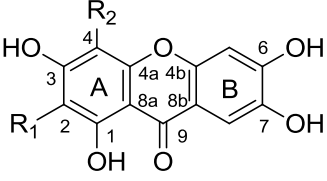
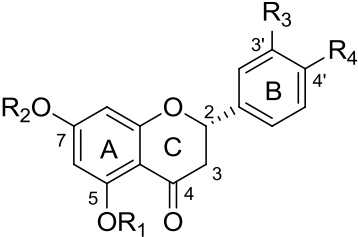
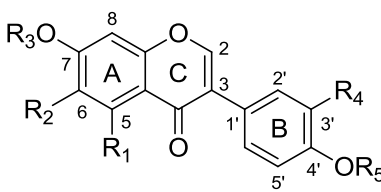
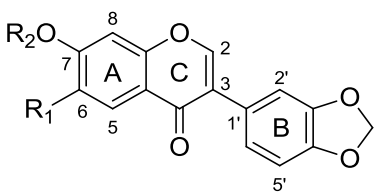
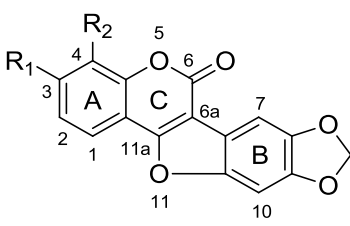
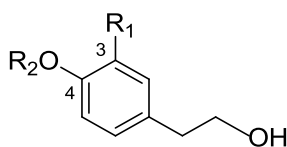
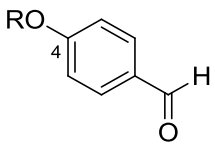
Basic Structure	Phenolic Sub-Class and Compound Name	Substituents
	Xanthones Mangiferin ^{a,c,d,e} Isomangiferin ^{a,e}	R ₁ = β -D-glucopyranosyl; R ₂ = H R ₁ = H; R ₂ = β -D-glucopyranosyl
	Flavanones 7-Rutinosyloxyhesperetin (Hesperidin) ^{a,c,d,e} Hesperetin ^a 7-Rutinosyloxyeriodictyol (Eriocitrin) ^c Eriodictyol ^a 7-Rutinosyloxynaringenin (Narirutin) ^{c,d} Naringenin ^a 7- β -D-Glucopyranosyloxynaringenin (Prunin) ^b 5-Rutinosyloxynaringenin ^b 5- β -D-Glucopyranosyloxyeriodictyol ^b 7- β -D-Glucopyranosyloxyeriodictyol ^b	R ₁ = H; R ₂ = rutinosyl; R ₃ = OH; R ₄ = OCH ₃ R ₁ = R ₂ = H; R ₃ = OH; R ₄ = OCH ₃ R ₁ = H; R ₂ = rutinosyl; R ₃ = R ₄ = OH R ₁ = R ₂ = H; R ₃ = R ₄ = OH R ₁ = R ₃ = H; R ₂ = rutinosyl; R ₄ = OH R ₁ = R ₂ = R ₃ = H; R ₄ = OH R ₁ = R ₃ = H; R ₂ = β -D-glucopyranosyl; R ₄ = OH R ₁ = rutinosyl; R ₂ = R ₃ = H; R ₄ = OH R ₁ = β -D-glucopyranosyl; R ₂ = H; R ₃ = R ₄ = OH R ₁ = H; R ₂ = β -D-glucopyranosyl; R ₃ = R ₄ = OH
	Isoflavones Formononetin ^d 7- β -D-Glucopyranosyloxyformononetin (ononin) ^d 7-[α -D-apiofuranosyl-(1 ^{'''} →6 ^{''})- β -D-glucopyranosyloxy]formononetin ^b Afromosin ^a Calycosin ^a 7- β -D-Glucopyranosyloxyalcalycosin ^d	R ₁ = R ₂ = R ₃ = R ₄ = H; R ₅ = CH ₃ R ₁ = β -D-glucopyranosyloxy; R ₂ = R ₃ = R ₄ = H; R ₅ = CH ₃ R ₁ = α -D-apiofuranosyl-(1 ^{'''} →6 ^{''})- β -D-glucopyranosyloxy; R ₂ = R ₃ = R ₄ = H; R ₅ = CH ₃ R ₁ = R ₃ = R ₄ = H; R ₂ = OCH ₃ ; R ₅ = CH ₃ R ₁ = R ₂ = R ₃ = H; R ₄ = OH; R ₅ = CH ₃ R ₁ = R ₂ = H; R ₃ = β -D-glucopyranosyl; R ₄ = OH; R ₅ = CH ₃ R ₁ = R ₄ = H; R ₂ = OCH ₃ ; R ₃ = β -D-glucopyranosyl; R ₅ = CH ₃ R ₁ = R ₄ = OH; R ₂ = R ₃ = R ₅ = H
	Methylenedioxyisoflavone derivatives Pseudobaptigen ^a 7- β -D-Glucopyranosyloxy pseudobaptigen (rothindin) ^d Fujikinetin ^a	R ₁ = R ₂ = H R ₁ = H; R ₂ = β -D-glucopyranosyl R ₁ = OH; R ₂ = OCH ₃
	Coumestans Medicagol ^a Flemichapparin ^a Sophoracoumestan B ^a	R ₁ = OH; R ₂ = H R ₁ = OCH ₃ ; R ₂ = H R ₁ = OH; R ₂ = OCH ₃
	Phenylethanol derivatives Tyrosol ^b 3-Methoxytyrosol ^b 4- β -D-Glucopyranosyloxytyrosol ^c 4-[α -D-apiofuranosyl-(1 ^{''} →6 ['])- β -D-glucopyranosyloxy]tyrosol ^b	R ₁ = R ₂ = H R ₁ = OCH ₃ ; R ₂ = H R ₁ = H; R ₂ = β -D-glucopyranosyl R ₁ = H; R ₂ = α -D-apiofuranosyl-(1 ^{''} →6 ['])- β -D-glucopyranosyl
	Benzaldehyde derivative 4-[α -D-apiofuranosyl-(1 ^{''} →2 ['])- β -D-glucopyranosyloxy]benzaldehyde ^b	R = α -D-apiofuranosyl-(1 ^{''} →2 ['])- β -D-glucopyranosyl

Table 1 cont.

Basic Structure	Phenolic Sub-Class and Compound Name	Substituents
	Flavones Luteolin ^{a,c,e} Diosmetin ^b 5-Deoxyluteolin ^{b,c} 7-Rutinosyloxyluteolin (Scolymoside) ^{c,d} 7-Rutinosyloxyapigenin (Isorhoifolin) ^d	R ₁ = R ₃ = OH; R ₂ = R ₄ = H R ₁ = R ₃ = OH; R ₂ = H; R ₄ = CH ₃ R ₁ = R ₂ = R ₄ = H; R ₃ = OH R ₁ = R ₃ = OH; R ₂ = rutinosyl; R ₄ = H R ₁ = OH; R ₂ = rutinosyl; R ₃ = R ₄ = H
	Flavonols 5- α -D-Glucopyranosyloxykaempferol ^b 6- β -D-Glucopyranosylkaempferol ^{b,c} 8- β -D-Glucopyranosylkaempferol ^b 3- β -D-Glucopyranosyloxy-6- β -D-glucopyranosylkaempferol ^b	R ₁ = R ₃ = R ₄ = H; R ₂ = α -D-glucopyranosyl R ₁ = R ₂ = R ₄ = H; R ₃ = β -D-glucopyranosyl R ₁ = R ₂ = R ₃ = H; R ₄ = β -D-glucopyranosyl R ₁ = R ₃ = β -D-glucopyranosyl; R ₂ = R ₄ = H
	Methylenedioxyflavonol derivative 6-[α -D-apiofuranosyl-(1''' \rightarrow 6'')- β -D-glucopyranosyloxy]-3-hydroxy-3',4'-methylenedioxyflavonol ^b	R = α -D-apiofuranosyl-(1''' \rightarrow 6'')- β -D-glucopyranosyl
	Flavan-3-ol epigallocatechin gallate ^c	
	Benzoic acid p-coumaric acid ^{a,c}	
	Benzophenones 3- β -D-Glucopyranosyliriflophenone ^{d,e} 3- β -D-Glucopyranosylmaclurin ^f	R ₁ = β -D-glucopyranosyl; R ₂ = H R ₁ = β -D-glucopyranosyl; R ₂ = OH
	Dihydrochalcone 3',5'-di- β -D-Glucopyranosylphloretin ^d	R = β -D-glucopyranosyl

^aFerreira et al. (1998); ^bKamara et al. (2003); ^cKamara et al. (2004); ^dKokotkiewicz et al. (2012); ^eKokotkiewicz et al. (2013); ^fMalherbe et al. (2014).

Continued investigation into the phenolic composition of the methanolic extract of fermented *C. intermedia* by Kamara *et al.* (2003) led to the identification of a considerable number and variety of additional flavonoids. The following compounds were identified for the first time (Table 1): three phenylethanol derivatives (tyrosol, 3-methoxytyrosol, 4-[α -D-apiofuranosyl-(1'' \rightarrow 6')- β -D-glucopyranosyloxy]tyrosol), four glycosylated flavonols (5- α -D-glucopyranosyloxykaempferol, 6- β -D-glucopyranosylkaempferol, 8- β -D-glucopyranosylkaempferol and 3- β -D-glucopyranosyloxy-6- β -D-glucopyranosylkaempferol) and a methylenedioxyflavonol derivative (6-[α -D-apiofuranosyl-(1''' \rightarrow 6'')- β -D-glucopyranosyloxy]-3-hydroxy-3',4'-methylenedioxyflavonol), two isoflavones (7-[α -D-apiofuranosyl-(1''' \rightarrow 6'')- β -D-glucopyranosyloxy]formononetin and wistin), four glycosylated flavanones (7- β -D-glucopyranosyloxynaringenin, 5-rutinosyloxynaringenin, 5- β -D-glucopyranosyloxyeriodictyol and 7- β -D-glucopyranosyloxyeriodictyol), and two flavones (5-deoxyluteolin and diosmetin).

Kamara *et al.* (2004) conducted a study on the phenolic composition of acetone and methanolic extracts of unfermented *C. subternata*. The presence of various phenolic compounds, previously identified in fermented *C. intermedia* extracts, was also confirmed in the species under investigation. These compounds included the flavanone hesperidin, the flavone luteolin and its 5-deoxy analogue, the flavonol 6- β -D-glucopyranosylkaempferol, the xanthone mangiferin and the benzoic acid *p*-coumaric acid. Two flavanones (narirutin and eriocitrin), one flavone (scolymoside), an isoflavone (orobol), a flavan-3-ol (epigallocatechin gallate) and a phenylethanol derivative (4- β -D-glucopyranosyloxytyrosol) were identified for the first time in *C. subternata* (Table 1).

Kokotkiewicz *et al.* (2012) isolated phenolic compounds from unfermented *C. subternata* intact plant material and callus. Their study re-established the presence of previously described honeybush constituents (mangiferin, scolymoside, hesperidin and narirutin) in *C. subternata*. Compounds identified for the first time in *C. subternata* included the benzophenone 3- β -D-glucopyranosyliriflophenone, the dihydrochalcone 3',5'-di- β -D-glucopyranosylphloretin and the flavone analogue of narirutin, isorhoifolin. This was notably also the first report of the presence of compounds from the benzophenone and dihydrochalcone phenolic subclasses in the genus *Cyclopia*. Furthermore, two glucosylated derivatives of previously isolated isoflavone aglycones (fermented *C. intermedia*; Ferreira *et al.*, 1998) were identified in the callus of *C. subternata*, *i.e.* 7- β -D-glucopyranosyloxycalycosin and 7- β -D-glucopyranosyloxyformononetin, together with the glucosylated methylenedioxyisoflavone derivative, 7- β -D-glucopyranosyloxypseudobaptigen.

Over the past two years, researchers have also selectively isolated compounds from *C. genistoides* (Table 1) with the explicit aim of assessing their potential biological activities. Kokotkiewicz *et al.* (2013) developed a fast and efficient method for the isolation of the *C*-glucosylated xanthones mangiferin and isomangiferin from unfermented *C. genistoides*, selected specifically due to their high contents in this species. The procedure involved extraction, liquid-liquid partitioning with ethyl acetate and subsequent precipitation of mangiferin and isomangiferin from methanol and acetonitrile-water fractions, respectively. Additionally, two benzophenone derivatives, 3- β -D-glucopyranosylmaclurin and 3- β -D-glucopyranosyliriflophenone, were also isolated from *C. genistoides* extracts using semi-preparative HPLC. Apart from the above, the isolation procedure also yielded hesperidin and small amounts of luteolin. The structures of these isolated compounds were confirmed on the basis of their LC diode-array (DAD) and electrospray ionisation-mass spectrometric (ESI-MS) spectra and/or by co-chromatography with authentic reference standards. Isomangiferin and 3- β -D-glucopyranosylmaclurin were furthermore subjected to 1D and 2D NMR analyses. This was the first report on the presence of 3- β -D-glucopyranosylmaclurin in the genus *Cyclopia*. Selected *Cyclopia* constituents were subsequently screened for pro-apoptotic activity on tumor necrosis factor- α -stimulated synovial cells isolated from rheumatoid arthritis patients.

3- β -D-Glucopyranosyliriflophenone was subsequently also isolated from a methanolic extract of unfermented *C. genistoides* using a combination of liquid-liquid extraction, high performance counter-current chromatography

(HPLC) and semi-preparative HPLC (Malherbe *et al.*, 2014). The antioxidant capacity of 3- β -D-glucopyranosyliriflophenone was assessed by on-line HPLC antioxidant assays and compared with those of mangiferin and isomangiferin.

Recently, the phenolic compositions of aqueous extracts of unfermented and fermented *C. subternata* (De Beer *et al.*, 2012) and *C. maculata* (Schulze *et al.*, 2014) were comprehensively characterised by LC-DAD-ESI-MS and –MS/MS. These studies employed “species-specific” HPLC methods (refer to section 2.2) which provided optimised separation of the phenolic compounds present in each of the individual species and enabled the characterisation and identification of a large number of constituents. The identities of mangiferin, eriocitrin and hesperidin in *C. subternata* extracts were determined by comparison of retention times, UV-Vis spectroscopic properties, LC-MS and LC-MS/MS fragmentation patterns with those of commercial standards, whereas the identity of isomangiferin was confirmed by comparison with isolated isomangiferin, authenticated by NMR spectroscopic data (De Beer *et al.*, 2009). The presence of the following compounds in *C. subternata* was re-affirmed in accordance with literature reports on the phenolic composition of *Cyclopia* spp.: 3- β -D-glucopyranosyliriflophenone, 3',5'-di- β -D-glucopyranosylphloretin, two eriodictyol-*O*-glucosides and scolymoside (Kamara *et al.*, 2003; Kamara *et al.*, 2004; Kokotkiewicz *et al.*, 2012). A hexosyloxy derivative of 3- β -D-glucopyranosyliriflophenone, termed iriflophenone-di-*O*,*C*-hexoside, was newly identified in aqueous extracts of *C. subternata*. The UV-VIS, LC-MS and –MS/MS characteristics of two additional flavanone derivatives, proposed to be naringenin-di-*C*-hexoside and naringenin-*O*-dihexoside, were also provided.

Moreover, the study by De Beer *et al.* (2012) also demonstrated novel similarities between the phenolic composition of *C. subternata* and *Aspalathus linearis*, both endemic Cape fynbos plants belonging to the Fabaceae family and used for herbal tea production. The presence of the dihydrochalcone 3-hydroxyphloretin-3',5'-di-*C*-hexoside (Beelders *et al.*, 2012a; Beelders *et al.*, 2012b) and the flavone 6,8-di- β -D-glucopyranosylapigenin (vicenin-2; Breiter *et al.*, 2011; Iswaldi *et al.*, 2011; Beelders *et al.*, 2012a) in the genus *Cyclopia* was demonstrated for the first time, whereas the flavanones (*S*)- and (*R*)-eriodictyol-di-*C*-hexoside were also tentatively identified for the first time, based on the presence of 6- β -D-glucopyranosyleriodictyol (Marais *et al.*, 2000) and 8- β -D-glucopyranosyleriodictyol (Krafczyk & Glomb, 2008) in *Aspalathus linearis* (rooibos).

The study conducted by Schulze *et al.* (2014) provided the first glimpse into the distribution of phenolic compounds in aqueous extract of *C. maculata*. Two xanthenes (hydroxymangiferin and hydroxyisomangiferin; position of extra hydroxy group unknown) were tentatively identified for the first time in the genus *Cyclopia*, whereas an additional four compounds (3- β -D-glucopyranosylmaclurin, 3-hydroxyphloretin-3',5'-di-*C*-hexoside and two eriodictyol-*O*-hexosides) were tentatively identified for the first time in *C. maculata* (Schulze *et al.*, 2014).

Collectively the aforementioned studies indicate that *Cyclopia* extracts principally contain glycosylated compounds from the xanthone, benzophenone, dihydrochalcone, flavanone, flavone, isoflavone and flavonol phenolic sub-classes. Major compounds present in aqueous infusions prepared from fermented *Cyclopia* spp. plant material include mangiferin, isomangiferin, vicenin-2, scolymoside, eriocitrin, hesperidin, 3- β -D-glucopyranosyliriflophenone and 3',5'-di- β -D-glucopyranosylphloretin.

2.2. Quantitative Analysis of the Phenolic Composition of *Cyclopia* spp. by LC-DAD

Reversed-phase HPLC (RP-HPLC) coupled with ultraviolet-visible (UV-VIS) spectroscopy and/or MS is the dominant analytical technique for the separation and characterisation of phenolic compounds (Stalikas, 2007). To date, various RP-LC methods have been employed in the quantitative analysis of *Cyclopia* polyphenols and these methods have found wide-spread application. Joubert *et al.* (2003) presented the first reversed-phase HPLC method for the separation of polyphenols in honeybush tea. The method was mainly required to screen unfermented *Cyclopia* plant material for high

levels of mangiferin. This method was suitable for the separation of a standard mixture of commercially available polyphenols reported to be present in honeybush tea samples, *i.e.* eriodictyol, medicagol, formononetin, mangiferin, isomangiferin, hesperitin and hesperidin (Figure 2A). Separation was achieved on a Phenomenex Synergy MAX-RP C₁₂ 80Å column with TMS end-capping (4 µm; 150 × 4.6 mm ID), with gradient elution using 2% acetic acid in water (v.v⁻¹) and acetonitrile as binary mobile phase. Separation was carried out at room temperature at a flow rate of 1 mL.min⁻¹, with a chromatographic run time of 29 min (excluding time for column re-equilibration). The method was subsequently used for the quantification of the three major polyphenols, mangiferin, isomangiferin and hesperidin in methanolic extracts of unfermented *Cyclopia* spp. (*C. genistoides*, *C. intermedia*, *C. maculata* and *C. sessiliflora*) (Figure 2B).

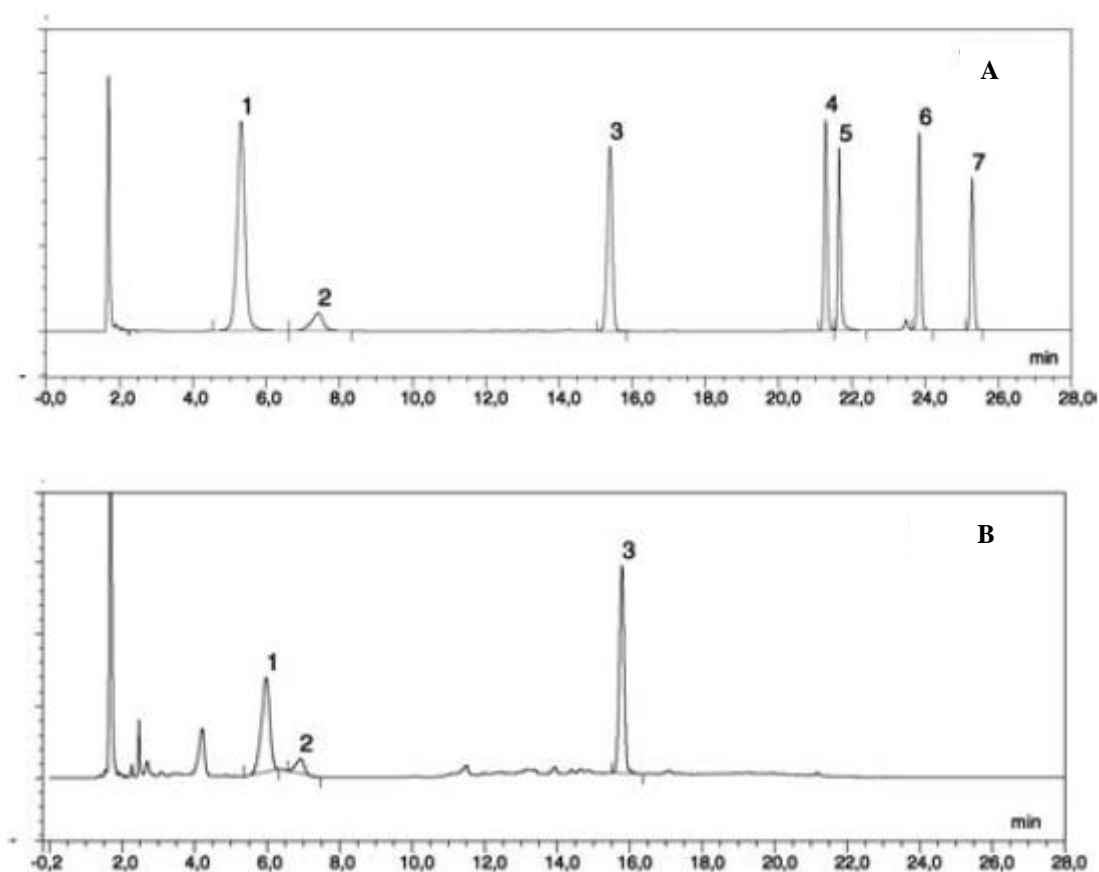


Figure 2 (A) Chromatogram of a standard mixture of commercially available polyphenols reported to be present in honeybush tea samples: 1 mangiferin, 2 impurity of mangiferin (later identified as homomangiferin; Van der Merwe *et al.*, 2012), 3 hesperidin, 4 eriodictyol, 5 luteolin, 6 hesperetin, 7 formononetin. Isomangiferin and medicagol would appear in the same chromatogram at 6.5 and 27.5 min, respectively (Joubert *et al.*, 2003). (B) Chromatogram (280 nm) of an unfermented honeybush sample 1 mangiferin, 2 isomangiferin, 3 hesperidin (Joubert *et al.*, 2003).

However, this method proved to be problematic when applied to aqueous samples. The gradient set up to facilitate rapid elution of mangiferin resulted in elution of several, poorly separated and/or co-eluted compounds in or near the column void volume. Eriocitrin, present in aqueous *C. subternata* extracts, was found to co-elute with one or more unknown compounds (*e.g.* Joubert *et al.*, 2008b).

The HPLC method of Joubert *et al.* (2003) was therefore subsequently modified by De Beer & Joubert (2010) by switching to a different stationary phase (Agilent Zorbax Eclipse XDB-C₁₈ column, extra-dense C₁₈ bonding with double endcapping, 5 µm, 80 Å, 150 mm × 4.6 mm) and changing the aqueous phase to 0.1% formic acid in water (v.v⁻¹). A comparison of the HPLC-DAD analysis of the same unfermented *C. subternata* extract, using the method of Joubert *et al.* (2003) and the modified method of De Beer & Joubert (2010), is depicted in Figure 3. The modified method was validated for the quantification of the major phenolic compounds present in hot water extracts of unfermented and fermented *C. subternata*, and specificity was also verified for *C. intermedia*, *C. genistoides* and *C. sessiliflora* by LC-MS. The method was suitable for the quantification of mangiferin, isomangiferin, eriocitrin, hesperidin and eriodictyol in *C. subternata* extracts, as well as five compounds that were not yet identified at that time (Figure 3B).

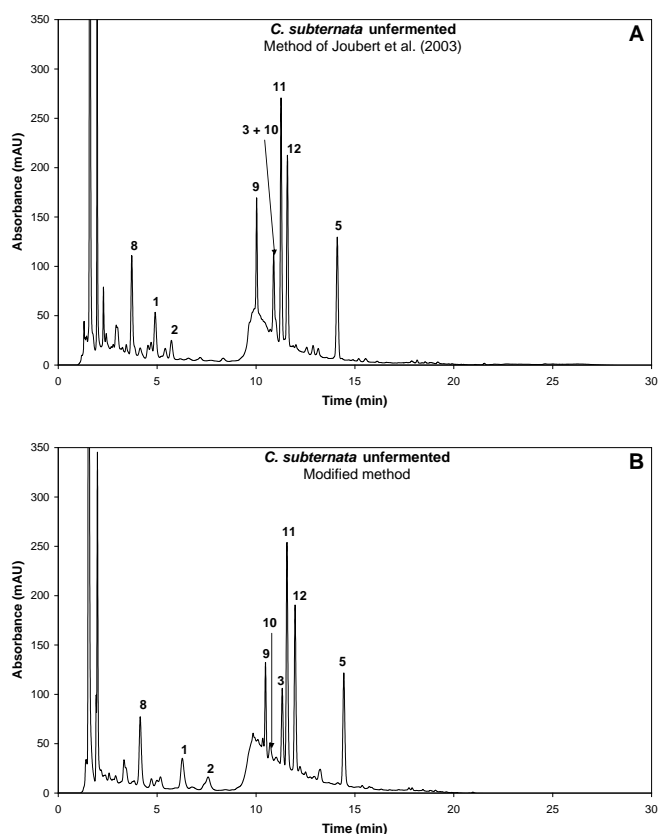


Figure 3 HPLC-DAD profiles of an unfermented *C. subternata* extract using (A) the method described in Joubert *et al.* (2003) and (B) the modified method of De Beer & Joubert (2010). 1 mangiferin, 2 isomangiferin, 3 eriocitrin, 5 hesperidin, 8-12 unidentified compounds.

The HPLC method described by De Beer & Joubert (2010), however, also suffered from a few limitations such as partial co-elution of isomangiferin with other unidentified compound(s) and a complicated integration process required for eriocitrin and two unidentified compounds (later identified as scolyoside and 3',5'-di-β-D-glucopyranosylphloretin) which eluted on a “polymeric hump” (Figure 3B). A new method for the analysis of aqueous *C. subternata* extracts was therefore developed by De Beer *et al.* (2012) to address these limitations. The potential benefits provided by new column formats, *i.e.*, sub-2 µm totally porous and superficially porous, prompted the selection of an Agilent Zorbax SB-C₁₈ column (100 × 4.6 mm, 1.8 µm) and a Phenomenex Kinetex C₁₈ column (150 × 4.6 mm, 2.6 µm, 100 Å), respectively, for testing. A Phenomenex Gemini-NX C₁₈ column (polymer-silica hybrid; 150 × 4.6 mm, 3 µm, 110 Å) was also evaluated as alternative chromatographic support due to its high stability at low pH values. Other factors investigated

were different acidified aqueous phases (2% acetic acid, 1% acetic acid and 0.1% formic acid in water, v.v⁻¹), organic modifiers (acetonitrile vs methanol) and a range of column temperatures (25-50 °C). Due to best chromatographic resolution, the 3 µm Gemini-NX column and a binary mobile phase comprising of 2% acetic acid and acetonitrile were selected. The multi-linear gradient described by De Beer & Joubert (2010) was essentially changed to include a shorter isocratic hold period at a lower initial percentage organic modifier, followed by a more gradual increase in solvent strength, with total run time amounting to 40 min. Separation was carried out at 30 °C and the flow rate was 1 mL.min⁻¹.

This HPLC method was successfully validated in terms of specificity (peak purity), linearity, intra- and inter-day analytical precision, as well as compound stability, and was subsequently applied to the quantification of eight phenolic compounds in aqueous extracts of unfermented *C. subternata*. The extracts were prepared from the leaves ($n = 10$) and stems ($n = 10$) of unfermented *C. subternata*, as well as plant material comprising a mixture of leaf and stem material ($n = 64$, individual seedlings). The compounds quantified included a benzophenone (6 3-β-D-glucopyranosyliriflophenone), two xanthenes (7 mangiferin, 8 isomangiferin), two flavanones (15 eriocitrin, 19 hesperidin), a flavone (16 scolymoside) and two dihydrochalcones (14 3-hydroxyphloretin-3',5'-di-C-hexoside, 17 3',5'-di-β-D-glucopyranosylphloretin) (De Beer *et al.*, 2012; Figure 4).

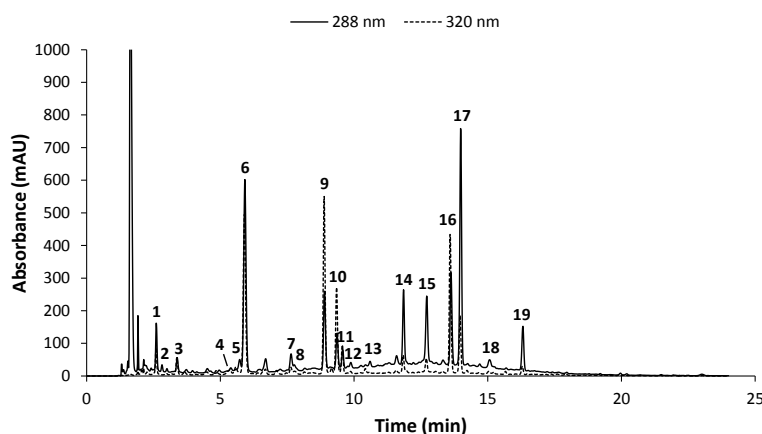


Figure 4 HPLC-DAD chromatogram showing phenolic compounds identified and/or quantified in aqueous extracts of unfermented *Cyclopia subternata*. 6 3-β-D-glucopyranosyliriflophenone, 7 mangiferin, 8 isomangiferin, 14 3-hydroxyphloretin-3',5'-di-C-hexoside, 15 eriocitrin, 16 scolymoside, 17 3',5'-di-β-D-glucopyranosylphloretin and 19 hesperidin (De Beer *et al.*, 2012).

Recent interest in *C. maculata* for commercial cultivation prompted the development of a species-specific HPLC method for the analysis of its phenolic composition (Schulze *et al.*, 2014). It was evident that the HPLC method developed for the analysis of *C. subternata* (De Beer *et al.*, 2012) was not suitable for *C. maculata* due to co-elution of minor, unidentified compounds with mangiferin and isomangiferin in *C. maculata* extracts. Improved resolution was achieved by optimising the gradient parameters, while the column format, column temperature and binary mobile phase components remained unchanged (Schulze *et al.*, 2014). The optimised method was successfully validated and allowed quantification of the major compounds present in extracts of unfermented and fermented *C. maculata* within 44 min. The compounds quantified included 1 3-β-D-glucopyranosylmaclurin, 2 3-β-D-glucopyranosyliriflophenone, 4 mangiferin, 6 isomangiferin, 7 vicenin-2, 8 eriodictyl-O-hexoside, 12 eriocitrin and 15 hesperidin (Figure 5).

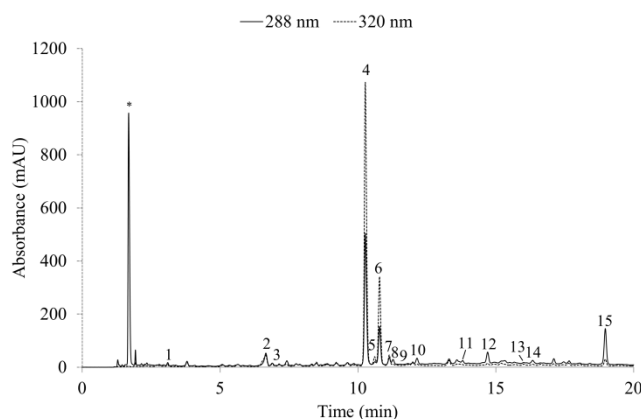


Figure 5 HPLC-DAD chromatogram of an aqueous extract prepared from unfermented *Cyclopia maculata* plant material using the optimised method (Schulze *et al.*, 2014), with compounds quantified comprising 1 3- β -D-glucopyranosylmaclurin, 2 3- β -D-glucopyranosyliriflophenone, 4 mangiferin, 6 isomangiferin, 7 vicenin-2, 8 eriodictyl-*O*-hexoside, 12 eriocitrin and 15 hesperidin.

These two examples clearly demonstrate that a species-specific HPLC-DAD method would be required for the analysis of *C. genistoides* as a species of commercial importance. Such a species-specific HPLC-DAD method should provide high-resolution chromatographic separation of the polyphenols inherently present in, and characteristic of, *C. genistoides*. This would enable accurate quantification of the major phenolic constituents and would also provide more detailed information on minor phenolic compounds possibly impacting on bio-activity.

2.3. Factors Affecting the Phenolic Composition of *Cyclopia* spp.

The phenolic composition of *Cyclopia* extracts is principally influenced by the specific species used for extract preparation, as evident from the preceding text. Using the “generic” HPLC method (Joubert *et al.*, 2003), Joubert *et al.* (2008b) demonstrated qualitative and quantitative differences in the phenolic compositions of *C. subternata*, *C. intermedia*, *C. genistoides* and *C. sessiliflora*. Large variation in the contents of individual phenolic compounds between different *Cyclopia* spp. have also been demonstrated by other researchers (De Beer & Joubert, 2010; Theron 2012). For instance, the levels of mangiferin in unfermented dried aqueous extracts may typically range from *ca.* 1-3% in *C. subternata* to *ca.* 9-10% in *C. genistoides* (Joubert *et al.*, 2008b; De Beer & Joubert, 2010).

As a result of the interest in *C. genistoides* as a rich source of the *C*-glucosyl xanthone mangiferin (Joubert *et al.*, 2003), a follow-up study screened 240 samples of *C. genistoides* for their mangiferin and hesperidin contents for the development of near-infrared spectroscopy (NIRS) calibration models (Joubert *et al.*, 2006). Large intra-species variation was observed (Joubert *et al.*, 2006). These samples, however, represented different types of *C. genistoides*, harvested over different years and at different harvest times, specifically to ensure large variation (as will be discussed in the ensuing text). Similarly, De Beer *et al.* (2012) demonstrated large variation in the individual phenolic contents of aqueous extracts prepared from unfermented *C. subternata*. The plant material was harvested from individual seedling plants ($n = 64$, of the same age; harvested in the same plantation on the same date) and the observed level of variation was thus attributed to a high level of genetic variation between seedlings. Conversely, a low level of variation has been observed in the individual phenolic contents of aqueous extracts of unfermented *C. maculata* ($n = 40$; Schulze *et al.*, 2014).

The effect of harvest time on the phenolic content of *C. genistoides* has been the subject of two studies, prompted by the need to harvest the plant material at optimum mangiferin content. A preliminary study on *C. genistoides*, covering a harvesting period spanning the end of March until mid-July, with harvest intervals of 5 weeks, showed that the mangiferin content of the shoots progressively decreased over this period, while their isomangiferin and hesperidin contents did not change significantly (Joubert *et al.*, 2003). The effect of harvest time on the phenolic composition of *C. genistoides* was revisited with a more comprehensive study by Joubert *et al.* (2014). In this study, the phenolic content of only the leaves of three types of *C. genistoides*, planted at the same location, was assessed to exclude the effect of variation in leaf-to-stem ratio that could occur over time. For instance, plants, established from seeds originating from a wild population near Darling on the West Coast, have a higher tendency to shed leaves to form a protective “mulch” when they are drought-stressed, resulting in a lower leaf-to-stem ratio (M. Joubert, ARC Cultivar Development Division, personal communication). Sampling was done over a full production year to gain insight into the role of climate in modulating the biosynthesis of the two major xanthenes, mangiferin and isomangiferin. The benzophenone 3- β -D-glucopyranosylriflophenone and the flavanone hesperidin present distinct flavonoid and benzophenone/xanthone biosynthetic pathways (Joubert *et al.*, 2014) which might also be differentially affected by climate and other factors. Results presented subsequently confirmed that the mangiferin levels in *C. genistoides* leaves decrease from March to mid-July (start of autumn to mid-winter) and that hesperidin show no clear seasonal variation as monitored over a full production year. Harvesting during summer (high solar radiation, high temperature, high “growing degree days” and water deficit) resulted in the highest levels of the benzophenone and xanthenes in the leaves of *C. genistoides* (Joubert *et al.*, 2014). The same study also demonstrated that harvest-interval has a significant impact on the mangiferin and hesperidin levels of *C. genistoides* leaves. Leaves from 19-month-old shoots (“old” re-growth) had significantly lower mangiferin levels than those from 12-month-old shoots (“young” re-growth), while hesperidin levels in leaves from old re-growth were significantly higher than those from young re-growth. In contrast, isomangiferin and 3- β -D-glucopyranosylriflophenone levels did not differ among samples from different harvest intervals (Joubert *et al.*, 2014).

Large quantitative differences in the phenolic composition between two types of *C. genistoides*, namely the Overberg and West Coast types, have also been demonstrated (Joubert *et al.*, 2003). The Overberg type contained significantly more mangiferin, but less hesperidin, than the West Coast type, whereas the isomangiferin content did not differ significantly between the two types. Similar findings were reported by Joubert *et al.* (2014), where initial seed source, *i.e.* wild population, strongly affected the mangiferin, isomangiferin and 3- β -D-glucopyranosylriflophenone levels in the leaves of *C. genistoides* when the seedlings were cultivated at the same location in the Overberg. The xanthone and benzophenone levels of the leaves were highest in plants grown from seeds collected from a natural population growing at a Cape Peninsula location, although their average mangiferin and 3- β -D-glucopyranosylriflophenone levels were not significantly higher than those of the Overberg and West Coast types, respectively. Seeds sourced from the Overberg population and planted at the same location as those from the West Coast and Cape Peninsula, produced plants with leaves containing significantly lower isomangiferin, 3- β -D-glucopyranosylriflophenone and hesperidin levels than the other two seed sources. West Coast plants had the highest hesperidin levels. Moreover, seed source determined the plant response to environmental factors in terms of composition (Joubert *et al.*, 2014).

In addition to these factors, processing of *Cyclopia* plant material under high-temperature oxidative conditions (generally referred to as fermentation) also affects the phenolic content of the plant material. This process, essential for the development of the desired brown colour, and the characteristically sweet, honey-like taste and aroma of the herbal tea product (Joubert *et al.*, 2011), briefly entails processing of moist, shredded plant material at elevated temperatures (> 60 °C), followed by drying, sieving and packing. Conditions currently in use by industry range from 70 °C/60 h for *C. intermedia* to 80–85 °C/18–24 h for a number of species such as *C. genistoides*, *C. maculata* and *C. subternata* (Joubert

et al., 2011). High-temperature oxidation, however, also leads to a significant reduction in the soluble matter of the plant material, as well as extracts with reduced total polyphenol and individual polyphenol contents (Joubert *et al.*, 2008b; De Beer & Joubert, 2010; Schulze *et al.*, 2014). It could be postulated that oxidation at such high temperatures may also introduce additional variation with the formation of new phenolic compounds, given the results of studies on other plant materials, *e.g.* roasting of green coffee beans (Farah & Donangelo, 2006). The latter aspect has not yet been studied for honeybush.

2.4. Bio-activity of *Cyclopia* Xanthone and Benzophenone Constituents

Cyclopia genistoides is characterised by exceptionally high levels of the xanthone mangiferin, present in amounts of up to 10% dry weight in the leaves (Joubert *et al.* 2014). Mangiferin is known to exert a number of biological activities including antioxidant, anti-inflammatory, antidiabetic and chemopreventative (as reviewed by Vyas *et al.*, 2012), thereby contributing to the health-promoting properties of honeybush tea. *Cyclopia genistoides* also represents a rich source of the xanthone isomangiferin and the benzophenone 3- β -D-glucopyranosyliriflophenone, constituting *ca.* 2% and *ca.* 1% of the dry weight of the leaves, respectively (Joubert *et al.* 2014). These compounds have thus far not been extensively studied with regard to their biological properties. The abilities of isomangiferin and 3- β -D-glucopyranosyliriflophenone to scavenge peroxy radicals were respectively shown to be similar to and substantially higher than that of mangiferin (Malherbe *et al.*, 2014). The on-line HPLC antioxidant assays employed by Malherbe *et al.* (2014) also indicated antioxidant activity for 3- β -D-glucopyranosylmaclurin, present in small quantities in the *C. genistoides* extract analysed, but the activity could not be quantified due to lack of an authentic standard. Both isomangiferin and 3- β -D-glucopyranosyliriflophenone have also demonstrated strong pro-apoptotic activity on rheumatoid arthritis synoviocytes (Kokotkiewicz *et al.*, 2013).

Mangiferin and its benzophenone precursors, 3- β -D-glucopyranosyliriflophenone and 3- β -D-glucopyranosylmaclurin, are considered to be potent anti-obesity agents. Zhang *et al.* (2011) demonstrated that mangiferin, in particular, as well as 3- β -D-glucopyranosyliriflophenone and 3- β -D-glucopyranosylmaclurin, significantly inhibit triglyceride synthesis and the expression of associated genes in mature 3T3-L1 cells. *Cyclopia* extracts have also been shown to inhibit adipogenesis in 3T3-L1 pre-adipocytes (Dudhia *et al.*, 2013).

Polyhydroxybenzophenones and polyhydroxyxanthenes together with their glycosylated derivatives are also gaining prominence in light of their α -glucosidase inhibitory (Liu *et al.*, 2006; Hu *et al.*, 2011; Liu *et al.*, 2012) and glucose-uptake stimulatory activities (Zhang *et al.*, 2013a). Studies have shown that mangiferin (Prashanth *et al.*, 2001; Yoshikawa *et al.*, 2001; Sanugul *et al.*, 2005; Feng *et al.*, 2011; Phoboo *et al.*, 2012) and 3- β -D-glucopyranosyliriflophenone (Feng *et al.*, 2011) serve as α -glucosidase inhibitors. Girón *et al.* (2009) furthermore reported that mangiferin exerts an antidiabetic effect by increasing glucose transporter 4 (GLUT4) expression and translocation in muscle cells. Recently, isomangiferin was shown to increase glucose uptake in C2C12 muscle cells with an efficacy similar to that of mangiferin (Schulze *et al.*, 2015).

The established biological effects of xanthone and benzophenone constituents of *C. genistoides* indicate that this species has potential value in the management of life-style diseases such as obesity and diabetes. For the production of enriched extracts, unfermented *C. genistoides* plant material is preferred (Joubert *et al.*, 2003; Bosman, 2014), as fermentation leads to significant reductions in the mangiferin (*ca.* 57-83%) and isomangiferin (*ca.* 46-59%) contents, and also lowers the antioxidant activity of the aqueous extracts (Joubert *et al.*, 2008b; De Beer & Joubert, 2010). Bosman (2014) obtained an aqueous ethanolic extract of unfermented *C. genistoides* containing more than 17% xanthenes by optimising extraction conditions and applying ultrafiltration.

2.5. Concluding Remarks

To conclude, a literature survey on *Cyclopia* spp. has underscored the need for a species-specific HPLC-DAD method for *C. genistoides* to accommodate for inter-species variation impacting on polyphenolic composition. *Cyclopia genistoides* is a species of commercial importance and is also of interest due to its high xanthone and benzophenone contents. In spite of this increasing interest in *C. genistoides*, the fate of its bio-active xanthone and benzophenone constituents during high-temperature processes is not known. Not only is the plant material subjected to a high-temperature oxidation process in the manufacture of fermented honeybush, but the compounds are also exposed to elevated temperatures during food ingredient extract preparation (> 90 °C for 30 min) and other food processes such as pasteurisation of iced teas, for example. A recent new application of honeybush extract as food ingredient is its use in bread (“Sasko Rosehip and Honeybush Brown Bread”). Knowledge regarding the thermal stability of the major xanthenes and benzophenones present in *Cyclopia* is therefore needed so that their losses during different thermal treatments may be predicted, and subsequently also minimised, to obtain a honeybush product with maximum biofunctionality. Towards this end, thermal degradation kinetics modelling can be used as a tool to establish the kinetic parameters that govern their degradation. To date, the thermal stability of compounds from the xanthone and benzophenone phenolic sub-classes have not been assessed kinetically.

3. THERMAL DEGRADATION KINETICS MODELLING OF PHENOLIC ACIDS AND FLAVONOIDS

Over the last few decades, links between non-nutritive dietary constituents such as polyphenols and general well-being have been demonstrated. Polyphenols have gained much attention due to their beneficial physiological properties, including their antioxidant properties. Their role in the prevention of cancer, cardiovascular diseases and diabetes has been the subject of many reviews (*e.g.* Scalbert *et al.*, 2005; Pandey & Rizvi, 2009).

The nutritional value of a food product, and the potential health-benefits that can be derived from its consumption, are influenced by the chemical changes that occur during food processing and storage. As such, kinetics modelling has increasingly found application to derive the basic kinetic information for a system in order to predict the chemical changes that occur within a particular food system during processing and storage. Two excellent reviews on this topic has been provided by Van Boekel (1996; 2008).

However, interest in the fate of these bio-active polyphenolic constituents during thermal treatments of food and beverage products mostly lag behind those of other food constituents such as ascorbic acid and carotenoids. The thermal stability of ascorbic acid has mostly been assessed in citrus juices (*e.g.* Lima *et al.*, 1999; Vikram *et al.*, 2005; Dhuique-Mayer *et al.*, 2007), due to its relation to non-enzymatic browning reactions which leads to major losses in the commercial value in citrus products. On the other hand, the thermal stability of carotenoids is of importance due to their use as natural colourants (Downham & Collins, 2000) and functional food ingredients in light of their purported health benefits (as reviewed by Stahl & Sies, 2005; Rao & Rao, 2007; Chatterjee *et al.*, 2012). The kinetic aspects of carotene degradation and isomerisation during thermal processing was recently reviewed by Colle *et al.* (2015).

The only phenolic sub-class that has received extensive attention is the anthocyanins and this is also related to their role as natural colourants and their beneficial effects on human health (Downham & Collins, 2000; Pazmiño-Durán *et al.*, 2001; Stintzing & Carle, 2004). As such, many studies have been conducted to evaluate the thermal stability of anthocyanins in order to minimise their degradation during thermal processing, and to secure optimal colour and biofunctionality. The focus has thus far been on structure-stability relationships, degradation mechanisms and the impact of thermal processing on the colour and antioxidant activity of anthocyanin-rich samples (as reviewed by Patras *et al.*, 2010 and Ioannou *et al.*, 2012).

Conversely, comparatively few studies have been conducted on the thermal stability of compounds from other phenolic sub-classes, such as the dihydrochalcones, for instance. Valorisation of agriculture by-products as a source of valuable nutraceuticals, in many instances, less common phenolic compounds such as xanthenes and benzophenones (*e.g.* mango stem bark, leaves, peels & seed kernels, Masibo & He, 2008; agarwood leaves, Feng *et al.*, 2011, Ito *et al.*, 2012), broaden the scope further, not only in terms of the types of phenolic compounds, but also the different thermal processes that these compounds are exposed to. Unit processing operations such as extraction, concentration and drying are just some. Whilst thermal degradation of phenolic compounds are mostly to be avoided or minimised, cases exist when thermal treatments are specifically applied to induce conversion of compounds to more active derivatives (*e.g.* the conversion of salvianolic acid B into salvianolic acid A in aqueous solution of *Radix Salviae Miltiorrhizae*; Xia *et al.*, 2014).

Processing techniques may have an impact on the chemical structure, resulting in changes in the bio-availability and bio-activity of these phytochemicals. The degradation of phytochemicals in plant material are influenced by factors such as the composition of the matrix and inherent factors such as pH and oxygen content. Matrix effects are further complicated in a food product due to the presence of food ingredients that may accelerate or slow down degradation. In spite of these, modelling of degradation kinetics of specific constituents or a quality parameter such as colour is useful to predict the effect of thermal treatment on food product quality, particularly nutrient losses. It allows expression of pseudo reaction mechanisms and the estimation of degradation rates and activation energies, which can subsequently be applied to minimise undesirable changes, and to optimise process design and food formulation.

The aim of this section of the literature review is to provide insight into the thermal stability of phenolic compounds, with specific emphasis on structure-stability relationships and factors that impact on the degradation rates and mechanisms. Major findings relating to the thermal degradation and/or conversion of phenolic acids and flavonoids are discussed. Tables are employed to summarise experimental conditions, details of reaction kinetics and the major findings of a large number of studies.

3.1. Phenolic Acids

Phenolic acids are important dietary constituents, as evident from their wide range of biological properties (Khadem & Marles, 2010; El-Seedi *et al.*, 2012; Heleno *et al.*, 2015). Coffee, apple juice and maté tea represent some of the richest dietary sources of chlorogenic acids, and consequently the thermal stability of their phenolic acid constituents during associated thermal processes have been investigated. In light of the application of sub- and supercritical water as extraction solvent for functional ingredients from different natural sources (Herrero *et al.*, 2006), the thermal stability of phenolic acids has also been investigated under these conditions.

3.1.1. Thermal Stability of Chlorogenic Acids and Other Phenolic Acid Derivatives

Kinetic studies, to date, have focused on the thermal degradation of total chlorogenic acids during the roasting of whole green coffee beans (Perrone *et al.*, 2010), and the degradation of 5-*O*-caffeylquinic acid (5-CQA; Figure 6) during accelerated storage (Van der Sluis *et al.*, 2005) and conventional thermal processing of apple juice (De Paepe *et al.*, 2014) (Table 2). Similarly, Zanoelo & Benincá (2009) used 5-CQA as target compound to assess the viability of superheated steam as an alternative drying medium for *Illex paraguayensis* (maté) leaves (Table 2).

Table 2 Thermal degradation kinetic studies on phenolic acids during roasting of coffee beans, accelerated storage and conventional thermal processing of apple juices, and in aqueous model solutions in the presence of superheated steam.

Phenolic acid and matrix	Operating conditions	Mathematical model, kinetic order and kinetic parameters	Major findings	Reference
Green coffee beans (<i>Coffea canephora</i> & <i>Coffea arabica</i>)				
Total chlorogenic acids	Roasting in a commercial spouted bed roaster: 170, 180, 190 or 200 °C 4, 5, 6, 7, 8 or 9 min	First-order degradation kinetic model; Arrhenius equation C. canephora: $k_{170\text{ °C}} = 0.4116 \text{ min}^{-1}$; $k_{180\text{ °C}} = 0.5457 \text{ min}^{-1}$; $k_{190\text{ °C}} = 0.6774 \text{ min}^{-1}$; $k_{200\text{ °C}} = 0.9691 \text{ min}^{-1}$; $E_a = 48.4 \text{ kJ.mol}^{-1}$; $A = 2.10 \times 10^5 \text{ min}^{-1}$ C. arabica: $k_{170\text{ °C}} = 0.2665 \text{ min}^{-1}$; $k_{180\text{ °C}} = 0.3123 \text{ min}^{-1}$; $k_{190\text{ °C}} = 0.3772 \text{ min}^{-1}$; $k_{200\text{ °C}} = 0.5875 \text{ min}^{-1}$; $E_a = 44.4 \text{ kJ.mol}^{-1}$; $A = 4.27 \times 10^4 \text{ min}^{-1}$	Distinct kinetic models were calculated for the different species due to intrinsic differences in their cell wall structures. Higher degradation k and E_a were calculated for the degradation of total chlorogenic acids in <i>C. canephora</i> in comparison with <i>C. arabica</i> .	Perrone <i>et al.</i> , 2010
Apple Juice				
5-CQA	Accelerated storage conditions: 70-100 °C, 4 days Effect of oxygen concentration: 0, 21 and 100%	First-order degradation kinetic model; Arrhenius equation Reaction rate constant for non-oxidative degradation at 70 °C (T_{ref}): $k_d = 1.8 \times 10^{-3} \text{ h}^{-1}$; Activation energy, $E_{a,d} = 52 \text{ kJ.mol}^{-1}$ Reaction rate constants for oxidative degradation at 70 °C (T_{ref}): $k_o = 1.0 \times 10^{-4} \text{ h}^{-1}$; Activation energy, $E_{a,o} = 187 \text{ kJ.mol}^{-1}$	5-CQA was amongst the more thermally stable compounds in apple juice. 5-CQA exhibited only minor degradation (20-30%) during accelerated storage (80 °C/100 h). The presence of oxygen did not influence the thermal stability of 5-CQA. For temperatures lower than 90 °C, the main degradation route of 5-CQA was the non-oxidative pathway; oxidative degradation was only observed at 90 and 100 °C.	Van der Sluis <i>et al.</i> , 2005
a hydroxycinnamic acid hexoside, two methoxybenzoic acid hexosides, <i>p</i> -coumaroylquinic acid, and 5-CQA.	Conventional thermal processing, isothermal: 85-145 °C for 7200 s	First-order degradation kinetic model; Arrhenius equation hydroxycinnamic acid hexoside: $k_{100\text{ °C}} = 0.38 \times 10^{-2} \text{ min}^{-1}$; $k_{120\text{ °C}} = 5.36 \times 10^{-2} \text{ min}^{-1}$; $k_{135\text{ °C}} = 31.0 \times 10^{-2} \text{ min}^{-1}$; $k_{140\text{ °C}} = 54.2 \times 10^{-2} \text{ min}^{-1}$; $k_{145\text{ °C}} = 93.3 \times 10^{-2} \text{ min}^{-1}$; $E_a = 162 \text{ kJ.mol}^{-1}$ methoxybenzoic acid hexoside (I): $k_{120\text{ °C}} = 0.24 \times 10^{-2} \text{ min}^{-1}$; $k_{135\text{ °C}} = 1.14 \times 10^{-2} \text{ min}^{-1}$; $k_{140\text{ °C}} = 1.86 \times 10^{-2} \text{ min}^{-1}$; $k_{145\text{ °C}} = 3.00 \times 10^{-2} \text{ min}^{-1}$; $E_a = 84.3 \text{ kJ.mol}^{-1}$ methoxybenzoic acid hexoside (II): $k_{135\text{ °C}} = 4.30 \times 10^{-2} \text{ min}^{-1}$; $k_{140\text{ °C}} = 11.2 \times 10^{-2} \text{ min}^{-1}$; $k_{145\text{ °C}} = 28.6 \times 10^{-2} \text{ min}^{-1}$; $E_a = 180 \text{ kJ.mol}^{-1}$ <i>p</i>-coumaroylquinic acid: $k_{135\text{ °C}} = 0.98 \times 10^{-2} \text{ min}^{-1}$; $k_{140\text{ °C}} = 1.33 \times 10^{-2} \text{ min}^{-1}$; $k_{145\text{ °C}} = 1.99 \times 10^{-2} \text{ min}^{-1}$; $E_a = 67.8 \text{ kJ.mol}^{-1}$ 5-CQA: $k_{135\text{ °C}} = 0.53 \times 10^{-2} \text{ min}^{-1}$; $k_{140\text{ °C}} = 0.80 \times 10^{-2} \text{ min}^{-1}$; $k_{145\text{ °C}} = 1.18 \times 10^{-2} \text{ min}^{-1}$; $E_a = 107 \text{ kJ.mol}^{-1}$	Some of the most heat-resistant compounds in cloudy apple juice belong to the hydroxycinnamic acid sub-class, of which 5-CQA was the most thermally stable.	De Paepe <i>et al.</i> , 2014
Aqueous model solutions				
5-CQA (0.099-0.101 mg.L ⁻¹ ultra pure water)	Isothermal treatments Performed in a glass cylindrical batch reactor Superheated steam: 125-226 °C Reaction times up to 5400 s	Reversible pseudofirst-order reaction of isomerisation; Arrhenius equation Frequency factor times the superheated steam concentration: ($A \times [\text{H}_2\text{O}] = 4.88 \times 10^6 \text{ s}^{-1}$) $-E_a/R = 2284 \text{ K}$. Therefore, $E_a = 18.98 \text{ kJ.mol}^{-1}$ Equilibrium constant at 298 K, $K_{298} = 1.68$ Ratio of heat of reaction to universal gas constant at 298 K: $-\Delta H_{298}/R = 1013 \text{ K}$	5-CQA presented negligible rates of oxidation when in contact with superheated steam; it was rather subject to isomerisation to 4-CQA. Isomerisation of 5-CQA will not be detrimental for the quality of manufactured leaves and branches of maté (<i>Ilex paraguariensis</i>), since the total concentration of chlorogenic acids would remain unchanged.	Zanoelo & Benincá, 2009

Results presented by Perrone *et al.* (2010), Van der Sluis *et al.* (2005) and De Paepe *et al.* (2014) indicated that the thermal degradation of total chlorogenic acids, individual chlorogenic acids (including 5-CQA) and other phenolic acids follow first-order^a, Arrhenius-compliant^b, kinetic models. The thermal degradation of total chlorogenic acids in green coffee beans was affected by the coffee species due to intrinsic differences in their cell wall structures (Perrone *et al.*, 2010), as observed previously for individual chlorogenic acid isomers in Arabica and Robusta coffees (Trugo & Macrae, 1984a). 5-CQA was identified as one of the most heat-resistant compounds in apple juice (Van der Sluis *et al.*, 2005; De Paepe *et al.*, 2014) and its thermal stability was not affected by the presence of oxygen (Van der Sluis *et al.*, 2005). Zanoelo & Benincá (2009) demonstrated that 5-CQA presented negligible rates of oxidation when in contact with superheated steam and that it was rather subject to a reversible isomerisation reaction (Table 2).

To date, much effort has been expended towards characterising the chemical changes that occur upon thermal treatment of phenolic acid-rich matrices. This is particularly true with regard to the roasting of coffee beans, as it is during the roasting process that the desired colour, taste and aroma of the beans are produced (Sivetz & Desrosier, 1979; Mwithiga & Jindal, 2003; Farah *et al.*, 2006a). During roasting, chlorogenic acids are lost as a consequence of the thermal breakage of the carbon-carbon covalent bonds, resulting in isomerisation or hydrolysis of the ester bond in the initial roasting stages. Later, chemical transformation such as decarboxylation of the cinnamoyl moieties, epimerisation at the quinic acid moiety of chlorogenic acids, dehydration to produce lactones and cyclohexene derivatives, and degradation into low molecular weight compounds occur (as reviewed by Farah & Donangelo, 2006; Perrone *et al.*, 2008; Jaiswal *et al.*, 2012). Chlorogenic acids may also participate in the formation of melanoidins (Bekedam *et al.*, 2008; Jaiswal *et al.*, 2012), loosely defined as brown, nitrogenous macromolecular compounds that absorb light at 405 nm. In a recent study, Deshpande and co-workers (2014) observed positional isomerisation in mono- and di-caffeoylquinic acids under basic and acidic aqueous conditions, as well as dry roasting conditions (180 °C/12 min), which are all relevant to the processing of coffee.

^aFor a first-order reaction, the mathematical expression that relates concentration C with time t is given by:

$$C = C_0 \exp(-kt) \quad (1)$$

where C_0 is the initial concentration of the compound, and k is the reaction rate constant in units of time^{-1} .

Frequently, the logarithmic form of eq. 1 is used instead of the exponential equation, giving:

$$\ln C = \ln C_0 - kt \quad (2)$$

or
$$\ln \left(\frac{C}{C_0} \right) = -kt \quad (3)$$

^bThe model is based on the classical approach used for chemical reactions, which defines a reaction rate constant (k) that depends on temperature (T) according to an Arrhenius law (Peleg *et al.*, 2012; Van Boekel, 1996; 2008):

$$k = A \exp \left(-\frac{E_a}{RT} \right) \quad (4)$$

The linearised form is:

$$\ln k = \ln A - \frac{E_a}{RT} \quad (5)$$

Where A is the so-called 'pre-exponential factor' (sometimes called the frequency factor, k_0), E_a the activation energy (J mol^{-1}), T the absolute temperature in °K, and R the ideal gas constant ($8.3145 \text{ J mol}^{-1} \text{ K}^{-1}$). The dimension of A should be the same as that of k .

The effect of temperature on the rate constant can also be evaluated by means of the Arrhenius equation with a simple reparameterisation by introducing a reference temperature, T_{ref} (eq. 6):

$$k = k_{ref} \exp \left[-\frac{E_a}{R} \left(\frac{1}{T} - \frac{1}{T_{ref}} \right) \right] \quad (6)$$

In which k_{ref} is the reaction rate constant at the reference temperature; also known as the reparameterised pre-exponential factor (k_0').

The reference temperature should preferentially be chosen in the middle of the studied temperature range.

The chemical changes of chlorogenic acids that occur during decaffeination (Farah *et al.*, 2006b) and coffee brewing (Matei *et al.*, 2012), both high-temperature processes, have also been investigated. Farah *et al.* (2006b) reported an average loss of 10% in the total chlorogenic acid content of decaffeinated, roasted Arabica coffee samples, in comparison with non-decaffeinated samples roasted under the same conditions. On the other hand, an average increase of 7% in lactone content was observed in the same samples. From a qualitative perspective, Matei *et al.* (2012) investigated novel compounds formed from chlorogenic acids during the brewing process. Hydroxylation of the chlorogenic acid cinnamoyl substituent by conjugate addition of water was reported and, following this, a reversible water elimination reaction was observed, yielding *cis*-cinnamoyl derivatives accompanied by acyl migration products.

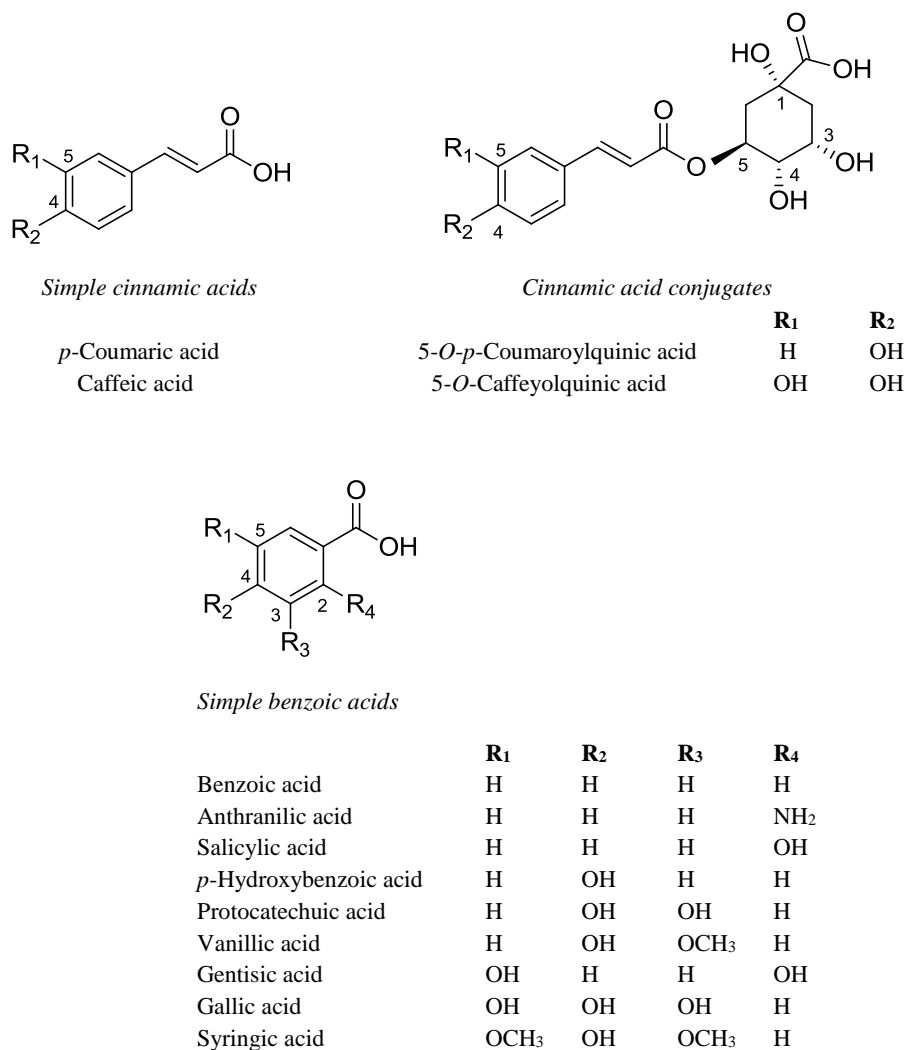


Figure 6 Substitution patterns of selected simple cinnamic acids and cinnamic acid conjugates, as well as simple benzoic acids.

The research group of Dawidowicz and Typek has provided fundamental insight into the reactions of *trans*-5-CQA (Figure 6) upon thermal treatment in aqueous solution. Heating of an aqueous solution of *trans*-5-CQA under different heat and pH conditions resulted in isomerisation, esterification, hydroxylation and/or hydrolysis leading to the formation of several compounds (Dawidowicz & Typek, 2010; 2011). The amount of each component formed strongly depended upon the heating time and temperature, as well as the pH of the solution. Hydrolysis of *trans*-5-CQA led to the formation

of caffeic acid and quinic acid, and subsequent transformation of quinic acid produced protocatechuic acid (Dawidowicz & Typek, 2010; 2011).

Two isomerisation behaviours may be observed for *trans*-5-CQA, namely *trans-cis* isomerisation and positional isomerisation. *Trans-cis* isomerisation is more commonly induced by UV irradiation (e.g. Karaköse *et al.*, 2015), but high-temperature thermal treatment may also induce isomerisation of the C-C double bond. Upon thermal treatment, positional isomerisation of *trans*-5-CQA in aqueous model solutions (Trugo & Macrae, 1984b; Zanoelo & Benincá, 2009; Dawidowicz & Typek, 2010; 2011) and in blueberry pulp (Dawidowicz & Typek, 2014) lead to the formation of *trans*-4-CQA and *trans*-3-CQA. These positional isomers are also formed upon incubation of *trans*-5-CQA at relatively low temperatures under alkaline conditions (Clifford *et al.*, 1989; Narita & Inouye, 2013), and under physiological pH and temperature conditions (Xie *et al.*, 2011). These studies indicated that the formation of 4-CQA predominates over that of 3-CQA, which is in accordance with the conversion mechanism proposed by Xie *et al.* (2011). They postulated that *trans*-5-CQA first isomerises to *trans*-4-CQA, and then to *trans*-3-CQA via intramolecular trans-esterification. Small amounts of the *trans*-1-CQA isomer has also been identified in *trans*-5-CQA buffered aqueous solutions (pH 4.0-9.0) heated under reflux for 10-300 min (Dawidowicz & Typek, 2011), while treatment of *trans*-5-CQA with the strong base, tetramethylammonium hydroxide, for 5 min at 20 °C also resulted in formation of *trans*-1-CQA.

While all the studies in the abovementioned section have concentrated on the thermal stability of 5-CQA, there are only a few reports on the thermal stability of other mono- and di-caffeoylquinic acids. Most recently, Li *et al.* (2015) investigated the thermal stability of six caffeoylquinic acids, including 5-CQA, 4-CQA, 3-CQA, 3,4-di-CQA, 4,5-di-CQA and 3,5-di-CQA, by heating a dilute aqueous solution of each compound in boiling water for 0-6 h. Mono-CQAs were shown to be thermally more stable than the di-CQAs with the relative order of stability for the individual mono-CQAs established as 5-CQA > 3-CQA > 4-CQA, and that of the di-CQAs as 4,5-di-CQA > 3,5-di-CQA > 3,4-di-CQA. In accordance with the findings of Dawidowicz & Typek (2010; 2011), the mono-CQAs underwent transformations such as isomerisation, hydroxylation and/or hydrolysis to caffeic acid and quinic acid. The di-CQAs could also isomerise and/or degrade to form mono-CQAs, caffeic acid and unidentified compounds. The extent of conversion depended on the heating time. Positional isomerisation of the mono- and di-CQAs proceeded via intramolecular trans-esterification (Li *et al.*, 2015). Similarly, positional isomerisation has also been observed for cinnamoylquinic acids and hydroxycinnamoylquinic acids under basic and high temperature (90 °C) conditions (Hanson, 1965; Haslam *et al.*, 1964).

While data from the kinetic studies indicate that increased temperatures increase the degradation rates of phenolic acids (Table 2), other factors relevant in the production of food products may also affect the transformation and degradation rates of phenolic acids during thermal processing. For instance, it has been shown that the stability of 5-CQA during high-temperature processing is greatly improved in the presence of sucrose (Dawidowicz & Typek, 2014), and by the addition of epigallocatechin gallate (EGCG) and ascorbic acid during incubation at 37 °C under alkaline conditions (Narita & Inouye, 2013). The protective effects of EGCG or ascorbic acid on 5-CQA were shown to be dose-dependent (0.002-1.2 mM) and were also stronger at higher pH values (Narita & Inouye, 2013). Other studies have found that matrix composition have no impact on the degradation; the transformation and degradation of *trans*-5-CQA in thermally processed blueberry pulp was almost the same as in an acidic aqueous model system (Dawidowicz & Typek, 2014).

Several studies have demonstrated the effect of pH on the transformation and isomerisation of phenolic acids. While these studies were carried out at relatively low temperatures considering thermal processing of food products, they provided insight into the stability of chlorogenic acids at different pH levels. *Trans*-3-, -4-, and -5-CQA are stable in acidic conditions (pH ≤ 5) during incubation at 37 °C for 2 h (Xie *et al.*, 2011), while 5-CQA in alkaline aqueous solution undergoes isomerisation and transformation even at room temperature (Clifford *et al.*, 1989). Indeed, an increase in pH

towards the alkaline region (pH ~ 9) has been shown to increase the degradation rate constant of 5-CQA in aqueous buffer solution (37 °C) significantly (Xie *et al.*, 2011; Narita & Inouye, 2013).

3.1.2. Thermal Stability of Phenolic Acids under Sub- and Supercritical Water Conditions

The stability of phenolic acids under sub- and supercritical water conditions has been assessed by several researchers (González *et al.*, 2004; Lindquist & Yang, 2011; Khuwijitjaru *et al.*, 2014a, 2014b). Under sub-critical water conditions, the main decomposition reaction of benzoic acids is thermal decarboxylation (González *et al.*, 2004; Lindquist & Yang, 2011; Khuwijitjaru *et al.*, 2014a, 2014b), which proceeds according to the reaction mechanism proposed by Chunchev & BelBruno (2007) for the decarboxylation of *ortho*-substituted benzoic acids under neutral conditions. In addition to decarboxylation, other reactions may also occur under sub-critical water conditions. González *et al.* (2004) demonstrated that 2-methoxyphenol (guaiacol), formed as primary product from the decarboxylation of vanillic acid, may also participate in secondary reactions, leading to the formation of catechol and phenol. The authors postulated that catechol originates from the hydrolysis of the methoxy group of guaiacol through an S_N2 mechanism, while phenol is formed through pyrolytic free radical decomposition of guaiacol. Similarly, caffeic acid subjected to sub-critical water treatment (Khuwijitjaru *et al.*, 2014a; 2014b) and mild pyrolysis (225-226 °C/15 min; Stadler *et al.*, 1996), resulted in rapid decarboxylation with the formation of simple catechol monomers, *i.e.* 4-vinylcatechol, 4-ethylpyrocatechol and pyrocatechol, while hydroxytyrosol and protocatechuic aldehyde (Khuwijitjaru *et al.*, 2014b), as well as more complex cyclocondensed dimers and polymers (Stadler *et al.*, 1996), were also identified. Stadler *et al.* (1996) furthermore reported that the thermal degradation products of caffeic acid, subjected to pyrolysis under atmospheric conditions, showed more products of oligomeric/polymeric nature compared to thermal treatment under vacuum (*i.e.* oxygen-free) conditions. Oxygen could thus have catalysed oxidative coupling reactions, leading to a broader spectrum of products and the formation of polymeric substances (Stadler *et al.*, 1996).

Decarboxylation of phenolic acids under sub- and supercritical water conditions follows first-order kinetics (Table 3) as observed for other organic acids, including formic (Yu & Savage, 1998) and acetic acids (Meyer *et al.*, 1995). The reaction rate constant for decarboxylation of vanillic acid is independent of pressure below the critical temperature (375 °C), while it decreases with increasing pressure at supercritical temperatures, indicative of a unimolecular dissociation mechanism (González *et al.*, 2004). The evolution of degradation products over time can also be adequately described by a first-order kinetic model, while the temperature dependence of the rate constants for both the degradation and formation reactions obeys the Arrhenius law (Table 3). The activation energy for the degradation of phenolic acids under sub-critical water conditions has been reported to range between 28 and 93 kJ.mol⁻¹ (Table 3).

Table 3 Thermal degradation kinetic studies on phenolic acids under sub- and supercritical water conditions

Phenolic acid and matrix	Operating conditions	Mathematical model, kinetic order and kinetic parameters	Major findings	Reference
Aqueous model system				
Vanillic acid (200 ppm) (1.19×10^{-3} mol.L ⁻¹ degassed and deionised water)	Continuous tubular reactor Sub- and supercritical water conditions Isothermal: 280, 300, 350, 375, 400, 425, 450 and 500 °C Isobaric: 225, 250 and 300 bar Treatment times < 160 s	First-order (irreversible) degradation kinetic model; Arrhenius equation Sub-critical water: k (300 °C, 250 bar) = 0.054 s ⁻¹ ; k (300 °C, 300 bar) = 0.055 s ⁻¹ ; k (350 °C, 250 bar) = 0.127 s ⁻¹ ; k (350 °C, 300 bar) = 0.126 s ⁻¹ ; Average E_a = 57 kJ.mol ⁻¹ ; ln A = 9.0 s ⁻¹ Supercritical water: k (400 °C, 250 bar): 0.367 s ⁻¹ ; k (400 °C, 300 bar): 0.277 s ⁻¹ ; k (425 °C, 250 bar): 0.694 s ⁻¹ ; k (425 °C, 300 bar): 0.505 s ⁻¹ ; Average E_a = 95 kJ.mol ⁻¹ ; ln A = 16.0 s ⁻¹	The main decomposition reaction was decarboxylation of vanillic acid with the formation of 2-methoxyphenol (guaiacol) as primary product. Guaiacol further reacted to form phenol and catechol. The isothermal decarboxylation k was independent of pressure below the critical temperature (375 °C). The isothermal decarboxylation k decreased with increasing pressure at supercritical temperatures, indicating direct elimination of carbon dioxide. Different values for the Arrhenius parameters suggested that two different reaction mechanisms exist, dominating below and above the critical temperature, respectively.	González <i>et al.</i> , 2004
Benzoic acids: gallic, gentisic, protocatechuic, syringic, <i>p</i> -hydroxybenzoic and vanillic acids. Cinnamic acids: 5-CQA, caffeic and <i>p</i> -coumaric acids. (100 mg.L ⁻¹ distilled water)	Batch-type reactor Sub-critical water at 100, 150, 200 and 250 °C Pressure inside the vessel was equal to the saturated vapour pressure of water at each of the respective treatment temperatures. Treatment times: 30, 60, 90 and 120 min.	First-order degradation kinetic model; Arrhenius equation gallic acid: $k_{100\text{ °C}} = 5.9 \times 10^3 \text{ min}^{-1}$; $k_{150\text{ °C}} = 32.2 \times 10^3 \text{ min}^{-1}$ gentisic acid: $k_{100\text{ °C}} = 4.3 \times 10^3 \text{ min}^{-1}$; $k_{150\text{ °C}} = 16.1 \times 10^3 \text{ min}^{-1}$ <i>p</i>-hydroxybenzoic acid: $k_{100\text{ °C}} = 0.7 \times 10^3 \text{ min}^{-1}$; $k_{150\text{ °C}} = 3.8 \times 10^3 \text{ min}^{-1}$; $k_{200\text{ °C}} = 18.8 \times 10^3 \text{ min}^{-1}$; $E_a = 48.1 \text{ kJ.mol}^{-1}$ protocatechuic acid: $k_{100\text{ °C}} = 3.3 \times 10^3 \text{ min}^{-1}$; $k_{150\text{ °C}} = 8.3 \times 10^3 \text{ min}^{-1}$; $k_{200\text{ °C}} = 60.7 \times 10^3 \text{ min}^{-1}$; $E_a = 41.9 \text{ kJ.mol}^{-1}$ syringic acid: $k_{100\text{ °C}} = 1.9 \times 10^3 \text{ min}^{-1}$; $k_{150\text{ °C}} = 6.6 \times 10^3 \text{ min}^{-1}$; $k_{200\text{ °C}} = 21.2 \times 10^3 \text{ min}^{-1}$; $E_a = 35.3 \text{ kJ.mol}^{-1}$ vanillic acid: $k_{100\text{ °C}} = 0.8 \times 10^3 \text{ min}^{-1}$; $k_{150\text{ °C}} = 1.6 \times 10^3 \text{ min}^{-1}$ caffeic acid: $k_{100\text{ °C}} = 7.8 \times 10^3 \text{ min}^{-1}$; $k_{150\text{ °C}} = 28.0 \times 10^3 \text{ min}^{-1}$ 5-CQA: $k_{100\text{ °C}} = 6.1 \times 10^3 \text{ min}^{-1}$; $k_{150\text{ °C}} = 18.4 \times 10^3 \text{ min}^{-1}$; $k_{200\text{ °C}} = 42.3 \times 10^3 \text{ min}^{-1}$; $E_a = 28.4 \text{ kJ.mol}^{-1}$ <i>p</i>-coumaric acid: $k_{100\text{ °C}} = 1.7 \times 10^3 \text{ min}^{-1}$; $k_{150\text{ °C}} = 7.1 \times 10^3 \text{ min}^{-1}$	All phenolic acids were completely degraded within 30 min at 250 °C, but at different degradation k . Gallic acid was the most labile phenolic acid at 150 °C. The degree of hydroxylation and methoxylation, and the position of hydroxylation affected thermal stability. Cinnamic acids were more easily decarboxylated than the benzoic acids. Caffeic acid degraded to form the decarboxylated product, pyrocatechol. Half of the DPPH radical scavenging activity of the original caffeic acid solution was retained after sub-critical water treatment (250 °C/120 min). The degradation products were quite stable at high temperature and exhibited a high DPPH radical scavenging activity.	Khuwijitjaru <i>et al.</i> , 2014a
Caffeic acid (100 mg.L ⁻¹ degassed and distilled water)	Continuous flow-type/tubular reactor Sub-critical water: 160, 180, 200, 220 and 240 °C. Constant pressure: 5 MPa. Treatment times: 5-1080 s.	First-order kinetic model; Arrhenius equation Degradation of caffeic acid: $E_a = 93 \text{ kJ.mol}^{-1}$; $A = 1.78 \times 10^8 \text{ s}^{-1}$ Formation of 4-vinylcatechol: $E_a = 87 \text{ kJ.mol}^{-1}$; $A = 2.46 \times 10^7 \text{ s}^{-1}$ Formation of hydroxytyrosol: $E_a = 103 \text{ kJ.mol}^{-1}$; $A = 8.24 \times 10^8 \text{ s}^{-1}$ Formation of protocatechuic aldehyde: $E_a = 85 \text{ kJ.mol}^{-1}$; $A = 1.06 \times 10^6 \text{ s}^{-1}$	The major degradation products of caffeic acid was 4-vinylcatechol (decarboxylated product), hydroxytyrosol and protocatechuic aldehyde. The total antioxidant activity of the treated caffeic acid solution (online HPLC-DPPH assay) did not change. The degradation products also exhibited strong DPPH radical scavenging activity.	Khuwijitjaru <i>et al.</i> , 2014b

The thermal stability of benzoic acid derivatives under sub- and supercritical water conditions depends on their substitution pattern (Figure 6). Under sub-critical water conditions, benzoic acid was the most stable, followed by syringic acid, salicylic acid and anthranilic acid (Lindquist & Yang, 2011). It was concluded that the methoxy, hydroxy and amino groups of syringic acid, salicylic acid and anthranilic acid, respectively, are activating groups that facilitate thermal decarboxylation, causing their degradation in sub-critical water. The decreased thermal stability of benzoic acids, attributed to the presence of additional hydroxy and methoxy groups, has also been confirmed kinetically. Comparison of the degradation rate constants of selected benzoic acid derivatives at 150 °C (Khuwijitjaru *et al.*, 2014a; Table 3) indicated that gallic acid, with three hydroxy groups on its benzene ring, is the most thermally labile phenolic acid. Indeed, an increase in the degree of hydroxylation increased the degradation rate of benzoic acids, and their stability was found to decrease in the order *p*-hydroxybenzoic acid ($k_{150\text{ °C}} = 3.8 \times 10^3 \text{ min}^{-1}$) > protocatechuic acid ($k_{150\text{ °C}} = 8.3 \times 10^3 \text{ min}^{-1}$) > gallic acid ($k_{150\text{ °C}} = 32.2 \times 10^3 \text{ min}^{-1}$) (Table 3). However, replacement of hydroxy groups with methoxy groups confers increased thermal stability to the phenolic acids. This is exemplified by the lower degradation rate of syringic acid at 100 and 150 °C compared to that of gallic acid at the same temperatures (Table 3). The position(s) of hydroxylation may also affect the thermal stability of the benzoic acids. The degradation rate constant of gentisic acid (with OH groups at C-2 and C-5) was almost twice that of protocatechuic acid (with OH groups at C-3 and C-4) at 150 °C (Table 3). Comparison of the degradation rate constants of *p*-coumaric acid and *p*-hydroxybenzoic acid with similar substitution patterns furthermore indicates that the carboxylic group on the acrylic side chain of cinnamic acids might be more easily decarboxylated than the carboxylic group directly attached to the benzene ring as is the case for benzoic acids (Table 3).

3.2. Flavan-3-ols and Proanthocyanidins

Flavan-3-ols are the major phenolic constituents of fresh tea leaves and extracts of *Camellia sinensis*. The numerous health benefits associated with the consumption of green tea, including preventative effects against cancer and cardiovascular disease (as reviewed by Zaveri, 2006 and Khan & Mukhtar, 2007) are mainly attributed to these compounds. The major flavan-3-ols present in green tea include epigallocatechin gallate (EGCG), epicatechin gallate (ECG), epicatechin (EC) and epigallocatechin (EGC) (Tounekti *et al.*, 2013). These compounds occur in the 2,3-*cis* configuration (2*R*,3*R*) and differ with regard to the presence/absence of a hydroxy group at C-5' and/or a galloyl group at C-3 (Figure 7).

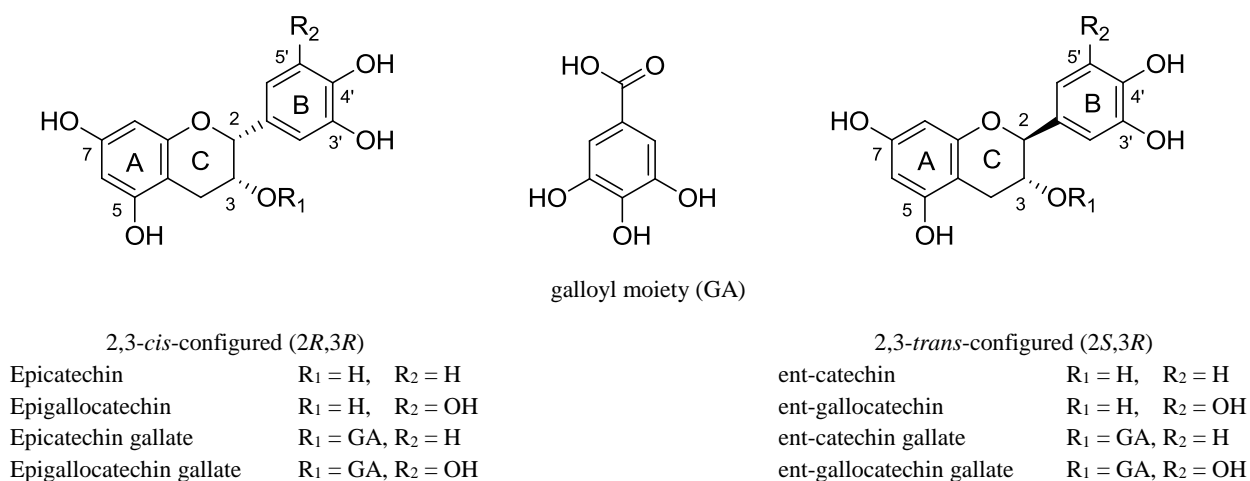


Figure 7 Structures of the major green tea flavan-3-ols, epicatechin, epigallocatechin, epicatechin gallate and epigallocatechin gallate, and their corresponding C-2 epimers that are formed upon thermal treatment.

Interest in the health-promoting properties of green tea flavan-3-ols has motivated several studies on their stability during tea preparation, food processing and storage (as reviewed by Ananingsih *et al.*, 2013). The thermal stabilities of other flavan-3-ols, including proanthocyanidins, have also been investigated in apple juice, grape seed extract and cocoa beans. In these studies, thermal conditions were selected to simulate relevant thermal processes to which these products are commonly exposed to. This included shelf-life testing under accelerated conditions, conventional thermal processing and roasting, amongst others. Selected studies have also been conducted in aqueous model solutions to provide fundamental insight into structure-stability relationships and reaction pathways, and to elucidate the effects of factors such as pH and oxygen concentration on the thermal stability of monomeric flavan-3-ols and proanthocyanidins.

3.2.1. Green Tea Flavan-3-ols

During high-temperature processing, green tea flavan-3-ols simultaneously undergo epimerisation and thermal degradation. This phenomenon has been observed by numerous researchers (Seto *et al.*, 1997; Wang & Helliwell, 2000; Wang *et al.*, 2000; Chen *et al.*, 2001; Xu *et al.*, 2003; Lee *et al.*, 2010; Li *et al.* 2011; 2012) and has also been characterised kinetically (Wang *et al.*, 2006; 2008a; 2008b). The 2,3-*cis*-configured catechins EGCG, ECG, EC and EGC are converted to their corresponding C-2 epimers in the 2,3-*trans* configuration (2*S*,3*R*), *i.e.* ent-gallocatechin gallate (ent-GCG), ent-catechin gallate (ent-CG), ent-catechin (ent-C) and ent-gallocatechin (ent-GC), respectively (Figure 7). This epimerisation between compound pairs is reversible. At high temperatures, the epimerisation of monomeric flavan-3-ols from the 2,3-*cis* configuration to the 2,3-*trans* configuration, rather than the reversed epimerisation, is the predominant reaction. This has been ascribed to the fact that ent-GCG and ent-CG in the 2,3-*trans* configuration are thermodynamically more stable than EGCG and ECG in the 2,3-*cis* configuration. The rate of epimerisation also increases with increasing temperature. During prolonged heating, however, the predominant change becomes the degradation or oxidation of the flavan-3-ols.

Thermally-induced degradation reactions of flavan-3-ols may include cleavage of the galloyl moiety of galloylated flavan-3-ols, as well as dimerisation. Lee *et al.* (2010) found that the increasing amount of gallic acid in a thermally treated sample of EGCG can be ascribed to the release of gallic acid from EGCG and, more importantly, to its release from EGCG dimers that were also formed upon heating. Li *et al.* (2013) found that heating of an EGCG solution induced cleavage and epimerisation reactions, leading to the formation of flavan-3-ol monomers and gallic acid. A schematic of the possible degradation pathways of EGCG and ECG in aqueous solution was proposed (Figure 8).

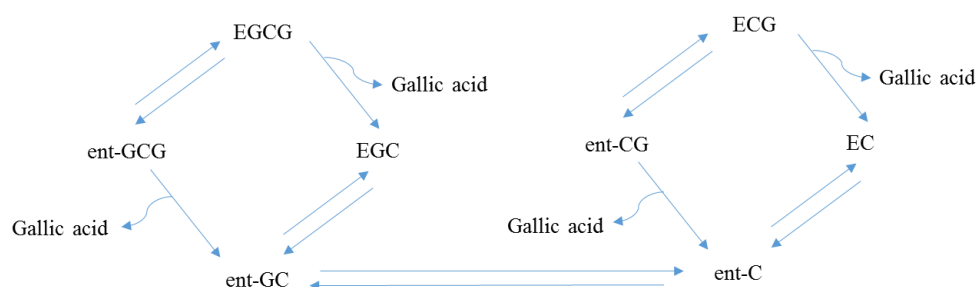
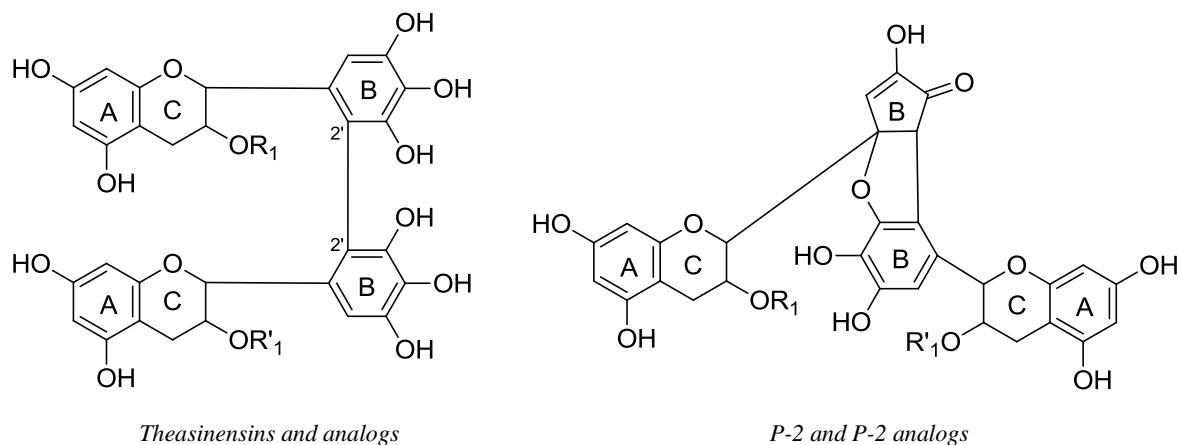


Figure 8 Possible degradation pathways for EGCG and ECG in solution (adapted from Li *et al.*, 2013).

Thermally-induced autoxidation of green tea flavan-3-ols with trihydroxy substitution of the B-ring leads to the formation of dimeric products, and colourless bisflavanols (theasinensins, THSNs; linked through C-2'-C-2' in the B-ring) and their P-2 analogs (linked by B-ring opening/condensation and elimination reaction in the B-ring) (Figure 9). Incubation of EGCG in 0.1 M acetate buffer (pH 5) at 120 °C for 5 h led to the formation of an EGCG dimer that contained two galloyl groups [linkage through C-4 (C-ring) and C-8 (A-ring) of the EGCG units] and an EGCG dimer in which one galloyl

moiety was lost, together with the formation of another dimeric product (Lee *et al.*, 2010). Storage of EGCG in solid state samples at elevated temperature (80 °C) led to the formation of the EGCG B-ring homodimer THSN A/D (Li *et al.*, 2013). Heating of green tea flavan-3-ols in model dairy beverages at 37 and 62 °C led to the formation of EGC and EGCG homo- and heterodimers (THSN A/D, C/E and B) and P-2 analogs (Song *et al.*, 2015). These B-ring dimers also form upon incubation of EGCG in different cell culture media and phosphate buffer solution (pH 7.4, 37 °C; Sang *et al.*, 2005). Epimerisation of flavan-3-ol monomers prior to dimerisation may also contribute to stereochemical variation in the THSNs and P-2 analogs. For instance, Song *et al.* (2015) identified three different THSN C/E analogues corresponding to ent-GC–ent-GC, ent-GC–EGC and EGC–EGC.



Linkage	Type	Compound	Precursors	Nominal Molecular Weight, g.mol ⁻¹	Substitution	
					R ₁	R ₁ '
C-2'-C-2'	Homo	THSN A/D	2 EGCG	914	GA	GA
	Homo	THSN C/E	2 EGC	610	OH	OH
	Hetero	THSN B	EGCG + EGC	762	GA	OH
B-ring opening	Homo	P-2	2 EGCG	884	GA	GA
	Homo	P-2 analog	2 EGC	580	OH	OH
	Hetero	P-2 analog	EGCG + EGC	732	GA/OH	OH/GA

Figure 9 Structures of the autoxidation products of epigallocatechin gallate (EGCG) and epigallocatechin (EGC). GA = galloyl moiety (reproduced from Neilson *et al.*, 2010).

The thermal stability of monomeric flavan-3-ols depends upon their chemical structure, *i.e.*, the number of hydroxy groups on the B-ring and esterification with a galloyl moiety at C-3. Results presented by Wang *et al.* (2000) indicated that flavan-3-ols with three hydroxy groups in their B-ring (EGCG and EGC) are more prone to oxidation than those with only two hydroxy groups (ECG and EC) during thermal processing (121 °C/1 min) and storage (50 °C/12 days) of green tea extracts. Galloylated flavan-3-ols (EGCG and EGC) are also more prone to oxidation than their non-galloylated derivatives (EGC and EC). The thermal stability of the flavan-3-ols was thus found to decrease in the order EC > ECG > EGC > EGCG (Wang *et al.*, 2000).

Likewise, other studies showed that EGCG and EGC were less stable than ECG and EC during incubation (room temperature to 37 °C) in alkaline solution (sodium phosphate buffer solution, pH 7.4) (Zhu *et al.*, 1997; Chen *et al.*, 1998; Su *et al.*, 2003). Sang *et al.* (2005) demonstrated that EGCG and EGC had a similar stability, and that they were both less stable than ECG and EC during the incubation of different concentrations of green tea extract in nanopure water (0.05-0.6%) at room temperature. The difference in the relative stability of these flavan-3-ols was especially prominent at the

lowest concentration of the green tea extract. Conversely, the individual epicatechin derivatives appear to have similar rates of degradation during boiling in deionised water at 100 °C/6 h (Su *et al.*, 2003).

To date, most kinetic studies on the thermal stability of green tea flavan-3-ols have been conducted in aqueous model solutions and aqueous green tea infusions (Komatsu *et al.*, 1993; Zimeri & Tong, 1999; Wang *et al.*, 2006, 2008a; Li *et al.*, 2012). These studies were conducted over a wide range of temperatures ranging from typical shelf-life (25 °C) up to pasteurisation/sterilisation/UHT (~ 100-135 °C) and baking (165 °C) temperatures (Table 4). Other studies include the assessment of the thermal stability of catechin under sub-critical water conditions (100-150 °C; Khuwijtjaru *et al.*, 2014a), and that of EGCG and other 2,3-*cis*-configured flavan-3-ols in the solid state upon storage (25-60 °C; Li *et al.*, 2011) (Table 4). Limited information is, however, available on the thermal stability of green tea extract/green tea flavan-3-ols when used as functional ingredients in food products. Wang *et al.* (2008b) kinetically assessed the thermal stability of EGCG in fortified bread during the baking process with designated oven temperatures of 200-240 °C, while Song *et al.* (2015) investigated the degradation of monomeric flavan-3-ols and the formation of dimers in model dairy beverages at 37 and 62 °C (Table 5). Most of the aforementioned studies indicated that the thermal degradation and epimerisation of monomeric flavan-3-ols can adequately be described by first-order reaction kinetics, and that the temperature dependence of the rate constants follow the Arrhenius equation (Tables 4 and 5). Conversely, Song *et al.* (2015) demonstrated that the degradation of flavan-3-ols in model dairy beverages will not accurately fit the Arrhenius model. The observed increase in the first-order degradation rates of all flavan-3-ols with increasing temperature was ascribed not only to typical Arrhenius behaviour of the flavan-3-ols, but also to the weakening of non-covalent interactions between milk proteins and flavan-3-ols at elevated temperature (Song *et al.*, 2015).

Komatsu *et al.* (1993) demonstrated that epimerisation and thermal degradation of flavan-3-ols in green tea infusions occur simultaneously, and that the dominant reaction of EC in slightly acidic media (pH 4.0-5.0) following thermal processing (121 °C/15 min) is isomerisation to (\pm)-catechin. Because of the complexity of the kinetic reactions, independent first-order reactions, which were incapable of handling simultaneous epimerisation and degradation, were assumed. Results presented by Komatsu *et al.* (1993) indicated the existence of a specific “turning point temperature” on the Arrhenius plots. The activation energies for the overall degradation of individual and total flavan-3-ols in green tea infusion were much higher at temperatures above the turning point temperature of 82 °C (Table 4). Komatsu *et al.* (1993) stated that the turning point temperature on the Arrhenius plot suggests that “there might exist two competing reactions of the same reaction products and a different temperature dependence, or two or more reactions of different reaction products and different temperature dependence”.

Table 4 Thermal degradation kinetics modelling of green tea flavan-3-ols.

Flavan-3-ols ^a and matrix	Operating conditions	Mathematical model, kinetic order and kinetic parameters	Major findings	Reference
Green tea ('Yabukita') infusion				
EC, ECG, EGC and EGCG	<p><i>Individual flavan-3-ols</i></p> <p>Thermal degradation kinetics of individual catechins in green tea infusion (pH 6.12) over a temperature range 25-95 °C</p> <p><i>Total flavan-3-ols</i></p> <p>Effect of pH (4.93 vs 6.12) on the thermal degradation kinetics of total catechins in green tea infusion at 25-95 °C.</p> <p>pH 6.12: without addition of ascorbic acid</p> <p>pH 4.93: with ascorbic acid (20 mg.100 mL⁻¹)</p>	<p>First-order degradation kinetic model; Arrhenius equation</p> <p><i>Individual flavan-3-ols::</i></p> <p>ECG: $E_a (< 82\text{ °C}) = 13.39\text{ kJ.mol}^{-1}$; $E_a (> 82\text{ °C}) = 149.79\text{ kJ.mol}^{-1}$</p> <p>EC: $E_a (< 82\text{ °C}) = 21.76\text{ kJ.mol}^{-1}$; $E_a (> 82\text{ °C}) = 159.41\text{ kJ.mol}^{-1}$</p> <p>EGC: $E_a (< 82\text{ °C}) = 15.06\text{ kJ.mol}^{-1}$; $E_a (> 82\text{ °C}) = 171.96\text{ kJ.mol}^{-1}$</p> <p>EGCG: $E_a (< 82\text{ °C}) = 19.66\text{ kJ.mol}^{-1}$; $E_a (> 82\text{ °C}) = 158.57\text{ kJ.mol}^{-1}$</p> <p><i>Total flavan-3-ols:</i></p> <p>Ascorbic-added green tea infusion, pH 4.93: $E_a (< 82\text{ °C}) = 10.46\text{ kJ.mol}^{-1}$; $E_a (> 82\text{ °C}) = 147.28\text{ kJ.mol}^{-1}$</p> <p>Original green tea infusion, pH 6.12: $E_a (< 82\text{ °C}) = 15.90\text{ kJ.mol}^{-1}$; $E_a (> 82\text{ °C}) = 160.67\text{ kJ.mol}^{-1}$</p>	<p><i>Individual flavan-3-ols:</i></p> <p>The k values of the individual flavan-3-ols were different with k of EGCG the lowest, and that of ECG the highest.</p> <p>Arrhenius plot showed a concave line which consisted of two straight lines which crossed each other at 82 °C ("turning point temperature").</p> <p>E_a values for the degradation of individual flavan-3-ols in green tea infusions were slightly different.</p> <p>For all flavan-3-ols, E_a values at temperatures > 82 °C were 7-11 times larger than E_a values at temperatures < 82 °C.</p> <p><i>Total flavan-3-ols:</i></p> <p>The apparent k of total flavan-3-ols in the ascorbic-added infusion was less than half that in the original infusion due to the role of ascorbic as acidulant, which lowered the pH and inhibited isomerisation.</p> <p>The "turning point temperature" on the Arrhenius plot was also observed in the slightly acidic and original media at 82 °C.</p>	Komatsu <i>et al.</i> , 1993 ^b
Citrate buffer solution (0.1 M)				
EGCG (20 mg.L ⁻¹)	<p>Heating in agitated, constant temperature water baths</p> <p>For each pH and dissolved oxygen concentration, three temperatures (between 30 and 100 °C, $\Delta T = 10\text{ °C}$) were selected</p> <p>Length of heating time = $2 \times D$ value</p> <p>pH: 3, 4, 5 and 6</p> <p>Initial dissolved oxygen concentrations (% oxygen saturation): 0 (0%), 2.50 (33%), 5.01 (66%) and 7.59 mg.L⁻¹ (100%)</p>	<p>First-order kinetic model, with the application of a fractional conversion technique ($[EGCG]_0 = 2\text{ mg.L}^{-1}$); Arrhenius equation</p> <p>Average $E_a = 78.24\text{ kJ.mol}^{-1}$</p>	<p>The non-zero equilibrium concentration ($[EGCG]_{\infty}$) had a significant effect on kinetic data analysis.</p> <p>The k at 80 °C increased log-linearly with respect to both pH and dissolved oxygen concentration.</p> <p>E_a was independent of pH and dissolved oxygen concentration.</p> <p>A mathematical model relating k to temperature, pH and dissolved oxygen concentration was developed and validated.</p> <p>The model indicated that k will increase by 180, 800 and 175% when temperature, pH and dissolved oxygen concentration is increased by 10 °C, 1 unit, and 33% respectively.</p>	Zimeri & Tong, 1999 ^{b,c}

^aAbbreviations for flavan-3-ols: EC = epicatechin; ECG = epicatechin gallate; EGC = epigallocatechin; EGCG = epigallocatechin gallate.

^bValues for the activation energy (E_a) converted from kcal.mol⁻¹ to kJ.mol⁻¹ with a factor 4.184.

^cValues for kinetic data not given in Tabular form, refer to the original study by Zimeri & Tong (1999) for graphical representations.

Table 4 cont.

Flavan-3-ols ^a and matrix	Operating conditions	Mathematical model, kinetic order and kinetic parameters	Major findings	Reference
Purified EGCG powder (PEP) in deionised water (pH 5.1); and green tea extract (GTE) and green tea polyphenols (GTP) in deionised water (pH 3.5-3.7) EGCG and ent-GCG ECG and ent-CG	Microwave conductor	First-order kinetic models; Arrhenius equation	Epimerisation and degradation occurred concurrently at temperatures ≥ 100 °C. 2,3- <i>cis</i> -configured flavan-3-ols (EGCG and ECG) decreased, while the levels of their C-2 epimers (ent-GCG and ent-CG) increased exponentially with time. Levels of the 2,3- <i>trans</i> -configured flavan-3-ols (2 <i>S</i> ,3 <i>R</i>) (ent-GCG, in particular) reached a maximum and then decreased, indicating subsequent degradation. Epimerisation was a reversible reaction, but the epimerisation of flavan-3-ols from the 2,3- <i>cis</i> (2 <i>R</i> ,3 <i>R</i>) to the 2,3- <i>trans</i> (2 <i>S</i> ,3 <i>R</i>) configuration was the predominant reaction at high temperatures. Predominant isomerisation from the 2,3- <i>cis</i> (2 <i>R</i> ,3 <i>R</i>) to the 2,3- <i>trans</i> (2 <i>S</i> ,3 <i>R</i>) configuration was reflected in the higher values of <i>A</i> (ca 10 ¹³). EGCG + ent-GCG was more susceptible to thermal degradation than ECG + ent-CG as shown by higher values of <i>A</i> for the former pair, due to their increased degree of hydroxylation. <i>E_a</i> values for the degradation of paired flavan-3-ols and the isomerisation reactions were independent of the medium environment. <i>k</i> and <i>A</i> for the degradation of paired flavan-3-ols and epimerisation reactions were pH sensitive: values for <i>k</i> and <i>A</i> were much greater in the PEP solution (pH 5.1) than those in the GTE and GTP solutions (pH 3.5-3.7)	Wang <i>et al.</i> , 2006
	Isothermal heat treatments: 100 °C/120 min; 121 °C/60 min; 135 °C/45 min; 165 °C/20 min	<p><i>Total degradation of paired flavan-3-ols</i> EGCG + ent-GCG, PEP: $E_a = 42.78 \text{ kJ}\cdot\text{mol}^{-1}$, $A = 2.56 \times 10^3$ EGCG + ent-GCG, GTE: $E_a = 42.78 \text{ kJ}\cdot\text{mol}^{-1}$, $A = 0.88 \times 10^3$ EGCG + ent-GCG, GTP: $E_a = 42.78 \text{ kJ}\cdot\text{mol}^{-1}$, $A = 0.67 \times 10^3$ ECG + ent-CG, GTE: $E_a = 41.58 \text{ kJ}\cdot\text{mol}^{-1}$, $A = 0.41 \times 10^3$ ECG + ent-CG, GTP: $E_a = 41.58 \text{ kJ}\cdot\text{mol}^{-1}$, $A = 0.31 \times 10^3$</p> <p><i>Epimerisation of 2,3-<i>cis</i>-configured flavan-3-ols to their C-2 epimers</i> EGCG → ent-GCG, PEP: $E_a = 117.59 \text{ kJ}\cdot\text{mol}^{-1}$, $A = 7.29 \times 10^{13}$ EGCG → ent-GCG, GTE: $E_a = 117.59 \text{ kJ}\cdot\text{mol}^{-1}$, $A = 0.85 \times 10^{13}$ EGCG → ent-GCG, GTP: $E_a = 117.59 \text{ kJ}\cdot\text{mol}^{-1}$, $A = 1.42 \times 10^{13}$ ECG → ent-CG, GTE: $E_a = 119.25 \text{ kJ}\cdot\text{mol}^{-1}$, $A = 1.14 \times 10^{13}$ ECG → ent-CG GTP: $E_a = 119.25 \text{ kJ}\cdot\text{mol}^{-1}$, $A = 0.96 \times 10^{13}$</p> <p><i>Epimerisation of 2,3-<i>trans</i>- (2<i>S</i>,3<i>R</i>) to 2,3-<i>cis</i>-configured flavan-3-ols</i> ent-GCG → EGCG, PEP: $E_a = 84.15 \text{ kJ}\cdot\text{mol}^{-1}$, $A = 8.97 \times 10^9$ ent-GCG → EGCG, GTE: $E_a = 84.15 \text{ kJ}\cdot\text{mol}^{-1}$, $A = 0.66 \times 10^9$ ent-GCG → EGCG, GTP: $E_a = 84.15 \text{ kJ}\cdot\text{mol}^{-1}$, $A = 0.93 \times 10^9$ ent-CG → ECG, GTE: $E_a = 96.22 \text{ kJ}\cdot\text{mol}^{-1}$, $A = 28.0 \times 10^9$ ent-CG → ECG, GTP: $E_a = 96.22 \text{ kJ}\cdot\text{mol}^{-1}$, $A = 19.0 \times 10^9$</p>		
Purified EGCG powder (PEP) in deionised water (pH 5.1) EGCG and ent-GCG	Isothermal treatments Storage at ambient conditions: 25 °C/16 days Heating in a water bath: 40 °C/960 min; 60 °C/540 min; 80 °C/360 min; 100 °C/120 min	First-order kinetic models; Arrhenius equation. <i>Total degradation of paired flavan-3-ols</i> EGCG + ent-GCG, PEP: $E_a = 43.09 \text{ kJ}\cdot\text{mol}^{-1}$, $A = 2.70 \times 10^3$ <i>Epimerisation of 2,3-<i>cis</i>-configured flavan-3-ols to their C-2 epimers</i> EGCG → ent-GCG, PEP: $E_a = 105.07 \text{ kJ}\cdot\text{mol}^{-1}$, $A = 1.42 \times 10^{12}$ <i>Epimerisation of 2,3-<i>trans</i>- (2<i>S</i>,3<i>R</i>) to 2,3-<i>cis</i>-configured flavan-3-ols</i> ent-GCG → EGCG, PEP: $E_a = 84.33 \text{ kJ}\cdot\text{mol}^{-1}$, $A = 1.70 \times 10^{10}$	Epimerisation and degradation occurred concurrently at temperatures ≤ 100 °C. The levels of EGCG decreased with increases in temperature and time, while ent-GCG first increased to a maximum and then decreased. Values for <i>E_a</i> and <i>A</i> for the degradation and isomerisation reactions in PEP aqueous solution at low temperatures (25-100 °C) were the same as those obtained at high temperatures (100-165 °C, Wang <i>et al.</i> , 2006), regardless of the heating method. Two specific points (44 and 98 °C) in the reaction kinetics were identified, corresponding to the points of intersection of the Arrhenius curves for the total degradation of EGCG and ent-GCG, for the epimerisation of EGCG to ent-GCG, and for the epimerisation of ent-GCG to EGCG.	Wang <i>et al.</i> 2008a

^aAbbreviations for flavan-3-ols: ECG = epicatechin gallate; EGCG = epigallocatechin gallate; ent-CG = ent-catechin gallate; ent-GCG = ent-gallocatechin gallate

Table 4 cont.

Flavan-3-ols ^a and matrix	Operating conditions	Mathematical model, kinetic order and kinetic parameters	Major findings	Reference
Spray-dried green tea extract powder				
EGCG, EGC, ECG and EC	Storage for up to 16 weeks in temperature-controlled incubators at various RH (41-97% RH) and temperature (25, 35, 40, 50 and 60 °C) conditions.	First-order degradation kinetic model; Arrhenius equation <i>Rate constants for EGCG in green tea powders</i> 43% RH: $k_{40\text{ °C}} = 0.0577 \times 10^2 \text{ day}^{-1}$, $k_{50\text{ °C}} = 0.077 \times 10^2 \text{ day}^{-1}$, $k_{60\text{ °C}} = 0.500 \times 10^2 \text{ day}^{-1}$; $E_a = 92.86 \text{ kJ.mol}^{-1}$ 49-58% RH: $k_{35\text{ °C}} = 0.0530 \times 10^2 \text{ day}^{-1}$, $k_{40\text{ °C}} = 0.158 \times 10^2 \text{ day}^{-1}$, $k_{50\text{ °C}} = 0.236 \times 10^2 \text{ day}^{-1}$, $k_{60\text{ °C}} = 0.758 \times 10^2 \text{ day}^{-1}$ 75% RH: $k_{25\text{ °C}} = 0.0628 \times 10^2 \text{ day}^{-1}$, $k_{35\text{ °C}} = 0.164 \times 10^2 \text{ day}^{-1}$, $k_{40\text{ °C}} = 0.357 \times 10^2 \text{ day}^{-1}$, $k_{50\text{ °C}} = 1.144 \times 10^2 \text{ day}^{-1}$, $k_{60\text{ °C}} = 3.543 \times 10^2 \text{ day}^{-1}$; $E_a = 97.16 \text{ kJ.mol}^{-1}$ 80% RH: $k_{25\text{ °C}} = 0.0754 \times 10^2 \text{ day}^{-1}$, $k_{35\text{ °C}} = 0.289 \times 10^2 \text{ day}^{-1}$, $k_{40\text{ °C}} = 0.448 \times 10^2 \text{ day}^{-1}$, $k_{50\text{ °C}} = 1.634 \times 10^2 \text{ day}^{-1}$, $k_{60\text{ °C}} = 3.957 \times 10^2 \text{ day}^{-1}$; $E_a = 94.05 \text{ kJ.mol}^{-1}$ 97% RH: $k_{25\text{ °C}} = 0.321 \times 10^2 \text{ day}^{-1}$, $k_{35\text{ °C}} = 1.461 \times 10^2 \text{ day}^{-1}$, $k_{40\text{ °C}} = 2.221 \times 10^2 \text{ day}^{-1}$, $k_{50\text{ °C}} = 5.581 \times 10^2 \text{ day}^{-1}$, $k_{60\text{ °C}} = 9.604 \times 10^2 \text{ day}^{-1}$; $E_a = 79.27 \text{ kJ.mol}^{-1}$	Flavan-3-ol degradation kinetics were affected by temperature and RH, with temperature as the dominant factor. A log-linear increase in k with increasing RH was observed at all temperatures. The k of flavan-3-ol degradation also followed the Williams-Landel-Ferry relationship. Upon storage (60 °C/97% RH), the <i>trans</i> -configured flavan-3-ols (ent-CG, ent-GCG) first increased, and then decreased.	Li <i>et al.</i> , 2011
Green tea concentrated solutions (1666.7 mg green tea powder.mL⁻¹ water)				
EGCG	Storage up to 35 days in sealed glass vials at 25, 40, 60, 100 and 120 °C. pH adjusted to 1.5, 2, 3, 4, 5.2, 6 and 7 using NaOH-HCL solutions.	First-order degradation kinetic model; Arrhenius equation <i>Kinetic parameters for EGCG in green tea concentrated solution (1666.7 mg.mL⁻¹) at different pH and temperature conditions:</i> pH 1.5: $k_{25\text{ °C}} = 0.290 \times 10^5 \text{ min}^{-1}$, $k_{40\text{ °C}} = 3.361 \times 10^5 \text{ min}^{-1}$, $k_{60\text{ °C}} = 16.00 \times 10^5 \text{ min}^{-1}$, $k_{100\text{ °C}} = 1566 \times 10^5 \text{ min}^{-1}$, $k_{120\text{ °C}} = 6660 \times 10^5 \text{ min}^{-1}$; $E_a = 102.54 \text{ kJ.mol}^{-1}$, $\ln A = 28.70$. pH 2: $k_{25\text{ °C}} = 0.241 \times 10^5 \text{ min}^{-1}$, $k_{40\text{ °C}} = 1.450 \times 10^5 \text{ min}^{-1}$, $k_{60\text{ °C}} = 10.12 \times 10^5 \text{ min}^{-1}$, $k_{100\text{ °C}} = 669.0 \times 10^5 \text{ min}^{-1}$, $k_{120\text{ °C}} = 5482 \times 10^5 \text{ min}^{-1}$; $E_a = 102.23 \text{ kJ.mol}^{-1}$, $\ln A = 28.09$. pH 3: $k_{25\text{ °C}} = 0.132 \times 10^5 \text{ min}^{-1}$, $k_{40\text{ °C}} = 1.109 \times 10^5 \text{ min}^{-1}$, $k_{60\text{ °C}} = 6.646 \times 10^5 \text{ min}^{-1}$, $k_{100\text{ °C}} = 613.0 \times 10^5 \text{ min}^{-1}$, $k_{120\text{ °C}} = 2595 \times 10^5 \text{ min}^{-1}$; $E_a = 102.11 \text{ kJ.mol}^{-1}$, $\ln A = 27.62$. pH 4: $k_{25\text{ °C}} = 0.098 \times 10^5 \text{ min}^{-1}$, $k_{40\text{ °C}} = 0.553 \times 10^5 \text{ min}^{-1}$, $k_{60\text{ °C}} = 4.479 \times 10^5 \text{ min}^{-1}$, $k_{100\text{ °C}} = 250.0 \times 10^5 \text{ min}^{-1}$, $k_{120\text{ °C}} = 1538 \times 10^5 \text{ min}^{-1}$; $E_a = 99.36 \text{ kJ.mol}^{-1}$, $\ln A = 26.08$. pH 5.2: $k_{25\text{ °C}} = 0.222 \times 10^5 \text{ min}^{-1}$, $k_{40\text{ °C}} = 0.879 \times 10^5 \text{ min}^{-1}$, $k_{60\text{ °C}} = 5.586 \times 10^5 \text{ min}^{-1}$, $k_{100\text{ °C}} = 347.4 \times 10^5 \text{ min}^{-1}$, $k_{120\text{ °C}} = 1278 \times 10^5 \text{ min}^{-1}$; $E_a = 95.32 \text{ kJ.mol}^{-1}$, $\ln A = 24.90$. pH 6: $k_{25\text{ °C}} = 0.193 \times 10^5 \text{ min}^{-1}$, $k_{40\text{ °C}} = 1.939 \times 10^5 \text{ min}^{-1}$, $k_{60\text{ °C}} = 0.979 \times 10^5 \text{ min}^{-1}$, $k_{100\text{ °C}} = 441.0 \times 10^5 \text{ min}^{-1}$, $k_{120\text{ °C}} = 1794 \times 10^5 \text{ min}^{-1}$; $E_a = 90.88 \text{ kJ.mol}^{-1}$, $\ln A = 23.72$. pH 7: $k_{25\text{ °C}} = 0.629 \times 10^5 \text{ min}^{-1}$, $k_{40\text{ °C}} = 5.146 \times 10^5 \text{ min}^{-1}$, $k_{60\text{ °C}} = 11.03 \times 10^5 \text{ min}^{-1}$, $k_{100\text{ °C}} = 649.0 \times 10^5 \text{ min}^{-1}$, $k_{120\text{ °C}} = 3542 \times 10^5 \text{ min}^{-1}$; $E_a = 85.68 \text{ kJ.mol}^{-1}$, $\ln A = 22.55$.	<i>Trans</i> -configured flavan-3-ols (ent-GCG and ent-CG) were produced as isomerisation products, and were also consumed as reactants in degradation reactions. The production of <i>trans</i> -configured flavan-3-ols increased with increasing pH levels, suggesting that isomerisation is more favoured with increases in pH. The loss of flavan-3-ols was dependent on the pH. <i>Cis</i> -configured flavan-3-ols were most stable at pH levels from 4 to 5.2; k increased as the pH was increased above pH 5.2, and also as the pH was decreased below 4. The extent of physical instability and chemical degradation pathways of flavan-3-ols were altered due to elevated pH levels, and this was reflected in the Arrhenius parameters: both E_a and A reached their maximum values at a pH level of 1.5.	Li <i>et al.</i> , 2012
Aqueous model solution Catechin (unspecified) (100 mg.L ⁻¹ distilled water)	Batch-type reactor Sub-critical water at 100, 150, 200 and 250 °C Treatment times: 30, 60, 90 and 120 min.	First-order degradation kinetic model $k_{100\text{ °C}} = 11.7 \times 10^3 \text{ min}^{-1}$ $k_{150\text{ °C}} = 20.6 \times 10^3 \text{ min}^{-1}$	An increase in temperature increased the k of catechin under sub-critical water conditions; no kinetic data could be derived at 200 or 250 °C. Catechin was completely degraded within 30 min at 250 °C.	Khuwijitjaru <i>et al.</i> , 2014a

^aAbbreviations for flavan-3-ols: EC = epicatechin; ECG = epicatechin gallate; EGC = epigallocatechin; EGCG = epigallocatechin gallate; ent-CG = ent-catechin gallate; ent-GCG = ent-gallocatechin gallate.

Table 5 Thermal stability of green tea extract/green tea flavan-3-ols when used as functional ingredient in bread and dairy beverages.

Flavan-3-ols ^a and matrix	Operating conditions	Mathematical model, kinetic order and kinetic parameters	Major findings	Reference
Fortified bread^b (pH 5.5)				
EGCG and ent-GCG	Bread baked with designated oven temperatures: 200 °C (15 min), 215 °C (20 min), 240 °C (20 min).	First-order kinetic models; Arrhenius equation. <i>Total degradation of paired flavan-3-ols</i> EGCG + ent-GCG, crumb: $E_a = 43.1 \text{ kJ.mol}^{-1}$, $A = 4.95 \times 10^3$ EGCG + ent-GCG, crust: $E_a = 43.1 \text{ kJ.mol}^{-1}$, $A = 2.48 \times 10^3$ <i>Epimerisation of 2,3-cis-configured flavan-3-ols to their C-2 epimers</i> EGCG → ent-GCG, crumb: $E_a = 105.1 \text{ kJ.mol}^{-1}$, $A = 2.33 \times 10^{12}$ EGCG → ent-GCG, crust: $E_a = 105.1 \text{ kJ.mol}^{-1}$, $A = 3.10 \times 10^9$ <i>Epimerisation of 2,3-trans- (2S,3R) to 2,3-cis-configured flavan-3-ols</i> ent-GCG → EGCG, crumb: $E_a = 84.3 \text{ kJ.mol}^{-1}$, $A = 1.21 \times 10^{11}$ ent-GCG → EGCG, crust: $E_a = 84.3 \text{ kJ.mol}^{-1}$, $A = 3.16 \times 10^6$	EGCG simultaneously underwent thermal degradation and epimerisation. E_a values for the thermal degradation and epimerisation reactions were independent of the medium environment; differences in the reaction kinetics between the crumb and crust are reflected in A . Values for A for the degradation of paired flavan-3-ols and individual epimerisation reactions in the crust were lower than in the crumb. Values for A for the degradation of paired flavan-3-ols and the individual epimerisation reactions in the crumb were greater than the values in the aqueous system (Wang <i>et al.</i> , 2008a) In both the crumb and the crust, the values of A for the epimerisation of EGCG to ent-GCG were much greater than those from ent-GCG to EGCG.	Wang <i>et al.</i> 2008b
Model dairy beverages				
EC, EGC, ECG and EGCG	Single strength milk (SSM, 36.2 mg protein.L ⁻¹), quarter strength milk (QSM, 9.0 mg protein.L ⁻¹) and control model beverages (buffer solution, pH 6.30), incubated with isolated EGCG and green tea extract (GTE) at different concentrations, and heated in a water bath at 37 °C and 62 °C for 180 min.	First-order degradation kinetic model <i>Isolated EGCG at 37 °C:</i> SSM: $k_{100 \mu\text{M EGCG}} = 5.83 \times 10^{-4} \text{ min}^{-1}$; $k_{10 \mu\text{M EGCG}} = 5.66 \times 10^{-4} \text{ min}^{-1}$; $k_{1 \mu\text{M EGCG}} = 5.34 \times 10^{-4} \text{ min}^{-1}$; $k_{0.1 \mu\text{M EGCG}} = 5.31 \times 10^{-4} \text{ min}^{-1}$; QSM: $k_{100 \mu\text{M EGCG}} = 4.05 \times 10^{-3} \text{ min}^{-1}$; $k_{10 \mu\text{M EGCG}} = 3.83 \times 10^{-3} \text{ min}^{-1}$; $k_{1 \mu\text{M EGCG}} = 3.25 \times 10^{-3} \text{ min}^{-1}$; $k_{0.1 \mu\text{M EGCG}} = 3.32 \times 10^{-3} \text{ min}^{-1}$; Control: $k_{100 \mu\text{M EGCG}} = 4.58 \times 10^{-3} \text{ min}^{-1}$; $k_{10 \mu\text{M EGCG}} = 4.62 \times 10^{-3} \text{ min}^{-1}$; $k_{1 \mu\text{M EGCG}} = 4.86 \times 10^{-3} \text{ min}^{-1}$; $k_{0.1 \mu\text{M EGCG}} = 5.29 \times 10^{-3} \text{ min}^{-1}$. <i>Isolated EGCG at 62 °C:</i> SSM: $k_{100 \mu\text{M EGCG}} = 2.83 \times 10^{-3} \text{ min}^{-1}$; $k_{10 \mu\text{M EGCG}} = 2.26 \times 10^{-3} \text{ min}^{-1}$; $k_{1 \mu\text{M EGCG}} = 1.31 \times 10^{-3} \text{ min}^{-1}$; $k_{0.1 \mu\text{M EGCG}} = 1.32 \times 10^{-3} \text{ min}^{-1}$; QSM: $k_{100 \mu\text{M EGCG}} = 4.15 \times 10^{-3} \text{ min}^{-1}$; $k_{10 \mu\text{M EGCG}} = 4.50 \times 10^{-3} \text{ min}^{-1}$; $k_{1 \mu\text{M EGCG}} = 3.26 \times 10^{-3} \text{ min}^{-1}$; $k_{0.1 \mu\text{M EGCG}} = 3.24 \times 10^{-3} \text{ min}^{-1}$; Control: $k_{100 \mu\text{M EGCG}} = 8.67 \times 10^{-4} \text{ min}^{-1}$; $k_{10 \mu\text{M EGCG}} = 8.45 \times 10^{-4} \text{ min}^{-1}$; $k_{1 \mu\text{M EGCG}} = 8.96 \times 10^{-4} \text{ min}^{-1}$; $k_{0.1 \mu\text{M EGCG}} = 9.62 \times 10^{-4} \text{ min}^{-1}$. <i>EGCG in green tea extract at 37 °C:</i> SSM: $k_{120.1 \mu\text{M EGCG}} = 6.88 \times 10^{-3} \text{ min}^{-1}$; $k_{24.0 \mu\text{M EGCG}} = 6.43 \times 10^{-3} \text{ min}^{-1}$; $k_{120.1 \text{ nM EGCG}} = 4.07 \times 10^{-3} \text{ min}^{-1}$; $k_{24.0 \text{ nM EGCG}} = 4.11 \times 10^{-3} \text{ min}^{-1}$; QSM: $k_{120.1 \mu\text{M EGCG}} = 7.93 \times 10^{-3} \text{ min}^{-1}$; $k_{24.0 \mu\text{M EGCG}} = 7.87 \times 10^{-3} \text{ min}^{-1}$; $k_{120.1 \text{ nM EGCG}} = 6.16 \times 10^{-3} \text{ min}^{-1}$; $k_{24.0 \text{ nM EGCG}} = 6.38 \times 10^{-3} \text{ min}^{-1}$; Control: $k_{120.1 \mu\text{M EGCG}} = 8.28 \times 10^{-3} \text{ min}^{-1}$; $k_{24.0 \mu\text{M EGCG}} = 8.25 \times 10^{-3} \text{ min}^{-1}$; $k_{120.1 \text{ nM EGCG}} = 1.24 \times 10^{-2} \text{ min}^{-1}$; $k_{24.0 \text{ nM EGCG}} = 1.19 \times 10^{-2} \text{ min}^{-1}$. <i>EGCG in green tea extract at 62 °C:</i> SSM: $k_{120.1 \mu\text{M EGCG}} = 2.91 \times 10^{-3} \text{ min}^{-1}$; $k_{24.0 \mu\text{M EGCG}} = 2.61 \times 10^{-3} \text{ min}^{-1}$; $k_{120.1 \text{ nM EGCG}} = 1.92 \times 10^{-3} \text{ min}^{-1}$; $k_{24.0 \text{ nM EGCG}} = 1.95 \times 10^{-3} \text{ min}^{-1}$; QSM: $k_{120.1 \mu\text{M EGCG}} = 6.59 \times 10^{-3} \text{ min}^{-1}$; $k_{24.0 \mu\text{M EGCG}} = 6.24 \times 10^{-3} \text{ min}^{-1}$; $k_{120.1 \text{ nM EGCG}} = 4.11 \times 10^{-3} \text{ min}^{-1}$; $k_{24.0 \text{ nM EGCG}} = 4.45 \times 10^{-3} \text{ min}^{-1}$; Control: $k_{120.1 \mu\text{M EGCG}} = 2.60 \times 10^{-2} \text{ min}^{-1}$; $k_{24.0 \mu\text{M EGCG}} = 2.91 \times 10^{-2} \text{ min}^{-1}$; $k_{120.1 \text{ nM EGCG}} = 4.04 \times 10^{-2} \text{ min}^{-1}$; $k_{24.0 \text{ nM EGCG}} = 3.88 \times 10^{-2} \text{ min}^{-1}$.	Differences in the k of EGCG in model dairy beverages were related to the binding of polyphenols to proline rich proteins. Generally, higher polyphenol-to-protein ratios increased the EGCG degradation, due to a smaller probability that a free EGCG molecule will interact with an available binding site on a protein. Higher polyphenol-to-protein ratios also decreased the formation of oxidation products. Theasinensin A/D, C/E and B and P-2 dimers were detected; EC or ECG homo- or heterodimers were not detected. Significant differences for the degradation of isolated EGCG and EGCG from GTE across model dairy beverages were similar. The presence of the galloyl and hydroxy moieties increased the binding of flavan-3-ols to proteins, thereby stabilising them with increasing protein concentration. The presence of the galloyl moiety at C-3 influenced polyphenol-protein interactions to a greater extent than the presence of the hydroxy group on the B-ring. The increase in k of all flavan-3-ols with increasing temperature was not only caused by typical Arrhenius behaviour of the flavan-3-ols, but likely also by the weakening of non-covalent interactions between milk proteins and flavan-3-ols at elevated temperature. The degradation of flavan-3-ols will therefore not accurately fit the Arrhenius model.	Song <i>et al.</i> , 2015 ^c

^aAbbreviations for flavan-3-ols: EC = epicatechin; ECG = epicatechin gallate; EGC = epigallocatechin; EGCG = epigallocatechin gallate; ent-GCG = ent-gallocatechin gallate.

^bBread fortified with purified EGCG powder (PEP). 500 mg PEP (comprising of 89.2% EGCG and 0.017% of ent-GCG) per 100 g flour.

^cOnly selected data are presented in Table 5, for the complete experimental data set (first-order degradation rate constants of epicatechin, epigallocatechin, and epicatechin gallate in different concentrations of green tea extract and different dairy beverages at 62 °C) refer to the original study by Song *et al.* (2015).

However, Zimeri & Tong (1999) questioned the validity of these values, as Komatsu and co-workers (1993) failed to consider the non-zero equilibrium concentration in their kinetic data analysis. They subsequently developed a first-order kinetic model that predicted the loss of EGCG in a liquid model system during thermal treatment (temperatures < 100 °C) with the application of a fractional conversion technique^c. These authors obtained an average activation energy for the thermal degradation of EGCG of 78.24 kJ.mol⁻¹ (Table 4).

Unfortunately the study by Zimeri & Tong (1999) did not consider the epimerisation of EGCG to its C2-epimer ent-GCG, and vice versa. Wang and co-workers subsequently overcame these limitations and developed mathematical models, which accounted for the simultaneous degradation and epimerisation of green tea flavan-3-ols in aqueous systems during thermal treatment (Wang *et al.*, 2006, 2008a; Table 4), and in fortified bread during the baking process (Wang *et al.*, 2008b; Table 5). This group showed that the activation energies for the degradation of paired flavan-3-ols [EGCG + ent-GCG, and ECG + ent-CG] and isomerisation reactions are independent of the reaction medium, and that the impact of the medium is reflected in the frequency factor of the Arrhenius equation (Wang *et al.*, 2006; Wang *et al.*, 2008b).

They furthermore demonstrated that both the activation energy and frequency factor for the total degradation of EGCG and its C-2 epimer, as well as the corresponding values for the epimerisation reactions, in the same solution remain unchanged over a wide temperature range, regardless of the heating method. This can be seen by comparison of the kinetic data generated in a purified EGCG powder (PEP) solution during high temperature processing using a microwave conductor (100-165 °C; Wang *et al.*, 2006), and heating at low temperatures using conventional techniques (25-100 °C; Wang *et al.*, 2008a) (Table 4). In accordance with previous findings, Wang *et al.* (2006) demonstrated that the flavan-3-ol pair, EGCC + ent-GCG was more prone to thermal degradation than ECG + ent-CG, due to an increase in the degree of B-ring hydroxylation. While the activation energy for the thermal degradation of these flavan-3-ol pairs were approximately similar, the value of the frequency factor (A) for EGCG + ent-GCG was *ca.* twice that of ECG + ent-CG (Table 4).

Wang *et al.* (2008a) conducted a study to re-examine the “turning point temperature” of 82 °C in the reaction kinetics of brewing tea as proposed by Komatsu *et al.* in 1993. Two specific temperature points were identified, at 44 and 98 °C, respectively. These points were visualised as the points of intersection of the Arrhenius curves for the reactions of EGCG and ent-GCG in PEP solution. At temperatures below 44 °C, the total degradation reaction dominated the two epimerisation reactions, whereas at temperatures above 98 °C, the epimerisation reactions dominated. At temperatures between 44 and 98 °C, the epimerisation from 2,3-*trans*-configured flavan-3-ols (2*S*,3*R*; ent-GCG) to 2,3-*cis*-configured flavan-3-ols (2*R*,3*R*; EGCG) occurred the fastest, followed by the total degradation of the flavan-3-ol pair, and the epimerisation from 2,3-*cis*- to 2,3-*trans*-configured flavan-3-ols.

^cFor an irreversible first-order reaction, with a non-zero equilibrium concentration, concentration is related to time as follows:

$$\ln \left[\frac{(C - C_{\infty})}{(C_0 - C_{\infty})} \right] = -kt \quad (7)$$

Where C_{∞} is the equilibrium concentration of the reactant after prolonged heating.

Since:

$$\frac{(C - C_{\infty})}{(C_0 - C_{\infty})} = 1 - f \quad (8)$$

where f is the fractional conversion or extent of the reaction, eq. 8 can further be simplified as:

$$\ln(1 - f) = -kt \quad (9)$$

Wang *et al.* (2008b) successfully established mathematical models for the stability of EGCG during the bread baking process, which not only accounted for simultaneous degradation and epimerisation reactions, but also for varying moisture content and temperature profiles in the crumb and crust. The frequency factors for the degradation of total flavan-3-ols and the individual epimerisation reactions in the crumb were greater than the previously calculated values in the aqueous system (Wang *et al.* 2008a). This was ascribed to a higher pH and the natural presence of metal ions in the former matrix. The frequency factors for the degradation of total flavan-3-ols and individual epimerisation reactions in the crust were lower than the corresponding values in the crumb. This could be due to much lower moisture content in the crust that confined the collision of molecules associated with degradations.

The first study on the reaction kinetics of green tea flavan-3-ols in the solid state was conducted by Li *et al.* (2011), where the effect of various relative humidity (43-97% RH) and temperature (25-60 °C) conditions on the degradation kinetics of individual 2,3-*cis*-configured flavan-3-ols (EGCG, EGC, EC and ECG) during storage of spray-dried green tea extract was investigated. Their degradation followed first-order reaction kinetics under all experimental conditions, with temperature exerting the largest effect on flavan-3-ol loss (Table 4).

Li *et al.* (2012) kinetically assessed the degradation behaviour of individual 2,3-*cis*-configured flavan-3-ols in concentrated solutions of green tea as a function of pH, temperature and concentration. Their results demonstrated that the kinetic models developed for these concentrated solutions (1666.7 mg.mL⁻¹) and green tea powder systems (Li *et al.*, 2011) could possibly be interchangeable. This can be seen by comparable rate constants and activation energies for the degradation of EGCG at 25 °C in these systems (Table 4).

Most recently, Song *et al.* (2015) investigated the thermal degradation of green tea flavan-3-ols in model dairy beverages at 37 and 62 °C (Table 5). Single strength (36.2 g protein.L⁻¹), quarter strength (9.0 g protein.L⁻¹) and control model beverages were incubated with different concentrations of isolated EGCG (0.1-100 µM) and green tea extract (0.1-500 mg.L⁻¹). Generally, higher polyphenol-to-protein ratios increased flavan-3-ol degradation, attributed to a smaller probability that a free flavan-3-ol molecule will interact with an available binding site on a protein. The presence of the galloyl and hydroxyl moieties increased the binding of flavan-3-ols to proteins, thus stabilising them with increasing protein concentration. The presence of the galloyl moiety at C-3 influenced polyphenol-to-protein interactions to a greater extent than the presence of the (additional) hydroxyl group on the B-ring (Song *et al.*, 2015).

While the thermal stability of monomeric flavan-3-ols is principally determined by their chemical structure, other factors, showing interplay, may also impact on their stability. This includes the physical state (crystalline vs amorphous; solid vs liquid state), the percentage relative humidity (% RH, for solid state samples), the concentration of dissolved oxygen, and the concentration of the green tea catechin/extract. Crystalline EGCG is more stable than the amorphous form, and is also more stable in the powders than when in solution (Li *et al.*, 2013). The lowered reaction rate in the solid state has been ascribed to the limited molecular mobility and diffusion rate, as well as an increased concentration in the solid state as compared with the dilute solution systems (Li *et al.*, 2013). For amorphous powders stored at 85% RH, crystallisation occurs rapidly, resulting in a higher stability of EGCG at 85% RH compared to that at 0% RH (where the powder remained amorphous) (Li *et al.*, 2013). However, an increase in the % RH has generally been associated with increased degradation of individual 2,3-*cis*-configured flavan-3-ols: Li *et al.* (2011) reported a log-linear increase in the first-order degradation constants of EGCG with increasing % RH during storage of spray-dried green tea extract (25-60 °C; Table 4). The first-order degradation rate constant of EGCG in aqueous model solutions has also been shown to increase log-linearly with respect to dissolved oxygen concentration (Zimeri & Tong, 1999; Table 4). This is in accordance with results showing that, under low O₂ partial pressure, EGCG was greatly stabilised during incubation in phosphate buffer solution (pH 7.4) at 37 °C (Sang *et al.*, 2005).

Numerous studies have reported increased stability of pure EGCG and EGCG in green tea extract at increased concentrations (Sang *et al.*, 2005; Li *et al.*, 2012; Li *et al.*, 2013). The increase in the reaction rates as more water is present in the system has been ascribed to increased levels in dissolved oxygen, increased pH and increased molecular mobility. It has also been suggested that the concentration dependence of flavan-3-ol degradation might suggest different reaction kinetics consisting of multiple degradation pathways. This is supported by the fact that the concentration of EGCG determines the predominant reaction responsible for the thermal degradation of EGCG in solution (epimerisation vs cleavage reactions) (Li *et al.*, 2013). Also, the activation energy for EGCG degradation in a 1 mg.mL⁻¹ green tea solution (57.34 kJ.mol⁻¹) was significantly lower than that in the green tea extract concentrate (1666.7 mg.mL⁻¹; 98.52 kJ.mol⁻¹) (Li *et al.*, 2012). Consequently, a crossing point in the Arrhenius curves was observed at approximately 120 °C. Extrapolations to temperatures higher than 120 °C suggest that reactions would probably proceed faster in concentrated green tea solutions than in dilute solutions at these elevated temperatures. The lowered E_a in dilute green tea solutions was ascribed to (potentially) altered reaction mechanisms in systems with differences in water content, or to increased diffusion rates due to the presence of bulk water. This finding is not in agreement with a previous study that revealed that the activation energies for thermal degradation and epimerisation of green tea flavan-3-ols in aqueous systems remained unchanged with varied concentrations of EGCG and ECG (Wang *et al.*, 2006).

In addition to the aforementioned factors, pH quite possibly represents the most crucial factor affecting the stability of green tea flavan-3-ols. Kinetic studies have shown that the thermal degradation and epimerisation of flavan-3-ols depend upon the pH of the solvent system, and that the first-order rate constants typically increase with an increase in pH (Komatsu *et al.*, 1993; Zimeri & Tong, 1999; Wang *et al.*, 2006; Li *et al.*, 2012). Zimeri & Tong (1999) reported that the rate constant increased log-linearly with respect to pH (pH 4-7). This is in accordance with other studies on the thermal stability of tea flavan-3-ols, indicating increased epimerisation (Seto *et al.*, 1997; Chen *et al.*, 2001) and increased degradation (Zhu *et al.*, 1997; Chen *et al.*, 2001; Su *et al.*, 2003) at higher pH values. Within the same ionic environment, catechins are less stable at higher pH values (pH 7.1 vs 5.9) (Wang & Helliwell, 2000).

While it is generally accepted that green tea flavan-3-ols are stable in acidic pH environments (pH < 5; Komatsu *et al.*, 1993; Su *et al.*, 2003), extremely low pH conditions might also enhance flavan-3-ol loss in solution. Results presented by Li *et al.* (2012) demonstrated that the lowest rate constants for degradation of EGCG in green tea concentrates were at pH ~ 4, and this was taken as the approximate minimum for pH dependency. As expected, degradation was accelerated as the pH was raised above 5.2, but flavan-3-ol loss also occurred faster at pH levels below 4 (Li *et al.*, 2012). Tu *et al.* (2005) also reported that most flavan-3-ols were much less stable at pH 2.6 than at pH 3.6-5.6 during incubation of citric acid buffer solutions at 25 °C/18 h.

Although studies by numerous researchers showed that the activation energy for the thermal degradation of tea flavan-3-ols is independent of pH (Komatsu *et al.*, 1993; Zimeri & Tong, 1999; Wang *et al.*, 2006), Li *et al.* (2012) demonstrated that the extent of physical instability and chemical degradation pathways of flavan-3-ols were altered due to elevated pH levels, and this was reflected in the Arrhenius parameter: both the activation energy and the frequency factor reached their maximum values at a pH level of 1.5, with minima at pH 7 (Table 4). The higher values for E_a at lower pH levels indicate that the degradation rate of flavan-3-ols is more sensitive to temperature changes under acidic conditions.

3.2.2. Thermal Stability of Monomeric Flavan-3-ols in Apple Juice, Grape Seed Extract and Cocoa

Kinetic data for the thermal degradation of catechin and/or epicatechin in apple juice, commercial grape seed extract and cocoa beans are summarised in Table 6. Van der Sluis *et al.* (2005) showed that the degradation of epicatechin (unspecified) during the accelerated storage (80 °C/4 days) of apple juice follows a first-order kinetic model. In contrast to previous findings on the effect of dissolved oxygen on flavan-3-ol stability (Zimeri & Tong, 1999; Table 4), the non-oxidative degradation of epicatechin in apple juice was slightly higher than the oxidative degradation at 100% oxygen (Table 6).

Investigation of the kinetics of thermal modifications in a commercial grape seed extract, under conditions simulating those commonly used in the food industry, showed that the levels of catechin (2,3-*trans*-configured; 2*R*,3*S*) and epicatechin decreased, while those of gallic acid, and procyanidins B1 and B2 (Figure 10), increased (Davidov-Pardo *et al.*, 2011; Table 6). They postulated that the main source of gallic acid units was from the excision of the gallate group attached to the C-ring of flavonoids [*e.g.* catechin gallate and epicatechin gallate] as observed for green tea flavan-3-ols (Lee *et al.*, 2010; Li *et al.*, 2013). Nevertheless, Davidov-Pardo *et al.* (2011) stated that grape seed extracts only contain a small amount of gallotannins so that these compounds present a much smaller source of gallic acid.

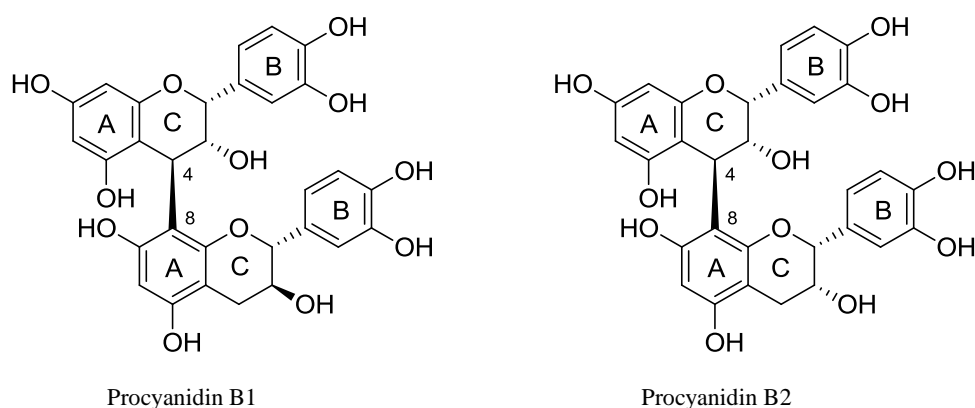


Figure 10 Structures of the B-type proanthocyanidins, procyanidins B1 and B2, linked through a C-4–C-8 bond in the A- and C-rings of the catechin (2,3-*trans*-configured; 2*R*,3*S*) and epicatechin (2,3-*cis*-configured; 2*R*,3*R*) units.

The degradation of flavan-3-ol monomers and the formation of products during thermal processing of grape seed extract were accurately modelled using the Weibull equation^d that takes a C_m value (maximum or minimum concentration) and shape constant, β , into account. The Arrhenius activation energies for the degradation of catechin and epicatechin, and the formation of gallic acid, procyanidin B1 and procyanidin B2 were calculated as 286, 42, 102, 249 and 95 $\text{kJ}\cdot\text{mol}^{-1}$, respectively (Table 6). The lower activation energy for the thermal degradation of epicatechin compared to catechin was ascribed to the lower stability of epicatechin in the 2,3-*cis* configuration as opposed to catechin in the 2,3-*trans* configuration. This fact was also partially responsible for the lower energy needed for the formation of procyanidin B2 (comprising of two epicatechin units) compared to procyanidin B1 (comprising of one epicatechin and one catechin unit) (Figure 10).

^dWeibull model (Davidov-Pardo *et al.*, 2011):

$$C = C_m + (C_0 - C_m) \exp[-(kt)^\beta] \quad (10)$$

Where C , C_m and C_0 is the concentration at time t , the minimum or maximum concentration, and the initial concentration, respectively; k is the reaction rate constant, t is time and β is the shape constant in the Weibull model.

Table 6 Thermal degradation kinetics modeling of monomeric flavan-3-ols in apple juice, commercial grape seed extract, and cocoa beans.

Flavan-3-ols and matrix	Operating conditions	Mathematical model, kinetic order and kinetic parameters	Major findings	Reference
Apple Juice (pH 3.6/3.7)				
Epicatechin (unspecified)	Accelerated storage conditions: 70-100 °C, 4 days Effect of oxygen concentration: 0, 21 and 100%	First-order kinetic model; Arrhenius equation Reaction rate constants for the non-oxidative (k_a) and oxidative (k_o) degradation of epicatechin at 80 °C: $k_a = 31.2 \times 10^{-3} \text{ h}^{-1}$; $k_o = 11.3 \times 10^{-3} \text{ h}^{-1}$ The formation rate constant (k_f) of epicatechin at 80 °C: $k_f = 8.7 \times 10^{-4} \text{ h}^{-1}$	EC was amongst the most thermally sensitive compounds in apple juice. EC decreased by 80% after 50-100 h (depending on the oxygen pressure), whereafter it remained stable. The seemingly stable levels of EC are a quasi-steady state as a consequence of a formation and degradation reactions. It was postulated that EC was formed from the hydrolysis of procyanidins, inherently present in apples. The k for non-oxidative degradation of EC was slightly higher than that for oxidative degradation at 100% oxygen.	Van der Sluis <i>et al.</i> , 2005
Commercial Grape Seed Extract (GSE, pH 4.22)				
GSE dissolved in an aqueous alcoholic solution (4%, v.v ⁻¹) at a concentration of 2.5 g.L ⁻¹ . Degradation of C and EC. Formation of gallic acid, procyanidin B1 and procyanidin B2.	GSE solution placed in hermetically closed glass bottles and subjected to heat treatments (60, 90 and 120 °C/60 min) using a water bath pressure autoclave.	Weibull model; Arrhenius equation. Degradation of C: $E_a = 286 \text{ kJ.mol}^{-1}$ Degradation of EC: $E_a = 42 \text{ kJ.mol}^{-1}$ Formation of gallic acid: $E_a = 102 \text{ kJ.mol}^{-1}$ Formation of procyanidin B1: $E_a = 249 \text{ kJ.mol}^{-1}$ Formation of procyanidin B2: $E_a = 95 \text{ kJ.mol}^{-1}$	The levels of C and EC decreased, while those of gallic acid, and procyanidins B1 and B2 increased. The Weibull model more accurately described the quantitative changes than a combined zero- and first-order model, especially when the k values were fitted to the Arrhenius equation. The model was validated by independent experiments (70, 95 and 110 °C, for 10, 25, 40 and 55 min).	Davidov-Pardo <i>et al.</i> , 2011
Cocoa (<i>Theobroma cacao</i> L.) beans				
Epicatechin to catechin ratio (EC/C ratio)	Roasting process (isothermal) conducted in a ventilated electric oven at constant air-flow rate (1 m.s ⁻¹) and relative humidity (0.4%). Fermented and dried cocoa beans (35 g) were roasted at 125 °C/74 min, 135 °C/35 min and 145 °C/40 min until they reached a residual moisture content of ca. 1.8 g.100 g ⁻¹ . Portions of roasted cocoa were taken from the oven at predetermined time limits.	Weibull model; Arrhenius equation. <i>EC/C ratio</i> 125 °C: $\alpha = 21.9$; $\beta = 27.2 \text{ min}$; $C_E = 0.47 \text{ mg.mg}^{-1}$ 135 °C: $\alpha = 1.03$; $\beta = 4.22 \text{ min}$; $C_E = 0.45 \text{ mg.mg}^{-1}$ 145 °C: $\alpha = 0.68$; $\beta = 1.13 \text{ min}$; $C_E = 0.40 \text{ mg.mg}^{-1}$ Pre-exponential factor, $K_0 = 6.93 \times 10^{16} \text{ min}^{-1}$ Activation energy, $E_a = 133 \text{ kJ.mol}^{-1}$	Decrease in the levels of C and EC were observed upon roasting. Contents of GC (unspecified) and EGC (unspecified) increased during the first stages of roasting, and then decreased. The EC/C ratio decreased during roasting time, thereby suggesting that EC degradation is faster than that of C, possibly due to epimerisation of EC to C. An increase in roasting temperature increased the overall rate of EC/C decrease. With moisture content equal, the EC/C ratio was inversely related to roasting temperature. This result suggested that high temperature-short time processes induce a higher EC epimerisation than do low temperature-long time processes. With roasting times equal, temperature negatively affected the EC/C ratio, indicating increased epimerisation of EC to C at higher roasting temperatures.	Ioannone <i>et al.</i> , 2015

Ioannone *et al.* (2015) studied the evolution of monomeric flavan-3-ols (Table 6) and total proanthocyanidins (Table 7) during the cocoa roasting process as a function of roasting temperature and time. A general reduction of catechin and epicatechin levels was observed during cocoa roasting, with losses exacerbated at increased roasting temperatures and times. The EC/C ratio, which was proposed as a useful and sensitive indicator for the processing history of cocoa beans by Payne *et al.* (2010), also decreased with increasing roasting time. This result suggested that epicatechin degradation is faster than that of catechin, possibly due to the formation of catechin (via the thermally-induced epimerisation of epicatechin to catechin) which offset losses in catechin. It should, however, be noted that C-3 epimerisation of epicatechin (2*R*,3*R*), with the formation of catechin (2*R*,3*S*), is much less likely than C-2 epimerisation with the formation of ent-catechin (2*S*,3*R*). The evolution of the EC/C ratio during the roasting of cocoa beans was well described by the cumulative function of the Weibull probabilistic model^c ($R^2 > 0.98$). An increase in roasting temperature increased the overall rate of epicatechin/catechin decrease, as described by decreases of the shape parameter (α) and the rate parameter (β) (Table 6).

3.2.3. Proanthocyanidins

The thermal degradation of individual procyanidin oligomers in apple juice (De Paepe *et al.*, 2014), and procyanidin and prodelfphinidin dimers in aqueous model systems (Xu *et al.*, 2015) follow first-order degradation kinetics. Ioannone *et al.* (2015) demonstrated that the loss of total proanthocyanidins during the roasting of cocoa beans is well described by the Weibull model^c (Table 7). An increase in temperature typically increased the rate of individual and total proanthocyanidin loss in accordance with the Arrhenius equation. The activation energy for the degradation of procyanidin oligomers at 85-145 °C ranged between 93 and 149 kJ.mol⁻¹, and that of proanthocyanidin dimers at temperatures of 4-40 °C was substantially lower at 6-40 kJ.mol⁻¹. The activation energy for the thermal degradation of total proanthocyanidins during roasting of cocoa beans at 125-145 °C was calculated as 59 kJ.mol⁻¹ (Table 7).

Under influence of temperature, procyanidins with a high degree of polymerisation hydrolyse to form monomers (catechin and epicatechin) and dimeric compounds such as procyanidin B2. De Paepe *et al.* (2014) demonstrated a remarkable increase in the levels of catechin and epicatechin (temperatures > 90 °C), and procyanidin B2 (temperatures > 100 °C). The thermal resistance of the B-type procyanidins was found to increase with a decreasing degree of polymerisation, as exemplified by comparison of the thermal degradation constants of procyanidin hexamers and a procyanidin trimer at 100 °C (Table 7). This is in accordance with findings by Hong *et al.* (2004) showing that pasteurisation (93 °C, 10 min) resulted in a 5-11% reduction in procyanidin monomers through to pentamers, a *ca.* 30% reduction of hexamers and heptamers, and the octamers could no longer be detected. However, due to the complexity of the reactions involved, including thermally-induced degradation, formation reactions and polymerisation reactions, the thermal stabilities of procyanidin oligomers with differing degrees of polymerisation should be assessed individually to better elucidate the effect of the degree of polymerisation.

^cWeibull model, rewritten by Ioannone *et al.* (2015) as:

$$\frac{C_0 - C_t}{C_0 - C_E} = 1 - e^{-\left(\frac{t}{\beta}\right)^\alpha} \quad (11)$$

Where C_t , C_E and C_0 is the concentration at time t , the equilibrium concentration, and the initial concentration, respectively; t is time, α is the shape parameter, and β is the rate parameter

Table 7 Thermal degradation kinetics modelling of oligomeric proanthocyanidins

Proanthocyanidins and matrix	Operating conditions	Mathematical model, kinetic order and kinetic parameters	Major findings	Reference
Apple juice procyanidin hexamer (B-type, isomer I, II and III), procyanidin pentamer derivative, procyanidin pentamer (B-type), procyanidin derivative, procyanidin tetramer (B-type, isomer I and II), procyanidin trimer (B-type), methylated procyanidin dimer (A-type, isomer I and II),	Conventional thermal processing, isothermal: 85-145 °C for 7200 s	First-order degradation kinetic model; Arrhenius equation Procyanidin hexamer I (B-type): $k_{85\text{ °C}} = 0.33 \times 10^{-2} \text{ min}^{-1}$; $k_{90\text{ °C}} = 0.56 \times 10^{-2} \text{ min}^{-1}$; $k_{100\text{ °C}} = 1.58 \times 10^{-2} \text{ min}^{-1}$; $k_{120\text{ °C}} = 10.6 \times 10^{-2} \text{ min}^{-1}$; $k_{135\text{ °C}} = 39.4 \times 10^{-2} \text{ min}^{-1}$; $k_{140\text{ °C}} = 59.6 \times 10^{-2} \text{ min}^{-1}$; $k_{145\text{ °C}} = 89.5 \times 10^{-2} \text{ min}^{-1}$; $E_a = 116 \text{ kJ.mol}^{-1}$ Procyanidin hexamer II (B-type): $k_{85\text{ °C}} = 0.28 \times 10^{-2} \text{ min}^{-1}$; $k_{90\text{ °C}} = 0.47 \times 10^{-2} \text{ min}^{-1}$; $k_{100\text{ °C}} = 1.22 \times 10^{-2} \text{ min}^{-1}$; $k_{120\text{ °C}} = 7.26 \times 10^{-2} \text{ min}^{-1}$; $k_{135\text{ °C}} = 24.8 \times 10^{-2} \text{ min}^{-1}$; $k_{140\text{ °C}} = 36.6 \times 10^{-2} \text{ min}^{-1}$; $k_{145\text{ °C}} = 53.6 \times 10^{-2} \text{ min}^{-1}$; $E_a = 109 \text{ kJ.mol}^{-1}$ Procyanidin hexamer III (B-type): $k_{85\text{ °C}} = 0.22 \times 10^{-2} \text{ min}^{-1}$; $k_{90\text{ °C}} = 0.39 \times 10^{-2} \text{ min}^{-1}$; $k_{100\text{ °C}} = 1.09 \times 10^{-2} \text{ min}^{-1}$; $k_{120\text{ °C}} = 7.36 \times 10^{-2} \text{ min}^{-1}$; $k_{135\text{ °C}} = 25.6 \times 10^{-2} \text{ min}^{-1}$; $k_{140\text{ °C}} = 38.0 \times 10^{-2} \text{ min}^{-1}$; $k_{145\text{ °C}} = 55.9 \times 10^{-2} \text{ min}^{-1}$; $E_a = 117 \text{ kJ.mol}^{-1}$ Procyanidin pentamer derivative: $k_{90\text{ °C}} = 0.90 \times 10^{-2} \text{ min}^{-1}$; $k_{100\text{ °C}} = 2.05 \times 10^{-2} \text{ min}^{-1}$; $k_{120\text{ °C}} = 9.47 \times 10^{-2} \text{ min}^{-1}$; $k_{135\text{ °C}} = 29.9 \times 10^{-2} \text{ min}^{-1}$; $k_{140\text{ °C}} = 43.0 \times 10^{-2} \text{ min}^{-1}$; $k_{145\text{ °C}} = 61.4 \times 10^{-2} \text{ min}^{-1}$; $E_a = 93.3 \text{ kJ.mol}^{-1}$ Procyanidin pentamer I (B-type): $k_{90\text{ °C}} = 0.59 \times 10^{-2} \text{ min}^{-1}$; $k_{100\text{ °C}} = 1.47 \times 10^{-2} \text{ min}^{-1}$; $k_{120\text{ °C}} = 8.02 \times 10^{-2} \text{ min}^{-1}$; $k_{135\text{ °C}} = 28.1 \times 10^{-2} \text{ min}^{-1}$; $k_{140\text{ °C}} = 41.8 \times 10^{-2} \text{ min}^{-1}$; $k_{145\text{ °C}} = 61.6 \times 10^{-2} \text{ min}^{-1}$; $E_a = 104 \text{ kJ.mol}^{-1}$ Procyanidin derivative: $k_{90\text{ °C}} = 0.45 \times 10^{-2} \text{ min}^{-1}$; $k_{100\text{ °C}} = 1.15 \times 10^{-2} \text{ min}^{-1}$; $k_{120\text{ °C}} = 6.61 \times 10^{-2} \text{ min}^{-1}$; $k_{135\text{ °C}} = 23.2 \times 10^{-2} \text{ min}^{-1}$; $k_{140\text{ °C}} = 34.6 \times 10^{-2} \text{ min}^{-1}$; $k_{145\text{ °C}} = 51.1 \times 10^{-2} \text{ min}^{-1}$; $E_a = 106 \text{ kJ.mol}^{-1}$ Procyanidin tetramer I (B-type): $k_{100\text{ °C}} = 0.93 \times 10^{-2} \text{ min}^{-1}$; $k_{120\text{ °C}} = 5.68 \times 10^{-2} \text{ min}^{-1}$; $k_{135\text{ °C}} = 22.5 \times 10^{-2} \text{ min}^{-1}$; $k_{140\text{ °C}} = 34.9 \times 10^{-2} \text{ min}^{-1}$; $k_{145\text{ °C}} = 53.4 \times 10^{-2} \text{ min}^{-1}$; $E_a = 111 \text{ kJ.mol}^{-1}$ Procyanidin tetramer II (B-type): $k_{100\text{ °C}} = 0.87 \times 10^{-2} \text{ min}^{-1}$; $k_{120\text{ °C}} = 5.33 \times 10^{-2} \text{ min}^{-1}$; $k_{135\text{ °C}} = 23.3 \times 10^{-2} \text{ min}^{-1}$; $k_{140\text{ °C}} = 37.1 \times 10^{-2} \text{ min}^{-1}$; $k_{145\text{ °C}} = 58.5 \times 10^{-2} \text{ min}^{-1}$; $E_a = 110 \text{ kJ.mol}^{-1}$ Procyanidin trimer I (B-type): $k_{100\text{ °C}} = 0.50 \times 10^{-2} \text{ min}^{-1}$; $k_{120\text{ °C}} = 5.75 \times 10^{-2} \text{ min}^{-1}$; $k_{135\text{ °C}} = 30.9 \times 10^{-2} \text{ min}^{-1}$; $k_{140\text{ °C}} = 52.6 \times 10^{-2} \text{ min}^{-1}$; $k_{145\text{ °C}} = 88.5 \times 10^{-2} \text{ min}^{-1}$; $E_a = 149 \text{ kJ.mol}^{-1}$ Methylated procyanidin dimer I (A-type): $k_{100\text{ °C}} = 0.49 \times 10^{-2} \text{ min}^{-1}$; $k_{120\text{ °C}} = 2.73 \times 10^{-2} \text{ min}^{-1}$; $k_{135\text{ °C}} = 9.67 \times 10^{-2} \text{ min}^{-1}$; $k_{140\text{ °C}} = 14.4 \times 10^{-2} \text{ min}^{-1}$; $k_{145\text{ °C}} = 21.4 \times 10^{-2} \text{ min}^{-1}$; $E_a = 105 \text{ kJ.mol}^{-1}$ Methylated procyanidin dimer II (A-type): $k_{120\text{ °C}} = 3.63 \times 10^{-2} \text{ min}^{-1}$; $k_{135\text{ °C}} = 12.9 \times 10^{-2} \text{ min}^{-1}$; $k_{140\text{ °C}} = 19.2 \times 10^{-2} \text{ min}^{-1}$; $k_{145\text{ °C}} = 28.5 \times 10^{-2} \text{ min}^{-1}$; $E_a = 107 \text{ kJ.mol}^{-1}$	Procyanidin oligomers are the most heat labile phenolic constituents in cloudy apple juice. Thermal resistance (of the B-type procyanidins) increased with a decreasing degree of polymerisation. Procyanidins with a high degree of polymerisation hydrolyse under the influence of temperature into monomers (C and EC) and dimeric compounds such as procyanidin B2. A remarkable increase in the levels of C and EC (> 90 °C), and for procyanidin B2 (> 100 °C) was demonstrated.	De Paepe <i>et al.</i> , 2014

Table 7 cont.

Proanthocyanidins and matrix	Operating conditions	Mathematical model, kinetic order and kinetic parameters	Major findings	Reference
Cocoa (<i>Theobroma cacao</i> L.) beans				
Total proanthocyanidins (monomers P1 through to high molecular weight polymers P10)	Roasting process (isothermal) conducted in a ventilated electric oven at constant air-flow rate (1 m.s ⁻¹) and relative humidity (0.4%). Fermented and dried cocoa beans (35 g) were roasted at 125 °C/74 min, 135 °C/35 min and 145 °C/40 min until they reached a residual moisture content of ca. 1.8 g.100 g ⁻¹ . Portions of roasted cocoa were taken from the oven at predetermined time limits.	Weibull model; Arrhenius equation. <i>Total proanthocyanidin loss</i> 125 °C: $\alpha = 4.80$; $\beta = 24.5$ min; $C_E = 5.35$ mg.g _{dw} ⁻¹ 135 °C: $\alpha = 2.11$; $\beta = 18.8$ min; $C_E = 5.32$ mg.g _{dw} ⁻¹ 145 °C: $\alpha = 0.87$; $\beta = 7.03$ min; $C_E = 4.92$ mg.g _{dw} ⁻¹ Pre-exponential factor, $K_0 = 2.16 \times 10^6$ min ⁻¹ Activation energy, $E_a = 59$ kJ.mol ⁻¹	No changes in the relative abundance of P1 and P2 were observed between the unroasted beans and beans roasted for 30 min. The relative abundance of P3, P4 and P5 decreased during roasting. The relative abundance of the high molecular weight proanthocyanidins (P6-P10) decreased in the first stages of roasting, but then increased as a result of the polymerisation of proanthocyanidins with a lower molecular weight. The total proanthocyanidins content decreased upon heat treatment, and an increase in roasting temperature increased the overall rate of total proanthocyanidin loss. High temperature-short time processes minimised total proanthocyanidin loss.	Ioannone <i>et al.</i> 2015
Aqueous model solutions				
B-type (E)C dimer A-type (E)C dimer A-type (E)CG dimer A-type (E)GCG dimer	<i>Effect of temperature</i> Proanthocyanidin dimers (0.67 mg.mL ⁻¹ distilled water) kept at 4 °C (refrigerator), and 25 and 40 °C (water bath) for 11.25 h. <i>Effect of pH*</i> Proanthocyanidin dimers (final concentration 0.3 mg.mL ⁻¹ aqueous buffer solution) kept at 4 °C (refrigerator), and 25 and 40 °C (water bath) for 11.25 h. pH of the aqueous solutions were adjusted to 1.5, 6.8, 7.4 and 10.0. <i>*Results were only given for experiments at 25 °C, and pH 1.5 and 7.4</i>	First-order kinetic model; Arrhenius equation <i>Effect of temperature</i> B-type (E)C dimer: $k_{4\text{ }^\circ\text{C}} = 8.352 \times 10^{-3}$ h ⁻¹ , $t_{1/2}^{\text{a}}$ = 82.964 h; $k_{25\text{ }^\circ\text{C}} = 10.67 \times 10^{-3}$ h ⁻¹ , $t_{1/2} = 64.948$ h; $k_{40\text{ }^\circ\text{C}} = 12.57 \times 10^{-3}$ h ⁻¹ , $t_{1/2} = 55.131$ h; $E_a = 8.281$ kJ.mol ⁻¹ A-type (E)C dimer: $k_{4\text{ }^\circ\text{C}} = 2.668 \times 10^{-3}$ h ⁻¹ , $t_{1/2} = 259.746$ h; $k_{25\text{ }^\circ\text{C}} = 3.001 \times 10^{-3}$ h ⁻¹ , $t_{1/2} = 230.923$ h; $k_{40\text{ }^\circ\text{C}} = 12.012 \times 10^{-3}$ h ⁻¹ , $t_{1/2} = 57.708$ h; $E_a = 40.224$ kJ.mol ⁻¹ A-type (E)CG dimer: $k_{4\text{ }^\circ\text{C}} = 2.375 \times 10^{-3}$ h ⁻¹ , $t_{1/2} = 291.790$ h; $k_{25\text{ }^\circ\text{C}} = 8.985 \times 10^{-3}$ h ⁻¹ , $t_{1/2} = 77.129$ h; $k_{40\text{ }^\circ\text{C}} = 11.86 \times 10^{-3}$ h ⁻¹ , $t_{1/2} = 58.432$ h; $E_a = 33.112$ kJ.mol ⁻¹ A-type (E)GCG dimer: $k_{4\text{ }^\circ\text{C}} = 8.366 \times 10^{-3}$ h ⁻¹ , $t_{1/2} = 82.835$ h; $k_{25\text{ }^\circ\text{C}} = 10.38 \times 10^{-3}$ h ⁻¹ , $t_{1/2} = 66.763$ h; $k_{40\text{ }^\circ\text{C}} = 11.74 \times 10^{-3}$ h ⁻¹ , $t_{1/2} = 59.029$ h; $E_a = 6.726$ kJ.mol ⁻¹ <i>Effect of pH</i> B-type (E)C dimer: pH 1.5: $k_{25\text{ }^\circ\text{C}} = 20.37 \times 10^{-3}$ h ⁻¹ , $t_{1/2, 25\text{ }^\circ\text{C}} = 34.021$ h, $E_a = 5.354$ kJ.mol ⁻¹ ; pH 7.4: $k_{25\text{ }^\circ\text{C}} = 14.42 \times 10^{-3}$ h ⁻¹ , $t_{1/2, 25\text{ }^\circ\text{C}} = 48.058$ h, $E_a = 6.163$ kJ.mol ⁻¹ . A-type (E)C dimer: pH 1.5: $k_{25\text{ }^\circ\text{C}} = 2.675 \times 10^{-3}$ h ⁻¹ , $t_{1/2, 25\text{ }^\circ\text{C}} = 259.06$ h, $E_a = 41.743$ kJ.mol ⁻¹ ; pH 7.4: $k_{25\text{ }^\circ\text{C}} = 13.48 \times 10^{-3}$ h ⁻¹ , $t_{1/2, 25\text{ }^\circ\text{C}} = 51.410$ h, $E_a = 37.901$ kJ.mol ⁻¹ . A-type (E)CG dimer: pH 1.5: $k_{25\text{ }^\circ\text{C}} = 3.128 \times 10^{-3}$ h ⁻¹ , $t_{1/2, 25\text{ }^\circ\text{C}} = 221.55$ h, $E_a = 35.727$ kJ.mol ⁻¹ ; pH 7.4: $k_{25\text{ }^\circ\text{C}} = 10.99 \times 10^{-3}$ h ⁻¹ , $t_{1/2, 25\text{ }^\circ\text{C}} = 63.057$ h, $E_a = 32.608$ kJ.mol ⁻¹ . A-type (E)GCG dimer: pH 1.5: $k_{25\text{ }^\circ\text{C}} = 2.149 \times 10^{-3}$ h ⁻¹ , $t_{1/2, 25\text{ }^\circ\text{C}} = 319.50$ h, $E_a = 19.856$ kJ.mol ⁻¹ ; pH 7.4: $k_{25\text{ }^\circ\text{C}} = 14.87 \times 10^{-3}$ h ⁻¹ , $t_{1/2, 25\text{ }^\circ\text{C}} = 46.604$ h, $E_a = 15.056$ kJ.mol ⁻¹ .	Stability of proanthocyanidin dimers was temperature, structure and pH dependent. The higher the temperature, the less stable the dimers. In general, A-type dimers were more stable than the B-type dimer. A-type (E)C dimer was more stable than the B-type (E)C dimer with the same monomer composition, due to the additional C-2-O-C-7 ether linkage in the A-type (E)C dimer, instead of a phenolic hydroxy group as in the B-type (E)C dimer. Amongst the A-type dimers, (E)GCG dimer was the least stable, and this was attributed to the presence of an extra hydroxy group and a galloyl group. Proanthocyanidins dimers were unstable at pH as low as 1.5 (gastric pH) and physiological conditions (intestinal pH, 7.4), and were extremely unstable at alkaline conditions (pH 10.0). Increase in k with increasing pH for the A-type dimers, while the half-life values decreased. A-type dimers were more stable at pH 1.5 than pH 7.4, while the B-type dimer was less stable under the acidic pH conditions. Higher stability of A-type dimers under acidic conditions was attributed to the fact that the A-type linkage is not susceptible to degradation under acidic conditions.	Xu <i>et al.</i> , 2015

^aHalf-life value, $t_{1/2}$, calculated according to eq. 12:

$$t_{1/2} = \frac{\ln 2}{k} \quad (12)$$

A recent study by Xu *et al.* (2015) compared the degradation kinetics of A-type and B-type proanthocyanidin dimers (Figure 11) as a function of pH and temperature (Table 7). While this study was conducted at relatively low temperatures, it provided fundamental insight into the effect of structure and pH on the thermal stability of proanthocyanidin dimers. Both the linkage type of the interflavan bonds and the structural features of the monomers affected their thermal stability over a temperature range of 4–40 °C. The A-type (E)C dimer was more stable than the B-type (E)C dimer with the same monomer composition, due to the presence of an additional C-2–O–C-7 ether linkage in the former. In accordance with findings of the impact of structural features on the thermal stability of flavan-3-ol monomers, the presence of an additional hydroxy group and a galloyl moiety decreased the thermal stability of the A-type proanthocyanidin dimers (Xu *et al.*, 2015; Table 7).

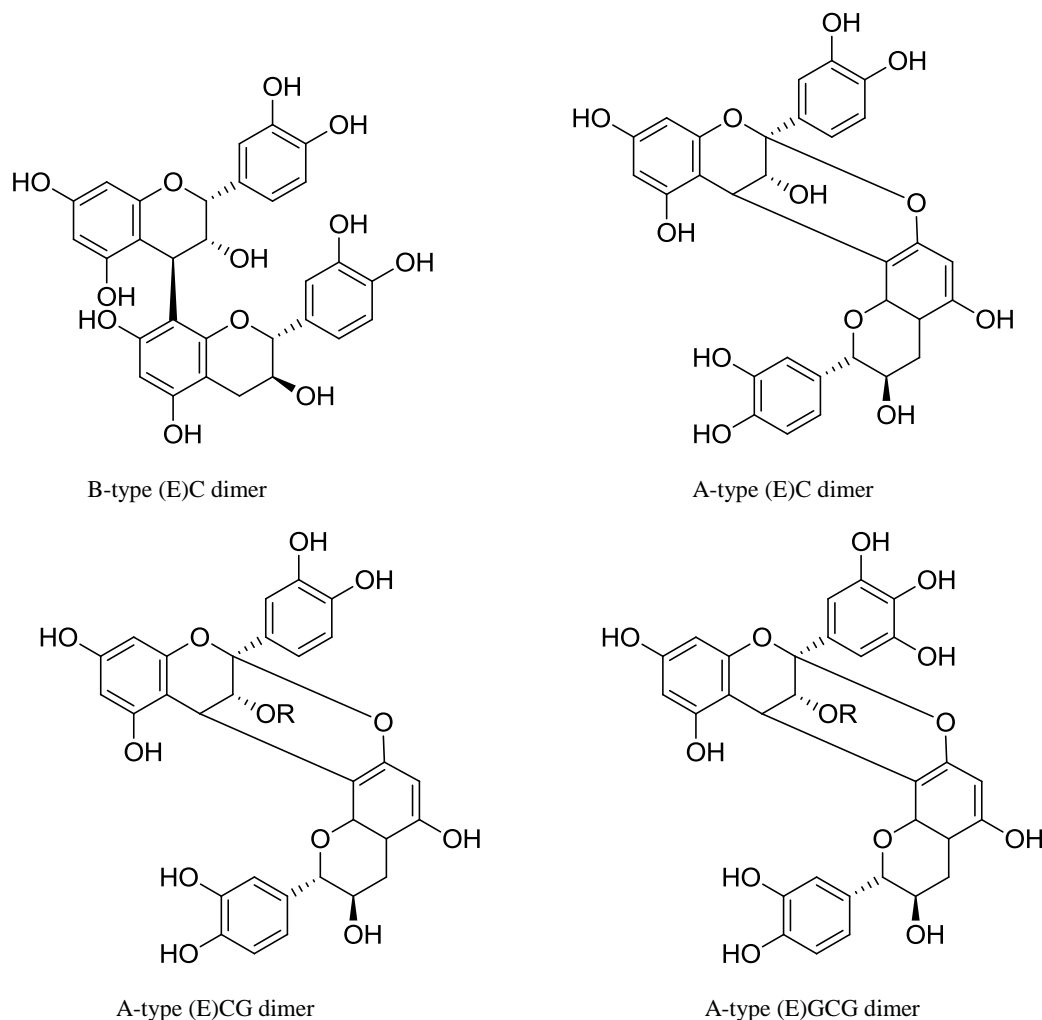


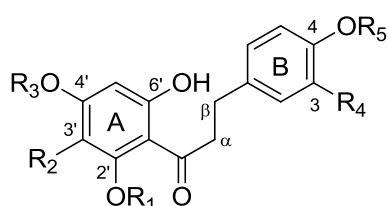
Figure 11 Structures of the four proanthocyanidin dimers, with R = galloyl moiety (reproduced from Xu *et al.*, 2015).

As observed for monomeric flavan-3-ols, pH had a significant effect on the thermal stability of proanthocyanidin dimers. Both A- and B-type dimers were unstable at pH as low as 1.5 (gastric pH) and physiological conditions (intestinal pH, 7.4), and were extremely unstable at alkaline conditions (pH 10.0) upon incubation in aqueous buffer solutions at 25 °C (Xu *et al.*, 2015). For the A-type dimers, an increase in the first-order degradation rate constants was observed with an increase in pH from 1.5 to 7.4, while the half-life values correspondingly decreased (Table 7). Conversely, the B-type dimer was less stable at pH 1.5 than at pH 7.4. The higher stability of the A-type dimers compared to the B-type dimer under acidic conditions was attributed to the fact that the A-type linkage is not susceptible to degradation under acidic conditions (Xu *et al.*, 2015).

3.3. Dihydrochalcones, Flavanones, Dihydroflavonols, Flavonols and Flavones

3.3.1. Dihydrochalcones

To date, studies on the thermal stability of compounds from the dihydrochalcone flavonoid sub-class have focused on a few target compounds (Figure 12). In light of its importance as an artificial sweetener, the thermal stability of neohesperidin dihydrochalcone has been investigated comprehensively, and kinetic data from literature are summarised in Table 8. The thermal stabilities of 2'- β -D-glucopyranosyloxyphloretin (phloridzin) and its derivatives, 2'- β -D-glucopyranosyloxy-3-hydroxyphloretin and 2'-(6- β -D-xylopyranosyl- β -D-glucopyranosyloxy)-3-hydroxyphloretin, have mostly been assessed in apple juice (Table 9). While the C-glucosyl dihydrochalcone aspalathin and its 3-deoxy derivative nothofagin represent important phenolic constituents of rooibos (*Aspalathus linearis*), their thermal stabilities have not yet been investigated kinetically. Selected findings from literature regarding general trends in their thermal stabilities will thus be highlighted.



	R₁	R₂	R₃	R₄	R₅
Neohesperidin dihydrochalcone	H	H	neohesperidosyl*	OH	CH ₃
2'- β -D-Glucopyranosyloxyphloretin (phloridzin)	glucopyranosyl	H	H	H	H
2'- β -D-Glucopyranosyloxy-3-hydroxyphloretin	glucopyranosyl	H	H	OH	H
2'-(6- β -D-Xylopyranosyl- β -D-glucopyranosyloxy)-3-hydroxyphloretin	xylopyranosylglucoside	H	H	OH	H
3'- β -D-Glucopyranosyl-3-hydroxyphloretin (aspalathin)	H	glucopyranosyl	H	OH	H
3'- β -D-Glucopyranosylphloretin (nothofagin)	H	glucopyranosyl	H	H	H

Figure 12 Substitution pattern of selected dihydrochalcones. *2- α -L-rhamnopyranosyloxy- β -D-glucopyranosyl.

Neohesperidin dihydrochalcone

Neohesperidin dihydrochalcone (Figure 12) is an intense sweetener and flavour modifier obtained by simple modification of citrus flavanones (hydrogenation of naringin or neohesperidin) and was first prepared by Horowitz and Gentili in 1963 (Horowitz & Gentili, 1963). The thermal stability of neohesperidin dihydrochalcone has been studied in aqueous model systems (Inglett *et al.*, 1969; Canales *et al.*, 1993; Coiffard *et al.*, 1998), during pasteurisation of milk (Montijano *et al.*, 1995) and representative model beverages (Montijano *et al.*, 1996), and also during processing and storage of complex food systems including blackcurrant jams (Tomás-Barberán *et al.*, 1995). Storage stability studies include storage of a carbonated lemonade formulation under normal (20-25 °C/12 months), accelerated (40 °C/3 months), and extreme (90 °C /58 h) conditions (Montijano *et al.*, 1997). The degradation of neohesperidin dihydrochalcone was found to follow pseudo-first order kinetics across different temperature (30-95 °C) and pH (0.5-7.0) ranges, and the temperature-dependence of the reaction rate constant follows the Arrhenius law (Canales *et al.*, 1993; Montijano *et al.*, 1995, 1997; Coiffard *et al.*, 1998; Table 8).

Table 8 Thermal degradation kinetic studies on neohesperidin dihydrochalcone.

Dihydrochalcone and matrix	Operating conditions	Mathematical model, kinetic order and kinetic parameters	Major findings	Reference
Aqueous buffer solutions				
neohesperidin dihydrochalcone (300 ppm)	Incubation of neohesperidin dihydrochalcone solutions in temperature-controlled circulating water baths at 30 °C (140 days), 40 °C (86 days), 50 °C (56 days), 60 °C (28 days) and 90 °C. Buffer compositions were adjusted to obtain pH values between 1 and 7.	First-order kinetic model; Arrhenius equation. pH 1: $k_{30\text{ °C}} = 3.03 \times 10^3 \text{ day}^{-1}$; $k_{40\text{ °C}} = 12.60 \times 10^3 \text{ day}^{-1}$; $k_{50\text{ °C}} = 57.88 \times 10^3 \text{ day}^{-1}$; $k_{60\text{ °C}} = 271.44 \times 10^3 \text{ day}^{-1}$; $E_a = ca. 126 \text{ kJ.mol}^{-1}$ pH 2: $k_{30\text{ °C}} = NA$; $k_{40\text{ °C}} = 2.80 \times 10^3 \text{ day}^{-1}$; $k_{50\text{ °C}} = 9.03 \times 10^3 \text{ day}^{-1}$; $k_{60\text{ °C}} = 20.96 \times 10^3 \text{ day}^{-1}$; $E_a = ca. 88 \text{ kJ.mol}^{-1}$ pH 3: $k_{30\text{ °C}} = NA$; $k_{40\text{ °C}} = 0.63 \times 10^3 \text{ day}^{-1}$; $k_{50\text{ °C}} = 2.23 \times 10^3 \text{ day}^{-1}$; $k_{60\text{ °C}} = 4.03 \times 10^3 \text{ day}^{-1}$; $E_a = ca. 79 \text{ kJ.mol}^{-1}$ pH 4: $k_{30\text{ °C}} = NA$; $k_{40\text{ °C}} = 0.36 \times 10^3 \text{ day}^{-1}$; $k_{50\text{ °C}} = 0.82 \times 10^3 \text{ day}^{-1}$; $k_{60\text{ °C}} = 1.46 \times 10^3 \text{ day}^{-1}$; $E_a = ca. 59 \text{ kJ.mol}^{-1}$ pH 5: $k_{30\text{ °C}} = 0.41 \times 10^3 \text{ day}^{-1}$; $k_{40\text{ °C}} = 0.71 \times 10^3 \text{ day}^{-1}$; $k_{50\text{ °C}} = 1.54 \times 10^3 \text{ day}^{-1}$; $k_{60\text{ °C}} = 1.94 \times 10^3 \text{ day}^{-1}$; $E_a = ca. 46 \text{ kJ.mol}^{-1}$ pH 6: $k_{30\text{ °C}} = 0.65 \times 10^3 \text{ day}^{-1}$; $k_{40\text{ °C}} = 1.11 \times 10^3 \text{ day}^{-1}$; $k_{50\text{ °C}} = 2.21 \times 10^3 \text{ day}^{-1}$; $k_{60\text{ °C}} = 6.76 \times 10^3 \text{ day}^{-1}$; $E_a = ca. 65 \text{ kJ.mol}^{-1}$ pH 7: $k_{30\text{ °C}} = 4.98 \times 10^3 \text{ day}^{-1}$; $k_{40\text{ °C}} = 13.88 \times 10^3 \text{ day}^{-1}$; $k_{50\text{ °C}} = 36.15 \times 10^3 \text{ day}^{-1}$; $k_{60\text{ °C}} = 70.19 \times 10^3 \text{ day}^{-1}$; $E_a = ca. 75 \text{ kJ.mol}^{-1}$	Maximum stability of neohesperidin dihydrochalcone was observed at pH 4. At pH levels below the optimum pH, acid catalysis was dominant, and at pH levels above the optimum, base-catalysed reactions occurred. The reactions became more temperature-sensitive (<i>i.e.</i> , higher E_a) at $5 > \text{pH} > 5$.	Canales <i>et al.</i> , 1993 ^a
Skimmed milk				
0.0050% (w.v ⁻¹) neohesperidin dihydrochalcone and 10% (w.v ⁻¹) powdered skimmed milk in distilled water	Heating in a temperature-controlled circulating water bath at 85 and 95 °C for 8 h.	First-order kinetic model $k_{85\text{ °C}} = 0.06029 \text{ h}^{-1}$; $k_{95\text{ °C}} = 0.12205 \text{ h}^{-1}$	No significant decomposition was detected after milk pasteurisation (85 °C /30 min and 95 °C /5 min).	Montijano <i>et al.</i> , 1995
Carbonated lemonade system (pH 3.3)				
neohesperidin dihydrochalcone (20 mg.L ⁻¹)	Heating in a temperature-controlled circulating polyethylene glycol 400 bath at 90 °C.	First-order kinetic model $k_{90\text{ °C}} = 0.00318 \text{ h}^{-1}$; $t_{1/2} = 9.1 \text{ days}$	The stability of neohesperidin dihydrochalcone in the beverage studied was similar to that in the aqueous model systems (Canales <i>et al.</i> , 1993).	Montijano <i>et al.</i> , 1997
Aqueous model solutions				
neohesperidin dihydrochalcone (3.26 × 10 ⁻⁵ M)	Isothermal treatment for 65 days Solutions stored in thermostatically controlled ovens at 50, 70 and 90 °C. Samples were withdrawn periodically. The effect of pH (0.50-6.50) was assessed.	First-order kinetic model; Arrhenius equation pH = 0.50: $k_{50\text{ °C}} = 13.27 \times 10^{-3} \text{ days}^{-1}$; $k_{70\text{ °C}} = 37.66 \times 10^{-3} \text{ days}^{-1}$; $k_{90\text{ °C}} = 95.25 \times 10^{-3} \text{ days}^{-1}$. pH = 2.50: $k_{50\text{ °C}} = 5.10 \times 10^{-3} \text{ days}^{-1}$; $k_{70\text{ °C}} = 10.33 \times 10^{-3} \text{ days}^{-1}$; $k_{90\text{ °C}} = 19.43 \times 10^{-3} \text{ days}^{-1}$. pH = 4.50: $k_{50\text{ °C}} = 3.71 \times 10^{-3} \text{ days}^{-1}$, $t_{1/2} = 195.41 \text{ days}$; $k_{70\text{ °C}} = 10.06 \times 10^{-3} \text{ days}^{-1}$; $t_{1/2} = 62.40 \text{ days}$; $k_{90\text{ °C}} = 24.50 \times 10^{-3} \text{ days}^{-1}$; $t_{1/2} = 23.00 \text{ days}$. $E_a = 45.8 \text{ kJ.mol}^{-1}$ pH = 6.50: $k_{50\text{ °C}} = 9.60 \times 10^{-3} \text{ days}^{-1}$; $k_{70\text{ °C}} = 31.80 \times 10^{-3} \text{ days}^{-1}$; $k_{90\text{ °C}} = 93.15 \times 10^{-3} \text{ days}^{-1}$.	Thermal degradation of neohesperidin dihydrochalcone in dilute aqueous solution was pH-dependent. The optimum pH for stability was 4.50.	Coiffard <i>et al.</i> , 1998

^aValues for the activation energy (E_a) converted from kcal.mol⁻¹ to kJ.mol⁻¹ with a factor 4.184.

Canales *et al.* (1993) conducted the first study on the degradation kinetics of neohesperidin dihydrochalcone in aqueous buffer solutions at elevated temperatures (30-60 °C) as a function of pH (1.0-7.0) (Table 8). The kinetic data were subsequently extrapolated to 20 and 25 °C to predict the half-life values for neohesperidin dihydrochalcone degradation at different pH values during normal shelf-life conditions. The high half-life values for neohesperidin dihydrochalcone from pH 2 to 6 indicated that this sweetener would be stable throughout the normal shelf-life of soft drinks (6-12 months) (Canales *et al.*, 1993). An additional set of experiments was also conducted by Canales *et al.* (1993) at 90 °C (pH 2, 3, 6 and 7) to check the validity of their thermal degradation kinetics model (using data from the experiments performed at 30-60 °C) to predict half-life values for neohesperidin dihydrochalcone degradation at pasteurisation temperatures. Large differences between the extrapolated and experimental half-life values were observed, and this was ascribed to the lack of intermediate temperatures or by a change in the slope of the Arrhenius curve from lower to higher temperatures. The experimental data at 90 °C confirmed that neohesperidin dihydrochalcone would be able to withstand pasteurisation (Canales *et al.*, 1993).

The high stability of neohesperidin dihydrochalcone during storage and thermal treatments has since been confirmed by numerous researchers. Non-significant degradation of neohesperidin dihydrochalcone was found to occur during the manufacturing process (102-106 °C/35-40 min) and storage (room temperature/18 months) of black current jams (pH 3.08) (Tomás-Barberán *et al.*, 1995). A kinetic study conducted by Montijano *et al.* (1995) indicated that normal heat treatments of milk used for yoghurt manufacture, *i.e.*, 85 °C/30 min or 95 °C/5 min, would hardly influence the levels of neohesperidin dihydrochalcone, with 97 and 99% remaining after the respective heat treatments (Table 8). Similarly, no significant loss in neohesperidin dihydrochalcone content was observed in different model beverages (orange, lemon, apple and pineapple, pH 2.7-3.1) after pasteurisation (90 °C/1 h), or during pasteurisation of the lemon-based drink at temperatures ranging from 60 °C (4 h) to 100 °C (45 min) (Montijano *et al.*, 1996). No losses in neohesperidin dihydrochalcone content of a carbonated lemonade formulation (pH 3.3) was observed after a one year storage period at room temperature, or after three months at 40 °C (Montijano *et al.*, 1997). Degradation of neohesperidin dihydrochalcone only occurred under more drastic conditions, *i.e.*, prolonged storage at 90 °C (Montijano *et al.*, 1997). The reaction rate constant at 90 °C was calculated as 0.00318 h⁻¹, with a corresponding half-life value of 9.1 days (Table 8).

The aforementioned studies indicated that exposure to light at ambient temperature (Montijano *et al.*, 1997) and matrix components at ambient and elevated temperatures (Tomás-Barberán *et al.*, 1995; Montijano *et al.*, 1996; Montijano *et al.*, 1997) have no impact on the thermal stability of neohesperidin dihydrochalcone in different systems with pH ~ 3. Its thermal stability is, however, pH-dependent. Under conditions combining high acidity with high temperature, neohesperidin dihydrochalcone is hydrolysed to form a mixture of hesperetin dihydrochalcone, 4'-β-D-glucopyranosyloxyhesperetin, and the sugars rhamnose and glucose. Results presented by Inglett *et al.* (1969) indicated that the glycosidic bonds of neohesperidin dihydrochalcone in solution are resistant to hydrolysis by various acids (hydrochloric-, sulphuric-, phosphoric-, acetic- and citric acids) above pH 2 (pH range 2.0 to 3.8) at normal room temperature. An increase in temperature from 25 to 100 °C (at constant pH) typically decreased the time for detection of the free sugars, indicative of an increased rate of hydrolysis (Inglett *et al.*, 1969). Montijano *et al.* (1996) also demonstrated that a pH range of 2.5 to 3.5 did not affect the thermal stability of neohesperidin dihydrochalcone in a lemon-based juice; a significant loss in neohesperidin dihydrochalcone content (8%) was only observed upon thermal treatment (90 °C/1 h) of the lemon-based juice with pH adjusted to 2.0, with hydrolysis products only detectable after 12 h (Montijano *et al.*, 1996).

Maximum stability of neohesperidin dihydrochalcone in aqueous buffer solutions adjusted to different pH levels (1.0-7.0) has been observed at pH 4 (Canales *et al.*, 1993; Table 8). A plot of natural log/l_n half-life values for neohesperidin dihydrochalcone degradation vs pH resulted in a “bell-shaped” curve which defined two different regions: one below the

optimum pH where acid catalysis was dominant, and one above the optimum pH characterised by base-catalysed reactions. This is in accordance with a study by Coiffard *et al.* (1998), who found that the first-order degradation rate constant of neohesperidin dihydrochalcone in dilute aqueous solutions typically increased as the pH was increased above 4.50 (pH < 6.50), and also as the pH was decreased to 0.50 (Table 8). Under the best stability conditions (pH = 4.50), the activation energy was calculated as 45.8 kJ.mol⁻¹. The critical effect of pH on neohesperidin dihydrochalcone stability is also reflected in the Arrhenius activation energy. The hydrolysis reactions became more temperature-sensitive (*i.e.*, higher E_a) as the pH decreased (1 < pH < 5), but also as the pH increased towards the near neutral region (5 < pH < 7) (Canales *et al.*, 1993; Table 8).

Dihydrochalcone O-glycosyl compounds and apples

Apples are one of the few sources of dihydrochalcones in the human diet (Tomás-Barberán & Clifford, 2000). As a result, studies on the thermal stability of dihydrochalcones deal mainly with those present in apple juice. The dihydrochalcones, and, in particular 2'- β -D-glucopyranosyloxyphloretin (phloridzin, Figure 12), represent some of the most heat-resistant compounds in apple juice, second only to the phenolic acids. Van der Sluis *et al.* (2005) demonstrated that the main degradation route for phloridzin in apple juice during accelerated storage (70-100 °C/4 days) is a non-oxidative pathway. Different levels of oxygen bubbled through apple juice (0, 21 and 100%) had no effect on the thermal stability of phloridzin at any of the temperatures studied. This compound only exhibited minor degradation, with a degradation rate of $2.3 \times 10^{-3} \text{ h}^{-1}$ at 70 °C and an activation energy of 73 kJ.mol⁻¹ (Table 9).

Similarly, De Paepe *et al.* (2014) demonstrated that 2'- β -D-glucopyranosyloxyphloretin in cloudy apple juice was very resistant to thermal degradation at increased temperatures of 135–145 °C. The thermal degradation of phloretin-2'- O -glucoside and two derivatives (Figure 12) followed first-order degradation kinetics, with increased temperatures leading to increased degradation rates in accordance with the Arrhenius law (Table 9). By comparing the values of k for 2'- β -D-glucopyranosyloxy-3-hydroxyphloretin, 2'-(6- β -D-xylopyranosyl- β -D-glucopyranosyloxy)-3-hydroxyphloretin and 2'- β -D-glucopyranosyloxyphloretin at each of the respective temperatures, certain trends were observed: a slight decrease in k with the presence of an extra hydroxy group at C-3 on the B-ring of the dihydrochalcone structure, and an increase in k with an increase in the degree of glycosylation (from an O -monoglucosyl to an O -diglycosyl compound). Based on the cut-off temperature whereupon significant degradation was observed in the studied time range of 7200 s, and the comparative values of the reaction rate constants at each of the temperatures, De Paepe *et al.* (2014) ranked the thermostability of the dihydrochalcones in the following order: 2'- β -D-glucopyranosyloxyphloretin > 2'-(6- β -D-xylopyranosyl- β -D-glucopyranosyloxy)-3-hydroxyphloretin > 2'- β -D-glucopyranosyloxy-3-hydroxyphloretin. Activation energies for these dihydrochalcones over the studied temperature range ranged between 120-140 kJ.mol⁻¹ (Table 9).

Dihydrochalcone C-glucosyl compounds and rooibos

The C-glucosyl dihydrochalcone aspalathin (Figure 12) is unique to the fynbos plant *Aspalathus linearis* (rooibos) and also represents its most abundant phenolic constituent. Its 3-deoxy derivative, nothofagin (Figure 12), represents the second most abundant dihydrochalcone in the plant material (as reviewed by Joubert *et al.*, 2008a). Aspalathin and nothofagin are both valuable bio-active compounds, as demonstrated by their antioxidant (Snijman *et al.*, 2009), antimutagenic (Snijman *et al.*, 2007) and anti-inflammatory (Ku *et al.*, 2015) activities. Aspalathin is also well-known for its antidiabetic properties (Kawano *et al.*, 2009; Muller *et al.*, 2012; Son *et al.*, 2013; Mazibuko *et al.*, 2015). Retaining high dihydrochalcone content levels during processing of the rooibos plant material, and also during subsequent thermal treatment of the infusions, are therefore paramount to ensure a rooibos product with maximum biofunctionality.

Table 9 Thermal degradation kinetic studies on other dihydrochalcones and flavonols.

Flavonoids and matrix	Operating conditions	Mathematical model, kinetic order and kinetic parameters	Major findings	Reference
0.05 M phosphate buffer solution (pH 8.0)				
Flavonols quercetin and rutin (1 mM)	Heating under reflux: 97 °C/15-240 min Investigated the effect of dissolved oxygen. Non-oxidative conditions: solutions purged with argon Oxidative conditions: air bubbled into the solution with a sparger during refluxing Investigated the effect of the transition metal ions Fe ²⁺ and Cu ²⁺ on degradation rates (ion concentrations: 0.05-0.2 mM)	First-order kinetic model *Salt-to-flavonol ratios Quercetin non-oxidative: $k_{97\text{ °C}} = 4.3 \times 10^{-5} \text{ s}^{-1}$; oxidative: $k_{97\text{ °C}} = 18.7 \times 10^{-5} \text{ s}^{-1}$. Fe (1:20)*: $k_{97\text{ °C}} = 57.8 \times 10^{-5} \text{ s}^{-1}$; Fe (1:10)*: $k_{97\text{ °C}} = 47.7 \times 10^{-5} \text{ s}^{-1}$; Fe (1:5)*: $k_{97\text{ °C}} = 55.8 \times 10^{-5} \text{ s}^{-1}$. Cu (1:20)*: $k_{97\text{ °C}} = 44.0 \times 10^{-5} \text{ s}^{-1}$; Cu (1:10)*: $k_{97\text{ °C}} = 66.8 \times 10^{-5} \text{ s}^{-1}$; Cu (1:5)*: $k_{97\text{ °C}} = 88.0 \times 10^{-5} \text{ s}^{-1}$. Rutin non-oxidative: $k_{97\text{ °C}} = 6.3 \times 10^{-5} \text{ s}^{-1}$. oxidative: $k_{97\text{ °C}} = 10.3 \times 10^{-5} \text{ s}^{-1}$. Fe (1:20)*: $k_{97\text{ °C}} = 4.0 \times 10^{-5} \text{ s}^{-1}$; Fe (1:10)*: $k_{97\text{ °C}} = 10.8 \times 10^{-5} \text{ s}^{-1}$; Fe (1:5)*: $k_{97\text{ °C}} = 16.2 \times 10^{-5} \text{ s}^{-1}$. Cu (1:20)*: $k_{97\text{ °C}} = 17.5 \times 10^{-5} \text{ s}^{-1}$; Cu (1:10)*: $k_{97\text{ °C}} = 21.0 \times 10^{-5} \text{ s}^{-1}$; Cu (1:5)*: $k_{97\text{ °C}} = 26.3 \times 10^{-5} \text{ s}^{-1}$.	Quercetin and rutin exhibited excellent stability under non-oxidative conditions. The presence of oxygen accelerated the degradation rates, with the degradation rate of quercetin higher than that of rutin. The major degradation product of quercetin was protocatechuic acid. Oxidative conditions provoked a more extensive degradation of rutin, with the formation of a series of products (quercetin not formed). Addition of Fe ²⁺ and Cu ²⁺ increased the oxidative degradation rates for both flavonols. The manner in which Cu ²⁺ acted was dose-dependent. Metal ions could interact more profoundly with quercetin than with rutin, yielding higher <i>k</i> values.	Makris & Rossiter, 2000
Enriched apple juice (11 °Brix, pH 3.6/3.7)				
Dihydrochalcone 2'-β-D-glucopyranosyloxyphloretin (phloridzin)	Accelerated storage conditions: 70-100 °C, 4 days Effect of oxygen concentration: 0, 21 and 100%	First-order kinetic model; Arrhenius equation Dihydrochalcone Reaction rate constant for the non-oxidative degradation ($k_{d,70\text{ °C}}$) of phloridzin at 70 °C (T_{ref}) and the corresponding activation energy ($E_{a,d}$): $k_{d,70\text{ °C}} = 2.3 \times 10^{-3} \text{ h}^{-1}$; $E_{a,d} = 73 \text{ kJ.mol}^{-1}$ Flavonols Reaction rate constants for the hydrolysis ($k_{h,70\text{ °C}}$) of quercetin glycosides at 70 °C (T_{ref}) and the corresponding activation energies ($E_{a,h}$): quercetin-galactoside: $k_{h,70\text{ °C}} = 2.2 \times 10^{-3} \text{ h}^{-1}$; $E_{a,h} = 78 \text{ kJ.mol}^{-1}$ quercetin-rhamnoside: $k_{h,70\text{ °C}} = 2.9 \times 10^{-3} \text{ h}^{-1}$; $E_{a,h} = 74 \text{ kJ.mol}^{-1}$ quercetin-glucoside/rutinoside: $k_{h,70\text{ °C}} = 4.3 \times 10^{-3} \text{ h}^{-1}$; $E_{a,h} = 66 \text{ kJ.mol}^{-1}$ quercetin-arabinoside: $k_{h,70\text{ °C}} = 11.8 \times 10^{-3} \text{ h}^{-1}$; $E_{a,h} = 57 \text{ kJ.mol}^{-1}$ Reaction rate constants for the non-oxidative ($k_{d,70\text{ °C}}$) and oxidative ($k_{o,70\text{ °C}}$) degradation of quercetin at 70 °C (T_{ref}) and the corresponding activation energies: $k_{d,70\text{ °C}} = 1.1 \times 10^{-2} \text{ h}^{-1}$; $E_{a,d} = 31 \text{ kJ.mol}^{-1}$ $k_{o,70\text{ °C}} = 3.8 \times 10^{-2} \text{ h}^{-1}$; $E_{a,o} = 30 \text{ kJ.mol}^{-1}$	Dihydrochalcone Phloridzin only exhibited minor degradation, and was amongst the more thermally stable compounds in apple juice. The presence of oxygen did not affect the thermal stability of phloridzin. The main degradation route for phloridzin in apple juice during accelerated storage was a non-oxidative pathway. Flavonols Quercetin glycosides were amongst the most thermally sensitive compounds in apple juice. Quercetin glycosides showed clear differences in their stability. The stability decreased in the order quercetin-galactoside ≈ quercetin-rhamnoside > quercetin-glucoside/rutinoside > quercetin-arabinoside. The breakdown of quercetin glycosides showed no dependency on oxygen pressure. Quercetin aglycone was formed during the incubation, presumably due to the hydrolysis of quercetin glycosides. Degradation of quercetin showed a clear dependency on the amount of oxygen, indicating an oxidative pathway.	Van der Sluis <i>et al.</i> , 2005

Table 9 cont.

Flavonoids and matrix	Operating conditions	Mathematical model, kinetic order and kinetic parameters	Major findings	Reference
Cloudy apple juice Dihydrochalcones 2'- β -D-glucopyranosyloxy-3-hydroxyphloretin, 2'-(6- β -D-xylopyranosyl- β -D-glucopyranosyloxy)-3-hydroxyphloretin, 2'- β -D-glucopyranosyloxyphloretin Flavonols 3- α -L-arabinopyranosyloxyquercetin, 3- β -D-glucopyranosyloxyquercetin, 3- β -D-xylopyranosyloxyquercetin, 3- α -L-rhamnopyranosyloxyquercetin, 3- β -D-galactopyranosyloxyquercetin	Conventional thermal processing, isothermal: 85-145 °C for 7200 s.	First-order kinetic model; Arrhenius equation ($T_{ref} = 120$ °C) Dihydrochalcones 2'- β -D-glucopyranosyloxy-3-hydroxyphloretin: $k_{120\text{ °C}} = 0.26 \times 10^{-2} \text{ min}^{-1}$; $k_{135\text{ °C}} = 1.01 \times 10^{-2} \text{ min}^{-1}$; $k_{140\text{ °C}} = 1.54 \times 10^{-2} \text{ min}^{-1}$; $k_{145\text{ °C}} = 2.33 \times 10^{-2} \text{ min}^{-1}$; $E_a = 120 \text{ kJ.mol}^{-1}$ 2'-(6- β -D-xylopyranosyl- β -D-glucopyranosyloxy)-3-hydroxyphloretin: $k_{135\text{ °C}} = 1.31 \times 10^{-2} \text{ min}^{-1}$; $k_{140\text{ °C}} = 2.03 \times 10^{-2} \text{ min}^{-1}$; $k_{145\text{ °C}} = 3.13 \times 10^{-2} \text{ min}^{-1}$; $E_a = 124 \text{ kJ.mol}^{-1}$ 2'- β -D-glucopyranosyloxyphloretin: $k_{135\text{ °C}} = 1.08 \times 10^{-2} \text{ min}^{-1}$; $k_{140\text{ °C}} = 1.76 \times 10^{-2} \text{ min}^{-1}$; $k_{145\text{ °C}} = 2.82 \times 10^{-2} \text{ min}^{-1}$; $E_a = 140 \text{ kJ.mol}^{-1}$ Flavonols 3- α -L-arabinopyranosyloxyquercetin: $k_{90\text{ °C}} = 0.37 \times 10^{-2} \text{ min}^{-1}$; $k_{100\text{ °C}} = 0.72 \times 10^{-2} \text{ min}^{-1}$; $k_{120\text{ °C}} = 2.53 \times 10^{-2} \text{ min}^{-1}$; $k_{135\text{ °C}} = 6.48 \times 10^{-2} \text{ min}^{-1}$; $k_{140\text{ °C}} = 8.74 \times 10^{-2} \text{ min}^{-1}$; $k_{145\text{ °C}} = 11.7 \times 10^{-2} \text{ min}^{-1}$; $E_a = 75.9 \text{ kJ.mol}^{-1}$ 3- β -D-glucopyranosyloxyquercetin: $k_{90\text{ °C}} = 0.33 \times 10^{-2} \text{ min}^{-1}$; $k_{100\text{ °C}} = 0.79 \times 10^{-2} \text{ min}^{-1}$; $k_{120\text{ °C}} = 3.88 \times 10^{-2} \text{ min}^{-1}$; $k_{135\text{ °C}} = 11.7 \times 10^{-2} \text{ min}^{-1}$; $k_{140\text{ °C}} = 16.5 \times 10^{-2} \text{ min}^{-1}$; $k_{145\text{ °C}} = 23.2 \times 10^{-2} \text{ min}^{-1}$; $E_a = 97.3 \text{ kJ.mol}^{-1}$ 3- β -D-xylopyranosyloxyquercetin: $k_{90\text{ °C}} = 0.31 \times 10^{-2} \text{ min}^{-1}$; $k_{100\text{ °C}} = 0.80 \times 10^{-2} \text{ min}^{-1}$; $k_{120\text{ °C}} = 4.65 \times 10^{-2} \text{ min}^{-1}$; $k_{135\text{ °C}} = 15.5 \times 10^{-2} \text{ min}^{-1}$; $k_{140\text{ °C}} = 22.7 \times 10^{-2} \text{ min}^{-1}$; $k_{145\text{ °C}} = 32.9 \times 10^{-2} \text{ min}^{-1}$; $E_a = 107 \text{ kJ.mol}^{-1}$ 3- α -L-rhamnopyranosyloxyquercetin: $k_{120\text{ °C}} = 0.77 \times 10^{-2} \text{ min}^{-1}$; $k_{135\text{ °C}} = 3.2 \times 10^{-2} \text{ min}^{-1}$; $k_{140\text{ °C}} = 5.02 \times 10^{-2} \text{ min}^{-1}$; $k_{145\text{ °C}} = 7.81 \times 10^{-2} \text{ min}^{-1}$; $E_a = 169 \text{ kJ.mol}^{-1}$ 3- β -D-galactopyranosyloxyquercetin: $k_{120\text{ °C}} = 0.30 \times 10^{-2} \text{ min}^{-1}$; $k_{135\text{ °C}} = 1.69 \times 10^{-2} \text{ min}^{-1}$; $k_{140\text{ °C}} = 2.91 \times 10^{-2} \text{ min}^{-1}$; $k_{145\text{ °C}} = 4.95 \times 10^{-2} \text{ min}^{-1}$; $E_a = 162 \text{ kJ.mol}^{-1}$	Dihydrochalcones Some of the most heat-resistant compounds in cloudy apple juice belong to the dihydrochalcone phenolic sub-class; only started degrading at temperatures ≥ 120 °C 2'- β -D-glucopyranosyloxyphloretin, in particular, was found to be very resistant to thermal degradation over a temperature range of 135-145 °C. The thermal stability decreased in the order: 2'- β -D-glucopyranosyloxyphloretin > 2'-(6- β -D-xylopyranosyl- β -D-glucopyranosyloxy)-3-hydroxyphloretin > 2'- β -D-glucopyranosyloxy-3-hydroxyphloretin. Flavonols A clear difference in k between the various quercetin glycosides was observed. The stability decreased in the order: 3- β -D-galactopyranosyloxyquercetin > 3- α -L-rhamnopyranosyloxyquercetin > 3- β -D-xylopyranosyloxyquercetin > 3- β -D-glucopyranosyloxyquercetin > 3- α -L-arabinopyranosyloxyquercetin.	De Paepe <i>et al.</i> , 2014

Rooibos plant material is “fermented” to develop the characteristic sensory qualities associated with the traditional herbal tea (oxidised form). The fermentation process typically entails shredding and bruising of the plant material, followed by open-air heap fermentation and sun drying. The process induces substantial quantitative changes in the phenolic composition of rooibos; in particular, significant reductions in the dihydrochalcone contents (Joubert, 1996). During fermentation, aspalathin is photochemically and enzymatically converted via its flavanone analogues [(*R*)- and (*S*)-6- β -D-glucopyranosyl-eriodictyol (dihydro-isoorientin), and (*R*)- and (*S*)-8- β -D-glucopyranosyl-eriodictyol (dihydro-orientin)] to isoorientin and orientin. Whereas dihydro-isoorientin oxidises to form isoorientin, the same conversion does not occur for dihydro-orientin and orientin; rather, orientin is formed irreversibly by the Wessely-Moser rearrangement from isoorientin (as reviewed by Joubert & De Beer, 2014).

During oxidation under non-enzymatic and aerated conditions (0.2 M phosphate buffer solution, pH 7.4; 37 °C), aspalathin and nothofagin are also degraded to higher molecular weight browning products (as reviewed by Joubert & De Beer, 2014). Colourless aspalathin dimers were identified in the reaction mixture and these dimers eventually completely degraded to brown end products with the characteristic absorbance maximum at 450 nm. Several other compounds formed in parallel in the reaction mixture, of which two were identified as the colored dibenzofurans, (*S*)- and (*R*)-3-(7,9-dihydroxy-2,3-dioxo-6- β -D-glucopyranosyl-3, 4-dihydrobenzo[*b,d*]furan-4*a*(2*H*)-yl) propionic acid, with maximum absorbance at 430 nm. These compounds were reactive intermediates and were degraded within 60 h, giving rise to high-molecular weight tannin-like structures. Oxidation of nothofagin, differing only from aspalathin by lacking the ortho-dihydroxy function on the B-ring, proceeded much more slowly, and this comparably slow degradation was also observed for orientin and isoorientin. It was therefore concluded that, in addition to the *o*-hydroquinone moiety of the B-ring, the C-2 configuration is of major importance to oxidation (Joubert & De Beer, 2014).

All fermented (oxidised) rooibos plant material that is exported, is also subjected to elevated temperatures during steam-pasteurisation, required as a de-contamination step to ensure microbial loads of an acceptable level. A study by Koch *et al.* (2013), regarding the effect of steam-pasteurisation (96 °C for 1 min) of rooibos leaves on the composition of aqueous rooibos infusions, demonstrated small, but significant, reductions in the aspalathin content.

The stability of aspalathin and its corresponding flavones, orientin and isoorientin, in fermented (Joubert *et al.*, 2009) and green (Joubert *et al.*, 2010) rooibos iced tea formulations has been assessed during different heat treatments including pasteurisation (93 °C/30 min), normal-temperature sterilisation (NTS, 121 °C/15 min) and high-temperature sterilisation (HTS, 135 °C/4 min). Sterilisation treatments were conducted in an autoclave and therefore included additional heat exposure during heating and cooling phases. Whereas pasteurisation had no or little effect on the flavonoid content, sterilisation significantly reduced the aspalathin, orientin and isoorientin contents of the rooibos iced tea formulations. Heat-induced losses of isoorientin and orientin were lower than those observed for aspalathin and conversion of aspalathin to its flavone analogues, off-setting their degradation, was implicated. Similarly, orientin appeared to be more thermally stable than its regio-isomer isoorientin during sterilisation, but this was attributed to the irreversible conversion of isoorientin to orientin (Krafczyk & Glomb, 2008), which would have off-set losses in orientin during heating. The addition of ascorbic acid and/or citric acid to the base iced tea formulations (containing only green or fermented rooibos extract and sugar) improved the thermal stability of the flavonoids and proved to be beneficial for the retention of aspalathin, especially during the sterilisation treatments (Joubert *et al.*, 2009, 2010). This was attributed to the lower pH of the iced tea formulations containing ascorbic acid and/or citric acid (*ca.* 2.80-2.95 as opposed to a pH of 4.40-5.05 of the base iced tea formulations), and to the role of ascorbic acid as reducing agent. Lowering of the pH confers greater stability to aspalathin due to protonation of the hydroxy groups at lower pH, which reduces its oxidation potential (Lemańska *et al.*, 2001). Interestingly, aspalathin was more thermally stable in rooibos iced tea formulations

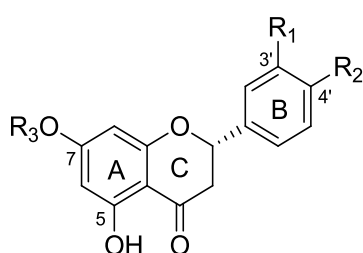
containing the aspalathin-enriched green rooibos extract, compared to formulations with the fermented rooibos extract. Compositional differences between the extract types were implicated (Joubert *et al.*, 2009; 2010).

In accordance with the high-temperature findings, the stability of aspalathin during subsequent storage of the (heat-treated) rooibos iced tea formulations (25 °C/12 weeks) was also shown to depend on product formulation and extract type (De Beer *et al.*, 2011). During short-term storage (48 h) of the same iced tea formulations, storage temperature and pH were shown to be crucial factors for aspalathin stability (De Beer *et al.*, 2011). The aspalathin content in fermented rooibos iced teas generally decreased with increasing pH (pH 3 to 5) and storage temperature (from 5 to 40 °C), while these factors did not affect the levels of aspalathin in iced tea formulations containing green rooibos extract or green rooibos extract/ascorbic acid solubilisate (*i.e.*, nano-emulsion). In a recent study by De Beer and co-workers (De Beer *et al.*, 2015), the effect of pH on the stability of aspalathin and nothofagin in sodium phosphate buffers (0.2 M) was assessed at room temperature/25 °C over a period of 29 h. Both aspalathin and nothofagin were completely stable at pH 3, while nothofagin was also stable at pH 5 and 6. The increased stability of nothofagin was attributed to the absence of a catechol group on the B-ring, which decreases its oxidation potential (Bors *et al.*, 1995). Aspalathin was extremely sensitive to changes in pH, with losses amounting to 9, 14 and 55% after 29 h in phosphate buffer solutions with pH adjusted to 5, 6 and 7, respectively (De Beer *et al.*, 2015).

3.3.2. Flavanones

Flavanones represent the major citrus polyphenols and are primarily responsible for the beneficial effects associated with the consumption of *Citrus* fruits and juices (Khan *et al.*, 2014). Honeybush herbal tea, prepared from various *Cyclopia* species, also contains a number of flavanones (refer to Table 1, page 9), of which hesperidin, with well-known pharmacological activity (as reviewed by Garg *et al.*, 2001), represents one of the major phenolic constituents.

Information on the thermal degradation kinetics of flavanones is very limited – only the degradation of hesperidin (7-rutinosyloxyhesperetin; Figure 13) has been kinetically assessed to date. Dhuique-Mayer *et al.* (2007) showed no significant degradation of hesperidin in citrus juice upon thermal treatment (losses < 2% after 240 min at 90 °C), and consequently no kinetic parameters could be derived. The thermal stability of hesperidin therefore appears to be very high in the temperature range of 70-90 °C.



	R₁	R₂	R₃
Hesperetin	OH	OCH ₃	H
Hesperidin (7-rutinosyloxyhesperetin)	OH	OCH ₃	rutinosyl*
Naringenin	H	OH	H
Naringin (7-neohesperidosyloxynaringenin)	H	OH	neohesperidosyl**
Eriocitrin (7-rutinosyloxyeriodictyol)	OH	OH	rutinosyl*
Neocitrin (7-neohesperidosyloxyeriodictyol)	OH	OH	neohesperidosyl**

Figure 13 Substitution pattern of selected flavanones. *6- α -L-rhamnopyranosyloxy- β -D-glucopyranosyl. **2- α -L-rhamnopyranosyloxy- β -D-glucopyranosyl.

This high thermal stability of hesperidin has also been demonstrated in a flavanone glycoside-enriched extract of *C. maculata*, where it remained stable upon heating of an aqueous ethanolic extract at 90 °C for 90 min (Du Preez, 2014). However, subjecting the same extract to the same thermal conditions, but with acidification (0.295 M HCl), induced hydrolysis of hesperidin to 7- β -D-glucopyranosyloxyhesperetin, followed by further deglycosylation and formation of hesperetin aglycone. These conversion reactions were significantly accelerated at increased acid concentration and increased temperatures (Du Preez, 2014). The content of hesperidin in aqueous extract prepared from unfermented (green) *Cyclopia* plant material has also been shown to be reduced following “fermentation” (high-temperature oxidation; 70 °C/60 h) of *Cyclopia* plant material. Aqueous extracts prepared from fermented *C. intermedia*, *C. subternata* and *C. genistoides* contained significantly less hesperidin (ca. 36-60%) than extracts prepared from their unfermented counterparts, while the content of hesperidin in *C. sessiliflora* extracts was not significantly reduced (ca. 10% loss) (Joubert *et al.*, 2008b).

No studies have been conducted to explore structure-stability relationships for the flavanone phenolic sub-class, but investigation of the effect of thermal pasteurisation on the contents of individual flavanones (Figure 13) in orange juice indicated that substituents on the A- and B-rings significantly affect the thermal stability of flavanones. Sánchez-Moreno *et al.* (2005) reported that low temperature pasteurisation (70 °C/30 s) and high temperature pasteurisation (90 °C/60 s) treatments did not affect the hesperetin content of orange juice, but significantly reduced its naringenin content. Agcam *et al.* (2014) showed that thermal pasteurisation (90 °C/10 s) had no significant effect on the contents of hesperidin, neohesperidin, eriocitrin and neoeriocitrin in orange juice, while the naringenin content was significantly reduced and that of naringin significantly increased. Further research is, however, required to elucidate structure-stability relationships for these flavanones.

3.3.3. Dihydroflavonols

Zhang *et al.* (2013b) investigated the effect of B-ring substitution on the thermal stability of the dihydroflavonol rhamnosides astilbin and engeletin (Figure 14) over the temperature range 4-55 °C. Their degradation in aqueous media (0.2 M phosphate buffer, pH 7.0) followed a first-order kinetic model and the degradation rates increased with increasing temperature. Engeletin, with a 4'-hydroxy-substituted B-ring, was more stable than astilbin with a 3',4'-dihydroxy-substituted B-ring. The main isomerisation product of astilbin was neoastilbin, while neoastilbin and isoastilbin only formed at elevated temperatures (> 45 °C). Subsequent decomposition of neoastilbin also occurred and this too was accelerated by increased temperature.

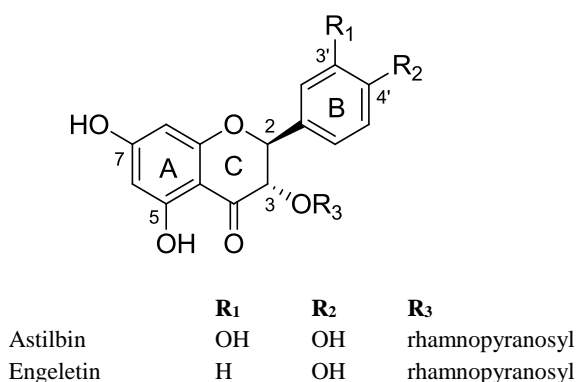


Figure 14 Substitution pattern of the dihydroflavonol rhamnosides, astilbin and engeletin.

The degradation of astilbin and engeletin were found to be pH-dependent, while the stability of astilbin was also affected by the type of solvent (Zhang *et al.*, 2013b). Astilbin and engeletin were fairly stable during storage at 18 °C in aqueous

solutions with pH 3.0-5.0, while their first-order degradation rate constants increased as the pH increased from 7.0 to 10.0. Under alkaline conditions, preferential isomerisation of astilbin to neoastilbin occurred, together with hydrolysis of the rhamnose moiety of astilbin leading to the formation of the aglycone, taxifolin. The stability of astilbin in different solvents, assessed at 85 °C, followed the order 50% aqueous ethanol > ethanol > methanol > 50% aqueous methanol > water. Astilbin was furthermore shown to be less stable in cultural media than in water, even at 25 °C, and the stability followed the order RPMI 1640 > high-glucose Dulbecco's modified Eagle's medium (DMEM) > low-glucose DMEM. A possible explanation was given that cultural media contain many metal ions, such as Fe²⁺, Ca²⁺, and Mg²⁺, which may chelate the B-ring *o*-dihydroxy groups of astilbin and accelerate its oxidation.

3.3.4. Flavonols

The thermal stability of flavonol aglycones (Figure 15) appear to be quite high and, as such, losses during thermal pasteurisation of fruit juices have been shown to be quite small. Thermal pasteurisation treatment of strawberry juice (90 °C/30 and 60 s) did not affect its kaempferol, quercetin and myricetin contents (Odriozola-Serrano *et al.*, 2008). Similarly thermal pasteurisation of orange juice (90 °C/10 and 20 s) had no significant effect on the contents of kaempferol, quercetin and quercetin *O*-glycosyl compounds (Agcam *et al.*, 2014). Rohn *et al.* (2007) demonstrated that application of dry heat (180 °C/60 min) did not induce significant degradation in quercetin.

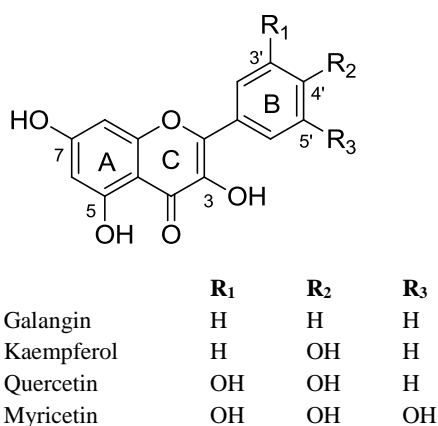


Figure 15 Substitution pattern of selected flavonol aglycones.

Rutin (3-rutinosyloxyquercetin) is relatively stable during heating of an aqueous ethanolic solution at 100 °C, but it rapidly decomposes at elevated temperatures of 180 °C (Murakami *et al.*, 2004). The low stability of rutin during roasting of buckwheat (*Fagopyrum esculentum* Moench L.) groats at high temperature (160 °C/30 min) has also been reported, with the rutin content of raw groats approximately six-fold higher than that found in the roasted groats. However, under these conditions, rutin was thermally more stable than the flavone glucosides isovitexin, orientin and isoorientin (Zielinski *et al.*, 2009). An increase in the dehulling time (10-130 min) at 150 °C leads to greater losses of rutin in the same product grains (Dietrych-Szostak & Oleszek, 1999).

The thermal stability of quercetin and its glycosides have been studied widely, and selected findings from those studies that utilised thermal degradation kinetics modelling are presented in Table 9 (pp. 48-49). Makris & Rossiter (2000) studied the oxidative degradation of quercetin and its corresponding 3-rutinosyloxy derivative, rutin, in phosphate buffer solutions (pH 8.0) at 97 °C over a period of 240 min. Kinetic data have also been reported, describing the stability of quercetin and various glycosylated derivatives during accelerated storage (70-100 °C/4 days; Van der Sluis *et al.*, 2005) and conventional thermal processing (85-145 °C/7200 s; De Paepe *et al.*, 2014) of apple juices. Collectively, these studies

indicate that the thermal degradation of quercetin derivatives follow first-order reactions, and that the effect of temperature on the reaction rate constants can adequately be described by the Arrhenius equation (Table 9).

Oxidative reaction pathways for the degradation of quercetin in aqueous solution have been proposed by Buchner *et al.* (2006). Cleavage of quercetin is possible (pathway I), leading to the formation of 3-(3,4-dihydroxyphenyl)-3-hydroxy-2-oxopropanal and protocatechuic acid as degradation products. Nucleophilic addition products of quercetin were, however, also detected by HPLC/DAD/MSⁿ, and thus a second reaction pathway was proposed. It was postulated that quercetin is oxidised to a quinoic structure, followed by the addition of solvent molecules (pathway II). Evidence for such behaviour has also been given by Hvattum *et al.* (2004). Buchner *et al.* (2006) identified hydroxylated and methoxylated derivatives, stemming from the oxidation of the 2,3-double bond of the flavonol C-ring, and a furanone. Makris & Rossiter (2000) identified protocatechuic acid as the major degradation product of quercetin, supporting pathway I.

With regard to quercetin *O*-glycosyl compounds, reaction conditions markedly affect their degradation pathways. Under dry heating conditions (roasting at 180 °C), quercetin monoglycosides are typically deglycosylated to form the aglycone, which then remains stable upon further heating (Rohn *et al.*, 2007). Degradation of rutin and 3,4'-di- β -D-glucopyranosyloxyquercetin first proceeds via mono-glucopyranosyloxy intermediates, namely 3- β -D-glucopyranosyloxyquercetin and 4'- β -D-glucopyranosyloxyquercetin, respectively (Rohn *et al.*, 2007). Quercetin aglycone was also formed during the accelerated storage of apple juice (70-100 °C), presumably due to the hydrolysis of quercetin glycosides (Van der Sluis *et al.*, 2005). Conversely, heating of rutin in aqueous model systems (pH 8.0) does not lead to the formation of the aglycone, but rather to the formation of a series of products (Makris & Rossiter, 2000; Buchner *et al.*, 2006).

It has furthermore been suggested that the reaction pathways are independent of the flavonol concentration in an aqueous model system (Buchner *et al.*, 2006), but that they are affected by the type of organic solvent (*e.g.* methanol vs acetonitrile; Hvattum *et al.*, 2004). The food matrix can also affect the nature of the flavonol degradation products (Rohn *et al.*, 2007). To investigate the influence of the food matrix, lyophilized onions were roasted under the same conditions as used for model experiments (dry roasting, 180 °C). Although the changes in 3,4'-di- β -D-glucopyranosyloxyquercetin, 4'- β -D-glucopyranosyloxyquercetin and quercetin contents were similar to what was expected from the model experiments, several other reaction products arose. Since the food matrix is very complex it was suggested that the new products resulted from reactions with other food constituents. It is known from literature that the oxidation of flavonoids leads to semiquinoid intermediates and the respective quinones. The quinone, being a highly reactive electrophile intermediate, can easily undergo attack by nucleophilic food components. Proteins, in particular, have been shown to interact in diverse mechanisms with phenolic compounds and their respective quinones (as reviewed by Kroll *et al.*, 2003).

The stability of flavonols is principally determined by their structure, while the effects of transition metal ions (Fe²⁺ and Cu²⁺) and oxygen on the degradation rates of selected flavonols have also been assessed kinetically (Table 9). During thermal processing, under oxidative conditions in aqueous media, quercetin is typically degraded more extensively than rutin (Makris & Rossiter, 2000; Buchner *et al.*, 2006). The higher stability of rutin has been attributed to the blockage of the C-3 hydroxy group by the sugar moiety, which prevents the formation of the carbanion (Tournaire *et al.*, 1994, as cited by Buchner *et al.*, 2006). The thermal stability of quercetin glycosides depends both on the position of glycosylation and the nature of the sugar moiety. Under dry roasting conditions (180 °C), the sugar attached to the C-ring of the flavan skeleton (3-*O*-position) was more susceptible to deglycosylation than when attached to the B-ring (4'-*O*-position), leading to the higher thermal stability of 4'- β -D-glucopyranosyloxyquercetin as opposed to 3- β -D-glucopyranosyloxyquercetin (Rohn *et al.*, 2007). Under these conditions, the stability of quercetin glycosides with the same bond position decreased in the order: 3- β -D-galactopyranosyloxyquercetin > 3-rutinosyloxyquercetin > 3- β -D-glucopyranosyloxyquercetin > 3- α -L-rhamnopyranosyloxyquercetin (Rohn *et al.*, 2007). Van der Sluis *et al.* (2005) and De Paepe *et al.* (2014) also

observed clear differences in the degradation kinetic parameters of different quercetin glycosides in apple juices during heat treatments, and this was attributed to the differences in susceptibility of the glycosidic bond to hydrolysis in an acidic environment. The thermal stability of quercetin glycosides typically decreased in the order: 3- β -D-galactopyranosyloxyquercetin > 3- α -L-rhamnopyranosyloxyquercetin > 3- β -D-xylopyranosyloxyquercetin > 3- β -D-glucopyranosyloxyquercetin > 3- α -L-arabinopyranosyloxyquercetin (Van der Sluis *et al.*, 2005; De Paepe *et al.*, 2014). While no research has been conducted to investigate the effect of B-ring substitution on the thermal stability of flavonols, data presented by Maini *et al.* (2012) demonstrated that the number of B-ring hydroxy groups is inversely related to flavonol UVA stability. The general pattern of flavonol stability was established as galangin > kaempferol > quercetin > myricetin (Maini *et al.*, 2012).

Iron(II) and copper(II) are the most abundant transition metal ions in plant tissues and, as such, their impact on the thermal stability of bio-active compounds in actual plant products and model systems has been assessed. Addition of Fe²⁺ and Cu²⁺ caused an increase in the oxidative degradation rate of quercetin and rutin in aqueous model systems (Makris & Rossiter, 2000; Table 9). The manner in which Cu²⁺ acted was dose-dependent, with increasing ion concentration (0.05-0.2 mM) leading to increased degradation rates. With regard to the effect of oxygen, Van der Sluis *et al.* (2005) demonstrated that the hydrolysis of quercetin glycosides showed no dependency on oxygen pressure, while the degradation of quercetin showed a clear dependency on the amount of oxygen, indicative of an oxidative pathway. Conversely, Makris & Rossiter (2000) and Buchner *et al.* (2006) demonstrated that both quercetin and rutin are very susceptible to thermally induced degradation under oxidative conditions as assessed in aqueous model solutions (pH 8.0) at 97-100 °C. Metal ions were postulated to promote flavonol oxidation through the formation of reactive oxygen species (ROS; Makris & Rossiter, 2000). Similarly, the accelerated decay of quercetin and rutin in the presence of oxygen has also been attributed to ROS (Buchner *et al.*, 2006).

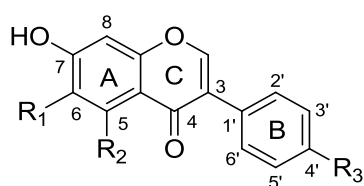
Other factors such as the pH of the reaction medium, the presence of other phytochemicals in the reaction medium, and the composition of the atmosphere (in a closed system) also have a significant impact on the thermal stability of flavonols. Thermal degradation of quercetin and rutin increased under weak basic conditions (pH 8) as opposed to near neutral conditions (pH 5) upon thermal treatment of aqueous solutions at 100 °C with air perfusion (Buchner *et al.*, 2006). Decomposition of rutin in aqueous ethanolic solution was almost totally inhibited at 100 °C by the presence of chlorogenic acid and markedly reduced at 180 °C (Murakami *et al.*, 2004). This protective effect offered by chlorogenic acid was attributed to the fact that chlorogenic acid is an ester, and that it is thereby probably more easily decomposed than rutin. As stated previously, the degradation of 3,4'-di- β -D-glucopyranosyloxyquercetin under dry heating conditions (180 °C) proceeds via a mono-glucopyranosyloxy intermediate, 4'- β -D-glucopyranosyloxyquercetin, which is further converted to the respective aglycone (Rohn *et al.*, 2007). By flushing the ampoules with gaseous nitrogen instead of free exposure to air, the second step proceeded much slower, indicating that (besides differences in the stability of the glycosidic bonds, as discussed previously) oxidative effects might play a role during deglycosylation (Rohn *et al.*, 2007).

3.3.5. Flavones

To date, no kinetic studies on the thermal stability of flavones, either in model systems, natural plant extracts or food and beverage products, have been conducted at elevated temperatures. Results presented by Murakami *et al.* (2004) have, however, demonstrated that luteolin and 7- β -D-glucopyranosyloxy-luteolin (Figure 16) are generally stable during heating of aqueous ethanolic solutions at 100 °C for 360 min. It has also been reported that luteolin and its 3'-deoxy derivative, apigenin, remained stable during pasteurisation of orange juice at 90 °C for 10 or 20 s (Agcam *et al.*, 2014). Similarly, pasteurisation (93 °C/30 min) had no or little effect on the levels of orientin (8- β -D-glucopyranosylluteolin; Figure 16) and isoorientin (6- β -D-glucopyranosylluteolin; Figure 16) in rooibos iced tea formulations (Joubert *et al.*, 2009; 2010).

3.4. Isoflavones

Isoflavones are phytoestrogens with potent estrogenic activity (as reviewed by Vitale *et al.*, 2013), and their greatest dietary source is soy (*Glycine max* L. Merrill) (Manach *et al.*, 2004). The main isoflavones found in soybeans are genistein, daidzein and glycitein, each of which exists in four different chemical forms, namely as an aglycone (genistein, daidzein and glycitein; Figure 17), a β -glucoside (genistin, daidzin and glycitin), an acetylglucoside (6''-O-acetylgenistin, 6''-O-acetyl daidzin and 6''-O-acetylglycitin) and a malonylglucoside (6''-O-malonylgenistin, 6''-O-malonyl daidzin and 6''-O-malonylglycitin). The glycosidic forms have a β -D-glucopyranosyl moiety linked to the C-7 hydroxy group (Figure 17) and the conjugated forms have either a malonyl group (-COCH₂COOH) or an acetyl group (-COCH₃) esterified at the 6''-O- of the sugar moiety. Red clover (*Trifolium pratense* L.), used for preparation of phytoestrogenic nutraceuticals (Dornstauder *et al.*, 2001; Beck *et al.*, 2005), also represents a rich source of isoflavones, of which the most common aglycones include formononetin and biochanin A. They differ from the soy isoflavone aglycones with regard to the B-ring substituent at C-4' (Figure 17).



	R₁	R₂	R₃
Daidzein	H	H	OH
Genistein	H	OH	OH
Glycitein	OCH ₃	H	OH
Formononetin	H	H	OCH ₃
Biochanin A	H	OH	OCH ₃

Figure 17 Substitution pattern of the major soy and red clover isoflavone aglycones.

The production of soy-based foods involves several types and intensities of processing conditions, which have a substantial effect on its isoflavone constituents (as reviewed by Villares *et al.*, 2011). The thermal stability of isoflavones has been assessed during a wide range of processes including extrusion processing of soy protein mixtures (Mahungu *et al.*, 1999; Singletary *et al.*, 2000), dry heating (Yuan *et al.*, 2009), drying (Lee & Lee, 2009; Niamnuy *et al.*, 2011) and steaming (Huang & Chou, 2008) of whole soybeans, dry heating of steamed black soybeans and black soybean koji (Huang & Chou, 2008), roasting and explosive puffing processing of soybean (Lee & Lee, 2009), heating of soy milk (Murphy *et al.*, 2002; Huang *et al.*, 2006), toasting of soybean powder (Murphy *et al.*, 2002) and extraction of isoflavones from commercially available soy food materials at elevated temperatures (Kudou *et al.*, 1991; Coward *et al.*, 1993; Barnes *et al.*, 1994; Coward *et al.*, 1998). The effects of processing techniques on the distribution of isoflavones (*i.e.*, changes in the respective compound pattern/different chemical forms) have also been investigated during the preparation of tempeh, soymilk, tofu and protein isolate, where the production of the first three products utilised heat processing (Wang & Murphy, 1996). Coward *et al.* (1998) studied the chemical modification of isoflavones in soy foods during cooking and processing. Grün *et al.* (2001) assessed the thermal stabilities of daidzein, genistein and their conjugates during thermal treatment of tofu. Zhang *et al.* (2004) characterised the changes in isoflavone isomer distribution during the soy breadmaking process. Due to the complex nature of these soy matrices, studies on the thermal stability of isoflavones have also been conducted on isolated soy isoflavones as a dry residu (Xu *et al.*, 2002) and in aqueous model systems (Mathias *et al.*, 2006).

These studies indicated that both the content and profile of isoflavones depend on processing temperature and time. Upon mild thermal treatment, soy isoflavones are subject to interconversion reactions between different chemical forms, and the total isoflavone content generally remains constant or is reduced only slightly. The major chemical reactions that occur include decarboxylation of malonylglucosides to produce acetylglucosides, while both malonyl- and acetylglucosides can be transformed to underivatized/non-conjugated β -glucosides via a de-esterification reaction. Also, the glucopyranosyl moiety of malonyl-, acetyl- and β -glucosides can be hydrolysed to generate the basic aglycone structure. These interconversion and degradation reactions (with concomitant losses in total isoflavone content) are accelerated at elevated temperatures.

Other thermally-induced chemical reactions may include acetylation of underivatized β -glucosides (Xu *et al.*, 2002), and the Maillard reaction (Davies *et al.*, 1998). Xu *et al.* (2002) reported that heating of a dry residue of daidzin, genistin and glycitin (temperatures > 135 °C) produced acetyldaidzin and acetylgenistin, as well as the aglycones daidzein, genistein and glycitein. The generation of acetyldaidzin and acetylgenistin was unexpected and the authors postulated that acetyl groups may have been produced during thermal degradation of the original glucosides, with subsequent acetylation of daidzin and genistin during heating. The rate of binding of an acetyl group to form acetyldaidzin or acetylgenistin from daidzin and genistin, respectively, was found to be higher than the rate of loss of a glucoside group to form the corresponding aglycones, daidzein and genistein. Davies *et al.* (1998) reported that genistein forms Maillard browning products during its autodegradation or reaction with the available amino acid groups of lysine during incubation at 60 °C and pH 9. This non-enzymatic browning reaction followed zero-order reactions (based on spectrophotometric absorbance measurement at 420 nm), and the addition of lysine approximately doubled the rate of browning. The rate of browning paralleled the rate of genistein loss, suggesting that genistein is a reactant in non-enzymatic browning reactions. This is in accordance with the results of a previous study by Wang *et al.* (1990), showing that genistein formed conjugates with very high UV absorption when mixed with dextrose, fructose, maltose, or sucrose, and the amount of conjugate formed was proportional to the amount of sugar added.

In addition to heat, the interconversion and degradation reactions of isoflavones can be accelerated or prompted into a particular direction by altering the pH (Wang *et al.*, 1990; Mathias *et al.*, 2006; Vaidya *et al.*, 2007), by matrix effects (Huang & Chou, 2008; Yuan *et al.*, 2009), the presence of other components (*e.g.* sugar and butter; Coward *et al.*, 1998), as well as moist heating (liquid soy foods) vs dry heating (solid soy matrix) conditions. For instance, decarboxylation of malonylglucosides and the concomitant formation of acetylglucoside conjugates is normally favoured under dry heating conditions, whilst moist heat typically produces conversion to the β -glucoside conjugates (de-esterification) (Coward *et al.*, 1998; Grün *et al.*, 2001; Murphy *et al.*, 2002; Zhang *et al.*, 2004). These observations have been confirmed in a study where the effect of moist vs dry heating on the conversion and degradation of isoflavones was kinetically assessed in model systems (Chien *et al.*, 2005).

While numerous researchers have characterised the changes in isoflavone content and distribution as a function of thermal processes, kinetic data that mathematically explain the interconversion and degradation reactions remain rather limited. To date, most kinetic studies have been conducted in aqueous model systems or on dry residues of isoflavones during heat treatment over a temperature range of 60-200 °C (Ungar *et al.*, 2003; Chien *et al.*, 2005; Stintzing *et al.*, 2006; Vaidya *et al.*, 2007; Yue *et al.*, 2010) (Table 10). In most of these studies, the specific temperature-time regimes were selected to represent thermal processing conditions of real soy products and isoflavones from the genistein- and daidzein-series were used as target compounds. Eisen *et al.* (2003) assessed the thermal stability of genistin during storage of soymilk at elevated temperatures (70-90 °C) and more recently Niamnuy *et al.* (2012) studied the conversion and degradation of the genistein-series isoflavones during drying of soybean (50-150 °C) (Table 10).

Table 10 Kinetic data for thermal degradation and interconversion reactions of isoflavones.

Isoflavone and matrix	Operating conditions	Mathematical model, kinetic order and kinetic parameters	Major findings	Reference
FOOD PRODUCTS				
UHT soy milk (pH 6.6)				
Genistin	Storage at elevated temperatures: 70 °C/59 days, 80 °C/35 days, 90 °C/35 days.	First-order degradation kinetic model; Arrhenius equation $k_{70\text{ °C}} = 61.055 \times 10^3 \text{ days}^{-1}$; $k_{80\text{ °C}} = 77.845 \times 10^3 \text{ days}^{-1}$; $k_{90\text{ °C}} = 109.162 \times 10^3 \text{ days}^{-1}$; $E_a = 73.64 \text{ kJ.mol}^{-1}$	A similar experimental setup for ambient temperature (15-37 °C) revealed the same degradation pattern. The low value for E_a may indicate some type of oxidation reaction.	Eisen <i>et al.</i> , 2003 ^a
Fresh soybean (<i>Glycine max</i> L. Merrill)				
Malonylgenistin, acetylgenistin, genistin and genistein.	Gas-fired infrared combined with hot air vibrating drying (GFIR-HAVD). Drying temperatures: 50, 70, 130 and 150 °C.	First-order kinetic models; Arrhenius equation. k_1 , malonylgenistin → acetylgenistin: $k_{50\text{ °C}} = 0.02 \times 10^5 \text{ s}^{-1}$; $k_{70\text{ °C}} = 0.07 \times 10^5 \text{ s}^{-1}$; $k_{130\text{ °C}} = 0.15 \times 10^5 \text{ s}^{-1}$; $k_{150\text{ °C}} = 0.25 \times 10^5 \text{ s}^{-1}$; $E_a = 24.82 \text{ kJ.mol}^{-1}$ k_2 , malonylgenistin → genistin: $k_{50\text{ °C}} = 13.23 \times 10^5 \text{ s}^{-1}$; $k_{70\text{ °C}} = 25.17 \times 10^5 \text{ s}^{-1}$; $k_{130\text{ °C}} = 73.35 \times 10^5 \text{ s}^{-1}$; $k_{150\text{ °C}} = 198.53 \times 10^5 \text{ s}^{-1}$; $E_a = 27.91 \text{ kJ.mol}^{-1}$ k_3 , malonylgenistin → genistein: $k_{50\text{ °C}} = 2.43 \times 10^5 \text{ s}^{-1}$; $k_{70\text{ °C}} = 4.83 \times 10^5 \text{ s}^{-1}$; $k_{130\text{ °C}} = 18.17 \times 10^5 \text{ s}^{-1}$; $k_{150\text{ °C}} = 20.53 \times 10^5 \text{ s}^{-1}$; $E_a = 24.66 \text{ kJ.mol}^{-1}$ k_4 , malonylgenistin → degraded products D ₁ : $k_{50\text{ °C}} = 1.80 \times 10^5 \text{ s}^{-1}$; $k_{70\text{ °C}} = 2.77 \times 10^5 \text{ s}^{-1}$; $k_{130\text{ °C}} = 5.85 \times 10^5 \text{ s}^{-1}$; $k_{150\text{ °C}} = 14.22 \times 10^5 \text{ s}^{-1}$; $E_a = 23.15 \text{ kJ.mol}^{-1}$ k_5 , acetylgenistin → genistin: $k_{50\text{ °C}} = 11.35 \times 10^5 \text{ s}^{-1}$; $k_{70\text{ °C}} = 21.68 \times 10^5 \text{ s}^{-1}$; $k_{130\text{ °C}} = 60.03 \times 10^5 \text{ s}^{-1}$; $k_{150\text{ °C}} = 161.72 \times 10^5 \text{ s}^{-1}$; $E_a = 27.20 \text{ kJ.mol}^{-1}$ k_6 , acetylgenistin → genistein: $k_{50\text{ °C}} = 2.05 \times 10^5 \text{ s}^{-1}$; $k_{70\text{ °C}} = 6.17 \times 10^5 \text{ s}^{-1}$; $k_{130\text{ °C}} = 16.15 \times 10^5 \text{ s}^{-1}$; $k_{150\text{ °C}} = 18.07 \times 10^5 \text{ s}^{-1}$; $E_a = 23.37 \text{ kJ.mol}^{-1}$ k_7 , acetylgenistin → degraded products D ₂ : $k_{50\text{ °C}} = 1.28 \times 10^5 \text{ s}^{-1}$; $k_{70\text{ °C}} = 2.35 \times 10^5 \text{ s}^{-1}$; $k_{130\text{ °C}} = 3.85 \times 10^5 \text{ s}^{-1}$; $k_{150\text{ °C}} = 12.77 \times 10^5 \text{ s}^{-1}$; $E_a = 23.46 \text{ kJ.mol}^{-1}$ k_8 , genistin → genistein: $k_{50\text{ °C}} = 1.25 \times 10^5 \text{ s}^{-1}$; $k_{70\text{ °C}} = 2.13 \times 10^5 \text{ s}^{-1}$; $k_{130\text{ °C}} = 6.87 \times 10^5 \text{ s}^{-1}$; $k_{150\text{ °C}} = 13.55 \times 10^5 \text{ s}^{-1}$; $E_a = 25.64 \text{ kJ.mol}^{-1}$ k_9 , genistin → degraded products D ₃ : $k_{50\text{ °C}} = 1.18 \times 10^5 \text{ s}^{-1}$; $k_{70\text{ °C}} = 1.87 \times 10^5 \text{ s}^{-1}$; $k_{130\text{ °C}} = 4.82 \times 10^5 \text{ s}^{-1}$; $k_{150\text{ °C}} = 11.02 \times 10^5 \text{ s}^{-1}$; $E_a = 23.33 \text{ kJ.mol}^{-1}$ k_{10} , genistein → degraded products D ₄ : $k_{50\text{ °C}} = 1.08 \times 10^5 \text{ s}^{-1}$; $k_{70\text{ °C}} = 1.71 \times 10^5 \text{ s}^{-1}$; $k_{130\text{ °C}} = 3.50 \times 10^5 \text{ s}^{-1}$; $k_{150\text{ °C}} = 10.07 \times 10^5 \text{ s}^{-1}$; $E_a = 22.47 \text{ kJ.mol}^{-1}$	De-esterification was the predominant reaction during infrared drying. The ester bond appeared to be less stable than the glycosidic bond. Drying did not provide a good condition for decarboxylation reactions. Malonylgenistin was the most thermally labile genistin derivative, and was readily converted to its stable corresponding forms. All isoflavones were more susceptible to interconversion reactions than to thermal and oxidative degradation reactions during drying.	Niamnuy <i>et al.</i> , 2012
MODEL SOLUTIONS				
Aqueous buffer solutions (pH 7 and 9)				
Genistein and daidzein	Thermal treatment: autoclave, 120 °C/20min [0.25 mM in 0.1 M phosphate buffer (pH 7) and 0.1 mM in 0.1 M borate buffer (pH 9)]. Incubation under isothermal conditions at 70, 80, 90 °C [30 μM in 0.1 M phosphate buffer (pH 7) and 30 μM in 0.1 M borate buffer (pH 9)]. Microcalorimetric stability tests: aqueous solutions of genistein and daidzein [1.0 mM in 0.1 M borate buffer (pH 9)] were de-aerated and scanned from 50-120 °C at the scanning rate of 3.8 °C.h ⁻¹ .	First-order degradation kinetic model; Arrhenius equation. Incubation under isothermal conditions (aerobic): genistein, pH 7: $k_{70\text{ °C}} = 0.022 \text{ day}^{-1}$, $k_{80\text{ °C}} = 0.025 \text{ day}^{-1}$, $k_{90\text{ °C}} = 0.030 \text{ day}^{-1}$; $E_a = 16.23 \text{ kJ.mol}^{-1}$ genistein, pH 9: $k_{70\text{ °C}} = 0.087 \text{ day}^{-1}$, $k_{80\text{ °C}} = 0.102 \text{ day}^{-1}$, $k_{90\text{ °C}} = 0.222 \text{ day}^{-1}$; $E_a = 48.41 \text{ kJ.mol}^{-1}$ daidzein, pH 7: $k_{70\text{ °C}} = 0.045 \text{ day}^{-1}$, $k_{80\text{ °C}} = 0.091 \text{ day}^{-1}$, $k_{90\text{ °C}} = 0.262 \text{ day}^{-1}$; $E_a = 90.75 \text{ kJ.mol}^{-1}$ daidzein, pH 9: $k_{70\text{ °C}} = 0.277 \text{ day}^{-1}$, $k_{80\text{ °C}} = 0.323 \text{ day}^{-1}$, $k_{90\text{ °C}} = 0.547 \text{ day}^{-1}$; $E_a = 35.06 \text{ kJ.mol}^{-1}$ Microcalorimetric stability tests (anaerobic): genistein, pH 9: degraded concentration = 0.29 mM; $\Delta H = 75.14 \text{ kJ.mol}^{-1}$; $E_a = 308.36 \text{ mol}^{-1}$ daidzein, pH 9: degraded concentration = 0.58 mM; $\Delta H = 104.77 \text{ kJ.mol}^{-1}$; $E_a = 142.84 \text{ kJ.mol}^{-1}$	Genistein and daidzein were degraded when exposed to high temperatures under conditions simulating a commercial sterilisation process. The degradation rates of genistein and daidzein were higher at pH 9 than at pH 7. Daidzein was more susceptible to thermal degradation than genistein. Isoflavone degradation proceeded much faster under anaerobic than under aerobic conditions, and the E_a was also much higher under anaerobic conditions, suggesting different degradation mechanisms.	Ungar <i>et al.</i> , 2003 ^a

^aValues for the activation energies (E_a) and the enthalpy of the reactions (ΔH , where applicable) were converted from kcal.mol⁻¹ to kJ.mol⁻¹ using a conversion factor of 4.184.

Table 10 *cont.*

Isoflavone and matrix	Operating conditions	Mathematical model, kinetic order and kinetic parameters	Major findings	Reference
Methanolic solution and dry residu of isoflavone standards				
Malonylgenistin, acetylgenistin, genistin and genistein	Isothermal heating in an oil-bath at 100, 150 and 200 °C for heating times of 5, 15, 30, 60, 120 and 180 min.	<p>First-order kinetic models; Arrhenius equation.</p> <p>Dry heating: malonylgenistin → acetylgenistin, k_1: $k_{100\text{ °C}} = 0.0445\text{ h}^{-1}$; $k_{150\text{ °C}} = 1.43\text{ h}^{-1}$; $k_{200\text{ °C}} = 7.86\text{ h}^{-1}$; $E_a = 76.57\text{ kJ.mol}^{-1}$ malonylgenistin → genistin, k_6: $k_{150\text{ °C}} = 2.31\text{ h}^{-1}$; $k_{200\text{ °C}} = 9.71\text{ h}^{-1}$; $E_a = 50.00\text{ kJ.mol}^{-1}$ malonylgenistin → genistein, k_7: $k_{200\text{ °C}} = 0.000\text{ h}^{-1}$ malonylgenistin → degraded products D₁, k_5: $k_{150\text{ °C}} = 0.206\text{ h}^{-1}$; $k_{200\text{ °C}} = 5.808\text{ h}^{-1}$; $E_a = 116.15\text{ kJ.mol}^{-1}$ acetylgenistin → genistin, k_2: $k_{150\text{ °C}} = 0.221\text{ h}^{-1}$; $k_{200\text{ °C}} = 0.585\text{ h}^{-1}$; $E_a = 33.89\text{ kJ.mol}^{-1}$ acetylgenistin → genistein, k_8: $k_{00\text{ °C}} = 0.2766\text{ h}^{-1}$ acetylgenistin → degraded products D₂, k_9: $k_{150\text{ °C}} = 0.219\text{ h}^{-1}$; $k_{200\text{ °C}} = 0.00\text{ h}^{-1}$ genistin → genistein, k_3: $k_{200\text{ °C}} = 0.0157\text{ h}^{-1}$ genistin → degraded products D₃, k_{10}: $k_{150\text{ °C}} = 0.0368\text{ h}^{-1}$; $k_{200\text{ °C}} = 4.61\text{ h}^{-1}$; $E_a = 167.99\text{ kJ.mol}^{-1}$ genistein → degraded products D₄, k_4: $k_{150\text{ °C}} = 0.0338\text{ h}^{-1}$; $k_{200\text{ °C}} = 0.853\text{ h}^{-1}$; $E_a = 112.30\text{ kJ.mol}^{-1}$</p> <p>Moist heating: malonylgenistin → acetylgenistin, k_1: $k_{100\text{ °C}} = 0.773\text{ h}^{-1}$; $k_{150\text{ °C}} = 46.7\text{ h}^{-1}$; $k_{200\text{ °C}} = 76.0\text{ h}^{-1}$; $E_a = 69.45\text{ kJ.mol}^{-1}$ malonylgenistin → genistin, k_6: $k_{100\text{ °C}} = 1.80\text{ h}^{-1}$; $k_{150\text{ °C}} = 265\text{ h}^{-1}$; $k_{200\text{ °C}} = 318\text{ h}^{-1}$; $E_a = 79.08\text{ kJ.mol}^{-1}$ malonylgenistin → degraded products D₁, k_5: $k_{100\text{ °C}} = 0.422\text{ h}^{-1}$; $k_{150\text{ °C}} = 0.012\text{ h}^{-1}$; $k_{200\text{ °C}} = 0.000\text{ h}^{-1}$ acetylgenistin → genistin, k_2: $k_{100\text{ °C}} = 0.211\text{ h}^{-1}$; $k_{150\text{ °C}} = 2.54\text{ h}^{-1}$; $k_{200\text{ °C}} = 6.60\text{ h}^{-1}$; $E_a = 51.04\text{ kJ.mol}^{-1}$ acetylgenistin → degraded products D₂, k_9: $k_{150\text{ °C}} = 4.40\text{ h}^{-1}$; $k_{200\text{ °C}} = 19.0\text{ h}^{-1}$; $E_a = 50.63\text{ kJ.mol}^{-1}$ genistin → degraded products D₃, k_{10}: $k_{150\text{ °C}} = 1.23\text{ h}^{-1}$; $k_{200\text{ °C}} = 11.6\text{ h}^{-1}$; $E_a = 77.82\text{ kJ.mol}^{-1}$ genistein → degraded products D₄, k_4: $k_{100\text{ °C}} = 0.0743\text{ h}^{-1}$; $k_{150\text{ °C}} = 5.53\text{ h}^{-1}$; $k_{200\text{ °C}} = 12.6\text{ h}^{-1}$; $E_a = 77.40\text{ kJ.mol}^{-1}$</p>	<p>Isoflavones were more susceptible to conversion and degradation reactions under moist heating conditions than during dry heating.</p> <p>Generally, under both heating conditions, the conversion rate constants were substantially higher than the degradation rate constants.</p> <p>The heating treatment (dry vs moist heating) influenced the type of conversions that occurred, and the relative stability of the isoflavones towards thermal degradation.</p> <p>During both moist and dry heating, the conversion reactions of malonylgenistin was very fast, demonstrating that the stability of malonylgenistin is extremely low compared to the other three isoflavones.</p> <p>Under moist heating, the malonyl type of isoflavone was preferentially converted to the β-glycoside, while under dry heating the acetyl derivative was favoured.</p> <p>The conversion and degradation reactions in moist heating had energy barriers similar to dry heating.</p>	Chien <i>et al.</i> , 2005 ^a
80% Aqueous methanolic solution (pH 3.1, 5.6 and 7)				
Daidzein, genistein, glycitein, formononetin, biochanin A, isoflavone and flavone (0.3-0.6 mM)	Heating in a laboratory oven at 150 °C for heating times of 1, 3, 5 and 7 h	<p>Regression fits for isoflavone and flavone aglycone degradation at pH 3.1:</p> <p>Exponential [\equiv First-order kinetic model, where $A = C_0$ and $B = k\text{ (h}^{-1}\text{)}$] Glycitein: $A = 0.3294$; $B = 0.2096$; Flavone: $A = 0.4608$; $B = 0.0658$</p> <p>Sigmoidal^b Daidzein: $A = 0.3973$; $B = 0.5318$; $X_0 = 3.138$; Genistein: $A = 0.3907$; $B = -0.7253$; $X_0 = 4.102$ Formononetin: $A = 0.4160$; $B = -0.4481$; $X_0 = 3.941$; Biochanin A: $A = 0.3537$; $B = -0.3308$; $X_0 = 3.377$ Isoflavone: $A = 0.5064$; $B = -0.3140$; $X_0 = 3.853$</p>	<p>Daidzein was the most thermally labile isoflavone aglycone.</p> <p>The number and nature of the substituent(s), as well as position of substitution affected the relative thermal stability of isoflavone aglycones.</p> <p>Thermal degradation was negligible at pH 7.0 and 5.6, and most prominent at pH 3.1</p> <p>Overall compound retention depended on the duration of heat exposure.</p>	Stintzing <i>et al.</i> , 2006

^aValues for the activation energies (E_a) were converted from kcal.mol⁻¹ to kJ.mol⁻¹ using a conversion factor of 4.184.

^bMathematical expression for sigmoidal degradation pattern given by eq. 14 (terms not defined by Stintzing *et al.*, 2006):

$$Y = A / [1 + \exp(-(X - X_0) / B)] \quad (14)$$

Table 10 *cont.*

Isoflavone and matrix	Operating conditions	Mathematical model, kinetic order and kinetic parameters	Major findings	Reference
0.01 M Borax solution (pH 8.5, 9.0 and 9.5) Malonylgenistin and malonyldaidzin (7.5 μL of a 500 ppm solution, added to 192.5 μL buffer solution)	Heating in a waterbath at 60, 80 and 100 °C for three different time intervals (ranging from 0.50 to 300 min)	First-order kinetic models; Arrhenius equation. k_1 = conversion reactions, and k_2 = degradation reactions	Malonylglucosides were only converted to their respective β -glucosides under alkaline conditions. Malonylglucosides were also degraded into unknown products, albeit to a lesser extent. An increase in the rate constants of both the conversion and degradation reactions was observed as the temperature and pH increased. The conversion rate constants and corresponding activation energies of malonylgenistin and malonyldaidzin were comparable. At elevated temperature, malonyldaidzin was more susceptible to thermal degradation reactions than malonylgenistin.	Vaidya <i>et al.</i> , 2007 ^a
		Malonylgenistin 100 °C, pH 9.5: $k_1 = 1.27 \text{ min}^{-1}$, $k_2 = 0.325 \text{ min}^{-1}$ 100 °C, pH 9.0: $k_1 = 0.570 \text{ min}^{-1}$, $k_2 = 0.159 \text{ min}^{-1}$ 100 °C, pH 8.5: $k_1 = 0.191 \text{ min}^{-1}$, $k_2 = 0.042 \text{ min}^{-1}$ 80 °C, pH 9.5: $k_1 = 0.339 \text{ min}^{-1}$, $k_2 = 0.049 \text{ min}^{-1}$ 80 °C, pH 9.0: $k_1 = 0.111 \text{ min}^{-1}$, $k_2 = 0.033 \text{ min}^{-1}$ 80 °C, pH 8.5: $k_1 = 0.037 \text{ min}^{-1}$, $k_2 = 0.016 \text{ min}^{-1}$ 60 °C, pH 9.5: $k_1 = 0.039 \text{ min}^{-1}$, $k_2 = 0.016 \text{ min}^{-1}$ 60 °C, pH 9.0: $k_1 = 0.012 \text{ min}^{-1}$, $k_2 = 0.004 \text{ min}^{-1}$ 60 °C, pH 8.5: $k_1 = 0.006 \text{ min}^{-1}$, $k_2 = 0.002 \text{ min}^{-1}$ Activation energy for k_1 : 93.01 $\text{kJ}\cdot\text{mol}^{-1}$ Malonyldaidzin 100 °C, pH 9.5: $k_1 = 1.30 \text{ min}^{-1}$, $k_2 = 0.669 \text{ min}^{-1}$ 100 °C, pH 9.0: $k_1 = 0.592 \text{ min}^{-1}$, $k_2 = 0.354 \text{ min}^{-1}$ 100 °C, pH 8.5: $k_1 = 0.217 \text{ min}^{-1}$, $k_2 = 0.132 \text{ min}^{-1}$ 80 °C, pH 9.5: $k_1 = 0.263 \text{ min}^{-1}$, $k_2 = 0.058 \text{ min}^{-1}$ 80 °C, pH 9.0: $k_1 = 0.104 \text{ min}^{-1}$, $k_2 = 0.016 \text{ min}^{-1}$ 80 °C, pH 8.5: $k_1 = 0.041 \text{ min}^{-1}$, $k_2 = 0.013 \text{ min}^{-1}$ 60 °C, pH 9.5: $k_1 = 0.037 \text{ min}^{-1}$, $k_2 = 0.029 \text{ min}^{-1}$ 60 °C, pH 9.0: $k_1 = 0.012 \text{ min}^{-1}$, $k_2 = 0.007 \text{ min}^{-1}$ 60 °C, pH 8.5: $k_1 = 0.005 \text{ min}^{-1}$, $k_2 = 0.002 \text{ min}^{-1}$ Activation energy for k_1 : 97.49 $\text{kJ}\cdot\text{mol}^{-1}$		
Dry residu of isoflavone standards	Dry-heating in a sand bath at 100, 150 and 200 °C, for heating times of 10, 20 and 30 min.	First-order kinetic model. Refer to the publication of Yue <i>et al.</i> (2010) for graphical representation of data.	The degradation rate constants of the isoflavones were not significantly different from one another at 100 °C. The reaction rate constants increased with increasing temperature. Upon thermal treatment at 150 °C or higher, the glycosidic linkages of the isoflavone β -glucosides were cleaved, leading to the formation of the corresponding aglycones.	Yue <i>et al.</i> , 2010
Daidzein, glycitein, genistein, daidzin, glycitin and genistin.				

^aValues for the activation energies (E_a) were converted from $\text{kcal}\cdot\text{mol}^{-1}$ to $\text{kJ}\cdot\text{mol}^{-1}$ using a conversion factor of 4.184.

These studies showed that isoflavone conversion and degradation typically follows first-order reaction kinetics, while curve fitting of the data presented by Stintzing *et al.* (2006) only revealed first-order degradation kinetics for glycitein; the remaining aglycones (genistein, formononetin, biochanin A and daidzein) exhibited a sigmoidal degradation pattern. The first-order rate constants of both the conversion and degradation reactions increase with increasing temperature and the effect of temperature on the reaction rate constants follows the Arrhenius law (Table 10).

A study by Chien *et al.* (2005) provided fundamental insight into the degradation and, in particular, the conversion mechanism among the various forms of isoflavones during dry and moist heating. The authors took all possible reactions (*i.e.*, consecutive conversions and degradation to other products) into account and developed complex consecutive reaction models under the different heating conditions (Figure 18).

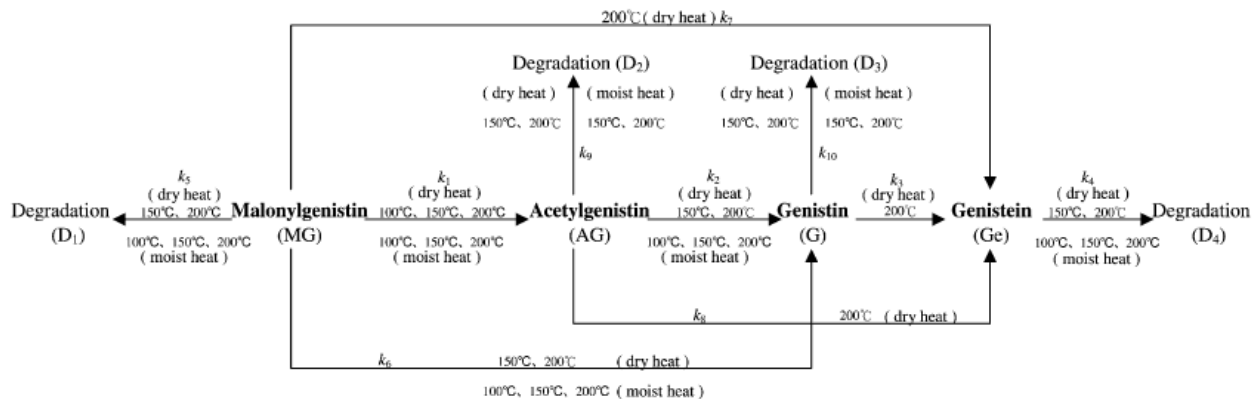


Figure 18 Influence of dry and moist heating on the conversion and degradation of the different chemical forms of genistin (reproduced from Chien *et al.*, 2005).

The different heating conditions markedly affected the susceptibility of the isoflavones towards thermally-induced chemical reactions, as well as the type of conversions that occurred (Chien *et al.*, 2005). The isoflavones were more susceptible to conversion and degradation under moist heating conditions than during dry heating, whilst the conversions of malonylgenistin, acetylgenistin and genistin to genistein (*i.e.*, production of the aglycone) only occurred during dry heating (200 °C) and not under moist heating conditions.

Generally, under both heating conditions, the conversion rate constants were substantially higher than the degradation rate constants (Chien *et al.*, 2005). Similar findings were later reported by Vaidya *et al.* (2007), showing that the rate constants for the conversion of malonylgenistin and malonyldaidzin into their respective non-conjugated β -glycosides were substantially higher than the rate constants for their degradation into unknown products. Chien *et al.* (2005) reported rate constants of 1.80 h^{-1} for the conversion of malonylgenistin to genistin, and 0.422 h^{-1} for the degradation of malonylgenistin to unknown products upon heating a methanolic solution at 100 °C. The corresponding values calculated by Vaidya *et al.* (2007) for the conversion and degradation of malonylgenistin in a 0.01 M borax solution (pH 8.5-9.5) at the same temperature ranged between 0.191 and 1.27 min^{-1} , and 0.042 and 0.325 min^{-1} , respectively. The values of the rate constants differ significantly between the two studies, suggesting that the nature of the reaction medium and/or other experimental parameters may have a profound effect on kinetic data.

Niamny *et al.* (2012) also established that the rate constants for the degradation of genistein-series isoflavones were lower than the corresponding rate constants of the de-esterification and hydrolysis reactions during gas-fired infrared combined with hot air vibrating drying (GFIR-HAVD) of soybean at 50-150 °C. Collectively these results indicate that isoflavones are more susceptible to interconversion reactions than thermal and oxidative degradation reactions during thermal treatment.

In terms of the evolution of isoflavones during GFIR-HAVD of soybean, Niamnuy *et al.* (2012) reported that the contents of 6''-*O*-malonylgenistin and 6''-*O*-acetylgenistin decreased, while those of genistin and genistein increased with an increase in drying temperature and time. At all drying temperatures, the conversion of malonylgenistin to genistin exhibited the highest rate constant, followed by the conversion of acetylgenistin to genistin, indicating that de-esterification was the predominant reaction during infrared drying. This is contradictory to previous studies (*vide supra*), which showed that decarboxylation, as opposed to de-esterification, is typically favoured under dry heating conditions. Indeed, considering all the conversion reactions of malonylgenistin in soybean, it was found that k_2 (malonylgenistin \rightarrow genistin) $>$ k_3 (malonylgenistin \rightarrow genistein) $>$ k_1 (malonylgenistin \rightarrow acetylgenistin) (Niamnuy *et al.*, 2012; Table 10). The conversion of malonylgenistin to genistin via de-esterification thus exhibited a higher rate constant than the conversion of malonylgenistin to genistein via hydrolysis. A similar trend also occurred with the conversion reactions of acetylgenistin, with k_5 (acetylgenistin \rightarrow genistin) $>$ k_6 (acetylgenistin \rightarrow genistein) (Table 10).

Several studies have highlighted the significance of chemical structure with regard to the thermal stability of isoflavones. Concerning the isoflavone phenolic sub-class as a whole, a study by Stintzing and co-workers (2006) indicated that isoflavones are thermally less stable than the flavones. Stintzing *et al.* (2006) also established key structure-stability relationships amongst the isoflavone aglycones daidzein, genistein, glycitein, formononetin and biochanin A with regard to nature of the substituent(s), as well as the substitution pattern. Among the 7,4'-disubstituted isoflavone aglycones, the 4'-methoxy-substitution resulted in increased stability of formononetin compared to daidzein (4'-hydroxy-substitution). Conversely, the thermal stability of the 5,7,4'-trisubstituted isoflavone aglycones was reduced when C-4' carried a methoxy (biochanin A) instead of a hydroxy group (genistein). Genistein was thermally more stable than daidzein, suggesting that hydroxylation at C-5 enhances the stability of 7,4'-dihydroxylated structures. In contrast, these findings did not hold true for the 7-hydroxy-4'-methoxylated isoflavones, since biochanin A (containing an additional hydroxy group at C-5) exhibited lower thermal stability than formononetin (Stintzing *et al.*, 2006).

The higher thermal stability of genistein and its derivatives compared to the daidzein-series of isoflavones has also been reported by many other researchers (Mahungu *et al.*, 1999; Grün *et al.*, 2001; Ungar *et al.*, 2003; Huang *et al.*, 2006; Mathias *et al.*, 2006; Vaidya *et al.*, 2007; Lee & Lee, 2009). This observation, that increased hydroxylation on the A-ring confers higher thermal stability to the 7,4'-dihydroxylated isoflavone structure, contradicts other literature data, as an increase in the number of hydroxy groups of the aromatic B-ring has typically been associated with decreased thermal stability of polyphenols (*e.g.* flavan-3-ols; Wang *et al.*, 2000). It has thus been suggested that the location of the additional hydroxy group of genistein (*i.e.*, at C-5), and its proximity to the C-4-oxo moiety, may stabilise the hydroxy groups on the A-ring of genistein, leading to increased stability (Ungar *et al.*, 2003).

In terms of the relative thermal stability of genistein and its derivatives, compared to that of the daidzein-series of isoflavones, selected studies have indicated just the opposite, with a higher thermal stability reported for the latter (Wang *et al.*, 1990; Xu *et al.*, 2002; Yue *et al.*, 2010). For instance, Wang *et al.* (1990) reported higher stability of daidzein compared to genistein upon thermal treatment under acidic conditions (Wang *et al.*, 1990). During dry heating at 135-215 °C, the thermal stability of isolated soy isoflavones decreased in the order daidzin $>$ genistin $>$ glycitin; the stability of daidzein was also higher than that of glycitein or genistein (Xu *et al.*, 2002). Under similar dry heating conditions, the thermal stability of a dry residu of isolated soy isoflavones decreased in the order daidzein $>$ genistein $>$ glycitein $>$ daidzin $>$ genistin $>$ glycitin (temperatures $<$ 150 °C; Yue *et al.*, 2010). Compared with the three isoflavone glucosides, the aglycone isoflavones were more stable at heating temperatures of 150 and 200 °C (Yue *et al.*, 2010).

The exceptional thermal stability of isoflavone aglycones has been demonstrated during dry heating at 200 °C, where the contents of daidzein, genistein and glycitein remained relatively stable over a 30 min period (Xu *et al.*, 2002). Conversely, Huang & Chou (2008) noted that the percentages of individual and total isoflavone aglycones in steamed black soybeans significantly decreased after heating at 60 °C or higher for merely 30 min, indicating the crucial role of moisture in decreasing thermal stability.

The principal chemical forms of isoflavones in soybean are their 6''-*O*-malonylglucoside conjugates and these conjugates are affected the most when exposed to heat. This has been observed during solvent extraction from soyfoods (Coward *et al.*, 1998), extrusion processing of soy/corn/mixtures (Mahungu *et al.*, 1999) and dry heating of whole soybeans (Yuan *et al.*, 2009) to name but a few examples. Indeed, Coward and co-workers (1998) even found that prolonged storage of an 80% aqueous methanol extract of soybeans at 4 °C induced conversion of 6''-*O*-malonylglucosides to the β -glucosyl conjugates.

Considering the interconversion reactions of the genistein-series of isoflavones under dry and moist heating conditions, Chien *et al.* (2005) reported that the conversion reactions of malonylgenistin was the most rapid, demonstrating that the stability of malonylgenistin is extremely low compared to the other genistein derivatives. Similarly, the specific conversion of malonylgenistin to genistein aglycone during infrared drying of soybean was shown to proceed at a much faster rate than the conversions of both acetylgenistin and genistin to genistein (Niamnuy *et al.*, 2012). Malonylgenistin also exhibited the highest degradation rate constant during infrared drying, followed by acetylgenistin, genistin and genistein in descending order (Niamnuy *et al.*, 2012). Different heating conditions may, however, influence the relative thermal stability of the different chemical forms of isoflavones with respect to degradation reactions. Chien *et al.* (2005) showed that during dry heating, malonylgenistin had the highest degradation rate, followed by genistin, genistein and acetylgenistin, while the reversed trend occurred for moist heating. It thus appear that, under certain conditions, malonylgenistin may actually be more stable than the other chemical forms of genistin. This is supported by findings of Mathias and co-workers (2006), where malonyldaidzin and malonylgenistin exhibited higher thermal stability than their corresponding acetylglucosides upon thermal treatment in aqueous model systems, especially under acidic conditions.

Indeed, the thermal stability of isoflavones is markedly influenced by the pH of the reaction medium. Mathias *et al.* (2006) investigated the effect of pH on the conjugated forms of genistin and daidzin isoflavones. Malonyldaidzin and malonylgenistin were most stable at pH 2 and least stable at pH 10, whereas acetyldaidzin was most stable at pH 7 and least stable at pH 10. Although acetylgenistin was most stable under neutral conditions, overall minimal loss was observed under acidic conditions (Mathias *et al.*, 2006). The effect of pH on the thermal degradation of isoflavone aglycones and their malonyl-derivatives in aqueous model systems has also been assessed kinetically (Ungar *et al.*, 2003; Stintzing *et al.*, 2006; Vaidya *et al.*, 2007; Table 10). The thermal degradation rate constants of genistein and daidzein were found to be pH dependent, with lower degradation rate constants for both compounds observed in neutral media (pH 7) as opposed to alkaline media (pH 9) (Ungar *et al.*, 2003). Similarly, Vaidya *et al.* (2007) showed the first-order rate constants of both the conversion and degradation reactions of malonylglucosides (malonylgenistin and malonyldaidzin) increased as the pH increased from 8.5 to 9.5. In the latter case, an increase in the rate of de-esterification at the higher pH values was ascribed to the fact that more hydroxy groups, from the buffer, were available to attack the carbonyl carbon participating in the ester bond of malonylglucosides. Upon heating, isoflavone aglycones (glycitein, genistein, formononetin, biochanin A and daidzein) in aqueous model solutions showed virtually no degradation at pH 7.0 and 5.6, while it was most prominent at pH 3.1 (Stintzing *et al.*, 2006). It therefore appears that isoflavones are at their most stable under neutral to slightly acidic conditions, while highly acidic and alkaline conditions exacerbates thermally-induced chemical reactions. More comprehensive studies, over a wide range of pH values and identical thermal processing conditions, are, however, required to better elucidate the effect of pH on the thermal stability of isoflavones under standardised conditions.

To date, studies regarding the effect of oxygen (or lack thereof) on the conversion and degradation of isoflavones during thermal treatment is limited to a single study by Ungar and co-workers (Ungar *et al.*, 2003). They compared the degradation of genistein and daidzein in aqueous buffer solution (0.1 M borate buffer, pH 9) during incubation under isothermal conditions (aerobic; 70-90 °C), with results obtained in a de-aerated solution subjected to microcalorimetric stability testing. Differential scanning calorimetry (DSC) was used to evaluate the stability of these isoflavone aglycones, and to assess the enthalpies and activation energies of the degradation reactions. Isoflavone degradation in the de-aerated solutions during the microcalorimetric tests was found to be much faster than that during aerobic isothermal experiments, and higher activation energies were also calculated under anaerobic conditions. The higher stability of isoflavones under aerobic conditions is contradictory to the findings of previous studies on flavonols (Makris & Rossiter, 2000) and monomeric flavan-3-ols (Zimeri & Tong, 1999), for instance, showing that increased levels of oxygen increased the first-order degradation rate constants. Ungar *et al.* (2003) concluded that the differences in the degradation rates and the activation energies under aerobic and anaerobic conditions imply that two or more reactions exist, and that these reactions likely differ with respect to their mechanism, their products, and thus also their temperature dependencies.

3.5. Concluding Remarks

From the large number of kinetic studies scrutinised in this review, certain trends were observed across all phenolic sub-classes. Irrespective of the conditions of the applied thermal treatments (*e.g.* accelerated storage, conventional thermal processing, microwave heating, sub- and supercritical water conditions, etc.), the degradation of most phenolic compounds could adequately be described by first-order kinetic models. Within the same phenolic sub-class, the thermal stability of individual compounds was principally defined by their chemical structure, and it appears that B-ring hydroxylation, in particular, is a defining factor. In general, increased temperature, pH and dissolved oxygen concentration led to increased reaction rate constants. The temperature-dependence of the reaction rate constant was shown to comply with the Arrhenius law in most cases, while the effect of pH and dissolved oxygen concentration on the degradation rate constant also exhibited log-linear relationships over certain ranges. Optimum stability of the phenolic compounds was usually at a pH level ~ 4; further reductions or increase in pH were associated with decreased thermal stability. Other factors that affected the thermal stability of phenolic compounds included the concentration and physical state of the phenolic compound (amorphous vs crystalline; solid vs solution), the % RH of the environment (solid state samples), and the presence of metal ions, additives and other phytochemicals in the reaction medium. The presence of metal ions promoted degradation, while the presence of additives (*e.g.* citric and ascorbic acids) and other phytochemicals mostly offered protective effects. Matrix effects were also profound, and the occurrence of epimerisation (flavan-3-ols) and interconversion reactions (isoflavones) underlined the necessity of using model systems for accurate estimation of kinetic parameters and elucidation of reaction pathways. To conclude, a great deal of research is still required to better understand the thermal stability of phenolic compounds as affected by chemical structure and external factors, and this is particularly true for the dihydrochalcones, flavanones, dihydroflavonols and flavones, which are entirely under-represented. Furthermore, kinetic data on the thermal stability of compounds from the benzophenone and xanthone phenolic sub-classes are not available to date.

REFERENCES

- Agcam, E., Akyildiz, A. & Evrendilek, G.A. (2014). Comparison of phenolic compounds of orange juice processed by pulsed electric fields (PEF) and conventional thermal pasteurisation. *Food Chemistry*, **143**, 354-361.
- Ananingsih, V.K., Sharma, A. & Zhou, W. (2013). Green tea catechins during food processing and storage: A review on stability and detection. *Food Research International*, **50**, 469-479.
- Barnes, S., Kirk, M. & Coward, L. (1994). Isoflavones and their conjugates in soy foods: extraction conditions and analysis by HPLC-mass spectrometry. *Journal of Agricultural and Food Chemistry*, **42**, 2466-2474.
- Beelders, T., Sigge, G.O., Joubert, E., De Beer, D. & De Villiers, A. (2012a). Kinetic optimisation of the reversed phase liquid chromatographic separation of rooibos tea (*Aspalathus linearis*) phenolics on conventional high performance liquid chromatographic instrumentation. *Journal of Chromatography A*, **1219**, 128-139.
- Beelders, T., Sigge, G.O., Joubert, E., De Beer, D. & De Villiers, A. (2012b). Erratum to “Kinetic optimisation of the reversed phase liquid chromatographic separation of rooibos tea (*Aspalathus linearis*) phenolics on conventional high performance liquid chromatographic instrumentation.” [*Journal of Chromatography A*, **1219**, 128-139]. *Journal of Chromatography A*, **1241**, 128.
- Beck, V., Rohr, U. & Jungbauer, A. (2005). Phytoestrogens derived from red clover: An alternative to estrogen replacement therapy? *Journal of Steroid Biochemistry & Molecular Biology*, **94**, 499-518.
- Bekedam, E.K., Loots, M.J., Schols, H.A., Van Boekel, M.A.J.S. & Smit, G. (2008). Roasting effects on formation mechanisms of coffee brew melanoidins. *Journal of Agricultural and Food Chemistry*, **56**, 7138-7145.
- Bors, W., Michel, C. & Schikora, S. (1995). Interaction of flavonoids with ascorbate and determination of their univalent redox potentials: A pulse radiolysis study. *Free Radical Biology and Medicine*, **19**, 45-52.
- Bosman, S.C. (2014). Development of a xanthone-enriched honeybush tea extract. MSc (Food Science) Thesis, Stellenbosch University, Stellenbosch, South Africa.
- Bott, R.F., Labuza, T.P. & Oliveira, W.P. (2010). Stability testing of spray- and spouted bed-dried extracts of *Passiflora alata*. *Drying Technology*, **28**, 1255-1265.
- Breiter, T., Laue, C., Kressel, G., Gröll, S., Engelhardt, U.H. & Hahn, A. (2011). Bioavailability and antioxidant potential of rooibos flavonoids in humans following the consumption of different rooibos formulations. *Food Chemistry*, **128**, 338-347.
- Buchner, N., Krumbein, A., Rohn, S. & Kroh, L.W. (2006). Effect of thermal processing on the flavonols rutin and quercetin. *Rapid Communications in Mass Spectrometry*, **20**, 3229-3235.
- Canales, I., Borrego, F. & Lindley, M.G. (1993). Neohesperidin dihydrochalcone stability in aqueous buffer solutions. *Journal of Food Science*, **57**, 589-591, 643.
- Chatterjee, M., Roy, K., Janarthan, M., Das, S. & Chatterjee, M. (2012). Biological activity of carotenoids: its implications in cancer risk and prevention. *Current Pharmaceutical Biotechnology*, **13**, 180-190.
- Chen, Z.-Y., Zhu, Q.Y., Wong, Y.F., Zhang, Z. & Chung, H.Y. (1998). Stabilizing effect of ascorbic acid on green tea catechins. *Journal of Agricultural and Food Chemistry*, **46**, 2512-2516.
- Chen, Z.-Y., Zhu, Q.Y., Tsang, D. & Huang, Y. (2001). Degradation of green tea catechins in tea drinks. *Journal of Agricultural and Food Chemistry*, **49**, 477-482.
- Chien, J.T., Hsieh, H.C., Kao, T.H. & Chen, B.-H. (2005). Kinetic model for studying the conversion and degradation of isoflavones during heating. *Food Chemistry*, **91**, 425-434.
- Chunchev, K. & BelBruno, J.J. (2007). Mechanisms of decarboxylation of *ortho*-substituted benzoic acids. *Journal of Molecular Structure: THEOCHEM*, **807**, 1-9.

- Clifford, M.N., Kellard, B. & Birch, G.G. (1989). Characterisation of chlorogenic acids by simultaneous isomerisation and transesterification with tetramethylammonium hydroxide. *Food Chemistry*, **33**, 115-123.
- Colle, I.J.P., Lemmens, L., Knockaert, G., Van Loey, A. & Hendrickx, M. (2015). Carotene degradation and isomerisation during thermal processing: a review on the kinetic aspects. *Critical Reviews in Food Science and Nutrition*, DOI: 10.1080/10408398.2013.790779.
- Coiffard, C., Coiffard, L., Peigné, F. & De Roeck-Holtzhauer, Y. (1998). Effect of pH on neohesperidin dihydrochalcone thermostability in aqueous solutions. *Analisis*, **25**, 150-153.
- Coward, L., Barnes, N., Setchell, K. & Barnes, S. (1993). Genistein, daidzein, and their β -glycoside conjugates: antitumor isoflavones in soybean foods from American and Asian diets. *Journal of Agricultural and Food Chemistry*, **41**, 1961-1967.
- Coward, L., Smith, M., Kirk, M. & Barnes, S. (1998). Chemical modification of isoflavones in soyfoods during cooking and processing. *American Journal of Clinical Nutrition*, **68** (suppl), 1486S-1491S.
- Davidov-Pardo, G., Arozarena, I. & Marín-Arroyo, M.R. (2011). Kinetics of thermal modifications in a grape seed extract. *Journal of Agricultural and Food Chemistry*, **59**, 7211-7217.
- Davies, C.G.A., Netto, F.M., Glassenap, N., Gallaher, C.M., Labuza, T.P. & Gallaher, D.D. (1998). Indication of the Maillard reaction during storage of protein isolates. *Journal of Agricultural and Food Chemistry*, **46**, 2485-2489.
- Dawidowicz, A.L. & Typek, R. (2010). Thermal stability of 5-*O*-caffeoylquinic acid in aqueous solutions at different heating conditions. *Journal of Agricultural and Food Chemistry*, **58**, 12578-12584.
- Dawidowicz, A.L. & Typek, R. (2011). The influence of pH on the thermal stability of 5-*O*-caffeoylquinic acids in aqueous solutions. *European Food Research and Technology*, **233**, 223-232.
- Dawidowicz, A.L. & Typek, R. (2014). Transformation of 5-*O*-caffeoylquinic acid in blueberries during high-temperature processing. *Journal of Agricultural and Food Chemistry*, **62**, 10889-10895.
- De Beer, D., Jerz, G., Joubert, E., Wray, V. & Winterhalter, P. (2009). Isolation of isomangiferin from honeybush (*Cyclopia subternata*) using high-speed counter-current chromatography and high-performance liquid chromatography. *Journal of Chromatography A*, **1216**, 4282-4289.
- De Beer, D. & Joubert, E. (2010). Development of HPLC method for *Cyclopia subternata* phenolic compound analysis and application to other *Cyclopia* spp. *Journal of Food Composition and Analysis*, **23**, 289-297
- De Beer, D., Joubert, E., Viljoen, M. & Manley, M. (2011). Enhancing aspalathin stability in rooibos (*Aspalathus linearis*) ready-to-drink iced teas during storage: the role of nano-emulsification and beverage ingredients, citric and ascorbic acids. *Journal of the Science of Food and Agriculture*, **92**, 274-282.
- De Beer, D., Schulze, A.E., Joubert, E., De Villiers, A., Malherbe, C.J. & Stander, M.A. (2012). Food Ingredient Extracts of *Cyclopia subternata* (Honeybush): Variation in Phenolic Composition and Antioxidant Capacity. *Molecules*, **17**, 14602-14624.
- De Beer, D., Malherbe, C.J., Beelders, T., Willenburg, E.L., Brand, D.J. & Joubert, E. (2015). Isolation of aspalathin and nothofagin from rooibos (*Aspalathus linearis*) using high-performance countercurrent chromatography: Sample loading and compound stability considerations. *Journal of Chromatography A*, **1381**, 29-36.
- De Paepe, D., Valkenburg, D., Coudijzer, K., Noten, B., Servaes, K., De Loose, M., Voorspoels, S., Diels, L. & Van Droogenbroeck, B. (2014). Thermal degradation of cloudy apple juice phenolic constituents. *Food Chemistry*, **162**, 176-185.
- Deshpande, S., Jaiswal, R., Matei, M.F. & Kuhnert, N. (2014). Investigation of acyl migration in mono- and dicaffeoylquinic acids under aqueous basic, aqueous acidic, and dry roasting conditions. *Journal of Agricultural and Food Chemistry*, **62**, 9160-9170.

- Dhuique-Mayer, C., Tbatou, M., Carail, M., Caris-Veyrat, C., Dornier, M. & Amiot, M.J. (2007). Thermal degradation of antioxidant micronutrients in *Citrus* juice: kinetics and newly formed compounds. *Journal of Agricultural and Food Chemistry*, **55**, 4209-4216.
- Dietrych-Szostak, D. & Oleszek, W. (1999). Effect of processing on the flavonoid content of buckwheat (*Fagopyrum esculentum* Möench) grain. *Journal of Agricultural and Food Chemistry*, **47**, 4384-4387.
- Dornstauder, E., Jisa, E., Unterrieder, I., Krenn, L., Kubelka, W. & Jungbauer, A. (2001). Estrogenic activity of two standardized red clover extracts (Menoflavon[®]) intended for large scale use in hormone therapy replacement. *Journal of Steroid Biochemistry & Molecular Biology*, **78**, 67-75.
- Downham, A. & Collins, P. (2000). Colouring our foods in the last and next millennium. *International Journal of Food Science and Technology*, **35**, 5-22.
- Dudhia, Z., Louw, J., Muller, C., Joubert, E., De Beer, D., Kinnear, C. & Pheiffer, C. (2013). *Cyclopia maculata* and *Cyclopia subternata* (honeybush tea) inhibits adipogenesis in 3T3-L1 pre-adipocytes. *Phytomedicine*, **20**, 401-408.
- Du Preez, B.V.P. (2014). *Cyclopia maculata* – Source of flavanone glycosides as precursors of taste-modulating aglycones. Master of Science in Food Science. Stellenbosch University, Stellenbosch, South Africa.
- Du Toit, J. & Joubert, E. (1999). Optimization of the fermentation parameters of honeybush tea (*Cyclopia*). *Journal of Food Quality*, **22**, 241-256.
- Eisen, B., Ungar, Y. & Shimoni, E. (2003). Stability of isoflavones in soy milk stored at elevated and ambient temperatures. *Journal of Agricultural and Food Chemistry*, **51**, 2212-2215.
- El-Seedi, H.R., El-Said, A.M.A., Khalifa, S.A.M., Göransson, U., Bohlin, L., Borg-Karlson, A.-K. & Verpoorte, R. (2012). Biosynthesis, natural sources, dietary intake, pharmacokinetic properties, and biological activities of hydroxycinnamic acids. *Journal of Agricultural and Food Chemistry*, **60**, 10877-10895.
- Farah, A. & Donangelo, C.M. (2006). Phenolic compounds in coffee. *Brazilian Journal of Plant Physiology*, **18**, 23-36.
- Farah, A., Monteiro, M.C., Calado, V., Franca, A.S. & Trugo, L.C. (2006a). Correlation between cup quality and chemical attributes of Brazilian coffee. *Food Chemistry*, **98**, 373-380.
- Farah, A., De Paulis, T., Moreira, D.P., Trugo, L.C. & Martin, P.R. (2006b). Chlorogenic acids and lactones in regular and water-decaffeinated Arabica coffees. *Journal of Agricultural and Food Chemistry*, **54**, 374-381.
- Feng, J., Yang, X.-W. & Wang, R.-F. (2011). Bio-assay guided isolation and identification of α -glucosidase inhibitors from the leaves of *Aquilaria sinensis*. *Phytochemistry*, **72**, 242-247.
- Ferreira, D., Kamara, B.I., Brandt, E.V. & Joubert, E. (1998). Phenolic compounds from *Cyclopia intermedia* (honeybush tea). 1. *Journal of Agricultural and Food Chemistry*, **46**, 3406-4310.
- Garg, A., Garg, S., Zaneveld, L.J.D. & Singla, A.K. (2001). Chemistry and pharmacology of the citrus bioflavonoid hesperidin. *Phytotherapy Research*, **15**, 655-669.
- Girón, M.D., Sevillano, N., Salto, R., Haidour, A., Manzano, M., Jiménez, M.L., Rueda, R. & López-Pedrosa, J.M. (2009). *Salacia oblonga* extract increase glucose transporter 4-mediated glucose uptake in L6 rat myotubes: Role of mangiferin. *Clinical Nutrition*, **28**, 565-574.
- González, G., Salvadó, J. & Montané, D. (2004). Reactions of vanillic acid in sub- and supercritical water. *Journal of Supercritical Fluids*, **31**, 57-66.
- Goppel, M. & Franz, G. (2004). Stability control of senna leaves and senna extracts. *Planta Medica*, **70**, 432-436.
- Greenish, H.G. (1881). Cape tea. *The Pharmaceutical Journal and Transactions*, **11**, 549-551.
- Grün, I.U., Adhikari, K., Li, C., Li, Y., Lin, B., Zhang, J. & Fernando, L.N. (2001). Changes in the profile of genistein, daidzein, and their conjugates during thermal processing of tofu. *Journal of Agricultural and Food Chemistry*, **49**, 2839-2843.

- Hanson, K.R. (1965). Chlorogenic acid biosynthesis. Chemical synthesis and properties of the mono-*O*-cinnamoylquinic acids. *Biochemistry* (Moscow), **4**, 2719-2731.
- Haslam, E., Makinson, G.K., Naumann, M.O. & Cunningham, J. (1964). Synthesis and properties of some hydroxycinnamoyl esters of quinic acid. *Journal of the Chemical Society*, 2137-2146.
- Heleno, S.A., Martins, A., Queiroz, M.J.R.P. & Ferreira, I.C.F.R. (2015). Bioactivity of phenolic acids. Metabolites *versus* parent compounds: A review. *Food Chemistry*, **173**, 501-513.
- Herrero, M., Cifuentes, A. & Ibañez, E. (2006). Sub- and supercritical fluid extraction of functional ingredients from different natural sources: Plants, food-by-products, algae and microalgae. A review. *Food Chemistry*, **98**, 136-148.
- Hong, Y.-J., Barrett, D.M. & Mitchell, A.E. (2004). Liquid chromatography/mass spectrometry investigation of the impact of thermal processing and storage on peach procyanidins. *Journal of Agricultural and Food Chemistry*, **52**, 2366-2371.
- Horowitz, R.M. & Gentili, B. (1963). Dihydrochalcone derivatives and their use as sweetening agents. U.S. Patent **3,087,821** (April 30, 1963).
- Hu, X., Xiao, Y., Wu, J. & Ma, L. (2011). Evaluation of polyhydroxybenzophenones as α -glucosidase inhibitors. *Archiv der Pharmazie – Chemistry in Life Sciences*, **344**, 71-77.
- Huang, H., Liang, H. & Kwok, K.-C. (2006). Effect of thermal processing on genistein, daidzein and glycitein content in soymilk. *Journal of the Science of Food and Agriculture*, **86**, 1110-1114.
- Huang, R.-Y. & Chou, C.-C. (2008). Heating affects the content and distribution profile of isoflavones in steamed black soybeans and black soybean koji. *Journal of Agricultural and Food Chemistry*, **56**, 8484-8489.
- Hvattum, E., Stenstrøm, Y. & Ekeberg, D. (2004). Study of the reaction products of flavonols with 2,2-diphenyl-1-picrylhydrazyl using liquid chromatography coupled with negative electrospray ionization tandem mass spectrometry. *Journal of Mass Spectrometry*, **39**, 1570-1581.
- Inglett, G.E., Krbeček, L., Dowling, B. & Wagner, R. (1969). Dihydrochalcone sweeteners – sensory and stability evaluation. *Journal of Food Science*, **34**, 101-103.
- Ioannone, F., Di Mattia, C.D., De Gregorio, M., Sergi, M., Serafini, M. & Sacchetti, G. (2015). Flavanols, proanthocyanidins and antioxidant activity changes during cocoa (*Theobroma cacao* L.) roasting as affected by temperature and time of processing. *Food Chemistry*, **174**, 256-262.
- Ioannou, I., Hafsa, I., Hamdi, S., Charbonnel, C. & Ghoul, M. (2012). Review of the effects of food processing and formulation on flavonol and anthocyanin behaviour. *Journal of Food Engineering*, **111**, 208-217.
- Iswaldi, I., Arráez-Román, D., Rodríguez-Medina, I., Beltrán-Debón, R., Joven, J., Segura-Carretero, A. & Fernández-Gutiérrez, A. (2011). Identification of phenolic compounds in aqueous and ethanolic rooibos extracts (*Aspalathus linearis*) by HPLC-ESI-MS (TOF/IT). *Analytical and Bioanalytical Chemistry*, **400**, 3643-3654.
- Ito, T., Kakino, M., Tazawa, S., Watarai, T., Oyama, M., Maruyama, H., Araki, Y., Hara, H. & Inuma, M. (2012). Quantification of polyphenols and pharmacological analysis of water and ethanol-based extracts and cultivated agarwood leaves. *Journal of Nutritional Science and Vitaminology*, **58**, 136-142.
- Jaiswal, R., Matei, M.F., Golon, A., Witt, M. & Kuhnert, N. (2012). Understanding the fate of chlorogenic acids in coffee roasting using mass spectrometry based targeted and non-targeted analytical strategies. *Food & Function*, **3**, 976-984.
- Joubert, E. (1996). HPLC quantification of the dihydrochalcones, aspalathin and nothofagin in rooibos tea (*Aspalathus linearis*) as affected by processing. *Food Chemistry*, **55**, 403-411.
- Joubert, E., Otto, F., Grüner, S. & Weinreich, B. (2003). Reversed-phase HPLC determination of mangiferin, isomangiferin and hesperidin in *Cyclopia* and the effect of harvesting date on the phenolic composition of *C. genistoides*. *European Food Research and Technology*, **216**, 270-273.

- Joubert, E., Manley, M. & Botha, M. (2006). Use of NIRS for quantification of mangiferin and hesperidin contents of dried green honeybush (*Cyclopia genistoides*) plant material. *Journal of Agricultural and Food Chemistry*, **54**, 5279-5283.
- Joubert, E., Gelderblom, W.C.A., Louw, A. & De Beer, D. (2008a). South African herbal teas: *Aspalathus linearis*, *Cyclopia* spp. and *Athrixia phylicoides* – A review. *Journal of Ethnopharmacology*, **119**, 376-412.
- Joubert, E., Richards, E.S., Van der Merwe, J.D., De Beer, D., Manley, M. & Gelderblom, W.C.A. (2008b). Effect of species variation and processing on phenolic composition and *in vitro* antioxidant activity of aqueous extracts of *Cyclopia* spp. (honeybush tea). *Journal of Agricultural and Food Chemistry*, **56**, 954-963.
- Joubert, E., Viljoen, M., De Beer, D. & Manley, M. (2009). Effect of heat on aspalathin, iso-orientin and orientin contents and color of fermented rooibos (*Aspalathus linearis*) iced tea. *Journal of Agricultural and Food Chemistry*, **57**, 4204-4211.
- Joubert, E., Viljoen, M., De Beer, D., Malherbe, C.J., Brand, D.J. & Manley, M. (2010). Use of green rooibos (*Aspalathus linearis*) extract and water-soluble nanomicelles of green rooibos extract encapsulated with ascorbic acid for enhanced aspalathin content in ready-to-drink iced teas. *Journal of Agricultural and Food Chemistry*, **58**, 10965-10971.
- Joubert, E., Joubert, M.E., Bester, C., De Beer, D. & De Lange, J.H. (2011). Honeybush (*Cyclopia* spp.): From local cottage industry to global markets – the catalytic and supporting role of research. *South African Journal of Botany*, **77**, 887-907.
- Joubert, E. & De Beer, D. (2014). Antioxidants of Rooibos Beverages: Role of Plant Composition and Processing, in: Preedy, V. (Ed.), *Processing and Impact on Antioxidants in Beverages*. Academic Press, San Diego, pp. 131-144.
- Joubert, E., De Beer, D., Hernández, I. & Munné-Bosch, S. (2014). Accumulation of mangiferin, isomangiferin, iriflophenone-3-*C*- β -glucoside and hesperidin in honeybush leaves (*Cyclopia genistoides* Vent.) in response to harvest time, harvest interval and seed source. *Industrial Crops and Products*, **56**, 74-82.
- Kamara, B.I., Brandt, E.V., Ferreira, D. & Joubert, E. (2003). Polyphenols from honeybush tea (*Cyclopia intermedia*). *Journal of Agricultural and Food Chemistry*, **51**, 3874-3879.
- Kamara, B.I., Brand, D.J., Brandt, E.V. & Joubert, E. (2004). Phenolic metabolites from honeybush tea (*Cyclopia intermedia*). *Journal of Agricultural and Food Chemistry*, **52**, 5391-5395.
- Karaköse, H., Jaiswal, R., Deshpande, S. & Kuhnert, N. (2015). An investigation of the photochemical changes of chlorogenic acids induced by UV light in model systems and in agricultural practice with *Stevia rebaudiana* cultivation as an example. *Journal of Agricultural and Food Chemistry*, DOI: 10.1021/acs.jafc.5b00838.
- Kawano, A., Nakamura, H., Hata, S.-I., Minakawa, M., Miura, Y. & Yagasaki, K. (2009). Hypoglycemic effect of aspalathin, a rooibos tea component from *Aspalathus linearis*, in type 2 diabetic model *db/db* mice. *Phytomedicine*, **16**, 437-443.
- Khadem, S. & Marles, R.J. (2010). Monocyclic phenolic acids; hydroxy- and polyhydroxybenzoic acids: occurrence and recent bioactivity studies. *Molecules*, **15**, 7985-8005.
- Khan, N. & Mukhtar, H. (2007). Tea polyphenols for health promotion. *Life Sciences*, **81**, 519-533.
- Khan, M.K., Zill-E-Huma & Dangles, O. (2014). A comprehensive review on flavanones, the major citrus polyphenols. *Journal of Food Composition and Analysis*, **33**, 85-104.
- Khuwijitjaru, P., Plernjit, J., Suaylam, B., Samuhaseneetoo, S., Pongsawatmanit, R. & Adachi, S. (2014a). Degradation kinetics of some phenolic compounds in subcritical water and radical scavenging activity of their degradation products. *The Canadian Journal of Chemical Engineering*, **92**, 810-815.
- Khuwijitjaru, P., Suaylam, B. & Adachi, S. (2014b). Degradation of caffeic acid in subcritical water and online HPLC-DPPH assay of degradation products. *Journal of Agricultural Food Chemistry*, **62**, 1945-1949.

- Koch, I.S., Muller, N., De Beer, D., Naes, T. & Joubert, E. (2013). Impact of steam pasteurization on the sensory profile and phenolic composition of rooibos (*Aspalathus linearis*) herbal tea infusions. *Food Research International*, **53**, 704-712.
- Kokotkiewicz, A., Luczkiewicz, M., Sowinski, P., Glod, D., Gorynski, K. & Bucinski, A. (2012). Isolation and structure elucidation of phenolic compounds from *Cyclopia subternata* Vogel (honeybush) intact plant and *in vitro* cultures. *Food Chemistry*, **133**, 1373-1382.
- Kokotkiewicz, A., Luczkiewicz, M., Pawlowska, J., Luczkiewicz, P., Sowinski, P., Witkowski, J., Bryl, E. & Bucinski, A. (2013). Isolation of xanthone and benzophenone derivatives from *Cyclopia genistoides* (L.) Vent. (honeybush) and their pro-apoptotic activity on synoviocytes from patients with rheumatoid arthritis. *Fitoterapia*, **90**, 199-208.
- Komatsu, Y., Suematsu, S., Hisanobu, Y., Saigo, H., Matsuda, R. & Hara, K. (1993). Effects of pH and temperature on reaction kinetics of catechins in green tea infusion. *Bioscience, Biotechnology, and Biochemistry*, **57**, 907-910.
- Kraczyk, N. & Glomb, M.A. (2008). Characterization of phenolic compounds in rooibos tea. *Journal of Agricultural and Food Chemistry*, **56**, 3368-3376.
- Kroll, J., Rawel, H.M. & Rohn, S. (2003). Reactions of plant phenolics with food proteins and enzymes under special consideration of covalent bonds. *Food Science and Technology Research*, **9**, 205-218.
- Ku, S.-K., Kwak, S., Kim, Y. & Bae, J.-S. (2015). Aspalathin and nothofagin from rooibos (*Aspalathus linearis*) inhibits high glucose-induced inflammation *in vitro* and *in vivo*. *Inflammation*, **38**, 445-455.
- Kudou, S., Fleury, Y., Welti, D., Magnolato, D., Uchida, T., Kitamura, K. & Okubo, K. (1991). Malonyl isoflavone glycosides in soybean seeds (*Glycine max* Merrill). *Agricultural and Biological Chemistry*, **55**, 2227-2233.
- Lee, S.W. & Lee, J.H. (2009). Effects of oven-drying, roasting, and explosive puffing process on isoflavone distributions in soybeans. *Food Chemistry*, **112**, 316-320.
- Lee, R.-Y., Lee, V.S.Y., Tzen, J.T.C. & Lee, M.-R. (2010). Study of the release of gallic acid from (-)-epigallocatechin gallate in old oolong tea by mass spectrometry. *Rapid Communications in Mass Spectrometry*, **24**, 851-858.
- Lemańska, K., Szymusiak, H., Tyrakowska, B., Zieliński, R., Soffers, A.E.M.F. & Rietjens, I.M.C.M. (2001). The influence of pH on antioxidant properties and the mechanism of antioxidant action of hydroxyflavones. *Free Biology and Medicine*, **31**, 869-881.
- Li, N., Taylor, L.S. & Mauer, L.J. (2011). Degradation kinetics of catechins in green tea powder: Effects of temperature and relative humidity. *Journal of Agricultural and Food Chemistry*, **59**, 6082-6090.
- Li, N., Taylor, L.S., Ferruzzi, M.G. & Mauer, L.J. (2012). Kinetic study of catechin stability: Effects of pH, concentration, and temperature. *Journal of Agricultural and Food Chemistry*, **60**, 12531-12539.
- Li, N., Taylor, L.S., Taylor, L.S., Ferruzzi, M.G. & Mauer, L.J. (2013). Color and chemical stability of tea polyphenol (-)-epigallocatechin-3-gallate in solution and solid states. *Food Research International*, **53**, 909-921.
- Li, Y.-J., Zhang, C.-F., Ding, G., Huang, W.-Z., Wang, Z.-Z., Bi, Y.-A. & Xiao, W. (2015). Investigating the thermal stability of six caffeoylquinic acids employing rapid-resolution liquid chromatography with quadrupole time-of-flight tandem mass spectrometry. *European Food Research and Technology*, **240**, 1225-1234.
- Lima, M., Heskitt, B.F., Burianek, L.L., Nokes, S.E. & Sastry, S.K. (1999). Ascorbic acid degradation kinetics during conventional and ohmic heating. *Journal of Food Processing and Preservation*, **23**, 421-434.
- Lindquist, E. & Yang, Y. (2011). Degradation of benzoic acid and its derivatives in subcritical water. *Journal of Chromatography A*, **1218**, 2146-2152.
- Liu, Y. Zou, L., Ma, L., Chen, W.-H., Wang, B. & Xu, Z.-L. (2006). Synthesis and pharmacological activities of xanthone derivatives as α -glucosidase inhibitors. *Bioorganic and Medicinal Chemistry*, **14**, 5683-5690.

- Liu, Q., Guo, T., Li, W., Li, D. & Feng, Z. (2012). Synthesis and evaluation of benzophenone *O*-glycosides as α -glucosidase inhibitors. *Archiv der Pharmazie – Chemistry in Life Sciences*, **345**, 771-783.
- Mahungu, S.M., Diaz-Mercado, S., Li, J., Schwenk, M., Singletary, K. & Faller, J. (1999). Stability of isoflavones during extrusion processing of corn/soy mixture. *Journal of Agricultural and Food Chemistry*, **47**, 279-284.
- Maini, S., Hodgson, H.L. & Krol, E.S. (2012). The UVA and aqueous stability of flavonoids is dependent on B-ring substitution. *Journal of Agricultural and Food Chemistry*, **60**, 6966-6976.
- Makris, D.P. & Rossiter, J.T. (2000). Heat-induced, metal-catalyzed oxidative degradation of quercetin and rutin (quercetin 3-*O*-rhamnosylglucoside) in aqueous model systems. *Journal of Agricultural and Food Chemistry*, **48**, 3830-3838.
- Malherbe, C.J., Willenburg, E., De Beer, D., Bonnet, S.L., Van der Westhuizen, J.H. & Joubert, E. (2014). Iriflophenone-3-*C*-glucoside from *Cyclopia genistoides*: Isolation and quantitative comparison of antioxidant capacity with mangiferin and isomangiferin using on-line HPLC antioxidant assays. *Journal of Chromatography B*, **951–952C**, 164-171.
- Manach, C., Scalbert, A., Morand, C., Rémésy, C. & Jiménez, L. (2004). Polyphenols: food sources and bioavailability. *American Journal of Clinical Nutrition*, **79**, 727-747.
- Marais, C., Van Rensburg, W.J., Ferreira, D. & Steenkamp, J.A. (2000). (*S*)- and (*R*)-Eriodictyol-6-*C*- β -*D*-glucopyranoside, novel keys to fermentation of rooibos (*Aspalathus linearis*). *Phytochemistry*, **55**, 43-49.
- Marloth, R. (1913). The Chemistry of South African Plants and Plant Products. *Cape Chemical Society*, p.9. Cape Town, South Africa.
- Marloth, R. (1925). *The Flora of South Africa with Synoptical Tables of the Genera of the Higher Plants*. Pp.69-72. Cape Town: Darter Bros & Co.
- Masibo, M & He, Q. (2008). Major mango polyphenols and their potential significance to human health. *Comprehensive Reviews in Food Science and Food Safety*, **7**, 309-319.
- Matei, M.F., Jaiswal, R. & Kuhnert, N. (2012). Investigating the chemical changes of chlorogenic acids during coffee brewing: Conjugate addition of water to the olefinic moiety of chlorogenic acids and their quinides. *Journal of Agricultural and Food Chemistry*, **60**, 12105-12115.
- Mathias, K., Ismail, B., Corvalan, C.M. & Hayes, K.D. (2006). Heat and pH effects on the conjugated forms of genistin and daidzin isoflavones. *Journal of Agricultural and Food Chemistry*, **54**, 7495-7502.
- Mazibuko, S.E., Joubert, E., Johnson, R., Louw, J., Opoku, A.R. & Muller, C.J.F. (2015). Aspalathin improves glucose and lipid metabolism in 3T3-L1 adipocytes exposed to palmitate. *Molecular Nutrition & Food Research*, doi: 10.1002/mnfr.201500258.
- Meyer, J.C., Marrone, P.A. & Tester, J.W. (1995). Acetic acid oxidation and hydrolysis in supercritical water. *AIChE Journal*, **41**, 2108-2121.
- Montijano, H., Tomás-Barberán, F.A. & Borrego, F. (1995). Stability of the intense sweetener neohesperidine DC during yoghurt manufacture and storage. *Zeitschrift für Lebensmittel-Untersuchung und-Forschung: European Food Research and Technology*, **201**, 541-543.
- Montijano, H., Coll, M.D. & Borrego, F. (1996). Assessment of neohesperidine DC stability during pasteurization of juice-based drinks. *International Journal of Food Science and Technology*, **31**, 397-401.
- Montijano, H., Borrego, F., Tomás-Barberán, F.A. & Lindley, M.G. (1997). Stability of neohesperidin dihydrochalcone in a lemonade system. *Food Chemistry*, **58**, 13-15.

- Muller, C.J.F., Joubert, E., De Beer, D., Sanderson, M., Malherbe, C.J., Fey, S.J. & Louw, J. (2012). Acute assessment of an aspalathin-enriched green rooibos (*Aspalathus linearis*) extract with hypoglycemic potential. *Phytomedicine*, **20**, 32-39.
- Murakami, M., Yamaguchi, T., Takamura, H. & Matoba, T. (2004). Effects of thermal treatment on radical-scavenging activity of single and mixed polyphenolic compounds. *Journal of Food Science*, **69**, FCT7-FCT10.
- Murphy, P.A., Barua, K. & Hauck, C.C. (2002). Solvent extraction selection in the determination of isoflavones in soy foods. *Journal of Chromatography B.*, **777**, 129-138.
- Mwithiga, G. & Jindal, V.K. (2003). Physical changes during coffee roasting in rotary conduction-type heating units. *Journal of Food Process Engineering*, **26**, 543-558.
- Narita, Y. & Inouye, K. (2013). Degradation kinetics of chlorogenic acid at various pH values and effects of ascorbic acid and epigallocatechin gallate on its stability under alkaline conditions. *Journal of Agricultural and Food Chemistry*, **61**, 966-972.
- Neilson, A.P, Song, B.J., Sapper, T.N., Bomser, J.A. & Ferruzzi, M.G. (2010). Tea catechin auto-oxidation dimers are accumulated and retained by Caco-2 human intestinal cells. *Nutrition Research*, **30**, 327-340.
- Niamnuy, C., Nachaisin, M., Laohavanich, J. & Devahastin, S. (2011). Evaluation of bioactive compounds and bioactivities of soybean dried by different methods and conditions. *Food Chemistry*, **129**, 899-906.
- Niamnuy, C., Nachaisin, M., Poomsa-ad, N. & Devahastin, S. (2012). Kinetic modelling of drying and conversion/degradation of isoflavones during infrared drying of soybean. *Food Chemistry*, **133**, 946-952.
- Odriozola-Serrano, I., Soliva-Fortuny, R. & Martín-Belloso, O. (2008). Phenolic acids, flavonoids, vitamin C and antioxidant capacity of strawberry juices processed by high-intensity pulsed electric fields or heat treatments. *European Food Research and Technology*, **228**, 239-248.
- Pandey, K. B. & Rizvi, S.I. (2009). Plant polyphenols as dietary antioxidants in human health and disease. *Oxidative Medicine and Cellular Longevity*, **2**, 270-278.
- Patras, A., Brunton, N.P., O'Donnell, C. & Tiwari, B.K. (2010). Effect of thermal processing on anthocyanin stability in foods; mechanisms and kinetics of degradation. *Trends in Food Science and Technology*, **21**, 3-11.
- Payne, M.J., Hurst, W.J., Miller, K.B., Rank, C. & Stuart, D.A. (2010). Impact of fermentation, drying, roasting, and dutch processing on epicatechin and catechin content of cacao beans and cocoa ingredients. *Journal of Agricultural and Food Chemistry*, **58**, 10518-10527.
- Pazmiño-Durán, E.A., Giusti, M.M., Wrolstad, R.E. & Glória, M.B.A (2001). Anthocyanins from *Oxalis triangularis* as potential food colorants. *Food Chemistry*, **75**, 211-216.
- Peleg, M., Normand, M.D. and Corradini, M.G. (2012). The Arrhenius equation revisited. *Critical Reviews in Food Science and Nutrition*, **52**, 830-851.
- Perrone, D., Farah, A., Donangelo, C.M., De Paulis, T. & Martin, P.R. (2008). Comprehensive analysis of major and minor chlorogenic acids and lactones in economically relevant Brazilian coffee cultivars. *Food Chemistry*, **106**, 859-867.
- Perrone, D., Donangelo, R., Donangelo, C.M. & Farah, A. (2010). Modeling weight loss and chlorogenic acids content in coffee during roasting. *Journal of Agricultural and Food Chemistry*, **58**, 12238-12243.
- Phoboo, S., Da Silva Pinto, M., Barbosa, A.C.L., Sarkar, D., Bhowmik, P.C., Jha, P.K. & Shetty, K. (2012). Phenolic-linked biochemical rationale for the anti-diabetic properties of *Swertia chirayita* (Roxb. ex Flem.) karst. *Phytotherapy Research*, Published online in Wiley Online Library (wileyonlinelibrary.com) DOI: 10.1002/ptr.4714
- Prashanth, D., Amit, A., Samiulla, D.S., Asha, M.K. & Padmaja, R. (2001). α -Glucosidase inhibitory activity of *Mangifera indica* bark. *Fitoterapia*, **72**, 686-688.

- Rao, A.V. & Rao, L.G. (2007). Carotenoids and human health. *Pharmacological Research*, **55**, 207-216.
- Rohn, S., Buchner, N., Driemel, G., Rauser, M. & Kroh, L.W. (2007). Thermal degradation of onion quercetin glucosides under roasting conditions. *Journal of Agricultural and Food Chemistry*, **55**, 1568-1573.
- Sánchez-Moreno, C., Plaza, L., Elez-Martínez, P., De Ancos, B., Martín-Belloso, O. & Cano, M.P. (2005). Impact of high pressure and pulsed electric fields on bioactive compounds and antioxidant activity of orange juice in comparison with traditional thermal processing. *Journal of Agricultural and Food Chemistry*, **53**, 4403-4409.
- Sang, S., Lee, M.-J., Hou, Z., Ho, C.-T. & Yang, C.S. (2005). Stability of tea polyphenol (-)-epigallocatechin-3-gallate and formation of dimers and epimers under common experimental conditions. *Journal of Agricultural and Food Chemistry*, **53**, 9478-9484.
- Sanugul, K., Akao, T., Li, Y., Kakiuchi, N., Nakamura, N. & Hattori, M. (2005). Isolation of a human intestinal bacterium that transforms mangiferin to norathyriol and inducibility of the enzyme that cleaves a C-glucosyl bond. *Biological and Pharmaceutical Bulletin*, **28**, 1672-1678.
- Scalbert, A., Johnson, I.T. & Saltmarsh, M. (2005). Polyphenols: antioxidants and beyond. *The American Journal of Clinical Nutrition*, **81**(suppl), 215S-217S.
- Schulze, A.E., De Beer, D., De Villiers, A., Manley, M. & Joubert, E. (2014). Chemometric analysis of chromatographic fingerprints shows potential of *Cyclopia maculata* (Andrews) Kies for production of standardized extracts with high xanthone content. *Journal of Agricultural and Food Chemistry*, **62**, 10542-10551.
- Schulze, A.E., De Beer, D., Mazibuko, S.E., Muller, C.J.F., Roux, C., Willenburg, E.L., Nyunai, N., Louw, J., Manley, M. & Joubert, E. (2015). Assessing similarity analysis of chromatographic fingerprints of *Cyclopia subternata* extracts as potential screening tool for *in vitro* glucose utilization. *Analytical and Bioanalytical Chemistry*, DOI 10.1007/s00216-015-9147-7.
- Seto, R., Nakamura, H., Nanjo, F. & Hara, Y. (1997). Preparation of epimers of tea catechins by heat treatment. *Bioscience, Biotechnology, and Biochemistry*, **61**, 1434-1439.
- Singletary, K., Faller, J., Li, J.Y. & Mahungu, S. (2000). Effect of extrusion on isoflavone content and antiproliferative bioactivity of soy/corn mixtures. *Journal of Agricultural and Food Chemistry*, **48**, 3566-3571.
- Sivetz, M. & Desrosier, N.W. (1979). Coffee bean processing. IN: *Coffee Technology*. Connecticut, USA: The AVI Publishing Company Inc.
- Snijman, P.W., Swanevelder, S., Joubert, E., Green, I.R. & Gelderblom, W.C.A. (2007). The antimutagenic activity of the major flavonoids of rooibos (*Aspalathus linearis*): Some dose-response effects on mutagen activation-flavonoid interactions. *Mutation Research*, **631**, 111-123.
- Snijman, P.W., Joubert, E., Ferreira, D., Li, X.-C., Ding, Y., Green, I.R. & Gelderblom, W.C.A. (2009). Antioxidant activity of the dihydrochalcones aspalathin and nothofagin and their corresponding flavones in relation to other rooibos (*Aspalathus linearis*) flavonoids, epigallocatechin gallate, and trolox. *Journal of Agricultural and Food Chemistry*, **57**, 6678-6684.
- Son, M., Minakawa, M., Miura, Y. & Yagasaki, K. (2013). Aspalathin improves hyperglycemia and glucose intolerance in obese diabetic *ob/ob* mice. *European Journal of Nutrition*, **52**, 1607-1619.
- Song, B.J., Manganais, C. & Ferruzzi, M.G. (2015). Thermal degradation of green tea flavan-3-ols and formation of hetero- and homocatechin dimers in model dairy beverages. *Food Chemistry*, **173**, 305-312.
- Stadler, R.H., Welti, D.H., Stämpfli, A.A. & Fay, L.B. (1996). Thermal decomposition of caffeic acid in model systems: identification of novel tetraoxygenated phenylindan isomers and their stability in aqueous solution. *Journal of Agricultural and Food Chemistry*, **44**, 898-905.

- Stahl, W. & Sies, H. (2005). Bioactivity and protective effects of natural carotenoids. *Biochimica et Biophysica Acta*, **1740**, 101-107.
- Stalikas, C.D. (2007). Review: Extraction, separation and detection methods for phenolic acids and flavonoids. *Journal of Separation Science*, **30**, 3268-3295.
- Stintzing, F.C. & Carle, R. (2004). Functional properties of anthocyanins and betalains in plants, food, and in human nutrition. *Trends in Food Science and Technology*, **15**, 19-38.
- Stintzing, F.C., Hoffmann, M. & Carle, R. (2006). Thermal degradation kinetics of isoflavone aglycones from soy and red clover. *Molecular Nutrition and Food Research*, **50**, 373-377.
- Su, Y.L., Leung, L.K., Huang, Y. & Chen, Z.-Y. (2003). Stability of tea theaflavins and catechins. *Food Chemistry*, **83**, 189-195.
- Theron, K.A. (2012). Sensory and Phenolic Profiling of Cyclopia Species (Honeybush) and Optimisation of the Fermentation Conditions. MSc (Food Science) Thesis, Stellenbosch University, Stellenbosch, South Africa.
- Tomás-Barberán, F.A., Borrego, F., Ferreres, F. & Lindley, M.G. (1995). Stability of the intense sweetener neohesperidine dihydrochalcone in blackcurrent jams. *Food Chemistry*, **52**, 263-265.
- Tomás-Barberán, F.A. & Clifford, M.N. (2000). Flavanones, chalcones and dihydrochalcones – nature, occurrence and dietary burden. *Journal of the Science of Food and Agriculture*, **80**, 1073-1080.
- Tounekti, T., Joubert, E., Hernández, I. & Munné-Bosch, S. (2013). Improving the polyphenol content of tea. *Critical Reviews in Plant Sciences*, **32**, 192-215.
- Tournaire, C., Hocquaux, M., Beck, I., Oliveros, E. & Maurette, M.-T. (1994). "Activité anti-oxydante de flavonoids. Réactivité avec le superoxide de potassium en phase hétérogène." (Article in French). *Tetrahedron*, **50**, 9303-9314.
- Trugo, L.C. & Macrae, R. (1984a). A study of the effect of roasting on the chlorogenic acid composition of coffee using HPLC. *Food Chemistry*, **15**, 219-227.
- Trugo, L.C. & Macrae, R. (1984b). Chlorogenic acid composition of instant coffees. *Analyst*, **109**, 263-266.
- Tu, Y.Y., Xia, H.L. & Watanabe, N. (2005). Changes in catechins during the fermentation of green tea. *Applied Biochemistry and Microbiology*, **41**, 574-577.
- Ungar, Y., Osundahunsi, O.F. & Shimoni, E. (2003). Thermal stability of genistein and daidzein and its effect on their antioxidant activity. *Journal of Agricultural and Food Chemistry*, **51**, 4394-4399.
- Vaidya, N.A., Mathias, K., Ismail, B., Hayes, K.D. & Corvalan, C.M. (2007). Kinetic modeling of malonylgenistin and malonyldaidzin conversions under alkaline conditions and elevated temperatures. *Journal of Agricultural and Food Chemistry*, **55**, 3408-3413.
- Van Boekel, M.A.J.S. (1996). Statistical aspects of kinetic modelling for food science problems. *Journal of Food Science*, **6**, 477-486.
- Van Boekel, M.A.J.S. (2008). Kinetic modeling of food quality: a critical review. *Comprehensive Reviews in Food Science and Food Safety*, **7**, 144-158.
- Van der Merwe, J.D., Joubert, E., Manley, M., De Beer, D., Malherbe, C.J. & Gelderblom, W.C.A. (2012). Mangiferin glucuronidation: important hepatic modulation of antioxidant activity. *Food and Chemical Toxicology*, **50**, 808-815.
- Van der Sluis, A.A., Dekker, M. & Van Boekel, M.A.J.S. (2005). Activity and concentration of polyphenolic antioxidants in apple juice. 3. Stability during storage. *Journal of Agricultural and Food Chemistry*, **53**, 1073-1080.
- Vikram, V.B., Ramesh, M.N. & Prapulla, S.G. (2005). Thermal degradation kinetics of nutrients in orange juice heated by electromagnetic and conventional methods. *Journal of Food Engineering*, **69**, 31-40.
- Villares, A., Rostagno, M.A., García-Lafuente, Guillamón, E. & Martínez, J.A. (2011). Content and profile of isoflavones in soy-based foods as a function of production process. *Food and Bioprocess Technology*, **4**, 27-38.

- Vitale, D.C., Piazza, C., Melilli, B., Drago, F. & Salomone, S. (2013). Isoflavones: estrogenic activity, biological effect and bioavailability. *European Journal of Drug Metabolism and Pharmacokinetics*, **38**, 15-25.
- Vyas, A., Syeda, K., Ahmad, A., Padhye, S. & Sarkar, F.H. (2012). Perspectives on medicinal properties of mangiferin. *Mini-Reviews in Medicinal Chemistry*, **12**, 412-425.
- Wang, G., Kuan, S.S., Francis, O.J., Ware, G.M. & Carman, A.S. (1990). A simplified HPLC method for the determination of phytoestrogens in soybean and its processed products. *Journal of Agricultural and Food Chemistry*, **38**, 185-190.
- Wang, H.-J. & Murphy, P.A. (1996). Mass balance study of isoflavones during soybean processing. *Journal of Agricultural and Food Chemistry*, **44**, 2377-2383.
- Wang, H. & Helliwell, K. (2000). Epimerisation of catechins in green tea infusions. *Food Chemistry*, **70**, 337-344.
- Wang, L.-F., Kim, D.-M. & Lee, C.Y. (2000). Effects of heat processing and storage on flavanols and sensory qualities of green tea beverage. *Journal of Agricultural and Food Chemistry*, **48**, 4227-4232.
- Wang, R., Zhou, W. & Wen, R.-A.H. (2006). Kinetic study of the thermal stability of tea catechins in aqueous systems using a microwave reactor. *Journal of Agricultural and Food Chemistry*, **54**, 5924-5932.
- Wang, R., Zhou, W. & Jiang, X. (2008a). Reaction kinetics of degradation and epimerization of epigallocatechin gallate (EGCG) in aqueous system over a wide temperature range. *Journal of Agricultural and Food Chemistry*, **56**, 2694-2701.
- Wang, R., Zhou, W. & Jiang, X. (2008b). Mathematical modeling of the stability of green tea catechin epigallocatechin gallate (EGCG) during bread baking. *Journal of Food Engineering*, **87**, 505-513.
- Watt, J.M. & Breyer-Brandwijk, M.G. (1962). *The Medicinal and Poisonous Plants of Southern and Eastern Africa*, 2nd ed. Edinburgh: E & S Livingstone.
- Xia, H., Sun, L., Lou, H. & Rahman, M.M. (2014). Conversion of salvianolic acid B into salvianolic acid A in tissues of *Radix Salviae Miltiorrhizae* using high temperature, high pressure and high humidity. *Phytomedicine*, **21**, 906-911.
- Xie, C., Yu, K., Zhong, D., Yuan, T., Ye, F., Jarrell, J.A., Millar, A. & Chen, X. (2011). Investigation of isomeric transformations of chlorogenic acid in buffers and biological matrixes by ultraperformance liquid chromatography coupled with hybrid quadrupole/ion mobility/orthogonal acceleration time-of-flight mass spectrometry. *Journal of Agricultural and Food Chemistry*, **59**, 11078-11087.
- Xu, Z., Wu, Q. & Godber, J.S. (2002). Stabilities of daidzin, glycitin, genistin, and generation of derivatives during heating. *Journal of Agricultural and Food Chemistry*, **50**, 7402-7406.
- Xu, J.Z., Leung, L.K., Huang, Y. & Chen, Z.-Y. (2003). Epimerisation of tea polyphenols in tea drinks. *Journal of the Science of Food and Agriculture*, **83**, 1617-1621.
- Xu., Z., Wei, L.-h., Ge, X.-z., Zhu, W. & Li, C.-m. (2015). Comparison of the degradation kinetics of A-type and B-type proanthocyanidins dimers as a function of pH and temperature. *European Food Research and Technology*, **240**, 707-717.
- Yoshikawa, M., Nishida, N., Shimoda, H., Takada, M., Kawahara, Y. & Matsuda, H. (2001). Polyphenol constituents from *Salacia* species: quantitative analysis of mangiferin with α -glucosidase and aldose reductase inhibitory activities. *Yakugaku Zasshi*, **121**, 371-378.
- Yu, J. & Savage, P.E. (1998). Decomposition of formic acid under hydrothermal conditions. *Industrial and Engineering Chemistry Research*, **37**, 2-10.
- Yuan, J.-P., Liu, Y.-B., Peng, J., Wang, J.-H. & Liu, X. (2009). Changes of isoflavone profile in the hypocotyls and cotyledons of soybeans during dry heating and germination. *Journal of Agricultural and Food Chemistry*, **57**, 9002-9010.

- Yue, X., Abdallah, A.M. & Xu, Z. (2010). Thermal dynamic properties of isoflavones during dry heating. *International Journal of Food Science and Technology*, **45**, 1878-1882.
- Zanoelo, E.F. & Benincá, C. (2009). Chemical kinetics of 5-*O*-caffeoylquinic acid in superheated steam: effect of isomerization on mate (*Ilex paraguariensis*) manufacturing. *Journal of Agricultural and Food Chemistry*, **57**, 11564-11569.
- Zaveri, N.T. (2006). Green tea and its polyphenolic catechins: Medicinal uses in cancer and noncancer applications. *Life Sciences*, **78**, 2073-2080.
- Zhang, Y.C., Lee, J.H., Vodovotz, Y. & Schwartz, S.J. (2004). Changes in distribution of isoflavones and β -glucosidase activity during soy bread proofing and baking. *Cereal Chemistry*, **81**, 741-745.
- Zhang, Y., Qian, Q., Ge, D., Li, Y., Wang, X., Chen, Q., Gao, X. & Wang, T. (2011). Identification of benzophenone *C*-glucosides from mango tree leaves and their inhibitory effect on triglyceride accumulation in 3T3-L1 adipocytes. *Journal of Agricultural and Food Chemistry*, **59**, 11526-11533.
- Zhang, Y., Liu, X., Han, L., Gao, X., Liu, E. & Wang, T. (2013a). Regulation of lipid and glucose homeostasis by mango tree leaf extract is mediated by AMPK and PI3K/AKT signaling pathways. *Food Chemistry*, **141**, 2896-2905.
- Zhang, Q.-F., Fu, Y.-J., Huang, Z.-W., Shangguang, X.-C. & Guo, Y.-X (2013b). Aqueous stability of astilbin: effects of pH, temperature, and solvent. *Journal of Agricultural and Food Chemistry*, **61**, 12085-12091.
- Zhu, Q.Y., Zhang, A., Tsang, D., Huang, Y. & Chen, Z.-Y. (1997). Stability of green tea catechins. *Journal of Agricultural and Food Chemistry*, **45**, 4624-4628.
- Zielinski, H., Michalska, A., Amigo-Benavent, M., Del Castillo, M. D. & Piskula, M.K. (2009). Changes in protein quality and antioxidant properties of buckwheat seeds and groats induced by roasting. *Journal of Agricultural and Food Chemistry*, **57**, 4771-4776.
- Zimeri, J. & Tong, C.H. (1999). Degradation kinetics of (-)-epigallocatechin gallate as a function of pH and dissolved oxygen in a liquid model system. *Journal of Food Science*, **64**, 753-758.

CHAPTER 3

Comprehensive Phenolic Profiling of *Cyclopia genistoides* (L.) Vent. by LC-DAD-ESI-MS and –MS/MS Reveals Novel Xanthone and Benzophenone Constituents

* **Published**

Beelders, T., De Beer, D., Stander, M.A. & Joubert, E. (2014). Comprehensive phenolic profiling of *Cyclopia genistoides* (L.) Vent. by LC-DAD-MS and –MS/MS reveals novel xanthone and benzophenone constituents. *Molecules*, **19**, 11760-11790.

DECLARATION

With regard to Chapter 3 (pp. 78-108), the nature and scope of my contribution were as follows:

Nature of Contribution	Extent of Contribution (%)
Conducted all experimental work, including HPLC method development, method validation and quantitative application, as well as LC-DAD-ESI-MS and –MS/MS analyses and data interpretation.	80%
Wrote the entire manuscript, and edited the document in its entirety during the different stages of the publication process.	

The following co-authors have contributed to Chapter 3 (pp. 78-108):

Name	E-mail address	Nature of Contribution	Extent of Contribution (%)
Dr Dalene de Beer (Co-supervisor)	DBeerD@arc.agric.za	Assisted in editing the document in its entirety during the different stages of publication.	10%
Dr Marietjie Stander	lcms@sun.ac.za	Assisted in LC-DAD-ESI-MS and –MS/MS analyses, and the optimisation of the MS and –MS/MS parameters. Also provided input with regard to the identification of unknown constituents.	5%
Dr Elizabeth Joubert (Supervisor)	JoubertL@arc.agric.za	Assisted in editing the document in its entirety during the different stages of publication.	5%

Signature of candidate: **Declaration with signature in possession of candidate and supervisor*

Date: February 2016

Declaration by co-authors:

The undersigned hereby confirm that

1. the declaration above accurately reflects the nature and extent of the contribution of the candidate and the co-authors to Chapter 3 (pp. 78-108),
2. no other authors contributed to Chapter 3 (pp. 78-108) besides those specified above, and
3. potential conflicts of interest have been revealed to all interested parties and that the necessary arrangements have been made to use the material in Chapter 3 (pp. 78-108) of this dissertation.

Signature*	Institutional Affiliation	Date
Dr Dalene de Beer	Post-Harvest and Wine Technology Division, Agricultural Research Council Infruitec-Nietvoorbij	
Dr Marietjie Stander	Central Analytical Facility, Mass Spectrometry Unit, Stellenbosch	
Dr Elizabeth Joubert	Post-Harvest and Wine Technology Division, Agricultural Research Council Infruitec-Nietvoorbij; Department of Food Science, Stellenbosch University	

ABSTRACT

A high-performance liquid chromatographic (HPLC) method coupled with diode-array detection (DAD) was optimised for the qualitative analysis of aqueous extracts of *Cyclopia genistoides*. Comprehensive insight into the phenolic profile of unfermented and fermented sample extracts was achieved with the identification of 10 compounds based on comparison with authentic reference standards and the tentative identification of 30 additional compounds by means of electrospray ionisation mass spectrometry (ESI-MS) and tandem MS detection. Three iriflophenone-di-*O,C*-hexoside isomers, three xanthone-dihydrochalcone derivatives and one dihydrochalcone are herein tentatively identified for the first time in *C. genistoides*. Of special interest is one iriflophenone-di-*O,C*-hexoside derivative present in large amounts. New compounds (tentatively) identified for the first time in this species, and also in the genus *Cyclopia*, include two aromatic amino acids, one flavone, an iriflophenone-di-*C*-hexoside, a maclurin-di-*O,C*-hexoside, two tetrahydroxyxanthone-*C*-hexoside isomers, a tetrahydroxyxanthone-di-*O,C*-hexoside, two symmetric tetrahydroxyxanthone-*C*-hexoside dimers, nine glycosylated flavanone derivatives and five glycosylated phenolic acid derivatives. The presence of new compound sub-classes in *Cyclopia*, namely aromatic amino acids and glycosylated phenolic acids, was demonstrated. The HPLC DAD method was successfully validated and applied for the quantitative analysis of the paired sample extracts. In-depth analysis of the chemical composition of *C. genistoides* hot water extracts gave a better understanding of the chemistry of this species that will guide further research into its medicinal properties and potential uses.

1. INTRODUCTION

Globally the market share of herbal teas is growing, driven by key factors such as increasing consumer awareness regarding their health benefits and caffeine-free status. The genus *Cyclopia* (family Fabaceae; tribe Podalyriaceae), commonly known as honeybush, has a long history of localised use as herbal tea. Concerted efforts towards cultivation, improved quality and value-adding resulted in its transition from a herbal tea, drunk solely in South Africa, to a product enjoyed world-wide (Joubert *et al.*, 2011). For the commercial development of the industry, a number of *Cyclopia* species including *C. genistoides*, which was used as a tea prior to 1900 (Greenish, 1881), were selected. *Cyclopia genistoides* contains high levels of the pharmacologically active xanthone, mangiferin, and its regio-isomer, isomangiferin (Joubert *et al.*, 2003). This fact motivated several investigations aimed at the use of *C. genistoides* as a source material for production of xanthone-rich extracts for the food ingredient and nutraceutical markets (Joubert *et al.*, 2008a, 2014). Mangiferin is valued for its antioxidant and antidiabetic properties (as reviewed by Vyas *et al.*, 2012). The related benzophenone 3- β -D-glucopyranosylriflophenone, recently shown to be present in *C. genistoides* by Kokotkiewicz *et al.* (2013), has the ability to regulate sugar and lipid homeostasis in vitro (Zhang *et al.*, 2013). Furthermore, among four *Cyclopia* species tested, all batches of *C. genistoides* demonstrated phytoestrogenic activity (Verhoog *et al.*, 2007), which clearly supports the value of this *Cyclopia* species as source of bio-active constituents. In spite of the interest in *C. genistoides*, a comprehensive characterisation of the phenolic profile of *C. genistoides* has not been performed to date.

The objective of the present work was thus to elucidate the phenolic profile of hot water extracts of *C. genistoides* using high-performance liquid chromatography (HPLC) coupled with diode-array detection (DAD), as well as electrospray ionisation mass spectrometry (ESI-MS) and tandem MS (MS/MS) detection. The focus fell on hot water extracts due to their similarity to a “cup of tea”. Furthermore, this type of extract is prepared by extract manufacturers for the food and nutraceutical industries. As both “unfermented” (green) and “fermented” (oxidised) processed plant materials are produced by the honeybush industry, samples of both types were analysed to incorporate the additional variation introduced with high-temperature fermentation (Joubert *et al.*, 2008b). Optimisation and validation of an HPLC-DAD method for the qualitative and quantitative analysis of extracts was performed, as a species-specific method for *C. genistoides* was not available. A “generic” *Cyclopia* HPLC method used to date for analysis of *C. genistoides* (De Beer & Joubert, 2010) suffers from several disadvantages, including poor separation of minor constituents and the elution of highly polar constituents in the void volume. Previous investigations of the phenolic profiles of aqueous extracts of *C. subternata* (De Beer *et al.*, 2012) and *C. maculata* (Schulze *et al.*, 2014) highlighted the need for species-specific HPLC methods to accommodate qualitative and quantitative differences between *Cyclopia* species.

2. MATERIALS AND METHODS

2.1. Chemicals

HPLC gradient-grade methanol and acetonitrile were purchased from Merck Millipore (Darmstadt, Germany) and Sigma-Aldrich (St. Louis, MO, USA), respectively. HPLC-grade water was prepared using Elix and Milli-Q academic (Merck Millipore) water purification systems in tandem. Authentic reference standards with purity > 95% were supplied by Sigma-Aldrich (maclurin, mangiferin, naringin, hesperidin), Extrasynthese (Genay, France; eriocitrin, narirutin, diosmin), Chemos GmbH (Regenstauf, Germany; isomangiferin), Apin Chemicals (Oxfordshire, UK; neomangiferin) and Phytolab (Vestenbergsgreuth, Germany; vicenin-2). Tyrosine and phenylalanine were constituents of an amino acid standard mixture (Waters, Milford, MA, USA). Aspalathin (3'- β -D-glucopyranosyl-3-hydroxyphloretin) and nothofagin (3'- β -D-glucopyranosylphloretin) (> 95%) were supplied by the PROMEC Unit of the Medical Research Council of South Africa (Tygerberg, Cape Town, South Africa). 3- β -D-Glucopyranosylriflophenone (97%) was isolated (Malherbe *et al.*, 2014)

and supplied by the Agricultural Research Council of South Africa (Post-Harvest and Wine Technology Division, ARC Infruitec-Nietvoorbij, Stellenbosch, South Africa). Other chemicals were reagent grade from Sigma-Aldrich or Merck Millipore.

Stock solutions of the phenolic standards were prepared in dimethylsulfoxide (DMSO) at concentrations of approximately $1 \text{ mg}\cdot\text{mL}^{-1}$ and diluted with purified water according to experimental requirements. All diluted standard solutions contained ascorbic acid (Sigma-Aldrich) at a final concentration of *ca.* $5 \text{ mg}\cdot\text{mL}^{-1}$ and were filtered using $0.22 \text{ }\mu\text{m}$ pore-size Millex-HV syringe filters (4 mm diameter, Millipore) prior to use.

2.2. Sample Preparation

The shoots from a single plant of *C. genistoides* (Overberg type) were harvested from a commercial plantation situated in Pearly Beach (Western Cape, South Africa). The shoots were mechanically shredded ($\leq 3 \text{ mm}$) and divided into two sub-batches for preparation of unfermented and fermented plant material. The unfermented plant material was produced by drying one sub-batch without delay in a cross-flow drying tunnel at $40 \text{ }^\circ\text{C}$ for 16 h to less than 10% moisture content, followed by sieving for 90 s through a 1.4 mm (12 mesh) sieve using a SMC Mini-sifter (JM Quality Services, Cape Town, South Africa) to obtain the “tea bag” fraction. The fermented plant material was prepared by adding water to the other sub-batch to achieve a moisture content of *ca.* 60-65%, followed by fermentation at $90 \text{ }^\circ\text{C}$ for 16 h. Drying and sieving were accomplished as described for the unfermented plant material. These laboratory-scale processing procedures are in accordance with industry practice.

An extract of each plant material sample was prepared by adding 100 mL freshly-boiled deionised water to 10 g sieved plant material in a screw-cap glass bottle. The bottle was placed in a water bath at $93 \text{ }^\circ\text{C}$ for 30 min, while the mixture was swirled every 5 min. The warm extracts were filtered through Whatman #4 filter paper and cooled to room temperature. The filtrates were frozen and freeze-dried using a VirTis Advantage Plus freeze-drier (SP Scientific, Warminster, PA, USA).

Prior to HPLC analysis, the freeze-dried extracts were reconstituted in deionised water (*ca.* $6 \text{ mg}\cdot\text{mL}^{-1}$), followed by the addition of 10% aqueous ascorbic acid ($\text{m}\cdot\text{v}^{-1}$, final concentration = $9 \text{ mg}\cdot\text{mL}^{-1}$). Samples were filtered using $0.45 \text{ }\mu\text{m}$ pore-size Millex-HV syringe filters (33 mm diameter; Merck Millipore) and analysed.

2.3. HPLC-DAD Method Development

HPLC-DAD method development was conducted on an Agilent 1200 instrument equipped with an in-line degasser, quaternary pump, autosampler, column thermostat and DAD controlled by Openlab Chemstation software (Agilent Technologies Inc., Santa Clara, CA, USA). The following 4.6 mm ID columns were evaluated: 150 mm $3 \text{ }\mu\text{m}$ d_p Gemini-NX C_{18} (Phenomenex, Santa Clara, CA, USA); 100 mm $1.8 \text{ }\mu\text{m}$ d_p Zorbax SB- C_{18} (Agilent Technologies Inc.); and 150 mm $2.6 \text{ }\mu\text{m}$ d_p Kinetex C_{18} (Phenomenex). Methanol, acetonitrile and mixtures of methanol and acetonitrile were investigated as potential organic modifiers. For the aqueous phase, 2% aqueous acetic acid ($\text{v}\cdot\text{v}^{-1}$) and different concentrations of aqueous formic acid (0.1 and 1.0%, $\text{v}\cdot\text{v}^{-1}$) were evaluated. Gradient parameters were adjusted by systematically changing the percentage organic modifier at initial conditions, and/or the isocratic hold period at initial conditions, and/or gradient steepness. Different column temperatures were furthermore evaluated in $5 \text{ }^\circ\text{C}$ intervals ranging from 25-40 $^\circ\text{C}$.

2.4. Optimised HPLC-DAD Method

Optimum chromatographic separation of the phenolic constituents of *C. genistoides* extracts was achieved using the Kinetex column protected with an HPLC Krudkratcher Ultra in-line filter ($0.5 \text{ }\mu\text{m}$; Phenomenex). The column was

thermostatted at 30 °C and the mobile phase comprised of (A) 1% aqueous formic acid (v.v⁻¹), (B) methanol and (C) acetonitrile. The flow rate was 1.0 mL.min⁻¹ and a multi-linear gradient was performed as follows: 0 min (95.0% A, 2.5% B, 2.5% C), 5 min (95.0% A, 2.5% B, 2.5% C), 45 min (75% A, 12.5% B, 12.5% C), 55 min (50% A, 25.0% B, 25.0% C), 56 min (50% A, 25.0% B, 25.0% C), 57 min (95.0% A, 2.5% B, 2.5% C), 65 min (95.0% A, 2.5% B, 2.5% C).

2.5. LC-DAD-ESI-MS and –MS/MS Analyses

LC-DAD-ESI-MS and -MS/MS analyses were conducted on an Acquity UPLC system equipped with a binary solvent manager, sample manager, column heating compartment and photodiode-array detector coupled to a Synapt G2 Q-TOF system equipped with an electrospray ionisation source (Waters, Milford, MA). For front end separation, the optimised HPLC method and a premix of methanol and acetonitrile (45:55, v.v⁻¹) was used. Data were acquired in resolution mode (scanning from 150-1500 amu) and MS/MS scanning mode and processed using MassLynx v.4.1 software (Waters). The instrument was operated in positive and negative ionisation modes and calibrated using a sodium formate solution. Leucine enkephalin was used for lockspray (lock mass 556.2771). The MS parameters were as follows: capillary voltage 2.5 kV, sampling cone voltage 15.0 V, source temperature 120 °C, desolvation temperature 275 °C, desolvation gas flow (N₂) 650 L.h⁻¹, cone gas flow (N₂) 50 L.h⁻¹. For MS/MS experiments, the trap collision energy (CE) was set to obtain sufficient fragmentation for selected precursor ions (30 or 45 V). The eluent was split 3:1 prior to introduction into the ionisation chamber. The injection volume was 10 µL and UV-Vis spectra were acquired over 220–400 nm at 20 Hz.

2.6. HPLC-DAD Method Validation

Method validation was performed in terms of specificity, linearity and range, analyte stability, as well as intra- and inter-day analytical precision. The paired sample extracts of unfermented and fermented *C. genistoides* and a standard calibration mixture were used.

LC-DAD-ESI-MS data were used to identify compounds suitable for quantification. In both sample extracts, peak purity of the selected compounds was established by comparing their MS spectra with those of the authentic reference standards, where possible. For the additional phenolic compounds, specificity was determined by critically evaluating both the UV-Vis and MS spectra of the peaks in the sample extracts.

Calibration curves were set up for the selected standard compounds to test the linearity of the DAD response. UV-Vis spectra were recorded between 200–700 nm with selective wavelength monitoring at 288 and 320 nm. The dihydrochalcone aspalathin, and the flavanones eriocitrin, narirutin and hesperidin were monitored at 288 nm, while the xanthone mangiferin, the benzophenone maclurin, and the flavone vicenin-2 were monitored at 320 nm. The standard calibration mixture was diluted to obtain six different analyte concentrations which were injected at 10 µL each. The most diluted calibration mixture was also injected at 5 µL and the undiluted calibration mixture at 15 and 20 µL. On-column levels ranged between 0.0060 and 3.6422 µg. Concentration ranges were selected to cover the different quantities of the compounds present in the *C. genistoides* sample extracts. Linear regression, using the least squares method (Microsoft Excel 2010, Microsoft Corporation, Redmond, WA, USA), was performed to determine the slope, y-intercept and coefficient of determination (R^2).

The stability of the phenolic compounds, both as part of the standard calibration mixture and the *C. genistoides* extracts, was assessed by repeat injections over a 24 h period ($n = 6$). The percentage relative standard deviation (% RSD) over the time points during this period was used to evaluate the stability of the compounds.

Intra-day precision was determined by consecutive repeat injections ($n = 6$) of the calibration mixture and each of the extracts on the same day. To determine the inter-day precision, the same procedure was repeated over three consecutive days ($n = 3$). The % RSD was determined for replicate injections on each day (intra-day precision) and for mean values

per day (inter-day precision) by considering the respective peak areas.

2.7. Quantification of Phenolic Compounds in Freeze-Dried Aqueous Extracts of *C. genistoides*

Quantitative analyses were conducted on the Agilent 1200 instrument using the optimised HPLC-DAD method. Sample extracts were prepared for HPLC analyses as described in section 2.2 and injected in duplicate. Injection volumes of 5 and 15 μL were used for the unfermented *C. genistoides* extract, whilst the injection volumes were 10 and 25 μL for the fermented sample. The lower injection volumes were required to provide responses for the major constituents within the linear range. Calibration curves were constructed as described in section 2.6. Owing to limited quantities of the 3- β -D-glucopyranosylriflophenone, isomangiferin and nothofagin standards available, these and related compounds were quantified using previously determined response factors with regards to hesperidin, mangiferin and aspalathin, respectively. In the absence of authentic reference standards, additional phenolic compounds were quantified using calibration curves of the most closely related reference standard.

3. RESULTS AND DISCUSSION

3.1. HPLC-DAD Method Development

Method development was focused on optimising the selectivity on a high-efficiency column and thus the first step entailed selecting the optimum chromatographic support. Separation provided by the 3 μm Gemini-NX column, currently employed in the analysis of other *Cyclopia* species (De Beer *et al.*, 2012; Schulze *et al.*, 2014), was compared to that obtainable on the 1.8 μm Zorbax SB-C₁₈ column under constant gradient conditions and temperature. The 1.8 μm Zorbax column was included in this study due to the known benefits of sub-2 μm phases for speeding up reversed phase (RP) LC analyses (De Villiers *et al.*, 2006). The potential gain in efficiency provided by a core-shell column (2.6 μm Kinetex C₁₈) was also investigated. The best separation was ultimately achieved on this core-shell column, which is in line with a study on the RP-LC separation of proanthocyanidins showing that the Kinetex column kinetically outperforms solid supports over efficiencies in the practical range of *ca.* 25 000-250 000 plates (Kalili *et al.*, 2012).

Based exclusively on selectivity considerations, the aqueous phase was selected as 1% aqueous formic acid (v.v⁻¹) and the organic component as a 1:1 mixture of methanol and acetonitrile (obtained by on-line mixing). When assessed individually, the organic modifiers were both characterised by insufficient chromatographic resolution. For example, the use of 100% methanol led to perfect co-elution of the major constituent, mangiferin, and its C-4 regio-isomer isomangiferin, irrespective of gradient profile and temperature conditions. As opposed to 100% methanol, which is highly viscous, the mixture also served to lower the operating pressure, which is an important consideration for the Agilent 1200 instrument ($P_{\text{max}} = 400$ bar).

After selecting the optimal solid support and mobile phase components, the gradient profile and column temperature were optimised. Selectivity effects as a function of changes in mobile phase composition and temperature are often complementary (Dolan, 2002), and therefore these parameters were optimised simultaneously. An isocratic hold period at initial conditions, followed by a flat increase in solvent strength, were required to attain sufficient retention of the highly polar, early eluting compounds, whilst also improving band spacing and resolution of the later eluting compounds. This effect was more pronounced at lower temperatures. At the selected temperature of 30 °C, the optimised gradient profile comprised of a 5 min isocratic hold period at 5% organic modifier, followed by an increase to 25% organic modifier over 40 min. The second gradient step entailed an increase to 50% organic modifier over 10 min. The total chromatographic run time, including column re-equilibration, was 65 min.

The critical effect of mobile phase composition on the separation of honeybush phenolic compounds was demonstrated during method transfer from the Agilent 1200 instrument, where a quaternary pump provides low-pressure mixing of methanol and acetonitrile, to the Waters UPLC instrument equipped with a binary pump (high-pressure mixing). To achieve separation comparable to that of the Agilent instrument on the Waters instrument, methanol and acetonitrile had to be premixed using a ratio of 45% methanol to 55% acetonitrile (v.v⁻¹).

Under the optimised RP-LC conditions, a large number of phenolic compounds present in hot water extracts of *C. genistoides* were successfully separated (Figure 1a). Compounds that were only present in the fermented sample extract and/or only detected in positive ionisation mode during LC-ESI-MS analyses, are depicted in the extracted mass chromatograms ([M+H]⁺, Figures 1b–d). Exclusive detection of compounds in the fermented extract does not necessarily suggest their formation during fermentation, but may be related to the challenge of analysing samples which contain very high levels of certain compounds compared to other constituents. With fermentation a decrease in the content values of the former compounds allows minor compounds to be more easily observed due to a shift in the relative peak area ratios.

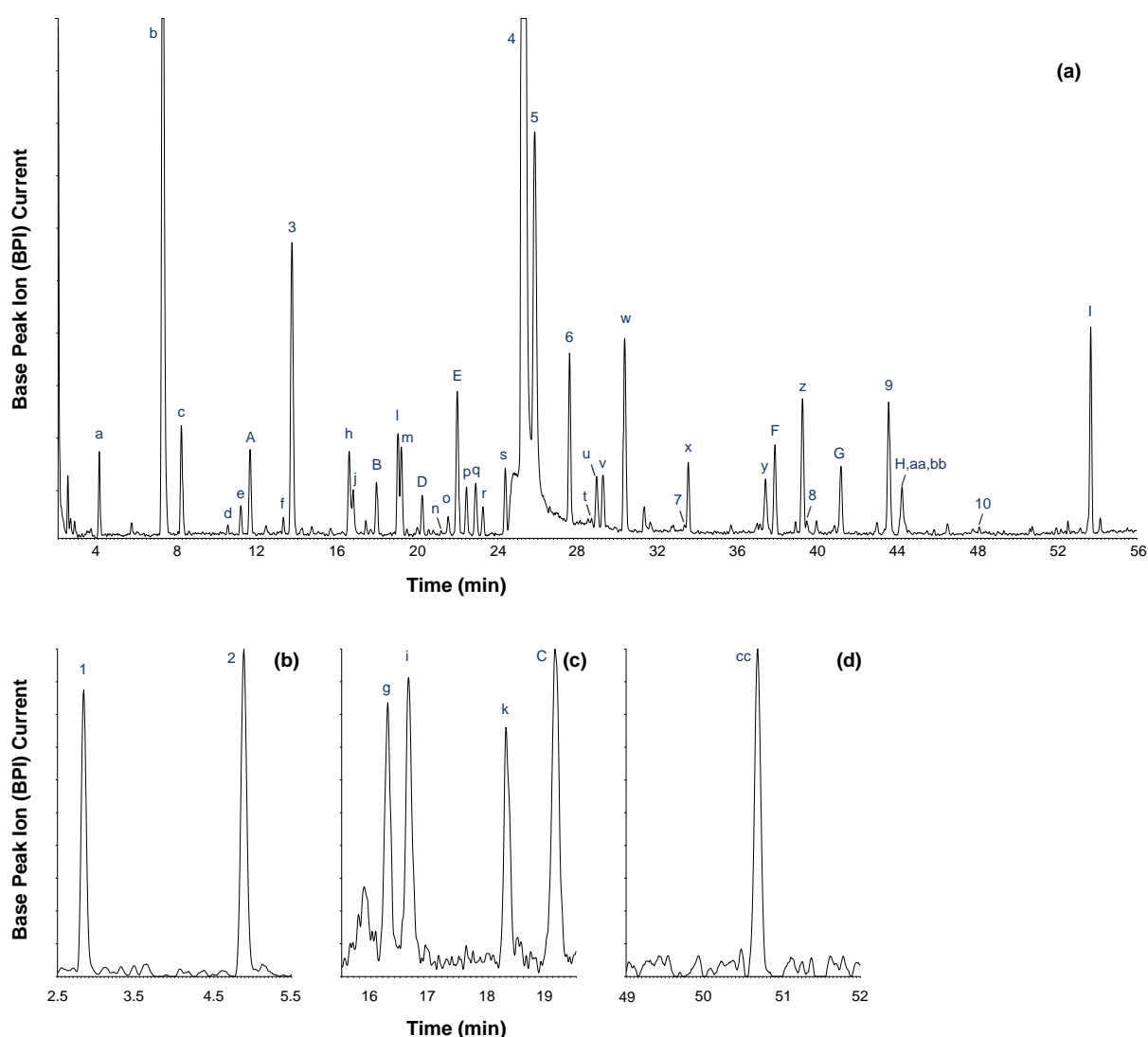


Figure 1 (a) LC-MS base peak chromatogram (ESI⁻) of an aqueous extract of unfermented *Cyclopia genistoides* and (b–d) extracted mass chromatograms (ESI⁺) of compounds that were only detected in the extract of the fermented sample and/or positive ionisation mode (Peak labels correspond to Tables 1–4; Table S1, Supplementary Material, page 106).

3.2. LC-DAD-ESI-MS and -MS/MS Identification of Compounds Present in Hot Water Extracts of Unfermented and Fermented *C. genistoides*

Identification of compounds was performed by assigning each peak to a compound sub-class based on their characteristic UV-Vis spectra, where possible (Abad-García *et al.*, 2009). Accurate mass measurement and MS/MS fragmentation patterns were then used to tentatively identify the molecular structures. Ten compounds **1–10** were identified by co-elution with the authentic reference standards, whilst 30 additional compounds **a–cc** were tentatively identified by interpretation of their UV-Vis spectroscopic and mass spectrometric data compared to relevant literature reports, as discussed per compound sub-class below. A further nine compounds **A–I** could not be identified based on the current data (Table S1, Supplementary Material, page 106). The characteristics of authentic reference standards, not present in sample extracts, but used in the identification of unidentified constituents, can be found in Table S2 (Supplementary Material, page 107). Structures for selected compounds and/or selected sub-classes are shown in Figure 2.

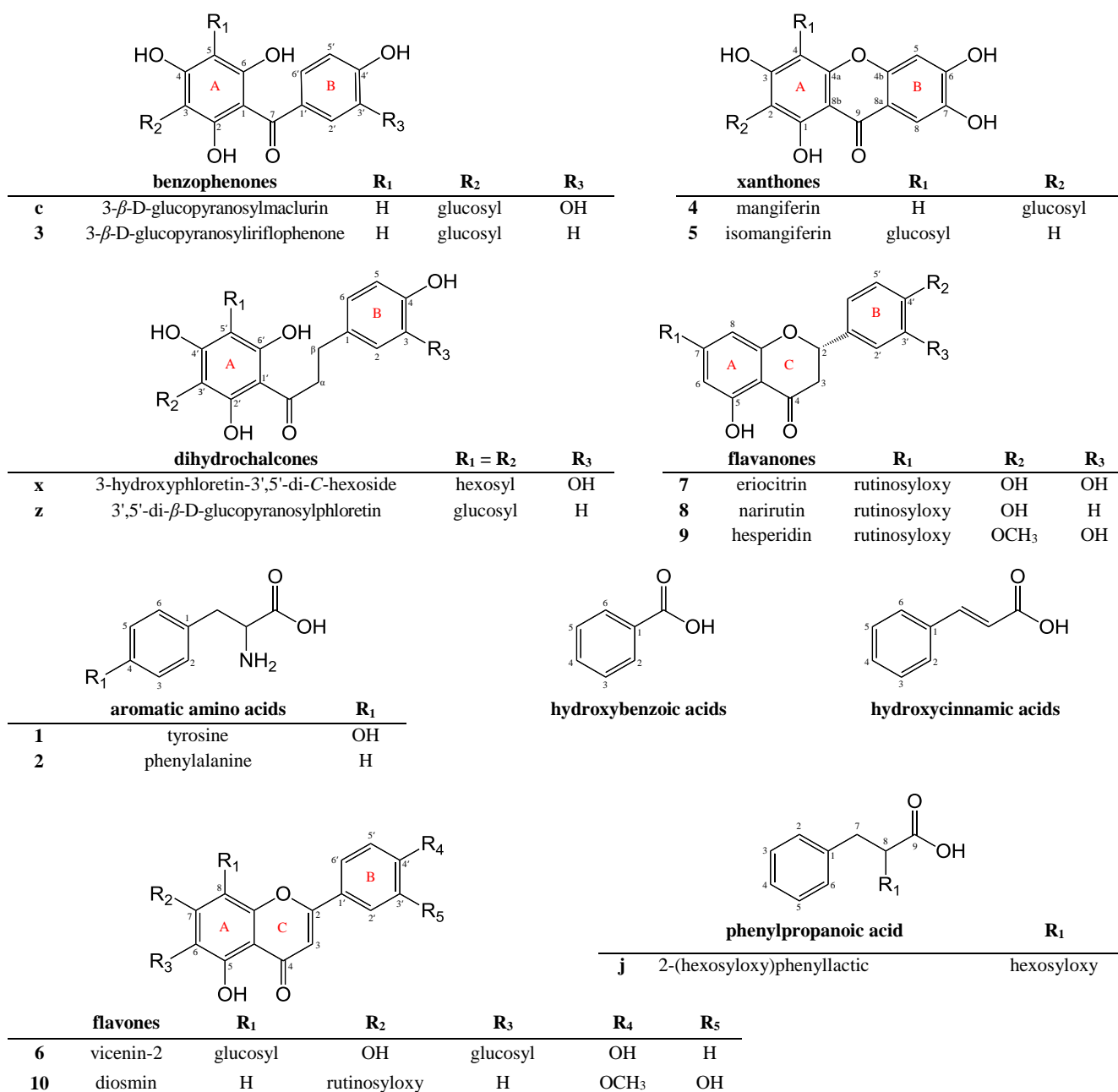


Figure 2 Structures for selected compounds and/or compound sub-classes identified in *Cyclopia genistoides* aqueous extracts.

3.2.1. Benzophenone Derivatives

Compound **3** was identified as 3- β -D-glucopyranosylriflophenone (Figure 2; Table 1), based on comparative data for the isolated reference compound. Six additional benzophenone derivatives were tentatively identified in aqueous extracts of unfermented and fermented *C. genistoides* (Table 1).

Four compounds, detected at t_R of 7.24 min (**b**), 10.49 min (**d**), 13.27 min (**f**) (Figure 1a) and 16.65 min (**i**) (Figure 1b), presented the same deprotonated molecule ($[M-H]^- = m/z$ 569). The experimental accurate masses of these compounds were in good agreement with the proposed molecular formula of $C_{25}H_{29}O_{15}$ ($[M-H]^-$). Compounds **b**, **d** and **f** exhibited maximum UV absorbance at 225 and 290 nm, whilst the second absorption maximum of compound **i** was shifted to a slightly higher value (302 nm).

The MS/MS fragmentation patterns of compounds **b**, **d** and **f** in negative ionisation mode were similar, with MS/MS base peak ions detected at m/z 287 ($[M-H-162-120]^-$). Compound **b** represents a major compound, as its peak area was among the four largest of the detected peaks, and thus this compound was selected for further discussion. The MS/MS spectrum of the deprotonated molecule (m/z 569, $[M-H]^-$) presented the following fragment ions (m/z): 479, 449, 407, 385, 355, 341, 329, 317, 311, 287, 245, 197, 193, 167 and 125 (Figure 3). The ions at m/z 479 and m/z 449 correspond to neutral losses of 90 amu ($[M-H-90]^-$) and 120 amu ($[M-H-120]^-$), respectively, signifying cross-ring cleavage of a hexoside moiety. The neutral loss of a hexoside moiety was also observed with the presence of a minor fragment ion at m/z 407 ($[M-H-162]^-$), whilst fragment ions detected at m/z 317 and m/z 287 signify subsequent losses of 90 amu ($[M-H-162-90]^-$) and 120 amu ($[M-H-162-120]^-$) from this “deglycosylated” fragment ion.

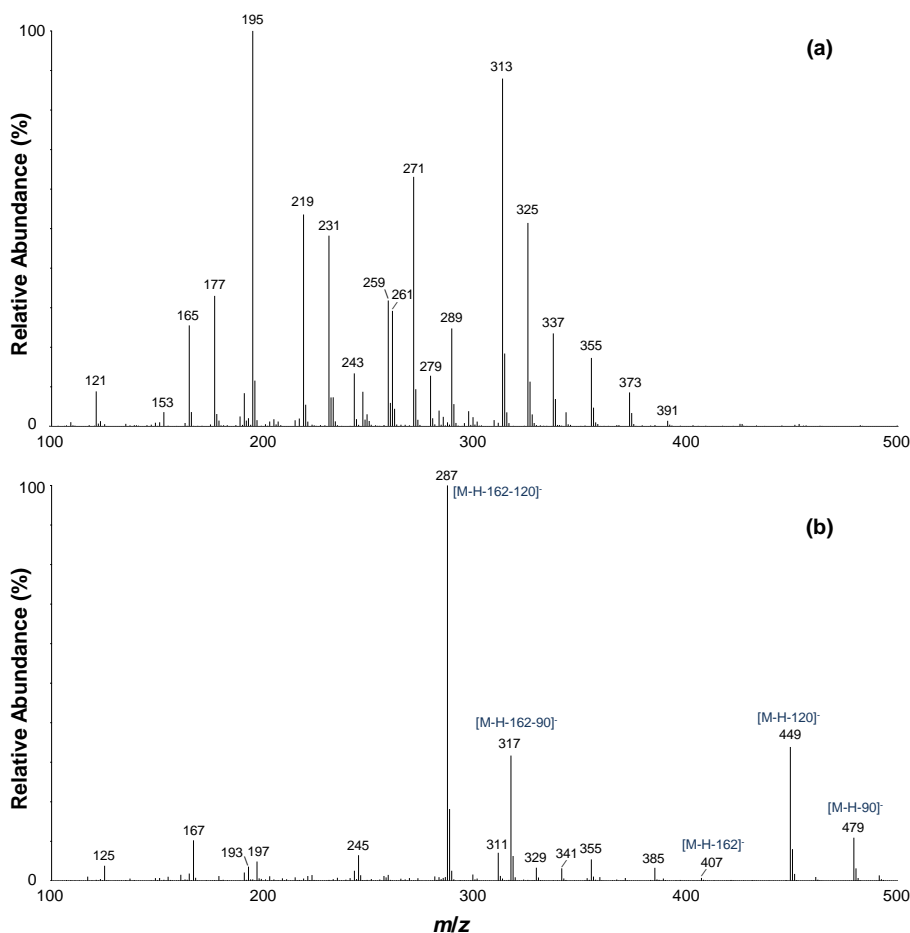


Figure 3 LC-ESI-MS/MS spectra of compound **b** in (a) positive ionisation mode (CE = 30 V) and (b) negative ionisation mode (CE = 30 V).

Table 1 Benzophenone derivatives identified in freeze-dried aqueous extracts of unfermented and fermented *Cyclopia genistoides*.

Nr	t _R (min)	Proposed Compound	λ _{max} (nm)	Mode	Accurate Mass, exp.	Proposed Formula	Error (ppm)	Precursor Ion	LC-MS/MS Ions ^{a,b}
a	4.06	maclurin-di- <i>O,C</i> -hexoside	235, 290, 320 sh	+	587.1625	C ₂₅ H ₃₁ O ₁₆	-2.2	587	425, 407, 389, 371, 353, 341, 329, 305, 287, 275, 261, 243, 231, 219, 195 , 177, 165, 153, 137, 121
				-	585.1469	C ₂₅ H ₂₉ O ₁₆	2.2	585	495, 465, 385, 355, 333, 303 , 285, 261, 223, 193, 165, 125
b	7.24	iriflophenone-di- <i>O,C</i> -hexoside isomer	234, 294	+	571.1664	C ₂₅ H ₃₁ O ₁₅	0.2	571	373, 355, 337, 325, 313, 289, 279, 271, 261, 243, 231, 219, 195 , 177, 165, 121
				-	569.1509	C ₂₅ H ₂₉ O ₁₅	0.5	569	479, 449, 407, 385, 355, 341, 329, 317, 311, 287 , 245, 197, 193, 167, 125
c	8.17	3-β-D-glucopyranosylmaclurin	235, 290, 318 sh	+	425.1080	C ₁₉ H ₂₁ O ₁₁	-0.4	425	353, 341, 329, 287, 261, 243, 231, 219, 195 , 177, 165, 153, 137, 121
				-	423.0923	C ₁₉ H ₁₉ O ₁₁	-0.9	423	333, 303, 261, 223, 205, 193 , 165, 151, 137, 125, 109
d	10.49	iriflophenone-di- <i>O,C</i> -hexoside isomer	225, 290	+	571.1503	C ₂₅ H ₃₁ O ₁₅	-5.6	571	373, 337, 325, 313, 289, 279, 271, 261, 243, 231, 219, 195 , 177, 165, 121
				-	569.1511	C ₂₅ H ₂₉ O ₁₅	0.9	569	479, 449, 385, 355, 317, 287 , 245, 193, 167, 125
f	13.27	iriflophenone-di- <i>O,C</i> -hexoside isomer	225, 290	+	571.1639	C ₂₅ H ₃₁ O ₁₅	-4.2	571	425, 355, 337, 325, 313, 289, 279, 271, 261, 247, 231, 219, 195 , 177, 165, 121
				-	569.1503	C ₂₅ H ₂₉ O ₁₅	-0.5	569	479, 449, 385, 355, 317, 287 , 245, 193, 167, 125
3	13.70	3-β-D-glucopyranosyliriflophenone	235, 295	+	409.1133	C ₁₉ H ₂₁ O ₁₀	-0.5	409	337, 325, 313, 279, 271, 261, 243, 231, 219, 195 , 177, 165, 153, 121
				-	407.0967	C ₁₉ H ₁₉ O ₁₀	-2.7	407	317, 299, 287 , 257, 245, 215, 201, 193, 167, 151, 137, 125
i	16.65	iriflophenone-di- <i>C</i> -hexoside ^c	225, 302 (weak)	+	571.1655	C ₂₅ H ₃₁ O ₁₅	-1.4	571	481, 470, 463, 451, 433, 421, 403, 391, 379 , 367, 355, 349, 337, 325, 313, 295, 285, 273, 261, 243, 231, 219, 189, 177, 121
				-	569.1509	C ₂₅ H ₂₉ O ₁₅	0.5	569	479, 461, 431, 389, 359, 329 , 317, 287, 239, 167

^aDefault collision energy (CE) of 30 V, unless otherwise stated. ^bValues in bold indicate the base peak ions. ^cOnly detected in the fermented *C. genistoides* sample extract. sh = shoulder.

The neutral loss of a hexoside moiety is characteristic of a flavonoid *O*-glycosyl compound, whilst the cross-ring cleavage of a hexoside moiety points toward a *C*-glycosyl compound (Abad-García *et al.*, 2009; Cuyckens & Claeys, 2004). In the lower molecular weight region of the MS/MS spectrum in negative ionisation mode, fragment ions characteristic of 3- β -D-glucopyranosyliriflophenone were observed (Zhang *et al.*, 2013). Compounds **b**, **d** and **f** were thus broadly assigned as iriflophenone-di-*O,C*-hexoside isomers, with the *O*-hexoside moiety either linked to a hydroxy group on the aglycone or to a hydroxy group of the *C*-bound hexoside residue. The data presented herein are in agreement with those of an iriflophenone-di-*O,C*-hexoside tentatively identified in *C. subternata* (De Beer *et al.*, 2012).

Conversely, tandem MS analysis of compound **i** in negative ionisation mode yielded a different MS/MS spectrum with major fragment ions detected at m/z 389 ($[M-H-2 \times 90]^-$), m/z 359 ($[M-H-90-120]^-$) and m/z 329 ($[M-H-2 \times 120]^-$, base peak ion). This fragmentation pattern is characteristic for the simultaneous fragmentation of two *C*-linked hexoside entities as described for 3,5-di- β -D-glucopyranosyliriflophenone (Ito *et al.*, 2012). Compound **i** was thus identified as an iriflophenone-di-*C*-hexoside.

Based on *in vitro* studies conducted on the mono 3-glucosyl and 3,5-di-glucosyl derivatives of iriflophenone, possible biological activities of the iriflophenone derivatives could include α -glucosidase inhibition (Feng *et al.*, 2011) and the inhibition of triglyceride accumulation (Zhang *et al.*, 2013), as well as pro-apoptotic activity (Kokotkiewicz *et al.*, 2013). In accordance with the antioxidant activity demonstrated for 3- β -D-glucopyranosyliriflophenone using on-line HPLC antioxidant assays (Malherbe *et al.*, 2014), these compounds could potentially also exhibit antioxidant activity and thus contribute to the antioxidant activity of *C. genistoides* extracts (Joubert *et al.*, 2008b).

The UV-Vis, ESI-MS and -MS/MS characteristics of compound **c** were in agreement with literature reports on 3- β -D-glucopyranosylmaclurin (Kokotkiewicz *et al.*, 2013; Zhang *et al.*, 2013). This compound has been identified previously in *C. genistoides* (Kokotkiewicz *et al.*, 2013; Malherbe *et al.*, 2014) and has also been tentatively identified in *C. maculata* hot water extracts (Schulze *et al.*, 2014). A compound with similar characteristics has likewise been observed in hot water extracts of *C. subternata* (unidentified compound **3**; De Beer *et al.*, 2012).

Compound **a**, detected at 4.06 min, exhibited deprotonated and protonated molecules at m/z 585 ($[M-H]^-$) and m/z 587 ($[M+H]^+$), respectively, and maximum UV absorbance at 235, 290 and 320 nm. The experimental accurate mass (585.1469, $[M-H]^-$) was in good agreement with the proposed molecular formula of $C_{25}H_{29}O_{16}$. The deprotonated molecule yielded a base peak fragment ion at m/z 303 ($[M-H-162-120]^-$) and major fragment ions at m/z 495 ($[M-H-90]^-$), m/z 465 ($[M-H-120]^-$) and m/z 333 ($[M-H-162-90]^-$). This fragmentation pattern is identical to that of compounds **b**, **d** and **f**, whilst fragment ions common to these isomers and compound **a** were also detected at m/z 385 and m/z 355. The molecular mass of compound **a** is 16 amu higher than that of an iriflophenone-di-*O,C*-hexoside which, together with the earlier elution time of compound **a**, points towards a hydroxylated derivative. Additional hydroxy groups on the B-ring of flavonoids cause bathochromic shifts of bands II (Abad-García *et al.*, 2009) as observed for compound **a**. Compound **a** was therefore tentatively assigned as a maclurin-di-*O,C*-hexoside.

3.2.2. Xanthone Derivatives

The glucosylxanthone mangiferin (2- β -D-glucopyranosylnorathyriol, **4**) and its regio-isomer, isomangiferin (4- β -D-glucopyranosylnorathyriol, **5**) were identified in sample extracts based on spectroscopic data and confirmation with the authentic reference standards (Table 2; Figure 2). In addition, eight other xanthone derivatives were also tentatively identified. These compounds all exhibited UV absorbance characteristics typical of the xanthone phenolic sub-class, with three high-intensity absorbance maxima in the region 250 to 370 nm (Table 2).

Table 2 Xanthone derivatives identified in freeze-dried aqueous extracts of unfermented and fermented *Cyclopia genistoides*.

Nr	tr (min)	Proposed Compound	λ_{\max} (nm)	Mode	Accurate Mass, exp.	Proposed Formula	Error (ppm)	Precursor Ion	LC-MS/MS Ions ^{a,b}
g	16.28	tetrahydroxyxanthone-C-hexoside dimer ^c	259, 317, 365	+	843.1610	C ₃₈ H ₃₅ O ₂₂	-0.5	843	843, 827, 807, 789, 772, 759, 743, 729, 711, 705 , 693, 687, 675, 669, 657, 651, 639, 627, 603, 598, 585, 573, 562, 555, 531, 479, 425, 417
				-	841.1494	C ₃₈ H ₃₃ O ₂₂	0.5	841, CE = 45 V	841, 823, 805, 751, 733, 721, 703, 673, 661, 631 , 613, 601, 589, 559, 527, 477, 437, 419, 401, 365, 359, 329, 313, 299, 271, 259
k	18.31	tetrahydroxyxanthone-C-hexoside dimer ^c	259, 318, 368	+	843.1597	C ₃₈ H ₃₅ O ₂₂	-2.7	843	843, 825, 808, 789, 771, 753, 729, 705 , 687, 669, 651, 639, 627, 603, 585, 573, 555, 472, 425
				-	841.1463	C ₃₈ H ₃₃ O ₂₂	0.0	841, CE = 45 V	841, 823, 805, 751, 733, 721, 703, 691, 673, 661, 631 , 613, 601, 589, 559, 437, 419, 407, 373, 359, 329, 313, 299, 271, 259
l	19.02	tetrahydroxyxanthone-di-O,C-hexoside	259, 314, 367	+	585.1454	C ₂₅ H ₂₉ O ₁₆	-0.3	585	405, 387, 369, 357, 351, 339, 327, 313, 303 , 299, 285, 273, 261
				-	583.1287	C ₂₅ H ₂₇ O ₁₆	-2.1	583	583, 565, 493, 463, 421, 403, 331, 313, 301 , 271, 259
n	21.17	aspalathin derivative of (iso)mangiferin	261, 319, 372	+	873.2104	C ₄₀ H ₄₁ O ₂₂	1.7	873	819, 807, 731, 694, 675, 658, 631, 627, 616, 604, 591, 573, 561, 541, 525, 507, 489, 475, 459, 447, 439, 423, 405, 387, 369, 357, 345, 327, 313, 303, 289 , 273, 261, 247, 217, 196, 163, 151, 149, 139, 123
				-	871.1948	C ₄₀ H ₃₉ O ₂₂	1.7	871	871 , 751, 691, 601, 571, 557, 539, 449, 437, 421, 331, 301, 269, 243
r	23.26	nothofagin derivative of (iso)mangiferin	261, 319, 372	+	857.2137	C ₄₀ H ₄₁ O ₂₁	-0.3	857	677, 659, 641, 623, 599, 575, 557, 541, 523, 509, 487, 475, 463, 447, 439, 423, 405, 387, 369, 357, 327, 303, 285, 273 , 257, 245, 231 , 151, 139, 119, 107
				-	855.1984	C ₄₀ H ₃₉ O ₂₁	0.8	855	855 , 837, 765, 735, 675, 657, 585, 555, 421, 403, 331, 313, 301
4	25.23	2- β -D-glucopyranosylnorathyriol	258, 318, 366	+	423.0931	C ₁₉ H ₁₉ O ₁₁	0.9	423	369, 351, 339, 327, 313, 303, 299, 285, 273 , 257
				-	421.0770	C ₁₉ H ₁₇ O ₁₁	-0.2	421	331, 313, 301 , 285, 271, 259
5	25.86	4- β -D-glucopyranosylnorathyriol	255, 316, 365	+	423.0929	C ₁₉ H ₁₉ O ₁₁	0.5	423	387, 369, 357, 341, 327, 313, 303 , 285, 273
				-	421.0762	C ₁₉ H ₁₇ O ₁₁	-2.1	421	331, 313, 301 , 285, 271, 259
y	37.41	tetrahydroxyxanthone-C-hexoside isomer	258, 317, 366	+	423.0930	C ₁₉ H ₁₉ O ₁₁	0.7	423	369, 351, 339, 327, 313, 303, 299, 285, 273 , 257
				-	421.0777	C ₁₉ H ₁₇ O ₁₁	1.4	421	331, 313, 301 , 285, 271, 259
aa	44.24	tetrahydroxyxanthone-C-hexoside isomer	258, 318, 366	+	423.0948	C ₁₉ H ₁₉ O ₁₁	5.0	423	351, 339, 327, 313, 303, 299, 285, 273 , 257
				-	421.0771	C ₁₉ H ₁₇ O ₁₁	0.0	421	331, 313, 301 , 285, 271, 259
cc	50.68	schoepfin A derivative of (iso)mangiferin ^c	261, 317, 368	+	841.2220	C ₄₀ H ₄₁ O ₂₀	3.4	841	661, 643, 621, 583, 559, 541, 523, 509, 491, 475, 463, 439, 431, 423, 405, 387, 357, 351, 327, 303, 273, 257 , 231
				-	839.2026	C ₄₀ H ₃₉ O ₂₀	-1.1	839	839 , 821, 749, 719, 677, 551, 539, 527, 461, 449, 431, 421, 403, 331, 301, 271

^aDefault collision energy (CE) of 30 V, unless otherwise stated. ^bValues in bold indicate the base peak ions. ^cOnly detected in the fermented *C. genistoides* sample extract.

Compounds **y** and **aa** eluted at t_R of 37.41 and 44.24 min, respectively, and were assigned the elemental composition $C_{19}H_{18}O_{11}$, indicating that they are possible isomers of (iso)mangiferin. The MS/MS spectra of the deprotonated molecules (m/z 421, $[M-H]^-$) were predominantly characterised by the presence of daughter ions at m/z 331 and m/z 301, corresponding to neutral losses of 90 Da ($C_3H_6O_3$) and 120 Da ($C_4H_8O_4$), respectively. Less abundant daughter ions were also detected at m/z 313 ($[M-H-90-H_2O]^-$), m/z 271 ($[M-H-150]^-$) and m/z 259 ($[M-H-162]^-$). This fragmentation pattern is characteristic of glycosyl xanthenes (Du *et al.*, 2012). In positive ionisation mode, the fragmentation pattern of compounds **y** and **aa** showed a stronger correlation with mangiferin than with isomangiferin, as the base peak ion was detected at m/z 273 as opposed to m/z 303. This would suggest that the position of glycosylation is at C-2 on the dibenzo- γ -pyrone skeleton. However, based on the available data, it was not possible to confirm the position of glycosylation, nor to ascertain the nature of the hexoside moiety or the hydroxylation pattern of the dibenzo- γ -pyrone skeleton. Compounds **y** and **aa** were thus broadly assigned as tetrahydroxyxanthone-*C*-hexoside isomers.

Compound **I** ($t_R = 19.02$ min) yielded an $[M-H]^-$ ion at m/z 583, which indicated the addition of one hexose unit (162 Da) to a tetrahydroxyxanthone-*C*-hexoside. The MS/MS spectrum of the deprotonated molecule presented the following fragment ions (m/z): 565 ($[M-H-H_2O]^-$), 493 ($[M-H-90]^-$), 463 ($[M-H-120]^-$), 421 ($[M-H-162]^-$), 403 ($[M-H-162-H_2O]^-$), 331 ($[M-H-162-90]^-$), 313 ($[M-H-162-90-H_2O]^-$), 301 ($[M-H-162-120]^-$, base peak ion), 271 ($[M-H-162-150]^-$) and 259 ($[M-H-2 \times 162]^-$). This fragmentation pattern is identical to that of the authentic reference standard neomangiferin (7- β -D-glucopyranosyloxymangiferin; Table S2, Supplementary Material, page 107), analysed under the same experimental conditions. On the other hand, compound **I** eluted before neomangiferin, which suggests an isomer. Compound **I** was thus tentatively identified as a tetrahydroxyxanthone-di-*O,C*-hexoside.

This is the first report of the presence of tetrahydroxyxanthone-*C*-hexoside isomers besides mangiferin and isomangiferin, as well as a tetrahydroxyxanthone-di-*O,C*-hexoside, in *Cyclopia* spp. extracts. Based on the established antidiabetic activity of mangiferin and neomangiferin (Ichiki *et al.*, 1998; Miura *et al.*, 2001; Muruganandan *et al.*, 2005), the aforementioned compounds could possibly contribute to the antidiabetic potential of *C. genistoides* aqueous extracts.

Compounds **g** ($t_R = 16.28$ min) and **k** ($t_R = 18.31$ min) were only present in significant amounts in the fermented sample (Figure 1c), and exhibited protonated and deprotonated precursor ions at m/z 843 ($[M+H]^+$) and m/z 841 ($[M-H]^-$), respectively. The experimental accurate masses were in good agreement with the proposed molecular formula of $C_{38}H_{33}O_{22}$ ($[M-H]^-$), which would correspond to two *C-C* linked tetrahydroxyxanthone-*C*-hexoside entities. Compounds **g** and **k** exhibited identical fragmentation behavior, with small differences observed in the relative intensities of the MS/MS ions. In negative ionisation mode, a CE of 45 V was needed to obtain significant fragmentation of the precursor ions. The following MS/MS ions were detected in the higher-molecular weight region for both compounds (m/z): 841 ($[M-H]^-$), 823 ($[M-H-H_2O]^-$), 805 ($[M-H-2 \times H_2O]^-$), 751 ($[M-H-90]^-$), 733 ($[M-H-90-H_2O]^-$), 721 ($[M-H-120]^-$), 703 ($[M-H-120-H_2O]^-$), 673 ($[M-H-150-H_2O]^-$), 661 ($[M-H-2 \times 90]^-$), 631 ($[M-H-90-120]^-$, base peak ion) and 601 ($[M-H-2 \times 120]^-$).

This fragmentation pattern, characterised by cross-ring cleavage of the saccharide residues and subsequent loss of water molecules, corresponds to the simultaneous fragmentation of two hexosyl groups. It was therefore postulated that each of the tetrahydroxyxanthone monomers contains a single *C*-linked hexosyl group. This was confirmed by the presence of a fragment ion at m/z 419 (30–40% intensity; $[M-H-422]^-$) in the negative ionisation mode MS/MS spectra, which corresponds to the neutral loss of a tetrahydroxyxanthone-*C*-hexosyl ($C_{19}H_{18}O_{11}$). Subsequent losses of 90 and 120 amu from this monomeric unit were observed at m/z 329 ($[M-H-C_{19}H_{18}O_{11}-90]^-$) and m/z 299 ($[M-H-C_{19}H_{18}O_{11}-120]^-$). The MS/MS spectra of compound **g** in (a) positive ionisation mode (CE = 30 V) and (b) negative ionisation mode (CE = 45 V) are illustrated in Figure 4.

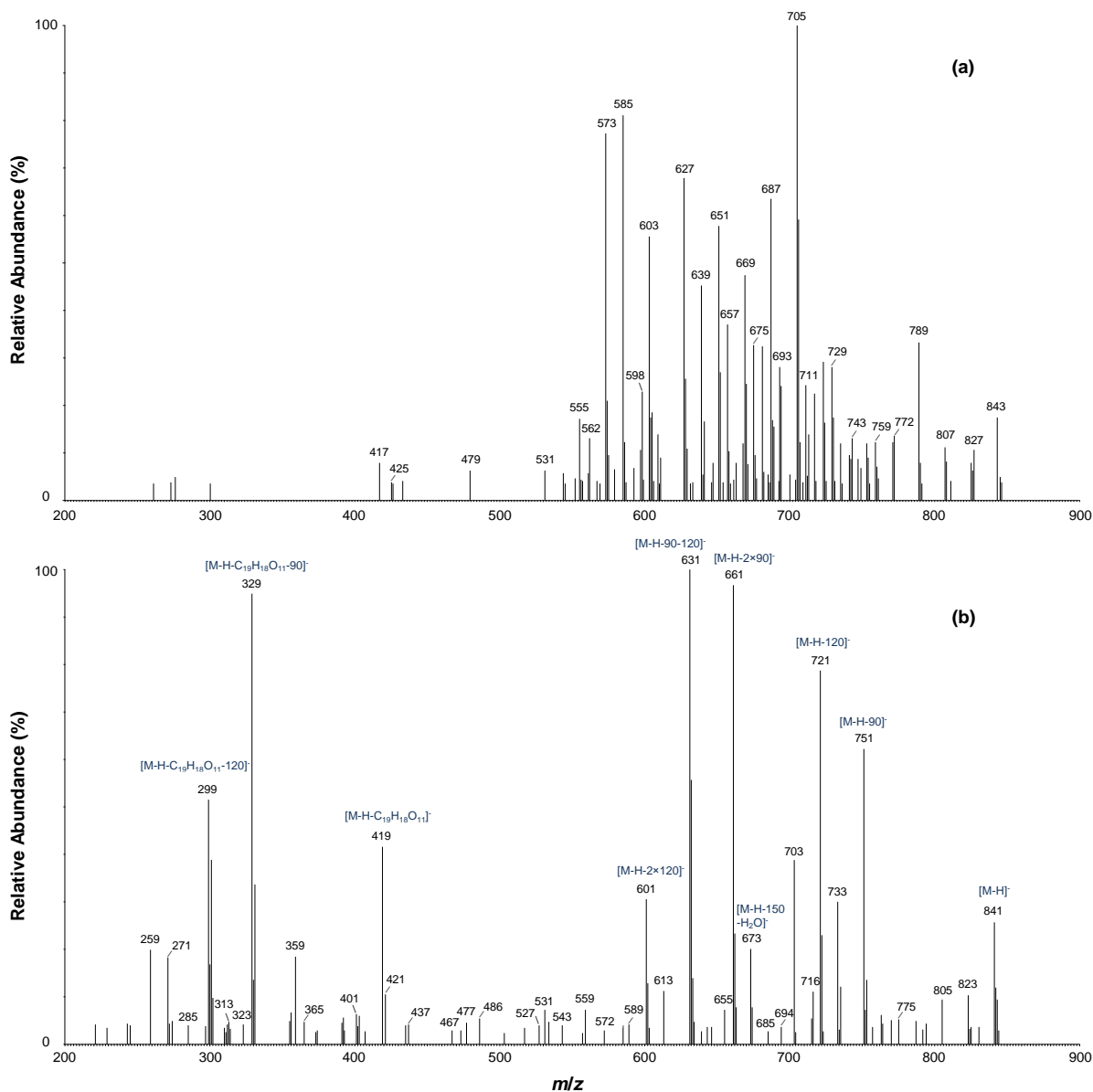


Figure 4 LC-ESI-MS/MS spectra of compound **g** in (a) positive ionisation mode (CE = 30 V) and (b) negative ionisation mode (CE = 45 V).

Compounds **g** and **k** were therefore tentatively assigned as tetrahydroxanthone-*C*-hexoside dimers. Such a symmetric homodimer of mangiferin, termed mangiferoxanthone A, was recently isolated from mango tree stem bark and exhibited moderate anti-viral activity (Abdel-Mageed *et al.*, 2014). Other xanthone dimers with a MW of 842 have thus far only been identified in *Swertia punicea* Hemsl. (Gentianaceae), namely swertiabixanthone diglucopyranoside and 3-glucosylpuniceaside A (Du *et al.*, 2012).

A molecular formula of C₄₀H₄₀O₂₂ was assigned to compound **n** with a retention time of 21.17 min. The deprotonated molecule (m/z 871, [M-H]⁻) presented the following daughter ions (m/z): 751, 691, 601, 571, 557, 539, 449, 437, 421, 331, 301, 269 and 243. These results correspond to data presented for an unidentified compound in extracts of *C. maculata* (compound **3**; Schulze *et al.*, 2014). The authors suggested that this compound could be a dimeric derivative of (iso)mangiferin, based on the common fragment ion detected at m/z 421, which represents the deprotonated molecule ion

of (iso)mangiferin ($[M-H]^-$), together with other characteristic ions at m/z 331 ($[M-H-90]^-$) and m/z 301 ($[M-H-120]^-$). High molecular weight fragments furthermore indicate the presence of more than one glycosyl group, for example m/z 751 ($[M-H-120]^-$), m/z 691 ($[M-H-2 \times 90]^-$), m/z 601 ($[M-H-120-150]^-$) and m/z 571 ($[M-H-2 \times 150]^-$). Based on the mass difference of 450 amu with regard to (iso)mangiferin, it is postulated that compound **n** could possibly be a C-C linked tetrahydroxyxanthone-C-hexoside [e.g. (iso)mangiferin] and a pentahydroxydihydrochalcone-C-hexoside (e.g. aspalathin).

Aspalathin (3'- β -D-glucopyranosyl-3-hydroxyphloretin) has not been detected in *Cyclopia* spp. to date, including the *C. genistoides* extracts of the present study. However, the related compounds, 3-hydroxyphloretin-3',5'-di-C-hexoside (compound **x**) and 3',5'-di- β -D-glucopyranosylphloretin (compound **z**), were shown to be present (Figure 2; Table 3). This hypothesis is further supported by the presence of fragment ions typical of aspalathin in the MS/MS spectrum of compound **n** in positive ionisation mode, i.e. m/z 151, m/z 139 and m/z 123 (Table S2, Supplementary Material, page 107). Most notable is the common fragment ion at m/z 123 ($[C_7H_7O_2]^+$), which represents the base peak ion in the MS/MS spectrum of aspalathin in positive ion mode. Based on the supporting evidence, compound **n** was tentatively identified as an aspalathin derivative of (iso)mangiferin.

Compound **r** with deprotonated and protonated molecules at m/z 855 ($[M-H]^-$) and m/z 857 ($[M+H]^+$), respectively, eluted at 23.26 min and was assigned a molecular formula of $C_{40}H_{40}O_{21}$ by HR-ESI-MS. This compound differs from compound **n** by the absence of a hydroxy group, which also explains the higher degree of retention observed for compound **r**. The deprotonated molecule exhibited the same fragmentation pattern as compound **n**. In positive ion mode, fragment ions with m/z 151, m/z 139 and m/z 107 were all common to compound **r** and nothofagin (3'- β -D-glucopyranosylphloretin), with the latter fragment ion representing the base peak MS/MS chromatogram of nothofagin ($[C_7H_7O]^+$; Table S2, Supplementary Material, page 107). These data led us to propose that compound **r** is a nothofagin derivative of (iso)mangiferin.

Compound **cc** ($t_R = 50.68$ min) has a molecular formula of $C_{40}H_{40}O_{20}$. The deprotonated molecule at m/z 839 ($[M-H]^-$) presented daughter ions at m/z 821 ($[M-H-H_2O]^-$), m/z 749 ($[M-H-90]^-$), m/z 719 ($[M-H-120]^-$), m/z 677 ($[M-H-162]^-$), m/z 551 ($[M-H-120-150-H_2O]^-$), m/z 539 ($[M-H-2 \times 150]^-$) and m/z 527 ($[M-H-162-150]^-$). The typical (iso)mangiferin fragment ions were also detected (Table 2). In the positive ionisation mode, the precursor ion at m/z 841 ($[M+H]^+$) furthermore presented product ions common to both compounds **n** and **r**, thereby suggesting another dihydrochalcone derivative of (iso)mangiferin. The deprotonated molecule ion of (iso)mangiferin detected at m/z 421 ($[M-H]^-$) represents the neutral loss of 418 amu from the deprotonated dimeric unit, which may correspond to a dihydroxydihydrochalcone-C-hexoside monomeric unit with a molecular formula of $C_{21}H_{24}O_9$ (420 Da). These data point towards schoepfin A (Huang *et al.*, 2008), which merely differs from nothofagin by the absence of a hydroxy group at C-6'. Compound **cc** was therefore tentatively identified as a schoepfin A derivative of (iso)mangiferin.

These dihydrochalcone derivatives of (iso)mangiferin are herein reported for the first time in *C. genistoides* extracts. The linkage of xanthenes to other phenolic compounds such as flavone C-glycosyl compounds (e.g. swertifrancheside; Wang *et al.*, 1994) has been reported previously, although the occurrence of bisxanthenes/tetrahydroxyxanthone dimers in higher plants and fungi are more common (e.g. Du *et al.*, 2012; Abdel-Mageed *et al.*, 2014).

Table 3 Amino acids, glycosylated phenolic acids, flavones and dihydrochalcones identified in freeze-dried aqueous extracts of unfermented and fermented *Cyclopia genistoides*.

Nr	t _R (min)	Proposed Compound	λ _{max} (nm)	Mode	Accurate Mass, exp.	Proposed Formula	Error (ppm)	Precursor Ion	LC-MS/MS Ions ^{a,b}
<i>Amino Acids</i>									
1	2.83	tyrosine	225, 233, 274 (weak)	+	182.0818	C ₉ H ₁₂ NO ₃	0.5	182	182, 148, 136, 119, 107, 95, 91 , 77
2	4.89	phenylalanine	225, 233, 259 (weak)	+	166.0871	C ₉ H ₁₂ NO ₂	1.8	166	120, 103 , 91, 77
<i>Glycosylated phenolic acids</i>									
e	11.14	dihydroxybenzoic acid- <i>O</i> -pentoside	247, 289 sh, 314	–	285.0607	C ₁₂ H ₁₃ O ₈	–1.1	285	153, 152, 109, 108
h	16.57	dihydroxybenzoic acid- <i>O</i> -dipentoside	290 (weak)	–	417.1032	C ₁₇ H ₂₁ O ₁₂	–0.2	417	417, 285, 241, 153, 152 , 109, 108
j	16.77	2-(hexosyloxy)phenyllactic acid	nd	–	327.1080	C ₁₅ H ₁₉ O ₈	0.0	327	165, 147 , 103
m	19.18	coumaric acid- <i>O</i> -(pentosyl)hexoside	nd ^c	–	457.1336	C ₂₀ H ₂₅ O ₁₂	–2.2	457	457, 325, 163 , 119
o	21.52	caffeic acid- <i>O</i> -(pentosyl)hexoside	225, 277	–	473.1281	C ₂₀ H ₂₅ O ₁₃	–3.0	473	473, 341, 323, 179 , 135
<i>Flavones</i>									
6	27.60	6,8-di-β-D-glucopyranosylapigenin (vicenin-2)	270, 330	+	595.1652	C ₂₇ H ₃₁ O ₁₅	–1.8	595	505, 457, 439, 427, 421, 409, 403, 391, 379, 355, 349, 337, 325 , 307, 295
				–	593.1514	C ₂₇ H ₂₉ O ₁₅	1.3	593	593 , 575, 503, 485, 473, 455, 413, 395, 383, 365, 353
10	48.10	7-rutinosyloxydiosmetin (diosmin)	260, 319 (weak)	+	609.1819	C ₂₈ H ₃₃ O ₁₅	0.0	609	301
				–	607.1673	C ₂₈ H ₃₁ O ₁₅	1.6	607	299 , 284
<i>Dihydrochalcones</i>									
x	33.54	3-hydroxyphloretin-3',5'-di- <i>C</i> -hexoside	285	+	615.1926	C ₂₇ H ₃₅ O ₁₆	0.2	615	513, 495, 477, 465, 447, 435, 423, 411 , 399, 381, 369, 357, 345, 327, 313, 301, 259, 247, 235, 217, 205, 193, 165, 123
				–	613.1771	C ₂₇ H ₃₃ O ₁₆	0.3	613	505, 493, 475, 433, 415, 403, 385, 373 , 361, 331, 251, 239, 209
z	39.26	3',5'-di-β-D-glucopyranosylphloretin	286	+	599.1971	C ₂₇ H ₃₅ O ₁₅	–0.8	599	497, 479, 461, 449, 431, 419, 413, 407, 395, 383, 377, 365, 353 , 341, 329, 301, 259, 247, 235, 107
				–	597.1830	C ₂₇ H ₃₃ O ₁₅	1.8	597	489, 477, 459, 429, 417, 399, 387, 369, 357 , 345, 327, 315

^aDefault collision energy (CE) of 30 V, unless otherwise stated. ^bValues in bold indicate the base peak ions. ^cCo-elution. sh = shoulder. nd = not detected.

3.2.3. Flavanones

Flavanones usually occur as glycosyloxy derivatives, with the sugar moiety preferentially bound to the aglycone hydroxy group at C-7 or C-3 (Andersen & Markham, 2005). Three known flavanone-7-*O*-disaccharides were identified in the sample extracts by co-elution with the authentic reference standards, namely 7-rutinosyloxyeriodictyol (eriodictin, **7**), 7-rutinosyloxynaringenin (narirutin, **8**) and 7-rutinosyloxyhesperetin (hesperidin, **9**) (Figure 2; Table 4). In addition to these compounds, nine additional flavanones were also tentatively identified (Table 4). The UV-Vis spectra of compounds **p**, **q**_{1,2}, **s**, **t**, **u**, **v**, **w** and **bb** showed maximum absorption at *ca.* 280 nm with an undefined shoulder at *ca.* 330 nm corresponding to a flavanone structure. In negative ionisation mode, the presence of the fragment ion at *m/z* 287 in the MS/MS spectra of compounds **p**, **q**_{1,2} and **s** indicated eriodictyol as the aglycone, while the fragment ion at *m/z* 271 indicated naringenin as the aglycone for compounds **t**, **u**, **v**, **w** and **bb**.

Full mass scan analysis of compound **bb** in negative ionisation mode showed a signal at *m/z* 579 ([M-H]⁻). The MS/MS spectrum from the parent ion at *m/z* 579 provided the following MS/MS ions (*m/z*): 579, 485, 459, 433, 415, 313, 271, 253, 209, 151, 149 and 125. The MS/MS base peak ion (*m/z* 271) represents the molecule ion of the aglycone, naringenin, after neutral loss of a disaccharide residue ([M-H-308]⁻). The most common flavonoid disaccharides include rutinoides [rhamnosyl-(α1→6)-glucose] and neohesperidosides [rhamnosyl-(α1→2)-glucose], which only differ with regard to the interglycosidic linkage type between the terminal rhamnose and internal glucose units. The neohesperidosides are typically more retained (Abad-García *et al.*, 2009; Cuyckens & Claeys, 2004; Djoukeng *et al.*, 2008), and show more pronounced fragmentation than their rutinoides analogues (Cuyckens *et al.*, 2001). In accordance with the systematic nomenclature described by Domon and Costello (1988), the interglycosidic linkage for compound **bb** was characterised as (1→2) based on the relatively high intensities of the Y₁⁻ (*m/z* 433 at 15% intensity) and Z₁⁻ (*m/z* 415 at 10% intensity) ions and the occurrence of the fragment ions ^{0,2}X₀⁻ (*m/z* 459 = [M-H-120]⁻) and ^{0,2}X₀Y⁻ (*m/z* 313 = [M-H-146-120]⁻) (Cuyckens *et al.*, 2001). The Y₁⁻ ion ([M-H-146]⁻) represents the neutral loss of a terminal rhamnose unit, allowing for the determination of the glycan sequence. The complementary monosaccharide ion was also detected (*m/z* 145 at 40% intensity). The observed loss of 120 amu could be attributed to the partial loss of a glucose unit as typical transition of neohesperidoside or could have resulted from the retro-Diels-Alder (RDA) cleavage of the C-ring of the flavanone (Djoukeng *et al.*, 2008; Cuyckens *et al.*, 2001). Compound **bb** was thus broadly assigned as a naringenin-*O*-deoxyhexose(1→2)hexoside. Compound **bb** is most likely an isomer of naringin (7-neohesperidosyloxynarirutin), as the fragmentation pattern and molecular formula matched, but the retention times differed (Table S2, Supplementary Material, page 107).

Compounds **v** (*t_R* = 29.28 min) and **w** (*t_R* = 30.36 min) were also assigned the elemental composition C₂₇H₃₁O₁₄ ([M-H]⁻) and presented exactly the same fragmentation pattern as compound **bb**, with characteristic ions detected at *m/z* 459 ([M-H-120]⁻), *m/z* 433 ([M-H-146]⁻), *m/z* 415 ([M-H-164]⁻), *m/z* 313 ([M-H-146-120]⁻), *m/z* 271 ([M-H-308]⁻) and *m/z* 145. Conversely, these compounds eluted at much earlier retention times in relation to compound **bb** (*t_R* = 44.43 min), suggesting that they are most likely di-*O*-saccharides as opposed to *O*-disaccharides (Abad-García *et al.*, 2009). Compounds **v** and **w** were thus tentatively identified as naringenin-*O*-hexose-*O*-deoxyhexoside isomers.

In negative ionisation mode, compounds **t** (*t_R* = 28.54 min) and **u** (*t_R* = 28.95 min) presented deprotonated molecule ions at *m/z* 565 ([M-H]⁻) with a corresponding molecular formula of C₂₆H₂₉O₁₄. The deprotonated molecules presented the following high-intensity ions in their MS/MS spectra (*m/z*): 565 ([M-H]⁻), 445 ([M-H-120]⁻), 419 ([M-H-146]⁻), 299 ([M-H-146-120]⁻), 271 ([M-H-294]⁻), 145 and 125. The UV-Vis spectra and fragment ions detected at *m/z* 271, formed by the successive loss of 146 amu (deoxyhexose) and 148 amu, point toward naringenin derivatives. The ion at *m/z* 419 ([M-H-146]⁻) showed an intensity of 60 and 100% in the MS/MS spectra of compounds **r** and **s**, respectively, and the corresponding monosaccharide ion at *m/z* 145 was also present at 90-100% relative abundance in both spectra.

The loss of 120 amu observed with ions at m/z 445 (20% intensity) and m/z 299 (20% intensity) could have resulted from the RDA reaction of the flavanone, although this has previously only been observed for the neohesperidosides (Djoukeng *et al.*, 2008). The loss of 148 amu could not be explained and therefore compounds **t** and **u** were only classified as naringenin derivatives.

Four eriodictyol derivatives (compounds **p**, **q_{1,2}** and **s**) were tentatively identified in the sample extracts based on their UV-Vis spectra and base peak ions detected at m/z 287 in negative ionisation mode. Compounds **p** and **q₁** eluted at 22.44 min and 22.90 min, respectively, and presented deprotonated molecules at m/z 581 (C₂₆H₂₉O₁₅, [M-H]⁻). During tandem MS analysis in negative ionisation mode, compounds **p** and **q₁** presented the following high-intensity MS/MS ions [m/z , (%): 581 ([M-H]⁻, 70–100), 445 ([M-H-136]⁻, 40–50), 419 ([M-H-162]⁻, 55–60) and 161 (85–100)]. Loss of 136 amu from the deprotonated molecules could signify retrocyclisation of the C-ring in the eriodictyol aglycone, whilst the neutral loss of 162 amu corresponds to a hexosyloxy moiety. The corresponding monosaccharide ion was also detected at m/z 161. The difference in mass between the fragment ion at m/z 419 and the molecule ion of the eriodictyol aglycone at m/z 287 (15–30% relative abundance) furthermore indicates the presence of a pentosyloxy moiety (132 amu). The position of these glycan substituents of different mass could not be determined, but preferential cleavage of the hexosyl-aglycone bond suggests that the hexosyl is bound at a position on the flavanone ring that is more susceptible to acid hydrolysis. Compounds **p** and **q₁** were thus tentatively identified as eriodictyol-*O*-hexose-*O*-pentoside isomers. Following a similar approach and based on the corresponding mass spectrometric data, compounds **q₂** (t_R = 22.90 min) and **s** (t_R = 24.38 min) were identified as eriodictyol-*O*-hexose-*O*-deoxyhexoside isomers. The presence of these flavanone derivatives in extracts of *C. genistoides* exemplifies the high degree of structural variation in natural plant extracts. Such glycosylated derivatives of eriodictyol and naringenin, other than the two most common compounds eriocitrin and narirutin, have been detected in extracts of *C. genistoides* (unidentified compound **7**; Malherbe *et al.*, 2014) and *C. subternata* (eriodictyol-di-*C*-hexoside, eriodictyol-*O*-glucoside, naringenin-di-*C*-hexoside and naringenin-*O*-dihexoside; De Beer *et al.*, 2012). The flavanone aglycones, eriodictyol and naringenin, as well as their rutinoside derivatives, have phytoestrogenic activity, indicating the potential of these glycosylated flavanone derivatives to contribute to the phytoestrogenic potential of *C. genistoides* extracts (as reviewed by Louw *et al.*, 2013).

3.2.4. Amino Acids

Compounds **1** (t_R = 2.83 min) and **2** (t_R = 4.89 min) were only detected in positive ionisation mode and produced protonated molecules at m/z 182 and m/z 166, respectively (Figure 1b; Table 3). Compounds **1** and **2** were identified as the aromatic amino acids tyrosine and phenylalanine (Figure 2), respectively, based on comparison with authentic standards. This is the first report of the presence of these aromatic amino acids in *Cyclopia* spp. The key role of phenylalanine as intermediate in the shikimate pathway, central to the biosynthesis of phenolic compounds in plants, could possibly explain the presence of these aromatic amino acids in the analysed honeybush extracts.

3.2.5. Glycosylated Phenolic Acids

Phenolic acids are aromatic secondary plant metabolites possessing at least one carboxylic acid functionality. This group of organic acids contains two distinctive carbon frameworks, namely the hydroxybenzoic acid structure (C₆.C₁) and hydroxycinnamic acid structure (C₆.C₃) (Figure 2). Two glycosylated hydroxybenzoic acid derivatives (compounds **e** and **h**) and two hydroxycinnamic acid derivatives (compounds **m** and **o**) were tentatively identified in *C. genistoides* hot water extracts (Table 3). Under the RP-LC conditions reported in this study, and in line with literature (Abad-García *et al.*, 2009), the hydroxybenzoic acids eluted first. The presence of these compounds in extracts of *Cyclopia* could impart additional health benefits, stemming from the potent antioxidant activity recorded for their underivatized counterparts (Natella *et al.*, 1999). One glycosylated phenylpropanoic acid (compound **j**) was also tentatively identified in the sample extracts (Table 3).

Table 4. Flavanone derivatives identified in freeze-dried aqueous extracts of unfermented and fermented *Cyclopia genistoides*.

Nr	tr (min)	Proposed Compound	λ_{\max} (nm) ^a	Mode	Accurate Mass, exp.	Proposed Formula	Error (ppm)	Precursor Ion	LC-MS/MS Ions ^{b,c}
p	22.44	eriodictyol- <i>O</i> -hexose- <i>O</i> -pentoside	225,	+	583.1705	C ₂₆ H ₃₁ O ₁₅	7.2	583	356, 289 , 219, 195, 154
			282	–	581.1508	C ₂₆ H ₂₉ O ₁₅	0.3	581	581, 445, 419, 401, 313, 299, 287, 161 , 151, 135, 125
q₁	22.90	eriodictyol- <i>O</i> -hexose- <i>O</i> -pentoside	225,	+	583.1436	nd ^e		583	289 , 261, 195, 163
			282 ^d	–	581.1519	C ₂₆ H ₂₉ O ₁₅	2.2	581	581 , 445, 419, 401, 299, 287, 161, 151, 135, 125
q₂	22.90	eriodictyol- <i>O</i> -hexose- <i>O</i> - deoxyhexoside	225,	+	597.1788	C ₂₇ H ₃₃ O ₁₅	–5.2	597	473, 313, 289 , 195, 163
			288 ^d	–	595.1656	C ₂₇ H ₃₁ O ₁₅	–1.2	595	595 , 459, 433, 313, 287, 169, 161, 151, 135, 125
s	24.38	eriodictyol- <i>O</i> -hexose- <i>O</i> - deoxyhexoside	225,	+	597.1826	C ₂₇ H ₃₃ O ₁₅	1.2	597	355, 289 , 219, 195, 163
			282	–	595.1666	C ₂₇ H ₃₁ O ₁₅	0.5	595	595 , 459, 433, 313, 287, 169, 161, 151, 135, 125
t	28.54	naringenin derivative	278	+	567.1711	C ₂₆ H ₃₁ O ₁₄	–0.5	567	573, 569, 478, 452, 414, 404, 381, 372, 352, 339, 330, 301, 285, 273 , 261, 236, 196, 173
			(weak)	–	565.1545	C ₂₆ H ₂₉ O ₁₄	–2.1	565	565, 445, 419, 299, 271, 257, 227, 199, 179, 169, 149, 145 , 125, 117
				+	567.1668	C ₂₆ H ₃₁ O ₁₄	–8.1	567	285, 273 , 261, 195
u	28.95	naringenin derivative		–	565.1558	C ₂₆ H ₂₉ O ₁₄	0.2	565	565, 445, 419 , 299, 271, 257, 209, 203, 169, 149, 145, 125
				+	581.1891	C ₂₇ H ₃₃ O ₁₄	3.6	581	351, 339, 315, 297, 285, 273 , 261, 231, 219, 195, 165, 153, 147
v	29.28	naringenin- <i>O</i> -hexose- <i>O</i> - deoxyhexoside	281	+	581.1891	C ₂₇ H ₃₃ O ₁₄	3.6	581	351, 339, 315, 297, 285, 273 , 261, 231, 219, 195, 165, 153, 147
				–	579.1722	C ₂₇ H ₃₁ O ₁₄	1.4	579	579 , 485, 459, 433, 415, 313, 271, 253, 209, 151, 145, 125
w	30.36	naringenin- <i>O</i> -hexose- <i>O</i> - deoxyhexoside	280	+	581.1866	C ₂₇ H ₃₃ O ₁₄	–0.7	581	351, 339, 315, 297, 285, 273 , 261, 251, 231, 219, 195, 147
				–	579.1722	C ₂₇ H ₃₁ O ₁₄	1.4	579	579 , 485, 459, 433, 415, 313, 271 , 253, 209, 169, 151, 145, 125
7	33.35	7-rutinosyloxyeriodictyol (eriocitrin)	281	+	597.1812	C ₂₇ H ₃₃ O ₁₅	–1.2	597	289
				–	595.1664	C ₂₇ H ₃₁ O ₁₅	0	595	595, 459, 287 , 175, 151, 135, 125, 107, 83
8	39.47	7-rutinosyloxynaringenin (narirutin)	280	+	581.1856	C ₂₇ H ₃₃ O ₁₄	–2.4	581	339, 315, 289, 285, 273 , 263, 245, 219, 195, 163, 153, 147
				–	579.1688	C ₂₇ H ₃₁ O ₁₄	–4.5	579	313, 295, 271 , 151
9	43.58	7-rutinosyloxyhesperetin (hesperidin)	283	+	611.1976	C ₂₈ H ₃₅ O ₁₅	0.0	611	303
				–	609.1834	C ₂₈ H ₃₃ O ₁₅	2.5	609	301
bb	44.43	naringenin- <i>O</i> -deoxyhexose(1→2) hexoside	nd ^d	+	581.1869	C ₂₇ H ₃₃ O ₁₄	–0.2	581	315, 273 , 231, 219, 195, 153, 147
				–	579.1691	C ₂₇ H ₃₁ O ₁₄	–4.0	579	579, 485, 459, 433, 415, 313, 271 , 253, 209, 177, 151, 145, 125

^aAll spectra also showed an undefined shoulder around 310-330 nm, however, the λ_{\max} could not be determined. ^bDefault collision energy (CE) of 30 V, unless otherwise stated. ^cValues in bold indicate the base peak ions. ^dCo-elution. ^eCompound **q₁** represented a very small peak, with the protonated molecule ion (m/z 583, [M+H]⁺) present at 5% relative abundance. The experimental accurate mass did not match the expected molecular formula of C₂₆H₃₁O₁₅. nd = not detected.

Compound **e** eluted at 11.14 min and exhibited maximum UV absorption at 314 nm. Its molecular formula was assigned as $C_{12}H_{13}O_8$ ($[M-H]^-$) based on the accurate mass of the deprotonated molecule ion. The MS/MS spectrum of the deprotonated molecule yielded the following ions [m/z (%): 153 (10), 152 (90), 109 (20), 108 (100)]. The ion at m/z 153 is compatible with, and characteristic of, a dihydroxybenzoic acid, while the ion at m/z 108 corresponds to a fragment of the latter that has lost the carboxy group (-COOH). Moreover, the ion at m/z 153 corresponds to the neutral loss of a pentose moiety from the deprotonated molecule ($[M-H-132]^-$). In accordance with literature (Bartsch *et al.*, 2010; Fayos *et al.*, 2006), compound **e** was tentatively identified as a dihydroxybenzoic acid-*O*-pentoside.

Compound **h** ($t_R = 16.57$ min) with m/z 417 ($[M-H]^-$) and the proposed molecular formula $C_{17}H_{21}O_{12}$ ($[M-H]^-$) was tentatively identified as a dihydroxybenzoic acid-*O*-dipentoside in a similar manner. The deprotonated molecule presented fragment ions at m/z 417 ($[M-H]^-$), m/z 285 ($[M-H-132]^-$), m/z 241 ($[M-H-132-44]^-$), m/z 153 ($[M-H-2 \times 132]^-$), m/z 152, m/z 109 and m/z 108. Thus far, only one dihydroxybenzoic acid-*O*-dipentoside has been reported, namely gentisic acid-5-*O*- $[\beta$ -D-apiofuranosyl-(1 \rightarrow 2)- β -D-xylopyranoside]. This compound has been isolated from the stems of *Spatholobus suberectus* (family Fabaceae; traditional Chinese medicine; Zhang & Xuan, 2006) and also from *Lens culinaris* Medik. (lentil cultivars; Tsopmo & Muir, 2010).

These two dihydroxybenzoic acid glycosides are herein tentatively identified for the first time in *Cyclopia* spp. Benzoate and 3-hydroxybenzoate are also key molecules in the biosynthetic pathway towards mangiferin, isomangiferin and 3- β -D-glucopyranosyliriflophenone (Joubert *et al.*, 2014), and therefore the presence of compounds **e** and **h** as hydroxylated and glycosylated derivatives of these key molecules (enhancing their water-solubility and storage in “inactive forms”; Andersen & Markham, 2005) is not unexpected.

In negative ionisation mode, the MS/MS spectrum of compound **m** ($t_R = 19.18$ min) showed the typical fragmentation of coumaric acid at m/z 163 and m/z 119 (Sánchez-Rabaneda *et al.*, 2003). The presence of a minor fragment ion at m/z 325 and the base peak ion at m/z 163 represents the neutral loss of a terminal pentose unit ($[M-H-132]^-$) and the subsequent loss of the internal hexose unit ($[M-H-132-162]^-$), respectively. Based on its MS/MS fragmentation pattern, compound **m** was tentatively identified as a coumaric acid *O*-(pentosyl)hexoside, which is supported by its experimental accurate mass and proposed molecular formula of $C_{20}H_{25}O_{12}$ ($[M-H]^-$). The only coumaric acid *O*-(pentosyl)hexoside that has been isolated and characterised in full is 4- $[\alpha$ -D-apiofuranosyl-(1 \rightarrow 2)- β -D-glucopyranosyloxy]-*p*-coumaric acid (Lu & Foo, 2000; Meng *et al.*, 2010), and thus it is very likely that compound **m** has the same glycosylation pattern. This is further supported by the presence of related compounds such as *p*-coumaric acid, 3- $[\alpha$ -D-apiofuranosyl-(1 \rightarrow 2)- β -D-glucopyranosyloxy]phenylethanol and 4- $[\alpha$ -D-apiofuranosyl-(1 \rightarrow 2)- β -D-glucopyranosyloxy]benzaldehyde in extracts of fermented *C. intermedia* (Ferreira *et al.*, 1998; Kamara *et al.*, 2003) and unfermented *C. subternata* (Kamara *et al.*, 2004). Based on the available data, however, it was not possible to establish the identity or the absolute configuration of the individual monosaccharides, nor the position of glycosylation or the type of interglycosidic linkage. The MS characteristics of compound **m** are in line with data reported for an unidentified compound **7** in extracts of *C. subternata* (De Beer *et al.*, 2012).

In a similar manner, the identity of compound **o** ($t_R = 21.52$ min) with a deprotonated molecule ion at m/z 473 ($[M-H]^-$), and fragment ions at m/z 179 and m/z 135 corresponding to a caffeic acid aglycone (Sánchez-Rabaneda *et al.*, 2003), was tentatively assigned to caffeic acid *O*-(pentosyl)hexoside. No information on such a compound could be found in the literature. The linkage of an apiosylglucoside to the propenoic side chain (esterification), rather than the hydroxy group on the aromatic ring of caffeic acid has, however, been reported [“1-*O*-caffeoyl- β -D-apiofuranosyl-(1 \rightarrow 6)- β -D-glucopyranoside”]; Wang *et al.*, 1999].

Compound **j** ($t_R = 16.77$ min) was assigned a molecular formula of $C_{15}H_{19}O_8$ ($[M-H]^-$) from the analysis of its HR-

ESI-MS data. The precursor ion at m/z 327 ($[M-H]^-$) exhibited typical fragmentation of cinnamic acid and presented the following daughter ions during tandem MS analysis: m/z 147 (cinnamic acid-H) and m/z 103 (cinnamic acid-COOH). The mass difference of 180 amu with regard to the cinnamic acid backbone could possibly be explained by an open degree of saturation in the C₃ side chain, with the presence of an 8-hexosyloxy moiety (Figure 2). By taking the accurate mass and proposed molecular formula into account, it is proposed that compound **j** is 2-(hexosyloxy)phenyllactic acid. The glucoside derivative, 2- β -D-glucopyranosyloxyphenyllactic acid, has previously been isolated from *Helleborus niger* L. leaves (Vitalini *et al.*, 2011).

3.2.6. Flavones

Compounds **6** ($t_R = 27.60$ min) and **10** ($t_R = 48.10$ min) were identified as 6,8-di- β -D-glucopyranosylapigenin (vicenin-2) and 7-rutinosyloxydiosmetin (diosmin), respectively, based on co-elution with the authentic reference standards (Table 3, Figure 2). The presence of vicenin-2 in extracts of *C. genistoides* (Malherbe *et al.*, 2014) and other *Cyclopia* species (De Beer *et al.*, 2012; Schulze *et al.*, 2014) has been proposed, but this is the first confirmation with an authentic reference standard. Diosmin is herein identified for the first time in *Cyclopia* spp., whereas its corresponding aglycone, diosmetin, has previously been identified in a methanol extract of fermented *C. intermedia* (Kamara *et al.*, 2003).

3.2.7. Dihydrochalcones

Compounds **x** and **z** were tentatively identified as the dihydrochalcones 3-hydroxyphloretin-3',5'-di-C-hexoside and 3',5'-di- β -D-glucopyranosylphloretin, respectively (Figure 2). Identification of these compounds was based on comparison of their UV-Vis, ESI-MS and -MS/MS characteristics (Table 3) with literature (Roowi & Crozier, 2011; Beelders *et al.*, 2012a, 2012b; De Beer *et al.*, 2012; Kokotkiewicz *et al.*, 2012; Malherbe *et al.*, 2014; Schulze *et al.*, 2014). 3-Hydroxyphloretin-3',5'-di-C-hexoside is herein identified for the first time in *C. genistoides*, whilst the presence of this compound in extracts of *C. subternata* (De Beer *et al.*, 2012) and *C. maculata* (Schulze *et al.*, 2014) has been proposed. This compound also occurs in *Aspalathus linearis* (family Fabaceae; rooibos) plant material (Beelders *et al.*, 2012a, 2012b), exemplifying distinct similarities between different *Cyclopia* species and also between different genera of the Fabaceae family. This compound has not been isolated and unambiguously identified to date. Conversely, 3',5'-di- β -D-glucopyranosylphloretin was recently isolated from *C. subternata* (Kokotkiewicz *et al.*, 2012) and has also been tentatively identified in extracts of *C. genistoides* (Malherbe *et al.*, 2014), *C. subternata* (De Beer *et al.*, 2012) and *C. maculata* (Schulze *et al.*, 2014).

3.3. HPLC-DAD Method Validation

Method validation was performed to ensure that the optimised HPLC-DAD method can produce reliable and reproducible quantitative results. The method was deemed specific for the 18 peaks selected for quantification as their UV-Vis and MS spectra matched those of authentic reference standards, or were in accordance with literature. Linearity was assessed by performing single measurements at several analyte concentrations (μg on-column). Six to eight concentration levels were considered which conform to guidelines specifying a minimum of five levels (Snyder *et al.*, 1997). Linearity of the calibration curves for authentic standards was excellent, with coefficients of determination (R^2) larger than 0.999. The y-intercept values were also relatively low (Table 5). The stability of the phenolic compounds in the standard calibration mixture and unfermented and fermented sample extracts was very good over the considered 24 h period (% RSD < 2%; Table S3, Supplementary Material, page 108). The intra- and inter-day precision values were also excellent for most phenolic compounds (Table S3), complying with the precision criteria of % RSD < 2% (Snyder *et al.*, 1997). The stability (% RSD < 3%) and precision (% RSD < 6%) for maclurin-di-*O,C*-hexoside (**a**) were, however, slightly poorer, but were still deemed acceptable for such a complex sample matrix.

Table 5 Characteristics of calibration curves obtained for HPLC analysis of phenolic standards.

Phenolic Standard	Number of Calibration Points, <i>n</i>	Wavelength, nm	Linearity Range, μg on-column	Regression Equation ^a	Coefficient of Determination, R^2
Maclurin ^b	6	320	0.0202–0.2527	$y = 2034.4 x + 1.3312$	0.9999
Mangiferin ^c	7	320	0.0364–3.6422	$y = 2114.9 x + 1.9834$	0.9999
Vicenin-2 ^c	8	320	0.0060–0.9008	$y = 1647.0 x - 2.3668$	0.9995
Aspalathin ^b	6	288	0.0301–0.3760	$y = 2305.6 x + 3.9468$	0.9999
Eriocitrin	6	288	0.0200–0.2500	$y = 1607.5 x + 1.7281$	0.9999
Narirutin	7	288	0.0200–0.3340	$y = 1584.9 x + 1.7940$	0.9999
Hesperidin	6	288	0.0776–0.9700	$y = 1631.5 x + 2.1973$	0.9999

^a y = analyte response (peak area in mAU) and x = amount of standard compound injected (μg). ^bMaclurin and aspalathin were representative of the benzophenone and dihydrochalcone phenolic sub-classes, respectively. ^cDiluted with DMSO, while other compounds were diluted with water.

3.4. Quantification of Phenolic Compounds

The validated HPLC-DAD method was subsequently applied to the analysis of freeze-dried hot water extracts of unfermented and fermented *C. genistoides* plant materials. The unfermented and fermented plant materials originated from the same individual plant. The content values of the major phenolic compounds, expressed as g of compound per 100 g of soluble solids, are summarised in Table 6.

The optimised, species-specific HPLC-DAD method was suitable for the quantification of 18 phenolic compounds, which is a major improvement with regard to other HPLC methods previously employed in the quantitative analysis of *C. genistoides* extracts (Joubert *et al.*, 2003; De Beer & Joubert, 2010). To date, quantitative data for the individual monomeric phenolic constituents of *C. genistoides* extracts have been mostly limited to four of the major compounds, *i.e.* mangiferin, isomangiferin, hesperidin and 3- β -D-glucopyranosyliriflophenone (Joubert *et al.*, 2003; Joubert *et al.*, 2008a; De Beer & Joubert, 2010; Joubert *et al.*, 2014).

The results in Table 6 show that the major constituents of freeze-dried hot water extracts of *C. genistoides* (> 1%) are the xanthenes, mangiferin and isomangiferin, and the benzophenones, iriflophenone-di-*O,C*-hexoside and 3- β -D-glucopyranosyliriflophenone. Collectively, these compounds comprised more than 20% of the aqueous soluble solids of the unfermented plant material, which enhances the nutraceutical potential of this species as a rich source of both xanthenes and benzophenones. These content values were, however, markedly reduced with fermentation. Interestingly, the new compound iriflophenone-di-*O,C*-hexoside represented the second most abundant phenolic constituent in both the unfermented and fermented sample extracts and appeared relatively stable during the high-temperature oxidation process (Table 6).

Other phenolic compounds present in significant amounts in the analysed *C. genistoides* sample extracts (> 3% in unfermented extract) include vicenin-2, hesperidin and compound **w**, tentatively identified as a naringenin-*O*-hexose-*O*-deoxyhexoside and quantified in terms of narirutin equivalents (Table 6).

Table 6 Content values (g of compound.100 g of soluble solids⁻¹) of the major phenolic compounds present in freeze-dried hot water extracts of unfermented and fermented *Cyclopia genistoides*.

Nr	Compound	Unfermented Extract	Fermented Extract
a	Maclurin-di- <i>O,C</i> -hexoside ^a	0.096	0.117
b	Iriflophenone-di- <i>O,C</i> -hexoside ^b	6.101	5.540
c	3- β -D-Glucopyranosylmaclurin ^a	0.173	0.041
A	Unidentified compound ^c	0.159	0.105
3	3- β -D-Glucopyranosyliriflophenone	1.222	0.498
k	Tetrahydroxyxanthone- <i>C</i> -hexoside dimer ^d	nq ^e	0.074
l	Tetrahydroxyxanthone-di- <i>O,C</i> -hexoside ^d	0.190	0.080
s	Eriodictyol- <i>O</i> -hexose- <i>O</i> -deoxyhexoside ^f	0.143	0.100
4	Mangiferin	13.791	6.966
5	Isomangiferin	1.617	0.907
6	Vicenin-2	0.493	0.420
v	Naringenin- <i>O</i> -hexose- <i>O</i> -deoxyhexoside ^g	0.147	0.206
w	Naringenin- <i>O</i> -hexose- <i>O</i> -deoxyhexoside ^g	0.441	0.219
7	Eriocitrin	0.045	0.041
x	3-Hydroxyphloretin-3',5'-di- <i>C</i> -hexoside ^h	0.125	0.029
y	Tetrahydroxyxanthone- <i>C</i> -hexoside isomer ^d	0.109	0.053
z	3',5'-di- β -D-Glucopyranosylphloretin ⁱ	0.273	0.145
9	Hesperidin	0.374	0.268

^ag of maclurin equivalents.100 g of soluble solids⁻¹. ^bg of 3- β -D-glucopyranosyliriflophenone equivalents.100 g of soluble solids⁻¹.

^cg of hesperidin equivalents.100 g of soluble solids⁻¹. ^dg of mangiferin equivalents.100 g of soluble solids⁻¹. ^enq = not quantified.

^fg of eriocitrin equivalents.100 g of soluble solids⁻¹. ^gg of narirutin equivalents.100 g of soluble solids⁻¹.

^hg of aspalathin equivalents.100 g of soluble solids⁻¹. ⁱg of nothofagin equivalents.100 g of soluble solids⁻¹.

4. CONCLUSIONS

Optimisation of a species-specific HPLC-DAD method for the analysis of hot water extracts of unfermented and fermented *C. genistoides* provided high-resolution chromatographic separation of a large number of phenolic compounds. Characteristic profiles for these two types of extracts were described. Ten compounds were identified by co-elution with the authentic reference standards, while MS data enabled tentative identification of 30 additional compounds. A total of 31 phenolic compounds were identified for the first time in *C. genistoides*, including 28 identified for the first time in *Cyclopia* spp. The optimised HPLC-DAD method was successfully validated and applied for the quantitative analysis of the same sample extracts. The major phenolic constituents were the well-known xanthenes, mangiferin and isomangiferin, the known benzophenone 3- β -D-glucopyranosyliriflophenone and an iriflophenone-di-*O,C*-hexoside (unidentified to date). Future applications of this method will include the quantification of a large number of samples to obtain representative content values and, from a qualitative perspective, authentication of nutraceutical extracts based on their phenolic profiles. Moreover, tentative identification of these phenolic compounds by ESI-MS and tandem MS detection will prove invaluable in subsequent studies on the bio-activity of *C. genistoides* hot water extracts.

REFERENCES

- Abad-García, B., Berrueta, L.A., Garmón-Lobato, S., Gallo, B. & Vicente, F. (2009). A general analytical strategy for the characterization of phenolic compounds in fruit juices by high-performance liquid chromatography with diode array detection coupled to electrospray ionization and triple quadrupole mass spectrometry. *Journal of Chromatography A*, **1216**, 5398-5415.
- Abdel-Mageed, W.M., Bayoumi, S.A.H., Chen, C., Vavricka, C.J., Li, L., Malik, A., Dai, H., Song, F., Wang, L., Zhang, J., Gao, G.F., Lv, Y., Liu, L., Liu, X., Sayed, H.M. & Zhang, L. (2014). Benzophenone C-glucosides and gallotannins from mango tree stem bark with broad-spectrum anti-viral activity. *Bioorganic and Medicinal Chemistry*, **22**, 2236-2243.
- Andersen, Ø.M. & Markham, K.R. (2005). *Flavonoids: Chemistry, Biochemistry and Applications*. CRC Press: Boca Raton, FL, USA.
- Bartsch, M., Bednarek, P., Vivancos, P.D., Schneider, B., Von Roepenack-Lahaye, E., Foyer, C.H., Kombrink, E., Scheel, D. & Parker, J.E. (2010). Accumulation of isochlorismate-derived 2,3-dihydroxybenzoic 3-O- β -D-xyloside in *Arabidopsis* resistance to pathogens and ageing of leaves. *Journal of Biological Chemistry*, **285**, 25654-25665.
- Beelders, T., Sigge, G.O., Joubert, E., De Beer, D. & De Villiers, A. (2012a) Kinetic optimisation of the reversed phase liquid chromatographic separation of rooibos tea (*Aspalathus linearis*) phenolics on conventional high performance liquid chromatographic instrumentation. *Journal of Chromatography A*, **1219**, 128-139.
- Beelders, T., Sigge, G.O., Joubert, E., De Beer, D. & De Villiers, A. (2012b). Erratum to “Kinetic optimisation of the reversed phase liquid chromatographic separation of rooibos tea (*Aspalathus linearis*) phenolics on conventional high performance liquid chromatographic instrumentation” [*Journal of Chromatography A*, **1219**, 128-139]. *Journal of Chromatography A*, **1241**, 128.
- Cuyckens, F., Rozenberg, R., De Hoffmann, E. & Claeys, M. (2001). Structure characterization of flavonoid O-diglycosides by positive and negative nano-electrospray ionization ion trap mass spectrometry. *Journal of Mass Spectrometry*, **36**, 1203-1210.
- Cuyckens, F. & Claeys, M. (2004). Mass spectrometry in the structural analysis of flavonoids. *Journal of Mass Spectrometry*, **39**, 1-15.
- De Beer, D. & Joubert, E. (2010). Development of HPLC method for *Cyclopia subternata* phenolic compound analysis and application to other *Cyclopia* spp. *Journal of Food Composition and Analysis*, **23**, 289-297
- De Beer, D., Schulze, A.E., Joubert, E., De Villiers, A., Malherbe, C.J. & Stander, M.A. (2012). Food Ingredient Extracts of *Cyclopia subternata* (Honeybush): Variation in Phenolic Composition and Antioxidant Capacity. *Molecules*, **17**, 14602-14624.
- De Villiers, A., Lestremau, F., Szucs, R., Gélébart, S., David, F. & Sandra, P. (2006). Evaluation of ultra performance liquid chromatography: Part I. Possibilities and limitations. *Journal of Chromatography A*, **1127**, 60-69.
- Djoukeng, J.D., Arbona, V., Argamasilla, R. & Gomez-Cadenas, A. (2008). Flavonoid profiling in leaves of citrus genotypes under different environmental situations. *Journal of Agricultural and Food Chemistry*, **56**, 11087-11097.
- Dolan, J.W. (2002). Temperature selectivity in reversed-phase high performance liquid chromatography. *Journal of Chromatography A*, **965**, 195-205.
- Domon, B. & Costello, C.E. (1988) A systematic nomenclature for carbohydrate fragmentations in FAB-MS/MS spectra of glycoconjugates. *Glycoconjugate Journal*, **5**, 397-409.

- Du, X.G., Wang, W., Zhang, Q.Y., Cheng, J., Avula, B., Khan, I.A. & Guo, D.A. (2012). Identification of xanthenes from *Swertia punicea* using high-performance liquid chromatography coupled with electrospray ionization tandem mass spectrometry. *Rapid Communications in Mass Spectrometry*, **26**, 2913-2923.
- Fayos, J., Bellés, J.M., López-Gresa, M.P., Primo, J. & Conejero, V. (2006). Induction of gentisic acid 5-*O*- β -D-xylopyranoside in tomato and cucumber plants infected by different pathogens. *Phytochemistry*, **67**, 142-148.
- Feng, J., Yang, X.W. & Wang, R.F. (2011). Bio-assay guided isolation and identification of α -glucosidase inhibitors from the leaves of *Aquilaria sinensis*. *Phytochemistry*, **72**, 242-247.
- Ferreira, D., Kamara, B.I., Brandt, E.V. & Joubert, E. (1998). Phenolic compounds from *Cyclopia intermedia* (honeybush tea). 1. *Journal of Agricultural and Food Chemistry*, **46**, 3406-3410.
- Greenish, H. (1881). Cape tea. *The Pharmaceutical Journal and Transactions*, **11**, 549-551.
- Huang, C.F., Gan, X.W., Bai, H.Y., Ma, L. & Hu, L.H. (2008). Schoepfin A, B, C: Three new chalcone C-glycosides from *Schoepfia chinensis*. *Natural Product Research*, **22**, 623-627.
- Ichiki, H., Miura, T., Kubo, M., Ishihara, E., Komatsu, Y., Tanigawa, K. & Okada, M. (1998). New antidiabetic compounds, mangiferin and its glucoside. *Biological and Pharmaceutical Bulletin*, **21**, 1389-1390.
- Ito, T., Kakino, M., Tazawa, S., Oyama, M., Maruyama, H., Araki, Y., Hara, H. & Inuma, M. (2012). Identification of phenolic compounds in *Aquilaria crassna* leaves via liquid chromatography-electrospray ionization mass spectroscopy. *Food Sci. Technol. Res.*, **18**, 259-262.
- Joubert, E., Otto, F., Grüner, S. & Weinreich, B. (2003). Reversed-phase HPLC determination of mangiferin, isomangiferin and hesperidin in *Cyclopia* and the effect of harvesting date on the phenolic composition of *C. genistoides*. *European Food Research and Technology*, **216**, 270-273.
- Joubert, E., Manley, M. & Botha, M. (2008a). Evaluation of spectrophotometric methods for screening of green rooibos (*Aspalathus linearis*) and green honeybush (*Cyclopia genistoides*) extracts for high levels of bio-active compounds. *Phytochemical Analysis*, **19**, 169-178.
- Joubert, E., Richards, E.S., Van der Merwe, J.D., De Beer, D., Manley, M. & Gelderblom, W.C.A. (2008b). Effect of species variation and processing on phenolic composition and *in vitro* antioxidant activity of aqueous extracts of *Cyclopia* spp. (honeybush tea). *Journal of Agricultural and Food Chemistry*, **56**, 954-963.
- Joubert, E., Joubert, M.E., Bester, C., De Beer, D. & De Lange, J.H. (2011). Honeybush (*Cyclopia* spp.): From local cottage industry to global markets – The catalytic and supporting role of research. *South African Journal of Botany*, **77**, 887-907.
- Joubert, E., De Beer, D., Hernández, I. & Munné-Bosch, S. (2014). Accumulation of mangiferin, isomangiferin, iriflophenone-3-*C*- β -glucoside and hesperidin in honeybush leaves (*Cyclopia genistoides* Vent.) in response to harvest time, harvest interval and seed source. *Industrial Crops and Products*, **56**, 74-82.
- Kalili, K.M., Cabooter, D., Desmet, G. & De Villiers, A. (2012). Kinetic optimisation of the reversed phase liquid chromatographic separation of proanthocyanidins on sub-2 μ m and superficially porous phases. *Journal of Chromatography A*, **1236**, 63-76.
- Kamara, B.I., Brandt, E.V., Ferreira, D. & Joubert, E. (2003). Polyphenols from honeybush tea (*Cyclopia intermedia*). *Journal of Agricultural and Food Chemistry*, **51**, 3874-3879.
- Kamara, B.I., Brand, D.J., Brandt, E.V. & Joubert, E. (2004). Phenolic metabolites from honeybush tea (*Cyclopia subternata*). *Journal of Agricultural and Food Chemistry*, **52**, 5391-5395.

- Kokotkiewicz, A., Luczkiewicz, M., Sowinski, P., Glod, D., Gorynski, K. & Bucinski, A. (2012). Isolation and structure elucidation of phenolic compounds from *Cyclopia subternata* Vogel (honeybush) intact plant and in vitro cultures. *Food Chemistry*, **133**, 1373-1382.
- Kokotkiewicz, A., Luczkiewicz, M., Pawlowska, J., Luczkiewicz, P., Sowinski, P., Witkowski, J., Bryl, E. & Bucinski, A. (2013). Isolation of xanthone and benzophenone derivatives from *Cyclopia genistoides* (L.) Vent. (honeybush) and their pro-apoptotic activity on synoviocytes from patients with rheumatoid arthritis. *Fitoterapia*, **90**, 199-208.
- Louw, A., Joubert, E. & Visser, K. P. (2013). Phytoestrogenic potential of *Cyclopia* extracts and polyphenols. *Planta Medica*, **79**, 580-590.
- Lu, Y. & Foo, L.Y. (2000). Flavonoid and phenolic glycosides from *Salvia officinalis*. *Phytochemistry*, **55**, 263-267.
- Malherbe, C.J., Willenburg, E., de Beer, D., Bonnet, S.L., van der Westhuizen, J.H. & Joubert, E. (2014). Iriflophenone-3-C-glucoside from *Cyclopia genistoides*: Isolation and quantitative comparison of antioxidant capacity with mangiferin and isomangiferin using on-line HPLC antioxidant assays. *Journal of Chromatography B*, **951-952C**, 164-171.
- Meng, D., Wu, J. & Zhao, W. (2010). Glycosides from *Breynia fruticosa* and *Breynia rostrata*. *Phytochemistry*, **71**, 325-331.
- Miura, T., Ichiki, H., Iwamoto, N., Kato, M., Kubo, M., Sasaki, H., Okada, M., Ishida, T., Seino, Y. & Tanigawa, K. (2001). Antidiabetic activity of the rhizoma of *Anemarrhena asphodeloides* and active components, mangiferin and its glucoside. *Biological and Pharmaceutical Bulletin*, **24**, 1009-1011.
- Muruganandan, S., Srinivasan, K., Gupta, S., Gupta, P.K. & Lal, J. (2005). Effect of mangiferin on hyperglycemia and atherogenicity in streptozotocin diabetic rats. *Journal of Ethnopharmacology*, **97**, 497-501.
- Natella, F., Nardini, M., Di Felice, M. & Scaccini, C. (1999). Benzoic and cinnamic acid derivatives as antioxidants: Structure–activity relation. *Journal of Agricultural and Food Chemistry*, **47**, 1453-1459.
- Roowi, S. & Crozier, A. (2011). Flavonoids in tropical citrus species. *Journal of Agricultural and Food Chemistry*, **59**, 12217-12225.
- Sánchez-Rababeda, F., Jáuregui, O., Lamuela-Raventós, R.M., Bastida, J., Viladomat, F. & Codina, C. (2003). Identification of phenolic compounds in artichoke waste by high-performance liquid chromatography–tandem mass spectrometry. *Journal of Chromatography A*, **1008**, 57-72.
- Schulze, A.E., De Beer, D., De Villiers, A., Manley, M. & Joubert, E. (2014). Chemometric analysis of chromatographic fingerprints shows potential of *Cyclopia maculata* (Andrews) Kies for production of standardized extracts with high xanthone content. *Journal of Agricultural and Food Chemistry*, **62**, 10542-10551.
- Snyder, L.R., Kirkland, J.J. & Glajch, J.L. (1997). *Practical HPLC Method Development*, 2th ed.; John Wiley & Sons, Inc.: New York, NY, USA.
- Tsopmo, A. & Muir, A.D. (2010). Chemical profiling of lentil (*Lens culinaris* Medik.) cultivars and isolation of compounds. *Journal of Agricultural and Food Chemistry*, **58**, 8715-8721.
- Verhoog, N.J.D., Joubert, E. & Louw, A. (2007). Screening of four *Cyclopia* (honeybush) species for putative phytoestrogenic activity by oestrogen receptor binding assays. *South African Journal of Science*, **103**, 13-21.
- Vitalini, S., Braca, A. & Fico, G. (2011). Study on secondary metabolite content of *Helleborus niger* L. leaves. *Fitoterapia*, **82**, 152-154.
- Vyas, A., Syeda, K., Ahmad, A., Padhye, S. & Sarkar, F.H. (2012). Perspectives on medicinal properties of mangiferin. *Mini-Reviews in Medicinal Chemistry*, **12**, 412-425.

- Wang, J.N., Hou, C.Y., Liu, Y.L., Lin, L.Z., Gil, R.R. & Cordell, G.A. (1994). Swertifrancheside, an HIV-Reverse transcriptase inhibitor and the first flavone-xanthone dimer, from *Swertia franchetiana*. *Journal of Natural Products*, **57**, 211-217.
- Wang, M., Shao, Y., Li, J., Zhu, N., Rangarajan, M., LaVoie, E.J. & Ho, C.T. (1999). Antioxidative phenolic glycosides from sage (*Salvia officinalis*). *Journal of Natural Products*, **62**, 454-456.
- Zhang, Y., Han, L., Ge, D., Liu, X., Liu, E., Wu, C., Gao, X. & Wang, T. (2013). Isolation, structural elucidation, MS profiling, and evaluation of triglyceride accumulation inhibitory effects of benzophenone C-glucosides from leaves of *Mangifera indica* L. *Journal of Agricultural and Food Chemistry*, **61**, 1884–1895.
- Zhang, S. & Xuan, L. (2006). New phenolic constituents from the stems of *Spatholobus suberectus*. *Helvetica Chimica Acta*, **89**, 1241-1245.

SUPPLEMENTARY MATERIAL CHAPTER 3

Table S1 Retention times, UV-Vis as well as ESI-MS and –MS/MS characteristics of additional compounds that could not be identified in *Cyclopia genistoides* sample extracts.

Nr	t _R (min)	Compound	λ _{max} (nm)	Mode	Accurate Mass, exp.	Proposed Formula	Error (ppm)	Precursor Ion	LC-MS/MS Ions ^{a,b}
A	11.61	unidentified	239, 283	+	397.1137	C ₁₈ H ₂₁ O ₁₀	0.5	397	325, 277, 259, 247 , 231, 193, 163, 149
				–	395.0963	C ₁₈ H ₁₉ O ₁₀	–3.8	395	287, 275, 259, 247 , 233, 124
B	17.94	unidentified	nd	+	425.1415	C ₁₈ H ₂₆ O ₁₀ Na	–2.1	425 [M+Na] ⁺	425
				–	447.1491	C ₁₉ H ₂₇ O ₁₂	–2.7	447 [M+formate] [–]	401, 269 , 233, 161, 143, 131, 125, 113, 101, 85, 71, 55
C	19.18	unidentified	nd, co-elution	+	476.1754	C ₂₀ H ₃₀ NO ₁₂	–2.9	476	481, 342, 165, 147 , 97
D	20.22	unidentified	nd	+	387.1989	C ₁₉ H ₃₁ O ₈	–7.7	387	149 , 137, 119, 109, 99, 95, 91, 79
				–	431.1906	C ₂₀ H ₃₁ O ₁₀	–2.6	431 [M+formate] [–]	347, 329, 317 , 301, 287, 275
E	21.98	unidentified	250, 316, 368 (weak)	+	519.2466	C ₂₄ H ₃₉ O ₁₂	4.6	519	207 , 189, 179, 165, 161, 149, 135, 123, 119, 113, 95, 67
				–	517.2287	C ₂₄ H ₃₇ O ₁₂	0.4	517	517, 505, 415, 347, 233, 205 , 191, 188, 153, 143, 125, 113, 108, 97, 89, 73
F	37.88	unidentified	nd	+	525.2296	C ₂₄ H ₃₈ O ₁₁ Na	–3.0	525 [M+Na] ⁺	525
				–	547.2405	C ₂₅ H ₃₉ O ₁₃	2.6	547 [M+formate] [–]	191, 175, 161, 149, 143, 131, 125, 119, 113, 99, 89 , 85, 71, 59, 43
G	41.19	unidentified	nd	+	527.2457	C ₂₄ H ₄₀ O ₁₁ Na	–2.1	527 [M+Na] ⁺	527
				–	549.2548	C ₂₅ H ₄₁ O ₁₃	0.2	549 [M+formate] [–]	503 , 371
H	44.24	unidentified	nd, co-elution	+	527.2468	C ₂₄ H ₄₀ O ₁₁ Na	0.0	527 [M+Na] ⁺	527
				–	549.2560	C ₂₅ H ₄₁ O ₁₃	2.4	549 [M+formate] [–]	503 , 371
I	53.69	unidentified	nd	+	471.2200	C ₂₁ H ₃₆ O ₁₀ Na	–0.6	471 [M+Na] ⁺	471 , 335
				–	493.2299	C ₂₂ H ₃₇ O ₁₂	2.8	493 [M+formate] [–]	447, 233, 191, 179, 161, 149, 143, 131, 125, 119, 113, 99 , 89, 85, 71, 59, 55, 43

^aDefault collision energy (CE) of 30 V, unless otherwise stated. ^bValues in bold indicate the base peak ions. nd = not detected.

Table S2 Retention times, UV-Vis as well as ESI-MS and –MS/MS characteristics of additional authentic reference standard compounds used in the identification of constituents.

t_R (min)	Compound	λ_{max} (nm)	Mode	Accurate Mass, exp.	Proposed Formula	Error (ppm)	Precursor Ion	LC-MS/MS Ions^{a,b}
19.83	7-β-D-glucopyranosyloxymangiferin (neomangiferin)	241, 256, 317, 357	+	585.1454	C ₂₅ H ₂₉ O ₁₆	-0.3	585	489, 465, 435, 405, 387, 369, 357, 351, 339, 327, 313, 303 , 299, 285, 273, 261
			-	583.1309	C ₂₅ H ₂₇ O ₁₆	1.7	583	583, 565, 493 , 463, 421, 403, 331, 313, 301, 271, 259
30.57	3'-β-D-glucopyranosyl-3- hydroxyphloretin (aspalathin)	287	+	453.1385	C ₂₁ H ₂₅ O ₁₁	-2.6	453	381, 369, 351, 315, 297, 285, 277, 259, 247, 235, 229, 217, 211, 205, 193, 181, 165, 151, 139, 123
			-	451.1241	C ₂₁ H ₂₃ O ₁₁	0.2	451	361, 343, 331, 313, 289, 239, 221, 209 , 197, 179, 167, 137, 125
38.96	3'-β-D-glucopyranosylphloretin (nothofagin)	287	+	437.1449	C ₂₁ H ₂₅ O ₁₀	0.2	437	365, 353, 335, 317, 299, 287, 277, 259, 247, 235, 229, 217, 211, 205, 193, 181, 163, 151, 139, 107
			-	435.1285	C ₂₁ H ₂₃ O ₁₀	-1.4	435	345, 327, 315 , 285, 273, 239, 221, 209, 197, 179, 167, 137, 125
41.08	7-neohesperidosyloxynaringenin (naringin)	280	+	581.1870	C ₂₇ H ₃₃ O ₁₄	0.0	581	603, 581, 488, 435, 419, 401, 383, 315, 311, 273, 245, 231, 219, 195, 153, 147
			-	579.1714	C ₂₇ H ₃₁ O ₁₄	0.0	579	579, 459, 271, 151

^aDefault collision energy (CE) of 30 V, unless otherwise stated. ^bValues in bold indicate the base peak ions.

Table S3 Percentage relative standard deviation (% RSD) values for the determination of analyte stability and analytical precision of phenolic constituents as part of a standard calibration mixture and unfermented and fermented *Cyclopia genistoides* extracts.

Nr	Compound	Stability	Analytical precision			
		24 hrs (n = 6)	day 1 (n = 6)	day 2 (n = 6)	day 3 (n = 6)	pooled (n = 3)
Standard calibration mixture						
na ^a	maclurin	0.31	0.47	0.28	0.32	1.02
4	mangiferin ^b	0.31	0.63	0.30	0.20	1.23
6	vicenin-2 ^b	1.44	0.51	0.68	0.74	1.07
na ^a	aspalathin	0.33	0.51	0.35	0.14	0.79
7	eriocitrin	0.58	0.68	0.49	0.69	0.52
8^a	narirutin	0.33	0.33	0.22	0.21	0.48
9	hesperidin	0.17	0.21	0.17	0.14	0.50
Unfermented extract						
a	maclurin-di- <i>O,C</i> -hexoside	5.89	2.24	2.39	2.55	0.88
b	iriflophenone-di- <i>O,C</i> -hexoside	0.51	0.12	0.14	0.22	0.18
c	3- β -D-glucopyranosylmaclurin	0.68	0.30	0.32	0.37	0.47
A	unidentified compound	0.55	0.75	0.70	0.39	0.38
3	3- β -D-glucopyranosyliriflophenone	0.24	0.17	0.18	0.11	0.15
k	tetrahydroxyxanthone- <i>C</i> -hexoside dimer	nq ^c	nq ^c	nq ^c	nq ^c	nq ^c
l	tetrahydroxyxanthone-di- <i>O,C</i> -hexoside	0.63	0.16	0.32	0.18	0.45
s	eriodictyol- <i>O</i> -hexose- <i>O</i> -deoxyhexoside	0.73	0.50	0.40	0.36	0.12
4	mangiferin	0.32	0.12	0.06	0.11	0.31
5	isomangiferin	0.13	0.26	0.25	0.24	0.26
6	vicenin-2	0.20	0.24	0.21	0.21	0.37
v	naringenin- <i>O</i> -hexose- <i>O</i> -deoxyhexoside	0.39	0.35	0.28	0.43	0.48
w	naringenin- <i>O</i> -hexose- <i>O</i> -deoxyhexoside	0.36	0.26	0.21	0.24	0.20
7	eriocitrin	1.05	1.21	0.93	1.63	0.24
x	3-hydroxyphloretin-3',5'-di- <i>C</i> -hexoside	0.40	0.58	0.55	0.50	0.38
y	tetrahydroxyxanthone- <i>C</i> -hexoside isomer	0.99	0.78	0.52	0.46	0.56
z	3',5'-di- β -D-glucopyranosylphloretin	0.57	0.45	0.37	0.23	0.23
9	hesperidin	0.34	0.52	0.27	0.25	0.29
Fermented extract						
a	maclurin-di- <i>O,C</i> -hexoside	5.75	2.02	2.71	2.14	0.78
b	iriflophenone-di- <i>O,C</i> -hexoside	0.40	0.14	0.22	0.15	0.40
c	3- β -D-glucopyranosylmaclurin	1.04	1.17	1.56	1.30	0.38
A	unidentified compound	0.58	0.45	0.91	0.78	0.49
3	3- β -D-glucopyranosyliriflophenone	0.27	0.11	0.33	0.23	0.24
k	tetrahydroxyxanthone- <i>C</i> -hexoside dimer	0.93	0.76	0.98	0.86	0.75
l	tetrahydroxyxanthone-di- <i>O,C</i> -hexoside	0.80	0.73	0.57	0.42	0.70
s	eriodictyol- <i>O</i> -hexose- <i>O</i> -deoxyhexoside	0.57	1.08	0.57	0.53	0.88
4	mangiferin	0.32	0.12	0.12	0.09	0.95
5	isomangiferin	0.42	0.23	0.27	0.15	0.64
6	vicenin-2	0.13	0.24	0.37	0.13	0.30
v	naringenin- <i>O</i> -hexose- <i>O</i> -deoxyhexoside	0.49	0.58	0.48	0.40	0.50
w	naringenin- <i>O</i> -hexose- <i>O</i> -deoxyhexoside	0.75	0.43	0.27	0.39	0.10
7	eriocitrin	1.00	1.15	1.85	1.78	1.14
x	3-hydroxyphloretin-3',5'-di- <i>C</i> -hexoside	1.03	0.86	1.67	1.29	0.84
y	tetrahydroxyxanthone- <i>C</i> -hexoside isomer	0.97	0.69	0.66	0.69	0.46
z	3',5'-di- β -D-glucopyranosylphloretin	0.74	0.68	0.23	0.73	0.44
9	hesperidin	0.28	0.24	0.51	0.28	0.15

^ana = not applicable, standard compound not detected and/or not quantified in the sample extracts, but used in the quantification of other phenolic constituents. ^bDiluted with DMSO, while other compounds were diluted with water. ^cnq = not quantified due to extremely small peak area (< 30 mAU) yielding large percentage error associated with difficult integration. Values in bold indicates % RSD values > 2.

CHAPTER 4

Structural Elucidation of the Novel *Cyclopia* Benzophenone 3- β -D-glucopyranosyl-4- β -D-glucopyranosyloxyiriflophenone and the Comparative Assessment of its Antidiabetic Potential

*** Published**

Beelders, T., Brand, D.J., De Beer, D., Malherbe, C.J., Mazibuko, S.E., Muller, C.J.F. & Joubert, E. (2014). Benzophenone C- and O-glucosides from *Cyclopia genistoides* (honeybush) inhibit mammalian α -glucosidase. *Journal of Natural Products*, **77**, 2694–2699.

DECLARATION

With regard to Chapter 4 (pp. 109-122), the nature and scope of my contribution were as follows:

Nature of Contribution	Extent of Contribution (%)
Conducted all experimental work pertaining to the isolation of the target compounds, and wrote the relevant sections.	74%
Compiled the manuscript, and edited the document in its entirety during the different stages of the publication process.	

The following co-authors have contributed to Chapter 4 (pp. 109-122):

Name	E-mail address	Nature of Contribution	Extent of Contribution (%)
Dr D. Jaco Brand	djbrand@sun.ac.za	Conducted the NMR experiments, and wrote the relevant sections.	5%
Dr Dalene de Beer (Co-supervisor)	DBeerD@arc.agric.za	Assisted in editing the document in its entirety during the different stages of publication.	5%
Dr Christiaan J. Malherbe	malherbech@arc.agric.za	Conducted the α -glucosidase inhibitory assays, and wrote the relevant sections.	3%
Dr Sithandiwe E. Mazibuko	sithandiwe.mazibuko@mrc.ac.za	Conducted the in vitro tests in cell models	5%
Dr Christo J.F. Muller	christo.muller@mrc.ac.za	Wrote the relevant sections pertaining to the in vitro tests in cell models.	3%
Dr Elizabeth Joubert (Supervisor)	JoubertL@arc.agric.za	Assisted in editing the document in its entirety during the different stages of publication.	5%

Signature of candidate: **Declaration with signature in possession of candidate and supervisor*

Date: February 2016

Declaration by co-authors:

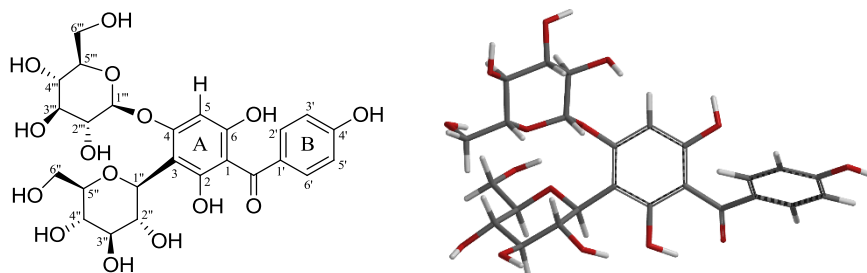
The undersigned hereby confirm that

1. the declaration above accurately reflects the nature and extent of the contribution of the candidate and the co-authors to Chapter 4 (pp. 109-122),
2. no other authors contributed to Chapter 4 (pp. 109-122) besides those specified above, and
3. potential conflicts of interest have been revealed to all interested parties and that the necessary arrangements have been made to use the material in Chapter 4 (pp. 109-122) of this dissertation.

Signature*	Institutional Affiliation	Date
Dr D. Jaco Brand	Central Analytical Facility, Nuclear Magnetic Resonance Unit Post-Harvest and Wine Technology Division, Agricultural Research Council	
Dr Dalene de Beer	Infruitec-Nietvoorbij Post-Harvest and Wine Technology Division, Agricultural Research Council	
Dr Christiaan J. Malherbe	Infruitec-Nietvoorbij	
Dr Sithandiwe E. Mazibuko	Diabetes Discovery Platform, South African Medical Research Council	
Dr Christo J.F. Muller	Diabetes Discovery Platform, South African Medical Research Council	
Dr Elizabeth Joubert	Post-Harvest and Wine Technology Division, Agricultural Research Council Infruitec-Nietvoorbij; Department of Food Science, Stellenbosch University	

ABSTRACT

An enriched fraction of an aqueous extract prepared from the aerial parts of *Cyclopia genistoides* (L.) Vent. yielded a new benzophenone di-*C,O*-glucosyl compound, 3- β -D-glucopyranosyl-4- β -D-glucopyranosyloxyriflophenone (**1**), together with small quantities of the known benzophenone *C*-glucoside, 3- β -D-glucopyranosylmaclurin (**2**).



3- β -D-glucopyranosyl-4- β -D-glucopyranosyloxyriflophenone

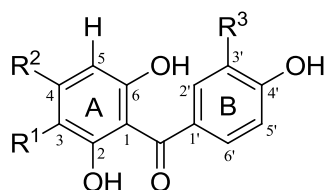
The isolated benzophenone glucosides were assessed for their α -glucosidase inhibitory activity against an enzyme mixture extracted from rat intestinal acetone powder, and their activities compared to that of 3- β -D-glucopyranosylriflophenone, maclurin and acarbose (positive control). The inhibitory activities of the benzophenones showed a clear dose-response, with higher activities observed at higher concentration levels. At equimolar concentration levels (200 μ M), compound **2** exhibited the highest inhibitory activity (54%), followed by 3- β -D-glucopyranosylriflophenone (49%) and **1** (43%), while maclurin showed the weakest activity (28%). The presence of an additional 3'-hydroxy group led to a significant increase in the α -glucosidase inhibitory activity of the polyhydroxybenzophenone *C*-glucosyl compounds. The presence of a single *C*-linked glucopyranosyl moiety on the A-ring of the diphenyl methanone structure was found to increase the inhibitory activity, while further *O*-glucosylation had the opposite effect. In vitro tests in several cell models showed that **1** and 3- β -D-glucopyranosylriflophenone were marginally effective ($p \geq 0.05$) in increasing glucose uptake.

1. INTRODUCTION

The global prevalence of diabetes is increasing at alarming rates leading to estimates of 439 million diabetics by 2030 (Shaw *et al.*, 2010). In Africa, South Africa tips the scale with a national prevalence of over 7% (International Diabetes Federation, 2013). It is projected that diabetes will rank as the ninth leading cause of death in low-income countries in the next few decades (Mathers & Loncar, 2006). A sedentary lifestyle together with an unhealthy diet, high in refined carbohydrates accompanied by a low intake of fruits and vegetables, are considered contributing factors. The search for natural and synthetic α -glucosidase inhibitors (Park *et al.*, 2008; Xiao *et al.*, 2013) that delay the breakdown and absorption of carbohydrates in the gut, thus mimicking the protective effect of the drug acarbose, but without its side-effects (Hollander, 2007), is escalating. Much prominence is given to polyphenols, with promising results in vitro (Xiao *et al.*, 2013). Synergistic effects between acarbose and polyphenols suggest benefits in terms of dose reduction of the drug (Boath *et al.*, 2012). Sub-classes of phenolic compounds that show promise as α -glucosidase inhibitors include the polyhydroxyxanthenes and polyhydroxybenzophenones, together with their glycosylated derivatives (Liu *et al.*, 2006; Feng *et al.*, 2011; Hu *et al.*, 2011; Liu *et al.*, 2012).

Extracts of *Cyclopia genistoides* (honeybush) are principally renowned for high levels of the tetrahydroxyxanthone *C*-glucoside, mangiferin (Joubert *et al.*, 2011), a bio-active compound (as reviewed by Vyas *et al.*, 2012) with potent α -glucosidase inhibitory activity (Feng *et al.*, 2011). Recent investigation of the phenolic constituents of *C. genistoides* revealed the presence of several benzophenone *C*-glucosyl compounds, including 3- β -D-glucopyranosyliriflophenone and 3- β -D-glucopyranosylmaclurin (Kokotkiewicz *et al.*, 2013; Malherbe *et al.*, 2014; Chapter 3). The major benzophenone glycoside present in hot water extracts of *C. genistoides* has been tentatively identified as an iriflophenone di-*O,C*-hexoside thus far (Chapter 3). A compound with similar mass spectrometric properties has also been observed in extracts of another *Cyclopia* species, *C. subternata* (De Beer *et al.*, 2012), albeit at lower concentrations.

In the present paper the isolation and structural elucidation of this benzophenone glucoside, identified as 3- β -D-glucopyranosyl-4- β -D-glucopyranosyloxyiriflophenone (**1**), is described. During the isolation process, small quantities of the known glucopyranosylbenzophenone 3- β -D-glucopyranosylmaclurin (**2**) was also obtained. These compounds were isolated from the aerial parts of *C. genistoides* using solid-phase extraction (SPE) for extract enrichment, followed by purification by semipreparative liquid chromatography (LC). The ability of **1** and **2** to inhibit mammalian α -glucosidase was assessed and compared to that of 3- β -D-glucopyranosyliriflophenone. Included in the α -glucosidase assay was the benzophenone aglucone, maclurin, with acarbose employed as positive control. To date, the α -glucosidase inhibitory activities of **1** and **2** as *C*- and *O*-glucosylated polyhydroxybenzophenones have not been assessed. In vitro tests in several cell models were conducted to investigate the ability of **1** and 3- β -D-glucopyranosyliriflophenone to increase glucose uptake in vitro.



Compound 1. R¹ = β -D-glucopyranosyl, R² = β -D-glucopyranosyloxy, R³ = H

Compound 2. R¹ = β -D-glucopyranosyl, R² = R³ = OH

3- β -D-glucopyranosyliriflophenone. R¹ = β -D-glucopyranosyl, R² = OH, R³ = H

Maclurin. R¹ = H, R² = R³ = OH

2. MATERIALS AND METHODS

2.1. General Experimental Procedures

NMR spectra were recorded on a Varian Unity Inova 600 NMR spectrometer with a ^1H frequency of 600 MHz and a ^{13}C frequency of 150 MHz using a 5 mm inverse detection PFG probe. The chemical shift frequencies are indicated on the δ scale. ^1H and ^{13}C NMR spectra were referenced to the residual DMSO- d_6 peak at δ 2.5 and 39.5, respectively. The spectra in acetone- d_6 have the residual acetone peaks referenced at δ 2.05 for ^1H NMR and at δ 29.84 for the ^{13}C NMR spectra. The spectra were recorded using the standard VnmrJ instrument software and processed and expanded further using the Mestrenova 9.0 software package. HRESIMS analyses were conducted on an Acquity UPLC system, fitted with a photodiode-array detector, and coupled to a Synapt G2 Q-TOF mass spectrometer equipped with an electrospray ionisation source (Waters, Milford, MA, USA). UV spectra were recorded online. Chromatographic conditions and MS parameters were as described in Chapter 3. Semipreparative LC was performed on a LaChrom HPLC system (Merck Hitachi, Hitachi High Technologies, Japan) comprising of a quaternary pump, autosampler, variable-wavelength detector and diode-array detector, and fitted with a Phenomenex Gemini C_{18} column (5 μm , 110 \AA , 150 \times 10 mm) (Phenomenex, Torrance, CA, USA). The column was protected by a guard column of the same stationary phase (10 \times 10 mm) and a high-pressure semipreparative in-line filter (IDEX Health & Science, Oak Harbor, WA, USA). Column temperature was maintained at 30 $^\circ\text{C}$ using an external HPLC column oven (LKB Bromma, Sweden). Gas chromatography was performed on an Agilent GC-MS instrument (Agilent 6890N GC and Agilent 5975 MSD, Agilent Technologies, Palo Alto, CA, USA) fitted with a 30 m Zebron ZB-SemiVolatiles column with 0.25 mm inner diameter and 0.25 μm film thickness (Phenomenex). The GC chromatograms and mass spectra were evaluated using Agilent MSD ChemStation (version D.02.00.237) software.

2.2. Plant Material

The leaves and fine stems from a selection of *Cyclopia genistoides* plants (Overberg type) were harvested from a commercial plantation situated near Pearly Beach (Western Cape, South Africa; GPS coor. -34.702, 19.618). The plant material was dried without delay in a cross-flow drying tunnel at 40 $^\circ\text{C}$ for 16 h to a moisture content less than 10%, and pulverised using a Retsch rotary mill (1.0 mm sieve; Retsch GmbH, Haan, Germany).

2.3. Extraction and Isolation

Plant material (420 g) was extracted with hot water (4.2 L, 93 $^\circ\text{C}$) for 30 min using a ratio of 1:10 (m.v $^{-1}$). The crude extract was filtered through Whatman #4 filter paper, frozen and freeze-dried using a VirTis Advantage Plus freeze-drier (SP Scientific, Warminster, PA, USA). The freeze-dried hot water extract (126.5 g) comprised of 6.31% of **1** and 0.53% of **2**.

Enrichment of the crude extract in terms of **1** and **2** was performed using C_{18} solid-phase extraction (Discovery DSC-18; 10 g.60 mL $^{-1}$; Sigma-Aldrich). The cartridge was conditioned sequentially with MeOH and deionised water (60 mL). A solution of freeze-dried extract (300 mg reconstituted in 50 mL of deionised water) was applied to the cartridge, followed by flushing with deionised water (100 mL). The target analytes were eluted with 5% aqueous MeOH (300 mL). This process was repeated 48 times with new cartridges (14.4 g of freeze-dried extract loaded), and the eluants were pooled, vacuum-evaporated, and freeze-dried, yielding *ca.* 1.2 g enriched fraction. The enriched fraction comprised of 56.5% of **1** and 4.8% of **2**. The average recovery of target analytes after SPE was 75%.

The enriched fraction was reconstituted in deionised water (*ca.* 6 mg.mL $^{-1}$), filtered, and subjected to semipreparative LC (MeCN–2% aqueous HOAc, 4:96, v.v $^{-1}$) using a flow rate of 4.8 mL.min $^{-1}$. Aliquots (400 μL) of the reconstituted, enriched fraction were injected repeatedly, equaling 880 mg. The fractions containing **1** and **2** were collected based on retention times

using a Gilson FC203B fraction collector (Gilson, Middleton, WI, USA) and pooled, and the organic solvent was evaporated under vacuum. The remaining aqueous solutions were filtered, frozen, and freeze-dried, yielding 370 mg of **1** (purity > 99% by HRESIMS; total yield of 74% from the enriched extract) and 30 mg of **2** (purity 95% by HRESIMS; total yield of 71% from the enriched extract).

2.4. Structural Elucidation

3- β -D-Glucopyranosyl-4- β -D-glucopyranosyloxiriflophenone (1): white amorphous powder; UV λ_{\max} online: 234, 294 nm; ^1H NMR 600 MHz (DMSO- d_6 , 298 K) δ 7.61 (2H, d, $J = 8.6$ Hz, H-2',6'), 6.78 (2H, d, $J = 8.6$ Hz, H-3',5'), 6.24 (1H, s, H-5), 4.73 (1H, d, $J = 7.8$ Hz, H-1'''), 4.66 (1H, d, $J = 9.8$ Hz, H-1''), 3.6 (3H, m, H-6'', 2 x H-6'''), 3.46 (2H, m, H-2'', H-6''), 3.25 (3H, m, H-3'', H-4'', H-5''), 3.18 (2H, m, H-3''', H-5'''), 3.08 (1H, t, $J = 9.2$ Hz, H-4'''), 2.88 (1H, t, $J = 8.4$ Hz, H-2''); ^{13}C NMR 150 MHz (DMSO- d_6 , 298 K) δ 193.1 (C, C=O), 161.8 (C, C-1'), 157.7 (C, C-1), 155.2 (C, C-2), 155.2 (C, C-4), 131.8 (CH, C-3', 5'), 130.2 (CH, C-4'), 114.8 (CH, C-2', 6'), 110.0 (C, C-6), 106.2 (C, C-3), 100.5 (CH, C-1'''), 94.8 (CH, C-5), 81.0 (CH, C-3''), 78.0 (CH, C-5''), 77.1 (CH, C-5'''), 76.6 (CH, C-3'''), 74.9 (CH, C-1''), 73.2 (CH, C-2'''), 72.3 (CH, C-2''), 69.3 (CH, C-4''), 69.3 (CH, C-4'''), 60.5 (CH₂, C-6'''), 60.1 (CH₂, C-6''); HRESIMS m/z 569.1503 [M-H]⁻ (calcd for C₂₅H₂₉O₁₅, 596.1506); ESIMS [m/z (%): 569 (100) [M-H]⁻, 1139 (20) [2M-H]⁻; HRESIMS m/z 571.1661 [M+H]⁺ (calcd for C₂₅H₃₁O₁₅, 571.1663); ESIMS [m/z (%): 1141 (10) [2M+H]⁺, 571 (60) [M+H]⁺, 409 (100) [M+H-162]⁺, 391 (60) [M+H-162-H₂O]⁺, 373 (10) [M+H-162-2 x H₂O]⁺, 355 (10) [M + H-162-3 x H₂O]⁺, 313 (10) [M+H-258]⁺, 289 (15) [M+H-162-120]⁺.

Acid Hydrolysis of 1. Aliquots of a solution of **1** (105 mg in 70 mL of 1.1 M HCl) were heated in 5 mL glass Reacti-vials at 60 °C in a Stuart heating block (Bibby Scientific Limited, Stone, UK) for 24 h. The hydrolysis reaction was monitored using HPLC-DAD (86% degradation at $t = 24$ h). The hydrolysed mixture was cooled to room temperature and adjusted to pH ~ 4 using 1.1 M NaHCO₃. One half of this hydrolysed mixture was vacuum-evaporated and subjected to semipreparative LC (MeCN-2% aqueous HOAc, 8:92, v.v⁻¹) to obtain intact **1** and iriflophenone-hexosyl. The fraction containing iriflophenone-hexosyl was collected based on retention time, pooled, vacuum-evaporated, and freeze-dried, followed by NMR analysis.

^1H NMR and ^{13}C NMR Data for 3- β -D-Glucopyranosyliriflophenone (Hydrolysed Product of 1): ^1H NMR 600 MHz (acetone- d_6 , 298 K) δ 7.64 (2H, d, $J = 8.6$ Hz, H-2', 6'), 6.85 (2H, d, $J = 8.6$ Hz, H-3', 5'), 5.99 (1H, s, H-5), 4.92 (1H, d, $J = 9.8$ Hz, H-1''), 3.85 (2H, d, $J = 3.1$ Hz, 2 x H-6''), 3.69 (H, t, $J = 9.2$ Hz, H-4''), 3.63 (H, t, $J = 9.2$ Hz, H-2''), 3.57 (H, t, $J = 8.9$ Hz, H-3''), 3.49 (H, m, H-5''); ^{13}C NMR 150 MHz (acetone- d_6 , 298 K) δ 197.8 (C=O), 162.6 (C-4'), 161.9 (C-4), 161.4 (C-2), 160.5 (C-6), 133.3 (C-1''), 132.5 (C-2', 6'), 115.3 (C-3', 5'), 106.6 (C-1), 104.7 (C-3), 96.9 (C-5), 82.1 (C-5''), 79.3 (C-3''), 76.6 (C-1''), 74.6 (C-4''), 70.6 (C-2''), 61.7 (C-6'').

Identification of the O-linked Hexose Residue in the Hydrolysed Product. The other half of the hydrolysed product was partially evaporated under vacuum, and a small volume of the concentrated liquid was removed for an enzyme robot assay. This assay was conducted on a Thermo Scientific Arena 20XT random access chemistry analyser (Thermo Fisher Scientific, Oy, Finland) with the use of an Enytec Fluid D-glucose no. 5140 enzyme reagent kit (AEC-Amersham, Kayalami, South Africa) for the identification of glucose according to the manufacturer's instructions.

The remaining sample volume was freeze-dried, derivatised with bis(trimethylsilyl)trifluoroacetamide (BSTFA) using the procedure described by Roessner *et al.* (2000), and subjected to GC-MS analysis. D-Glucose and D-galactose standards (Sigma-Aldrich) were also derivatised prior to analysis. Sample volumes of 1 μL were injected with a split ratio of 1:10. The injection temperature was 280 $^{\circ}\text{C}$, the interface set to 280 $^{\circ}\text{C}$ and the ion source adjusted to 240 $^{\circ}\text{C}$. The carrier gas was helium set at a constant flow rate of 1.0 $\text{mL}\cdot\text{min}^{-1}$. The temperature program comprised of a 6 $^{\circ}\text{C}$ oven temperature ramp from 70 to 76 $^{\circ}\text{C}$ within one min, followed by a 32 $^{\circ}\text{C}\cdot\text{min}^{-1}$ ramp to 300 $^{\circ}\text{C}$ and a final 5 min heating at 300 $^{\circ}\text{C}$. Mass spectra were recorded over an m/z scanning range of 40 to 650. Electron energy was 70 eV and solvent delay 8 min.

3- β -D-Glucopyranosylmaclurin (2): Light yellow amorphous powder; UV λ_{max} online: 236, 290 (sh), 318 nm; ^1H NMR 600 MHz (DMSO- d_6 , 298 K) δ 7.15 (1H, d, $J = 1.93$ Hz, H-2'), 7.06 (1H, dd, $J = 1.93, 8.24$ Hz, H-6'), 6.74 (1H, d, $J = 8.24$ Hz, H-5'), 5.94 (1H, s, H-5), 4.60 (1H, d, $J = 9.77$ Hz, H-1''), 3.61 (1H, d, 10.96 Hz, H-6a), 3.51 (2H, m, H-2'', 6''), 3.20 (3H, H-3'', 4'', 5''); ^{13}C NMR 150 MHz (DMSO- d_6 , 298 K) δ 194.6 (C, C=O), 158.4 (C, C-4), 156.7 (C, C-6), 156.3 (C, C-2), 150.0 (C, C-4'), 144.6 (C, C-3'), 131.0 (C, C-1'), 122.3 (CH, C-6'), 116.2 (CH, C-2'), 114.7 (CH, C-5'), 107.6 (C, C-3), 103.6 (C, C-1), 94.8 (CH, C-5), 81.1 (CH, C-5''), 78.3 (CH, C-3''), 74.8 (CH, C-1''), 72.1 (CH, C-4''), 69.6 (CH, C-2''), 60.4 (CH₂, C-6''); HRESIMS m/z 423.0933 [M-H]⁻ (calcd for C₁₉H₁₉O₁₁, 423.0927); ESIMS [m/z (%): 1271 (5) [3M-H]⁻, 847 (70) [2M-H]⁻, 423 (100) [M-H]⁻, 303 (20) [M-H-120]⁻; HRESIMS m/z 425.1075 [M+H]⁺ (calcd for C₁₉H₂₁O₁₁, 425.1084); ESIMS [m/z (%): 425 (80) [M+H]⁺, 407 (100) [M+H-H₂O]⁺, 389 (10) [M+H-2 \times H₂O]⁺, 371 (10) [M+H-3 \times H₂O]⁺, 341 (10) [M+H-84]⁺, 329 (15) [M+H-96]⁺, 305 (20) [M+H-120]⁺, 287 (5) [M+H-120-H₂O]⁺.

2.5. Determination of α -Glucosidase Inhibitory Activity

A method for the determination of α -glucosidase inhibitory effects (Azuma *et al.*, 2011) was adapted for use on a BioTek SynergyHT microplate reader with dispenser (BioTek Instruments, Winooski, VT, USA). A mixture containing α -glucosidase was extracted from rat intestinal acetone powder (Sigma-Aldrich) by suspending *ca.* 350 mg of powder in 10 mL of cold KH₂PO₄ buffer (200 mM KH₂PO₄, pH 6.8 with KOH) followed by repeated sonication on ice (sonication sequence repeated 12 times: 30 s sonication with 25% amplitude, 1 min rest) using a model VCX600 high-intensity ultrasonic processor with 3 mm stepped microtip (Sonics & Materials Inc., Newton, CT, USA). The crude mixture was centrifuged at 10000 g for 30 min at 4 $^{\circ}\text{C}$ in a Hettich Universal 320R refrigerated centrifuge (Hettich Holding GmbH & Co. oHG, Kirchlingern, Germany), and the supernatant was retrieved and filtered using 0.45 μm pore size, 33 mm Millex HV PVDF filter membranes (Merck Millipore). The supernatant was used as enzyme mixture after dilution to the standardised concentration based on activity testing.

Activity determination of the enzyme mixture was performed daily prior to each set of experiments, using the same procedure as for the inhibition assays, but with H₂O as sample controls and varying dilutions of the enzyme mixture. Fluorescence measurements were used to determine the correct concentration for optimal enzyme activity, *ca.* 15 to 20 $\text{mg}\cdot\text{mL}^{-1}$ of the original powder estimated as an FL-value of 50 000 (λ_{EX} : 360 nm; λ_{EM} : 460 nm), 20 min after addition of the substrate.

The inhibitory activities of **1**, **2**, 3- β -D-glucopyranosylriflophenone (Fluka, Sigma-Aldrich, St. Louis, MO, USA) and maclurin (Sigma-Aldrich) were assessed at three concentration levels ranging between 50 and 400 μM . Acarbose (Sigma-Aldrich), a known inhibitor of mammalian α -glucosidase, was used as positive control at 65 μM . The following test procedure was employed: 20 μL of the assay control (H₂O), positive control or target analyte at selected concentration was added to 125 μL of a 200 mM KH₂PO₄ buffer (pH 6.8) and 65 μL of the chosen enzyme dilution in 96-well black, flat-bottom microplates with clear bottom (Greiner Bio-One GmbH, Rainbach im Mühlkreis, Austria). The mixture was

preincubated at 37 °C for 15 min, followed by the addition of 40 µL of the substrate, 1.2 mM 7- α -D-glucopyranosyloxy-4-methylumbelliferone, by dispenser. Fluorescence (λ_{EX} : 360 nm; λ_{EM} : 460 nm) was monitored over 30 min and the net fluorescence (Net FL) and % enzyme activity were calculated using the following formulas:

$$\text{Net FL} = \text{Fluorescence}_{30 \text{ min}} - \text{Fluorescence}_{0 \text{ min}}$$

$$\% \text{ enzyme activity} = 100 \times \frac{\text{Net FL}_{\text{sample}}}{\text{Net FL}_{\text{assay control}}}$$

Statistical analysis was performed with GraphPad Prism version 5.00 for Windows (GraphPad Software, San Diego California USA, www.graphpad.com) using one way ANOVA with Tukey's multiple comparison post-hoc test to determine significant differences between values at the 95% confidence level ($p < 0.05$).

2.6. Assessment of Cellular 2-deoxy-[^3H]-D-glucose (^3H -2-DOG) Uptake

To estimate in vitro glucose uptake activity, cellular ^3H -2-DOG uptake was assessed by liquid scintillation counting, using the method described by Mazibuko (2013). Briefly, L6 myoblasts (2.5×10^4 cells.mL $^{-1}$) and 3T3-L1 fibroblasts (2.0×10^4 cells.mL $^{-1}$) were seeded into 24-well plates in Dulbecco's Modified Eagle's medium (DMEM) supplemented with 10% fetal or normal calf serum, respectively. C3A hepatocytes were seeded at 5.5×10^4 cells.mL $^{-1}$ in Eagle's minimal essential medium (EMEM) supplemented with 10% fetal calf serum. All cells were cultured at 37 °C in humidified air with 5% CO $_2$. Cell culture media DMEM, EMEM, fetal, and normal calf serum were obtained from (Lonza, Walkersville, MD, USA). The L6 myoblasts and 3T3-L1 fibroblasts were differentiated into myotubule-forming myocytes and adipocytes, respectively, while the C3A hepatocytes were used as semiconfluent cultures. For the ^3H -2-DOG uptake experiments, cells (1 h for L6 myocytes, and 3 h for 3T3-L1 adipocytes and C3A hepatocytes) were exposed to **1** and 3- β -D-glucopyranosylriflophenone at concentrations ranging from 0.001 to 100 µM. Compounds were dissolved in DMSO and diluted with Krebs-Ringer bicarbonate HEPES buffer (KRBH) containing 8 mM glucose (final DMSO concentrations < 0.004%). For glucose uptake determination, cells were pulse-labeled for 15 min with 0.5 µCi.mL $^{-1}$ ^3H -2-DOG (American Radiolabeled Chemicals, Inc., St. Louis, MO, USA) in glucose- and serum-free KRBH containing **1** and 3- β -D-glucopyranosylriflophenone at the relevant concentrations. Insulin and metformin (1,1-dimethylbiguanide hydrochloride) (Sigma-Aldrich) both at 1 µM were included as positive and drug reference controls, respectively. The amount of ^3H -2-DOG taken up by cells was measured using a liquid scintillation counter (2200CA Tricarb Series, Packard Instrument Company, Downers Grove, IL, USA) and the activity calculated as fmol (^3H -2-DOG).mg protein $^{-1}$. Statistical analysis was performed with GraphPad Prism version 5.00 for Windows using one way ANOVA with Dunnett's multiple comparison post hoc test to determine significant differences between values at the 95% confidence level ($p < 0.05$).

3. RESULTS AND DISCUSSION

3.1. Identification of Compounds 1 and 2

Compound **1** was obtained as a white, amorphous powder. Its molecular formula was established as $C_{25}H_{30}O_{15}$ from the analyses of its HRESIMS and ^{13}C NMR data. Initial LC-ESIMSMS analyses of this compound in a *C. genistoides* sample matrix (Chapter 3) had pointed to an iriflophenone di-*O,C*-hexoside derivative. The elucidation of the structure of **1** and, in particular, the identification of the hexoside moieties and their point of attachment to the aglycone, were done via 1D and 2D NMR experiments. The relative configurations of the glycoside units can normally be determined by a 1D/2D NOESY NMR experiment. However, NMR spectroscopic data for **1** proved inconclusive for unambiguous identification of the individual glycoside units, due to overlapping proton resonances. Since the NMR spectra of **1** closely resembled those of 3- β -D-glucopyranosyliriflophenone, it was essential to first selectively hydrolyse and identify the terminal O-linked sugar moiety, followed by comparison of the resulting iriflophenone-hexosyl to that of a commercial 3- β -D-glucopyranosyliriflophenone standard, also present in *C. genistoides* (Kokotkiewicz *et al.*, 2012).

The terminal O-linked hexoside moiety was identified as D-glucose by enzymatic hydrolysis and GC-MS analysis. The resulting iriflophenone-hexosyl was purified and its 1H and ^{13}C NMR data matched those of 3- β -D-glucopyranosyliriflophenone. Having identified the β -D-glucopyranosyl constituent units, the rest of the molecule and the point of attachment of the β -D-glucopyranosyloxy unit were defined by additional 1D NOESY, COSY, HSQC and HMBC NMR experiments.

The aromatic region between 6.0-8.5 ppm of the 1H NMR spectra showed two *o*-coupled doublets and a singlet, δ 7.61 (2H, d, $J = 8.6$ Hz), 6.78 (2H, d, $J = 8.6$ Hz), 6.24 (1H, s), reminiscent of an AA'BB' aromatic spin system with an uncoupled singlet on a separate aromatic ring and supported by the presence of aromatic carbons in the ^{13}C NMR spectra of **1**. The 1H NMR spectra also showed the resonances of two β -coupled (~ 8 Hz anomeric coupling constant) glucoside units in the characteristic 2.5-5.0 ppm region (Jay, 1993). The presence of a single carbon at δ 193.1 in addition to the 12 aromatic carbons in the ^{13}C NMR spectrum were reminiscent of a benzophenone aglycone unit (Jay, 1993). The anomeric protons of the two glucopyranosyl moieties at δ 4.73 (1H, d, $J = 7.8$ Hz) and 4.66 (1H, d, $J = 9.8$ Hz) were irradiated selectively utilising a 1D NOESY experiment to determine their position of attachment and other proton resonances of the individual glucopyranosyloxy and glucopyranosyl units. The anomeric proton of the glucopyranosyl residue at δ 4.73 (1H, d, $J = 7.8$ Hz, H-1''') displayed a strong NOE association with the H-5 singlet at δ 6.24. This assigned the O-linked glucosyl unit to C-4 of the benzophenone A-ring. A weak NOE association of H-1''' with H-4'' (δ 3.24) of the neighboring glucosyl moiety indicated the close proximity of the glucosyl entities.

An NOE association was also observed between the three axial H-1''', H-3''', and H-5''' protons (Figure 1), affirming the glucose configuration of the O-linked sugar unit. The nature of the C-linked sugar to the aglycone was confirmed by comparison of the hydrolytic products to the NMR spectra of the commercial 3- β -D-glucopyranosyliriflophenone standard.

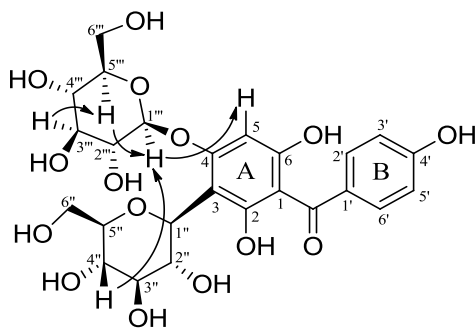


Figure 1 Relevant NOE associations in **1**.

A COSY experiment confirmed the AA'BB' aromatic spin system of the B-ring and the connectivity of some of the protons on the individual glucosyl moieties. This includes only the protons that are sufficiently resolved to be assigned by the COSY experiment and did not overlap with the glucosyl proton resonances.

The HSQC NMR experiment was used to assign all the directly bonded protons ($^1J_{\text{HC}}$) to their respective carbons. All the carbons were resolved successfully by an HMBC experiment showing the long range ($^2J_{\text{HC}}$, $^3J_{\text{HC}}$) connectivity between protons and carbons [up to four bonds ($^4J_{\text{HC}}$) in some cases]. Those structurally significant HMBC correlations are shown in Figure 2, enabling the assignment of the unprotonated carbons in the molecule. Compound **1** was thus identified as 3- β -D-glucopyranosyl-4- β -D-glucopyranosyloxyiriflophenone.

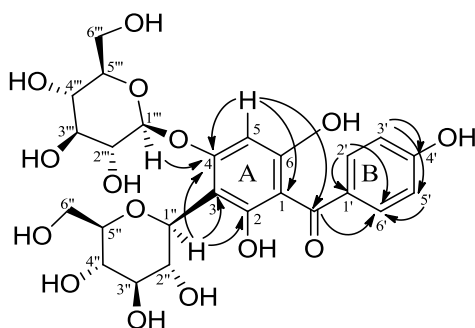


Figure 2 Relevant long range HMBC correlations in **1**.

Compound **2** was obtained as a light yellow, amorphous powder. Accurate measurement of the protonated and deprotonated molecule ions in the positive and negative HRESIMS data, respectively, in conjunction with ^{13}C NMR data, allowed a molecular formula of $\text{C}_{19}\text{H}_{20}\text{O}_{11}$ to be assigned to **2**. The structure of **2** was confirmed as 3- β -D-glucopyranosylmaclurin by comparison of its observed and reported ^1H NMR and ^{13}C NMR spectroscopic data (Tanaka *et al.*, 1984; Kokotkiewicz *et al.*, 2013).

3.2. α -Glucosidase Inhibitory Activity of Benzophenones

Both benzophenone derivatives **1** and **2**, together with the reference compounds, showed inhibitory activity against mammalian α -glucosidase at various concentrations with all values significantly differing ($p < 0.05$) from all other values. The observed inhibitory activities were both concentration- and compound-specific (Figure 3), showing a clear dose-response.

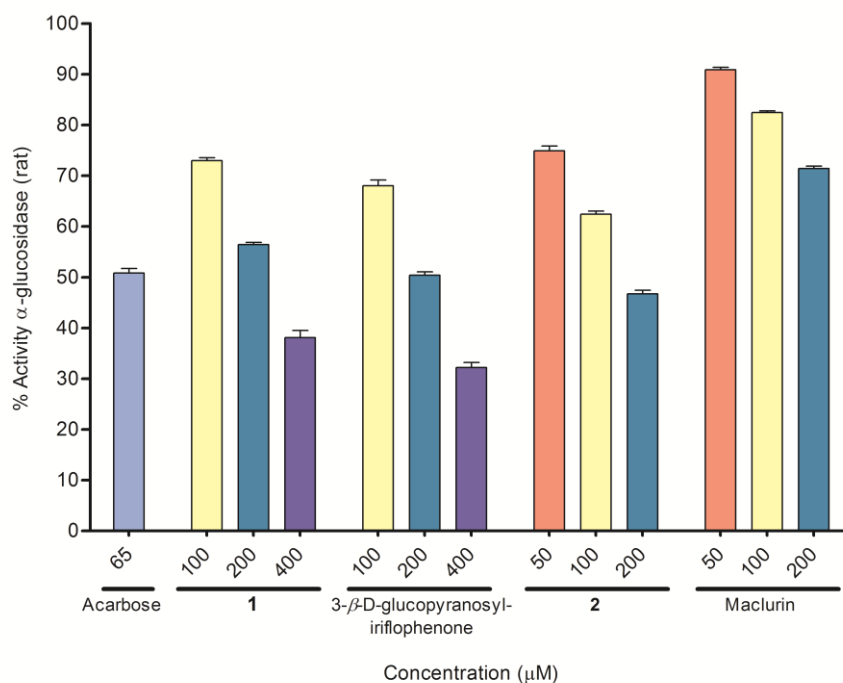


Figure 3 The percentage activity of rat α -glucosidase challenged with various concentrations of **1**, 3- β -D-glucopyranosyliriflophenone, **2**, and maclurin.

The activities of the benzophenones could thus be compared at equimolar concentration levels, which gave insight into possible structure-activity relationships. Compound **2** was the most active inhibitor, followed by 3- β -D-glucopyranosyliriflophenone and **1**, whilst maclurin showed the weakest inhibitory activity. It appears that C-monoglucosides tend to be more effective inhibitors than their corresponding aglucones; that is, **2** is significantly more active than maclurin ($p < 0.05$). This has also been observed previously for 3- β -D-glucopyranosyliriflophenone and its aglucone, iriflophenone (Feng *et al.*, 2011). Furthermore, the higher activity of **2** compared to that of 3- β -D-glucopyranosyliriflophenone was attributed to the additional 3'-hydroxy group of **2**. Previous studies on hydroxybenzophenones (Hu *et al.*, 2011) and hydroxyxanthenes (Liu *et al.*, 2006) have shown that increases in the number of phenolic hydroxy groups on the basic diphenyl methanone and dibenzo- γ -pyrone structures lead to significant increases in α -glucosidase inhibitory activities. Moreover, for hydroxyflavones it has been shown that a 3'-hydroxy group in particular leads to increased inhibitory activity (Li *et al.*, 2009). The presence of an additional glucopyranosyloxy moiety at C-4 on the diphenyl methanone structure of **1** significantly ($p < 0.05$) lowered α -glucosidase inhibitory activity compared to 3- β -D-glucopyranosyliriflophenone. A similar decrease in activity due to an additional glucopyranosyl moiety has also been reported for 3,5-di- β -D-glucopyranosyliriflophenone compared to 3- β -D-glucopyranosyliriflophenone (Feng *et al.*, 2011).

3.3. The Ability of Benzophenones to Increase Glucose Uptake In Vitro

The effect of **1** and 3- β -D-glucopyranosyliriflophenone on in vitro glucose uptake in L6 myocytes demonstrated marginal, but not significant, increases in glucose uptake relative to the vehicle control at concentrations of 10 μ M of **1** (*ca.* 22% increase; Figure 4A) and 100 μ M of 3- β -D-glucopyranosyliriflophenone (*ca.* 27% increase; Figure 4B). Similar marginal effects on glucose uptake were observed in 3T3-L1 adipocytes (Figure 4C and D) and in C3A hepatocytes (data not shown). It was anticipated that the isolated benzophenone glucoside (**1**) and 3- β -D-glucopyranosyliriflophenone could increase in vitro glucose uptake activity by activating the cellular energy regulator AMPK, as demonstrated for the latter compound

(Zhang *et al.*, 2011, 2013) in mature 3T3-L1 adipocytes and diabetic KK-A^y mice. The assessed compounds were, however, less effective at increasing cellular glucose uptake than the reference pharmacological agent metformin, mechanistically known to be an activator of AMPK (Zhou *et al.*, 2001).

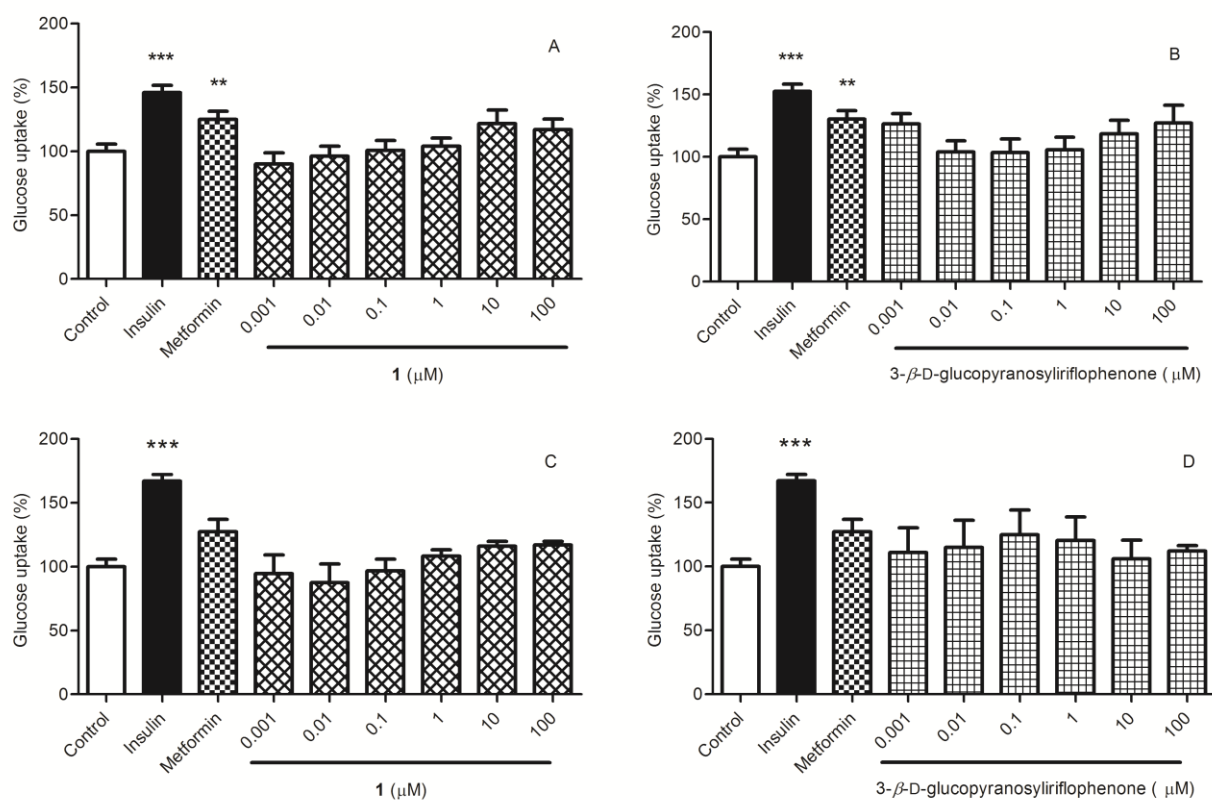


Figure 4 ³H-2-DOG uptake in L6 myocytes exposed to (A) **1** and (B) 3-β-D-glucopyranosyliriflophenone and 3T3-L1 adipocytes exposed to (C) **1** and (D) 3-β-D-glucopyranosyliriflophenone. Insulin (positive control) and metformin (reference drug control) were included at concentrations of 1 μM. Mean activity is expressed relative to the vehicle control at 100% ± standard error of the means. Three independent experiments were performed each with three technical repeats. ** *p* < 0.01; *** *p* < 0.001.

4. CONCLUSIONS

In this study, the presence of 3-β-D-glucopyranosyl-4-β-D-glucopyranosyloxyiriflophenone, a major and novel benzophenone was established for the first time in *C. genistoides* and also in the genus *Cyclopia*. Its potential as a major bioactive compound of *C. genistoides* was demonstrated in terms of α-glucosidase inhibitory activity and the ability to increase glucose uptake in vitro. Another benzophenone, 3-β-D-glucopyranosylmaclurin, present in minor quantities, was a more active inhibitor of α-glucosidase.

REFERENCES

- Azuma, T., Kayano, S., Matsumura Y., Konishi, Y., Tanaka, Y. & Kikuzaki, H. (2011). Antimutagenic and α -glucosidase inhibitory effects of constituents from *Kaempferia parviflora*. *Food Chemistry*, **125**, 471-475.
- Boath, A.S., Stewart, D. & McDougall, G.J. (2012). Berry components inhibit α -glucosidase *in vitro*: Synergies between acarbose and polyphenols from black currant and rowanberry *Food Chemistry*, **135**, 929-936.
- De Beer, D., Schulze, A.E., Joubert, E., De Villiers, A., Malherbe, C.J. & Stander, M.A. (2012). Food ingredient extracts of *Cyclopia subternata* (honeybush): variation in phenolic composition and antioxidant capacity. *Molecules*, **17**, 14602-14624.
- Feng, J., Yang, X.-W. & Wang, R.-F. (2011). Bio-assay guided isolation and identification of α -glucosidase inhibitors from the leaves of *Aquilaria sinensis*. *Phytochemistry*, **72**, 242-247.
- Hollander, P. (2007). Anti-diabetes and anti-obesity medications: effects on weight in people with diabetes. *Diabetes Spectrum*, **20**, 159-165.
- Hu, X., Xiao, Y., Wu, J. & Ma, L. (2011). Evaluation of polyhydroxybenzophenones as α -glucosidase inhibitors. *Archiv der Pharmazie – Chemistry in Life Sciences*, **2**, 71-77.
- International Diabetes Federation (2013). IDF Diabetes Atlas, 6th edition. International Diabetes Federation: Brussels, Belgium (accessible at <http://www.idf.org/diabetesatlas>).
- Jay, M. (1993). In *The Flavonoids: Advances in Research since 1986*; Harborne, J.B., Ed.; Chapman and Hall: London, p 85.
- Joubert, E., Joubert, M.E., Bester, C., De Beer, D. & De Lange, J.H. (2011). Honeybush (*Cyclopia* spp.): From local cottage industry to global markets – the catalytic and supporting role of research. *South African Journal of Botany*, **77**, 887-907.
- Kokotkiewicz, A., Luczkiewicz, M., Sowinski, P., Glod, D., Gorynski, K. & Bucinski, A. (2012). Isolation and structure elucidation of phenolic compounds from *Cyclopia subternata* Vogel (honeybush) intact plant and *in vitro* cultures. *Food Chemistry*, **133**, 1373-1382.
- Kokotkiewicz, A., Luczkiewicz, M., Pawlowska, J., Luczkiewicz, P., Sowinski, P., Witkowski, J., Bryl, E. & Bucinski, A. (2013). Isolation of xanthone and benzophenone derivatives from *Cyclopia genistoides* (L.) Vent. (honeybush) and their pro-apoptotic activity on synoviocytes from patients with rheumatoid arthritis. *Fitoterapia*, **90**, 199-208.
- Li, H., Song, F., Xing, J., Tsao, R., Liu, Z. & Liu, S. (2009). Screening and structural characterization of α -glucosidase inhibitors from hawthorn leaf flavonoids extract by ultrafiltration LC-DAD-MSⁿ and SORI-CID FTICR MS. *Journal of the American Society for Mass Spectrometry*, **20**, 1496-1503.
- Liu, Y., Zou, L., Ma, L., Chen, W.-H., Wang, B. & Xu, Z.-L. (2006). Synthesis and pharmacological activities of xanthone derivatives as α -glucosidase inhibitors. *Bioorganic and Medicinal Chemistry*, **14**, 5683-5690.
- Liu, Q., Guo, T., Li, W., Li, D. & Feng, Z. (2012). Synthesis and evaluation of benzophenone *O*-glycosides as α -glucosidase inhibitors. *Archiv der Pharmazie – Chemistry in Life Sciences*, **345**, 771-783.
- Malherbe, C.J., Willenburg, E., De Beer, D., Bonnet, S.L., Van der Westhuizen, J.H. & Joubert, E. (2014). Iriflophenone-3-*C*-glucoside from *Cyclopia genistoides*: Isolation and quantitative comparison of antioxidant capacity with mangiferin and isomangiferin using on-line HPLC antioxidant assays. *Journal of Chromatography B*, **951–952**, 164-171.
- Mathers, C.D. & Loncar, D. (2006). Projections of global mortality and burden of disease from 2002 to 2030. *PLoS Medicine*, **3**, 2011-2030.

- Mazibuko, M. E. (2013). In vitro and in vivo effect of *Aspalathus linearis* and its major polyphenols on carbohydrate and lipid metabolism in insulin resistant models. Ph.D. Thesis, University of Zululand, KwaDlangezwa, South Africa.
- Park, H., Hwang, K.Y., Oh, K.H., Kim, Y.H., Lee, J.Y. & Kim, K. (2008). Discovery of novel α -glucosidase inhibitors based on the virtual screening with the homology-modeled protein structure. *Bioorganic and Medicinal Chemistry*, **16**, 284-292.
- Roessner, U., Wagner, C., Kopka, J., Trethewey, R. N. & Willmitzer, L. (2000). Simultaneous analysis of metabolites in potato tuber by gas chromatography-mass spectrometry. *The Plant Journal*, **23**, 131-142.
- Shaw, J.E., Sicree, R.A. & Zimmet, P.Z. (2010). Global estimates of the prevalence of diabetes for 2010 and 2030. *Diabetes Research and Clinical Practice*, **87**, 4-14.
- Tanaka, T., Sueyasu, T., Nonaka, G.-I. & Nishioka, I. (1984). Tannins and related compounds. XXI. Isolation and characterization of galloyl and *p*-hydroxybenzoyl esters of benzophenone and xanthone C-glucosides from *Mangifera indica* L. *Chemical and Pharmaceutical Bulletin*, **32**, 2676-2686.
- Vyas, A., Syeda, K., Ahmad, A., Padhye, S. & Sarkar, F.H. (2012). Perspectives on medicinal properties of mangiferin. *Mini-Reviews in Medicinal Chemistry*, **12**, 412-425.
- Xiao, J., Kai, G., Yamamoto, K. & Chen, X. (2013). Advance in dietary polyphenols as α -glucosidases inhibitors: a review on structure-activity relationship aspect. *Critical Reviews in Food Science and Nutrition*, **53**, 818-836.
- Zhang, Y., Qian, Q., Ge, D., Li, Y., Wang, X., Chen, Q., Gao, X. & Wang, T. (2011). Identification of benzophenone C-glucosides from mango tree leaves and their inhibitory effect on triglyceride accumulation in 3T3-L1 adipocytes. *Journal of Agricultural and Food Chemistry*, **59**, 11526-11533.
- Zhang, Y., Liu, X., Han, L., Gao, X., Liu, E. & Wang, T. (2013). Regulation of lipid and glucose homeostasis by mango tree leaf extract is mediated by AMPK and PI3K/AKT signaling pathways. *Food Chemistry*, **141**, 2896-2905.
- Zhou, G., Myers, R., Li, Y., Chen, Y., Shen, X., Fenyk-Melody, J., Wu, M., Ventre, J., Doebber, T., Fujii, N., Musi, N., Hirshman, M.F., Goodyear, L.J. & Moller, D.E. (2001). Role of AMP-activated protein kinase in mechanism of metformin action. *The Journal of Clinical Investigation*, **108**, 1167-1174.

CHAPTER 5

Thermal Degradation Kinetics Modelling of Benzophenones and Xanthonenes during High-Temperature Oxidation of *Cyclopia genistoides* (L.) Vent. Plant Material and the Effect on the Total Antioxidant Capacity of Aqueous Extracts

*** Published**

Beelders, T., De Beer, D. & Joubert, E. (2015). Thermal degradation kinetics modeling of benzophenones and xanthonenes during high-temperature oxidation of *Cyclopia genistoides* (L.) Vent. plant material. *Journal of Agricultural and Food Chemistry*, **63**, 5518-5527.

DECLARATION

With regard to Chapter 5 (pp. 123-145), the nature and scope of my contribution were as follows:

Nature of Contribution	Extent of Contribution (%)
Conducted all experimental work, including high-temperature oxidation of plant material on small scale, quantification by HPLC-DAD, evaluation and validation of kinetic models, and antioxidant assays.	85%
Wrote the entire manuscript, and edited the document in its entirety during the different stages of the publication process.	

The following co-authors have contributed to Chapter 5 (pp. 123-145):

Name	E-mail address	Nature of Contribution	Extent of Contribution (%)
Dr Dalene de Beer (Co-supervisor)	DBeerD@arc.agric.za	Assisted in editing the document in its entirety during the different stages of publication.	5%
Dr Elizabeth Joubert (Supervisor)	JoubertL@arc.agric.za	Conceptualised the study. Assisted in editing the document in its entirety during the different stages of publication.	10%

Signature of candidate: **Declaration with signature in possession of candidate and supervisor*

Date: February 2016

Declaration by co-authors:

The undersigned hereby confirm that

1. the declaration above accurately reflects the nature and extent of the contribution of the candidate and the co-authors to Chapter 5 (pp. 123-145),
2. no other authors contributed to Chapter 5 (pp. 123-145) besides those specified above, and
3. potential conflicts of interest have been revealed to all interested parties and that the necessary arrangements have been made to use the material in Chapter 5 (pp. 123-145) of this dissertation.

Signature*	Institutional Affiliation	Date
Dr Dalene de Beer	Post-Harvest and Wine Technology Division, Agricultural Research Council Infruitec-Nietvoorbij	
Dr Elizabeth Joubert	Post-Harvest and Wine Technology Division, Agricultural Research Council Infruitec-Nietvoorbij; Department of Food Science, Stellenbosch University	

ABSTRACT

Degradation of the major benzophenones, 3- β -D-glucopyranosyl-4- β -D-glucopyranosyloxyiriflophenone and 3- β -D-glucopyranosyliriflophenone, and the major xanthenes, mangiferin and isomangiferin, of *Cyclopia genistoides* followed first-order reaction kinetics during high-temperature oxidation of the plant material at 80 and 90 °C. 3- β -D-Glucopyranosyl-4- β -D-glucopyranosyloxyiriflophenone was shown to be the most thermally stable compound. Isomangiferin was the second most stable compound at 80 °C, while its degradation rate constant was influenced the most by increased temperature. Mangiferin and 3- β -D-glucopyranosyliriflophenone had comparable degradation rate constants at 80 °C. The thermal degradation kinetics model was subsequently evaluated by subjecting different batches of plant material to oxidative conditions (90 °C/16 h). The model accurately predicted the individual contents of three of the compounds in aqueous extracts prepared from oxidised plant material. The impact of benzophenone and xanthone degradation was reflected in the decreased total antioxidant capacity of the aqueous extracts, as determined using the oxygen radical absorbance capacity and DPPH[•] scavenging assays.

1. INTRODUCTION

Cyclopia genistoides (family, Fabaceae; tribe, Podalyriaceae), a fynbos plant indigenous to South Africa, represents a rich source of xanthenes and benzophenones not typically consumed as part of the human diet (Chapter 3). *Cyclopia genistoides* is one of the major cultivated species contributing to the annual production of honeybush tea (Joubert *et al.*, 2011). The glucosylxanthone mangiferin and its regio-isomer isomangiferin represent the major xanthenes present in a hot water honeybush extract. The pharmacological activity of mangiferin is well-documented (as reviewed by Vyas *et al.* 2012), while only the pro-apoptotic (Kokotkiewicz *et al.*, 2013) and antioxidant (Malherbe *et al.*, 2014) activities of isomangiferin have been assessed to date. Most recently, a study by Schulze *et al.* (2015) showed that isomangiferin is also effective in increasing glucose uptake by C2C12 cells. The major benzophenones present in *Cyclopia* extracts include the novel constituent, 3- β -D-glucopyranosyl-4- β -D-glucopyranosyloxyiriflophenone, and 3- β -D-glucopyranosyliriflophenone, while the presence of 3- β -D-glucopyranosylmaclurin in *C. genistoides* has also been demonstrated (Kokotkiewicz *et al.*, 2013; Chapter 4). These benzophenones are gaining in prominence in light of their α -glucosidase inhibitory and glucose-uptake stimulatory activities (Feng *et al.*, 2011; Zhang *et al.*, 2011, 2013; Chapter 4).

The levels of these bio-active compounds in *C. genistoides* are, however, significantly reduced during agroprocessing (Joubert *et al.*, 2008; Chapter 3). Harvested plant material is typically subjected to a high-temperature oxidation process, commonly referred to as “fermentation”, required for the development of the sought-after sensory properties of the herbal tea product (honeybush) (Joubert *et al.*, 2011). The process employed by the honeybush industry briefly entails oxidation of prewetted, cut plant material at elevated temperature in rotary drums, followed by drying, sieving and packing. Oxidation typically occurs between 80 and 90 °C for periods ranging from 16 to 24 h. This process also leads to significant losses in the antioxidant capacity of aqueous extracts, which is associated with decreased levels of phenolic antioxidants present in the oxidised plant material (Joubert *et al.*, 2008).

The aim of this study was thus two-fold. One was to gain insight into the thermal degradation behaviour of the major xanthenes and benzophenones during processing of *C. genistoides* plant material so that their losses may be predicted, and subsequently also minimised. Towards this end, thermal degradation kinetics modelling was utilised as a tool to establish the kinetic parameters (reaction order and rate constant) governing their degradation in the plant material matrix. To date, no research on the thermal degradation kinetics of compounds from the benzophenone and xanthone phenolic sub-classes, either in plant material matrices or model solutions, has been conducted. The developed thermal degradation kinetics model was subsequently evaluated when different batches of plant material was subjected to high-temperature oxidation (90 °C/16 h).

The second aim was to evaluate the relevant importance of these four major constituents with regard to their individual contributions to the total antioxidant capacity (TAC) of aqueous extracts prepared from unoxidised and oxidised plant material. The TAC of aqueous extracts and the Trolox equivalent antioxidant capacity (TEAC) of the target compounds were assessed using the 2,2-diphenyl-1-picrylhydrazyl radical (DPPH \cdot) scavenging and oxygen radical absorbance capacity (ORAC) assays. These assays were selected as they are commonly used by extract manufacturers in South Africa for product specification and quality control of natural plant extracts. The TEAC of the minor benzophenone, 3- β -D-glucopyranosylmaclurin, was also calculated to determine the impact of increased B-ring hydroxylation on the antioxidant activity of the benzophenones.

2. MATERIALS AND METHODS

2.1. Chemicals

HPLC gradient-grade methanol was purchased from Merck Millipore (Darmstadt, Germany). Acetonitrile and acetic acid ($\geq 99.8\%$) were obtained from Riedel-de Haën (Sigma-Aldrich, St. Louis, MO, USA). Analytical grade reagents and chemicals, *i.e.*, 2,2-diphenyl-1-picrylhydrazyl (DPPH), 2,2'-azobis-(2-methylpropionamide)dihydrochloride (AAPH), (\pm)-6-hydroxy-2,5,7,8-tetramethylchromane-2-carboxylic acid (Trolox), potassium dihydrogen phosphate (KH_2PO_4), potassium hydroxide (KOH), and ascorbic acid were supplied by Sigma-Aldrich. Fluorescein sodium ($\text{C}_{20}\text{H}_{10}\text{Na}_2\text{O}_5$) was obtained from Fluka (Sigma-Aldrich). Ethanol was analytical grade (99%) and sourced from Servochem (Cape Town, South Africa). HPLC-grade water was prepared using Elix and Milli-Q Academic (Merck Millipore) water purification systems in series.

Authentic reference standards with purities $> 95\%$ were supplied by Sigma-Aldrich (mangiferin, hesperidin, 3- β -D-glucopyranosylriflophenone), Extrasynthese (Genay, France; eriocitrin, narirutin), Chemos GmbH (Regenstauf, Germany; isomangiferin) and Phytolab (Vestenbergsgreuth, Germany; vicenin-2). 3- β -D-Glucopyranosylmaclurin (95%) and 3- β -D-glucopyranosyl-4- β -D-glucopyranosyloxyriflophenone (99%) were isolated from *C. genistoides* (Chapter 4). 3',5'-di- β -D-Glucopyranosylphloretin, isolated from *C. subternata* to a purity of 94% (as assessed by liquid chromatography coupled with diode-array and electrospray ionisation mass spectrometric detection, LC-DAD-ESI-MS), was unambiguously identified by nuclear magnetic resonance spectroscopy. Stock solutions of the phenolic standards were prepared in dimethylsulfoxide (DMSO) at concentrations of *ca.* $1 \text{ mg}\cdot\text{mL}^{-1}$, diluted with water as required, and filtered through $0.22 \mu\text{m}$ pore-size Millex-GV syringe filters (4 mm diameter; Merck Millipore) prior to use.

2.2. Thermal Degradation Kinetics Modelling

The levels of the major benzophenones, 3- β -D-glucopyranosyl-4- β -D-glucopyranosyloxyriflophenone and 3- β -D-glucopyranosylriflophenone, and the major xanthenes, mangiferin and isomangiferin, in *Cyclopia genistoides* plant material were monitored during high-temperature oxidation to establish kinetic parameters governing their degradation. Experiments were conducted on small-scale under highly controlled conditions. The two temperature-time combinations investigated, *i.e.* $80 \text{ }^\circ\text{C}/24 \text{ h}$ and $90 \text{ }^\circ\text{C}/16 \text{ h}$, are representative of the optimum temperature-time regimens recommended to the honeybush industry for the production of the oxidised herbal tea product.

The shoots (leaves and fine stems) from a single *C. genistoides* (L.) Vent (Overberg type) plant were harvested from a commercial plantation near Pearly Beach (Western Cape, South Africa; GPS coor. $-34.702, 19.618$). The shoots were dried intact in a forced-air laboratory oven at $40 \text{ }^\circ\text{C}$ to a moisture content of $< 10\%$, whereafter the plant material was pulverised using a Retsch rotary mill (1.0 mm sieve; Retsch GmbH, Haan, Germany). A sub-sample was then sieved to obtain the fraction < 50 mesh to ensure a homogenous sample. The sieved plant material (*ca.* 80 mg) was weighed off into 4 mL clear glass vials ($n = 4$ for each time point), followed by addition of $130 \mu\text{L}$ of deionised water to achieve a final moisture content of *ca.* 65% and water activity (a_w) of *ca.* 0.97. The a_w of the wetted plant material was measured using a Labmaster- a_w meter (Novasina AG, Lachen, Switzerland). The vial contents were vortexed, the vials were placed in pre-heated water baths at 80 and $90 \text{ }^\circ\text{C}$, and the required number of vials was removed at each time point. Samples were taken hourly until 16 h for both the 80 and $90 \text{ }^\circ\text{C}$ trials, followed by sampling at 2 h intervals until 24 h for the $80 \text{ }^\circ\text{C}$ trial. The control samples received no treatment.

The samples were cooled to room temperature, followed by the addition of 4 mL of 40% aqueous ethanol (v.v⁻¹) and sonication for 30 min (ultrasonic bath, Branson Ultrasonic Corporation, Danbury, CT, USA). The extracts were cooled, filtered ($0.45 \mu\text{m}$ pore-size, 33 mm diameter Millex-HV syringe filters; Merck Millipore) and an aliquot of each was diluted

10 times with deionised water. Sample extracts were prepared for high-performance liquid chromatographic (HPLC) analysis by adding 100 μL of 10% aqueous ascorbic acid (m.v^{-1}) to 1 mL of the diluted extract.

HPLC-DAD analyses were performed in duplicate on an Agilent 1200 series instrument according to the validated method developed in Chapter 3. The target benzophenones and xanthenes in the sample extracts were identified by co-elution with the authentic reference standards, and were quantified at 280 nm and 320 nm, respectively. Owing to the limited quantity of the isomangiferin standard available, this compound (**5**) was quantified using a previously determined response factor relative to mangiferin (1.1197). Calibration curves for 3- β -D-glucopyranosyl-4- β -D-glucopyranosyloxiriflophenone (**1**), 3- β -D-glucopyranosylriflophenone (**3**) and mangiferin (**4**) were constructed weekly ($R^2 > 0.9999$) with on-column levels ranging between 0.0166–3.3261 μg , 0.0512–1.4906 μg and 0.0734–2.1173 μg , respectively.

Modelling of benzophenone and xanthone degradation was performed using quantitative data for the period 0–16 h. For each oxidation temperature, a completely randomised experimental design was used with 4 replications for each of the 16 treatment times. Univariate analysis of variance (ANOVA) using SAS, version 9.2 (SAS Institute, Cary, NC, USA) was performed for each oxidation temperature separately, using the General Linear Models Procedure. The Shapiro-Wilk test was performed to test for normality. Outliers were removed when the residual for an observation deviated with more than three standard deviations from the standardised model value. Fisher's least significant difference was calculated at the 5% level ($p < 0.05$) to compare treatment means.

Regression analysis with time (h) as independent variable was performed for the data of each temperature treatment to describe the decrease in compound concentration over time. The order of the thermal degradation reaction of the xanthenes and benzophenones were predicted using the model:

$$\frac{dC}{dt} = -K_D(C)^n \quad (1)$$

Where K_D is the degradation rate constant, n is the reaction order, C is the concentration (g of compound.100 g of plant material⁻¹), and t is the treatment time (h). The order of the degradation reactions was determined by setting component n in eq 1 to 0, 1 and 2, followed by comparing the coefficients of determination (R^2). The integrated forms of zero-, first-, and second-order kinetic models are given in eqs 2–4, with C_0 equal to the initial concentration of the compound (g of compound.100 g of plant material⁻¹) at $t = 0$ h:

$$\text{Zero-order:} \quad C = C_0 - K_D t \quad (2)$$

$$\text{First-order:} \quad \ln C = \ln C_0 - K_D t \quad (3)$$

$$\text{Second-order:} \quad \frac{1}{C} - \frac{1}{C_0} = K_D t \quad (4)$$

The temperature dependence of the degradation rate constants was evaluated by calculating the temperature coefficient (Q_{10}) according to Eq. 5 (Bělehrádek, 1930):

$$Q_{10} = \frac{K_D(T+10\text{ }^\circ\text{C})}{K_D(T)} \quad (5)$$

where K_D is the degradation rate constants at temperatures T and $T + 10$ $^\circ\text{C}$.

2.3. Evaluation of the Thermal Degradation Kinetics Model

The developed kinetic model was subsequently applied to predict the levels of benzophenones and xanthenes remaining when coarsely cut plant material (leaves and stems) was oxidised at 90 $^\circ\text{C}$ /16 h under up-scaled conditions. This tested the robustness of the kinetic model by incorporating additional variation, *i.e.*, heterogeneity of the plant material due to the coarse cut and batch size.

The shoots from 10 individual *C. genistoides* plants were harvested from the aforementioned commercial plantation. The fresh shoots from each plant were mechanically shredded (≤ 3 mm), mixed thoroughly, and divided into two sub-batches for the preparation of unoxidised (control) and oxidised plant material to provide content values for 0 and 16 h processing time, respectively. For the latter, the cut plant material (1 kg) was moistened to a moisture content of *ca.* 65% and oxidised at 90 °C/16 h (Le Roux *et al.*, 2008). Both the control and oxidised samples were dried at 40 °C/6 h and coarsely sieved (Le Roux *et al.*, 2008), followed by the preparation of freeze-dried hot water extracts as described in Chapter 3.

For HPLC analyses, the freeze-dried extracts were reconstituted in deionised water (*ca.* 6 mg.mL⁻¹), followed by the addition of 10% aqueous ascorbic acid (m.v⁻¹, final concentration = 9 mg.mL⁻¹). Samples were filtered using 0.45 µm pore-size Millex-HV syringe filters (33 mm diameter; Merck Millipore) and analysed. The target xanthone and benzophenone constituents were quantified as described in the previous section.

Other phenolic compounds present in the extracts were also quantified to provide further insight into the quantitative changes that occur during high-temperature oxidation, with emphasis on structure-stability relationships. 3-β-D-Glucopyranosylmaclurin (**2**), vicenin-2 (**6**), eriocitrin (**7**), 3',5'-di-β-D-glucopyranosylphloretin (**8**) and hesperidin (**9**) in the sample extracts were identified by co-elution with the authentic reference standards. Additionally, compounds **A–I** in the sample extracts were identified by taking their characteristic UV-vis spectra and relative elution order into account, in accordance with LC-DAD-MS results presented in Chapter 3 (Table S1, Supplementary Material, page 143). 3-β-D-Glucopyranosylmaclurin and vicenin-2 were quantified at 320 nm, and calibration curves were constructed over the following ranges (µg on-column): 0.0157–0.6905 and 0.0721–0.9008, respectively. The flavanones eriocitrin and hesperidin were quantified at 288 nm, and the ranges for the calibration curves were 0.0200–0.2500 and 0.0776–0.9700 µg on-column, respectively. Owing to the limited quantity of the 3',5'-di-β-D-glucopyranosylphloretin standard available, this compound was quantified using a previously determined response factor relative to hesperidin (0.7902). Compounds **A–I** were quantified using calibration curves of the most closely related reference standard. For this purpose, an additional calibration curve for narirutin was constructed at 288 nm over a range of 0.0200–0.3340 µg on-column. The coefficients of determination (*R*²) of all calibration curves were larger than 0.9999.

Quantitative data generated for extracts prepared from the unoxidised and oxidised plant material (*n* = 10) were subjected to ANOVA with Fisher's least significant difference calculated at the 5% level to compare treatment means.

2.4. Antioxidant Capacity of Selected Xanthenes and Benzophenones and the Effect of High-Temperature Oxidation on TAC of Aqueous Extracts

The TAC of the reconstituted freeze-dried extracts (*n* = 10) was determined in triplicate using the DPPH[•] scavenging (Arthur *et al.*, 2011) and ORAC (Huang *et al.*, 2002) assays in 96-well microplate format. Corresponding absorbance and fluorescence values were measured using a BioTek SynergyHT microplate reader fitted with a dispenser (BioTek Instruments, Winooski, VT, USA). TAC data were subjected to ANOVA with Fisher's least significant difference calculated at the 5% level to compare treatment means.

The trolox equivalent antioxidant capacity (TEAC) of the target benzophenones and xanthenes was determined to calculate their individual contributions to the TAC of aqueous extracts prepared from unoxidised *C. genistoides*, and to quantify the impact of their degradation based on the TAC of aqueous extracts prepared from the oxidised plant material. The antioxidant capacity of the minor benzophenone, 3-β-D-glucopyranosylmaclurin, was also determined to provide insight into structure-activity relationships.

Dose-response curves were constructed for the aforementioned compounds and Trolox by plotting graphs of concentration (μM) vs percent DPPH $^{\cdot}$ scavenged (DPPH assay) and net area under curve (ORAC assay). The concentration ranges of the standard compounds were selected to ensure that the antioxidant dose-response curves remain linear. TEAC values for each individual compound were then calculated as follows (Eq. 6):

$$\text{TEAC}_{\text{compound}} = \text{slope}_{\text{compound}} / \text{slope}_{\text{Trolox}} \quad (6)$$

3. RESULTS

3.1. Thermal Degradation Kinetics Modelling

The high-temperature oxidation process significantly ($p < 0.05$) reduced the mean content values of the target compounds over the evaluated time-temperature combinations, and these losses were more pronounced at 90 than 80 °C (Table S2, Supplementary Material, page 144).

The decrease in the contents of these compounds over a 16 h period, as affected by temperature and chemical structure, is depicted in Figure 1. Analysis of the kinetic data at both temperatures indicated first-order degradation reactions ($0.898 < R^2 < 0.970$), with the exception of 3- β -D-glucopyranosyl-4- β -D-glucopyranosyloxyiriflophenone at 80 °C ($R^2 = 0.111$) (Table 1). The mean content value of the latter compound did not change significantly over 16 h at 80 °C ($p \geq 0.05$; Table S2), which explains the poor correlation. Straight lines were obtained for plots of $\ln C$ vs t for each of the assessed compounds at each temperature (Figure 2), where the individual slopes are representative of the first-order degradation rate constants (K_D) (Table 1).

Table 1 Degradation rate constants^a and coefficients of determination (R^2) for the isothermal degradation of benzophenones and xanthenes in *Cyclopia genistoides* plant material, estimated by means of a first-order kinetic model.

Compound	80 °C		90 °C		Q_{10}^b
	$K_D \pm \text{SE} (\text{h}^{-1})$	R^2	$K_D \pm \text{SE} (\text{h}^{-1})$	R^2	
3- β -D-Glucopyranosyl-4- β -D-glucopyranosyloxyiriflophenone	0.0004 \pm 0.0003	0.111	0.0061 \pm 0.0005	0.921	–
3- β -D-Glucopyranosyliriflophenone	0.0224 \pm 0.0018	0.914	0.0314 \pm 0.0015	0.970	1.40
Mangiferin	0.0248 \pm 0.0017	0.941	0.0427 \pm 0.0037	0.905	1.72
Isomangiferin	0.0116 \pm 0.0010	0.898	0.0313 \pm 0.0023	0.929	2.70

^aDegradation rate constants \pm standard error of regression ($K_D \pm \text{SE}$). ^b Q_{10} = Temperature coefficient.

3- β -D-Glucopyranosyl-4- β -D-glucopyranosyloxyiriflophenone was the most thermally stable compound, with a $K_{D,90\text{ °C}}$ value of 0.0061 h^{-1} (Table 1). Isomangiferin was the second most thermally stable compound at 80 °C ($K_{D,80\text{ °C}} = 0.0116 \text{ h}^{-1}$), while its degradation rate was influenced the most by increased temperature ($Q_{10} = 2.70$, Table 1). 3- β -D-Glucopyranosyliriflophenone and mangiferin had comparable degradation rate constants of 0.0224 h^{-1} and 0.0248 h^{-1} , respectively, at 80 °C (Table 1). The degradation rate constants for these compounds respectively showed 1.40- and 1.72-fold increases with an increase in temperature from 80 to 90 °C (Table 1).

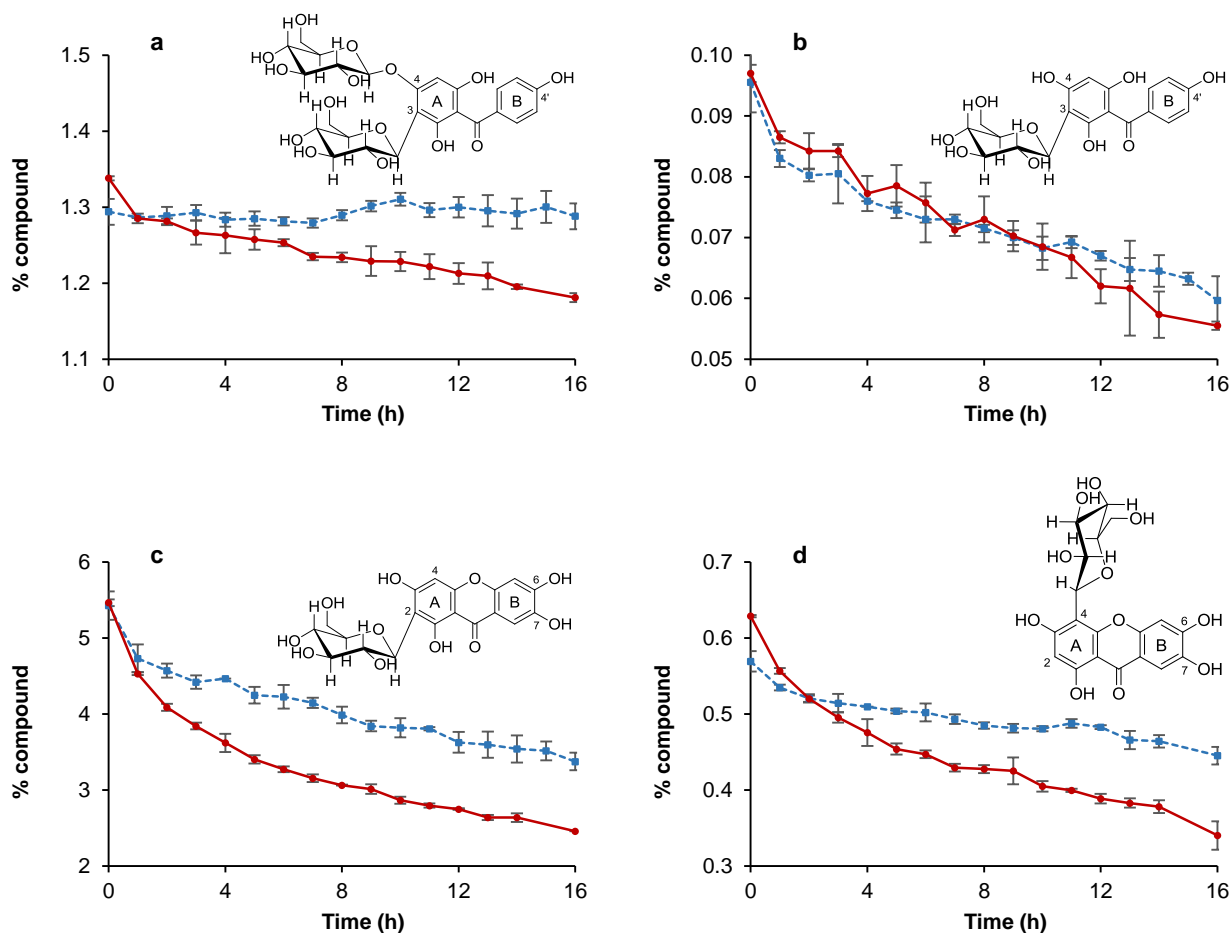


Figure 1 Changes in the mean percentage of compound in *Cyclopia genistoides* (g of compound.100 g of plant material⁻¹ ± standard deviation) for (a) 3-β-D-glucopyranosyl-4-β-D-glucopyranosyloxyiriflophenone, (b) 3-β-D-glucopyranosyliriflophenone, (c) mangiferin and (d) isomangiferin as a function of oxidation temperature over 16 h: (blue dotted curves) 80 °C; (red solid curves) 90 °C.

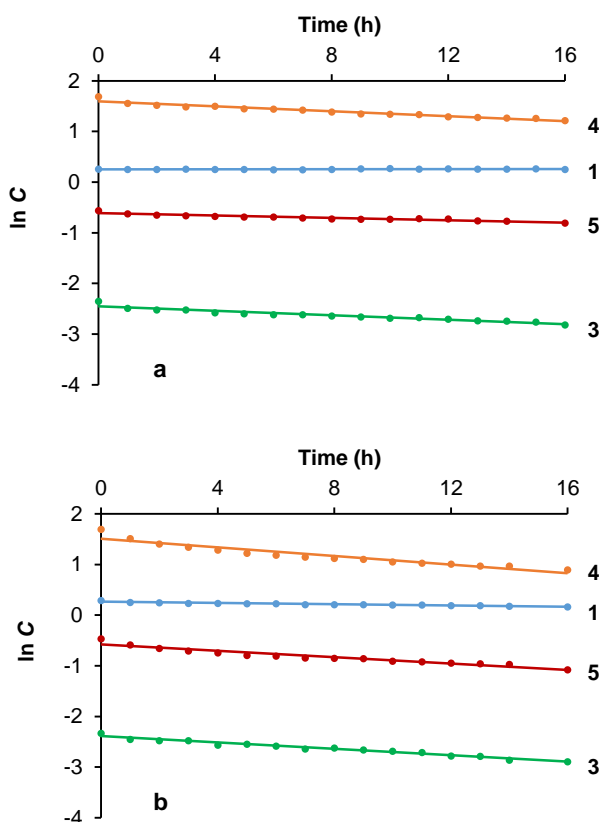


Figure 2 Kinetic degradation data for 3- β -D-glucopyranosyl-4- β -D-glucopyranosyloxiriflophenone (**1**), 3- β -D-glucopyranosylriflophenone (**3**), mangiferin (**4**) and isomangiferin (**5**) as fitted to a first-order kinetic model at (a) 80 °C and (b) 90 °C.

3.2. Evaluation of the Thermal Degradation Kinetics Model

Predicted content values for the target benzophenones and xanthenes in the oxidised plant material, based on their contents in the unoxidised plant material and their first-order $K_{D,90\text{ }^\circ\text{C}}$ values, were calculated for comparison with their actual content values in the oxidised plant material (Table 2).

Table 2 Mean values^a for the major benzophenones and xanthenes in *Cyclopia genistoides* plant material in relation to the values predicted using first-order degradation kinetics

Compound	Mean Content Value ($n = 10$)		Predicted Content Value	% Error
	Unoxidised	Oxidised ^b	Oxidised ^b	
3- β -D-Glucopyranosyl-4- β -D-glucopyranosyloxiriflophenone	1.3579	1.2927	1.2314	4.74
3- β -D-Glucopyranosylriflophenone	0.2691	0.0952	0.1629	-71.11
Mangiferin	2.7965	1.3486	1.4131	-4.78
Isomangiferin	0.3672	0.2039	0.2227	-9.22

^aIn units of g of compound.100 g of plant material⁻¹ ($n = 10$). ^bOxidation conditions: 90 °C/16 h.

The first-order kinetic model provided excellent (% error < 5%) prediction of 3- β -D-glucopyranosyl-4- β -D-glucopyranosyloxiriflophenone and mangiferin degradation, while it was acceptable (% error < 10%) for isomangiferin (Table 2). A poor fit was, however, obtained for 3- β -D-glucopyranosylriflophenone as the kinetic model greatly underestimated the degradation of this compound following oxidation at 90 °C for 16 h (Table 2).

3.3. Effect of High-Temperature Oxidation on the Levels of Individual Phenolic Compounds in Hot Water Extracts

Oxidation significantly decreased the content values of most phenolic compounds present in *C. genistoides* hot water extracts (refer to Figure 3 for a typical HPLC chromatogram), but some compounds either remained stable or showed a significant increase (Table 3).

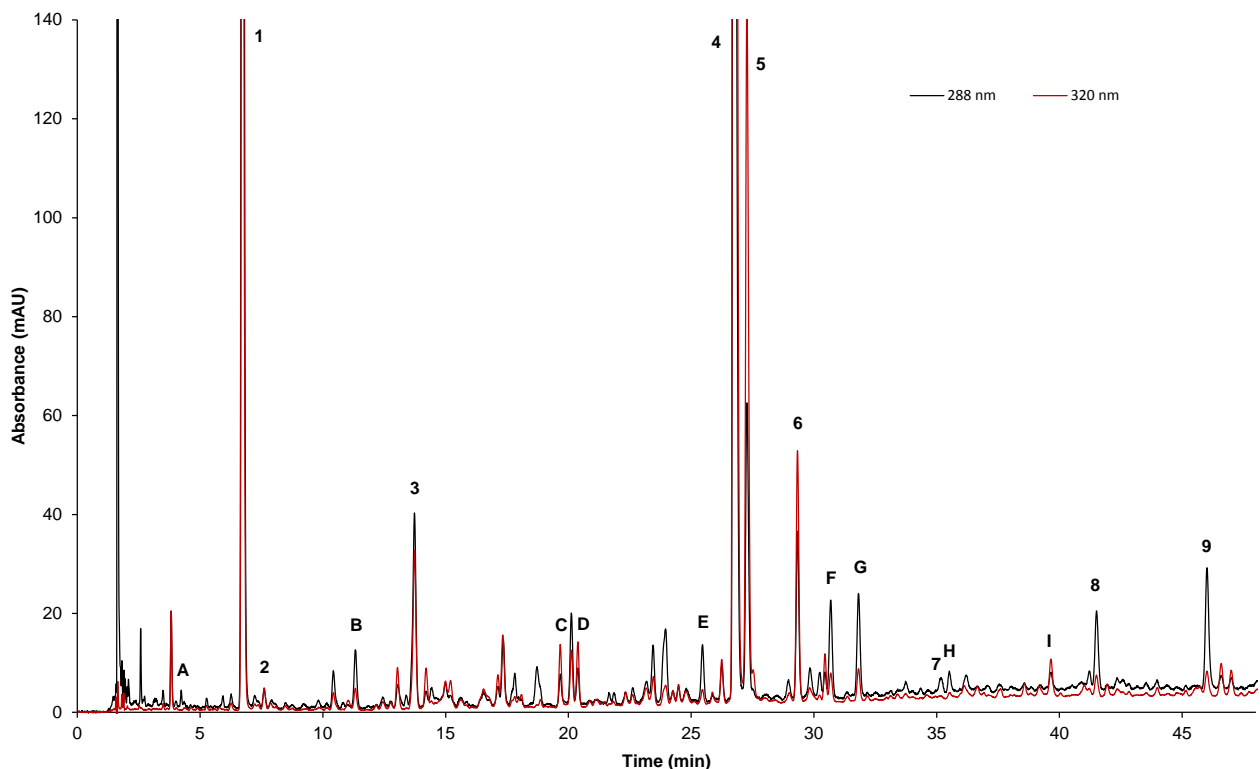


Figure 3 Typical HPLC chromatogram of an aqueous extract prepared from oxidised *Cyclopa genistoides* plant material. Peak labels correspond to Table 3. Refer to Table S1 (Supplementary Material, page 143) for the identification of compounds A–I.

The 2-glucosylxanthone mangiferin (**4**) was the major phenolic constituent of freeze-dried hot water extracts prepared from unoxidised (11.80%) and oxidised (6.04%) *C. genistoides* plant material (Table 3). Isomangiferin (**5**) represented the third most abundant phenolic constituent of *C. genistoides* at 1.54 and 0.91% of the unoxidised and oxidised extracts, respectively (Table 3). The mean content values of mangiferin and isomangiferin decreased by 49 and 41%, respectively, with oxidation (Table 3).

The second most abundant phenolic constituent of *C. genistoides* hot water extracts was the novel benzophenone, 3- β -D-glucopyranosyl-4- β -D-glucopyranosyloxyiriflophenone (**1**), and its mean content value was not significantly affected by oxidation ($p \geq 0.05$) (Table 3). 3- β -D-Glucopyranosyliriflophenone (**3**) represented the fourth and fifth most abundant phenolic constituent of aqueous extract prepared from the unoxidised (1.12%) and oxidised (0.42%) plant material, respectively. Contrary to compound **1**, the mean content value of 3- β -D-glucopyranosyliriflophenone showed a significant ($p < 0.05$) decrease with oxidation (62%; Table 3).

Table 3 Mean Values^a for the Major Phenolic Compounds and TAC of Hot Water Extracts Prepared from Unoxidised and Oxidised^b *Cyclopia genistoides* Plant Material.

Peak ^c	Compound	Unoxidised (n = 10)	Oxidised ^b (n = 10)	Mean Change (%)
A	Maclurin-di- <i>O,C</i> -hexoside ^d	0.1305 ± 0.03 a ^e	0.1114 ± 0.02 b	-14.64
1	3-β-D-Glucopyranosyl-4-β-D-glucopyranosyloxyiriflophenone	5.6950 ± 1.10 a	5.7840 ± 1.04 a	+1.56
2	3-β-D-Glucopyranosylmaclurin	0.3113 ± 0.14 a	0.0542 ± 0.03 b	-82.59
B	Unidentified compound ^f	0.1349 ± 0.03 a	0.1102 ± 0.03 b	-18.31
3	3-β-D-Glucopyranosyliriflophenone	1.1207 ± 0.67 a	0.4236 ± 0.22 b	-62.21
C	Tetrahydroxyxanthone- <i>C</i> -hexoside dimer ^g	nq ^h	0.0523 ± 0.02	-
D	Tetrahydroxyxanthone-di- <i>O,C</i> -hexoside ^g	0.1413 ± 0.04 a	0.0837 ± 0.02 b	-40.76
E	Eriodictyol- <i>O</i> -hexose- <i>O</i> -deoxyhexoside ⁱ	0.1685 ± 0.06 a	0.1155 ± 0.04 b	-31.45
4	Mangiferin	11.7983 ± 1.47 a	6.0362 ± 1.40 b	-48.84
5	Isomangiferin	1.5435 ± 0.24 a	0.9131 ± 0.16 b	-40.84
6	Vicenin-2	0.5014 ± 0.09 a	0.4470 ± 0.08 b	-10.85
F	Naringenin- <i>O</i> -hexose- <i>O</i> -deoxyhexoside ^j	0.2310 ± 0.08 b	0.3086 ± 0.09 a	+33.59
G	Naringenin- <i>O</i> -hexose- <i>O</i> -deoxyhexoside ^j	0.6733 ± 0.22 a	0.2891 ± 0.06 b	-57.06
7	Eriocitrin	0.0457 ± 0.01 a	0.0495 ± 0.01 a	+8.32
H	3-Hydroxyphloretin-3',5'-di- <i>C</i> -hexoside ^k	0.2579 ± 0.08 a	0.0416 ± 0.02 b	-83.87
I	Tetrahydroxyxanthone- <i>C</i> -hexoside isomer ^g	0.0964 ± 0.02 a	0.0620 ± 0.01 b	-35.68
8	3',5'-di-β-D-Glucopyranosylphloretin	0.4049 ± 0.12 a	0.1786 ± 0.05 b	-55.89
9	hesperidin	0.2984 ± 0.06 a	0.2120 ± 0.04 b	-28.95
	TAC ^l DPPH ^l	1350 ± 121 a	1164 ± 129 b	-13.78
	TAC ^l ORAC ^l	4460 ± 423 a	4406 ± 463 a	-1.21

^aIn units of g of compound.100 g of dried aqueous extract⁻¹ (DAE) ± standard deviation. ^bOxidation conditions: 90 °C/16 h. ^cRefer to Table S1 (Supplementary Material, page 141) for the identification of compounds **A-I**. ^dg of 3-β-D-glucopyranosylmaclurin equivalents.100 g of DAE⁻¹. ^emeans in the same row with different letters are significantly different ($p < 0.05$). ^fg of hesperidin equivalents.100 g of DAE⁻¹. ^gg of mangiferin equivalents.100 g of DAE⁻¹. ^hnq = not quantified due to extremely small peak area (< 30 mAU) yielding large percentage error associated with difficult integration. ⁱg of eriocitrin equivalents.100 g of DAE⁻¹. ^jg of narirutin equivalents.100 g of DAE⁻¹. ^kg of 3',5'-di-β-D-glucopyranosylphloretin equivalents.100 g of DAE⁻¹. ^lTotal antioxidant capacity (TAC) determined according to DPPH radical scavenging and ORAC assays, expressed as μmol of Trolox equivalents.g of DAE⁻¹.

In addition to these four major compounds, 14 additional compounds were also quantified to provide insight into the changes that occurred during oxidation (Table 3 and Figure 3). 3-β-D-Glucopyranosylmaclurin (**2**) and its glycosylated derivative, maclurin-di-*O,C*-hexoside (**A**), were quantified at levels of 0.31 and 0.13%, respectively, in extracts prepared from the unoxidised plant material. The former compound was extremely prone to degradation during the high-temperature oxidation process, exhibiting a decrease of 83%.

A tetrahydroxyxanthone-*C*-hexoside dimer (**C**), a tetrahydroxyxanthone-di-*O,C*-hexoside (**D**) and a tetrahydroxyxanthone-*C*-hexoside isomer (**J**) were also quantified as minor constituents of the *C. genistoides* extracts (Table 3). The mean content values of compounds **D** and **J** showed a reduction of 35-40% with oxidation, whilst the xanthone dimer (compound **C**) was only quantifiable in extracts prepared from the oxidised plant material.

Vicenin-2 (6,8-di-β-D-glucopyranosylapigenin, compound **6**) represented the sixth and fourth most abundant phenolic constituent of hot water extracts prepared from unoxidised (0.50%) and oxidised (0.45%) *C. genistoides* plant material, respectively. This represents a slight, but significant ($p < 0.05$) decrease with oxidation (*ca.* 10%).

The effect of processing on the flavanones was found to differ. The average content of eriocitrin (**7**) in the aqueous extract was not significantly ($p \geq 0.05$) affected by oxidation, whilst the hesperidin (**9**) and eriodictyol-*O*-hexose-*O*-deoxyhexoside (**E**) contents were significantly ($p < 0.05$) reduced. The average content of naringenin-*O*-hexose-*O*-deoxyhexoside (**G**) also

showed a significant ($p < 0.05$) decrease with oxidation (57%), which was accompanied by a significant ($p < 0.05$) increase in the content of another naringenin-*O*-hexose-*O*-deoxyhexoside derivative (compound **F**; 34%).

The mean content values of the dihydrochalcone 3',5'-di- β -D-glucopyranosylphloretin (**8**) and its hydroxylated derivative, 3-hydroxyphloretin-3',5'-di-*C*-hexoside (**H**), were both significantly ($p < 0.05$) reduced with oxidation. The former compound presented a decrease of 56%, whilst the latter was degraded more extensively (84%; Table 3).

3.4. Antioxidant Capacity of Selected Xanthenes and Benzophenones and the Effect of High-Temperature Oxidation on TAC of Aqueous Extracts

Oxidation significantly ($p < 0.05$) lowered the mean TAC of the extracts as assessed using the DPPH^{*} scavenging assay (TAC_{DPPH}, Table 3). Conversely, the TAC_{ORAC} of extracts was only slightly, but not significantly ($p \geq 0.05$) reduced with oxidation (Table 3).

Assessment of the TEAC of selected benzophenones and xanthenes provided some insight into the relative importance of these constituents in terms of the TAC of the extract. TEAC_{DPPH} values for the individual compounds (Table 4) indicated that 3- β -D-glucopyranosylmaclurin was the most efficient scavenger of DPPH^{*}. Its TEAC_{DPPH} value (2.19) was *ca.* three-fold higher than that of 3- β -D-glucopyranosyliriflophenone (0.65) (Table 4). Despite the low concentration of 3- β -D-glucopyranosylmaclurin in the unoxidised *C. genistoides* extract (Table 3), it almost contributed equally to the average TAC of the unoxidised extract compared to the much more abundant 3- β -D-glucopyranosyliriflophenone (Table 4). The radical scavenging ability of 3- β -D-glucopyranosyl-4- β -D-glucopyranosyloxyiriflophenone towards DPPH^{*} (0.01) was lower than that of its mono-glucosylated derivative, 3- β -D-glucopyranosyliriflophenone, and was also the lowest overall (Table 4).

Both mangiferin and isomangiferin exhibited moderate DPPH^{*} scavenging activity with TEAC values of 1.79 and 1.69, respectively. These xanthenes were the major contributors to the TAC of *C. genistoides* hot water extracts, collectively responsible for 41.7 and 25.2% of the TAC_{DPPH} of the extracts prepared from unoxidised and oxidised plant material, respectively (Table 4).

With regard to the ORAC assay, an entirely different ranking of phenolic antioxidants was obtained. The fluorescein fluorescence decay curve of 3- β -D-glucopyranosyl-4- β -D-glucopyranosyloxyiriflophenone showed a very different profile compared to those of the reference antioxidant, Trolox, and 3- β -D-glucopyranosylmaclurin (Figure S1, Supplementary Material, page 145). 3- β -D-Glucopyranosyl-4- β -D-glucopyranosyloxyiriflophenone exhibited the highest TEAC_{ORAC} value (4.76), followed by 3- β -D-glucopyranosyliriflophenone (4.06) (Table 4). Due to both its relative potency and high concentration in the *C. genistoides* extracts (Table 3), 3- β -D-glucopyranosyl-4- β -D-glucopyranosyloxyiriflophenone represented a major contributor (> 10%) to the average TAC_{ORAC} of the extracts. Conversely, the contribution of this compound to the TAC_{DPPH} of the extracts was almost negligible (*ca.* 0.1%) (Table 4). 3- β -D-Glucopyranosylmaclurin exhibited a moderate antioxidative effect in the ORAC assay (3.31) comparable to that of isomangiferin (3.38), and notably higher than that of mangiferin (2.80) (Table 4).

Table 4 Trolox equivalent antioxidant capacity (TEAC)^a of benzophenones and xanthenes in the DPPH radical scavenging and ORAC assays with their concentration ranges, slope and coefficients of determination (R^2), together with their individual contributions to the average total antioxidant capacity (TAC) of *Cyclopia genistoides* extracts.

Compound	Concentration Range (μM) ^b	Slope (R^2)	TEAC	Percentage Contribution to TAC of Extracts ^c	
				Unoxidised	Oxidised ^d
DPPH assay^e					
3- β -D-Glucopyranosyl-4- β -D-glucopyranosyloxyiriflophenone	260.6–695.0	0.0331 (0.997)	0.0147	0.109	0.128
3- β -D-Glucopyranosylmaclurin	3.0–16.3	4.8836 (0.999)	2.1876	1.188	0.240
3- β -D-Glucopyranosyliriflophenone	5.1–21.8	1.4614 (0.993)	0.6547	1.330	0.583
Mangiferin	4.1–17.0	4.1673 (0.995)	1.7945	37.117	22.023
Isomangiferin	2.9–19.5	3.7808 (0.998)	1.6936	4.583	3.144
% Contribution of benzophenones	–	–	–	2.627	0.951
% Contribution of xanthenes	–	–	–	41.700	25.167
TOTAL % contribution	–	–	–	44.327	26.119
ORAC assay^f					
3- β -D-Glucopyranosyl-4- β -D-glucopyranosyloxyiriflophenone	0.163–0.424	19.9054 (0.987)	4.7623	10.659	10.958
3- β -D-Glucopyranosylmaclurin	0.190–0.474	13.7585 (0.996)	3.3149	0.545	0.096
3- β -D-Glucopyranosyliriflophenone	0.101–0.228	18.0819 (0.987)	4.0559	2.496	0.955
Mangiferin	0.206–0.463	12.4914 (0.993)	2.8040	17.563	9.096
Isomangiferin	0.209–0.470	13.7753 (0.993)	3.3795	2.769	1.658
% Contribution of benzophenones	–	–	–	13.700	12.009
% Contribution of xanthenes	–	–	–	20.332	10.754
TOTAL % contribution	–	–	–	34.032	22.763

^aActivity of compound relative to that of Trolox: *i.e.*, concentration of Trolox solution in μM with equivalent antioxidant activity to a 1 μM concentration of the compound under investigation. ^bThe concentration range of a specific compound used in the dose-response curves (final concentrations in the reaction volume). ^cCalculated on the basis of content (Table 3) and TEAC values. ^dOxidation conditions: 90 °C/16 h. ^eTrolox assessed over a concentration range of 5.0–40.0 μM with an average slope ($n = 3$) of 2.2670 and $R^2 = 0.997$. ^fTrolox assessed over a concentration range of 0.6–3.7 μM with an average slope ($n = 6$) of 4.2240 and $R^2 = 0.999$. TEAC values for the xanthenes and benzophenones were determined in duplicate (% RSDs ≤ 5.6).

4. DISCUSSION

4.1. Thermal Degradation Kinetics Modelling and Evaluation of the Model

The thermal stabilities of 3- β -D-glucopyranosyl-4- β -D-glucopyranosyloxyiriflophenone, 3- β -D-glucopyranosyliriflophenone, mangiferin and isomangiferin were determined as these compounds represent the major phenolic constituents of *C. genistoides*. Due to the low levels of 3- β -D-glucopyranosylmaclurin present in the plant material, its thermal degradation behaviour could not be assessed kinetically. An isothermal method was used to estimate reaction kinetics, as the ramp-up time in the thin-walled glass vials was assumed to be negligible compared to the length of the holding phase. The kinetic data provided a good fit for first-order degradation reactions, which is in line with literature on the isothermal degradation of cloudy apple juice phenolic constituents (De Paepe *et al.*, 2014), anthocyanins (Sui *et al.*, 2014), and carotenoids (Dhuique-Mayer *et al.*, 2007), amongst others.

Addition of a 4-glucopyranosyloxy moiety conferred higher thermal stability to 3- β -D-glucopyranosyl-4- β -D-glucopyranosyloxyiriflophenone compared to 3- β -D-glucopyranosyliriflophenone during high-temperature oxidation of

C. genistoides plant material. Glucosylation at C-4 of the dibenzo- γ -pyrone structure, as opposed to C-2, also increased the stability of the tetrahydroxyxanthenes.

Previous studies on the thermal degradation of quercetin and rutin (3-rutinosyloxyquercetin) in aqueous model systems showed that rutin was more stable than its corresponding aglycone (Makris & Rossiter, 2000; Buchner *et al.*, 2006). This observation was attributed to the blockage of the 3-hydroxy group in the C-ring by the sugar moiety which prevents the formation of the carbanion (Tournaire *et al.*, 1994, as cited by Buchner *et al.*, 2006). It is thus possible that the hydroxy group at C-4 on the diphenyl methanone structure is a key parameter with respect to thermal degradation of benzophenones. Similarly, a study on the thermal stability of quercetin *O*-glycosyl compounds demonstrated that the position of glycosylation, and type of sugar determined susceptibility to deglycosylation (Rohn *et al.*, 2007). Zielinski and co-workers (Zielinski *et al.*, 2009) have demonstrated slight differences in the stability of the flavone *C*-glucosyl compounds vitexin (8- β -D-glucopyranosylapigenin; 72% degradation) and isovitexin (6- β -D-glucopyranosylapigenin; 84% degradation) in buckwheat groats during roasting.

In the current study, an increase in oxidation temperature from 80 to 90 °C increased the rate of degradation for all target compounds, as expected. Of interest is that this effect was more pronounced for 3- β -D-glucopyranosyl-4- β -D-glucopyranosyloxyiriflophenone which was stable under oxidative conditions at 80 °C for 16 h, but exhibited a decrease of 11.7% following oxidation at 90 °C after the same time period. The effect of temperature on the degradation rate constants was estimated by calculating the temperature coefficient (Q_{10}). The significance of this value is clear when considering the thermal degradation of isomangiferin. This compound had the lowest degradation rate constant at 80 °C, which, by itself would imply that this compound is more stable than mangiferin and 3- β -D-glucopyranosyliriflophenone. However, the degradation rate of isomangiferin showed a 2.7 fold increase with an increase in temperature from 80 to 90 °C, which implies greater susceptibility of this compound towards degradation at elevated temperature than mangiferin and 3- β -D-glucopyranosyliriflophenone.

The kinetic parameters derived for the first-order degradation reactions were subsequently used to predict the amounts of major compounds remaining in *C. genistoides* ($n = 10$) following oxidation (90 °C/16 h) of the coarsely cut plant material under conditions similar to those used in the industrial oxidation process. In spite of the procedure being less ‘controlled’ than the oxidation process carried out with very small quantities of homogenous material, the degradation kinetic model provided excellent estimates for the average amounts of 3- β -D-glucopyranosyl-4- β -D-glucopyranosyloxyiriflophenone and mangiferin in the oxidised plant material. The model, however, greatly underestimated the degradation of 3- β -D-glucopyranosyliriflophenone, and the reason for this still has to be established. In light of the apparent bitterness of *C. genistoides* infusions, associated with a high mangiferin content (Theron, 2012), the model could potentially be used to estimate the processing time needed to decrease the mangiferin content to a level where the infusions are not perceived as bitter, but without causing unnecessary losses in bio-activity. Another potential application is to “screen” new *C. genistoides* selections (unoxidised) of the ongoing Cultivar Development Programme of the Agricultural Research Council of South Africa for an unacceptable bitter taste by predicting the mangiferin content of the processed herbal tea.

4.2. Effect of High-Temperature Oxidation on the Levels of Individual Phenolic Compounds in Hot Water Extracts

It is well-known that the high-temperature oxidation process has a significant impact on the individual phenolic content values of *Cyclopia* extracts. Previous studies have, however, mostly been limited to a small data set of randomly selected or paired-processed samples and/or a limited number of quantifiable compounds (Joubert *et al.*, 2008; De Beer & Joubert, 2010; Chapter 3). In the present study, quantitative data were generated for nine known compounds and nine additional compounds in 10 individual batches of *C. genistoides* plant material.

The high-temperature oxidation process (90 °C/16 h), required for the development of the desirable sensory properties of honeybush herbal tea, significantly reduced the mean content values of most phenolic compounds of the aqueous extracts. The thermal stability of a number of minor compounds is worth highlighting. The tetrahydroxyxanthone-*C*-hexoside dimer (compound **C**) could only be quantified in extracts prepared from the oxidised plant material. Based on related studies regarding the dihydrochalcone aspalathin (Krafczyk *et al.*, 2009; Heinrich *et al.*, 2012), it is probable that this xanthone dimer is formed by the non-enzymatic, phenol oxidative coupling of two tetrahydroxyxanthone-*C*-hexoside monomers during high-temperature processing. The dimeric xanthone may be linked either through a rotatable or atropisomeric biaryl C-C bond, or a biaryl ether C-O-C linkage (Wezeman *et al.*, 2015). Storage of epigallocatechin gallate in solid state samples at elevated temperatures (80 °C) has also been shown to induce auto-oxidation with the formation of B-ring linked dimers (Li *et al.*, 2013).

Two naringenin derivatives, compounds **F** and **G**, also exhibited interesting behaviour during the oxidation process. A significant reduction in the mean content value of compound **G** was accompanied by a significant increase in the mean content value of compound **F**. These flavanones are potential isomers, and it is herein postulated that compound **G** is converted to the more stable structure of compound **F** during the oxidation process. Similar observations have been made with regard to the irreversible conversion of isoorientin to orientin via a Wessely-Moser rearrangement during incubation in phosphate buffer at 37 °C for 48 h (Krafczyk *et al.*, 2008).

In this study, 3',5'-di- β -D-glucopyranosylphloretin (**8**) was more stable than 3-hydroxyphloretin-3',5'-di-*C*-hexoside (**H**) during oxidation at 90 °C/16 h. The presence of an extra hydroxy group on the B-ring of the basic dihydrochalcone structure therefore decreased thermal stability. This effect was also prominent for 3- β -D-glucopyranosylriflophenone (**3**) (62% reduction) and its C-3' hydroxylated derivative, 3- β -D-glucopyranosylmaclurin (**2**) (82% reduction). Maini and co-workers (Maini *et al.*, 2012) found that the stability of flavonols in different cell culture media, and their stability to UVA irradiation, decreased with increasing B-ring substitution. Conversely, De Paepe *et al.* (2014) demonstrated a slight decrease in the K_D value with the presence of an additional hydroxy group at C-3' on the A-ring of the dihydrochalcone structure. These results therefore suggest that both the degree of hydroxylation and the position of hydroxylation, in particular, are key factors affecting the thermal stability of dihydrochalcones.

4.3. Antioxidant Capacity of Selected Xanthenes and Benzophenones and Effect of High-Temperature Oxidation on TAC of Aqueous Extracts

While a reduction in the contents of mangiferin and isomangiferin, for instance, may be desirable from a sensory perspective, the antioxidant activity of the extracts may also consequently be reduced. Given demonstration of the similar antioxidant capacity of three of these compounds in an on-line HPLC-ORAC assay (Malherbe *et al.*, 2014), their degradation was expected to have a major impact on TAC of hot water extracts of *C. genistoides*. This type of extract is of interest due to its use as an ingredient in food and nutraceutical products.

High-temperature oxidation significantly lowered the average TAC_{DPPH} value of the aqueous extracts, while their average TAC_{ORAC} value was only slightly reduced. These observations are in line with data presented by Joubert *et al.* (2008), in which oxidation significantly reduced the average antioxidant activity of six paired-processed samples of various *Cyclopia* species [as assessed using the ABTS^{•+} scavenging, ferric reducing antioxidant power (FRAP) and lipid peroxidation assays]. The same study showed, however, that the ability of the hot water extract of *C. genistoides* to inhibit lipid peroxidation was not affected (Joubert *et al.*, 2008). It is therefore possible that unknown degradation products may also possess antioxidant activity and thus could have contributed to the TAC_{ORAC} of extracts prepared from the oxidised plant material. Buchner *et al.* (2006) and Murakami *et al.* (2004) have previously demonstrated antioxidant activity for flavonol and other polyphenolic degradation products.

The higher TEAC_{DPPH} value of 3- β -D-glucopyranosylmaclurin compared to that of 3- β -D-glucopyranosyliriflophenone may be attributed to the presence of an extra hydroxy group at C-3' on the diphenyl methanone structure, which imparts a catechol-type structure to 3- β -D-glucopyranosylmaclurin, one of the structural features responsible for antioxidant activity of polyphenols (Rice-Evans *et al.*, 1996; Heim *et al.*, 2002). An increase in the degree of glucosylation was found to reduce the reactivity of the benzophenones towards DPPH[•] as previously observed for flavonoids (Rice-Evans *et al.*, 1996). The reduced reactivity of 3- β -D-glucopyranosyl-4- β -D-glucopyranosyloxyiriflophenone could possibly be attributed to the substitution of an active phenolic OH group, responsible for free radical scavenging. Furthermore, the additional glucopyranosyloxy moiety can sterically impede access of the remaining free phenolic OH groups to the hindered radical site of DPPH[•], thereby reducing reactivity (Xie & Schaich, 2014).

While data from the DPPH[•] scavenging assay inferred that 3- β -D-glucopyranosyl-4- β -D-glucopyranosyloxyiriflophenone is ineffective as radical scavenger, this compound had the highest TEAC_{ORAC} value among the five compounds assessed in this study. The difference in ranking of phenolic antioxidants in the ORAC assay compared to the DPPH assay may be related to the differences in the reaction mechanisms of the two assays, which underlines the importance of using more than one assay to assess the antioxidant capacity of natural extracts and/or phenolic compounds. To our knowledge, this is the first report on the antioxidant capacity of 3- β -D-glucopyranosyl-4- β -D-glucopyranosyloxyiriflophenone and 3- β -D-glucopyranosylmaclurin. Further research is thus required to understand the reaction mechanisms of these benzophenones with free radicals.

Similarly, the effect of glucosylation position on the antioxidant activity of the xanthenes differed between the two antioxidant assays. Mangiferin exhibited slightly higher reactivity towards DPPH[•] than its C-4 regio-isomer, isomangiferin, while the TEAC_{ORAC} of isomangiferin was slightly higher than that of mangiferin. These observations are in line with results presented by Malherbe *et al.* (2014) using online HPLC-DPPH and -ORAC assays. Similar antioxidant activities have also been demonstrated for positional isomers of chlorogenic acid (Nakatani *et al.*, 2000).

Collectively, the four major compounds and 3- β -D-glucopyranosylmaclurin contributed 44.3 and 26.1% to the TAC_{DPPH} of extracts prepared from unoxidised and oxidised plant material, respectively. Mangiferin was the major contributor, and this could be ascribed to both its high concentration in the sample extracts and its relatively high scavenging ability towards DPPH[•]. It is also clear that when using the DPPH assay, the contribution of the benzophenones to the TAC of the extracts was low, and that their degradation during oxidation would thus have little impact on the TAC_{DPPH} value. Using the ORAC assay, the same five compounds could only explain 34.0 and 22.8% of the TAC of extracts prepared from unoxidised and oxidised *C. genistoides* plant material, respectively. Here, mangiferin and 3- β -D-glucopyranosyl-4- β -D-glucopyranosyloxyiriflophenone contributed almost equally to the TAC_{ORAC} of extracts prepared from the oxidised plant material. The remarkable stability of 3- β -D-glucopyranosyl-4- β -D-glucopyranosyloxyiriflophenone during high-temperature oxidation was therefore paramount to retaining the high TAC_{ORAC} of the extracts, even after processing. A large percentage of the TAC of the hot water honeybush extracts still remains unaccounted for, and this may be ascribed to the antioxidant capacities of other phenolic constituents and other types of compounds present in the extracts (both known and unidentified compounds) which were not assessed in the current study.

5. CONCLUSION

The high-temperature oxidation process decreased the antioxidant capacity and individual content values of most phenolic compounds present in *C. genistoides* hot water extracts. Decreases in the individual phenolic contents were compound specific with factors such as the degree of hydroxylation, and the degree and position of glucosylation playing key roles. Insight into the thermal stability of selected xanthenes and benzophenones was obtained for the first time in this study, with the application of thermal degradation kinetics modelling. This includes kinetic data on the novel *Cyclopia* constituent, 3- β -D-glucopyranosyl-4- β -D-glucopyranosyloxyiriflophenone. Understanding these complex reaction mechanisms is a prerequisite to gain further insights into the chemical pathways during the high-temperature oxidation of *C. genistoides* plant material. Future studies will include assessing the thermal stability of the compounds in model solutions as opposed to the plant material, thereby eliminating matrix effects and interactions between phenolic constituents. Such degradation models will be useful to predict the stability of these compounds during pasteurisation/sterilisation of ready-to-drink herbal tea beverages, for instance.

REFERENCES

- Arthur, H., Joubert, E., De Beer, D., Malherbe, C.J. & Witthuhn, R.C. (2011). Phenylethanoid glycosides as major antioxidants in *Lippia multiflora* herbal infusion and their stability during steam pasteurisation of plant material. *Food Chemistry*, **127**, 581-588.
- Bělehrádek, J. (1930). Temperature coefficients in biology. *Biology Reviews*, **5**, 30-58.
- Buchner, N., Krumbein, A., Rohn, S. & Kroh, L.W. (2006). Effect of thermal processing on the flavonols rutin and quercetin. *Rapid Communications in Mass Spectrometry*, **20**, 3229-3235.
- De Beer, D. & Joubert, E. (2010). Development of HPLC method for *Cyclopia subternata* phenolic compound analysis and application to other *Cyclopia* spp. *Journal of Food Composition and Analysis*, **23**, 289-297.
- De Paepe, D., Valkenburg, D., Coudijzer, K., Noten, B., Servaes, K., De Loose, M., Voorspoels, S., Diels, L. & Van Droogenbroeck, B. (2014). Thermal degradation of cloudy apple juice phenolic constituents. *Food Chemistry*, **162**, 176-185.
- Dhuique-Mayer, C., Tbatou, M., Carail, M., Caris-Veyrat, C., Dornier, M. & Amiot, M.J. (2007). Thermal degradation of antioxidant micronutrients in citrus juice: kinetics and newly formed compounds. *Journal of Agricultural and Food Chemistry*, **55**, 4209-4216.
- Feng, J., Yang, X.-W. & Wang, R.-F. (2011). Bio-assay guided isolation and identification of α -glucosidase inhibitors from the leaves of *Aquilaria sinensis*. *Phytochemistry*, **72**, 242-247.
- Heim, K.E., Tagliaferro, A.R. & Bobilya, D.J. (2002). Flavonoid antioxidants: chemistry, metabolism and structure-activity relationships. *Journal of Nutritional Biochemistry*, **13**, 572-584.
- Heinrich, T., Willenberg, I. & Glomb, M.A. (2012). Chemistry of color formation during rooibos fermentation. *Journal of Agricultural and Food Chemistry*, **60**, 5221-5228.
- Huang, D., Ou, B., Hampsch-Woodill, M., Flanagan, J.A. & Prior, R.L. (2002). High-throughput assay of oxygen radical absorbance capacity (ORAC) using a multichannel liquid handling system coupled with a microplate fluorescence reader in 96-well format. *Journal of Agricultural and Food Chemistry*, **50**, 4437-4444.
- Joubert, E., Richards, E.S., Van der Merwe, J.D., De Beer, D., Manley, M. & Gelderblom, W.C.A. (2008). Effect of species variation and processing on phenolic composition and *in vitro* antioxidant activity of aqueous extracts of *Cyclopia* spp. (honeybush tea). *Journal of Agricultural and Food Chemistry*, **56**, 954-963.
- Joubert, E., Joubert, M.E., Bester, C., De Beer, D., De Lange, J.H. (2011). Honeybush (*Cyclopia* spp.): From local cottage industry to global markets – the catalytic and supporting role of research. *South African Journal of Botany*, **77**, 887-907.
- Kokotkiewicz, A., Luczkiewicz, M., Pawlowska, J., Luczkiewicz, P., Sowinski, P., Witkowski, J., Bryl, E. & Bucinski, A. (2013). Isolation of xanthone and benzophenone derivatives from *Cyclopia genistoides* (L.) Vent. (honeybush) and their pro-apoptotic activity on synoviocytes from patients with rheumatoid arthritis. *Fitoterapia*, **90**, 199-208.
- Krafczyk, N. & Glomb, M.A. (2008). Characterization of phenolic compounds in rooibos tea. *Journal of Agricultural and Food Chemistry*, **56**, 3368-3376.
- Krafczyk, N., Heinrich, T., Porzel, A. & Glomb, M.A. (2009). Oxidation of the dihydrochalcone aspalathin leads to dimerization. *Journal of Agricultural and Food Chemistry*, **57**, 6838-6843.
- Le Roux, M., Cronje, J.C., Joubert, E. & Burger, B.V. (2008). Chemical characterization of the constituents of the aroma of honeybush, *Cyclopia genistoides*. *South African Journal of Botany*, **74**, 139-143.
- Li, N., Taylor, L.S., Ferruzzi, M.G. & Mauer, L.J. (2013). Color and chemical stability of tea polyphenol (-)-epigallocatechin-3-gallate in solution and solid states. *Food Research International*, **53**, 909-921.
- Makris, D.P. & Rossiter, J.T. (2000). Heat-induced, metal-catalyzed oxidative degradation of quercetin and rutin (quercetin-3-O-rhamnosylglucoside) in aqueous model systems. *Journal of Agricultural and Food Chemistry*, **48**, 3830-3838.

- Malherbe, C.J., Willenburg, E., De Beer, D., Bonnet, S.L., Van der Westhuizen, J.H. & Joubert, E. (2014). Iriflophenone-3-C-glucoside from *Cyclopia genistoides*: Isolation and quantitative comparison of antioxidant capacity with mangiferin and isomangiferin using on-line HPLC antioxidant assays. *Journal of Chromatography B*, **951-952**, 164-171.
- Maini, S., Hodgson, H.L. & Krol, E.S. (2012). The UVA and aqueous stability of flavonoids is dependent on B-ring substitution. *Journal of Agricultural and Food Chemistry*, **60**, 6966-6976.
- Murakami, M., Yamaguchi, T., Takamura, H. & Matoba, T. (2004). Effects of thermal treatment on radical-scavenging activity of single and mixed polyphenolic compounds. *Journal of Food Sciences*, **69**, FCT7-FCT10.
- Nakatani, N., Kayano, S.I., Kikuzaki, H., Sumino, K., Katagiri, K. & Mitani, T. (2000). Identification, quantitative determination, and antioxidative activities of chlorogenic acid isomers in prune (*Prunus domestica* L.). *Journal of Agricultural and Food Chemistry*, **48**, 5512-5516.
- Rice-Evans, C.A., Miller, N.J. & Paganga, G. (1996). Structure-antioxidant activity relationships of flavonoids and phenolic acids. *Free Radical Biology and Medicine*, **20**, 933-956.
- Rohn, S., Bucher, N., Driemel, G., Rauser, M. & Kroh, L.W. (2007). Thermal degradation of onion quercetin glucosides under roasting conditions. *Journal of Agricultural and Food Chemistry*, **55**, 1568-1573.
- Schulze, A.E., De Beer, D., Mazibuko, S.E., Muller, C.J.F., Roux, C., Willenburg, E.L., Nyunai, N., Louw, J., Manley, M & Joubert, E. (2015). Assessing similarity analysis of chromatographic fingerprints of *Cyclopia subternata* extracts as potential screening tool for *in vitro* glucose utilization. *Analytical and Bioanalytical Chemistry*, accepted.
- Sui, X., Dong, X. & Zhou, W. (2014). Combined effect of pH and high temperature on the stability and antioxidant capacity of two anthocyanins in aqueous solution. *Food Chemistry*, **163**, 163-170.
- Theron, K.A. (2012). Sensory and phenolic profiling of *Cyclopia* species (honeybush) and optimisation of the fermentation conditions. MSc (Food Science) Thesis, Stellenbosch University, Stellenbosch, South Africa.
- Tournaire, C., Hocquaux, M., Beck, I., Oliveros, E. & Maurette, M.-T. (1994). "Activité anti-oxydante de flavonoids. Réactivité avec le superoxide de potassium en phase hétérogène." (Article in French). *Tetrahedron*, **50**, 9303-9314.
- Vyas, A., Syeda, K., Ahmad, A., Padhye, S. & Sarkar, F.H. (2012). Perspectives on medicinal properties of mangiferin. *Mini-Reviews in Medicinal Chemistry*, **12**, 412-425.
- Wezeman, T., Bräse, S. & Masters, K.-S. (2015). Xanthone dimers: a compound family which is both common and privileged. *Natural Product Reports*, **32**, 6-28.
- Xie, J. & Schaich, K.M. (2014). Re-evaluation of the 2,2-diphenyl-1-picrylhydrazyl free radical (DPPH) assay for antioxidant activity. *Journal of Agricultural and Food Chemistry*, **62**, 4251-4260.
- Zhang, Y., Qian, Q., Ge, D., Li, Y., Wang, X., Chen, Q., Gao, X. & Wang, T. (2011). Identification of benzophenone C-glucosides from mango tree leaves and their inhibitory effect on triglyceride accumulation in 3T3-L1 adipocytes. *Journal of Agricultural and Food Chemistry*, **59**, 11526-11533.
- Zhang, Y., Liu, X., Han, L., Gao, X., Liu, E. & Wang, T. (2013). Regulation of lipid and glucose homeostasis by mango tree leaf extract is mediated by AMPK and PI3K/AKT signaling pathways. *Food Chemistry*, **141**, 2896-2905.
- Zielinski, H., Michalska, A., Amigo-Benavent, M., Del Castillo, M.D. & Piskula, M.K. (2009). Changes in protein quality and antioxidant properties of buckwheat seeds and groats induced by roasting. *Journal of Agricultural and Food Chemistry*, **57**, 4771-4776.

SUPPLEMENTARY MATERIAL CHAPTER 5

Table S1 Retention times and UV-Vis characteristics of additional phenolic compounds (A–I) selected for quantification in the current study^a, based on previously reported data^b.

Current Study ^a			Previously Reported Data ^b				
Peak	t _R , min	λ _{max} , nm	Peak	t _R , min	Proposed Compound	MW	Molecular Formula
A	3.86	235, 290, 320 sh	a	4.06	Maclurin-di- <i>O,C</i> -hexoside	586	C ₂₅ H ₃₀ O ₁₆
B	11.40	240, 283	A	11.61	unidentified	396	C ₁₈ H ₂₀ O ₁₀
C	19.73	260, 320, 360	k	18.31	Tetrahydroxyxanthone- <i>C</i> -hexoside dimer	842	C ₃₈ H ₃₄ O ₂₂
D	20.45	260, 320, 360	l	19.02	Tetrahydroxyxanthone-di- <i>O,C</i> -hexoside	584	C ₂₅ H ₂₈ O ₁₆
E	25.54	280 ^c	s	24.38	Eriodictyol- <i>O</i> -hexose- <i>O</i> -deoxyhexoside	596	C ₂₇ H ₃₂ O ₁₅
F	30.76	280 ^c	v	29.28	Naringenin- <i>O</i> -hexose- <i>O</i> -deoxyhexoside	580	C ₂₇ H ₃₂ O ₁₄
G	31.89	280 ^c	w	30.36	Naringenin- <i>O</i> -hexose- <i>O</i> -deoxyhexoside	580	C ₂₇ H ₃₂ O ₁₄
H	35.58	288	x	33.54	3-Hydroxyphloretin-3',5'-di- <i>C</i> -hexoside	614	C ₂₇ H ₃₄ O ₁₆
I	39.70	260, 320, 360	y	37.41	Tetrahydroxyxanthone- <i>C</i> -hexoside isomer	422	C ₁₉ H ₁₈ O ₁₁

^aReversed phase-liquid chromatographic (RP-LC) separation achieved on an Agilent 1200 series HPLC, using the optimised chromatographic conditions and online mixing. ^bCompiled from Chapter 3. RP-LC separation achieved on a Waters UPLC system, using the optimised chromatographic conditions and a premix of 45 methanol:55 acetonitrile (v.v⁻¹). ^cSpectra of the flavanones also showed an undefined shoulder around 310-330 nm. sh = shoulder.

Table S2 Mean values^a for the major benzophenones and xanthenes in 40% aqueous ethanolic extracts of *Cyclopia genistoides* as a function of oxidation temperature and time.

Time (h)	Benzophenones				Xanthenes			
	3- β -D-Glucopyranosyl-4- β -D-glucopyranosyloxy-iriflophenone		3- β -D-Glucopyranosyl-iriflophenone		Mangiferin		Isomangiferin	
	80 °C	90 °C	80 °C	90 °C	80 °C	90 °C	80 °C	90 °C
0	1.2940 ab ^b	1.3380 a	0.0955 a	0.0970 a	5.4290 a	5.4665 a	0.5695 a	0.6290 a
1	1.2865 abc	1.2853 b	0.0830 b	0.0865 b	4.7343 b	4.5320 b	0.5350 b	0.5568 b
2	1.2885 abc	1.2815 bc	0.0803 bc	0.0843 b	4.5735 bc	4.0895 c	0.5208 c	0.5203 c
3	1.2927 abc	1.2665 bcd	0.0805 bc	0.0843 b	4.2375 de	3.8428 d	0.5145 cd	0.4955 d
4	1.2835 bc	1.2628 cd	0.0760 cd	0.0773 cd	4.4690 cd	3.6128 e	0.5100 cd	0.4758 e
5	1.2850 bc	1.2575 d	0.0745 de	0.0785 c	4.2493 de	3.4048 f	0.5040 de	0.4540 f
6	1.2813 bc	1.2533 de	0.0730 def	0.0758 cde	4.2278 e	3.2753 g	0.5023 de	0.4473 f
7	1.2793 bc	1.2350 ef	0.0730 def	0.0713 efg	4.1468 ef	3.1560 h	0.4933 ef	0.4295 g
8	1.2893 abc	1.2340 ef	0.0715 defg	0.0730 def	3.9890 fg	3.0663 i	0.4850 f	0.4278 g
9	1.3015 ab	1.2290 fg	0.0700 efg	0.0703 fg	3.8427 gh	3.0128 i	0.4815 f	0.4255 g
10	1.3105 a	1.2285 fg	0.0683 fghij	0.0685 fg	3.8208 ghi	2.8660 j	0.4808 f	0.4050 h
11	1.2960 ab	1.2218 fg	0.0693 efghi	0.0668 gh	3.8080 ghi	2.7965 jk	0.4878 f	0.3998 hi
12	1.3000 ab	1.2128 gh	0.0670 ghijk	0.0620 hi	3.6293 hij	2.7510 k	0.4830 f	0.3888 ij
13	1.2953 ab	1.2097 gh	0.0648 hijkl	0.0617 i	3.5970 ijk	2.6400 l	0.4660 g	0.3830 j
14	1.2915 abc	1.1953 hi	0.0645 ijkl	0.0573 ij	3.5413 jk	2.6387 l	0.4643 g	0.3783 j
15	1.3003 ab	x ^c	0.0633 jkl	x ^c	3.5163 jk	x ^c	x ^c	x ^c
16	1.2880 abc	1.1810 i	0.0597 lm	0.0555 j	3.3773 k	2.4580 m	0.4453 hi	0.3403 k
18	1.2530 de	–	0.0578 m	–	3.0218 lm	–	0.4458 h	–
20	1.2683 cd	–	0.0618 klm	–	2.7890 m	–	0.4315 ij	–
22	1.2528 de	–	0.0683 fghij	–	2.9995 lm	–	0.4245 j	–
24	1.2480 de	–	0.0650 hijkl	–	3.0620 l	–	0.4293 j	–
% Change	–3.55	–11.73	–31.94	–42.78	–43.60	–55.04	–24.62	–45.90

^aIn units of g of compound.100 g of plant material⁻¹. ^bMeans in the same column with different letters are significantly different ($p < 0.05$).

^cMean value for this time point removed as an outlier (refer to experimental section).

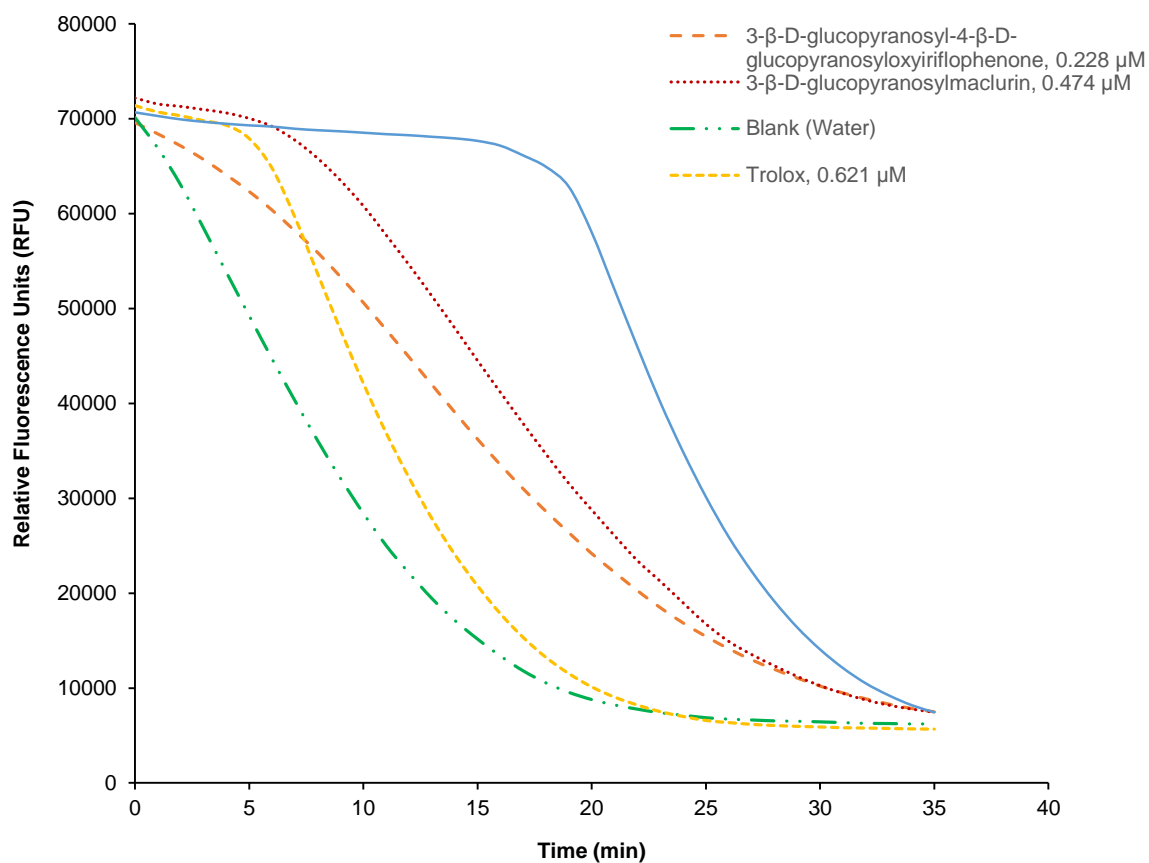


Figure S1 ORAC curves for the benzophenones 3- β -D-glucopyranosyl-4- β -D-glucopyranosyloxyiriflophenone (0.228 μ M) and 3- β -D-glucopyranosylmaclurin (0.474 μ M) in relation to the Trolox reference standard at 0.621 and 3.104 μ M.

CHAPTER 6

Thermal Degradation Kinetics Modelling
of Benzophenones and Xanthenes in Aqueous Model Systems:
Structure-Stability Relationships, and Temperature and pH Effects

ABSTRACT

The thermal stabilities of three benzophenones (3- β -D-glucopyranosyl-4- β -D-glucopyranosyloxyiriflophenone, 3- β -D-glucopyranosyliriflophenone and 3- β -D-glucopyranosylmaclurin) and two xanthones (mangiferin and isomangiferin) were kinetically assessed in aqueous model solutions at pH 5, which represents the pH of honeybush aqueous infusions and extracts. Kinetic studies were conducted over a wide temperature range, while the effect of pH (pH 3, 4, 5, 6 and 7) on the thermal stability of mangiferin was also investigated. The degradation of the target compounds followed first-order reaction kinetics under all evaluated conditions, and the temperature-dependence of the reaction rate constants could adequately be described by the Arrhenius equation. The thermal stability of the compounds (pH = 5, 110 °C) decreased in the order 3- β -D-glucopyranosyl-4- β -D-glucopyranosyloxyiriflophenone > isomangiferin > 3- β -D-glucopyranosyliriflophenone > mangiferin > 3- β -D-glucopyranosylmaclurin. Additional glucosylation on the A-ring of the benzophenones significantly increased thermal stability, whilst increased B-ring hydroxylation had the opposite effect. Isomangiferin was more stable than its regio-isomer, mangiferin, indicating that the position of glycosylation also affects the thermal stability of the xanthones. The higher thermal stabilities of mangiferin and isomangiferin compared to that of their benzophenone precursor, 3- β -D-glucopyranosylmaclurin, may be attributed to the presence of the xanthone nucleus (C-ring). The degradation rate of mangiferin rapidly increased as the pH was increased from 3 to 7, and the pH-dependence of the reaction rate constant at 100 °C followed an exponential relationship. Thermal degradation products were tentatively identified by LC-DAD-ESI-MS and –MS/MS. Thermally-induced degradation reactions principally comprised isomerisation and dimerisation, and the benzophenones were also converted to these xanthones. While 3- β -D-glucopyranosyl-4- β -D-glucopyranosyloxyiriflophenone and 3- β -D-glucopyranosyliriflophenone only formed trace quantities of mangiferin and isomangiferin upon thermal treatment, this was the primary conversion reaction for 3- β -D-glucopyranosylmaclurin. The corresponding rates of conversion of 3- β -D-glucopyranosylmaclurin to mangiferin and isomangiferin were also computed at selected temperatures, indicating that mangiferin, as the C-2 isomer, is formed preferentially.

1. INTRODUCTION

Benzophenones and xanthenes are phenolic compound sub-classes that are both privileged and unique. The benzophenones have a fairly limited distribution in nature, principally occurring in three Guttiferae genera, namely *Clusia*, *Garcinia* and *Hypericum* (Bagett *et al.*, 2005). The xanthenes also have a very restricted occurrence, with the majority of natural xanthenes found in just two families of higher plants – the Guttiferae and Gentianaceae (as reviewed by Sultanbawa, 1980; Bennett & Lee, 1989; and Vieira & Kijjoa, 2005). The benzophenones comprise a 13-carbon core (Figure 1) that can be prenylated and/or further cyclised producing numerous structurally unique compounds. Structurally, the xanthenes are characterised by a basic dibenzo- γ -pyrone structure (Figure 1), with varying degrees of hydroxylation, methoxylation, alkylation, prenylation, geranylation and/or glycosylation. In certain cases the prenyl group may undergo further change, including its characteristic oxidative cyclisation with an *ortho*-OH group to form a chromene ring.

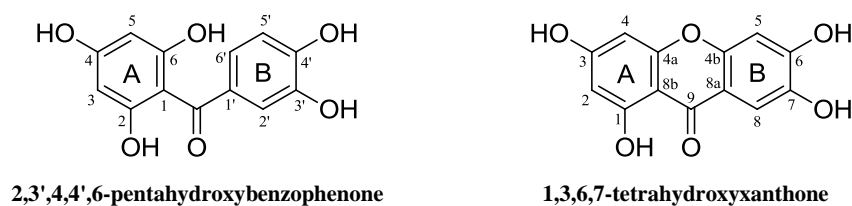


Figure 1 Chemical structures of a polyoxygenated benzophenone and xanthone.

It has been postulated that the polyoxygenated benzophenones are the precursors of the polyoxygenated xanthenes, and this biosynthetic relationship have been deliberated in numerous papers (as reviewed by Sultanbawa, 1980; Bennett & Lee, 1989; Negi *et al.*, 2013). A number of mechanisms have been suggested for the transformation of polyoxygenated benzophenones to their corresponding polyoxygenated xanthone analogues, of which direct/phenol oxidative coupling (Lewis, 1963; Atkinson & Lewis, 1969) involving radical intermediates appears to be most likely. Oxidative coupling can occur *ortho* or *para* only to an activating hydroxy group, leading to the formation of isomeric xanthenes.

Consequently, polyoxygenated xanthenes and their benzophenone precursor compounds have been found to co-occur in plant species, as reported for the traditional medicinal plants *Mangifera indica* (family Anacardiaceae; Tanaka *et al.*, 1986), *Aquilaria sinensis* (family Thymelaeaceae; Feng *et al.*, 2011) and *Cyclopia* spp. (family Fabaceae, Kokotkiewicz *et al.*, 2012, 2013), amongst others. The co-occurrence of xanthenes and benzophenones in the genus *Cyclopia* is of interest given the utilisation of *Cyclopia* as honeybush herbal tea, and its application as food ingredient and nutraceutical extracts (Joubert *et al.*, 2011). Schulze *et al.* (2015a) recently demonstrated that honeybush herbal tea represents a rich source of the glucosylxanthenes mangiferin and isomangiferin, and the benzophenones 3- β -D-glucopyranosyl-4- β -D-glucopyranosyloxyiriflophenone and 3- β -D-glucopyranosyliriflophenone, and could therefore contribute substantially to their dietary intake. Honeybush herbal tea can also contribute small amounts to the dietary exposure of the benzophenone 3- β -D-glucopyranosylmaclurin. Apart from mango, this compound is not commonly found in other food or beverage products.

These benzophenone and xanthone constituents have gradually risen in importance in light of their medicinal properties. Mangiferin is known to exert a wide range of biological properties including antioxidant and antidiabetic (as reviewed by Vyas *et al.*, 2012). Schulze *et al.* (2015b) recently showed a similar glucose lowering efficacy for mangiferin and its regio-isomer isomangiferin in vitro, using C2C12 muscle cells as model. The α -glucosidase inhibitory activities of these xanthenes, as well as those of 3- β -D-glucopyranosylmaclurin, 3- β -D-glucopyranosyliriflophenone and 3- β -D-glucopyranosyl-4- β -D-glucopyranosyloxyiriflophenone (Feng *et al.*, 2011; Zhang *et al.*, 2013a; Chapter 4), are also of

interest to the food and nutraceutical industries in light of their potential application as natural anti-obesity and antidiabetic agents.

Xanthone- and benzophenone-rich extracts from natural sources such as the fynbos plant *Cyclopia* therefore have tremendous potential for commercialisation. However, for the commercial development of such biofunctional ingredients/extracts or therapeutic agents, knowledge regarding the thermal stability of the principal bio-actives are required as these compounds may be subjected to elevated temperatures during various unit operations in their manufacture (*e.g.* extraction, concentration and spray-drying). Similarly, the bio-actives may also be exposed to severe thermal treatments during their incorporation into food and beverage products such as baking, extrusion processing, pasteurisation/sterilisation and so forth.

Thus far, investigations of the thermal stability of compounds from the benzophenone and xanthone phenolic subclasses have been very limited. In the present study (Chapter 5), it was demonstrated that mangiferin, isomangiferin, 3- β -D-glucopyranosyl-4- β -D-glucopyranosyloxyiriflophenone and 3- β -D-glucopyranosyliriflophenone are susceptible to thermal degradation upon high-temperature chemical oxidation of *C. genistoides* plant material, and that their degradation may adequately be described by first-order degradation kinetics. Preliminary insight into temperature effects was also provided and structure-stability relationships explored.

As *C. genistoides* plant material represents a complex matrix, the aim of the present work was to kinetically assess the thermal stability of the aforementioned compounds in aqueous model solutions, which would thereby minimise potential matrix effects. Even though 3- β -D-glucopyranosylmaclurin is not a major constituent of *C. genistoides* extracts (Chapter 3 and 5), it was also included as target compound in the current study based on its reported biological properties and biogenetic significance (Fujita & Inoue 1980a, 1980b, 1981). Inclusion of 3- β -D-glucopyranosylmaclurin will furthermore provide information on the impact of B-ring hydroxylation on the thermal stability of benzophenones, and enable a direct comparison of the thermal stabilities of 3- β -D-glucopyranosylmaclurin and its xanthone analogues, mangiferin and isomangiferin. Aqueous solutions of the individual target compounds (pH 5) were subjected to thermal treatments at five different temperatures, and their degradation followed by ultra-high performance liquid chromatography coupled with diode-array detection (UHPLC-DAD). Towards this end, a rapid UHPLC-DAD method was developed to provide optimised chromatographic separation of the target compounds and their degradation products. The degradation products were characterised by coupling of the optimised LC method to electrospray ionisation mass spectrometry (ESI-MS) and tandem MS detection. This provided the first glimpse into the thermal degradation pathways of these bio-active xanthenes and benzophenones in an aqueous environment. The reaction rate constants for the degradation of the target compounds, as well as the rate constants for selected conversion reactions, were computed using appropriate mathematical models. Hereby, the temperature-dependence of the degradation rate constants was also characterised mathematically by calculation of the Arrhenius activation energy. The role of pH in the stability of the xanthenes was explored by kinetically assessing the thermal stability of mangiferin as a function of pH (pH 3-7).

2. MATERIALS AND METHODS

2.1. Chemicals

General laboratory chemicals (ascorbic acid; potassium phosphate monobasic, KH_2PO_4 ; dimethylsulfoxide, DMSO) were reagent grade, provided by Sigma-Aldrich (St. Louis, MO, USA). HPLC gradient-grade acetonitrile and formic acid (98-100%) were purchased from Sigma-Aldrich and Merck Millipore (Darmstadt, Germany), respectively. HPLC-grade water was prepared using Elix and Milli-Q academic (Merck Millipore) water purification systems in tandem. Authentic reference standards with purities > 95%, namely mangiferin and 3- β -D-glucopyranosyliriflophenone, were obtained from Sigma-Aldrich. 3- β -D-Glucopyranosylmaclurin (95% purity by LC-ESI-MS) and 3- β -D-glucopyranosyl-4- β -D-glucopyranosyloxyiriflophenone (99% purity by LC-ESI-MS) were isolated from *C. genistoides* (Chapter 4). Isomangiferin, isolated from *C. genistoides* (ca. 99% purity by LC-DAD), was kindly supplied by Dr Elize Willenburg of the Agricultural Research Council of South Africa (Post-Harvest and Wine Technology Division, ARC Infruitec-Nietvoorbij, Stellenbosch, South Africa). Stock solutions (ca. 6 mM) of 3- β -D-glucopyranosyl-4- β -D-glucopyranosyloxyiriflophenone and 3- β -D-glucopyranosylmaclurin were prepared in HPLC-grade water, and those of 3- β -D-glucopyranosyliriflophenone, mangiferin and isomangiferin in 100% DMSO. Aliquots of the stock solutions were frozen at -20 °C until further use.

2.2. Optimisation and Validation of an UHPLC-DAD Method for Thermal Degradation Kinetics Experiments

UHPLC-DAD method development and validation were conducted on an Agilent 1290 UHPLC instrument (maximum pressure 1000 bar), equipped with an in-line degasser, binary pump, autosampler, column thermostat and diode-array detector controlled by OpenLab Chemstation software (Agilent Technologies Inc., Santa Clara, CA, USA).

A standard calibration mixture and one sample each of thermally-treated solutions of 3- β -D-glucopyranosyl-4- β -D-glucopyranosyloxyiriflophenone, 3- β -D-glucopyranosylmaclurin, 3- β -D-glucopyranosyliriflophenone, mangiferin and isomangiferin (generated during scouting experiments) were used for method development. Optimised separation of the target compounds and their degradation products was achieved on an Agilent Zorbax Eclipse Plus C_{18} column (Rapid Resolution HD; 1.8 μm , 2.1 \times 50 mm) thermostatted to 23 °C. The mobile phase comprised of (A) 0.1% formic acid in water (v.v⁻¹) and (B) acetonitrile. The flow rate was 0.7 mL.min⁻¹ and a multi-linear gradient was performed as follows: 5-22% B (0-2.2 min), 22-50% B (2.2-2.6 min), 50% B (2.6-4.1 min), 50-5% B (4.1-4.6 min). The column was re-equilibrated for 2 min.

The optimised UHPLC-DAD method was preliminary validated in terms of specificity, linearity and range, and analytical precision (Shabir *et al.*, 2007). In addition, the stability of the compounds in the reaction solvent (0.1 M phosphate buffer), used for thermal degradation experiments, was also assessed. For method validation purposes, a standard calibration mixture comprising of 3- β -D-glucopyranosyl-4- β -D-glucopyranosyloxyiriflophenone (0.0499 $\mu\text{g}.\mu\text{L}^{-1}$), 3- β -D-glucopyranosylmaclurin (0.0753 $\mu\text{g}.\mu\text{L}^{-1}$), 3- β -D-glucopyranosyliriflophenone (0.0414 $\mu\text{g}.\mu\text{L}^{-1}$), mangiferin (0.0363 $\mu\text{g}.\mu\text{L}^{-1}$) and isomangiferin (0.0415 $\mu\text{g}.\mu\text{L}^{-1}$) was prepared in HPLC-grade water or 0.1 M phosphate buffer solution, as required. The standard calibration mixtures contained ascorbic acid at a final concentration of ca. 9.5 mg.mL⁻¹ and were filtered using 0.22 μm pore-size Millex-GV syringe filters (4 mm diameter, Millipore) prior to use. Peak purity of the target compounds in the thermally-treated solutions was established by comparing their MS spectra with those of authentic reference standards in the aqueous calibration mixture. Calibration curves were set up for the target compounds to test the linearity of the DAD response. UV spectra were recorded between 200-500 nm at an acquisition rate of 20 Hz, with selective wavelength monitoring at 288 and 320 nm. 3- β -D-Glucopyranosyl-4- β -D-glucopyranosyloxyiriflophenone and 3- β -D-glucopyranosyliriflophenone were monitored at 288 nm, while 3- β -D-

glucopyranosylmaclurin, mangiferin and isomangiferin were monitored at 320 nm. The aqueous calibration mixture was injected at seven different injection volumes (0.5, 1, 2, 4, 7, 10 and 15 μL) to cover the different quantities of the compounds in the thermally-treated solutions over the different treatment times. Linear regression, using the least squares method (Microsoft Excel 2010, Microsoft Corporation, Redmond, WA, USA), was performed to determine the slope, y-intercept and coefficient of determination (R^2) (Table 1).

Table 1. Characteristics of calibration curves obtained for UHPLC analysis of phenolic standards.

Phenolic Standard	Wavelength, nm	Linearity Range, μg on-column	Regression Equation ^a	Coefficient of Determination, R^2
3- β -D-Glucopyranosyl-4- β -D-glucopyranosyloxiriflophenone (1)	288	0.0249 – 0.7484	$y = 2131.9x - 1.4838$	0.9999
3- β -D-Glucopyranosylmaclurin ^b (2)	320	0.0377 – 0.7532	$y = 1687.7x - 1.8687$	0.9999
3- β -D-Glucopyranosylriflophenone (3)	288	0.0207 – 0.6215	$y = 2632.8x - 1.7907$	0.9999
Mangiferin (4)	320	0.0182 – 0.5448	$y = 2968.6x - 2.1205$	0.9999
Isomangiferin (5)	320	0.0208 – 0.6231	$y = 2586.1x - 2.0792$	0.9999

^a y = analyte response (peak area in mAU) and x = amount of standard compound injected (μg).

^b Only six calibration points, with maximum injection volume equal to 10 μL .

Intra-day precision was determined by consecutive repeat injections ($n = 6$, $v_{\text{inj}} = 7 \mu\text{L}$) of the aqueous calibration mixture on the same day. The same procedure was repeated over three consecutive days ($n = 3$) to determine the inter-day precision. The percentage relative standard deviation (% RSD) was determined for replicate injections on each day (intra-day precision) and for mean values per day (inter-day precision) by considering the respective peak areas (Table S1, Supplementary Material, page 187).

The stability of the target compounds in 0.1 M aqueous phosphate buffer solution (pH 5) during UHPLC analysis was assessed by repeat injections of the calibration mixture over a 12 h period ($n = 6$, $v_{\text{inj}} = 7 \mu\text{L}$). The % RSD over the time points during this period was used to evaluate the stability of the compounds in the reaction solvent. The stability of mangiferin was also assessed in 0.1 M aqueous phosphate buffer solution with pH 3, 4, 6 and 7, using the aforementioned procedure (Table S2, Supplementary Material, page 187).

2.3. Thermal Degradation Kinetics Experiments

Thermal degradation experiments were conducted at five temperatures for each of the target compounds (0.1 mM in 0.1 M phosphate buffer solution, pH 5). The temperature range of each compound differed to accommodate thermal degradation within practically-feasible time periods (from 40 min/0.667 h to 164 h) and to fall within the capabilities of the heating block (Stuart, Bibby Scientific Limited, Stone, UK) and reaction vials. The selected temperatures ranged between 60 and 150 $^{\circ}\text{C}$, depending on the thermal stability of the specific compound, and the five selected temperatures differed by 10 $^{\circ}\text{C}$ each. The thermal stability of mangiferin in the aqueous buffer solution was also assessed at four additional pH levels (pH 3, 4, 6 and 7), with five temperatures at each evaluated pH. The temperature range for each pH was also varied to accommodate the lesser or higher thermal stability of mangiferin under the different conditions.

For each compound-temperature combination and each temperature-pH combination (only mangiferin), one aliquot of the appropriate stock solution was removed from the freezer and defrosted at room temperature. The stock solution was diluted with 0.1 M phosphate buffer solution to obtain 20 mL of a 0.1 mM working solution. Aliquots (0.8 mL) of the working solution were transferred to 5 mL glass micro reaction vessels (Supelco, Bellefonte, PA, USA) ($n = 24$), sealed, and placed in a pre-heated Stuart heating block equipped with digital temperature control (Figure 2). The remaining

sample volume received no thermal treatment (control sample). Each of the individual holes in the heating block contained approximately 1.5 mL of glycerin to improve heat transfer.



Figure 2 Photo depicting the experimental set-up – Stuart heating block, thermostatted to a specific temperature (110 °C), containing 24 micro reaction vessels.

Replicate samples ($n = 3$) were removed from the heating block at predetermined time points ($n = 8$) and cooled for 15 min in an ice bath. Each of the time points were selected to achieve successive reductions of *ca.* 0.01 mM in analyte concentration, with a final concentration of *ca.* 0.01 mM. The replicate samples were filtered (0.22 μm pore size, 4 mm diameter Millex-GV syringe filters; Merck Millipore) and an aliquot of each removed for immediate analysis by UHPLC-DAD. Samples were prepared for UHPLC analysis by adding 20 μL of 10% aqueous ascorbic acid (m.v^{-1}) to 200 μL of the filtrate (final concentration = 9.1 mg ascorbic acid. mL^{-1}). The remaining sample volume was aliquoted and frozen until further use. The control sample was also analysed by UHPLC to determine the initial concentration of the compound (C_0) before heating.

2.4. Quantitative Determination of Target Xanthenes and Benzophenones in Thermally-Treated Solutions by UHPLC-DAD

The evolution of the target xanthenes and benzophenones in the thermally-treated solutions were monitored using the newly-developed and validated UHPLC-DAD method (section 2.2.). All samples were analysed in duplicate using an injection volume of 10 μL , and calibration curves were constructed weekly as described in section 2.2.

Univariate analysis of variance (ANOVA) using the General Linear Models Procedure was performed for each compound-temperature and pH-temperature (only mangiferin) combination separately (SAS, version 9.2; SAS Institute, Cary, NC, USA). The Shapiro-Wilk test was performed to test for normality. Fisher's least significant difference was calculated at the 5% level ($p < 0.05$) to compare means across treatment times. The average concentrations of the target compounds as a function of treatment temperature and time is supplied in Tables S3-S11 (Supplementary Material, pp. 188-192).

2.5. Determination of Thermal Degradation Kinetic Parameters

Results from our previous study (*C. genistoides* plant material; Chapter 5), indicated that the degradation of benzophenones and xanthenes follows first-order degradation kinetics, and it was therefore assumed that similar first-

order degradation kinetics would apply in the current study (aqueous model systems). For a first-order reaction, the rate of degradation of a compound is given by

$$C = C_0 e^{(-kt)} \quad (1)$$

Where C is the concentration of the compound (mM) at time t , C_0 is the initial concentration of the compound (mM), k is the degradation rate constant (h^{-1}) and t is the treatment time (h).

The kinetic data generated in the current study (individual replicates) were fitted to eq 1, and the rate constants determined by non-linear regression using DRC package in R (R Foundation, Vienna, Austria). The goodness-of-fit was determined by evaluating the values for the coefficient of determination (R^2). For each compound (pH 5) and each pH level (only mangiferin), the computed values for k were compared over the different treatment temperatures ($n = 5$) to establish significant differences at the 5% significance level (DRC package in R). The values for k computed for all compounds (pH 5) at $110\text{ }^\circ\text{C}$ ($k_{110\text{ }^\circ\text{C}}$) were also compared across the different compounds to establish significant differences stemming from structural features. Similarly, the values for $k_{100\text{ }^\circ\text{C}}$ computed for mangiferin at pH 3, 4, 5, 6 and 7 were compared across the different pH levels to establish whether pH significantly affects the thermal stability of mangiferin.

The effect of temperature on the reaction rate constants of each compound (pH 5), and the effect of temperature on the reaction rate constants of mangiferin at various pH levels, were evaluated by calculating the activation energy according to the Arrhenius equation. This model is based on the classical approach used for chemical reactions, which defines a reaction rate constant (k) that depends on temperature (T) according to an Arrhenius law:

$$k = A e^{\left(-\frac{E_a}{RT}\right)} \quad (2)$$

The linearised form is:

$$\ln k = -\left(\frac{E_a}{R}\right) \cdot \frac{1}{T} + \ln A \quad (3)$$

Where A is the so-called ‘pre-exponential factor’ (sometimes called the frequency factor, and denoted as k_0), E_a the activation energy ($\text{J}\cdot\text{mol}^{-1}$), T the absolute temperature in $^\circ\text{K}$, and R the ideal gas constant ($8.31\text{ J}\cdot\text{mol}^{-1}\cdot\text{K}^{-1}$).

The activation parameters were estimated by substituting the estimated values of the degradation rate constants (k , eq 1) and the corresponding temperatures into eq 2, and performing non-linear regression (DRC Package in R). For a comparison, the activation parameters were also computed by estimation of the slope and y-intercept by a linear regression of $\ln k$ vs $1/T$ according to eq 3 (DRC Package in R).

2.6. Identification of Thermal Degradation Products by LC-DAD-ESI-MS and –MS/MS

One sample of each of the compounds (3- β -D-glucopyranosyl-4- β -D-glucopyranosyloxiriflophenone, 3- β -D-glucopyranosylmaclurin, 3- β -D-glucopyranosyliriflophenone, mangiferin and isomangiferin) in 0.1 M phosphate buffer solution (pH 5), thermally treated at $110\text{ }^\circ\text{C}$, was selected for LC-DAD-ESI-MS and –MS/MS analyses. An aqueous calibration mixture was also included for the assessment of peak purity (indicated in section 2.2) and confirmation of peak identities in the thermally-treated solutions.

LC-DAD-ESI-MS and –MS/MS analyses were conducted on an Acquity UPLC system equipped with a binary solvent manager, sample manager, column heating compartment and photodiode-array detector coupled to a Synapt G2 Q-TOF system equipped with an electrospray ionisation source (Waters; Milford, MA). For front end separation, the optimised UHPLC method was used. Data were acquired in resolution mode (scanning from 150-1500 amu) and MS/MS scanning mode and processed using MassLynx v.4.1 software (Waters). The instrument was operated in positive and negative ionisation modes and calibrated using a sodium formate solution. Leucine enkephalin was used for lockspray (ESI⁺, lock

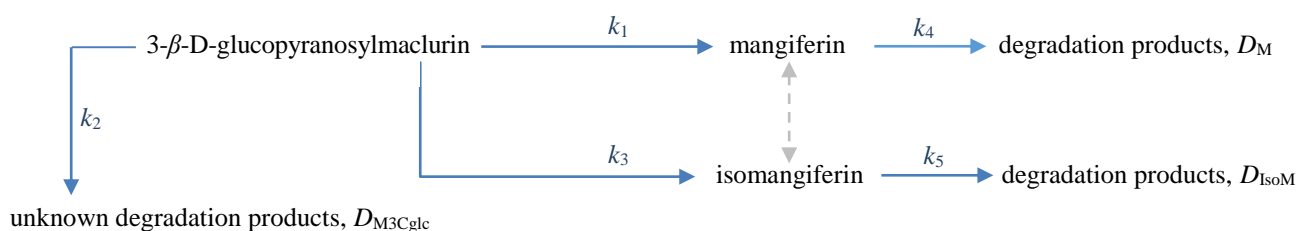
mass 556.2771 amu; ESI⁻, lock mass 554.2615 amu). The MS parameters were as follows: capillary voltage 2.5 kV, sampling cone voltage 15.0 V, source temperature 120 °C, desolvation temperature 275 °C, desolvation gas flow (N₂) 650 L.h⁻¹, cone gas flow (N₂) 50 L.h⁻¹. For MS/MS experiments, the trap collision energy (CE) was set to 30 V. The eluent was split *ca.* 1:1 prior to introduction into the ionisation chamber. The injection volume was 10 µL and UV-Vis spectra were acquired over 230–500 nm at 20 Hz.

2.7. Evolution of Mangiferin and Isomangiferin in Thermally-Treated Solutions of 3-β-D-Glucopyranosylmaclurin as a Function of Treatment Temperature and Time

Upon thermal treatment, 3-β-D-glucopyranosylmaclurin was predominantly converted to the xanthenes mangiferin and isomangiferin (from section 2.6), and it was of interest to calculate the rates of the individual conversion reactions. The evolution of mangiferin and isomangiferin in thermally-treated solutions of 3-β-D-glucopyranosylmaclurin was thus monitored as a function of treatment temperature (90, 100 and 110 °C) and time. For this purpose, additional calibration curves were constructed for mangiferin and isomangiferin in the lower concentration ranges of 0.0090–0.2700 and 0.0078–0.2337 µg on-column, respectively. The corresponding regression equations for mangiferin and isomangiferin were $y = 3066.0x - 0.7453$ and $y = 2617.1x - 0.7659$, respectively, with R^2 values larger than 0.9999 in both instances.

Univariate analysis of variance (ANOVA) using the General Linear Models Procedure was performed for each compound-temperature combination separately (SAS, version 9.2). The Shapiro-Wilk test was performed to test for normality. Fisher's least significant difference was calculated at the 5% level ($p < 0.05$) to compare means across treatment times. The average concentrations of mangiferin and isomangiferin as a function of treatment temperature and time are supplied in Tables S12 and S13 (Supplementary Material, page 193), respectively.

Kinetic assessment of the thermal stabilities of mangiferin and isomangiferin in aqueous model solutions (pH 5, section 2.5) had indicated that they are also prone to degradation upon thermal treatment. Thus, while mangiferin and isomangiferin are formed via a conversion reaction of 3-β-D-glucopyranosylmaclurin, they are degraded simultaneously. In addition, mangiferin and isomangiferin can also be converted to one another (from section 2.6), but this reaction was deemed negligible, and was not taken into account in the current mathematical model. Upon thermal treatment, 3-β-D-glucopyranosylmaclurin was also degraded to unknown degradation products, D_{M3Cglc} , albeit to a lesser extent (these minor compounds were not identified by LC-DAD-ESI-MS or monitored over thermal treatment time). This scenario can thus be depicted as follows:



Where the total rate of degradation for 3-β-D-glucopyranosylmaclurin (k_{total}) is equal to the sum of its degradation rate to unknown products D_{M3Cglc} (k_2) and its conversion to mangiferin (k_1) and isomangiferin (k_3):

$$k_{total} = k_1 + k_2 + k_3 \quad (4)$$

In accordance with eq 1, the change in the concentration (C) of 3- β -D-glucopyranosylmaclurin (M3Cglc) over time is given by:

$$\begin{aligned}\frac{d[M3Cglc]}{dt} &= -k_{total} [M3Cglc] \\ \text{thus: } [M3Cglc] &= [M3Cglc]_0 \cdot e^{-k_{total} \cdot t} \\ \text{thus: } \ln[M3Cglc] &= -k_{total} \cdot t + \ln[M3Cglc]_0\end{aligned}\quad (5)$$

For mangiferin (M) and isomangiferin (IsoM), changes in their concentrations over time are given by eqs 6 and 7, respectively:

$$\begin{aligned}\frac{d[M]}{dt} &= k_1 [M3Cglc] - k_4 [M] = k_1 ([M3Cglc]_0 \cdot e^{-k_{total} \cdot t}) - k_4 [M] \\ \text{thus, } [M] &= \frac{e^{-(k_{total} + k_4) \cdot t} \cdot (e^{k_{total} \cdot t} - e^{k_4 \cdot t}) \cdot k_1 [M3Cglc]_0}{k_{total} - k_4}\end{aligned}\quad (6)$$

$$\begin{aligned}\frac{d[IsoM]}{dt} &= k_3 [M3Cglc] - k_5 [IsoM] = k_3 ([M3Cglc]_0 \cdot e^{-k_{total} \cdot t}) - k_5 [IsoM] \\ \text{thus, } [IsoM] &= \frac{e^{-(k_{total} + k_5) \cdot t} \cdot (e^{k_{total} \cdot t} - e^{k_5 \cdot t}) \cdot k_3 [M3Cglc]_0}{k_{total} - k_5}\end{aligned}\quad (7)$$

Where k_1 and k_3 respectively represent the rates of conversion of 3- β -D-glucopyranosylmaclurin to mangiferin and isomangiferin, and k_4 , k_5 and k_{total} respectively represent the degradation rates of mangiferin, isomangiferin and 3- β -D-glucopyranosylmaclurin (as determined from section 2.5) at each of the respective temperatures. t denotes treatment time in h, and $[M3Cglc]_0$ the initial concentration of 3- β -D-glucopyranosylmaclurin at each of the respective temperatures.

We therefore only had to solve for k_1 and k_3 in eqs 6 and 7, respectively, by substituting the respective concentration values of mangiferin and isomangiferin at each of the selected time intervals t (DRC Package in R). The degradation rate of 3- β -D-glucopyranosylmaclurin to unknown degradation products D_{M3Cglc} (k_2) was then determined by solving for k_2 in eq 5. This process was repeated for each of the treatment temperatures.

3. RESULTS AND DISCUSSION

In this study, the thermal stabilities of glucosylated benzophenones and xanthenes were kinetically assessed in aqueous model solutions for the first time. Based on their dietary importance, the target compounds included three benzophenones, 3- β -D-glucopyranosyl-4- β -D-glucopyranosyloxyiriflophenone (**1**), 3- β -D-glucopyranosylmaclurin (**2**) and 3- β -D-glucopyranosyliriflophenone (**3**), and two xanthenes, mangiferin (**4**) and isomangiferin (**5**). Compounds **1**, **3**, **4** and **5** furthermore represent the major phenolic constituents of aqueous extracts and infusions prepared from *C. genistoides* (Chapter 5; Schulze *et al.*, 2015a). Knowledge regarding the thermally stability of the aforementioned compounds is paramount for the development of high-quality *C. genistoides* extracts destined for the food and nutraceutical industries, as they may be exposed to elevated temperatures during various unit operations in the production and subsequent application of such type extracts.

To enable stability assessment of individual compounds that were either not commercially available or not readily attainable, compounds **1** and **2** were isolated from *C. genistoides* (Chapter 4) and compound **3** was obtained from the compound library of ARC Infruitec-Nietvoorbij (Stellenbosch, South Africa) following its isolation from the same source

material. Herewith, stability assessments were conducted in a phosphate buffer solution of pH 5, as this pH represents the approximate pH of aqueous extracts prepared from “unfermented” and “fermented” (oxidised) *C. genistoides* plant material (results not shown). The thermal stability of mangiferin, as the major phenolic constituent and principal bioactive of *C. genistoides* extracts, was also investigated at pH 3, 4, 6 and 7. These experiments were to provide additional information on the thermal stability of mangiferin during its potential application as beverage ingredient where the pH of its environment might differ from that of the original extract. Aqueous solutions of the individual compounds were subjected to thermal treatments at five different temperatures (range of 50 °C) to establish the relationship between the degradation rate constants and temperature, and to affirm whether it complies with the Arrhenius equation (Peleg *et al.*, 2012). For each compound-temperature combination, and each pH-temperature combination (only mangiferin), the degradation rate constants were computed using non-linear regression (as suggested by Van Boekel, 1996; 2008).

3.1. Thermal Degradation Kinetics Modelling of Benzophenones and Xanthenes in Aqueous Model Systems (pH 5): Structure-Stability Relationships and Temperature Effects

The concentrations of the target compounds in the aqueous model solutions (0.1 M phosphate buffer, pH 5) were monitored as a function of treatment temperature and time (Tables S3-S7, Supplementary Material, pp. 188-190). The experimental data were fitted to eq 1 (page 153), yielding excellent values for the coefficient of determination under all evaluated conditions ($R^2 \geq 0.931$; Table 2), supporting first-order reaction kinetics. The computed degradation rate constants for each of the compounds at the different temperatures, together with the 95% confidence intervals, are provided in Table 2.

The thermal stabilities of the target compounds were found to differ, and therefore the temperature ranges over which the thermal treatments were conducted were compound-specific. For instance, 3- β -D-glucopyranosylmaclurin (**2**) was extremely prone to thermal degradation, and therefore temperatures between 70-110 °C were selected to achieve degradation rates that fell within the experimental domain (refer to section 2.2). Conversely, 3- β -D-glucopyranosyl-4- β -D-glucopyranosyloxiriflophenone (**1**) exhibited a high degree of thermal stability, requiring elevated temperatures of up to 150 °C to induce sufficient degradation for calculation of its degradation rate. The susceptibility of 3- β -D-glucopyranosylriflophenone (**3**), mangiferin (**4**) and isomangiferin (**5**) towards thermally-induced degradation was roughly similar, with experimental temperatures ranging between 90 and 130 °C. Consequently, the first-order degradation constants of the target xanthenes and benzophenones at matching temperatures differed substantially from one another (Table 2). Comparison of the first-order degradation rate constants at 110 °C ($k_{110\text{ }^\circ\text{C}}$), the only treatment temperature shared by all the compounds, indicated that thermal stability decreased in the order **1** > **5** > **3** > **4** > **2**, with **1** the most stable and **2** the least stable. Figure 3 depicts the degradation of the target xanthenes and benzophenones at 110 °C over time. From these degradation curves it is evident that degradation of **1** took more than 160 h to decrease to a final concentration of 0.01 mM, while **2** reached this concentration well within one hour.

The differences in the thermal stabilities of the assessed compounds are related to their chemical structures (Figure 3). For the benzophenones, addition of a glucopyranosyloxy moiety in the A-ring significantly increased thermal stability, whereas increased B-ring hydroxylation had the opposite effect. This is evident from comparison of the $k_{110\text{ }^\circ\text{C}}$ values of the benzophenone **1** (0.0141 h⁻¹) compared to that of its mono-glucopyranosyl analogue **3** (0.217 h⁻¹), differing by a factor of *ca.* 15 (Table 2). Similarly, the $k_{110\text{ }^\circ\text{C}}$ value of **3** compared to that of its 3'-hydroxylated derivative **2** (3.41 h⁻¹) differs by a factor of *ca.* 16 (Table 2). It is readily understood that the 4-*O*-glucosylation would stabilise **1** against high-temperature oxidative degradation. The 4-hydroxy group bears a *p*-relationship to the carbonyl group and is therefore the most susceptible to oxygen-radical formation. Blocking this process by glucosylation at C-4-OH would significantly stabilise this compound.

With regard to the xanthones, isomangiferin (**5**) was approximately one-and-a-half times more stable than its regio-isomer mangiferin (**4**) over the same temperature range (Table 2), indicating that glucosylation at C-4, as opposed to C-2, confers a higher thermal stability to the tetrahydroxanthones.

Table 2 Estimated values for the first-order rate constants (k , h^{-1})^a for the degradation of the target benzophenones (**1–3**) and xanthones (**4–5**) in aqueous model solutions (0.1 M phosphate buffer, pH 5). The values for the 95% confidence intervals and coefficient of determination (R^2) are provided in brackets.

Temperature (°C)	3- β -D-Glucopyranosyl-4- β -D-glucopyranosyloxy-iriflophenone (1)	3- β -D-Glucopyranosyl-maclurin (2)	3- β -D-Glucopyranosyl-iriflophenone (3)	Mangiferin (4)	Isomangiferin (5)
70	–	0.0775 e (0.0744 – 0.0805) ($R^2 = 0.999$)	–	–	–
80	–	0.230 d (0.221 – 0.240) ($R^2 = 0.999$)	–	–	–
90	–	0.677 c (0.649 – 0.704) ($R^2 = 0.998$)	0.0376 e (0.0354 – 0.0397) ($R^2 = 0.995$)	0.0532 e (0.0478 – 0.0586) ($R^2 = 0.997$)	0.0313 e (0.0297 – 0.0329) ($R^2 = 0.999$)
100	–	1.26 b (1.21 – 1.32) ($R^2 = 0.998$)	0.0877 d (0.0823 – 0.931) ($R^2 = 0.996$)	0.165 d (0.148 – 0.182) ($R^2 = 0.996$)	0.116 d (0.109 – 0.123) ($R^2 = 0.996$)
110	0.0141 e,E (0.0135 – 0.0147) ($R^2 = 0.998$)	3.41 a,A (3.27 – 3.56) ($R^2 = 0.990$)	0.217 c,C (0.205 – 0.229) ($R^2 = 0.995$)	0.352 c,B (0.313 – 0.390) ($R^2 = 0.991$)	0.197 c,D (0.185 – 0.208) ($R^2 = 0.995$)
120	0.0398 d (0.0380 – 0.0415) ($R^2 = 0.998$)	–	0.495 b (0.466 – 0.525) ($R^2 = 0.996$)	0.724 b (0.644 – 0.803) ($R^2 = 0.997$)	0.412 b (0.388 – 0.436) ($R^2 = 0.993$)
130	0.109 c (0.104 – 0.114) ($R^2 = 0.995$)	–	1.11 a (1.04 – 1.17) ($R^2 = 0.992$)	1.87 a (1.67 – 2.07) ($R^2 = 0.931$)	1.21 a (1.13 – 1.29) ($R^2 = 0.995$)
140	0.271 b (0.258 – 0.285) ($R^2 = 0.997$)	–	–	–	–
150	0.651 a (0.621 – 0.680) ($R^2 = 0.997$)	–	–	–	–

^aValues in the same column (lowercase) and values in the same row (at 110 °C, uppercase) with different letters are significantly different from one another ($p < 0.05$).

These observations are in accordance with findings on the thermal degradation kinetics modelling of **1**, **3**, **4** and **5** during high-temperature chemical oxidation of *C. genistoides* plant material (Chapter 5), while kinetic data for 3- β -D-glucopyranosylmaclurin (**2**) is presented herein for the first time. Inclusion of **2** in the current study provided additional insight into the thermal stability of the honeybush benzophenones, and in particular insight into the effect of B-ring hydroxylation. Its inclusion also enabled direct comparison of the thermal stability of **2** to that of its xanthone analogues **4** and **5**. The first-order degradation rate constant of **2** at 110 °C was approximately 10- and 17-fold higher than those of **4** and **5**, respectively (Table 2). It is clear that the central ring of the 1,3,6,7-tetrahydroxanthones **4** and **5**, formed by cyclisation of the 2,4,3',4',6-pentahydroxylated structure **2**, conferred a higher thermal stability to the xanthones.

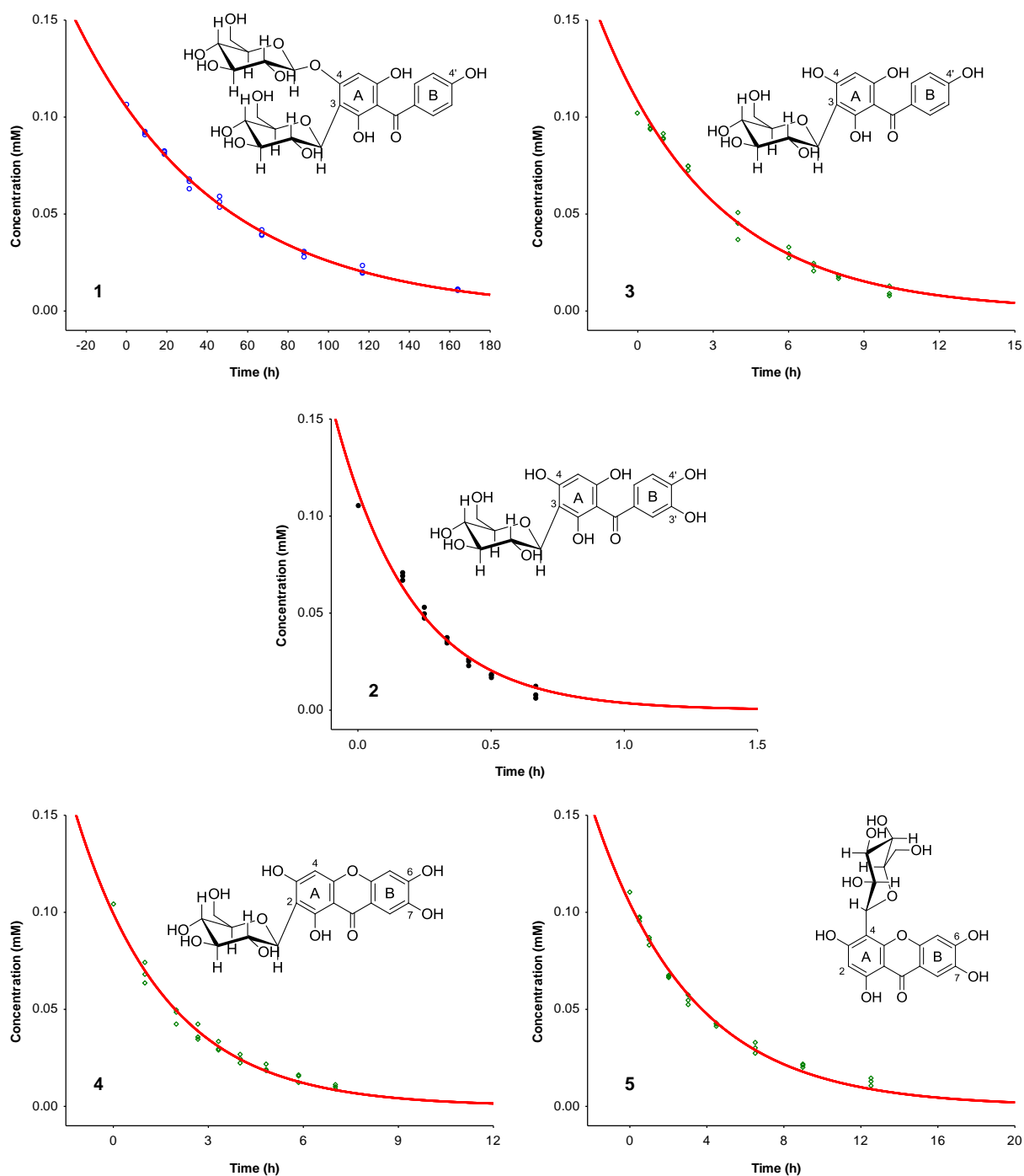


Figure 3 Degradation of the target benzophenones and xanthenes in aqueous model solutions (0.1 M phosphate buffer, pH 5) upon thermal treatment at 110 °C: 3-β-D-glucopyranosyl-4-β-D-glucopyranosyloxyriflophenone (1); 3-β-D-glucopyranosylmaclurin (2); 3-β-D-glucopyranosyliriflophenone (3); mangiferin (4); and isomangiferin (5).

Apart from the high-temperature oxidation study on *C. genistoides* plant material, described in Chapter 5, the thermal stability of compounds from the benzophenone and xanthenes phenolic sub-classes has not been investigated to date. The observations that the thermal stability of compounds from these sub-classes is affected by the position and degree of A-ring glycosylation, as well as the degree of B-ring hydroxylation, are supported by literature on other phenolic sub-classes. An increase in the number of hydroxy groups in the aromatic B-ring of flavonoids has typically been associated with decreased thermal stability of monomeric flavan-3-ols (Wang *et al.*, 2000) and dihydroflavonol rhamnosides (Zhang *et al.*, 2013b). Zielinski *et al.* (2009) also observed lower thermal stability for luteolin derivatives (3',4',5,7-

tetrahydroxyflavone) compared to apigenin derivatives (4',5,7-trihydroxyflavone) during roasting of buckwheat groats. The lower stability of the luteolin derivatives was associated with the presence of a C-3' hydroxy group. Similarly, an increase in the degree of hydroxylation has been found to increase the first-order degradation rate constants of benzoic acids upon thermal treatment under sub-critical water conditions (Khuwijtjaru *et al.*, 2014a). Conversely, higher thermal stability of genistein and its derivatives compared to the daidzein-series of isoflavones has been reported by numerous researchers (*e.g.* Stintzing *et al.*, 2006), suggesting that hydroxylation at C-5 of the A-ring confers a higher thermal stability to the 7,4'-dihydroxylated isoflavone structure.

Literature data pertaining to the effect of position and degree of glucosylation on the thermal stability of polyphenols are scarce. Up till now, this has only been investigated for flavonols and flavones. During processing, under oxidative conditions in aqueous media, the flavonol aglycone quercetin is typically degraded more extensively than its corresponding 3-rutinosyloxy derivative, rutin (Makris & Rossiter, 2000; Buchner *et al.*, 2006). The thermal stability of quercetin glucosides under dry roasting conditions depends on the position of glucosylation (3-*O*-position on the C-ring vs 4'-*O*-position on the B-ring; Rohn *et al.*, 2007). Slight differences in the thermal stabilities of the flavones, vitexin (8- β -D-glucopyranosylapigenin) and isovitexin (6- β -D-glucopyranosylapigenin), have also been observed upon roasting of buckwheat groats, indicating that the position of glucosylation affects the thermal stability of apigenin derivatives (Zielinski *et al.*, 2009).

In the current study, the first-order degradation rate constants of all compounds significantly ($p < 0.05$) increased with increasing temperature (Table 2), and this effect is illustrated for mangiferin in Figure 4. The temperature-dependence of the reaction rate constant obeyed the Arrhenius law, with all R^2 -values obtained for the estimation of A and E_a via non-linear regression (eq 2) > 0.972 , and those obtained for the estimation of $\ln A$ and the slope of the Arrhenius curve via linear regression (eq 3) > 0.991 (Table 3). The respective curves are depicted in Figures 5A and 5B.

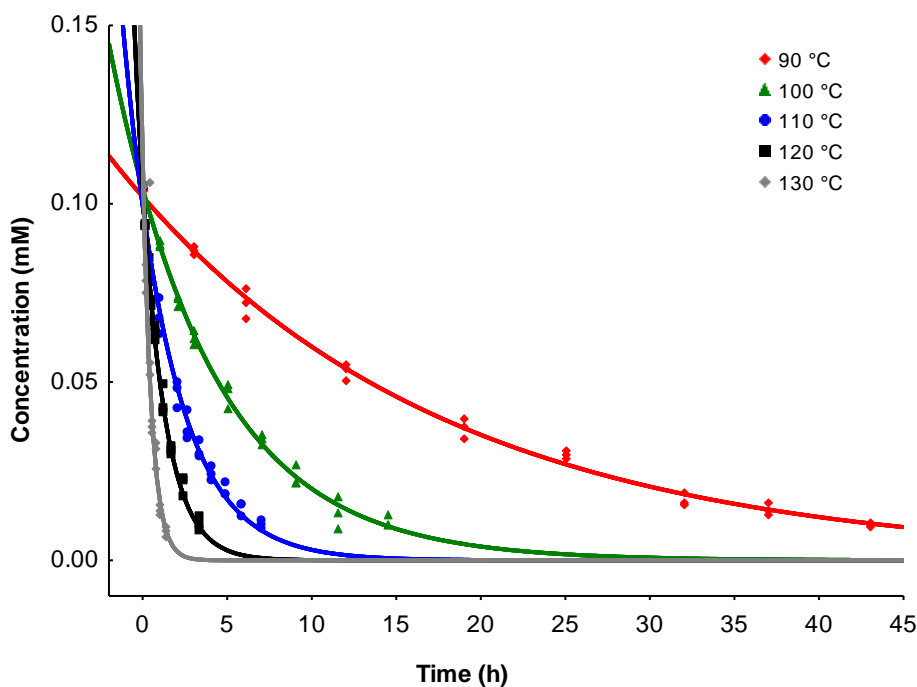


Figure 4 Thermal degradation of mangiferin in aqueous model solutions (0.1 M phosphate buffer, pH 5) at various temperatures over time: 90 °C (red), 100 °C (green), 110 °C (blue), 120 °C (black) and 130 °C (grey).

Table 3 Estimated values for the Arrhenius parameters (activation energy, E_a ; frequency factor, A ; and coefficient of determination, R^2) for the degradation of the target benzophenones (**1–3**) and xanthenes (**4–5**) in aqueous model solutions (0.1 M phosphate buffer, pH 5). The values for the 95% confidence intervals are provided in brackets.

Parameter	3- β -D-Glucopyranosyl-4- β -D-glucopyranosyloxy-iriflophenone (1)	3- β -D-Glucopyranosyl-maclurin (2)	3- β -D-Glucopyranosyl-iriflophenone (3)	Mangiferin (4)	Isomangiferin (5)
non-linear regression (eq 2)^a					
A , h ⁻¹	6.81 × 10 ⁸ e (6.64 – 6.97 × 10 ⁸)	6.80 × 10 ⁹ a	1.35 × 10 ⁹ d	3.96 × 10 ⁹ b	1.53 × 10 ⁹ c
E_a , kJ.mol ⁻¹	73.6 ab (71.1 – 76.1)	68.6 d (68.1 – 69.0)	70.7 c (69.2 – 72.1)	72.4 a (71.6 – 73.2)	70.8 bc (69.5 – 72.1)
R^2	0.986	0.986	0.992	0.985	0.972
linear regression (eq 3)^b					
ln A	35.2 a (31.8 – 38.6)	32.5 a (29.5 – 35.6)	31.5 a (28.2 – 34.7)	32.4 a (29.2 – 35.7)	31.8 a (28.6 – 35.1)
slope	-15096 b (-13722 – -16469)	-12013 a (-13124 – -10901)	-12665 a (-13901 – -11428)	-12827 a (-14062 – -11592)	-12790 a (-14026 – -11555)
R^2	1.00	0.998	1.00	0.998	0.991
<i>with computed values for</i>					
A , h ⁻¹	1.94 × 10 ¹⁵	1.35 × 10 ¹⁴	4.65 × 10 ¹³	1.21 × 10 ¹⁴	6.73 × 10 ¹³
E_a , kJ.mol ⁻¹	125	99.8	105	107	106

^aValues for A and E_a in the same row with different letters are significantly different from one another ($p < 0.05$).

^bValues for ln A and slope in the same row with different letters are significantly different from one another ($p < 0.05$).

Values for the frequency factor (A) and activation energy (E_a) for individual compounds differed considerably depending on whether the exponential (eq 2) or linear (eq 3) form of the Arrhenius equation was used for parameter estimation (Table 3). Based on the distribution of the data points on the Arrhenius curves for the individual compounds (exponential fit according to eq 2; Figure S1, Supplementary Material, page 195), in which most of the data points lies under the curve, it seems that the values estimated by means of linear regression might be more accurate. It is, however, recommended that the magnitudes of E_a be verified independently using calorimetry, for example (as proposed by Peleg *et al.*, 2012).

Proceeding with data obtained via linear regression, the activation energies for the thermal degradation of **2**, **3**, **4** and **5** ranged between 99.8 and 107 kJ.mol⁻¹, while that of **1** was significantly higher at 125 kJ.mol⁻¹ (Table 3). The activation energy can be interpreted as the energy barrier that molecules need to cross in order to be able to react or the change in potential energy of a chemical system that is required to convert reactants into products. The proportion of molecules able to do that increases with temperature, which qualitatively explains the effect of temperature on the reaction rates. This effect is quantitated by the Arrhenius equation (Peleg *et al.*, 2012). The higher activation energy of **1** compared to the other evaluated compounds (**2–5**) therefore indicates that this benzophenone is thermodynamically more stable, and that more energy is required for the molecules to react. As the A term in the Arrhenius equation deals with the frequency of molecules that collide in the correct orientation, and with enough energy to initiate a reaction, the higher value of A for the degradation of **1** (Table 3) could be attributed to its stereostructural properties. Compound **1**, characterised by two bulky glucopyranosyl substituents on the A-ring, has a larger steric compression than that of its mono-glucopyranosyl derivative (**3**), for example, and possibly exhibits a higher rate of collisions during thermal reactions.

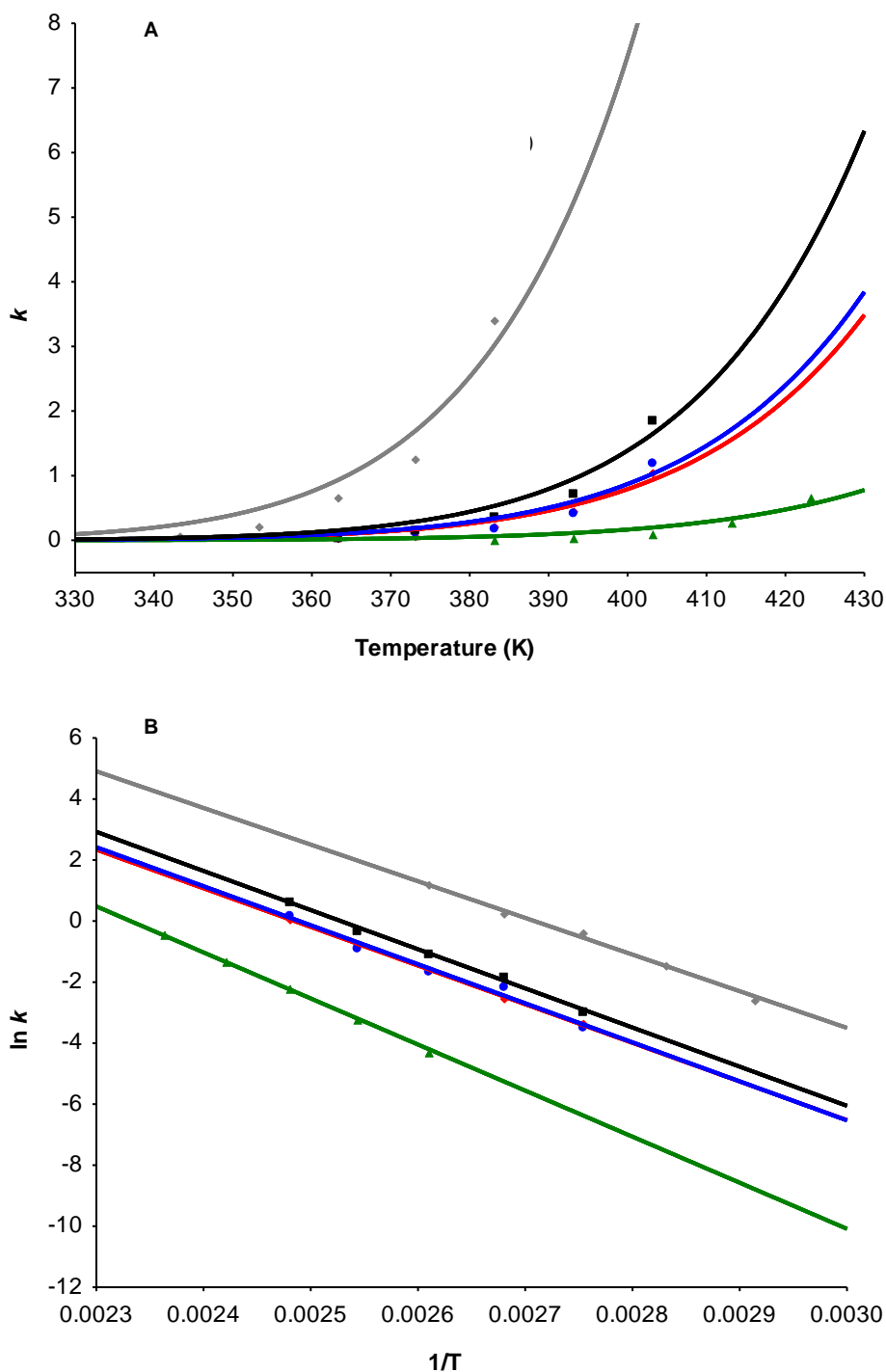


Figure 5 Arrhenius plots for the target benzophenones and xanthenes (0.1 M phosphate buffer, pH 5): 3- β -D-glucopyranosyl-4- β -D-glucopyranosyloxiriflophenone (**1**, green); 3- β -D-glucopyranosylmaclurin (**2**, grey); 3- β -D-glucopyranosyliriflophenone (**3**, red); mangiferin (**4**, black); and isomangiferin (**5**, blue). **A**) Exponential fit according to eq 2; **B**) Fit according to the linearised form of the Arrhenius equation, eq 3. Refer to Figure S1 (Supplementary Material, page 195) for the Arrhenius curves of the individual compounds (exponential fit according to eq 2).

The Arrhenius activation energies computed for the thermal degradation of the benzophenones and xanthenes over the collective temperature range of 70-150 °C (99.8-125 kJ.mol⁻¹, Table 3) are in line with literature values on various types of phenolic compounds, *i.e.* salvianolic acid B (E_a , 70-90 °C = 114 kJ.mol⁻¹; Pan *et al.*, 2013), 5-caffeoylquinic acid (E_a , 135-145 °C = 107 kJ.mol⁻¹; De Paepe *et al.*, 2014), oligomeric proanthocyanidins (E_a , 85-145 °C = 93-149 kJ.mol⁻¹; De Paepe *et al.*,

2014), dihydrochalcones ($E_{a, 120-145\text{ }^{\circ}\text{C}} = 120-140\text{ kJ.mol}^{-1}$; De Paepe *et al.*, 2014) and selected flavonols (3- β -D-glucopyranosyloxyquercetin and 3- β -D-xylopyranosyloxyquercetin, $E_{a, 90-145\text{ }^{\circ}\text{C}} = 97$ and 107 kJ.mol^{-1} , respectively; De Paepe *et al.*, 2014) at similar temperatures.

3.2. Thermal Degradation Kinetics Modelling of the Xanthone Mangiferin in Aqueous Model Systems: pH and Temperature Effects

The pH of the phosphate buffer solutions in which the stability assessments were conducted had a significant effect on the thermal stability of mangiferin (**4**). As the pH increased, mangiferin became more susceptible to thermal degradation; this was accommodated by the experimental temperature ranges chosen for each of the pH levels, and is also reflected in the magnitudes of the first-order degradation rate constants at matching temperatures (Table 4). The first-order degradation rate constants for mangiferin at $100\text{ }^{\circ}\text{C}$ ($k_{100\text{ }^{\circ}\text{C}}$) significantly ($p < 0.05$) increased with increasing pH (Table 4, Figure 6), and the pH-dependence of $k_{100\text{ }^{\circ}\text{C}}$ followed an exponential relationship (Figure 6 insert). 3D Contour and Surface plots, depicted in Figure S2 (Supplementary Material, page 196), illustrate the combined effect of pH and temperature on the reaction rate constant of mangiferin.

Table 4 Estimated values for the first-order rate constants (k, h^{-1})^a for the degradation of the xanthone mangiferin (**4**) in aqueous model solutions (0.1 M phosphate buffer) as a function of pH. The values for the 95% confidence intervals and coefficient of determination (R^2) are provided in brackets.

Temperature ($^{\circ}\text{C}$)	pH 3	pH 4	pH 5	pH 6	pH 7
60	–	–	–	–	0.0504 e (0.0484 – 0.0524) ($R^2 = 0.997$)
70	–	–	–	0.0433 e (0.0420 – 0.0447) ($R^2 = 0.999$)	0.165 d (0.159 – 0.172) ($R^2 = 0.999$)
80	–	–	–	0.0955 d (0.0926 – 0.0985) ($R^2 = 0.999$)	0.295 c (0.282 – 0.308) ($R^2 = 0.997$)
90	–	–	0.0532 e (0.0478 – 0.0586) ($R^2 = 0.997$)	0.210 c (0.203 – 0.216) ($R^2 = 1.00$)	0.773 b (0.741 – 0.805) ($R^2 = 0.998$)
100	0.0469 e,E (0.0432 – 0.0506) ($R^2 = 0.996$)	0.0628 e,D (0.0587 – 0.0670) ($R^2 = 0.996$)	0.165 d,C (0.148 – 0.182) ($R^2 = 0.996$)	0.461 b,B (0.446 – 0.475) ($R^2 = 0.998$)	1.67 a,A (1.61 – 1.74) ($R^2 = 0.997$)
110	0.109 d (0.0996 – 0.118) ($R^2 = 0.996$)	0.139 d (0.128 – 0.149) ($R^2 = 0.991$)	0.352 c (0.313 – 0.390) ($R^2 = 0.991$)	0.995 a (0.963 – 1.03) ($R^2 = 0.996$)	–
120	0.228 c (0.210 – 0.247) ($R^2 = 0.987$)	0.390 c (0.363 – 0.417) ($R^2 = 0.993$)	0.724 b (0.644 – 0.803) ($R^2 = 0.997$)	–	–
130	0.560 b (0.511 – 0.608) ($R^2 = 0.987$)	0.806 b (0.745 – 0.867) ($R^2 = 0.990$)	1.87 a (1.67 – 2.07) ($R^2 = 0.931$)	–	–
140	0.950 a (0.861 – 1.04) ($R^2 = 0.986$)	2.27 a (2.10 – 2.43) ($R^2 = 0.995$)	–	–	–

^aValues in the same column (lowercase) and values in the same row (at $100\text{ }^{\circ}\text{C}$, uppercase) with different letters are significantly different from one another ($p < 0.05$).

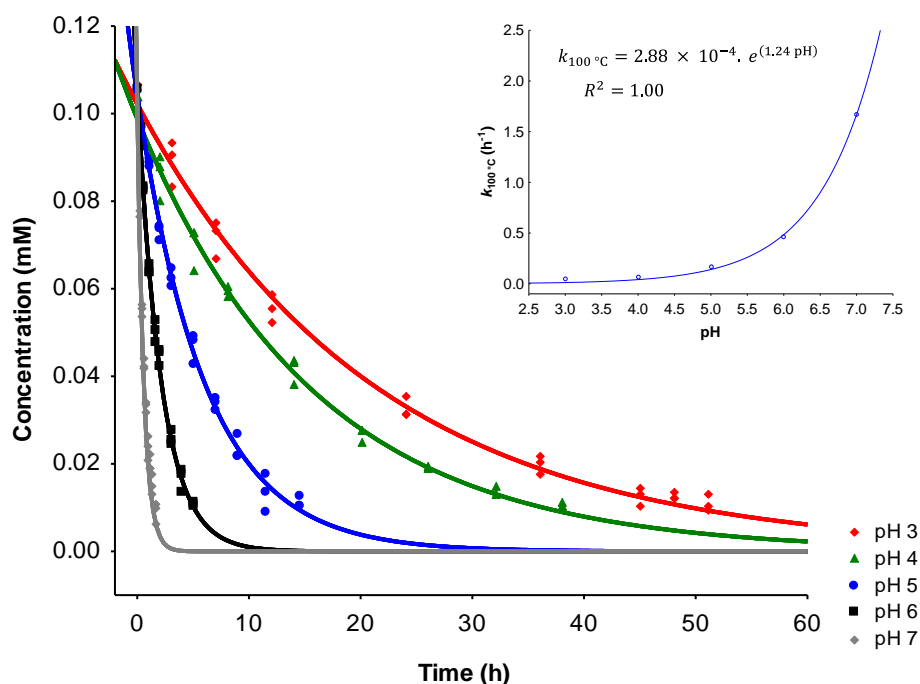


Figure 6 Thermal degradation of mangiferin in aqueous model solutions (0.1 M phosphate buffer; 100 °C) at various pH levels over time: pH 3 (red); pH 4 (green); pH 5 (blue); pH 6 (black); and pH 7 (grey). Insert indicates the relationship between $k_{100\text{ }^\circ\text{C}}$ and pH.

At pH 3, the degradation rate constants of mangiferin was slightly higher than expected, indicating that the optimum pH for mangiferin stability probably lies between 3 and 4. This is evident upon a linear regression of $\ln k_{100\text{ }^\circ\text{C}}$ vs pH (results not shown). It is thus expected that, as the pH is lowered below 3, the degradation rate of mangiferin would increase systematically. Further experiments at intermediate and additional pH levels are, however, required to support this hypothesis.

This is the first report on the effect of pH on the thermal stability of the xanthone mangiferin. Numerous researchers have, however, reported similar observations regarding the pH-dependence of the degradation rate constants for other phenolic sub-classes. For instance, Guo *et al.* (2007) found that the hydrolytic rate constant of salvianolic acid B in aqueous model systems at 90 °C increased as the pH increased from 2.0 to 7.05, but also as the pH was decreased from 2.0 to 0.51. Similarly, Li *et al.* (2012) found that the first-order degradation rate constants of the flavan-3-ol epigallocatechin gallate in concentrated green tea solutions increased as the pH was increased from 4 to 7, but also as the pH was decreased from 4 to 1.5. Maximum thermal stability of neohesperidin dihydrochalcone in aqueous solutions has been observed at a pH ~ 4.0-4.5 (Canales *et al.*, 1993; Coiffard *et al.*, 1998). With regard to the thermal stability of isoflavones in alkaline solution (0.01 M borax solution), increases in both the degradation and conversion rates have been observed as the pH was increased from 8.5 to 9.5 (Vaidya *et al.*, 2007).

The pH of the phosphate buffer solution did not distort the linear relationship between the rate constant k and temperature, as indicated in Figure 7B. The temperature-dependence of the first-order degradation rate constants for mangiferin still obeyed the Arrhenius law, with R^2 -values ≥ 0.979 (non-linear regression) and R^2 -values ≥ 0.996 (linear-regression) (Table 5). The Arrhenius activation energies for the thermal degradation of mangiferin in phosphate buffer solutions adjusted to pH 3, 4, 5, 6 and 7 were calculated as 97.0, 113, 107, 87.8 and 87.0 $\text{kJ}\cdot\text{mol}^{-1}$ (linear regression, eq 3), respectively. Comparison of the activation energies at pH 3 and 4, where the experiments were conducted over an identical temperature range of 100-140 °C, indicates a significantly ($p < 0.05$) higher value at pH 4.

This results in a crossing point in the Arrhenius curves of pH 3 and pH 4 (Figure 7B), indicative of stability inversion at temperatures $< ca. 85\text{ }^{\circ}\text{C}$. This effect is also exemplified in the 3D contour plot depicted in Figure S2 (Supplementary Material, page 196).

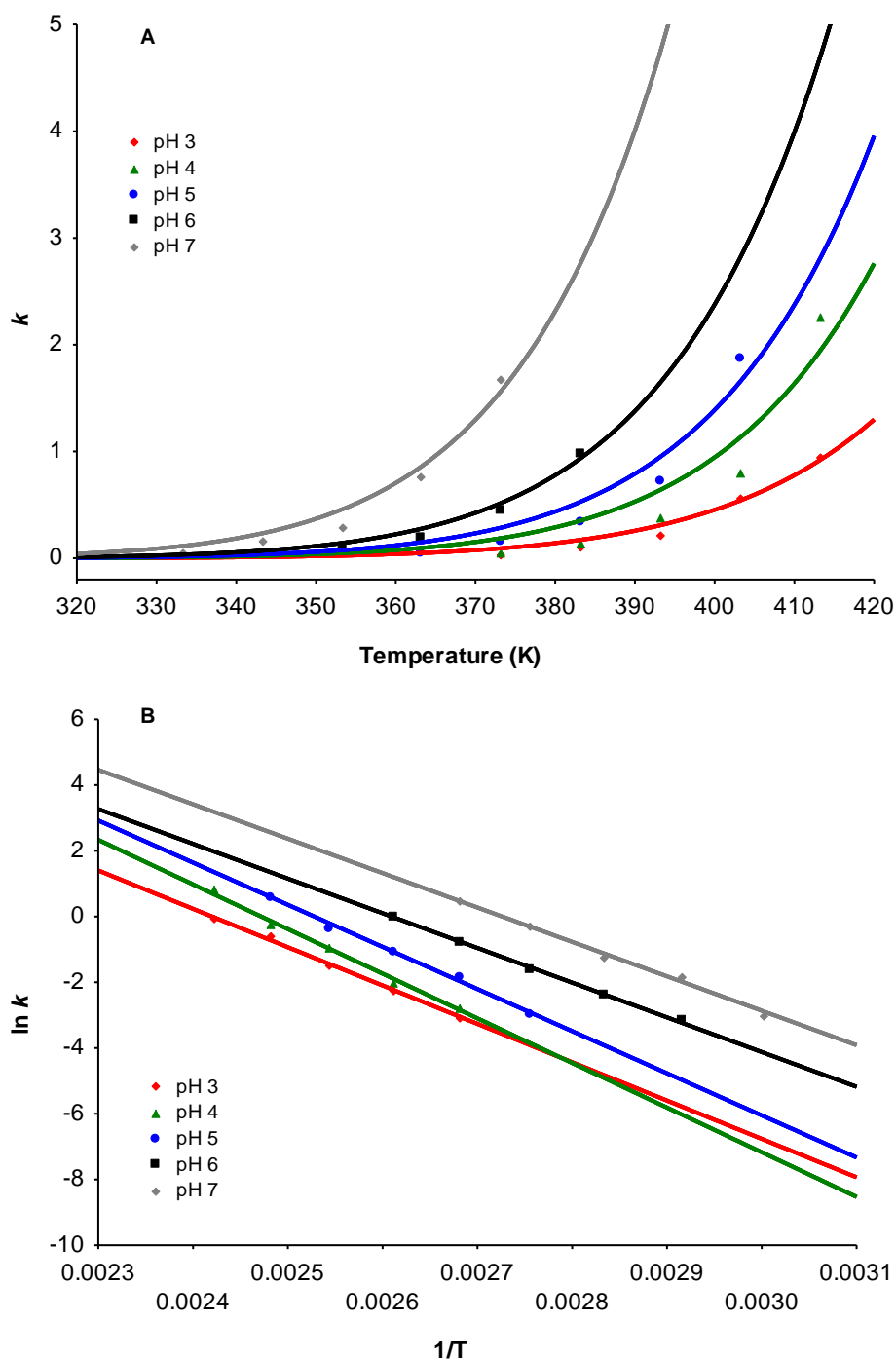


Figure 7 Arrhenius plots for mangiferin (**4**) (0.1 M phosphate buffer) as a function of pH: pH 3 (red), pH 4 (green), pH 5 (blue), pH 6 (black), pH 7 (grey). **A**) Exponential fit according to eq 2; **B**) Fit according to the linearised form of the Arrhenius equation, eq 3. Refer to Figure S3 (Supplementary Material, page 197) for the Arrhenius curves of mangiferin at the different pH levels (exponential fit according to eq 2).

Table 5 Estimated values for the Arrhenius parameters (activation energy, E_a ; frequency factor, A ; and coefficient of determination, R^2) for the degradation of the xanthone mangiferin (**4**) in aqueous model solutions (0.1 M phosphate buffer) as a function of pH. The values for the 95% confidence intervals are provided in brackets.

Parameter	pH 3	pH 4	pH 5	pH 6	pH 7
non-linear regression (eq. 2)^a					
A , h ⁻¹	1.79 × 10 ⁹ e (1.79 – 1.80 × 10 ⁹)	5.65 × 10 ⁹ a (5.64 – 5.65 × 10 ⁹)	4.87 × 10 ⁹ b (4.87 – 4.87 × 10 ⁹)	4.01 × 10 ⁹ d	4.63 × 10 ⁹ c (4.63 – 4.64 × 10 ⁹)
E_a , kJ.mol ⁻¹	73.5 ab (72.2 – 74.7)	74.8 a (74.2 – 75.4)	73.1 b (72.4 – 73.7)	70.6 c (69.5 – 71.8)	67.6 d (67.0 – 68.3)
R^2	0.9972	0.979	0.985	0.996	0.995
linear regression (eq. 3)^b					
ln A	28.2 c (25.5 – 31.0)	33.6 a (30.8 – 36.3)	32.4 ab (29.7 – 35.1)	27.6 c (25.0 – 30.1)	28.5 cb (26.1 – 31.0)
slope	-11666 ab (-12734 – -10599)	-13580 c (-14651 – -12509)	-12816 cb (-13838 – -11794)	-10559 a (-11472 – -9647)	-10470 a (-11335 – -9605)
R^2	0.998	0.998	0.998	1.00	0.996
<i>with corresponding values for</i>					
A , h ⁻¹	1.83 × 10 ¹²	3.79 × 10 ¹⁴	1.18 × 10 ¹⁴	9.28 × 10 ¹¹	2.49 × 10 ¹²
E_a , kJ.mol ⁻¹	97.0	113	107	87.8	87.0

^aValues for A and E_a in the same row with different letters are significantly different from one another ($p < 0.05$).

^bValues for ln A and slope in the same row with different letters are significantly different from one another ($p < 0.05$).

3.3. Identification of Thermal Degradation Products by LC-DAD-ESI-MS and –MS/MS

In this study, products formed upon thermal degradation of the target benzophenones **1**, **2** and **3** and xanthenes **4** and **5** were tentatively identified by LC-DAD-ESI-MS and –MS/MS. This provided the first glimpse into the thermal degradation pathways of these bio-active compounds in an aqueous environment. The compounds tentatively identified in thermally-treated solutions (110 °C) of 3- β -D-glucopyranosyl-4- β -D-glucopyranosyloxyiriflophenone (**1**), 3- β -D-glucopyranosylmaclurin (**2**), 3- β -D-glucopyranosyliriflophenone (**3**), mangiferin (**4**) and isomangiferin (**5**) are summarised in Tables 6, 7, 8, 9 and 10, respectively. The chromatographic profiles of the benzophenones **1**, **2** and **3** and the xanthenes **4** and **5** following thermal treatment at 110 °C are depicted in Figures 8 and 9, respectively. For reference purposes, the corresponding chromatograms of the control samples are provided in Figure S4 (Supplementary Material, page 198).

Upon thermal treatment, the benzophenones and xanthenes were subject to isomerisation, and each parent compound formed two later eluting isomers (Tables 6-10). In addition, mangiferin and isomangiferin were also converted to one another, but this reaction appeared to be negligible; mangiferin (**5D**) and isomangiferin (**4F**) could only be detected in trace quantities in thermally-treated solutions of isomangiferin and mangiferin, respectively, following extraction of their molecule ions (Figure 9; Tables 9 and 10). The isomeric compounds were assigned the same elemental compositions as those of their respective parent compounds by HRESIMS. The isomeric compounds also presented the same fragmentation patterns as those of their parent compounds during tandem MS analyses, but with slight differences observed in the relative intensities of the fragment ions. The presence of two iriflophenone-di- O,C -hexoside isomers (compounds **d** and **f**) and two tetrahydroxyxanthone- C -hexoside isomers (compounds **y** and **aa**) has been demonstrated previously in aqueous extracts of unfermented and fermented *C. genistoides* (Chapter 3).

Table 6 Retention times, UV-VIS characteristics, accurate masses, proposed molecular formulae and LC-MS/MS fragment ions of compounds (tentatively) identified in a thermally-treated sample (110 °C) of the benzophenone 3- β -D-glucopyranosyl-4- β -D-glucopyranosyloxyiriflophenone (**1**) in 0.1 M phosphate buffer solution (pH 5).

Nr.	t _R (min) ^a	Proposed Compound	λ_{\max} (nm)	Mode	Accurate Mass, exp.	Proposed Mol. Formula	Error (ppm)	LC-MS/MS Ions ^b
1	0.72	3-β-D-glucopyranosyl-4-β-D-glucopyranosyloxyiriflophenone	294	+	571.1668	C ₂₅ H ₃₁ O ₁₅	0.9	373 (15), 355 (20), 337 (25), 325 (70), 313 (100), 289 (30), 279 (15), 271 (70), 259 (40), 247 (10), 243 (15), 231 (45), 219 (45), 195 (100), 177 (30), 165 (25), 153 (5), 121 (10)
				-	569.1495	C ₂₅ H ₂₉ O ₁₅	-1.9	479 (10), 449 (30), 385 (5), 355 (5), 341 (5), 329 (5), 317 (30), 287 (100), 245 (10), 197 (5), 167 (10), 125 (5)
1A	0.85	iriflophenone-di- <i>O,C</i> -hexoside isomer	292	+	571.1658	C ₂₅ H ₃₁ O ₁₅	-0.9	373 (10), 355 (15), 337 (30), 325 (50), 313 (100), 289 (20), 279 (15), 271 (70), 259 (40), 247 (10), 231 (55), 219 (50), 195 (95), 177 (40), 165 (35), 153 (5), 121 (20)
				-	569.1489	C ₂₅ H ₂₉ O ₁₅	-3.0	479 (15), 449 (35), 355 (10), 341 (10), 329 (10), 317 (40), 287 (100), 245 (10), 197 (5), 167 (15), 125 (5)
1B	0.95	iriflophenone-di- <i>O,C</i> -hexoside isomer	292	+	571.1677	C ₂₅ H ₃₁ O ₁₅	2.5	373 (5), 355 (15), 337 (20), 325 (40), 313 (80), 289 (20), 271 (50), 259 (35), 231 (60), 219 (60), 195 (100), 177 (35), 165 (30), 153 (<5), 121 (10)
				-	569.1474	C ₂₅ H ₂₉ O ₁₅	-5.6	479 (5), 449 (30), 385 (5), 355 (10), 341 (5), 329 (10), 317 (35), 287 (100), 245 (5), 197 (10), 167 (10), 125 (5)
1C	1.12	unidentified	255	+	409.1116	C ₁₉ H ₂₁ O ₁₀	-4.6	247 (45), 203 (10), 153 (100), 121 (30), 105 (5).
				-	407.0977	C ₁₉ H ₁₉ O ₁₀	-0.2	245 (100), 201 (10), 161 (10), 151 (20), 107 (5)
1D	1.18	3- β -D-glucopyranosyliriflophenone	296	+	409.1107	C ₁₉ H ₂₁ O ₁₀	-6.8	339 (5), 329 (5), 313 (15), 301 (5), 283 (5), 271 (10), 261 (5), 243 (20), 231 (90), 219 (50), 205 (20), 195 (100), 191 (25), 177 (45), 165 (70), 159 (15), 149 (10), 137 (10), 121 (25)
				-	407.0953	C ₁₉ H ₁₉ O ₁₀	-6.1	374 (10), 317 (20), 300 (10), 287 (100), 271 (20), 259 (45), 245 (70), 215 (45), 201 (30), 193 (60), 177 (10), 173 (15), 165 (45), 149 (15), 139 (10), 125 (55), 108 (30)
1E	1.25	unidentified benzophenone	290	+	613.1742	C ₂₇ H ₃₃ O ₁₆	-4.4	413 (5), 401 (5), 391 (5), 377 (10), 373 (10), 355 (25), 343 (20), 337 (30), 329 (20), 325 (40), 313 (100), 301 (5), 298 (5), 289 (50), 280 (20), 271 (80), 260 (20), 243 (15), 232 (10), 219 (30), 205 (10), 195 (90), 187 (10), 177 (20), 165 (5), 149 (5), 127 (5), 121 (10)
				-	611.1611	C ₂₇ H ₃₁ O ₁₆	-0.2	521 (25), 491 (45), 427 (10), 397 (5), 385 (5), 329 (10), 317 (60), 287 (100), 245 (20), 167 (5), 151 (5), 125 (5)

Table 6 cont.

Nr.	t _R (min) ^a	Proposed Compound	λ _{max} (nm)	Mode	Accurate Mass, exp.	Proposed Mol. Formula	Error (ppm)	LC-MS/MS Ions ^b
1F	1.35	unidentified benzophenone	294	+	613.1808	C ₂₇ H ₃₃ O ₁₆	6.4	583 (5), 557 (5), 433 (5), 415 (10), 397 (10), 355 (95), 337 (40), 313 (100), 301 (5), 289 (40), 279 (10), 271 (80), 261 (65), 247 (10), 243 (45), 219 (20), 215 (15), 195 (90), 177 (20), 165 (5), 147 (5), 121 (5)
				–	611.1604	C ₂₇ H ₃₁ O ₁₆	-1.3	479 (15), 449 (35), 355 (5), 341 (5), 317 (30), 287 (100), 245 (5), 197 (10), 167 (10), 125 (5)
1G	1.38	unidentified benzophenone	295	+	497.1270	C ₂₂ H ₂₅ O ₁₃	-5.0	289 (15), 271 (5), 241 (40), 223 (5), 205 (10), 195 (100), 177 (15)
				–	495.1147	C ₂₂ H ₂₃ O ₁₃	1.6	495 (40), 477 (5), 401 (10), 375 (100), 357 (10), 339 (10), 333 (20), 315 (15), 295 (10), 289 (10), 271 (25), 255 (5), 237 (30), 213 (60), 195 (35), 177 (15), 169 (5), 151 (30), 127 (10)
1H	1.51	mangiferin	242, 257, 318, 365	+	423.0914	C ₁₉ H ₁₉ O ₁₁	-3.1	369 (10), 351 (15), 339 (40), 327 (25), 313 (20), 303 (90), 299 (70), 285 (25), 273 (100), 261 (15), 257 (20)
				–	421.0771	C ₁₉ H ₁₇ O ₁₁	0.0	385 (5), 355 (5), 343 (5), 331 (60), 313 (10), 301 (100), 285 (15), 271 (50), 259 (20)
1I	1.59	isomangiferin	255, 316, 365	+	423.0937	C ₁₉ H ₁₉ O ₁₁	2.4	387 (10), 369 (10), 357 (10), 341 (20), 333 (5), 327 (30), 313 (35), 303 (95), 287 (15), 273 (100), 261 (10)
				–	421.0759	C ₁₉ H ₁₇ O ₁₁	-2.8	343 (<5), 331 (50), 313 (20), 301 (100), 285 (<5), 273 (20), 258 (30)

^aLC-ESI-MS retention times. Refer to Table S14 (Supplementary Material, page 194) for the corresponding retention times on the Agilent UHPLC system and as depicted in Figure 8.

^bValues in bold indicate the base peak ions, and values in brackets indicate the relative intensity of the fragment ions.

Table 7 Retention times, UV-VIS characteristics, accurate masses, proposed molecular formulae and LC-MS/MS fragment ions of compounds (tentatively) identified in a thermally-treated sample (110 °C) of the benzophenone 3- β -D-glucopyranosylmaclurin (**2**) in 0.1 M phosphate buffer solution (pH 5).

Nr.	t _R (min) ^a	Proposed Compound	λ_{\max} (nm)	Mode	Accurate Mass, exp.	Proposed Mol. Formula	Error (ppm)	LC-MS/MS Ions ^b
*	0.72	3- β -D-glucopyranosyl-4- β -D-glucopyranosyloxiriflophenone (impurity)	292	+	571.1649	C ₂₅ H ₃₁ O ₁₅	-2.5	391 (5), 373 (15), 355 (15), 343 (5), 337 (10), 325 (50), 313 (100), 301 (5), 289 (10), 279 (5), 271 (35), 261 (30) / 259 (30), 247 (10), 243 (10), 231 (45), 219 (40), 195 (70), 177 (30), 165 (20), 153 (5), 123 (5) / 121 (5)
				-	569.1481	C ₂₅ H ₂₉ O ₁₅	-4.4	479 (10), 449 (35), 385 (5), 355 (5), 329 (5), 317 (35), 311 (10), 287 (100), 259 (<5), 245 (10), 197 (5), 193 (5), 179 (5), 167 (10), 151 (<5), 125 (5)
2	0.86	3-β-D-glucopyranosylmaclurin	231, 318	+	425.1065	C ₁₉ H ₂₁ O ₁₁	-4.5	353 (<5), 341 (<5), 329 (<5), 287 (10), 279 (5), 275 (5), 261 (15), 249 (5), 243 (25), 231 (90), 219 (65), 203 (5), 195 (100), 191 (35), 177 (70), 165 (50), 153 (10), 137 (15), 121 (10), 109 (<5)
				-	423.0910	C ₁₉ H ₁₉ O ₁₁	-4.0	343 (<5), 333 (<5), 303 (40), 261 (5), 223 (25), 205 (5), 193 (100), 165 (35), 151 (30), 137 (15), 125 (20), 121 (15), 109 (15)
2A	1.12	maclurin-C-hexoside isomer	320	+	425.1082	C ₁₉ H ₂₁ O ₁₁	-0.5	409 (10), 390 (5), 371 (5), 354 (5), 330 (15), 311 (10), 287 (10), 279 (20), 275 (10), 264 (10), 261 (10), 245 (15), 231 (100), 219 (20), 201 (5), 198 (10), 195 (80), 191 (20), 177 (40), 165 (45), 149 (10), 141 (10), 131 (5), 121 (10)
				-	423.0904	C ₁₉ H ₁₉ O ₁₁	-5.4	333 (5), 303 (35), 278 (5), 261 (20), 254 (5), 235 (10), 223 (30), 213 (10), 193 (100), 182 (5), 177 (5), 165 (40), 151 (35), 125 (25), 109 (10), 87 (5)
2B	1.32	maclurin-C-hexoside isomer	weak	+	425.1098	C ₁₉ H ₂₁ O ₁₁	3.3	409 (5), 372 (10), 354 (5), 340 (5), 330 (10), 323 (10), 314 (10), 303 (10), 293 (5), 277 (5), 265 (5), 261 (5), 250 (5), 237 (10), 231 (100), 219 (25), 207 (5), 200 (5), 195 (45), 191 (40), 189 (5), 177 (50), 166 (20), 157 (5), 149 (5), 137 (15), 122 (<5)
				-	423.0905	C ₁₉ H ₁₉ O ₁₁	-5.2	303 (15), 261 (10), 223 (20), 205 (10), 193 (100), 181 (10), 165 (40), 149 (15), 125 (15), 109 (10), 97 (10)
2C	1.51	mangiferin	240, 257, 318, 366	+	423.0920	C ₁₉ H ₁₉ O ₁₁	-1.7	369 (5), 351 (15), 339 (30), 327 (15), 323 (10), 313 (20), 303 (70), 299 (50), 295 (5), 285 (20), 273 (100), 261 (5), 257 (15), 245 (<5)
				-	421.0755	C ₁₉ H ₁₇ O ₁₁	-3.8	403 (<5), 373 (<5), 343 (5), 331 (70), 313 (10), 301 (100), 285 (10), 273 (10), 272 (30), 271 (30), 259 (40), 258 (15)

Table 7 cont.

Nr.	t _R (min) ^a	Proposed Compound	λ _{max} (nm)	Mode	Accurate Mass, exp.	Proposed Mol. Formula	Error (ppm)	LC-MS/MS Ions ^b
2D	1.59	isomangiferin	256, 316, 366	+	423.0929	C ₁₉ H ₁₉ O ₁₁	0.5	387 (10), 369 (15), 357 (10), 341 (10), 333 (5), 327 (30), 313 (30), 303 (100), 299 (10), 287 (10), 285 (15), 273 (85), 261 (10), 243 (5)
				-	421.0754	C ₁₉ H ₁₇ O ₁₁	-4.0	343 (<5), 331 (55), 313 (15), 301 (100), 285 (5), 273 (20), 272 (20), 271 (20), 259 (25), 258 (25)
2E	2.06	tetrahydroxyxanthone- <i>C</i> -hexoside isomer	258, 320, 368	+	423.0893	C ₁₉ H ₁₉ O ₁₁	-8.0	387 (5), 369 (10), 353 (5), 340 (15), 333 (5), 327 (10), 323 (10), 313 (15), 303 (65), 299 (35), 285 (25), 273 (100), 257 (10), 229 (10), 194 (10), 153 (10)
				-	421.0742	C ₁₉ H ₁₇ O ₁₁	-6.9	403 (10), 343 (<5), 331 (70), 313 (15), 301 (100), 285 (20), 273 (20) / 272 (25) / 273 (30), 259 (50)
2F	2.16	tetrahydroxyxanthone- <i>C</i> -hexoside isomer	256, 318, 370	+	423.0895	C ₁₉ H ₁₉ O ₁₁	-7.6	388 (5), 369 (15), 357 (10), 340 (10), 327 (30), 313 (30), 303 (95), 285 (15), 273 (100), 262 (10), 251 (10), 217 (910), 203 (10), 185 (10)
				-	421.0776	C ₁₉ H ₁₇ O ₁₁	1.2	403 (<5), 361 (<5), 344 (10), 331 (70), 313 (10), 301 (100), 285 (10), 272 (60), 259 (30) / 258 (30), 239 (10)
2G	2.35	unidentified xanthone derivative	258, 320, 370 ^c	+	465.1009	C ₂₁ H ₂₁ O ₁₂	-5.2	436 (10), 427 (5), 415 (5), 388 (15), 373 (5), 369 (30), 357 (5), 351 (50), 339 (5), 327 (40), 323 (10), 313 (30), 311 (30), 303 (100), 299 (35), 285 (10), 273 (40), 262 (5), 250 (5), 212 (5), 137 (5)
				-	463.0859	C ₂₁ H ₁₉ O ₁₂	-3.9	445 (5), 399 (<5), 367 (5), 343 (5), 331 (85), 313 (10), 301 (100), 285 (10), 272 (20), 259 (40)
2H	2.36	tetrahydroxyxanthone- <i>C</i> -hexoside isomer	258, 318, 370 ^c	+	423.0891	C ₁₉ H ₁₉ O ₁₁	-8.5	359 (5) / 357 (5), 339 (10), 333 (5), 327 (20), 313 (25), 303 (80), 299 (5), 285 (10), 273 (100), 257 (20), 243 (5), 231 (10)
				-	421.0724	C ₁₉ H ₁₇ O ₁₁	-11.2	403 (5), 343 (5), 331 (85), 313 (45), 301 (100), 286 (15), 272 (80), 259 (60)

^aLC-ESI-MS retention times. Refer to Table S14 (Supplementary Material, page 194) for the corresponding retention times on the Agilent UHPLC system and as depicted in Figure 8.

^bValues in bold indicate the base peak ions, and values in brackets indicate the relative intensity of the fragment ions.

^cVery weak signal and partial co-elution.

Table 8 Retention times, UV-VIS characteristics, accurate masses, proposed molecular formulae and LC-MS/MS fragment ions of compounds (tentatively) identified in a thermally-treated sample (110 °C) of the benzophenone 3- β -D-glucopyranosyliriflophenone (**3**) in 0.1 M phosphate buffer solution (pH 5).

Nr.	t _R (min) ^a	Proposed Compound	λ_{\max} (nm)	Mode	Accurate Mass, exp.	Proposed Mol. Formula	Error (ppm)	LC-MS/MS Ions ^b
3	1.18	3-β-D-glucopyranosyliriflophenone	295	+	409.1133	C ₁₉ H ₂₁ O ₁₀	-0.5	337 (<5), 325 (5), 313 (5), 279 (<5), 271 (10), 261 (10), 243 (25), 231 (90), 219 (60), 205 (5), 195 (100), 177 (55), 165 (55), 153 (5), 121 (20)
				-	407.0973	C ₁₉ H ₁₉ O ₁₀	-1.2	317 (10), 299 (10), 287 (100), 271 (10), 259 (10), 257 (20), 245 (55), 223 (10), 219 (5), 215 (15), 201 (20), 193 (30), 177 (5), 167 (15), 165 (15), 161 (10), 151 (10), 149 (5), 125 (15), 117 (10)
3A	1.47	unidentified	258, 288	+	391.1038	C ₁₉ H ₁₉ O ₉	2.3	373 (10), 355 (10), 323 (15), 297 (5), 279 (80), 255 (5), 248 (15), 235 (15), 231 (10), 219 (70), 215 (30), 209 (20), 200 (15), 191 (90), 189 (100), 182 (10), 177 (25), 165 (35), 161 (30), 155 (15), 151 (20), 147 (15), 145 (15), 137 (5), 134 (10), 128 (5), 121 (70), 109 (10), 107 (10), 73 (20)
				-	389.0870	C ₁₉ H ₁₇ O ₉	-0.8	359 (<5), 311 (55), 283 (<5), 269 (<5), 259 (<5), 247 (<5), 239 (<5), 217 (100), 189 (5), 173 (25), 161 (10), 149 (20), 145 (10), 129 (<5), 117 (5)
3B	1.50	iriflophenone-C-hexoside isomer	nd ^c	+	409.1071	no match for C ₁₉ H ₂₁ O ₁₀	-	very weak: 341 (20), 287 (10), 251 (20), 245 (15), 243 (20), 235 (60), 233 (65), 231 (100), 219 (20), 203 (50), 195 (45), 191 (15), 179 (20), 177 (30), 165 (25), 163 (25), 157 (30), 153 (10), 149 (20), 121 (50), 107 (10)
				-	407.0964	C ₁₉ H ₁₉ O ₁₀	-3.4	329 (10), 317 (25), 301 (10), 287 (90), 271 (15), 257 (20), 249 (15), 245 (100), 227 (15), 216 (10), 210 (15), 201 (30), 193 (70), 173 (15), 171 (20), 167 (30), 165 (30), 160 (10), 151 (20), 149 (30), 138 (25), 133 (15), 127 (15), 125 (20), 123 (25), 111 (25)
3C	1.51	mangiferin	nd ^c	+	423.0919	C ₁₉ H ₁₉ O ₁₁	-1.9	-
				-	421.0780	C ₁₉ H ₁₇ O ₁₁	2.1	-
3D	1.59	isomangiferin	255, 298, 347	+	423.0920	C ₁₉ H ₁₉ O ₁₁	-1.7	-
				-	421.0817	C ₁₉ H ₁₇ O ₁₁	10.9	-

Table 8 cont.

Nr.	t _R (min) ^a	Proposed Compound	λ _{max} (nm)	Mode	Accurate Mass, exp.	Proposed Mol. Formula	Error (ppm)	LC-MS/MS Ions ^b
3E	1.68	iriflophenone- <i>C</i> -hexoside isomer	295	+	409.0959	no match for C ₁₉ H ₂₁ O ₁₀	—	very weak: 342 (915), 337 (10), 292 (30), 267 (10), 261 (10), 249 (15), 243 (20), 235 (15), 231 (50), 221 (40), 219 (65), 216 (10), 207 (15), 203 (25), 195 (100), 190 (25), 189 (10), 177 (70), 165 (10), 153 (40), 137 (10), 135 (20), 131 (10), 125 (10), 121 (20)
				—	407.0947	C ₁₉ H ₁₉ O ₁₀	-7.6	328 (5), 297 (15), 287 (100), 257 (40), 245 (35), 225 (10), 215 (5), 201 (10), 195 (5), 173 (10), 171 (15), 165 (15), 159 (15), 151 (15), 149 (5), 125 (15), 117 (30), 108 (10), 105 (20)
3F	1.79	unidentified	nd ^c	+	391.1067	C ₁₉ H ₁₉ O ₉	9.7	—
				—	389.0861	C ₁₉ H ₁₇ O ₉	-3.1	295 (65), 287 (10), 277 (20), 265 (15), 257 (75), 245 (40), 224 (15), 205 (100), 177 (60), 163 (60), 151 (65), 137 (25), 123 (10), 117 (15), 109 (20), 107 (25), 81 (5), 66 (5)
3G	1.79	unidentified	nd ^c	+	829.2131	no match for C ₃₉ H ₄₁ O ₂₀	—	—
				—	827.2025	C ₃₉ H ₃₉ O ₂₀	-1.2	—
3H	1.89	unidentified	236, 306	+	501.1074	C ₁₇ H ₂₅ O ₁₇	-3.6	403 (<5), 385 (10), 367 (5), 356 (5), 325 (20), 301 (30), 291 (25), 283 (5), 273 (55), 259 (25), 243 (10), 231 (95), 207 (100), 189 (15), 177 (60), 165 (30), 151 (<5), 135 (5), 121 (5), 109 (<5)
				—	499.0922	C ₁₇ H ₂₃ O ₁₇	-2.6	419 (10), 329 (15), 299 (100), 271 (5), 257 (10), 235 (5), 205 (15)
3I	2.10	unidentified	262, 290	+	373.0911	C ₁₉ H ₁₇ O ₈	-3.2	—
				—	371.0779	C ₁₉ H ₁₅ O ₈	3.2	very weak: 311 (15), 273 (<5), 269 (<5), 217 (100), 191 (5), 179 (<5), 173 (5), 147 (5), 145 (5), 129 (20), 106 (5)
3J	2.13	unidentified	292	+	247.0618	C ₁₃ H ₁₁ O ₅	4.9	—
				—	245.0447	C ₁₃ H ₉ O ₅	-1.2	161 (45), 151 (100), 125 (40), 111 (55), 108 (50), 107 (30)
3K	2.22	unidentified	306	+	391.1038	C ₁₉ H ₁₉ O ₉	2.3	—
				—	389.087	C ₁₉ H ₁₇ O ₉	-0.8	317 (25), 313 (55), 311 (50), 299 (60), 295 (20), 287 (80), 283 (15), 275 (10), 271 (45), 257 (100), 245 (70), 217 (60), 205 (40), 193 (10), 187 (20), 173 (30), 163 (45), 151 (90), 139 (10), 135 (15), 131 (15), 125 (20), 118 (10), 109 (20), 90 (10), 75 (10)

Table 8 cont.

Nr.	t _R (min) ^a	Proposed Compound	λ _{max} (nm)	Mode	Accurate Mass, exp.	Proposed Mol. Formula	Error (ppm)	LC-MS/MS Ions ^b
3L	2.48	unidentified	320	+	305.0292	no match for C ₁₅ H ₁₃ O ₇	–	–
				–	303.0493	C ₁₅ H ₁₁ O ₇	-4.0	259 (20), 257 (20), 231 (25), 215 (60), 200 (20), 195 (20), 191 (80), 173 (60), 165 (100), 161 (85), 158 (70), 139 (40), 135 (30), 121 (60), 117 (80), 111 (35)
3M	2.64	unidentified benzophenone derivative	240, 295	+	829.2197	C ₃₉ H ₄₁ O ₂₀	0.7	774 (<5), 744 (<5), 685 (<5), 675 (<5), 571 (<5), 551 (<5), 421 (20), 403 (100), 391 (5), 385 (35), 367 (40), 355 (50), 337 (5), 325 (40), 309 (5), 301 (20), 291 (5), 271 (25), 259 (15), 255 (5), 243 (<5), 231 (40), 219 (5), 207 (20), 123 (<5)
				–	827.2053	C ₃₉ H ₃₉ O ₂₀	2.2	827 (40), 809 (5), 737 (<5), 707 (35), 689 (<5), 617 (10), 587 (20), 419 (100), 407 (50), 389 (5), 359 (<5), 329 (10), 317 (40), 299 (40), 287 (45)

^aLC-ESI-MS retention times. Refer to Table S14 (Supplementary Material, page 194) for the corresponding retention times on the Agilent UHPLC system and as depicted in Figure 8.

^bValues in bold indicate the base peak ions, and values in brackets indicate the relative intensity of the fragment ions.

^cNot detected; co-elution.

Table 9 Retention times, UV-VIS characteristics, accurate masses, proposed molecular formulae and LC-MS/MS fragment ions of compounds (tentatively) identified in a thermally-treated sample (110 °C) of the xanthone mangiferin (**4**) in 0.1 M phosphate buffer solution (pH 5).

Nr.	t _R (min) ^a	Proposed Compound	λ _{max} (nm)	Mode	Accurate Mass, exp.	Proposed Mol. Formula	Error (ppm)	LC-MS/MS Ions ^b
4A	0.70	tetrahydroxyxanthone- <i>C</i> -hexoside dimer	243, 258, 319, 364	+	843.1617	C ₃₈ H ₃₅ O ₂₂	-0.4	825 (15), 807 (30), 789 (30), 771 (40), 753 (25), 729 (40), 705 (80), 693 (70), 687 (55), 675 (50), 669 (100), 657 (45), 651 (40), 640 (30), 627 (75), 603 (65), 585 (25), 573 (45), 561 (15), 555 (10), 545 (15), 515 (<5), 497 (5), 473 (5), 445 (10)
				-	841.1434	C ₃₈ H ₃₃ O ₂₂	-3.4	841 (100), 823 (5), 805 (<5), 751 (5), 721 (10), 419 (5)
4B	0.92	tetrahydroxyxanthone- <i>C</i> -hexoside dimer	243, 259, 319, 364	+	843.1619	C ₃₈ H ₃₅ O ₂₂	-0.1	825 (5), 807 (10), 789 (15), 759 (15), 741 (25), 723 (35), 705 (75), 687 (40), 675 (30), 669 (70), 657 (45), 651 (20), 639 (30), 627 (55), 603 (100), 585 (20), 573 (50), 561 (10), 545 (15), 523 (5)
				-	841.1412	no match for C ₃₈ H ₃₃ O ₂₂	-	841 (100), 823 (10), 751 (10), 721 (20), 419 (5)
4C	0.96	tetrahydroxyxanthone- <i>C</i> -hexoside dimer	242, 258, 319, 367	+	843.1650	C ₃₈ H ₃₅ O ₂₂	3.6	843 (5), 825 (15), 807 (30), 789 (30), 771 (25), 759 (20), 741 (30), 735 (20), 729 (25), 723 (35), 711 (35), 705 (100), 693 (55), 687 (75), 675 (30), 669 (60), 657 (40), 651 (55), 639 (40), 627 (80), 609 (20), 603 (65), 597 (15), 585 (50), 573 (55), 561 (10), 555 (20), 545 (5), 531 (<5)
				-	841.1476	C ₃₈ H ₃₃ O ₂₂	1.5	841 (100), 823 (5), 751 (5), 721 (15)
4D	1.04	tetrahydroxyxanthone- <i>C</i> -hexoside dimer	243, 259, 319, 367	+	843.1657	C ₃₈ H ₃₅ O ₂₂	4.4	826 (20), 807 (30), 789 (20), 771 (20), 753 (15), 741 (20), 736 (20), 729 (25), 723 (35), 717 (20), 711 (25), 705 (100), 693 (45), 687 (80), 681 (25), 675 (25), 669 (55), 657 (30), 651 (30), 639 (65), 627 (80), 609 (10), 603 (60), 598 (10), 585 (40), 573 (60), 561 (20), 555 (15), 545 (15), 531 (10)
				-	841.1448	C ₃₈ H ₃₃ O ₂₂	-1.5	841 (100), 823 (5), 751 (5), 721 (20)
4E	1.35	tetrahydroxyxanthone- <i>C</i> -hexoside dimer	242, 260, 319, 367	+	843.1652	C ₃₈ H ₃₅ O ₂₂	3.8	825 (5), 807 (20), 789 (20), 771 (25), 753 (15), 741 (10), 735 (20), 729 (20), 723 (30), 717 (5), 711 (10), 705 (100), 693 (30), 687 (60), 675 (40), 669 (40), 657 (40), 651 (60), 639 (30), 627 (40), 609 (30), 603 (25), 597 (15), 585 (25), 573 (50), 555 (15), 543 (5), 525 (<5)
				-	841.1479	C ₃₈ H ₃₃ O ₂₂	1.9	841 (100), 823 (20), 805 (5), 787 (<5), 751 (15), 733 (5), 721 (40), 703 (10), 661 (<5), 631 (5), 601 (<5), 419 (5)

Table 9 cont.

Nr.	t _R (min) ^a	Proposed Compound	λ _{max} (nm)	Mode	Accurate Mass, exp.	Proposed Mol. Formula	Error (ppm)	LC-MS/MS Ions ^b
4	1.51	mangiferin	240, 257, 318, 366	+	423.0931	C ₁₉ H ₁₉ O ₁₁	0.9	369 (5), 351 (15), 339 (25), 327 (15), 323 (10), 313 (20), 303 (70), 299 (45), 285 (25), 273 (100), 261 (10), 257 (15), 245 (<5)
				-	421.0773	C ₁₉ H ₁₇ O ₁₁	0.5	331 (65), 313 (10), 301 (100), 285 (10), 271 (30), 259 (40)
4F	1.59	isomangiferin	256, 317, 365	+	423.0927	C ₁₉ H ₁₉ O ₁₁	0.0	387 (5), 369 (5), 357 (10), 351 (10), 339 (10), 327 (25), 313 (35), 303 (100), 299 (30), 287 (15), 285 (15), 273 (95), 261 (5), 257 (10), 245 (<5)
				-	421.0757	C ₁₉ H ₁₇ O ₁₁	-3.3	331 (50), 313 (15), 301 (100), 285 (10), 271 (25), 259 (25)
*	1.68	homomangiferin (impurity)	242, 259, 319, 364	+	437.1093	C ₂₀ H ₂₁ O ₁₁	2.1	-
				-	435.0923	C ₂₀ H ₁₉ O ₁₁	-0.9	-
4G	2.05	tetrahydroxyxanthone- <i>C</i> -hexoside isomer	258, 320, 369	+	423.0918	C ₁₉ H ₁₉ O ₁₁	-2.1	369 (5), 351 (15), 339 (25), 327 (20), 323 (10), 313 (25), 303 (45), 299 (35), 285 (15), 273 (100), 261 (10), 257 (10), 245 (<5)
				-	421.0775	C ₁₉ H ₁₇ O ₁₁	0.9	331 (60), 313 (10), 301 (100), 285 (10), 272 (35), 259 (35)
4H	2.35	tetrahydroxyxanthone- <i>C</i> -hexoside isomer	258, 320, 370	+	423.0912	C ₁₉ H ₁₉ O ₁₁	-3.5	369 (<5), 351 (20), 339 (20), 325 (10), 323 (10), 313 (20), 303 (35), 299 (35), 285 (25), 273 (100), 261 (10), 257 (15), 229 (10)
				-	421.0767	C ₁₉ H ₁₇ O ₁₁	-0.9	331 (60), 313 (20), 301 (100), 285 (15), 271 (35), 259 (40)

^aLC-ESI-MS retention times. Refer to Table S14 (Supplementary Material, page 194) for the corresponding retention times on the Agilent UHPLC system and as depicted in Figure 9.

^bValues in bold indicate the base peak ions, and values in brackets indicate the relative intensity of the fragment ions.

Table 10 Retention times, UV-VIS characteristics, accurate masses, proposed molecular formulae and LC-MS/MS fragment ions of compounds (tentatively) identified in a thermally-treated sample (110 °C) of the xanthone isomangiferin (**5**) in 0.1 M phosphate buffer solution (pH 5).

Nr.	t _R (min) ^a	Proposed Compound	λ _{max} (nm)	Mode	Accurate Mass, exp.	Proposed Mol. Formula	Error (ppm)	LC-MS/MS Ions ^b
5A	0.94	tetrahydroxyxanthone- <i>C</i> -hexoside dimer	257, 318, 363	+	843.1645	C ₃₈ H ₃₅ O ₂₂	3.0	825 (<5), 807 (5), 729 (5), 723 (20), 705 (65), 687 (15), 669 (10), 652 (5), 627 (30), 603 (100), 585 (20), 574 (5), 562 (5)
				-	841.1439	C ₃₈ H ₃₃ O ₂₂	-2.9	841 (100), 823 (<5), 751 (10), 721 (20), 419 (10)
5B	1.19	tetrahydroxyxanthone- <i>C</i> -hexoside dimer	257, 317, 366	+	843.1606	C ₃₈ H ₃₅ O ₂₂	-1.7	843 (100), 825 (40), 807 (20), 789 (5), 777 (5), 771 (5), 759 (5), 747 (5), 729 (20), 723 (65), 705 (85), 693 (15), 687 (40), 675 (10), 669 (30), 657 (10), 651 (20), 639 (10), 627 (20), 609 (10), 603 (90), 585 (40), 573 (25), 567 (15), 561 (10), 553 (5), 543 (5)
				-	841.1467	C ₃₈ H ₃₃ O ₂₂	0.5	841 (100), 823 (5), 805 (<5), 751 (20), 721 (20), 661 (5), 631 (5), 419 (<5)
5C	1.48	tetrahydroxyxanthone- <i>C</i> -hexoside dimer	- ^c	+	843.1611	C ₃₈ H ₃₅ O ₂₂	-1.1	843 (100), 825 (55), 807 (10), 789 (5), 777 (5), 771 (5), 759 (10), 753 (10), 747 (20), 735 (10), 730 (10), 723 (65), 705 (80), 693 (20), 687 (40), 675 (10), 669 (30), 663 (10), 651 (40), 639 (10), 633 (10), 627 (30), 609 (25), 603 (40), 585 (30), 573 (30), 567 (15), 561 (10), 555 (5), 543 (5), 531 (5)
				-	841.1458	C ₃₈ H ₃₃ O ₂₂	-0.6	841 (100), 823 (5), 751 (15), 721 (25), 661 (5), 631 (5), 601 (<5)
5D	1.51	mangiferin	- ^c	+	423.0912	C ₁₉ H ₁₉ O ₁₁	-3.5	369 (10), 351 (10), 339 (45), 327 (10), 323 (10), 313 (10), 303 (75), 299 (55), 285 (20), 273 (100), 261 (10), 257 (15), 245 (5)
				-	421.0754	C ₁₉ H ₁₇ O ₁₁	-4.0	403 (<5), 343 (5), 331 (80), 313 (10), 301 (100), 285 (10), 271 (30), 259 (35)
5	1.59	isomangiferin	256, 316, 366	+	423.0924	C ₁₉ H ₁₉ O ₁₁	-0.7	387 (15), 369 (10), 357 (10), 341 (5), 333 (5), 327 (25), 313 (30), 303 (100), 299 (5), 287 (10), 285 (10), 273 (75), 261 (5), 243 (<5)
				-	421.0764	C ₁₉ H ₁₇ O ₁₁	-1.7	343 (<5), 331 (55), 313 (20), 301 (100), 285 (10), 273 (20), 271 (20), 258 (30)

Table 10 *cont.*

Nr.	t _R (min) ^a	Proposed Compound	λ _{max} (nm)	Mode	Accurate Mass, exp.	Proposed Mol. Formula	Error (ppm)	LC-MS/MS Ions ^b
5E	2.17	tetrahydroxyxanthone- <i>C</i> -hexoside isomer	256, 316, 365	+	423.0921	C ₁₉ H ₁₉ O ₁₁	-1.4	387 (15), 369 (15), 357 (10), 341 (5), 334 (5), 327 (20), 313 (20), 303 (100), 299 (10), 287 (10), 285 (20), 273 (80), 261 (10), 243 (5)
				-	421.0762	C ₁₉ H ₁₇ O ₁₁	-2.1	331 (60), 313 (20), 301 (100), 285 (10), 273 (30), 271 (25), 259 (25), 258 (25)
5F	2.38	tetrahydroxyxanthone- <i>C</i> -hexoside isomer	256, 316, 366	+	423.0923	C ₁₉ H ₁₉ O ₁₁	-0.9	405 (<5), 387 (5), 369 (5), 357 (<5), 341 (5), 327 (30), 313 (40), 303 (70), 299 (5), 287 (15), 285 (10), 273 (100), 261 (5), 243 (5)
				-	421.0765	C ₁₉ H ₁₇ O ₁₁	-1.4	343 (5), 331 (50), 313 (30), 301 (100), 285 (10), 273 (20), 258 (40)

^aLC-ESI-MS retention times. Refer to Table S14 (Supplementary Material, page 194) for the corresponding retention times on the Agilent UHPLC system and as depicted in Figure 9.

^bValues in bold indicate the base peak ions, and values in brackets indicate the relative intensity of the fragment ions.

^cNot specified due to co-elution.

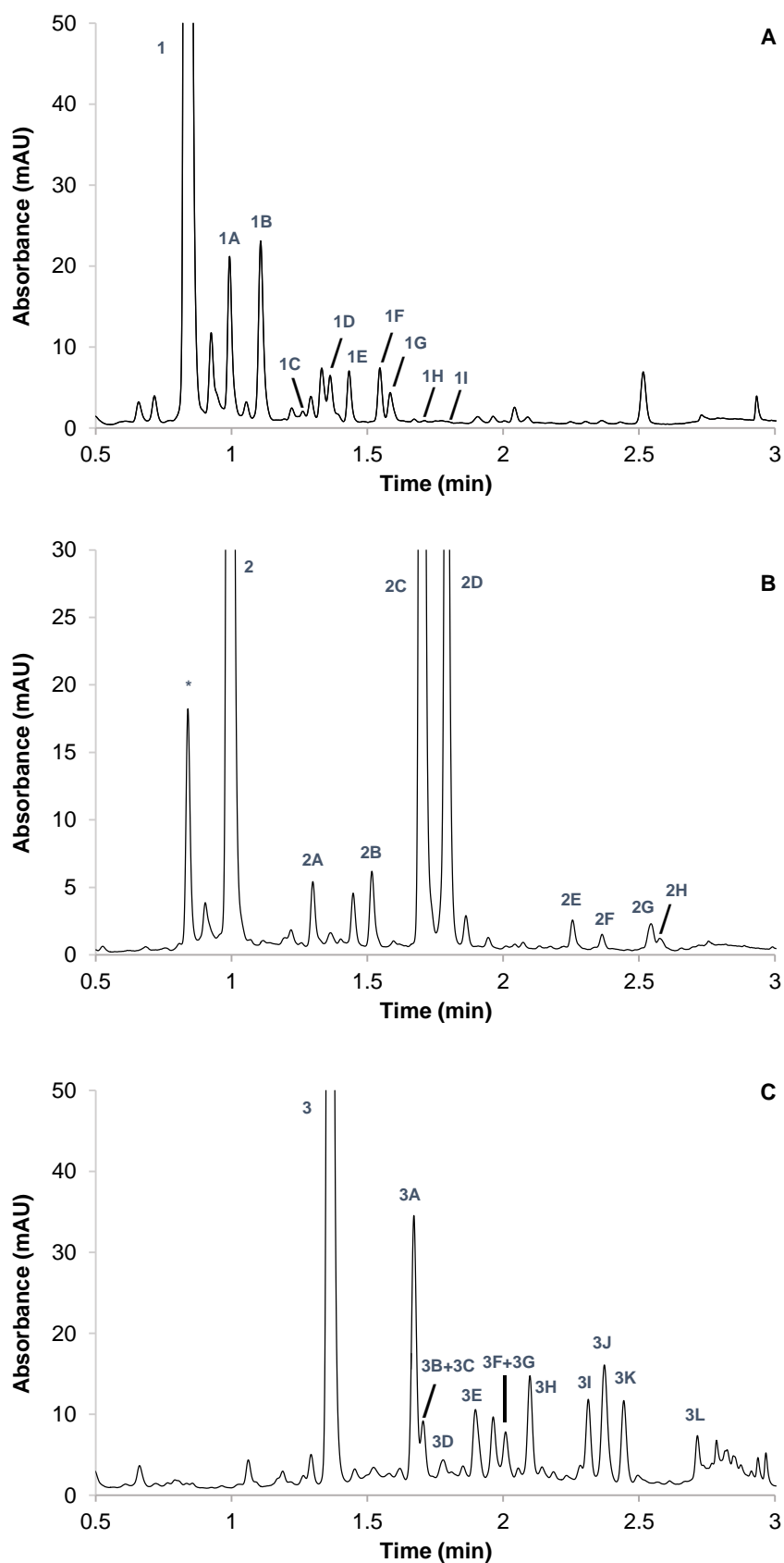


Figure 8 UHPLC-DAD chromatograms of thermally treated (110 °C) samples of the benzophenones (0.1 M phosphate buffer solution, pH 5): **A**) 3- β -D-glucopyranosyl-4- β -D-glucopyranosyloxyiriflophenone (**1**, $\lambda = 288$ nm); **B**) 3- β -D-glucopyranosylmaclurin (**2**, $\lambda = 320$ nm), *impurity (3- β -D-glucopyranosyl-4- β -D-glucopyranosyloxyiriflophenone); **C**) 3- β -D-glucopyranosyliriflophenone (**3**, $\lambda = 288$ nm). Peak labels correspond to Tables 6, 7 and 8, respectively.

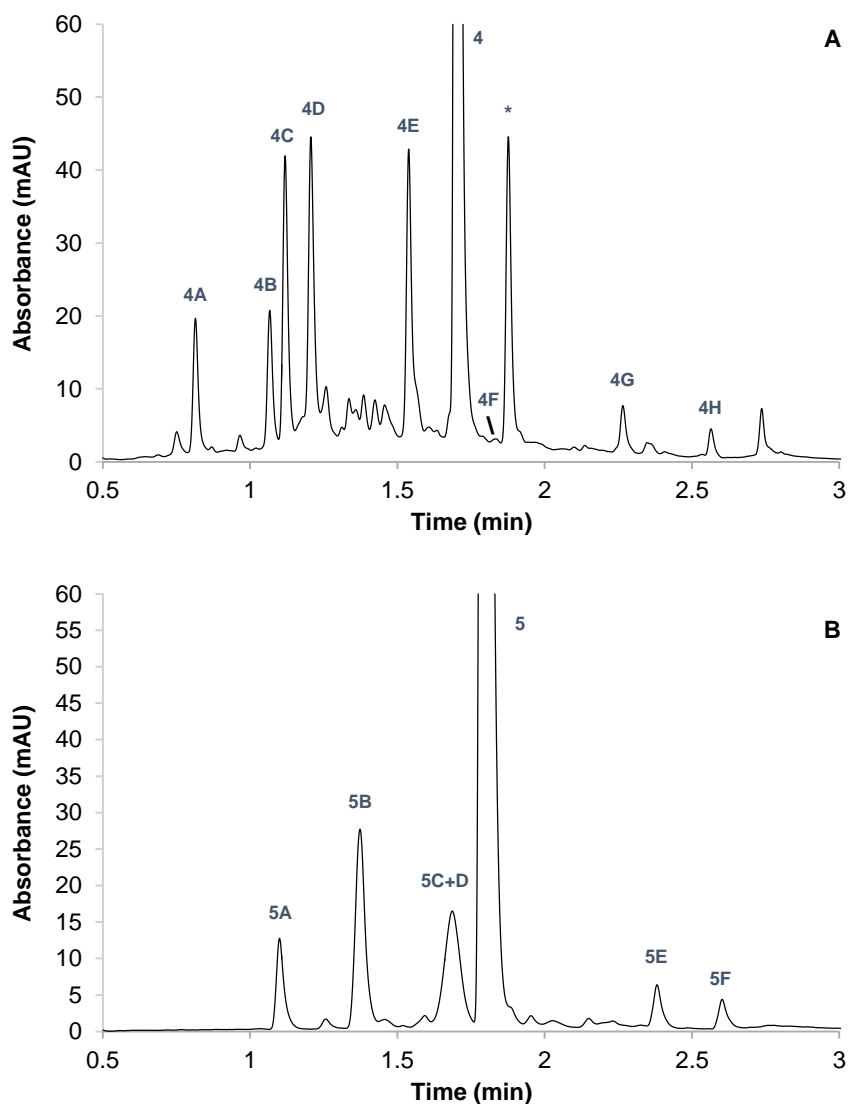


Figure 9 UHPLC-DAD chromatograms of thermally treated (110 °C) samples of the xanthenes (0.1 M phosphate buffer solution, pH 5): **A**) mangiferin (**4**, $\lambda = 320$ nm), *impurity (homomangiferin); **B**) isomangiferin (**5**, $\lambda = 320$ nm). Peak labels correspond to Tables 9 and 10, respectively.

Under the specific conditions employed in the current study, all benzophenones were also converted to mangiferin and isomangiferin. While these xanthenes were only present in trace quantities in the thermally-treated solutions of 3- β -D-glucopyranosyl-4- β -D-glucopyranosyloxiriflophenone and 3- β -D-glucopyranosyliriflophenone, mangiferin and isomangiferin represented the major constituents of a thermally-treated solution of 3- β -D-glucopyranosylmaclurin (Figure 8). The conversion of 3- β -D-glucopyranosylmaclurin to mangiferin and isomangiferin proceeded very rapidly, and was found to be the predominant reaction of 3- β -D-glucopyranosylmaclurin during thermal treatment. This interconversion reaction was subsequently also characterised kinetically, which will be discussed in section 3.4, together with the significance thereof. The presence of the tetrahydroxyxanthone-C-hexoside isomers **2E** ($t_R = 2.06$ min), **2F** ($t_R = 2.16$ min) and **2H** ($t_R = 2.36$ min) in the thermally-treated solution of 3- β -D-glucopyranosylmaclurin (Figure 8, Table 7) is ascribed to the secondary degradation reactions of mangiferin and isomangiferin, based on their co-occurrence in thermally-treated solutions of mangiferin (compounds **4G** and **4H**, Table 9) and isomangiferin (compound **5E**, Table 10).

In addition to isomerisation, the xanthenes were also subject to thermally-induced dimerisation reactions. Mangiferin (**4**) formed five prominent tetrahydroxyxanthone-*C*-hexoside dimers (**4A**, **4B**, **4C**, **4D** and **4E**; Table 9) and isomangiferin (**5**) formed three of these tetrahydroxyxanthone-*C*-hexoside dimers (**5A**, **5B** and **3C**; Table 10) (Figure 9). These compounds presented deprotonated molecule ions at m/z 841 ($[M-H]^-$) and were assigned a molecular formula of $C_{38}H_{33}O_{22}$ ($[M-H]^-$) by HRESIMS. The compounds all eluted at different times, suggesting slight differences in their molecular structures and therefore also their polarity. Interestingly, two such tetrahydroxyxanthone-*C*-hexoside dimers were previously detected in fermented *C. genistoides* extracts (compounds **g** and **k**; Table 2, Chapter 3), but not unfermented *C. genistoides* extracts. This is in accordance with the observation in the current study, namely that the dimeric xanthone compounds were only formed under high-temperature conditions. The co-occurrence of these tetrahydroxyxanthone-*C*-hexoside dimers in fermented *C. genistoides* extracts and thermally-treated solutions of mangiferin and isomangiferin should, however, be confirmed by analysing the respective samples with the same HPLC-DAD method, followed by comparison of their retention times. This also holds true for the co-occurrence of the iriflophenone-di-*O,C*-hexoside isomers and tetrahydroxyxanthone-*C*-hexoside isomers in aqueous *C. genistoides* extracts and their respective thermally-treatment solutions (as discussed in the preceding text).

A thermally-treated solution of 3- β -D-glucopyranosyl-4- β -D-glucopyranosyloxyiriflophenone (**1**) contained small quantities of 3- β -D-glucopyranosyliriflophenone (**1D**), indicating that hydrolysis of the glucopyranosyloxy moiety of **1** occurred upon thermal treatment in a slightly acidic aqueous environment (pH 5) (Table 6). Three other major degradation products (**1E**, **1F** and **1G**) were also detected in a thermally-treated solution of 3- β -D-glucopyranosyl-4- β -D-glucopyranosyloxyiriflophenone, but the exact identities of these compounds could not be established based on the available data (Table 6). They were, however, assigned as benzophenone derivatives, based on their characteristic UV spectra ($\lambda_{max} \sim 290$ -295 nm), and the presence of common and distinctive fragment ions in their MS/MS spectra. Compounds **1E** ($t_R = 1.25$ min) and **1F** ($t_R = 1.35$ min) presented deprotonated molecules at m/z 611 ($[M-H]^-$) and were assigned a molecular formula of $C_{27}H_{31}O_{16}$ ($[M-H]^-$) by HRESIMS. This represents a mass difference of 42 amu with respect to 3- β -D-glucopyranosyl-4- β -D-glucopyranosyloxyiriflophenone, corresponding to a C_2H_2O group. The MS/MS spectra of compounds **1E** and **1F** in positive ionisation mode (Figure S5, Supplementary Material, page 199) were almost exactly the same as that of the original compound, 3- β -D-glucopyranosyl-4- β -D-glucopyranosyloxyiriflophenone, but with slight differences in the relative intensities of the fragment ions. Conversely, slight differences were observed between the MS/MS spectrum of compound **1E** compared to those of compounds **1** and **1F** in negative ionisation mode (Figure S6, Supplementary Material, page 200). Compound **1G**, detected at 1.38 min, presented deprotonated and protonated molecules at m/z 495 ($[M-H]^-$) and 497 ($[M+H]^+$), respectively, and maximum UV absorbance at 295 nm. The experimental accurate mass (495.1147, $[M-H]^-$) was in good agreement with the proposed molecular formula of $C_{22}H_{23}O_{13}$. The deprotonated molecule yielded a base peak fragment ion at m/z 375 ($[M-H-120]^-$), while tandem MS analysis of compound **1G** in positive ionisation mode yielded a base peak fragment ion at m/z 195. The presence of this base peak ion at m/z 195, together with the fragment ions detected at m/z 289, 271 and 177, supports the identification of **1G** as a benzophenone derivative, as these fragment ions correspond to those detected in the lower molecular weight region of the MS/MS spectrum of compound **1** (both in positive ionisation mode; Table 6).

LC-DAD-ESI-MS analysis of a thermally treated solution of 3- β -D-glucopyranosylmaclurin (**2**) revealed the presence of a minor compound (compound **2G**), which exhibited UV-absorbance characteristics typical of the xanthone phenolic sub-class ($\lambda_{max} = 258, 329, 370$ nm; Table 7). This xanthone derivative **2G** ($t_R = 2.35$ min) presented a deprotonated molecule at m/z 463 ($[M-H]^-$) and was assigned a molecular formula of $C_{21}H_{19}O_{12}$ ($[M-H]^-$) by HRESIMS. This represents a mass difference of 42 amu ($\equiv C_2H_2O$ group) with respect to tetrahydroxyxanthone-hexosyl compounds such

as mangiferin, also detected in a thermally treated solution of 3- β -D-glucopyranosylmaclurin. The MS/MS spectra of compound **2G** in positive (Figure S7, Supplementary Material, page 201) and negative (Figure S8, Supplementary Material, page 201) ionisation modes were almost exactly the same as those of the tetrahydroxyxanthone-*C*-hexosides, but with slight differences observed in the relative intensities of the fragment ions. The corresponding MS/MS spectra of mangiferin (**2C**), as representative tetrahydroxyxanthone-*C*-hexoside, are also depicted in Figures S7 and S8.

The identification of degradation products **1E** and **1F** in a thermally treated solution of 3- β -D-glucopyranosyl-4- β -D-glucopyranosyloxyiriflophenone (**1**), and the presence of compound **2G** in a thermally treated solution of 3- β -D-glucopyranosylmaclurin (**2**), indicate that the addition of an O-linked C₂H₂O group (acetyl group), either to the parent compound **1** or to primary degradation products of **2**, may also occur upon thermal treatment. Further research is, however, required to elucidate the reaction mechanism and to determine the location of the additional C₂H₂O group. The thermally-induced acetylation of isoflavone β -glucosides has been reported previously (Xu *et al.*, 2002). Xu *et al.* (2002) reported that heating of a dry residue of daidzin, genistin and glycitin (temperatures > 135 °C) produced acetyldaidzin and acetylgenistin, as well as the aglycones daidzein, genistein and glycitein. The generation of acetyldaidzin and acetylgenistin was unexpected and the authors postulated that acetyl groups may have been produced during thermal degradation of the original glucosides, with subsequent acetylation of daidzin and genistin during heating.

Upon thermal treatment, 3- β -D-glucopyranosyliriflophenone (**3**) was subject to isomerisation with the formation of two iriflophenone-*C*-hexoside isomers **3B** and **3E**, while small quantities thereof was converted to the xanthenes mangiferin (**3C**) and isomangiferin (**3D**) (as discussed in the preceding text). In addition, 3- β -D-glucopyranosyliriflophenone formed a large number of degradation compounds which could not be identified based on the current data (Table 8). Of particular interest was one such compound (compound **3M**) that was only detected during LC-DAD-ESI-MS analysis (Figure 10).

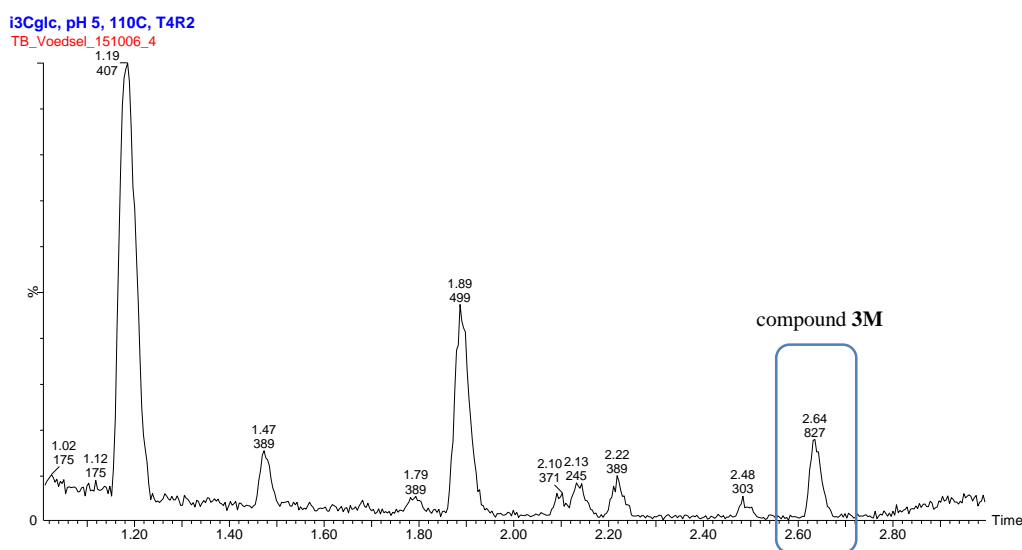


Figure 10 Base peak ion (BPI) chromatogram of a thermally-treated solution of 3- β -D-glucopyranosyliriflophenone (**3**) in negative ionisation mode showing the presence of compound **3M** ($t_R = 2.64$ min, m/z 827 [$M-H$]⁻).

Compound **3M** ($t_R = 2.64$ min) presented a deprotonated molecule at m/z 827 ([$M-H$]⁻) and was tentatively identified as a benzophenone derivative based on its UV-absorbance characteristics ($\lambda_{max} = 295$ nm; Table 8). The experimental accurate mass of the deprotonated molecule (827.2053, [$M-H$]⁻) was in good agreement with the proposed molecular formula of C₃₉H₃₉O₂₀. In the higher molecular weight region, the MS/MS spectrum of the deprotonated molecule was characterised by the presence of the following fragment ions (m/z): 827 ([$M-H$]⁻), 809 ([$M-H-H_2O$]⁻), 737 ([$M-H-90$]⁻),

719 ($[M-H-90-H_2O]^-$), 707 ($[M-H-120]^-$), 689 ($[M-H-120-H_2O]^-$), 617 ($[M-H-120-90]^-$), 599 ($[M-H-120-90-H_2O]^-$) and 587 ($[M-H-2 \times 120]^-$) (Figure 11).

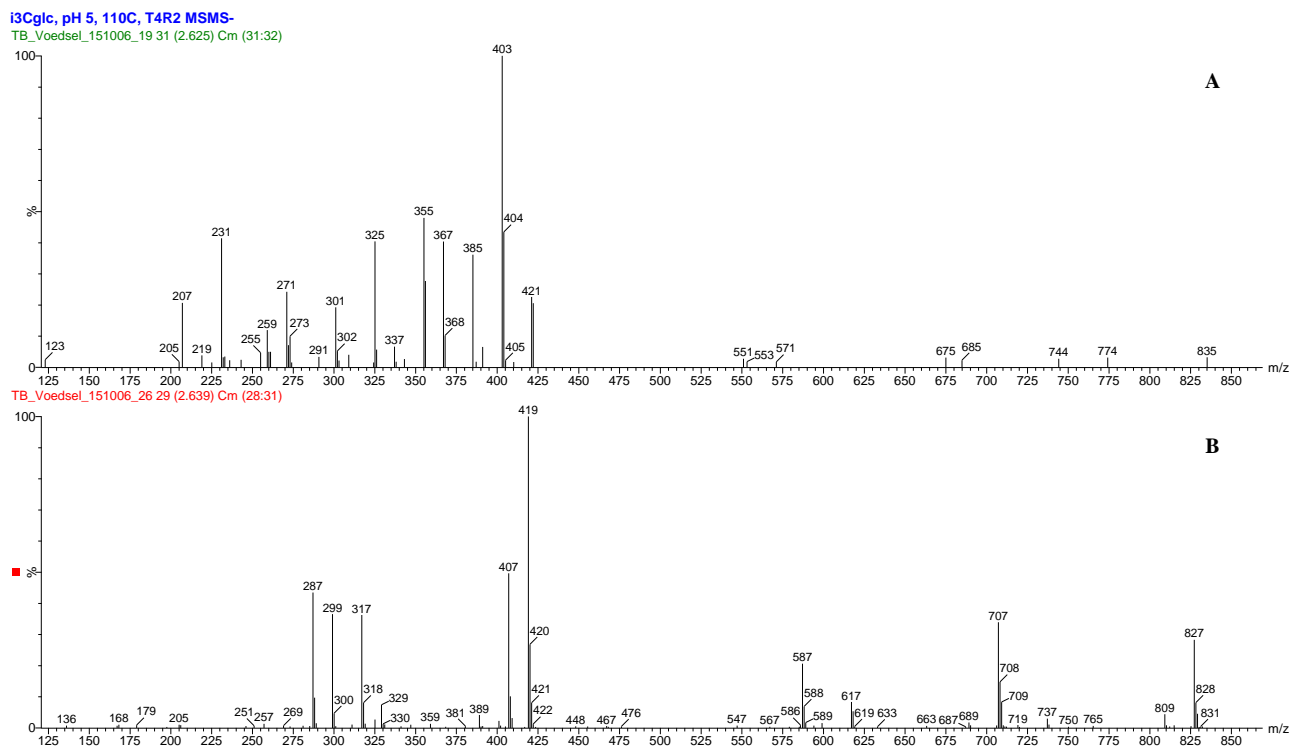


Figure 11 LC-ESI-MS/MS spectra of compound **3M** in **A**) positive ionisation mode and **B**) negative ionisation mode (Refer to Table 8 for additional information).

This fragmentation pattern is characteristic of the cross-ring cleavage of two hexosyl moieties. The base peak ion in the MS/MS spectrum of **3M** (negative ionisation mode) was detected at m/z 419 ($[M-H-408]^-$), which could correspond to the neutral loss of a 3- β -D-glucopyranosyliriflophenone molecule. This is supported by the presence of the corresponding deprotonated molecule detected at m/z 407 (Figure 11). The experimental accurate mass of the fragment ion at m/z 407 (407.0989, $[M-H]^-$) was in good agreement with the molecular formula of $C_{19}H_{19}O_{10}$, matching that of a deprotonated 3- β -D-glucopyranosyliriflophenone molecule. Similarly, the elemental composition of the base peak fragment ion at m/z 419 (exp. accurate mass: 419.0981, $[M-H]^-$) was assigned as $C_{20}H_{19}O_{10}$. It is herewith postulated that compound **3M** represents a benzophenone dimer, in which one monomeric unit is 3- β -D-glucopyranosyliriflophenone and the other monomer is a compound with the neutral molecular formula of $C_{20}H_{20}O_{10}$. The fragment ions detected at m/z 401, 329 and 299 would therefore respectively correspond to subsequent losses of 18 amu (H_2O), 90 amu and 120 amu from the monomeric unit at m/z 419 (Figure 11). Similarly, the fragment ions detected at m/z 389, 317, 299 and 287 would be the result of subsequent fragmentation of the 3- β -D-glucopyranosyliriflophenone monomeric unit, characterised by losses of water molecules and/or losses of 90 and 120 amu (Figure 11). This is supported by the presence of these fragment ions in the MS/MS spectrum of the authentic 3- β -D-glucopyranosyliriflophenone standard (Table 8). The tentative identification of the structure of compound **3M** is supported by its fragmentation pattern upon tandem MS analysis in positive ionisation mode (Figure 11). It would thus be of great interest to isolate this structurally-unique benzophenone dimer for unambiguous identification.

3.4. Evolution of Mangiferin and Isomangiferin in Thermally-Treated Solutions of 3- β -D-Glucopyranosylmaclurin as a Function of Treatment Temperature and Time

Upon thermal treatment, 3- β -D-glucopyranosylmaclurin was predominantly converted to the xanthenes mangiferin and isomangiferin (section 3.3). Typical formation curves of mangiferin and isomangiferin are depicted in Figure S9 (Supplementary Material, page 202) and the computed values for the conversion reactions are summarised in Table 11.

Table 11 Degradation and conversion rate constants of 3- β -D-glucopyranosylmaclurin (**2**) upon thermal treatment in aqueous model solutions (0.1 M phosphate buffer, pH 5).

Rate equation ^a		Treatment temperature					
		90 °C		100 °C		110 °C	
		<i>k</i> (h ⁻¹)	<i>R</i> ²	<i>k</i> (h ⁻¹)	<i>R</i> ²	<i>k</i> (h ⁻¹)	<i>R</i> ²
M3Cglc → M	<i>k</i> ₁	0.314 (0.310 – 0.318)	1.00	0.598 (0.588 – 0.609)	1.00	1.62 (1.58 – 1.67)	0.98
M3Cglc → IsoM	<i>k</i> ₃	0.128 (0.126 – 0.129)	1.00	0.263 (0.260 – 0.266)	1.00	0.719 (0.703 – 0.735)	0.99
M3Cglc → <i>D</i> _{M3Cglc}	<i>k</i> ₂	0.235	–	0.399	–	1.07	–

^aM3Cglc = 3- β -D-glucopyranosylmaclurin, *D*_{M3Cglc} = unknown degradation products, M = mangiferin, and IsoM = isomangiferin.

From this data, it is clear that 3- β -D-glucopyranosylmaclurin is predominantly converted to mangiferin under thermal stress, followed by its degradation to unknown products, and its conversion to isomangiferin in descending order (Table 11). The rates of conversion of 3- β -D-glucopyranosylmaclurin to mangiferin and isomangiferin presented a stoichiometric ratio of *ca.* 2:1, indicating that mangiferin, as the C-2 isomer, is formed preferentially. Increases in the rate constants of all reactions were observed as the temperature increased, but an insufficient number of temperature treatments were performed to accurately estimate the Arrhenius activation energy. The rate constants did, however, increase approximately two to three times as the temperature was increased by 10 °C (Table 11), which is in accordance with Van't Hoff's law (Bělehrádek, 1930).

The conversion reactions observed upon thermal treatment of an aqueous solution of 3- β -D-glucopyranosylmaclurin is in line with the biosynthetic pathway proposed for mangiferin and isomangiferin, where these xanthenes are biosynthesised via 3- β -D-glucopyranosylmaclurin in the plant material (Fujita & Inoue, 1980a, 1980b, 1981). This cyclisation (reaction) of benzophenones has also found application in the general synthesis of polyoxygenated xanthenes from benzophenone precursors (*e.g.* Quillinan & Scheinmann, 1973).

The conversion reactions observed for 3- β -D-glucopyranosylmaclurin in the current study underscores the importance of using individual model solutions for thermal stability assessments. If 3- β -D-glucopyranosylmaclurin, mangiferin and isomangiferin were subjected to thermal treatment as a mixture of compounds, the conversion of 3- β -D-glucopyranosylmaclurin to these xanthenes would have off-set losses in their content, thereby confounding reaction kinetics/under-estimating their respective degradation rates. This is also relevant to the thermal stability assessments conducted previously in the *C. genistoides* plant material (Chapter 5). However, as 3- β -D-glucopyranosylmaclurin is only present at low levels in the plant material, its conversion to mangiferin and isomangiferin in the plant material can be deemed insignificant. This also has implications for the selection of a compound as indicator of thermal stress for *Cyclopia* extracts containing xanthenes and benzophenones.

4. CONCLUSIONS

This work expanded the body of knowledge regarding the thermal stability of compounds from the benzophenone and xanthone phenolic sub-classes. The thermal stability of the xanthenes and benzophenones was principally determined by their chemical structures, and was also significantly affected by temperature. It was herein re-confirmed that increased glucosylation on the A-ring of the benzophenones significantly increases their thermal stability, and that the position of glucosylation affects the thermal stability of the xanthenes. While it is well known that increased B-ring hydroxylation decreases the thermal stability of phenolic compounds, this structure-stability relationship was affirmed for the first time for the benzophenones in the current study. The first-order degradation rate constants of all compounds significantly increased with temperature, and the temperature-dependence of the reaction rate constants could adequately be described by the linearised form of the Arrhenius equation. pH also had a significant effect on the thermal stability of mangiferin, with maximum stability observed at pH 3. The pH-dependence of the reaction rate constant of mangiferin at 100 °C presented an exponential relationship. The mathematical expressions describing the effect of temperature and pH on the rate constants can subsequently be used to compute the degradation rates of the target compounds at intermediate temperature (all compounds) and pH (only mangiferin) levels, making it useful tools to predict compound stability under common thermal treatment conditions (*e.g.* pasteurisation or sterilisation). It is, however, recommended that the models be validated in subsequent work. The current work also provided fundamental insight into the thermal degradation pathways of the xanthenes and benzophenones, which has not been addressed to date. Of particular interest was the thermally-induced conversion of 3- β -D-glucopyranosylmaclurin to its xanthone analogues mangiferin and isomangiferin, which is in accordance with the biosynthetic pathway proposed for these xanthenes in higher plants. Distinct similarities in the chromatographic profiles of thermally-treated solutions of the target compounds and aqueous extracts of fermented *C. genistoides* were also demonstrated, indicative of parallel degradation pathways under thermal stress in an aqueous environment and under high-temperature oxidative conditions in the plant material. Further research is, however, still required to elucidate the exact degradation mechanisms, and to elucidate the structures of the degradation products.

REFERENCES

- Atkinson, J.E. & Lewis, J.R. (1969). Oxidative coupling. Part VII. Biogenic type synthesis of naturally occurring xanthenes. *Journal of the Chemical Society C: Organic*, 281-287.
- Atkinson, J.E., Gupta, P. & Lewis, J.R. (1969). Some phenolic constituents of *Gentiana lutea*. *Tetrahedron*, **24**, 1507-1511.
- Baggett, S., Mazzola, E.P. & Kennelly, E.J. (2005). The benzophenones: isolation, structural elucidation and biological activities. In: *Studies in Natural Products Chemistry*, Vol. 32. Edited by Atta-ur-Rahman. Elsevier B.V., Amsterdam, The Netherlands.
- Beelders, T., Brand, D.J., De Beer, D., Malherbe, C.J., Mazibuko, S.E., Muller, C.J.F. & Joubert, E. (2014a). Benzophenone C- and O-glucosides from *Cyclopia genistoides* (honeybush) inhibit mammalian α -glucosidase. *Journal of Natural Products*, **77**, 2694-2699.
- Beelders, T., De Beer, D. & Joubert, E. (2015). Thermal degradation kinetics modelling of benzophenones and xanthenes during high-temperature oxidation of *Cyclopia genistoides* (L.) Vent. plant material. *Journal of Agricultural and Food Chemistry*, **63**, 5518-5527.
- Bélehrádek, J. (1930). Temperature coefficients in biology. *Biology Reviews*, **5**, 30-58.
- Bennett, G.J. & Lee, H.-H. (1989). Xanthenes from Guttiferae. *Phytochemistry*, **28**, 967-998.
- Buchner, N., Krumbein, A., Rohn, S. & Kroh, L.W. (2006). Effect of thermal processing on the flavonols rutin and quercetin. *Rapid Communications in Mass Spectrometry*, **20**, 3229-3235.
- Canales, I., Borrego, F. & Lindley, M.G. (1993). Neohesperidin dihydrochalcone stability in aqueous buffer solutions. *Journal of Food Science*, **57**, 589-591, 643.
- Coiffard, C., Coiffard, L., Peigné, F. & De Roeck-Holtzhauer, Y. (1998). Effect of pH on neohesperidin dihydrochalcone thermostability in aqueous solutions. *Analisis*, **25**, 150-153.
- De Paepe, D., Valkenburg, D., Coudijzer, K., Noten, B., Servaes, K., De Loose, M., Voorspoels, S., Diels, L. & Van Droogenbroeck, B. (2014). Thermal degradation of cloudy apple juice phenolic constituents. *Food Chemistry*, **162**, 176-185.
- Feng, J., Yang, X.-W. & Wang, R.-F. (2011). Bio-assay guided isolation and identification of α -glucosidase inhibitors from the leaves of *Aquilaria sinensis*. *Phytochemistry*, **72**, 242-247.
- Fujita, M. & Inoue, T. (1980a). Biosynthesis of mangiferin in *Anemarrhena asperoides* BUNGE. I. The origin of the xanthone nucleus. *Chemical and Pharmaceutical Bulletin*, **28**, 2476-2481.
- Fujita, M. & Inoue, T. (1980b). Biosynthesis of mangiferin in *Anemarrhena asperoides* BUNGE. II. C-glucosylation of mangiferin. *Chemical and Pharmaceutical Bulletin*, **28**, 2482-2486.
- Fujita, M. & Inoue, T. (1980). Further studies on the biosynthesis of mangiferin in *Anemarrhena asperoides*: hydroxylation of the shikimate-derived ring. *Phytochemistry*, **20**, 2183-2185.
- Guo, Y.-X., Zhang, D.-J., Wang, H., Xiu, Z.-L., Wang, L.-X. & Xiao, H.-B. (2007). Hydrolytic kinetics of lithospermic acid B extracted from roots of *Salvia miltiorrhiza*. *Journal of Pharmaceutical and Biomedical Analysis*, **43**, 435-439.
- Joubert, E., Joubert, M.E., Bester, C., De Beer, D., De Lange, J.H. (2011). Honeybush (*Cyclopia* spp.): From local cottage industry to global markets – the catalytic and supporting role of research. *South African Journal of Botany*, **77**, 887-907.
- Kokotkiewich, A., Luczkiewicz, M., Sowinski, P., Glod, D., Gorynski, K. & Bucinski, A. (2012). Isolation and structure elucidation of phenolic compounds from *Cyclopia subternata* Vogel (honeybush) intact plant and *in vitro* cultures. *Food Chemistry*, **133**, 1373-1382.

- Kokotkiewicz, A., Luczkiewicz, M., Pawlowska, J., Luczkiewicz, P., Sowinski, P., Witkowski, J., Bryl, E. & Bucinski, A. (2013). Isolation of xanthone and benzophenone derivatives from *Cyclopia genistoides* (L.) Vent. (honeybush) and their pro-apoptotic activity on synoviocytes from patients with rheumatoid arthritis. *Fitoterapia*, **90**, 199-208.
- Khuwijitjaru, P., Plernjit, J., Suaylam, B., Samuhaseneetoo, S., Pongsawatmanit, R. & Adachi, S. (2014). Degradation kinetics of some phenolic compounds in subcritical water and radical scavenging activity of their degradation products. *The Canadian Journal of Chemical Engineering*, **92**, 810-815.
- Lewis, J.R. (1963). Biogenetic type syntheses of the xanthone nucleus. *Proceedings of the Chemical Society*, 373.
- Li, N., Taylor, L.S., Ferruzzi, M.G. & Mauer, L.J. (2012). Kinetic study of catechin stability: Effects of pH, concentration, and temperature. *Journal of Agricultural and Food Chemistry*, **60**, 12531-12539.
- Makris, D.P. & Rossiter, J.T. (2000). Heat-induced, metal-catalyzed oxidative degradation of quercetin and rutin (quercetin 3-O-rhamnosylglucoside) in aqueous model systems. *Journal of Agricultural and Food Chemistry*, **48**, 3830-3838.
- Malherbe, C.J., Willenburg, E., de Beer, D., Bonnet, S.L., van der Westhuizen, J.H. & Joubert, E. (2014). Iriflophenone-3-C-glucoside from *Cyclopia genistoides*: Isolation and quantitative comparison of antioxidant capacity with mangiferin and isomangiferin using on-line HPLC antioxidant assays. *Journal of Chromatography B*, **951-952C**, 164-171.
- Murakami, T., Tanaka, N., Wada, H. Saiki, Y. & Chen, C.-M. (1986). Chemical and chemotaxonomical studies on filices. Xanthone derivatives of *Hypodematum fauriei* TAGAWA, *H. crenatum* KUHN and *Gymnocarpium robertianum* NEWM. (*G. jessoense* KOIDZ.). *Yakugaku Zasshi*, **106**, 378-382.
- Negi, J.S., Bisht, V.K., Singh, P., Rawat, M.S.M. & Joshi, G.P. (2013). Naturally occurring xanthenes: chemistry and biology. *Journal of Applied Chemistry*, **2013**, DOI: 10.1155/2013/621459.
- Pan, J., Gong, X. & Qu, H. (2013). Quantitative ¹H NMR method for hydrolytic kinetic investigation of salvianolic acid B. *Journal of Pharmaceutical and Biomedical Analysis*, **85**, 28-32.
- Peleg, M., Normand, M.D. & Corradini, M.G. (2012). The Arrhenius equation revisited. *Critical Reviews in Food Science and Nutrition*, **52**, 830-851.
- Quillinan, A.J. & Scheinmann, F. (1973). Studies in the xanthone series. Part XII. A general synthesis of polyoxygenated xanthenes from benzophenone precursors. *Journal of the Chemical Society, Perkin Transactions I*, 1329-1337.
- Rohn, S., Buchner, N., Driemel, G., Rauser, M. & Kroh, L.W. (2007). Thermal degradation of onion quercetin glucosides under roasting conditions. *Journal of Agricultural and Food Chemistry*, **55**, 1568-1573.
- Schulze, A.E., Beelders, T., Koch, I.S., Erasmus, L.M., De Beer, D. & Joubert, E. (2015a). Honeybush herbal teas (*Cyclopia* spp.) contribute to high levels of dietary exposure to xanthenes, benzophenones, dihydrochalcones and other bioactive phenolics. *Journal of Food Composition and Analysis*, **44**, 139-148.
- Schulze, A.E., De Beer, D., Mazibuko, S.E., Muller, C.J.F., Roux, C., Willenburg, E.L., Nyunai, N., Louw, J., Manley, M & Joubert, E. (2015b). Assessing similarity analysis of chromatographic fingerprints of *Cyclopia subternata* extracts as potential screening tool for *in vitro* glucose utilization. *Analytical and Bioanalytical Chemistry*, DOI: 10.1007/s00216-015-9147-7.
- Shabir, G.A., Lough, W.J., Arain, S.A. & Bradshaw, T.K. (2007). Evaluation and application of best practice in analytical method validation. *Journal of Liquid Chromatography & Related Technologies*, **30**, 311-333.
- Shaw, J.E., Sicree, R.A. & Zimmet, P.Z. (2010). Global estimates of the prevalence of diabetes for 2010 and 2030. *Diabetes Research and Clinical Practice*, **87**, 4-14.
- Stintzing, F.C., Hoffmann, M. & Carle, R. (2006). Thermal degradation kinetics of isoflavone aglycones from soy and red clover. *Molecular Nutrition and Food Research*, **50**, 373-377.

- Sultanbawa, M.U.S. (1980). Xanthonoids of tropical plants. *Tetrahedron*, **36**, 1465-1506.
- Tanaka, T., Sueyasu, T., Nonaka, G.-I. & Nishioka, I. (1984). Tannins and related compounds. XXI. Isolation and characterization of galloyl and *p*-hydroxybenzoyl esters of benzophenone and xanthone *C*-glucosides from *Mangifera indica* L. *Chemical and Pharmaceutical Bulletin*, **32**, 3676-2686.
- Vaidya, N.A., Mathias, K., Ismail, B., Hayes, K.D. & Corvalan, C.M. (2007). Kinetic modeling of malonylgenistin and malonyldaidzin conversions under alkaline conditions and elevated temperatures. *Journal of Agricultural and Food Chemistry*, **55**, 3408-3413.
- Van Boekel, M.A.J.S. (1996). Statistical aspects of kinetic modelling for food science problems. *Journal of Food Science*, **61**, 477-486.
- Van Boekel, M.A.J.S. (2008). Kinetic modeling of food quality: a critical review. *Comprehensive Reviews in Food Science and Food Safety*, **7**, 144-158.
- Vieira, L.M.M. & Kijjoo, A. (2005). Naturally-occurring xanthenes: recent developments. *Current Medicinal Chemistry*, **12**, 2413-2446.
- Vyas, A., Syeda, K., Ahmad, A., Padhye, S. & Sarkar, F.H. (2012). Perspectives on medicinal properties of mangiferin. *Mini-Reviews in Medicinal Chemistry*, **12**, 412-425.
- Wang, L.-F., Kim, D.-M. & Lee, C.Y. (2000). Effects of heat processing and storage on flavanols and sensory qualities of green tea beverage. *Journal of Agricultural and Food Chemistry*, **48**, 4227-4232.
- Xu, Z., Wu, Q. & Godber, J.S. (2002). Stabilities of daidzin, glycitin, genistin, and generation of derivatives during heating. *Journal of Agricultural and Food Chemistry*, **50**, 7402-7406.
- Zhang, Y., Liu, X., Han, L., Gao, X., Liu, E. & Wang, T. (2013a). Regulation of lipid and glucose homeostasis by mango tree leaf extract is mediated by AMPK and PI3K/AKT signalling pathways. *Food Chemistry*, **141**, 2896-2905.
- Zhang, Q.-F., Fu, Y.-J., Huang, Z.-W., Shangguang, X.-C. & Guo, Y.-X (2013b). Aqueous stability of astilbin: effects of pH, temperature, and solvent. *Journal of Agricultural and Food Chemistry*, **61**, 12085-12091.
- Zielinski, H., Michalska, A., Amigo-Benavent, M., Del Castillo, M. D. & Piskula, M.K. (2009). Changes in protein quality and antioxidant properties of buckwheat seeds and groats induced by roasting. *Journal of Agricultural and Food Chemistry*, **57**, 4771-4776.

SUPPLEMENTARY MATERIAL CHAPTER 6

Table S1 Percentage relative standard deviation (% RSD) values for the determination of analytical precision of phenolic compounds in a calibration mixture (0.1 M phosphate buffer solution, pH 5).

Compound	Concentration, µg on-column ^a	Analytical precision			
		day 1 (n = 6)	day 2 (n = 6)	day 3 (n = 6)	pooled (n = 3)
3-β-D-Glucopyranosyl-4-β-D-glucopyranosyloxyiriflophenone (1)	0.3492	0.07	0.11	0.14	0.20
3-β-D-Glucopyranosylmaclurin (2)	0.4284	0.17	0.06	0.16	2.72
3-β-D-Glucopyranosyliriflophenone (3)	0.2900	0.13	0.13	0.16	1.11
Mangiferin (4)	0.2543	0.15	0.16	0.14	1.16
Isomangiferin (5)	0.2908	0.10	0.10	0.12	0.63

^aCorresponding to an injection volume of 7 µL, roughly representing the midpoint in the range of the calibration curves. Value in bold does not conform to precision criteria of % RSD ≤ 2% (Shabir *et al.*, 2007).

Table S2 Percentage relative standard deviation (% RSD) values for the determination of analyte stability in the reaction solvent (0.1 M phosphate buffer solution) of varying pH.

Compound	Concentration, µg on-column ^a	pH	Stability
			12 h (n = 6)
3-β-D-Glucopyranosyl-4-β-D-glucopyranosyloxyiriflophenone (1)	0.3492	5	0.22
3-β-D-Glucopyranosylmaclurin (2)	0.4284	5	0.18
3-β-D-Glucopyranosyliriflophenone (3)	0.2900	5	0.20
Mangiferin (4)	0.2543	3	0.22
Mangiferin (4)	0.2543	4	0.17
Mangiferin (4)	0.2543	5	0.13
Mangiferin (4)	0.2543	6	0.15
Mangiferin (4)	0.2543	7	0.97
Isomangiferin (5)	0.2908	5	0.10

^aCorresponding to an injection volume of 7 µL, roughly representing the midpoint in the range of the calibration curves.

Table S3 Average concentration (mM, $n = 3$) \pm standard deviation for the benzophenone 3- β -D-glucopyranosyl-4- β -D-glucopyranosyloxyiriflophenone (**1**) in aqueous model solution (0.1 M phosphate buffer, pH 5) as a function of treatment temperature and time.

	110 °C		120 °C		130 °C		140 °C		150 °C	
	Time, h	Concentration	Time, h	Concentration	Time, h	Concentration	Time, h	Concentration	Time, h	Concentration
T0	0	0.1063a ^a	0	0.1013a ^a	0	0.1048a ^a	0	0.1064a ^a	0	0.1036a ^a
T1	9	0.09193b \pm 0.00086	3	0.08779b \pm 0.0010	2	0.08085b \pm 0.0019	0.5	0.09009b \pm 0.0016	0.167	0.09159b \pm 0.00091
T2	19	0.08184c \pm 0.00085	7	0.07536c \pm 0.0018	3	0.07338c \pm 0.0035	1	0.07784c \pm 0.0015	0.417 ^b	0.07927c \pm 0.0015
T3	31	0.06603d \pm 0.0027	12.5	0.05919d \pm 0.0023	4	0.06869c \pm 0.00097	1.5	0.06791d \pm 0.0023	0.667 ^b	0.06697d \pm 0.0033
T4	46	0.05653e \pm 0.0026	18	0.05043e \pm 0.0031	6	0.05215d \pm 0.0012	2	0.06200e \pm 0.0044	1	0.05496e \pm 0.00064
T5	67	0.04005f \pm 0.0014	25	0.03562f \pm 0.0022	8	0.04259e \pm 0.0050	3	0.04632f \pm 0.0030	1.333 ^b	0.04492f \pm 0.0055
T6	88	0.02963g \pm 0.0017	34	0.02626g \pm 0.0021	12	0.02620f \pm 0.0024	4.50 ^b	0.03027g \pm 0.00068	1.833	0.03048g \pm 0.0024
T7	117	0.02096h \pm 0.0021	44	0.01811h \pm 0.0013	16	0.02029g \pm 0.0015	6.5	0.01772h \pm 0.0023	2.667	0.01561h \pm 0.0020
T8	164	0.01105i \pm 0.00034	56	0.01073i \pm 0.00093	20	0.01096h \pm 0.00060	8.5	0.01144i \pm 0.0020	3.417	0.01206h \pm 0.0035
		89.60% degradation		89.41% degradation		89.54% degradation		89.25% degradation		88.36% degradation

^aValues with different letters in the same column are significantly different from one another ($p < 0.05$).

^bThe corresponding value at this time point represents the average of duplicate samples, as one replicate was lost during experimental procedures.

Table S4 Average concentration (mM, $n = 3$) \pm standard deviation of the benzophenone 3- β -D-glucopyranosylmaclurin (**2**) in aqueous model solution (0.1 M phosphate buffer, pH 5) as a function of treatment temperature and time.

	70 °C		80 °C		90 °C		100 °C		110 °C	
	Time, h	Concentration	Time, h	Concentration	Time, h	Concentration	Time, h	Concentration	Time, h	Concentration
T0	0	0.1050a ^a	0	0.1059a ^a	0	0.1045a ^a	0	0.1048a ^a	0	0.1055a ^a
T1	1	0.09910b \pm 0.00059	0.5	0.09547b \pm 0.00066	0.25	0.09174b \pm 0.0012	0.25	0.08028b \pm 0.00096	0.167	0.06900b \pm 0.0021
T2	3	0.08444c \pm 0.00087	1	0.08529c \pm 0.00077	0.5	0.07572c \pm 0.00044	0.5	0.05831c \pm 0.0019	0.25	0.04991c \pm 0.0028
T3	6	0.06787d \pm 0.0013	2	0.06793d \pm 0.0013	1	0.05402d \pm 0.0019	0.75	0.04333d \pm 0.0026	0.333	0.03586d \pm 0.0016
T4	10	0.05039e \pm 0.0021	3	0.05406e \pm 0.0024	1.5	0.03801e \pm 0.0036	1	0.03005e \pm 0.00071	0.417	0.02467e \pm 0.0015
T5	14	0.03597f \pm 0.0017	4	0.04285f \pm 0.0016	2	0.02964f \pm 0.0028	1.25	0.02186f \pm 0.0013	0.5	0.01782f \pm 0.0010
T6	19	0.02434g \pm 0.0014	5.5	0.03157g \pm 0.0018	2.5	0.01846g \pm 0.0015	1.5	0.01509g \pm 0.0018	0.667	0.008753g \pm 0.0031
T7	24	0.01601h \pm 0.0016	7.5	0.01752h \pm 0.0026	3	0.01366h \pm 0.0028	1.75	0.01136h \pm 0.0020	-	-
T8	29	0.01059i \pm 0.00071	9.75	0.01033i \pm 0.0013	3.333	0.01140h \pm 0.0012	-	-	-	-
		89.91% degradation		90.25% degradation		89.09% degradation		89.16% degradation		91.70% degradation

^aValues with different letters in the same column are significantly different from one another ($p < 0.05$).

Table S5 Average concentration (mM, $n = 3$) \pm standard deviation for the benzophenone 3- β -D-glucopyranosyliriflophenone (**3**) in aqueous model solution (0.1 M phosphate buffer, pH 5) as a function of treatment temperature and time.

	90 °C		100 °C		110 °C		120 °C		130 °C	
	Time, h	Concentration	Time, h	Concentration	Time, h	Concentration	Time, h	Concentration	Time, h	Concentration
T0	0	0.09982a ^a	0	0.1028a ^a	0	0.1024a ^a	0	0.1009a ^a	0	0.1010a ^a
T1	2	0.09564b \pm 0.00093	1	0.09666b \pm 0.00075	0.5	0.09467b \pm 0.00095	0.5	0.08382b \pm 0.0025	0.25	0.08521b \pm 0.0030
T2	4	0.09095c \pm 0.00089	2	0.09051c \pm 0.00090	1	0.08980b \pm 0.0017	1	0.06578c \pm 0.0011	0.5	0.06551c \pm 0.0069
T3	14	0.06722d \pm 0.0011	4	0.07881d \pm 0.00073	2	0.07410c \pm 0.0012	1.5	0.05280d \pm 0.0014	0.75	0.04777d \pm 0.0040
T4	24	0.04444e \pm 0.0021	8	0.05622e \pm 0.0021	4	0.04435d \pm 0.0070	2	0.03963e \pm 0.0032	1 ^b	0.03451e \pm 0.00011
T5	34	0.02953f \pm 0.0021	12	0.03817f \pm 0.00098	6	0.02990e \pm 0.0027	2.5	0.03133f \pm 0.0017	1.25	0.02896e \pm 0.0023
T6	43	0.01668g \pm 0.0012	17	0.02182g \pm 0.0023	7	0.02299f \pm 0.0019	3	0.02281g \pm 0.0013	1.5	0.02039f \pm 0.0021
T7	52	0.01116h \pm 0.0015	23	0.01035h \pm 0.0010	8	0.01762f \pm 0.00094	3.5	0.01717h \pm 0.0022	1.75	0.01335g \pm 0.0012
T8	-	-	-	-	10	0.009978g \pm 0.0024	4.333	0.01048i \pm 0.0017	2	0.01001g \pm 0.00056
		88.82% degradation		89.93% degradation		90.26% degradation		89.61% degradation		90.09% degradation

^aValues with different letters in the same column are significantly different from one another ($p < 0.05$).

^bThe corresponding value at this time point represents the average of duplicate samples, as one replicate was lost during experimental procedures.

Table S6 Average concentration (mM, $n = 3$) \pm standard deviation of the xanthone mangiferin (**4**) in aqueous model solution (0.1 M phosphate buffer, pH 5) as a function of treatment temperature and time.

	90 °C		100 °C		110 °C		120 °C		130 °C	
	Time, h	Concentration	Time, h	Concentration	Time, h	Concentration	Time, h	Concentration	Time, h	Concentration
T0	0	0.1040a ^a	0	0.1055a ^a	0	0.1044a ^a	0	0.1053a ^a	0	0.1053a ^a
T1	3	0.08721b \pm 0.0012	1	0.08912b \pm 0.00097	1	0.06862b \pm 0.0051	0.167	0.09408b \pm 0.00041	0.167	0.07908b \pm 0.0041
T2	6	0.07245c \pm 0.0043	2	0.07326c \pm 0.0016	2	0.04695c \pm 0.0038	0.333	0.08146c \pm 0.0034	0.333	0.07156b \pm 0.030
T3	12	0.05331d \pm 0.0022	3	0.06271d \pm 0.0020	2.667	0.03756d \pm 0.0042	0.5	0.07048d \pm 0.0031	0.5	0.03785c \pm 0.0017
T4	19	0.03730e \pm 0.0030	5	0.04689e \pm 0.0036	3.333	0.03087e \pm 0.0024	0.667	0.06406e \pm 0.0019	0.667	0.03025cd \pm 0.0039
T5	25	0.02985f \pm 0.00091	7	0.03410f \pm 0.0013	4	0.02455f \pm 0.0022	1.167	0.04466f \pm 0.0042	1	0.01431cd \pm 0.0017
T6	32	0.01693g \pm 0.0018	9	0.02376g \pm 0.0029	4.833	0.01968fg \pm 0.0018	1.667	0.03101g \pm 0.00090	1.333	0.008522d \pm 0.0013
T7	37	0.01455gh \pm 0.0019	11.5	0.01363h \pm 0.0044	5.833	0.01471gh \pm 0.0020	2.333	0.02144h \pm 0.0027	-	-
T8	43	0.01045h \pm 0.00056	14.5	0.01126h \pm 0.0015	7	0.01027h \pm 0.0010	3.333	0.01027i \pm 0.0019	-	-
		89.95% degradation		89.33% degradation		90.16% degradation		90.25% degradation		91.91% degradation

^aValues with different letters in the same column are significantly different from one another ($p < 0.05$).

Table S7 Average concentration (mM, $n = 3$) \pm standard deviation of the xanthone isomangiferin (**5**) in aqueous model solution (0.1 M phosphate buffer, pH 5) as a function of treatment temperature and time.

	90 °C		100 °C		110 °C		120 °C		130 °C	
	Time, h	Concentration	Time, h	Concentration	Time, h	Concentration	Time, h	Concentration	Time, h	Concentration
T0	0	0.1081a ^a	0	0.1112a ^a	0	0.1105a ^a	0	0.1106a ^a	0	0.1092a ^a
T1	4	0.09414b \pm 0.0015	2	0.08361b \pm 0.0018	0.5	0.09661b \pm 0.0011	0.25	0.09632b \pm 0.0013	0.25	0.07492b \pm 0.0012
T2	8	0.08314c \pm 0.0022	3	0.07230c \pm 0.0016	1	0.08537c \pm 0.0021	0.5	0.08187c \pm 0.0013	0.5 ^b	0.05558c \pm 0.0024
T3	16	0.06388d \pm 0.0028	5	0.05675d \pm 0.0018	2	0.06710d \pm 0.00045	1	0.06486d \pm 0.0024	0.75	0.03963d \pm 0.0035
T4	27	0.04535e \pm 0.0011	7.167	0.04616e \pm 0.0040	3	0.05495e \pm 0.0027	1.5	0.05513e \pm 0.0015	1	0.03203e \pm 0.0020
T5	38	0.03347f \pm 0.0020	10	0.03337f \pm 0.00035	4.5	0.04217f \pm 0.00096	2	0.04460f \pm 0.0030	1.5	0.01855f \pm 0.00065
T6	50	0.02227g \pm 0.0023	13	0.02297g \pm 0.00082	6.5	0.03005g \pm 0.0028	3	0.03226g \pm 0.0045	2	0.01175g \pm 0.0029
T7	62	0.01556h \pm 0.00084	16	0.01840h \pm 0.0017	9	0.02103h \pm 0.0010	4	0.02202h \pm 0.0024	-	-
T8	73	0.01140i \pm 0.00079	20	0.01281i \pm 0.00030	12.5	0.01289i \pm 0.0020	6 ^b	0.01301i \pm 0.0026	-	-
		89.45% degradation		88.48% degradation		88.33% degradation		88.24% degradation		89.24% degradation

^aValues with different letters in the same column are significantly different from one another ($p < 0.05$).

^bThe corresponding value at this time point represents the average of duplicate samples, as one replicate was lost during experimental procedures.

Table S8 Average concentration (mM, $n = 3$) \pm standard deviation of the xanthone mangiferin (**4**) in aqueous model solution (0.1 M phosphate buffer, **pH 3**) as a function of treatment temperature and time.

	100 °C		110 °C		120 °C		130 °C		140 °C	
	Time, h	Concentration	Time, h	Concentration	Time, h	Concentration	Time, h	Concentration	Time, h	Concentration
T0	0	0.1070a ^a	0	0.1069a ^a	0	0.1068a ^a	0	0.1068a ^a	0	0.1069a ^a
T1	3	0.08926b \pm 0.0054	2	0.08115b \pm 0.0013	1	0.07928b \pm 0.0043	0.5	0.07549b \pm 0.0018	0.5	0.06092b \pm 0.0065
T2	7	0.07204c \pm 0.0043	4	0.06480c \pm 0.0021	2	0.06116c \pm 0.0022	1	0.05700c \pm 0.0015	1	0.03686c \pm 0.0052
T3	12	0.05575d \pm 0.0032	6	0.05128d \pm 0.0011	3	0.04909d \pm 0.00018	1.5	0.03989d \pm 0.012	1.5	0.02471d \pm 0.0014
T4	24	0.03297e \pm 0.0022	8	0.04134e \pm 0.00099	4	0.04068e \pm 0.0019	2	0.03354d \pm 0.0057	2	0.01820de \pm 0.0042
T5	36	0.02011f \pm 0.0020	12	0.02790f \pm 0.0025	5	0.03301e \pm 0.0038	3	0.01889e \pm 0.0027	2.5	0.01097e \pm 0.0025
T6	45	0.01281g \pm 0.0021	16	0.01878g \pm 0.0038	6	0.02371f \pm 0.0091	4	0.01320ef \pm 0.0027	-	-
T7	48	0.01270g \pm 0.00081	21	0.01353h \pm 0.0031	8	0.01968f \pm 0.0026	5	0.008612f \pm 0.0019	-	-
T8	51	0.01114g \pm 0.0019 89.59% degradation	24	0.01021h \pm 0.0022 90.45% degradation	11	0.01130g \pm 0.00047 89.42% degradation	-	- 91.94% degradation	-	- 89.74% degradation

^aValues with different letters in the same column are significantly different from one another ($p < 0.05$).

Table S9 Average concentration (mM, $n = 3$) \pm standard deviation of the xanthone mangiferin (**4**) in aqueous model solution (0.1 M phosphate buffer, **pH 4**) as a function of treatment temperature and time.

	100 °C		110 °C		120 °C		130 °C		140 °C	
	Time, h	Concentration	Time, h	Concentration	Time, h	Concentration	Time, h	Concentration	Time, h	Concentration
T0	0	0.1041a ^a	0	0.1030a ^a	0	0.1036a ^a	0	0.1027a ^a	0	0.1038a ^a
T1	2	0.08641b \pm 0.0052	2	0.07183b \pm 0.0050	0.5	0.08349b \pm 0.00054	0.5	0.06544b \pm 0.0058	0.167	0.07251b \pm 0.0019
T2	5	0.07018c \pm 0.0049	4	0.05239c \pm 0.0024	1	0.06439c \pm 0.0034	1	0.04379c \pm 0.0029	0.333	0.04740c \pm 0.0052
T3	8	0.05973d \pm 0.0012	6	0.04238d \pm 0.00085	2	0.04403d \pm 0.0033	1.5	0.02765d \pm 0.0057	0.5	0.03346d \pm 0.0045
T4	14	0.04182e \pm 0.0029	8	0.03350e \pm 0.0013	3	0.02824e \pm 0.0064	2	0.02215de \pm 0.0011	0.667	0.02264e \pm 0.0026
T5	20	0.02686f \pm 0.0016	10	0.02253f \pm 0.0046	4	0.02355e \pm 0.0038	2.5	0.01449ef \pm 0.0018	0.917	0.01465f \pm 0.0013
T6	26	0.01951g \pm 0.00033	13	0.01840f \pm 0.0021	5	0.01569f \pm 0.00092	3	0.01041f \pm 0.0041	1.167	0.007155g \pm 0.0012
T7	32	0.01389h \pm 0.0010	18	0.009724g \pm 0.00086	6	0.01219fg \pm 0.0022	-	-	-	-
T8	38	0.01076h \pm 0.00046 89.66% degradation	-	- 90.56% degradation	6.75	0.008943g \pm 0.0011 91.37% degradation	-	- 89.86% degradation	-	- 93.11% degradation

^aValues with different letters in the same column are significantly different from one another ($p < 0.05$).

Table S10 Average concentration (mM, $n = 3$) \pm standard deviation of the xanthone mangiferin (**4**) in aqueous model solution (0.1 M phosphate buffer, **pH 6**) as a function of treatment temperature and time.

	70 °C		80 °C		90 °C		100 °C		110 °C	
	Time, h	Concentration	Time, h	Concentration	Time, h	Concentration	Time, h	Concentration	Time, h	Concentration
T0	0	0.1055a ^a	0	0.1053a ^a	0	0.1062a ^a	0	0.1060a ^a	0	0.1043a ^a
T1	2	0.09702b \pm 0.00047	1	0.09543b \pm 0.00061	0.5	0.09449b \pm 0.00051	0.25	0.09486b \pm 0.0026	0.25	0.08034b \pm 0.0043
T2	4	0.08878c \pm 0.00058	2	0.08594c \pm 0.00049	1	0.08432c \pm 0.00068	0.5	0.08325c \pm 0.00049	0.5	0.05960c \pm 0.0030
T3	8	0.07523d \pm 0.00071	4	0.07129d \pm 0.0016	2	0.06867d \pm 0.0010	1	0.06468d \pm 0.0010	0.75	0.04868d \pm 0.0012
T4	13.5	0.06053e \pm 0.00090	7	0.05454e \pm 0.0011	3	0.05653e \pm 0.00079	1.5	0.05055e \pm 0.0025	1	0.03843e \pm 0.0019
T5	22	0.04250f \pm 0.0011	11	0.03782f \pm 0.00024	5	0.03635f \pm 0.00090	2	0.04469f \pm 0.0019	1.25	0.02971f \pm 0.0010
T6	32	0.02627g \pm 0.0019	15	0.02520g \pm 0.00081	7	0.02332g \pm 0.00076	3	0.02610g \pm 0.0015	1.5	0.02216g \pm 0.0021
T7	44	0.01518h \pm 0.00046	20	0.01487h \pm 0.0014	9	0.01681h \pm 0.0014	4	0.01680h \pm 0.0026	1.75	0.01857g \pm 0.0016
T8	52.5	0.009481i \pm 0.00060	25	0.008278i \pm 0.00088	11	0.01089i \pm 0.0013	5	0.01096i \pm 0.00062	2.25	0.01189h \pm 0.0025
		91.01% degradation		92.14% degradation		89.75% degradation		89.66% degradation		88.60% degradation

^aValues with different letters in the same column are significantly different from one another ($p < 0.05$).

Table S11 Average concentration (mM, $n = 3$) \pm standard deviation of the xanthone mangiferin (**4**) in aqueous model solution (0.1 M phosphate buffer, **pH 7**) as a function of treatment temperature and time.

	60 °C		70 °C		80 °C		90 °C		100 °C	
	Time, h	Concentration	Time, h	Concentration	Time, h	Concentration	Time, h	Concentration	Time, h	Concentration
T0	0	0.1008a ^a	0	0.1003a ^a	0	0.1013a ^a	0	0.1002a ^a	0	0.1015a ^a
T1	2	0.08617b \pm 0.0048	0.5	0.09338b \pm 0.0011	0.5	0.08404b \pm 0.00052	0.167	0.08581b \pm 0.00076	0.167	0.07717b \pm 0.00066
T2	4	0.07813c \pm 0.0045	1	0.08459c \pm 0.00061	1	0.07047c \pm 0.0014	0.333	0.07401c \pm 0.00068	0.333	0.05557c \pm 0.0013
T3	8	0.06504d \pm 0.00015	3	0.05966d \pm 0.00055	1.5	0.06012d \pm 0.0015	0.667	0.05722d \pm 0.00063	0.5	0.04301d \pm 0.0010
T4	12	0.05405e \pm 0.0015	5	0.04333e \pm 0.00025	2	0.05376e \pm 0.0013	1.167	0.03870e \pm 0.0019	0.667	0.03327e \pm 0.0013
T5	20	0.03732f \pm 0.0010	7	0.03191f \pm 0.0016	3	0.04086f \pm 0.0013	1.667	0.02702f \pm 0.0033	0.833	0.02398f \pm 0.0028
T6	28	0.02295g \pm 0.00040	9	0.02413g \pm 0.0013	4	0.03101g \pm 0.0031	2.167	0.02016g \pm 0.0029	1	0.02024g \pm 0.0017
T7	36	0.01504h \pm 0.0010	12	0.01420h \pm 0.0014	6	0.01724h \pm 0.0034	2.833	0.01050h \pm 0.0015	1.167	0.01537h \pm 0.0022
T8	44.5	0.008528i \pm 0.0010	14.667	0.007859i \pm 0.00071	8	0.008803i \pm 0.0018	3.167	0.009051h \pm 0.0017	1.5	0.009178i \pm 0.0025
		91.54% degradation		92.16% degradation		91.31% degradation		90.97% degradation		90.96% degradation

^aValues with different letters in the same column are significantly different from one another ($p < 0.05$).

Table S12 Average concentration (mM, $n = 3$) \pm standard deviation for the xanthone mangiferin (**4**) upon thermal treatment of the benzophenone 3- β -D-glucopyranosylmaclurin (**2**) (0.1 M phosphate buffer, pH 5) as a function of treatment temperature and time.

	90 °C		100 °C		110 °C	
	Time, h	Concentration	Time, h	Concentration	Time, h	Concentration
T0	0	0.0000h ^a	0	0.0000g ^a	0	0.0000f ^a
T1	0.25	0.006234g \pm 0.00045	0.25	0.01114f \pm 0.00040	0.167	0.01670e \pm 0.00092
T2	0.5	0.01339f \pm 0.00022	0.5	0.02068e \pm 0.00080	0.25	0.02509d \pm 0.0014
T3	1	0.02307e \pm 0.00097	0.75	0.02704d \pm 0.0010	0.333	0.03106c \pm 0.00059
T4	1.5	0.02975d \pm 0.0017	1	0.03210c \pm 0.00023	0.417	0.03541b \pm 0.00046
T5	2	0.03290c \pm 0.0010	1.25	0.03477b \pm 0.00028	0.5	0.03776ab \pm 0.00052
T6	2.5	0.03671b \pm 0.00080	1.5	0.03679a \pm 0.00049	0.667	0.03919a \pm 0.00046
T7	3	0.03773ab \pm 0.00082	1.75	0.03748a \pm 0.00085	0.883	0.03917a \pm 0.00027
T8	3.333	0.03934a \pm 0.00074	2	0.03749a \pm 0.00041	1	0.03944a \pm 0.0036

^aValues with different letters in the same column are significantly different from one another ($p < 0.05$).

Table S13 Average concentration (mM, $n = 3$) \pm standard deviation for the xanthone isomangiferin (**5**) upon thermal treatment of the benzophenone 3- β -D-glucopyranosylmaclurin (**2**) (0.1 M phosphate buffer, pH 5) as a function of treatment temperature and time.

	90 °C		100 °C		110 °C	
	Time, h	Concentration	Time, h	Concentration	Time, h	Concentration
T0	0	0.0000h ^a	0	0.0000g ^a	0	0.0000f ^a
T1	0.25	0.002815g \pm 0.00018	0.25	0.005264f \pm 0.00021	0.167	0.007858e \pm 0.00047
T2	0.5	0.005791f \pm 0.00012	0.5	0.009605e \pm 0.00041	0.25	0.01177d \pm 0.00066
T3	1	0.009914e \pm 0.00040	0.75	0.01247d \pm 0.00049	0.333	0.01456c \pm 0.00026
T4	1.5	0.01251d \pm 0.00065	1	0.01470c \pm 0.00010	0.417	0.01651b \pm 0.00018
T5	2	0.01383c \pm 0.00040	1.25	0.01581b \pm 0.00019	0.5	0.01764ab \pm 0.00022
T6	2.5	0.01525b \pm 0.00020	1.5	0.01681a \pm 0.00023	0.667	0.01849a \pm 0.00033
T7	3	0.01583b \pm 0.00027	1.75	0.01718a \pm 0.00011	0.883	0.01849a \pm 0.000082
T8	3.333	0.01651a \pm 0.00028	2	0.01717a \pm 0.00013	1	0.01880a \pm 0.0015

^aValues with different letters in the same column are significantly different from one another ($p < 0.05$).

Table S14 Comparison of retention times of compounds identified in the thermally-treated solutions (pH 5, 110 °C) as obtained by analyses on an Agilent UHPLC-DAD system, and a Waters UPLC coupled with a photodiode-array detector (PDA) and an electrospray-ionisation mass spectrometer (ESI-MS).

Compound	Retention Time, min		
	UHPLC-DAD	UPLC-PDA	UPLC-ESI-MS
1 3-β-D-glucopyranosyl-4-β-D-glucopyranosyloxiriflophenone	0.836	0.67	0.72
1A iriflophenone-di- <i>O,C</i> -hexoside isomer	0.993	0.81	0.85
1B iriflophenone-di- <i>O,C</i> -hexoside isomer	1.107	0.91	0.95
1C unidentified (C ₁₉ H ₂₀ O ₁₀)	1.263	1.08	1.12
1D 3-β-D-glucopyranosyliriflophenone	1.363	1.14	1.18
1E unidentified (C ₂₇ H ₃₂ O ₁₆ isomer)	1.433	1.20	1.25
1F unidentified (C ₂₇ H ₃₂ O ₁₆ isomer)	1.546	1.31	1.35
1G unidentified (C ₂₂ H ₂₄ O ₁₃)	1.585	1.34	1.38
1H mangiferin	– ^a	1.47	1.51
1I isomangiferin	– ^a	1.55	1.59
* 3-β-D-glucopyranosyl-4-β-D-glucopyranosyloxiriflophenone (impurity)	0.840	0.68	0.72
2 3-β-D-glucopyranosylmaclurin	0.994	0.82	0.86
2A maclurin- <i>C</i> -hexoside isomer	1.300	1.08	1.12
2B maclurin- <i>C</i> -hexoside isomer	1.517	1.28	1.32
2C mangiferin	1.702	1.47	1.51
2D isomangiferin	1.792	1.55	1.59
2E tetrahydroxyxanthone- <i>C</i> -hexoside isomer	2.248	2.02	2.06
2F tetrahydroxyxanthone- <i>C</i> -hexoside isomer	2.357	2.12	2.16
2G unidentified xanthone derivative (C ₂₁ H ₂₀ O ₁₂)	2.537	2.30	2.35
2H tetrahydroxyxanthone- <i>C</i> -hexoside isomer	2.568	2.31	2.36
3 3-β-D-glucopyranosyliriflophenone	1.362	1.14	1.18
3A unidentified (C ₁₉ H ₁₈ O ₉ isomer)	1.671	1.43	1.47
3B iriflophenone- <i>C</i> -hexoside isomer	1.705	1.46	1.50
3C mangiferin	– ^a	1.47	1.51
3D isomangiferin	– ^a	1.54	1.59
3E iriflophenone- <i>C</i> -hexoside isomer	1.898	1.64	1.68
3F unidentified (C ₁₉ H ₁₈ O ₉ isomer)	2.009	1.75	1.79
3G unidentified (C ₃₉ H ₄₀ O ₂₀ isomer)	2.009	1.75	1.79
3H unidentified (C ₁₇ H ₂₄ O ₁₇)	2.098	1.84	1.89
3I unidentified (C ₁₉ H ₁₆ O ₈)	2.313	2.05	2.10
3J unidentified (C ₁₃ H ₁₀ O ₅)	2.373	2.09	2.13
3K unidentified (C ₁₉ H ₁₈ O ₉ isomer)	2.444	2.17	2.22
3L unidentified	2.715	2.44	2.48
3M unidentified (C ₃₉ H ₄₀ O ₂₀ isomer)	– ^a	2.59	2.64
4A tetrahydroxyxanthone- <i>C</i> -hexoside dimer	0.811	0.66	0.70
4B tetrahydroxyxanthone- <i>C</i> -hexoside dimer	1.062	0.88	0.92
4C tetrahydroxyxanthone- <i>C</i> -hexoside dimer	1.115	0.92	0.96
4D tetrahydroxyxanthone- <i>C</i> -hexoside dimer	1.203	0.99	1.04
4E tetrahydroxyxanthone- <i>C</i> -hexoside dimer	1.536	1.30	1.35
4 mangiferin	1.701	1.46	1.51
4F isomangiferin	– ^a	1.55	1.59
* homomangiferin (impurity)	1.878	1.63	1.68
4G tetrahydroxyxanthone- <i>C</i> -hexoside isomer	2.269	2.02	2.05
4H tetrahydroxyxanthone- <i>C</i> -hexoside isomer	2.569	2.32	2.35
5A tetrahydroxyxanthone- <i>C</i> -hexoside dimer	1.100	0.90	0.94
5B tetrahydroxyxanthone- <i>C</i> -hexoside dimer	1.372	1.14	1.19
5C tetrahydroxyxanthone- <i>C</i> -hexoside dimer	1.686	1.44	1.48
5D mangiferin	1.686	1.46	1.51
5 isomangiferin	1.796	1.55	1.59
5E tetrahydroxyxanthone- <i>C</i> -hexoside isomer	2.381	2.12	2.17
5F tetrahydroxyxanthone- <i>C</i> -hexoside isomer	2.602	2.33	2.38

^aNot detected on the Agilent UHPLC-DAD system.

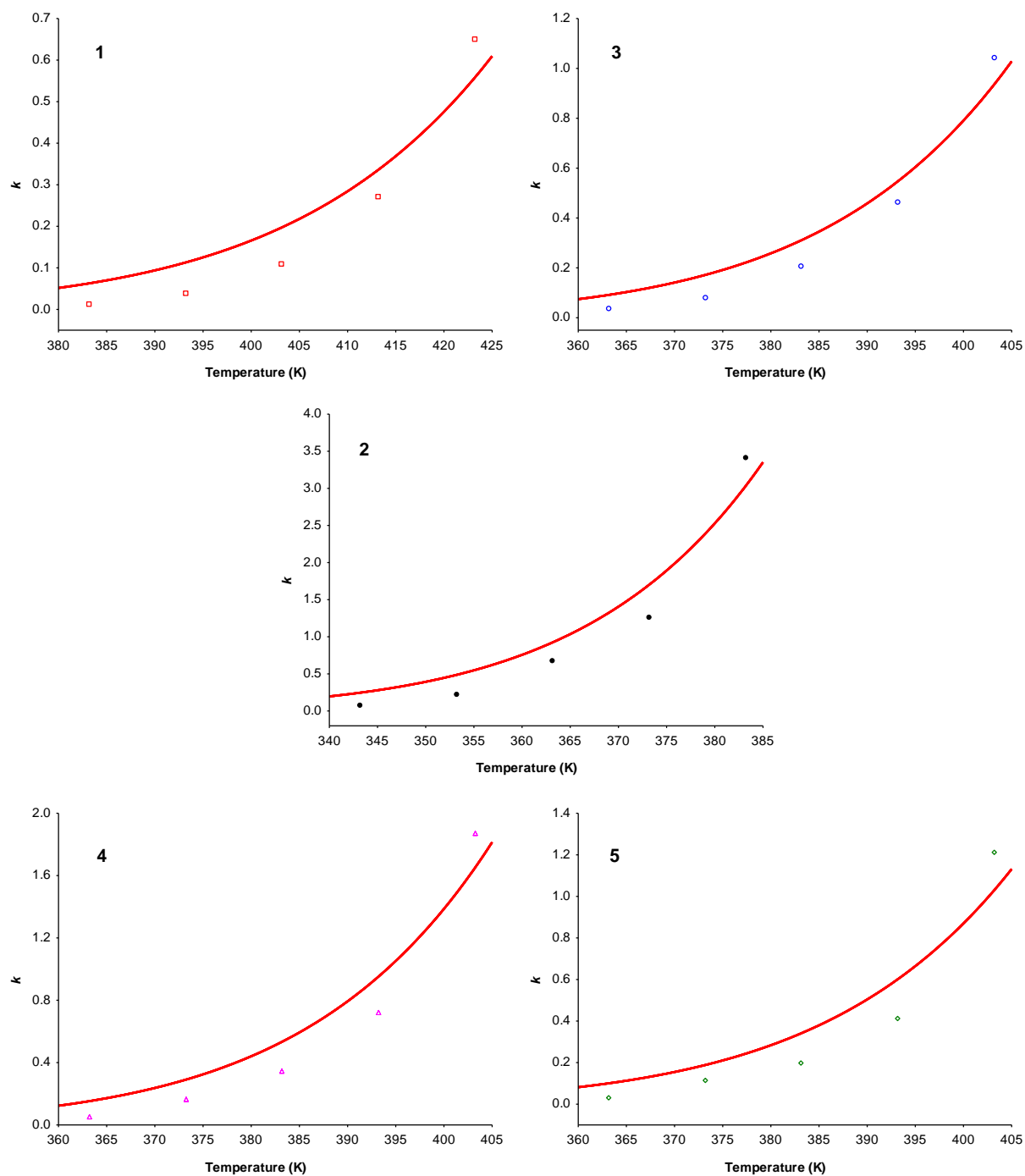


Figure S1 Arrhenius plots for the target benzophenones and xanthenes in aqueous model solutions (0.1 M phosphate buffer, pH 5), with exponential fit of data according to eq 2: 3- β -D-glucopyranosyl-4- β -D-glucopyranosyloxyiriflophenone (**1**); 3- β -D-glucopyranosylmaclurin (**2**); 3- β -D-glucopyranosyliriflophenone (**3**); mangiferin (**4**); and isomangiferin (**5**).

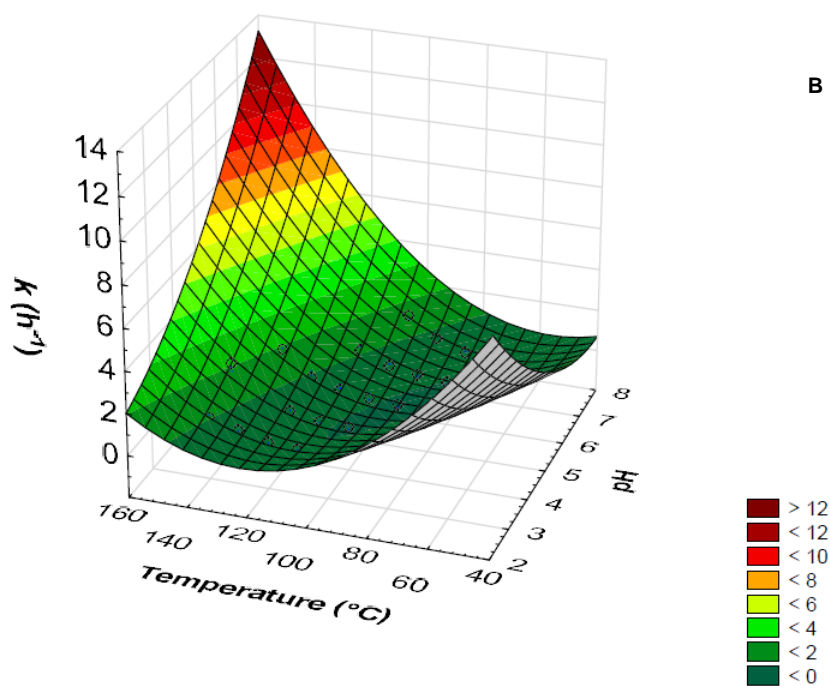
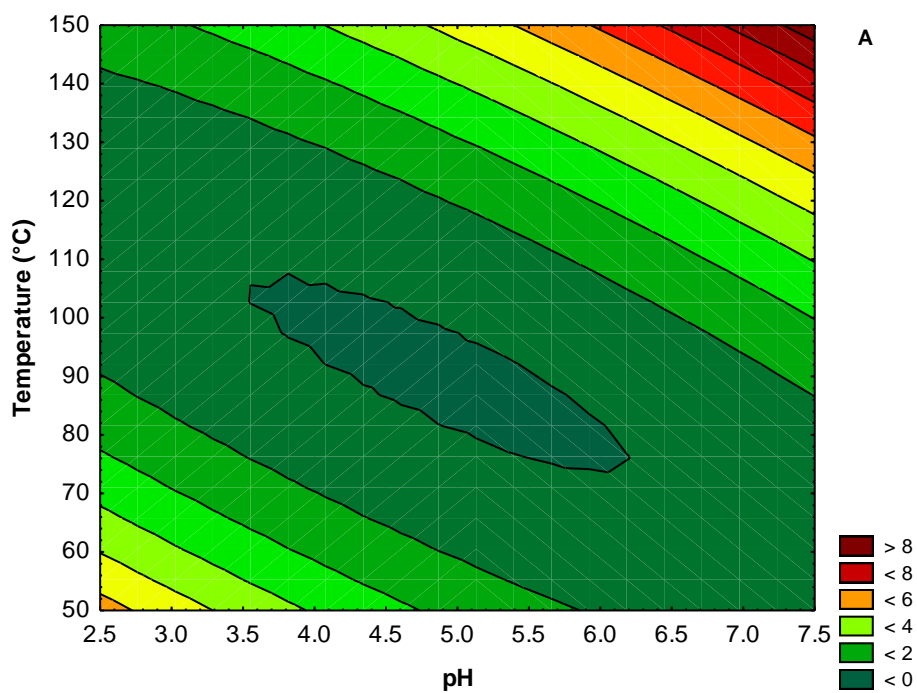


Figure S2 A) 3D Contour plot and B) 3D Surface plot showing the combined effect of temperature and pH on the degradation rate constant (k) of mangiferin.

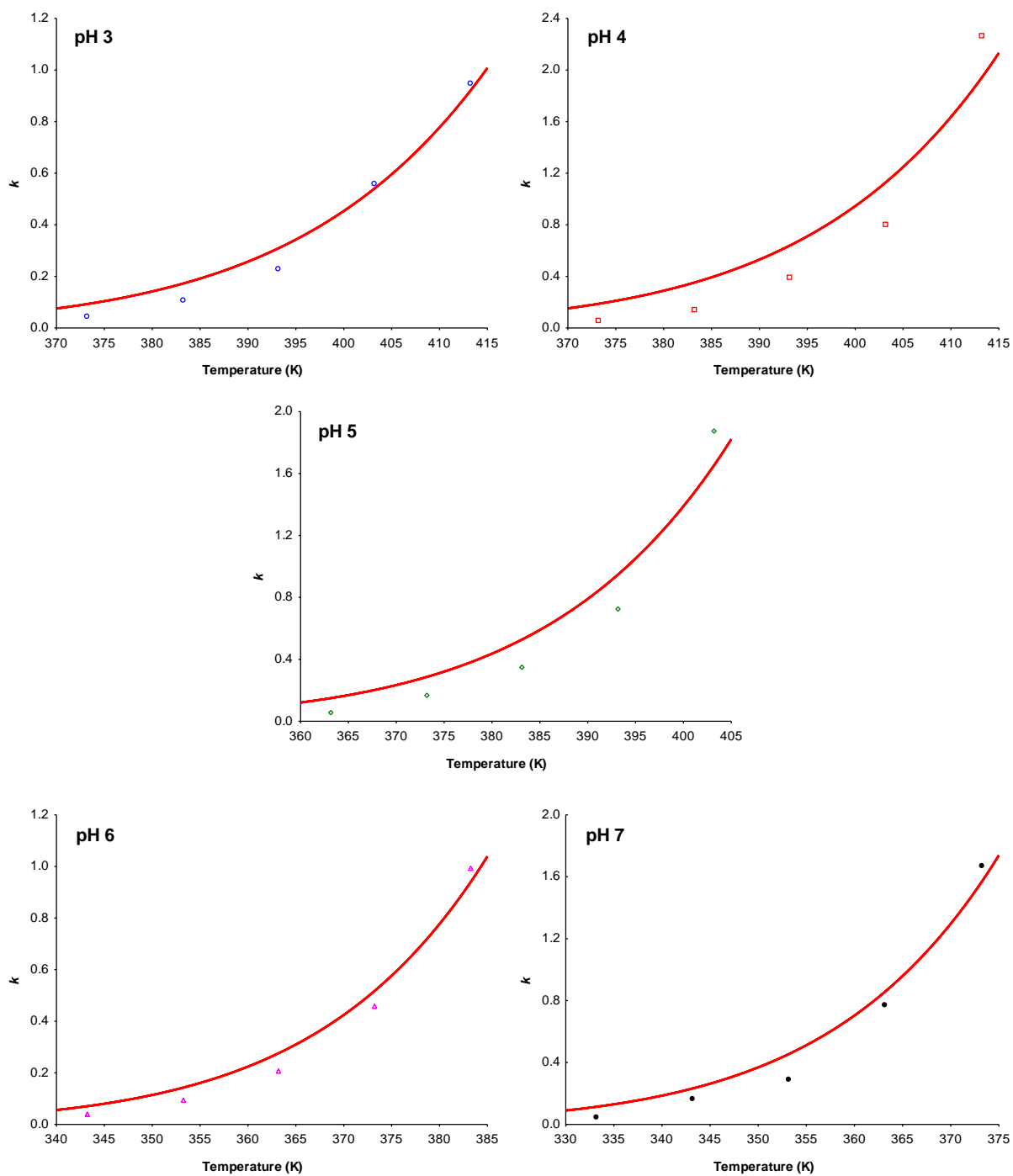


Figure S3 Arrhenius plots for mangiferin (4) (0.1 M phosphate buffer) at individual pH levels, with exponential fit according to equation 2.

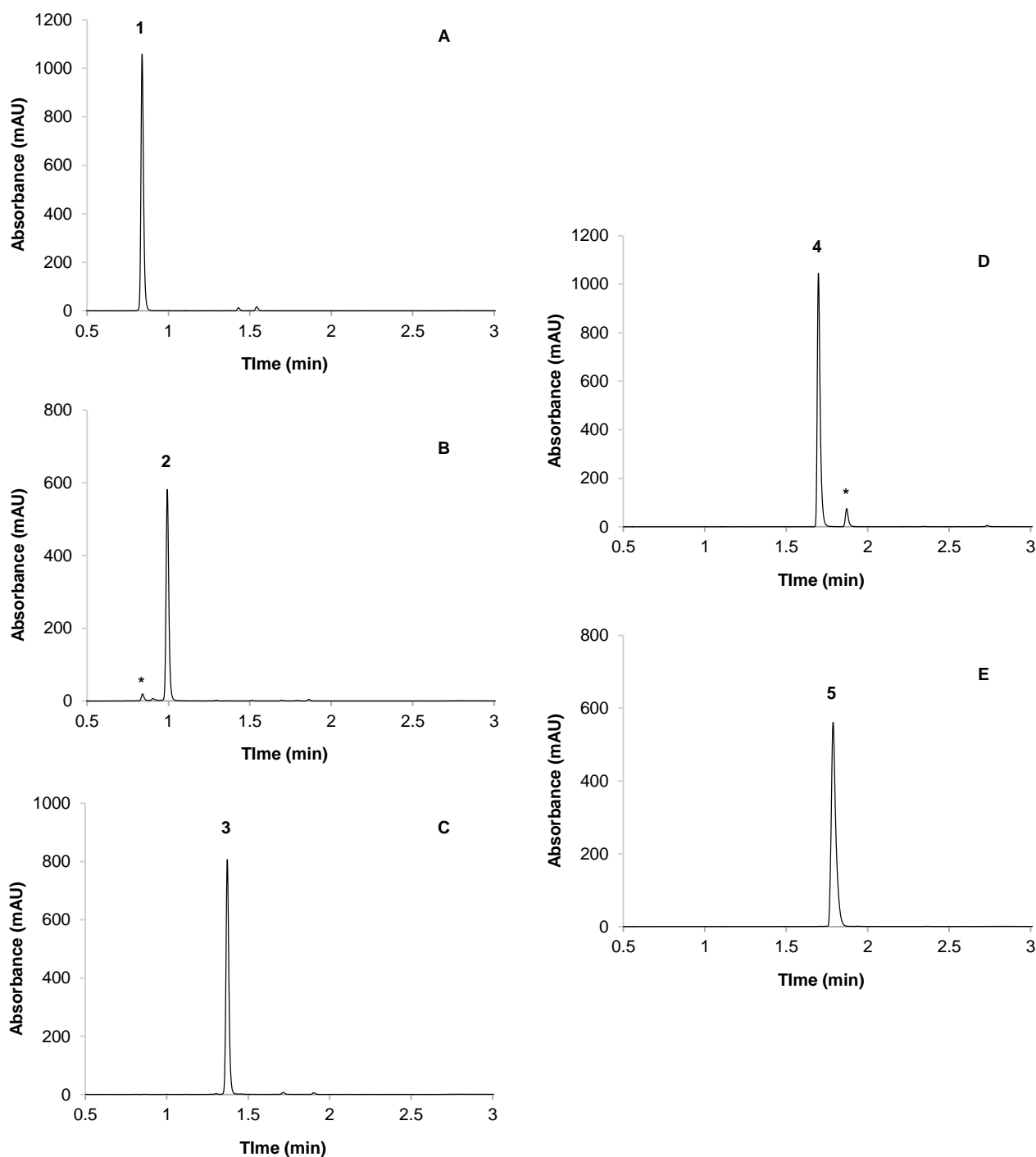


Figure S4 UHPLC-DAD chromatograms of control samples (untreated, 0.1 M phosphate buffer solution, pH 5): **A**) 3- β -D-glucopyranosyl-4- β -D-glucopyranosyloxiriflophenone (**1**, $\lambda = 288$ nm); **B**) 3- β -D-glucopyranosylmaclurin (**2**, $\lambda = 320$ nm), *impurity (3- β -D-glucopyranosyl-4- β -D-glucopyranosyloxiriflophenone); **C**) 3- β -D-glucopyranosylriflophenone (**3**, $\lambda = 288$ nm); **D**) mangiferin (**4**, $\lambda = 320$ nm), *impurity (homomangiferin); **E**) isomangiferin (**5**, $\lambda = 320$ nm).

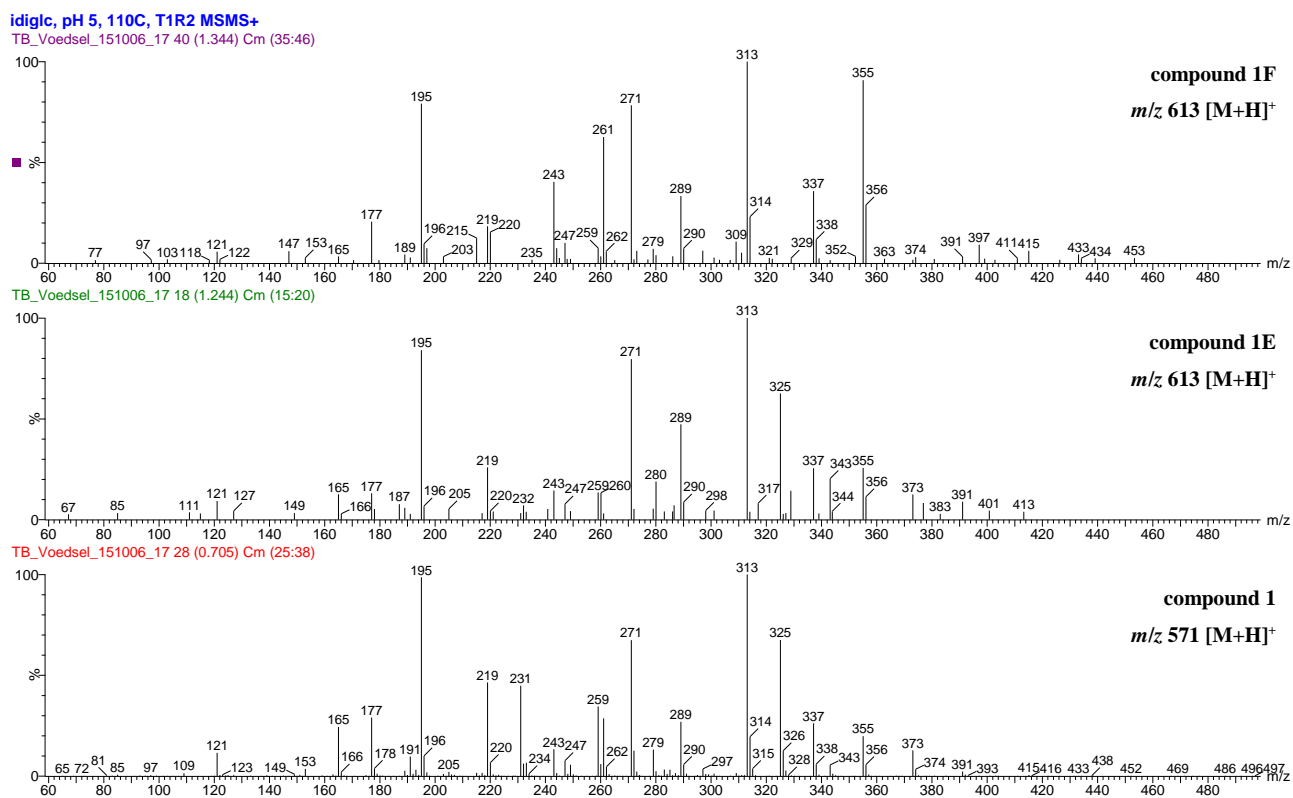


Figure S5 LC-ESI-MS/MS spectrum of 3- β -D-glucopyranosyl-4- β -D-glucopyranosyloxyiriflophenone (**1**), compared to those of the unidentified benzophenone derivatives **1E** and **1F**, in positive ionisation mode (Refer to Table 6 for additional information).

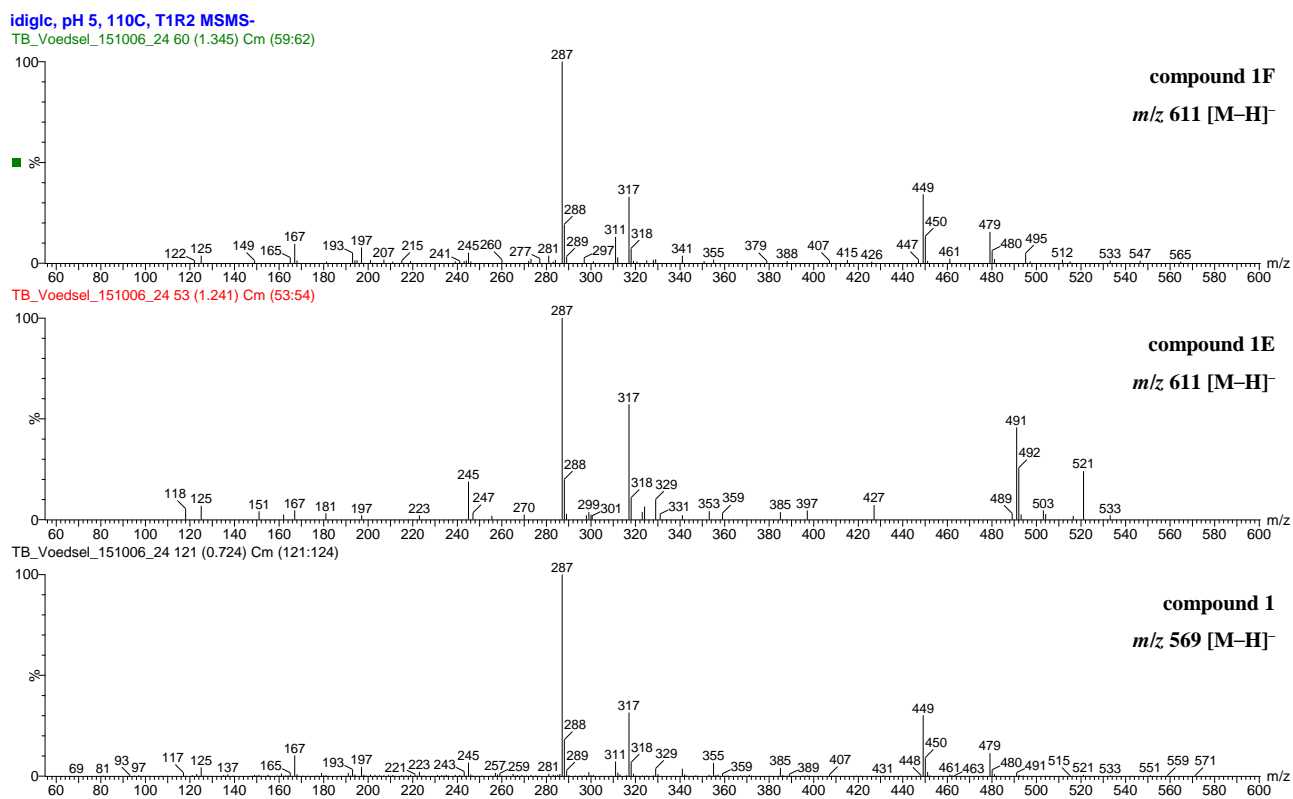


Figure S6 LC-ESI-MS/MS spectrum of 3- β -D-glucopyranosyl-4- β -D-glucopyranosyloxyiriflophenone (**1**), compared to those of the unidentified benzophenone derivatives **1E** and **1F**, in negative ionisation mode (Refer to Table 6 for additional information).

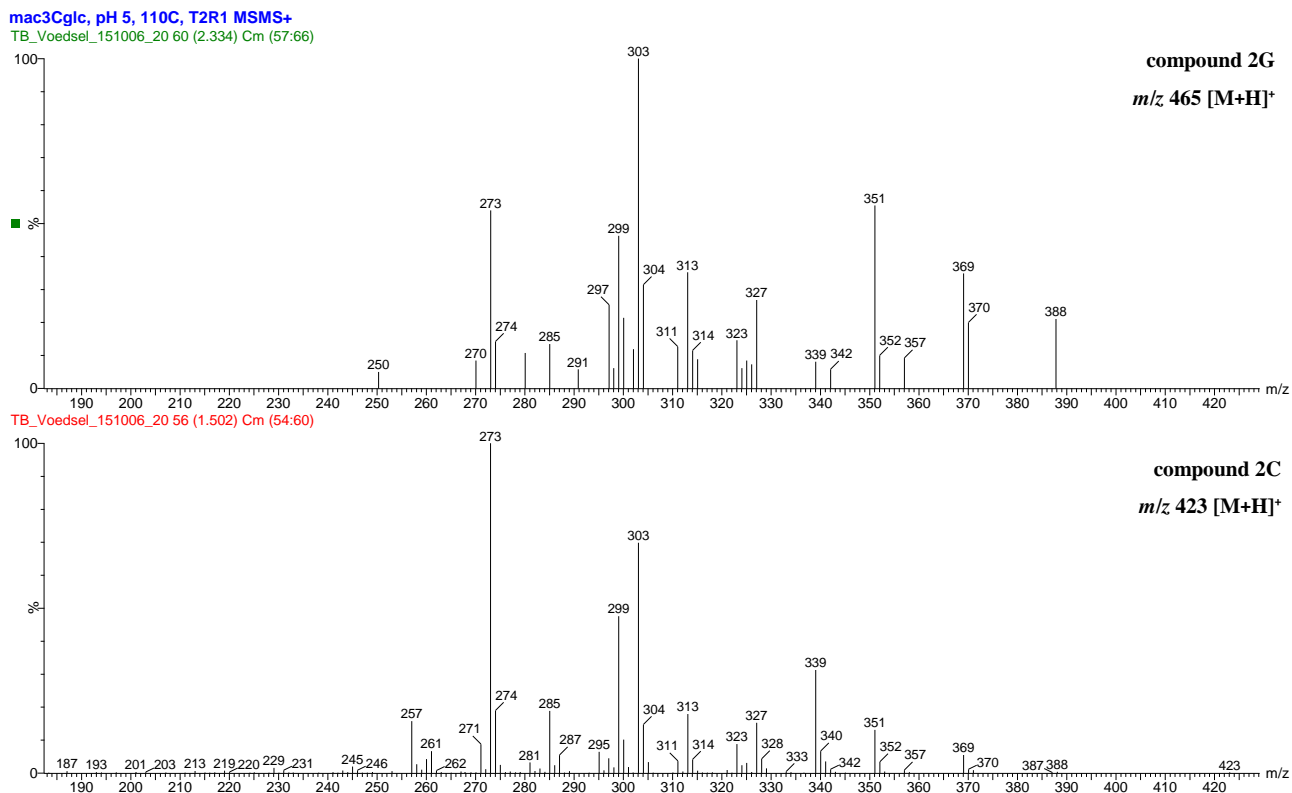


Figure S7 LC-ESI-MS/MS spectrum of the unidentified xanthone derivative (**2G**), compared to that of mangiferin (**2C**), in positive ionisation mode (Refer to Table 7 for additional information).

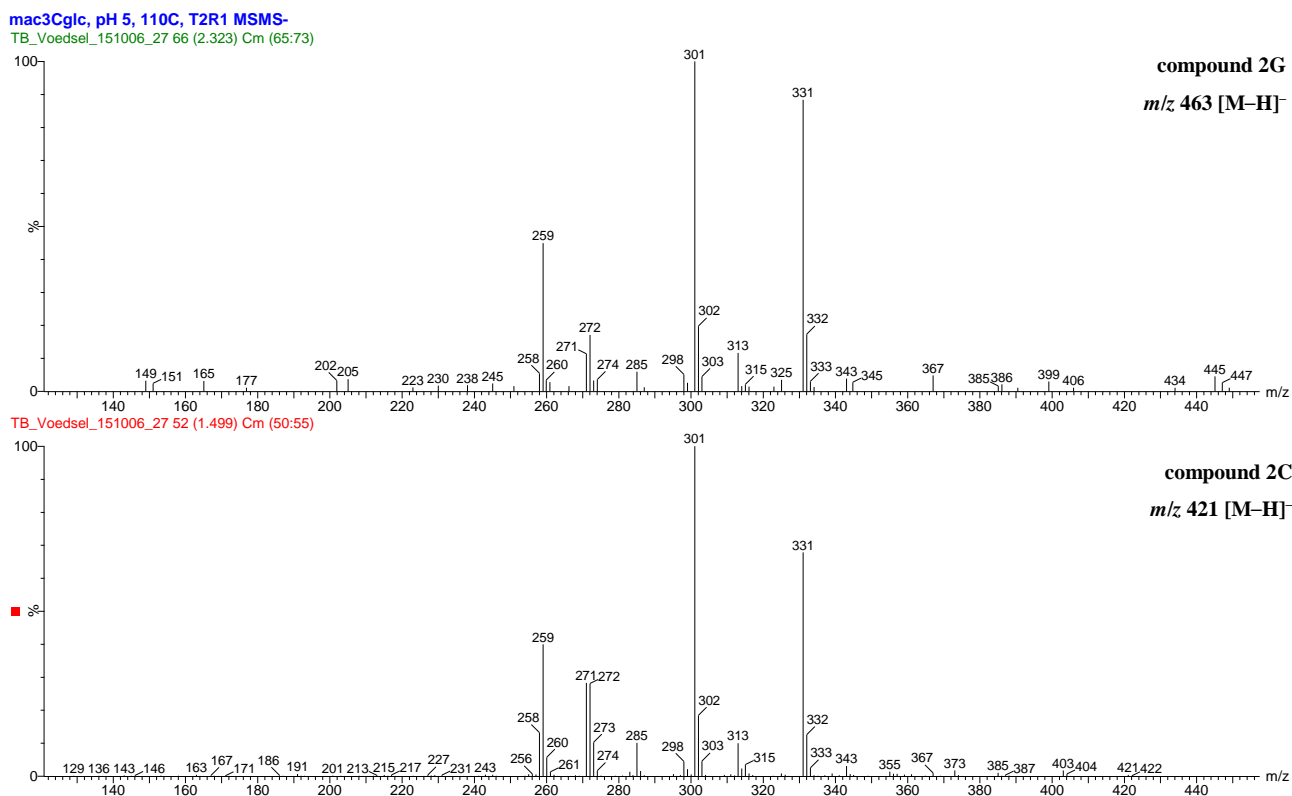


Figure S8 LC-ESI-MS/MS spectrum of the unidentified xanthone derivative (**2G**), compared to that of mangiferin (**2C**), in negative ionisation mode (Refer to Table 7 for additional information).

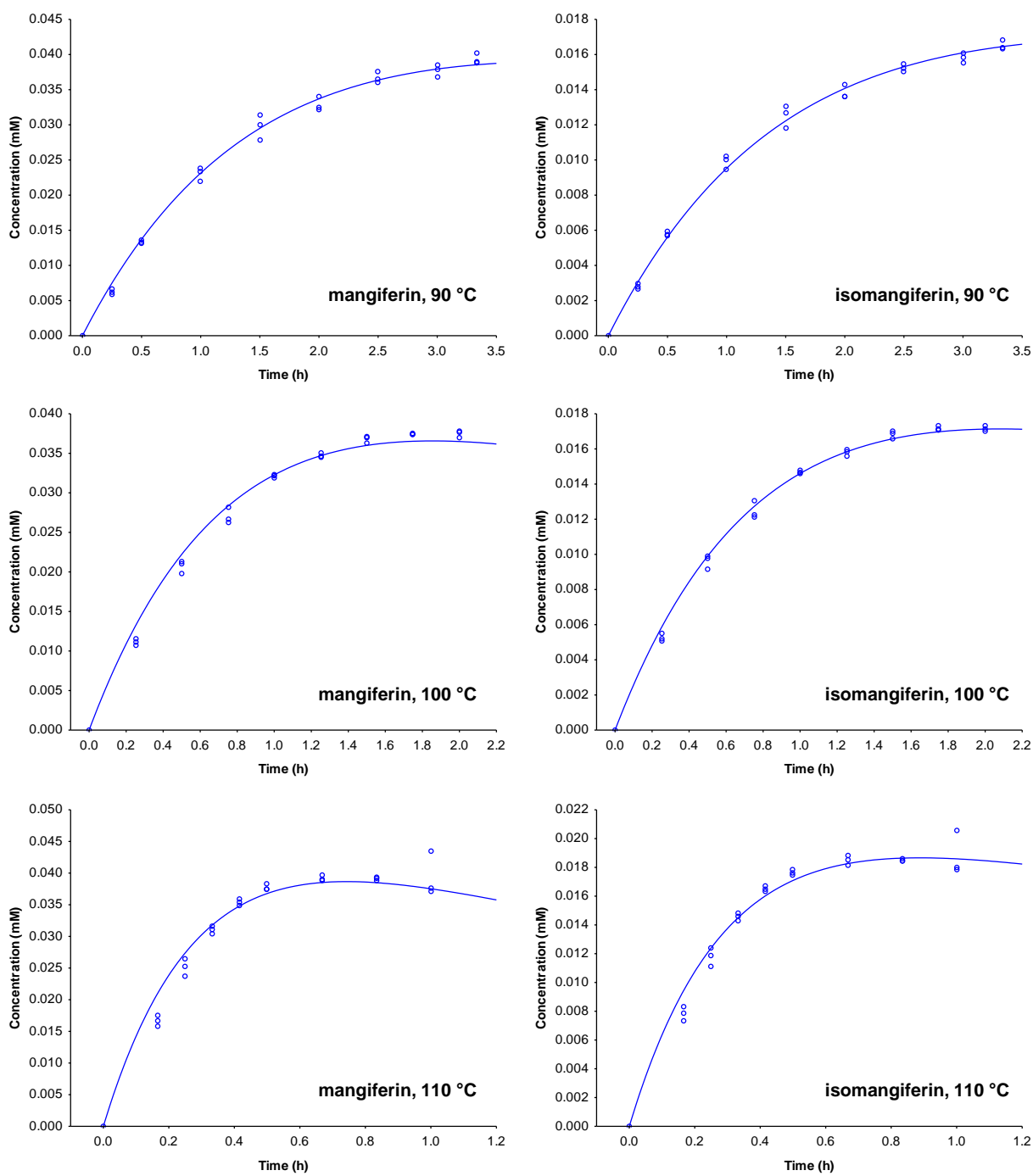


Figure S9 Formation curves of mangiferin and isomangiferin upon thermal treatment of 3- β -D-glucopyranosylmaclurin (2) (0.1 M phosphate buffer, pH 5) at 90, 100 and 110 °C.

CHAPTER 7

General Discussion and Conclusions

Cyclopia genistoides, one of the commercialised *Cyclopia* species, is of particular interest due to the presence of high levels of the bio-active xanthone, mangiferin. This makes *C. genistoides* the preferred *Cyclopia* species for the production of food ingredient and nutraceutical extracts rich in mangiferin (Joubert *et al.*, 2003). More recently, sensory analysis of infusions prepared from “fermented” (oxidised) *C. genistoides* revealed that some infusions had a noticeable bitter taste (Theron, 2012). A follow-up study that included *C. genistoides*, *C. longifolia*, *C. maculata* and *C. subternata* provided more insight into the association between phenolic compounds and taste modalities, as well as astringency of honeybush infusions. Once again mangiferin was identified as a potential predictor of bitter taste; other candidate predictors included isomangiferin and benzophenone compounds, including 3- β -D-glucopyranosylriflophenone (Erasmus, 2015). High levels of these phenolic compounds are desirable in terms of the nutraceutical value of the extracts due to their associated health-promoting benefits. Their maximum retention is therefore desirable during fermentation, the high-temperature oxidation process essential for the development of the characteristic sweet-associated aroma and flavour of honeybush herbal tea (Du Toit & Joubert, 1999). The challenge is thus to maximise polyphenol retention during fermentation, whilst reducing bitter intensity of the herbal tea infusion to acceptable levels. Similarly, losses during extract preparation and food processing, when the extract is used as a food ingredient, should be minimised to retain maximum health benefits. Kinetic modelling has proven to be a valuable tool to optimise processing conditions of complex chemical systems. The ultimate aim of the present study was thus to establish kinetic parameters and to elucidate the primary thermal degradation processes of the major *C. genistoides* xanthenes and benzophenones for eventual easy implementation in simulation models. Prediction of losses during fermentation and unit operations such as extraction, pasteurisation, etc. would therefore be possible, aiding process optimisation.

The first objective of this study was to gain insight into the phenolic composition of *C. genistoides*. To date, no comprehensive analysis of its phenolic constituents has been attempted. A high-performance liquid chromatographic (HPLC) method coupled with diode-array detection (DAD) was developed for the qualitative analysis of aqueous extracts prepared from “unfermented” (green/unoxidised) and fermented *C. genistoides* plant material. Both types of plant material were analysed to accommodate changes in phenolic composition with high-temperature oxidation. Optimised separation of the phenolic compounds present in the extracts was achieved by simultaneously optimising the gradient parameters and temperature on a high-efficiency 2.6 μ m Kinetex C₁₈ core-shell column. Identification of compounds was performed by assigning each peak to a phenolic compound sub-class based on its characteristic UV-Vis spectra, where possible. Accurate mass measurements by high-resolution electrospray ionisation-mass spectrometry (HR-ESI-MS) and MS/MS fragmentation patterns were then used to tentatively identify the molecular structures. Ten compounds were identified by comparing their retention times, UV-Vis spectra and MS characteristics with those of authentic reference standards. This included tyrosine, phenylalanine, 3- β -D-glucopyranosylriflophenone, mangiferin, isomangiferin, vicenin-2, eriocitrin, narirutin, hesperidin and diosmin. Herewith, the presence of the aromatic amino acids tyrosine and phenylalanine and the flavone diosmin (7-rutinosyloxydiosmetin) was demonstrated for the first time in *C. genistoides*, and also in the genus *Cyclopia*. Following publication of the current results (Beelders *et al.*, 2014), Moldoveanu *et al.* (2015) analysed honeybush (species not identified) for amino acids, showing that the plant material do contain these and other amino acids. The key role of phenylalanine as intermediate in the shikimate pathway, central to biosynthesis of phenolic compounds in plants, could possibly explain the presence of these aromatic amino acids in the analysed extracts. The presence of diosmin in *C. genistoides* could be expected based on the occurrence of the flavone aglycone diosmetin in *C. intermedia* (Kamara *et al.*, 2003). Mangiferin, isomangiferin and the rutinosyloxyflavanones, eriocitrin, narirutin and hesperidin, are well-known *Cyclopia* constituents (Ferreira *et al.*, 1998; Kamara *et al.*, 2004; Kokotkiewicz *et al.*, 2012, 2013), while the benzophenone 3- β -D-glucopyranosylriflophenone was only recently shown to be present in *C. subternata* (Kokotkiewicz *et al.*, 2012) and *C. genistoides* (Kokotkiewicz *et al.*, 2013; Malherbe *et al.*, 2014). The presence of the

flavone vicenin-2 (6,8-di- β -D-glucopyranosylapigenin) in *Cyclopia* spp. has been indicated previously by LC-DAD-ESI-MS analyses (De Beer *et al.*, 2012; Malherbe *et al.*, 2014; Schulze *et al.*, 2014), but the present study provided the first confirmation by co-chromatography with an authentic reference standard following its recent availability as a commercial authentic standard.

In lieu of the absence of authentic reference standards, the identity of the dihydrochalcone 3',5'-di- β -D-glucopyranosylphloretin and the benzophenone 3- β -D-glucopyranosylmaclurin, recently isolated from *C. subternata* (Kokotkiewicz *et al.*, 2012) and *C. genistoides* (Kokotkiewicz *et al.*, 2013), respectively, could only be tentatively reaffirmed in *C. genistoides* based on comparison of their UV-Vis and HR-ESI-MS data with reported data.

In addition, 28 compounds were tentatively identified in aqueous extracts of *C. genistoides*, which provided additional insight into the phenolic composition of this species for the first time. The compounds included three iriflophenone-di-*O,C*-hexoside isomers and an iriflophenone-di-*C*-hexoside, a maclurin-di-*O,C*-hexoside, two tetrahydroxyxanthone-*C*-hexoside isomers and two symmetric tetrahydroxyxanthone-*C*-hexoside dimers, a tetrahydroxyxanthone-di-*O,C*-hexoside, three xanthone-dihydrochalcone derivatives, one dihydrochalcone, nine glycosylated flavanone derivatives and five glycosylated phenolic acid derivatives. The benzophenone iriflophenone-di-*C*-hexoside, the symmetric tetrahydroxyxanthone-*C*-hexoside dimers and a xanthone-dihydrochalcone derivative [postulated to be a schoepfin A derivative of (iso)mangiferin] were only detected in the fermented sample extract. This may either be due to increased prominence in the fraction as the relative quantities of the polyphenolic constituents change upon fermentation or to their formation under such high-temperature oxidative conditions. Both situations are supported by literature; for example, the natural occurrence of a symmetric homodimer of mangiferin has been demonstrated in mango tree stem bark (Abdel-Mageed *et al.*, 2014), while the thermally-induced formation of dimeric compounds has been reported for other phenolic sub-classes (*e.g.* flavan-3-ols; Li *et al.*, 2013).

The results from the first research chapter focused the attention on one iriflophenone-di-*O,C*-hexoside isomer that was present in large quantities in both types of extracts. This compound was preliminary quantified in terms of 3- β -D-glucopyranosyliriflophenone equivalents, with corresponding values of 6.1 g per 100 g of dried aqueous extract (% DAE) prepared from the unfermented plant material (recalculated as 5.6% DAE, when quantified using the actual standard), and 5.5% DAE of the fermented sample (recalculated as 5.1% DAE). The high levels of this unknown benzophenone, together with its high thermal stability (only a decrease of *ca.* 9% with fermentation) provided the impetus for its isolation and identification. A protocol was thus developed for the specific isolation of this compound from *C. genistoides*. As a secondary aim, we hoped that the isolation protocol would simultaneously yield the minor benzophenone (tentatively identified as) 3- β -D-glucopyranosylmaclurin in its pure form for future in-house applications (identification, quantification, kinetic studies, bio-activity studies, and so forth).

The first-step entailed screening available batches of *C. genistoides* plant material to obtain starting material containing high levels of the target compounds. A preliminary screening indicated that *C. genistoides* of the Pearly Beach (Overberg) type contained substantially higher levels of the target compounds than plant material originating from the West Coast. Only one (randomly selected) sample of each were, however, analysed and further research is thus required to confirm that the Pearly Beach type does indeed contain higher levels of the “iriflophenone-di-*O,C*-hexoside” and 3- β -D-glucopyranosylmaclurin. This is also relevant in light of a recent study that demonstrated that *C. genistoides* seedling plants of the Overberg type (Southern Seaboard) contained significantly lower levels of the related benzophenone 3- β -D-glucopyranosyliriflophenone compared to seedling plants propagated from seeds originating respectively from a natural population located in the West Coast (Western Seaboard) and Cape Peninsula (Joubert *et al.*, 2014).

Hot water extracts (93 °C/30 min) of individual bushes of the Pearly Beach type harvested on different dates were subsequently screened, and plant material samples identified for the preparation of freeze-dried aqueous extract on large

scale. The levels of the target compounds in the extract were subsequently enriched using solid-phase extraction (SPE), following optimisation of sample loading and step-wise gradient elution conditions. While SPE is a relatively expensive technique, it provided significant enrichment of the target compounds (*ca.* nine-fold), with good recoveries of up to 75%. A similar approach, using open column chromatography, has since been adopted to obtain large quantities of a benzophenone-enriched fraction for biological activity and bio-availability studies in a related project by the ARC and MRC (Dr Christiaan Malherbe, ARC Infruitec-Nietvoorbij, personal communication).

For the final purification step, high-speed counter-current chromatography (HSCCC) was initially evaluated. Following mini shake flask experiments to test a wide range solvent systems, an optimum solvent was obtained (3 parts of EtOH, 5 parts of 2 M aq. ammonium sulphate), yielding partition coefficient (K) values of 0.67 for iriflophenone-di-*O,C*-hexoside and 0.48 for maclurin-3-*C*-glucoside. Although the ratio of the two K values or the separation factor ($\alpha = K_1/K_2$ where $K_1 > K_2$) was 1.398, and thus less than the required value of greater than 1.5 (Ito, 2005), an analytical run was still performed. The two target compounds were found to co-elute, which could not be improved by changing other experimental parameters such as temperature, flow rate of the mobile phase ($\text{mL}\cdot\text{min}^{-1}$) or revolution speed (rpm) as suggested by Ito (2005). As an alternative, semi-preparative LC was thus conducted to isolate the target compounds from the enriched *C. genistoides* extract. Even though it was a time-consuming process, with a high amount of solvent waste generated, the recovery values were still high at 71-74 %. Ultimately 370 mg of iriflophenone-di-*O,C*-hexoside (purity > 99% by HR-ESI-MS) and 30 mg of 3- β -D-glucopyranosylmaclurin (purity > 95% by HR-ESI-MS) were obtained from a starting material of 420 g of unfermented plant material. The minor benzophenone was confirmed to be 3- β -D-glucopyranosylmaclurin by comparison of its HR-ESI-MS data, and ^1H NMR and ^{13}C NMR spectroscopic data with literature data.

Structural elucidation of the iriflophenone-di-*O,C*-hexoside proved to be quite difficult. The relative configurations of the glycoside units can normally be determined by a 1D/2D NOESY NMR experiment. However, NMR spectroscopic data for the iriflophenone-di-*O,C*-hexoside proved inconclusive for unambiguous identification of the individual glycoside units, due to overlapping proton resonances. It was, however, postulated that the unknown benzophenone is a glucopyranosyloxy derivative of 3- β -D-glucopyranosyliriflophenone, and therefore the following methodology was employed: selective hydrolysis and identification of the terminal O-linked sugar moiety, together with purification of the liberated iriflophenone-hexosyl and comparison of its HR-ESI-MS and NMR spectroscopic data to those of a commercial 3- β -D-glucopyranosyliriflophenone standard. The terminal O-linked hexoside moiety was identified as D-glucose by enzymatic hydrolysis and GC-MS analysis. The resulting iriflophenone-hexosyl was purified, and its ^1H and ^{13}C NMR data compared to those of 3- β -D-glucopyranosyliriflophenone, which proved to be an excellent match. Having identified the β -D-glucopyranosyl units, the rest of the molecule and the point of attachment of the β -D-glucopyranosyloxy unit were defined by additional 1D NOESY, COSY, HSQC and HMBC NMR experiments. The unknown “iriflophenone-di-*O,C*-hexoside” was thus identified as 3- β -D-glucopyranosyl-4- β -D-glucopyranosyloxyiriflophenone, a new benzophenone unique to *Cyclopia*.

While it was not part of the initial objective of this dissertation, the isolated benzophenones were also characterised in terms of their biological activities. This included the assessment of their α -glucosidase inhibitory activities and their abilities to increase glucose uptake *in vitro*. These assays were specifically chosen in light of literature reports indicating that polyhydroxybenzophenones and their glycosylated derivatives have significant potential as natural α -glucosidase inhibitors (Feng *et al.*, 2011; Hu *et al.*, 2011; Liu *et al.*, 2012). Furthermore, data presented by Zhang *et al.* (2011, 2013) showed that the related benzophenone 3- β -D-glucopyranosyliriflophenone has the ability to increase glucose uptake activity *in vitro*.

The α -glucosidase inhibitory activities of the isolated benzophenones 3- β -D-glucopyranosyl-4- β -D-glucopyranosyloxyiriflophenone and 3- β -D-glucopyranosylmaclurin were assessed at three concentration levels ranging between 50 and 400 μ M, and compared to the activities of 3- β -D-glucopyranosyliriflophenone and maclurin (both obtained commercially). The inhibitory activity of the benzophenones showed a clear dose-response, with higher activity observed at higher concentration levels. At equimolar concentration levels (200 μ M), 3- β -D-glucopyranosylmaclurin exhibited the highest inhibitory activity (54%), followed by 3- β -D-glucopyranosyliriflophenone (49%) and 3- β -D-glucopyranosyl-4- β -D-glucopyranosyloxyiriflophenone (43%), while maclurin showed the weakest activity (28%). The presence of the 3'-hydroxy group led to a significant increase in the α -glucosidase inhibitory activity of the polyhydroxybenzophenone glucosyl compounds. The presence of a single glucopyranosyl moiety on the A-ring of the diphenyl methanone structure was found to increase the inhibitory activity, while further O-glucosylation had the opposite effect. While 3- β -D-glucopyranosylmaclurin exhibited the highest α -glucosidase inhibitory activity, limited availability meant that it could not be tested in the cell models (L6 myoblasts, 3T3-L1 fibroblasts, and C3A hepatocytes). 3- β -D-Glucopyranosyl-4- β -D-glucopyranosyloxyiriflophenone and 3- β -D-glucopyranosyliriflophenone were only marginally effective ($p \geq 0.05$) in increasing glucose uptake. The in vitro tests were undertaken by researchers of the Diabetes Discovery Platform (Medical Research Council of South Africa, Tygerberg).

In the present study, the isolated benzophenones were also characterised in terms of their antioxidant activity, in light of the prominence of oxidative stress playing a key role in the pathogenesis and progression of many diseases including obesity, diabetes and cardiovascular disease (Rains & Jain, 2011; Bandeira *et al.*, 2013; Pitocco *et al.*, 2013; Kayama *et al.*, 2015; Marseglia *et al.*, 2015). The Trolox equivalent antioxidant capacity (TEAC) of 3- β -D-glucopyranosyl-4- β -D-glucopyranosyloxyiriflophenone and 3- β -D-glucopyranosylmaclurin was determined using 96-well plate format of the 2,2-diphenyl-1-picrylhydrazyl radical (DPPH \bullet) scavenging and oxygen radical absorbance capacity (ORAC) assays. The TEAC values of these benzophenones were subsequently compared to that of 3- β -D-glucopyranosyliriflophenone, and to those of the two major *Cyclopia* xanthone constituents, namely mangiferin and isomangiferin. Assessment of the TEAC values of the selected benzophenones and xanthones provided some insight into the relative importance of these constituents in terms of the total antioxidant capacity (TAC) of the extract, and also enabled exploration of structure-activity relationships. TEAC_{DPPH \bullet} values for the individual compounds indicated that 3- β -D-glucopyranosylmaclurin was the most efficient scavenger of DPPH \bullet , while 3- β -D-glucopyranosyl-4- β -D-glucopyranosyloxyiriflophenone had the highest TEAC_{ORAC} value. Conversely, results from the DPPH \bullet assay showed that 3- β -D-glucopyranosyl-4- β -D-glucopyranosyloxyiriflophenone was ineffective as radical scavenger, which clearly underlines the importance of using more than one assay to assess the antioxidant capacity of natural extracts and/or phenolic compounds. This is the first report on the antioxidant capacity of 3- β -D-glucopyranosyl-4- β -D-glucopyranosyloxyiriflophenone and 3- β -D-glucopyranosylmaclurin. The impact of structural features (degree of glucosylation and hydroxylation, and the position of glucosylation) on the antioxidant capacity of the benzophenones and xanthones were found to differ between the two antioxidant assays. The different observations may be related to differences in the reaction mechanisms of the two assays, and further research is thus required to elucidate the reaction mechanisms of these benzophenones and xanthones with free radicals.

The optimised HPLC-DAD method developed in this study was subsequently validated and applied to the quantitative analysis of aqueous extracts prepared from unfermented and fermented *C. genistoides* plant material ($n = 10$). The plant material originated from the same individual plants ("paired-processed" samples), which enabled us to quantitatively assess the effect of fermentation on the content of individual phenolic compounds. This was the first "species-specific" HPLC-DAD method developed for the quantification of *C. genistoides* phenolic compounds, which overcame the limitations associated with the application of "generic" *Cyclopia* HPLC methods (Joubert *et al.*, 2003; De Beer & Joubert,

2010). The optimised method was suitable for the quantification of 18 phenolic compounds, which was a major improvement with regard to other HPLC methods previously employed in the quantitative analysis of *C. genistoides* extracts. Up to this point, quantitative data for the individual monomeric phenolic constituents of *C. genistoides* extracts was mostly limited to four of the major compounds, *i.e.* mangiferin, isomangiferin, hesperidin and 3- β -D-glucopyranosyliriflophenone (Joubert *et al.*, 2003, Joubert *et al.*, 2008; De Beer & Joubert, 2010; Joubert *et al.*, 2014). Analysis of the extracts indicated that the xanthones, mangiferin and isomangiferin, and the benzophenones, 3- β -D-glucopyranosyl-4- β -D-glucopyranosyloxiriflophenone and 3- β -D-glucopyranosyliriflophenone, were the four major constituents of aqueous extracts of unfermented *C. genistoides*, constituting on average 11.8, 1.5, 5.7 and 1.1 g per 100 g of extract, respectively. While *C. genistoides* is principally renowned for high levels of the bio-active xanthone mangiferin, as re-confirmed herein, the results of the current study also indicate that this species could be a good source material for the production of a benzophenone-enriched extract. The benzophenone 3- β -D-glucopyranosyliriflophenone is not commonly found in food or beverage products, with other dietary sources principally mango (Berardini *et al.*, 2004). The traditional medicinal plant, agarwood, is also a good source (Feng *et al.*, 2011). Furthermore, *Cyclopia* represents the only known natural source of the new benzophenone 3- β -D-glucopyranosyl-4- β -D-glucopyranosyloxiriflophenone.

Quantitative data were also generated for 14 additional minor compounds which provided further information on the composition of the paired-processed samples of *C. genistoides*. This included quantification of the known compounds vicenin-2, eriocitrin, narirutin, hesperidin, 3- β -D-glucopyranosylmaclurin, and 3',5'-di- β -D-glucopyranosylphloretin. Note that quantification of the latter two compounds was only made possible by their isolation from *Cyclopia* plant material, as discussed previously for 3- β -D-glucopyranosylmaclurin. 3',5'-di- β -D-Glucopyranosylphloretin was also isolated from *C. subternata* during the course of this study by a member of our research group for in-house use as authentic reference standard.

Nine compounds, tentatively identified by LC-DAD-ESI-MS and –MS/MS, were quantified in the *C. genistoides* extracts using calibration curves of the most closely related reference standard. This included the benzophenone maclurindi-*O,C*-hexoside, a tetrahydroxyxanthone-*C*-hexoside isomer, a tetrahydroxyxanthone-*C*-hexoside dimer, and a tetrahydroxyxanthone-di-*O,C*-hexoside, three flavanones comprising an eriodictyol-*O*-hexose-*O*-deoxyhexoside and two naringenin-*O*-hexose-*O*-deoxyhexoside isomers, the dihydrochalcone 3-hydroxyphloretin-3',5'-di-*C*-hexoside, and a compound that could not be identified based on the available data. Of these new compounds, one of the naringenin-*O*-hexose-*O*-deoxyhexoside isomers represented the fifth most abundant constituent of aqueous extract prepared from the unfermented plant material, which clearly underlines the necessity to isolate this compound for structural elucidation and identification purposes. This is further supported by the behaviour of this compound, and its isomer, upon fermentation of *C. genistoides* plant material (as discussed in the following section).

The HPLC-DAD method developed in this study has since been employed by our group to analyse a large number of aqueous infusions prepared from fermented *C. genistoides* ($n = 65$) to generate base-line content data for honeybush tea prepared from this species. The data were presented as part of a paper dealing with the contribution of honeybush herbal teas (*Cyclopia* spp.) to dietary exposure to xanthones and benzophenones, amongst others (Schulze *et al.*, 2015). For the same paper, the *C. genistoides* HPLC method was adapted for the analysis of *C. longifolia* extracts as the latter species is also characterised by exceptionally high levels of mangiferin in relation to its other phenolic constituents. Increasing evidence of the beneficial properties of polyphenols has led to a need for compositional data of foods and beverages to enable calculation of their dietary intake in epidemiological studies (Lyu *et al.*, 2008). This had led to the development of several databases on the content of polyphenols in food, including Phenol-Explorer (Nevue *et al.*, 2010), which has recently been updated to incorporate data on the effects of food processing on polyphenol content (Rothwell *et al.*, 2013; 2015).

Linking up with the quantitative data generated in the present study, it is clear that the levels of individual phenolic compounds in aqueous extracts of unfermented *C. genistoides* were considerably affected by high-temperature processing. In accordance with literature (Joubert *et al.*, 2008; De Beer & Joubert, 2010; Schulze *et al.*, 2014), the contents of most compounds were significantly reduced. The levels of 3- β -D-glucopyranosyl-4- β -D-glucopyranosyloxyiriflophenone remained relatively stable during fermentation, indicating that this compound has a high thermal stability. Interestingly, a tetrahydroxyxanthone-C-hexoside dimer could only be quantified in extracts prepared from the fermented sample, suggesting its formation with fermentation (as stated previously). Two compounds, tentatively identified as naringenin-O-hexose-O-deoxyhexosides, also exhibited interesting behaviour during the fermentation process. While the levels of one isomer decreased with fermentation that of the other isomer showed a corresponding increase, suggesting possible interconversion. It was also observed that compounds from the same phenolic sub-classes exhibited large differences in their thermal stability, and this was attributed to differences in their chemical structures; most notably, differences in the degree and position of glycosylation, as well as the degree of hydroxylation. It was therefore decided to investigate the thermal stability of the major benzophenones and xanthenes of *C. genistoides* more comprehensively, with the objective to better elucidate the effects of the degree of glycosylation and the position of glycosylation on their respective thermal stabilities.

The thermal stabilities of the benzophenones 3- β -D-glucopyranosyl-4- β -D-glucopyranosyloxyiriflophenone and 3- β -D-glucopyranosyliriflophenone and the xanthenes mangiferin and isomangiferin, when present in the plant matrix, were kinetically assessed under high-temperature oxidative conditions simulating the recommended fermentation conditions for the production of high quality fermented *C. genistoides* (Theron, 2012). The kinetic data provided a good fit for first-order degradation reactions, in accordance with literature reports on compounds from other phenolic sub-classes (refer to chapter 2). An increase in the oxidation temperature from 80 to 90 °C increased the rate of degradation for all target compounds in the plant matrix, as expected, and this effect was quantified by the temperature coefficient of Van't Hoff (the Q_{10} value). Thermal stability was found to decrease in the order 3- β -D-glucopyranosyl-4- β -D-glucopyranosyloxyiriflophenone > isomangiferin > 3- β -D-glucopyranosyliriflophenone > mangiferin. Addition of a glucopyranosyloxy moiety at C-4 inferred higher thermal stability to 3- β -D-glucopyranosyl-4- β -D-glucopyranosyloxyiriflophenone compared to 3- β -D-glucopyranosyliriflophenone during high-temperature oxidation of *C. genistoides* plant material. Glucosylation at C-4 of the dibenzo- γ -pyrone structure, as opposed to C-2, also increased the stability of the tetrahydroxyxanthenes.

The kinetic parameters derived for the first-order degradation reactions were subsequently used to predict the amounts of these compounds remaining in the plant material following oxidation under up-scaled conditions. The degradation kinetics model provided excellent estimates for the average amounts of three of the target compounds in the oxidised plant material, but greatly underestimated the degradation of 3- β -D-glucopyranosyliriflophenone. Further research and/or refinement of the model is thus required to obtain a more accurate prediction for the latter compound.

As the *C. genistoides* plant material represents a complex matrix, the thermal stabilities of the aforementioned compounds were also assessed in aqueous model solutions. This eliminated potential matrix effects, and also provided information on the degradation pathways of the individual compounds as degradation products could now be traced back to a "parent compound". Isolation of 3- β -D-glucopyranosylmaclurin from *C. genistoides*, described in the first part of this study, enabled us to kinetically assess its thermal stability, thereby providing additional insight into the thermal stability of the benzophenones as affected by B-ring hydroxylation. It also facilitated a direct comparison of its thermal stability with those of its xanthone analogues. The progression of the thermal degradation reactions was monitored by UHPLC-DAD and for this purpose a rapid method, specifically developed for the separation and quantification of target compounds and/or their degradation products, was developed and employed.

Kinetic data generated using aqueous model solutions confirmed the structure-stability relationships observed in the plant material. In addition, it was confirmed that increased B-ring hydroxylation significantly reduced the thermal stability of the benzophenones, making 3- β -D-glucopyranosylmaclurin the most thermally labile compound amongst those tested in the current study. While the ortho-diol structure in the B-ring appears to be key to increased biological activity (Rice-Evans *et al.*, 1996), as observed for the benzophenones in the present study, it also leads to decreased stability. However, cyclisation of this polyhydroxylated structure of 3- β -D-glucopyranosylmaclurin with the formation of a xanthone nucleus then confers a higher thermal stability to its xanthone analogues. This was exemplified by the large differences in the magnitudes of the first-order degradation rate constants calculated for 3- β -D-glucopyranosylmaclurin, mangiferin and isomangiferin.

As observed for the plant material, increased temperatures also increased the reaction rate constants of the target compounds in the model solutions, and this effect was quantified by computing the Arrhenius activation energy (E_a). This subsequently enabled estimation of the reaction rate constants at intermediate temperatures, and consequently also to predict losses under common thermal processing conditions. For instance, the reaction rate constant for 3- β -D-glucopyranosylmaclurin at 93 °C was calculated as 0.735 h⁻¹ (based on Arrhenius parameters computed via linear regression), signifying that hot water extraction or pasteurisation (93 °C/30 min) would lead to losses of *ca.* 31% in a similar medium. It is therefore clear that other methodologies should be evaluated for the extraction of this compound from the *C. genistoides* plant material (*e.g.* ultrasonication at lower temperatures or cold-water extraction) and for the preservation of food products or beverages containing this thermally-labile bio-active constituent (*e.g.* UV irradiation, or chemical agents). It is, however, suggested that the magnitude of E_a , calculated from the Arrhenius equation in this study, be verified independently using calorimetry, for example (as proposed by Peleg *et al.*, 2012).

Results from the current study also indicated that the pH of the aqueous environment significantly affects the thermal stability of mangiferin. Mangiferin was selected for this investigation due to availability of large quantities of the standard compound and due to its high levels in the plant material. Optimum thermal stability of mangiferin was observed at pH 3, and the degradation rate constant exponentially increased with increasing pH. Practically, this signifies that mangiferin will exert good stability in a fruit-based beverage (pH ~ 3-4), but that it will degrade quickly when subject to thermal treatment in a milk-based product (pH ~ 6.5). It should also be noted that the reaction rate constant of mangiferin at pH 3 was slightly higher than expected. This indicates that the optimum pH for mangiferin stability probably lies between pH 3 and 4, and that the degradation of mangiferin could also be accelerated when the pH is reduced below 3. It is therefore recommended that the thermal stability of mangiferin be assessed at intermediate pH levels between 3 and 4, and at pH levels lower than 3, to confirm these theories.

In the last section of the current study, identification of the degradation products by LC-DAD-ESI-MS and –MS/MS provided insight into possible thermal degradation reactions and pathways. Thermally-induced reactions principally comprised isomerisation, dimerisation, cleavage of the O-linked sugar moiety in 3- β -D-glucopyranosyl-4- β -D-glucopyranosyloxyiriflophenone, and conversion of the benzophenones to the xanthenes. While 3- β -D-glucopyranosyl-4- β -D-glucopyranosyloxyiriflophenone and 3- β -D-glucopyranosyliriflophenone only formed trace quantities of mangiferin and isomangiferin upon thermal treatment, this was the primary conversion reaction of 3- β -D-glucopyranosylmaclurin. The conversion of 3- β -D-glucopyranosylmaclurin to mangiferin and isomangiferin is in agreement with the biosynthetic pathway proposed for mangiferin and isomangiferin in *Anemarrhena asphodeloides* (Fujita and Inoue, 1980a, 1980b, 1981), which indicates that the conversion may be induced enzymatically in the plant material or under thermal stress in near-neutral aqueous conditions (pH 5). The fact that 3- β -D-glucopyranosylmaclurin is the biogenetic precursor of mangiferin and isomangiferin could therefore explain its relative low levels in *C. genistoides* (*ca.* 0.31 g per 100 g of DAE prepared from unfermented plant material) compared to those of the xanthenes (*ca.* 11.80% mangiferin and *ca.*

1.54% isomangiferin). What is also interesting is that mangiferin and isomangiferin formed in a stoichiometric ratio of *ca.* 2:1 upon thermal treatment of 3- β -D-glucopyranosylmaclurin, indicating that the formation of the C-2 isomer as opposed to the C-4 isomer is favoured, possibly due to thermodynamic considerations. Conversely, mangiferin and isomangiferin naturally occurs in the (unfermented) *C. genistoides* plant material in a much larger ratio of *ca.* 8:1. This indicates that the biosynthesis of mangiferin in the plant material (enzymatic reaction) is favoured to a much larger extent than the synthesis of isomangiferin, while other unknown factors might also play a role.

Based on the identification of tetrahydroxyxanthone-C-hexoside isomers and tetrahydroxyxanthone-C-hexoside dimers in thermally-treated solutions of mangiferin and isomangiferin, their presence in aqueous extract of fermented *C. genistoides* can now be directly traced back to isomerisation and dimerisation of their parent compounds (mangiferin and isomangiferin) upon high-temperature oxidation of the plant material. This is also supported by the co-occurrence of iriflophenone-di-*O,C*-hexoside isomers in thermally-treated solutions of 3- β -D-glucopyranosyl-4- β -D-glucopyranosyloxiriflophenone and in aqueous extract of fermented *C. genistoides*. It is, however, recommended that the thermally-treated solutions be analysed using the same HPLC-DAD method employed in the characterisation of the fermented extract to facilitate a direct comparison of retention times for the compounds of interest and thus tentative confirmation of their presence.

While it is clear that 3- β -D-glucopyranosylmaclurin is extremely susceptible to thermally-induced degradation/conversion reactions, it might not necessarily negatively impact on the biological properties of the thermally-treated solution, as mangiferin and isomangiferin are known to exert strong biological effects. While the degradation products of the other target compounds were only tentatively identified in this study, it is anticipated that they too could exert biological effects, and therefore offset losses in bio-activity associated with degradation of the parent compound. This has been observed previously for phenolic acids, where the thermal degradation products also exerted antioxidant activity (Khuwijitjaru *et al.*, 2014a, 2014b). It would thus be of great interest, for instance, to determine the antioxidant activity of the thermally-treated solutions of the target xanthenes and benzophenones in future studies. Furthermore, by conducting on-line HPLC antioxidant assays, peaks showing antioxidant activity, and thereby contributing to the antioxidant activity of the thermally-treated solutions, can be identified. The advantage of using this approach is that degradation reaction mixtures could be screened and new peaks with activity identified for targeted isolation and identification.

With regard to process control of *Cyclopia* extracts, the results from the current study clearly indicate that 3- β -D-glucopyranosyl-4- β -D-glucopyranosyloxiriflophenone would not be a good indicator of thermal stress, as it exhibits very good thermal stability. 3- β -D-Glucopyranosylmaclurin will also not be suitable, as it is only present at very low levels, and as it is extremely prone to thermally-induced conversion and degradation reactions. Consequently, mangiferin and isomangiferin will also not be good marker compounds, as their losses might be offset by their concurrent formation from 3- β -D-glucopyranosylmaclurin (when present in substantial quantities). These results point to 3- β -D-glucopyranosyliriflophenone as a suitable indicator of thermal stress, since it exhibited moderate degradation similar to those of the xanthenes.

To conclude, this study greatly expanded the knowledge of the phenolic composition of *C. genistoides*, highlighting the potential of this *Cyclopia* species as a source of interesting and diverse compounds. The presence of new xanthenes and benzophenones was demonstrated, including that of a novel benzophenone which was successfully isolated and characterised. Selected xanthenes and benzophenones were characterised in terms of biological activities, relevant to antidiabetic properties of *Cyclopia* extracts. The thermal stability of several of the major compounds was kinetically assessed for the first time, providing future researchers with kinetic models to predict losses during thermal food processes. A future application of the degradation kinetics model could be to adjust the fermentation time-temperature

combinations to reduce mangiferin in the plant material to a pre-determined "threshold" level, based on bitter taste of the herbal tea infusion, given the variation in content in the raw material. The HPLC-DAD method developed in the present study expands the number of species-specific HPLC methods available for analysis of *Cyclopia* species, forming an essential tool in the current Honeybush Research Programme of the Agricultural Research Council. This includes development of taste prediction models and evaluation of genotypes for plant breeding purposes, amongst others.

REFERENCES

- Abdel-Mageed, W.M., Bayoumi, S.A.H., Chen, C., Vavricka, C.J., Li, L., Malik, A., Dai, H., Song, F., Wang, L., Zhang, J., Gao, G.F., Lv, Y., Liu, L., Liu, X., Sayed, H.M. & Zhang, L. (2014). Benzophenone C-glucosides and gallotannins from mango tree stem bark with broad-spectrum anti-viral activity. *Bioorganic and Medicinal Chemistry*, **22**, 2236-2243.
- Bandeira, S. de M., Da Fonseca, L.J.S., Da S. Guedes, G., Rabelo, L.A., Goulart, M.O.F. & Vasconcelos, S.M.L. (2013). Oxidative stress as an underlying contributor in the development of chronic complications in diabetes mellitus. *International Journal of Molecular Sciences*, **14**, 3265-3284.
- Beelders, T., De Beer, D., Stander, M.A. & Joubert, E. (2014). Comprehensive phenolic profiling of *Cyclopia genistoides* (L.) Vent. by LC-DAD-MS and –MS/MS reveals novel xanthone and benzophenone constituents. *Molecules*, **19**, 11760-11790.
- Berardini, N., Carle, R. & Schieber, A. (2004). Characterization of gallotannins and benzophenone derivatives from mango (*Mangifera indica* L. cv. 'Tommy Atkins') peels, pulp and kernels by high-performance liquid chromatography/electrospray ionization mass spectrometry. *Rapid Communications in Mass Spectrometry*, **18**, 2208–2216.
- De Beer, D. & Joubert, E. (2010). Development of HPLC method for *Cyclopia subternata* phenolic compound analysis and application to other *Cyclopia* spp. *Journal of Food Composition and Analysis*, **23**, 289-297
- De Beer, D., Schulze, A.E., Joubert, E., De Villiers, A., Malherbe, C.J. & Stander, M.A. (2012). Food ingredient extracts of *Cyclopia subternata* (honeybush): variation in phenolic composition and antioxidant capacity. *Molecules*, **17**, 14602-14624.
- Du Toit, J. & Joubert, E. (1999). Optimization of the fermentation parameters of honeybush tea (*Cyclopia*). *Journal of Food Quality*, **22**, 241-256.
- Erasmus, L.M. (2015). Development of Sensory Tools for Quality Grading of *Cyclopia genistoides*, *C. longifolia*, *C. maculata* and *C. subternata* herbal teas MSc (Food Science) Thesis, Stellenbosch University, Stellenbosch, South Africa.
- Feng, J., Yang, X.-W. & Wang, R.-F. (2011). Bio-assay guided isolation and identification of α -glucosidase inhibitors from the leaves of *Aquilaria sinensis*. *Phytochemistry*, **72**, 242-247.
- Ferreira, D., Kamara, B.I., Brandt, E.V. & Joubert, E. (1998). Phenolic compounds from *Cyclopia intermedia* (honeybush tea). 1. *Journal of Agricultural and Food Chemistry*, **46**, 3406-4310.
- Fujita, M. & Inoue, T. (1980a). Biosynthesis of mangiferin in *Anemarrhena asperoides* BUNGE. I. The origin of the xanthone nucleus. *Chemical and Pharmaceutical Bulletin*, **28**, 2476-2481.
- Fujita, M. & Inoue, T. (1980b). Biosynthesis of mangiferin in *Anemarrhena asperoides* BUNGE. II. C-glucosylation of mangiferin. *Chemical and Pharmaceutical Bulletin*, **28**, 2482-2486.
- Fujita, M. & Inoue, T. (1980). Further studies on the biosynthesis of mangiferin in *Anemarrhena asperoides*: hydroxylation of the shikimate-derived ring. *Phytochemistry*, **20**, 2183-2185.
- Hu, X., Xiao, Y., Wu, J. & Ma, L. (2011). Evaluation of polyhydroxybenzophenones as α -glucosidase inhibitors. *Archiv der Pharmazie – Chemistry in Life Sciences*, **2**, 71-77.
- Ito, Y. (2005). Golden rules and pitfalls in selecting optimum conditions for high-speed counter-current chromatography. *Journal of Chromatography A*, **1065**, 145-168.
- Joubert, E., Otto, F., Grüner, S. & Weinreich, B. (2003). Reversed-phase HPLC determination of mangiferin, isomangiferin and hesperidin in *Cyclopia* and the effect of harvesting date on the phenolic composition of *C. genistoides*. *European Food Research and Technology*, **216**, 270-273.

- Joubert, E., Richards, E.S., Van der Merwe, J.D., De Beer, D., Manley, M. & Gelderblom, W.C.A. (2008). Effect of species variation and processing on phenolic composition and *in vitro* antioxidant activity of aqueous extracts of *Cyclopia* spp. (honeybush tea). *Journal of Agricultural and Food Chemistry*, **56**, 954-963.
- Joubert, E., De Beer, D., Hernández, I. & Munné-Bosch, S. (2014). Accumulation of mangiferin, isomangiferin, iriflophenone-3-*C*- β -glucoside and hesperidin in honeybush leaves (*Cyclopia genistoides* Vent.) in response to harvest time, harvest interval and seed source. *Industrial Crops and Products*, **56**, 74-82.
- Kamara, B.I., Brandt, E.V., Ferreira, D. & Joubert, E. (2003). Polyphenols from honeybush tea (*Cyclopia intermedia*). *Journal of Agricultural and Food Chemistry*, **51**, 3874-3879.
- Kamara, B.I., Brand, D.J., Brandt, E.V. & Joubert, E. (2004). Phenolic metabolites from honeybush tea (*Cyclopia intermedia*). *Journal of Agricultural and Food Chemistry*, **52**, 5391-5395.
- Kayama, Y., Raaz, U., Jagger, A., Adam, M., Schellinger, I.N., Sakamoto, M., Suzuki, H., Toyama, K., Spin, J.M. & Tsao, P.S. (2015). Diabetic cardiovascular disease induced by oxidative stress. *International Journal of Molecular Sciences*, **16**, 25234-25263.
- Khuwijitjaru, P., Plernjit, J., Suaylam, B., Samuhaseneetoo, S., Pongsawatmanit, R. & Adachi, S. (2014a). Degradation kinetics of some phenolic compounds in subcritical water and radical scavenging activity of their degradation products. *The Canadian Journal of Chemical Engineering*, **92**, 810-815.
- Khuwijitjaru, P., Suaylam, B. & Adachi, S. (2014b). Degradation of caffeic acid in subcritical water and online HPLC-DPPH assay of degradation products. *Journal of Agricultural Food Chemistry*, **62**, 1945-1949.
- Kokotkiewicz, A., Luczkiewicz, M., Sowinski, P., Glod, D., Gorynski, K. & Bucinski, A. (2012). Isolation and structure elucidation of phenolic compounds from *Cyclopia subternata* Vogel (honeybush) intact plant and *in vitro* cultures. *Food Chemistry*, **133**, 1373-1382.
- Kokotkiewicz, A., Luczkiewicz, M., Pawlowska, J., Luczkiewicz, P., Sowinski, P., Witkowski, J., Bryl, E. & Bucinski, A. (2013). Isolation of xanthone and benzophenone derivatives from *Cyclopia genistoides* (L.) Vent. (honeybush) and their pro-apoptotic activity on synoviocytes from patients with rheumatoid arthritis. *Fitoterapia*, **90**, 199-208.
- Li, N., Taylor, L.S., Ferruzzi, M.G. & Mauer, L.J. (2013). Color and chemical stability of tea polyphenol (-)-epigallocatechin-3-gallate in solution and solid states. *Food Research International*, **53**, 909-921.
- Liu, Q., Guo, T., Li, W., Li, D. & Feng, Z. (2012). Synthesis and evaluation of benzophenone *O*-glycosides as α -glucosidase inhibitors. *Archiv der Pharmazie – Chemistry in Life Sciences*, **345**, 771-783.
- Lyu, L.-C., Chi, I.-C., Huang, C.-K., Huang, L.-L., Lee, W.-J. & Lu, H.-C. (2008). Development of nutrient databases for epidemiological studies in Taiwan. *Asia Pacific Journal of Clinical Nutrition*, **17**, 302-305.
- Malherbe, C.J., Willenburg, E., De Beer, D., Bonnet, S.L., Van der Westhuizen, J.H. & Joubert, E. (2014). Iriflophenone-3-*C*-glucoside from *Cyclopia genistoides*: Isolation and quantitative comparison of antioxidant capacity with mangiferin and isomangiferin using on-line HPLC antioxidant assays. *Journal of Chromatography B*, **951-952C**, 164-171.
- Marseglia, L., Manti, S., D'Angelo, G., Nicotera, A., Parisi, E., Di Rosa, G., Gitto, E. & Arrigo, T. (2015). *International Journal of Molecular Sciences*, **16**, 378-400.
- Moldoveanu, S.C., Zhu, J. & Qian, N. (2015). Free amino acids analysis by liquid chromatography with tandem mass spectrometry in several botanicals with antioxidant character. *Journal of Separation Science*, **38**, 2208-2222.
- Neveu, V., Pérez-Jiménez, J., Vos, F., Crespy, V., Du Chaffaut, L., Mennen, L., Knox, C., Eisner, R., Cruz, J., Wishart, D. & Scalbert, A. (2010). Phenol-Explorer: an online comprehensive database on polyphenol contents in foods. Database 2010, bap024. DOI: 10.1093/database/bap024.

- Peleg, M., Normand, M.D. & Corradini, M.G. (2012). The Arrhenius equation revisited. *Critical Reviews in Food Science and Nutrition*, **52**, 830-851.
- Pitocco, D., Tesauro, M., Alessandro, R., Ghirlanda, G. & Cardillo, C. (2013). *International Journal of Molecular Sciences*, **14**, 21525-21550.
- Rains, J.L. & Jain, S.K. (2011). Oxidative stress, insulin signaling and diabetes. *Free Radical Biology and Medicine*, **50**, 567-575.
- Rice-Evans, C.A., Miller, N.J. & Paganga, G. (1996). Structure-antioxidant activity relationships of flavonoids and phenolic acids. *Free Radical Biology and Medicine*, **20**, 933-956.
- Rothwell, J.A., Pérez-Jiménez, J., Neveu, V., Medina-Remón, A., M'Hiri, N., García-Lobato, P., Manach, C., Knox, C., Eisner, R., Wishart, D.S. & Scalbert, A. (2013). Phenol-Explorer 3.0: a major update of the Phenol-Explorer database to incorporate data on the effects of food processing on polyphenol content. Database 2013, bat070. DOI:10.1093/database/bat070.
- Rothwell, J.A., Medina-Remón, A., Pérez-Jiménez, J., Neveu, V., Knaze, V., Slimani, N. & Scalbert, A. (2015). Effects of food processing on polyphenol contents: A systematic analysis using Phenol-Explorer data. *Molecular Nutrition Food Research*, **59**, 160-170.
- Schulze, A.E., De Beer, D., De Villiers, A., Manley, M. & Joubert, E. (2014). Chemometric analysis of chromatographic fingerprints shows potential of *Cyclopia maculata* (Andrews) Kies for production of standardized extracts with high xanthone content. *Journal of Agricultural and Food Chemistry*, **62**, 10542-10551.
- Schulze, A.E., Beelders, T., Koch, I.S., Erasmus, L.M., De Beer, D. & Joubert, E. (2015). Honeybush herbal teas (*Cyclopia* spp.) contribute to high levels of dietary exposure to xanthones, benzophenones, dihydrochalcones and other bioactive phenolics. *Journal of Food Composition and Analysis*, **44**, 139-148.
- Theron, K.A. (2012). Sensory and Phenolic Profiling of *Cyclopia* Species (Honeybush) and Optimisation of the Fermentation Conditions. MSc (Food Science) Thesis, Stellenbosch University, Stellenbosch, South Africa.
- Zhang, Y., Qian, Q., Ge, D., Li, Y., Wang, X., Chen, Q., Gao, X. & Wang, T. (2011). Identification of benzophenone C-glucosides from mango tree leaves and their inhibitory effect on triglyceride accumulation in 3T3-L1 adipocytes. *Journal of Agricultural and Food Chemistry*, **59**, 11526-11533.
- Zhang, Y., Liu, X., Han, L., Gao, X., Liu, E. & Wang, T. (2013). Regulation of lipid and glucose homeostasis by mango tree leaf extract is mediated by AMPK and PI3K/AKT signaling pathways. *Food Chemistry*, **141**, 2896-2905.